UNIVERSIDAD DE EXTREMADURA

Tesis Doctoral

Eliminación de contaminantes farmacéuticos en agua mediante procesos físicos, químicos y electroquímicos. Optimización de los sistemas.

Departamento de Ingeniería Química y Química Física

Patricia Palo Gil

2013

UNIVERSIDAD DE EXTREMADURA

DEPARTAMENTO DE INGENIERÍA QUÍMICA Y QUÍMICA FÍSICA

TESIS DOCTORAL

ELIMINACIÓN DE CONTAMINANTES FARMACÉUTICOS EN AGUA MEDIANTE PROCESOS FÍSICOS, QUÍMICOS Y ELECTROQUÍMICOS. OPTIMIZACIÓN DE LOS SISTEMAS.

PATRICIA PALO GIL

Conformidad de los directores de Tesis:

Fdo.: Teresa González Montero **Fdo.: Joaquín Ramón Domínguez Vargas**

Badajoz, 2013

A MIS PADRES

ÍNDICE

AGRADECIMIENTOS

La realización de esta Tesis Doctoral, no habría sido posible sin la participación y el apoyo de personas e instituciones que han facilitado este trabajo. Es para mí un verdadero placer escribir estas frases expresándoles mis agradecimientos.

En primer lugar, quisiera dar las gracias a mis directores, Teresa González Montero y Joaquín Ramón Domínguez Vargas, por darme la oportunidad de realizar esta Tesis Doctoral.

También he de exponer mi reconocimiento al Ministerio de Ciencia e Innovación a través de los Proyectos del plan Nacional CTQ 2007-60255 y CTQ 2010-14823, y a la Consejería de Ciencia y Tecnología de la Junta de Extremadura a través del Proyecto PRI-07A031. Sin el apoyo económico prestado no hubiera sido posible la realización de esta Tesis.

Al Departamento de Ingeniería Química de la Universidad de Castilla La Mancha por su estupenda aceptación durante la estancia realizada. A los que dirigieron mi trabajo, Manuel Andrés Rodrigo Rodrigo y Cristina Sáez Jiménez, y a los que fueron mis compañeros, Diego, Ángel, Mª José, Pedro Juan, Javi y Ana, os agradezco vuestro acogimiento y ayuda. Admiro vuestra profesionalidad y forma de trabajar.

Quiero agradecer enormemente a mis “compis” del Laboratorio 3, los cuales me robaron el corazón con su cariño, con su apoyo, con su verdadera amistad. Habéis hecho de mi lugar de trabajo mi segundo hogar. Gloria, mi gran apoyo, que tantas veces has ejercido de madre, de psicóloga, de consejera, se me quedan cortas las palabras de agradecimiento hacia ti. Fernando, mi protector, que tantas veces me has escuchado y comprendido, por tus consejos, por tus divertidos momentos de risas, eres una persona estupenda. Gracy, mi niña chica (te considero también parte de este laboratorio), que tantas veces hemos compartido momentos personales y

profesionales, por acompañarme en cada etapa de este camino que hemos recorrido juntas, eres muy especial para mí. Elenita, mi energía positiva, que tantas veces me has animado con tu optimismo, tus piropos y tus achuchones, eres un "sensible" encanto. Mª Jesús, mi compañera de batalla, que tantas veces me has apoyado y ayudado con tu sonrisa, con tus hechos, con tu escucha, eres genial. Paco, mi compañero de desayuno, que tantas veces me has hecho reír con tus coreografías, con tus canciones, eres una caja llena de sorpresas. Jesús Sánchez, mi colaborador, que tantas veces me has ofrecido tu ayuda y me has ayudado, sé que puedo contar contigo.

A mis otros compañeros de laboratorio, Azahara, Almudena, Sagasti, Ana, Fany, Rafa, Diego, Nuria y otros que ya se han ido como Ángel, Ruth, Gloria, Miriam, Juan Carlos y Lupe, gracias por vuestra ayuda y por los buenos momentos vividos a lo largo de todos estos años: risas, fiestas, comidas, desayunos, congresos…Ha sido un placer haberos conocido.

También agradecer a los profesores, Jesús Beltrán de Heredia, Francisco J. Real Moñino y Eduardo M. Cuerda Correa, que de una forma u otra me habéis ayudado y habéis hecho más fácil este camino.

Muchas gracias a mi marido Alex, por cuidarme, por mimarme, por quererme, por saber entenderme, por estar siempre ahí, por compartir tu vida conmigo. Y a mi preciosa hija Adriana por hacer tan felices los momentos que paso contigo y alegrarme sólo con verte la carita. Juntos "somos uno".

Finalmente, el agradecimiento más profundo y sentido va para mis padres, Ramón y Ángela, y mi hermano, Moncho. Sois un ejemplo de lucha y honestidad. Gracias porque siempre me he sentido arropada, querida y afortunada. Sin vuestro apoyo, ayuda y cariño habría sido imposible llevar a cabo todo esto. *Gracias, gracias y gracias.*

RESUMEN

Los compuestos farmacéuticos, considerados contaminantes emergentes, están presentes en efluentes de las estaciones depuradoras, en aguas naturales superficiales, subterráneas e incluso en agua potable. Dentro de estos contaminantes se encuentran analgésicos, antibióticos y antiepilépticos, entre otros. En la presente Tesis Doctoral se han estudiado diversos procesos físicos, químicos y electroquímicos con la finalidad de conseguir la eliminación de cuatro fármacos de uso común, cuya presencia en aguas está suficientemente documentada. Concretamente, se trata de trimetoprima (antibiótico), carbamacepina (antiepiléptico), ketoprofeno y naproxeno (analgésicos).

Los procesos de adsorción se han llevado a cabo utilizando resinas poliméricas sintéticas (*Amberlite XAD-7*) y adsorbentes naturales de base tanínica (acacia, quebracho, pino y ciprés). La síntesis de adsorbentes tanínicos ha sido estudiada teniendo en cuenta tanto su origen y la química de su formación como su posible aplicabilidad para la retirada de contaminantes farmacéuticos. Así se ha estudiado la influencia de variables en los procesos de adsorción y se ha llevado a cabo la modelización teórica haciendo uso de los modelos de pseudo-primer orden, pseudo-segundo orden, difusión intrapartícula, *Bangham* y *Elovich*, para el estudio de la cinética, y los modelos de *Langmuir*, *Freundlich* y *Dubbinin-Radushkevich* para el estudio del equilibrio de adsorción.

Por otra parte, se han tratado aguas contaminadas con estos compuestos farmacéuticos mediante electro-oxidación, concretamente oxidación anódica, empleando electrodos de diamante dopado con boro. Se ha comprobado la eficacia de este proceso en agua ultra-pura y en diferentes matrices acuosas (pantano, río, efluente de EDAR y residual de una industria farmacéutica). Los resultados obtenidos indican que esta técnica es muy eficaz y prometedora para la degradación de este tipo de contaminantes refractarios en aguas.

Otros Procesos de Oxidación Avanzada han sido estudiados para llevar a cabo la eliminación de los fármacos seleccionados. Se han aplicado las tecnologías de reactivo de Fenton, sistema Fenton-like, ozonación y radiación UV en presencia de peróxido de hidrógeno.

En la presente Tesis, además de demostrar la alta eficiencia de cada uno de los tratamientos aplicados y la influencia de las variables de operación, se ha llevado a cabo la optimización de los mismos y se ha estudiado la interacción de las variables en el proceso de retirada y degradación de fármacos, según diseños factoriales y metodología de la superficie de respuesta.

PUBLICACIONES

El trabajo realizado en esta Tesis Doctoral ha dado lugar a las siguientes publicaciones:

1. *"Removal of carbamazepine, naproxen and trimethoprim from water by Amberlite XAD-7: A kinetic study"*. Domínguez, J.R.; González, T.; Palo, P.; Cuerda-Correa, E.M. Clean. Air, Soil, Water. 10.1002/clen.201200245 **(2013)**.

2. *"Removal of common pharmaceuticals present in surface waters by Amberlite XAD-7 acrylic-ester-resin: Influence of pH and other drugs in solution"*. Domínguez, J.R.; González, T., Palo, P., y Sánchez-Martín, J. Desalination. 269, 231-238 **(2011)**.

3. *"Natural adsorbents derived from tannin extracts for pharmaceutical removal in water"*. Beltrán-Heredia, J.; Palo, P.; Sánchez-Martín, J.; Domínguez, J.R.; González, T. Industrial and Engineering Chemistry Research. 51, 50-57 **(2012)**.

4. *"Electrochemical advanced oxidation of carbamazepine on boron-doped diamond anodes. Influence of operating variables"*. Domínguez, J.R.; González, T.; Palo, P.; Sánchez-Martín, J. Industrial and Engineering Chemistry Research. 49, 8353-8359 **(2010)**.

5. *"Anodic oxidation of ketoprofen on boron-doped diamond (BDD) electrodes. Role of operative parameters"*. Domínguez, J.R.; González, T., Palo, P.; Sánchez-Martín, J. Chemical Engineering Journal. 162, 1012-1018 **(2010)**.

6. *"Conductive-diamond electrochemical advanced oxidation of naproxen in aqueous solution: optimizing the process"*. González, T.; Domínguez, J.R.; Palo,P.; Sánchez-Martín, J. Journal of Chemical Technology and Biotechnology. 86, 121-127 **(2011)**.

7. *"Development and optimization of the BDD-electrochemical oxidation of the antibiotic trimethoprim in aqueous solution".* González, T.; Domínguez, J.R.; Palo, P.; Sánchez-Martín, J. Desalination. 280, 197-202 **(2011)**.

8. *"Electrochemical degradation of a real pharmaceutical effluent".* Domínguez, J.R.; González, T.; Palo, P.; Sánchez-Martín, J.; Rodrigo, M. A.; Sáez, C. Water, Air and Soil Pollution. 223, 2685-2694 **(2012)**.

9. *"Conductive-diamond electrochemical oxidation of a pharmaceutical effluent with high COD. Kinetics and optimization of the process by RSM".* Domínguez, J.R.; González, T.; Palo, P.; Sánchez-Martín, J.; Rodrigo, M. A.; Sáez, C. Environmental Engineering and Management Journal. Aceptado para publicación **(2013)**.

10. *"Fenton + Fenton-like integrated process for carbamazepine degradation: optimizing the system".* Domínguez, J.R.; González, T.; Palo, P.; Cuerda-Correa, E.M. Industrial and Engineering Chemistry Research. 51, 2531-2538 **(2012)**.

11. *"Ozonation of a carbamazepine effluent. Designing the Operational Parameters".* Palo, P.; Domínguez, J.R.; Sánchez-Martín, J. Water, Air and Soil Pollution. 223, 5999-6007 **(2012)**.

Los siguientes artículos se encuentran en proceso de revisión:

12. *"Advanced Photochemical Oxidation of Carbamazepine in Aqueous Solution. Optimizing the System".* Palo, P.; Cuerda-Correa, E.M.; Domínguez, J.R.; González, T. Journal of Environmental Management. En revisión.

13. *"Electrochemical degradation of carbamazepine in aqueous solutions. Optimization of kinetic aspects by Design of Experiments".* Palo, P.; Domínguez, J.R.; Sánchez-Martín, J.; González, T. Water, Air and Soil Pollution. En revisión.

14. *"Feasibility of electrochemical degradation of pharmaceutical pollutants in different aqueous matrices. Optimization through Design of Experiments".* Palo,P.; Domínguez, J.R.; González, T.; Sánchez-Martín, J. Journal of Environmental Science and Health, part A. En revisión.

Primera Parte

Introducción

INTRODUCCIÓN

A. EL PROBLEMA DEL AGUA.

El agua es un recurso natural, escaso e indispensable para la vida humana que además permite la sostenibilidad del medio ambiente. Constituye una parte esencial de todo ecosistema, tanto en términos cualitativos como cuantitativos. Una reducción del agua disponible ya sea en cantidad, en calidad, o en ambas, provoca efectos negativos graves sobre los ecosistemas. El medio ambiente tiene una capacidad natural de absorción y de autolimpieza. Sin embargo, si se sobrepasa, la biodiversidad se altera, los medios de subsistencia disminuyen, las fuentes naturales de alimentos (por ejemplo, los peces) se deterioran y se generan costes de limpieza extremadamente elevados [1].

En el Decenio Internacional para la acción "El agua fuente de vida" 2005-2015 de la Organización de la Naciones Unidas (ONU), se expone que la calidad de cualquier masa de agua superficial o subterránea depende tanto de factores naturales como de la acción humana. Sin la acción humana, la calidad del agua vendría determinada por la erosión del substrato mineral, los procesos atmosféricos de evapotranspiración y sedimentación de lodos y sales, la lixiviación natural de la materia orgánica y los nutrientes del suelo, y los procesos biológicos en el medio acuático que puedan alterar la composición física y química del agua.

Según se constata en el segundo informe de las Naciones Unidas sobre el Desarrollo de los Recursos Hídricos en el Mundo [2], la mala calidad del agua frena el desarrollo económico, y puede tener efectos negativos sobre la salud y los medios de vida. La contaminación química de las aguas superficiales, principalmente debido a vertidos industriales y agrícolas, constituye también un gran riesgo para la salud en algunos países en vías de desarrollo. La contaminación y los residuos industriales están poniendo en peligro los recursos hídricos, dañando y destruyendo los

ecosistemas del mundo entero. Todo esto amenaza la seguridad hídrica de las personas y de las industrias consumidoras de agua. Los municipios están comprobando que la calidad del agua que suministran se ve comprometida por los residuos industriales. Las industrias en los países desarrollados y en vías de desarrollo que requieren agua no contaminada, comprueban que su seguridad hídrica se ve cada vez más afectada a causa del déficit y del deterioro de la calidad del agua.

La contaminación y la degradación del agua siguen creciendo a nivel mundial. Más del 80% de las aguas residuales de los países en vías de desarrollo se descargan sin tratamiento, contaminando ríos, lagos y zonas costeras. Muchas industrias, como la industria química y la del cuero, se están trasladando de los países desarrollados a los países de economía emergente. Se prevé que las poblaciones urbanas se incrementarán un 60% antes del año 2025, lo cual afectará a las previsiones acerca del estrés hídrico. En 1998, aproximadamente el 90% de los biotopos marinos y costeros del Mar Báltico estuvieron amenazados por una pérdida de la calidad del agua debido a problemas de contaminación, entre otros. En un estudio reciente sobre el agua potable en países desarrollados se observó que un 5,8% de la población estaba expuesta a aguas cuya calidad no estaba conforme con los estándares de la Organización Mundial de la Salud (OMS) [3].

Las medidas legislativas que se han ido adoptando progresivamente para evitar la contaminación química del agua y los riesgos que se derivan de ella han contribuido a paliar parcialmente esta situación. Sin embargo, la creciente demanda de agua y el descubrimiento continuo de nuevos contaminantes potencialmente peligrosos dejan clara la necesidad de seguir investigando en todas aquellas áreas que puedan contribuir a proteger la salud humana y la del medio ambiente. La aparición de elementos "no deseables" y tóxicos, y la variación en las concentraciones de los constituyentes comunes, tienen su origen en el denominado "ciclo del agua" (ver Figura 1). En alguna parte de este ciclo, en el cual confluyen distintos compartimentos ambientales y actividades humanas, es donde se produce la contaminación del agua, o mejor dicho, la alteración de su calidad. De acuerdo con este ciclo, las principales vías de entrada de contaminantes en el medio ambiente acuático son las aguas residuales, entre las que

se incluyen las urbanas, industriales, y las de origen agrícola o ganadero. La prevalencia de una u otra depende en gran medida del tipo de contaminación de que se trate y del nivel de depuración o atenuación natural (si existe) que experimentan [4].

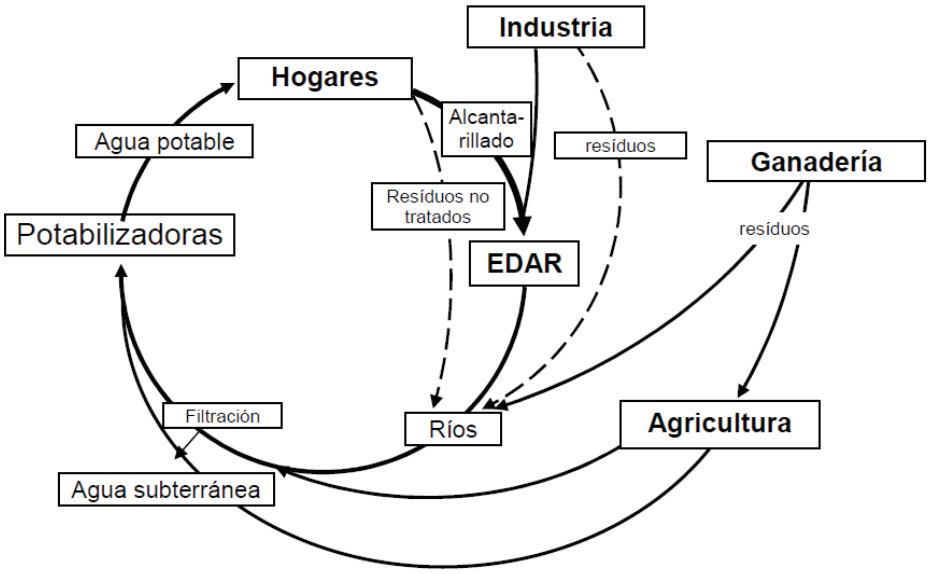

Fig.1. Ciclo del agua [4].

Las aguas residuales pueden tener diferentes orígenes, siendo las fuentes de contaminación más comunes las que se exponen a continuación:

- *Origen agrícola o ganadero:* Son el resultado del riego y de otras labores como la limpieza ganadera, que pueden aportar al agua grandes cantidades de estiércol y orines (materia orgánica, nutrientes y microorganismos). Uno de los mayores problemas es la contaminación con nitratos.
- *Origen doméstico:* Son las que provienen de núcleos urbanos. Contienen sustancias procedentes de la actividad humana (alimentos, deyecciones, basuras, productos de limpieza, jabones, etc.).
- *Origen pluvial:* Se origina por arrastre de la suciedad que encuentra a su paso el agua de lluvia.

- *Origen industrial:* Los procesos industriales generan una gran variedad de aguas residuales, y cada industria debe estudiarse individualmente.

Durante décadas, la comunidad científica ha centrado sus esfuerzos en el estudio de los contaminantes químicos cuya presencia en el medio ambiente ha estado o está regulada en las distintas legislaciones, contaminantes en su mayoría apolares, tóxicos, persistentes y bioacumulables, como los hidrocarburos policíclicos aromáticos (HPAs), los policlorobifenilos (PCBs) o las dioxinas. Sin embargo, en los últimos años, el desarrollo de nuevos y más sensibles métodos de análisis ha permitido alertar de la presencia de otros contaminantes, potencialmente peligrosos, denominados globalmente como "contaminantes emergentes" [4].

B. COMPUESTOS FARMACÉUTICOS Y SU IMPACTO AMBIENTAL.

B.1. Contaminantes emergentes.

Los contaminantes emergentes, cuyo estudio se encuentra entre las líneas de investigación prioritarias de los principales organismos dedicados a la protección de la salud pública y del medio ambiente, tales como la Organización Mundial de la Salud (OMS), la Agencia para la Protección del Medio Ambiente (EPA), o la Comisión Europea, se definen como contaminantes previamente desconocidos o no reconocidos como tales, cuya presencia en el medio ambiente no es necesariamente nueva pero sí la preocupación por las posibles consecuencias de la misma. Los contaminantes emergentes son compuestos de los cuales se sabe relativamente poco o nada acerca de su presencia e impacto en los distintos entornos ambientales, razón por la cual y a su vez consecuencia de que no hayan sido regulados, y de que la disponibilidad de métodos para su análisis sea nula o limitada. Otra particularidad de estos compuestos, es que debido a su elevada producción y consumo, y a la consecuente continua introducción de los mismos en el medio ambiente, no necesitan ser persistentes para ocasionar efectos negativos [5].

Algunos equipos científicos españoles han trabajado intensamente durante los últimos años en la investigación de algunos de estos contaminantes emergentes (detergentes del tipo alquilfenol etoxilado, estrógenos, retardantes de llama bromados, y algunos fármacos), como resultado de lo cual se han puesto a punto ya algunos métodos analíticos para su determinación en distintas matrices ambientales (fundamentalmente aguas superficiales y residuales, y sedimentos).

La lista de contaminantes emergentes incluye una amplia variedad de productos de uso diario con aplicaciones tanto industriales como domésticas. Las clases de contaminantes emergentes que demandan una mayor y más urgente atención debido a la escasez de datos ambientales ecotoxicológicos y de métodos para su análisis, y a las posibles consecuencias de su presencia en el medio ambiente son [4]:

- Retardantes de llama bromados
- Cloroalcanos
- Pesticidas polares
- Compuestos perfluorados
- Fármacos
- Drogas de abuso
- Metabolitos y/o productos de degradación de las clases de sustancias anteriores.

Como estos contaminantes emergentes no están regulados por la legislación, las depuradoras no realizan su análisis de forma rutinaria. En los últimos años, los fármacos han resultado ser los contaminantes emergentes que presentan una mayor preocupación siendo objeto de estudio. Ello es debido a que el elevado consumo de productos farmacéuticos produce contaminación y acumulación, afectando al ecosistema y a los humanos a través de la cadena trófica. Teniendo esto en cuenta, el trabajo de investigación realizado se centra en la eliminación de productos farmacéuticos presentes en aguas.

B.2. Productos farmacéuticos.

Se considera producto farmacéutico a toda sustancia medicinal y sus asociaciones o combinaciones, destinadas a prevenir, diagnosticar, curar o aliviar cualquier tipo de enfermedad. Es un compuesto bien definido, puro, natural o sintético, dotado de una actividad biológica, que puede ser aprovechable, o no, por sus efectos terapéuticos. Por lo tanto, un fármaco es el principio activo del medicamento.

Uno de los factores que condicionan fuertemente el efecto biológico de los fármacos es su metabolismo. De él dependen en gran parte, la velocidad de aparición del efecto (periodo de latencia) y la duración del mismo, la toxicidad del fármaco y la elección de la vía de administración. Cuando un fármaco entra en el organismo es transformado parcial o totalmente en otras sustancias para facilitar su excreción. Las reacciones químicas causantes del metabolismo son las encargadas de transformar el fármaco gracias a enzimas que catalizan las reacciones.

Dentro de las sustancias farmacológicamente activas, pueden considerarse como más representativos los siguientes grupos terapéuticos [6]:

- Antiinflamatorios y analgésicos. Se emplean fundamentalmente para combatir el dolor. La mayor parte de estos fármacos tienen también propiedades analgésicas y antipiréticas. Su forma de actuar es inhibiendo la síntesis de compuestos involucrados en la respuesta inflamatoria. Dentro de este grupo los compuestos más empleados son el paracetamol, ácido acetilsalicílico, ibuprofeno, diclofenaco, **naproxeno** y **ketoprofeno**.

- Antidepresivos. Los más frecuentes son las benzodiacepinas que son fármacos que aumentan la actividad de ciertos neurotransmisores inhibidores, reduciendo así el funcionamiento de ciertas áreas del cerebro. Producen somnolencia, descenso en la ansiedad y relajación de los músculos.

- Antiepilépticos. El más común es la **carbamacepina**. El cerebro y los nervios están formados por una gran cantidad de células nerviosas, que se comunican entre sí a través de impulsos eléctricos. La carbamacepina evita el cúmulo

excesivo, rápido y repetitivo de impulsos eléctricos, manteniendo normal la actividad cerebral.

- Antineoplásicos. Son fármacos empleados para el tratamiento del cáncer, entre los que se encuentran el bisulfan, ciclofosfamidas, etc.
- Antilipemiantes. Se aplican fundamentalmente para bajar los niveles de colesterol en sangre en personas con arterioesclerosis. Los fármacos mas frecuentes son fibratos (derivados del ácido fíbrico) y estatinas. Los fibratos reducen los niveles de triglicéridos y aumentan los niveles de HDL, mientras que las estatinas son más efectivas sobre el LDL.
- Betabloqueantes. Bloquean los receptores beta que existen en el corazón, consiguiendo disminuir la necesidad de oxígeno del corazón, reducir el ritmo cardíaco, disminuir la fuerza de contracción del corazón, y reducir la contracción de los vasos sanguíneos. Están indicados para combatir la hipertensión arterial, angina de pecho, arritmias cardíacas, etc. Los más utilizados son el atenolol, propanolol, metoprolol, etc.
- Antiulcerosos y antihistamínicos. Se emplean contra la acidez de estómago, úlceras y otras alteraciones estomacales. Son bloqueadores de receptores H1 y H2 de la histamina. Estos receptores se encuentran en unas células que recubren el estómago, cuando la histamina se une a ellos las células producen ácido. Estos fármacos reducen la unión de la histamina a estos receptores, por lo que la producción de ácido disminuye. (Ej. Ranitidina, famotidina).
- Antibióticos. Entre los antibióticos más importantes se encuentran las sulfonamidas, fluoroquinolonas, cloranfenicol, tilosina y **trimetoprima**.
- Otras sustancias. Se pueden incluir aquí sustancias que alteran la mente sin una necesidad médica y que con frecuencia son objeto de abuso como por ejemplo el alcohol, marihuana, cocaína, barbitúricos, metadona, heroína y otros narcóticos, anfetaminas, LSD (dietilamina del acido lisérgico) y la PCP (fenilciclidina).

Los productos farmacéuticos seleccionados en el presente trabajo han sido: ketoprofeno, naproxeno, carbamacepina y trimetoprima. A continuación, se describe brevemente la naturaleza química y las principales aplicaciones de dichos compuestos.

B.2.1. Carbamacepina, ketoprofeno, naproxeno y trimetoprima.

La **carbamacepina** es un fármaco antiepiléptico psicótropo en cuya estructura se aprecia una subunidad de urea o carbamida, de ahí su nombre [5H-dibenzo-(b,f)-azepina-5-carboxamida]. Es un derivado tricíclico del iminoestilbeno. La fórmula molecular es $C_{15}H_{12}N_2O$. La estructura química se puede observar en la Figura 2. Es un estabilizador del ánimo, usado principalmente para el tratamiento de la epilepsia y del trastorno bipolar. También es un fármaco antimaníaco, para el tratamiento de la crisis maníaca aguda. En ocasiones también se utiliza para tratar la esquizofrenia y la neuralgia del trigémino.

La carbamacepina es el compuesto farmacéutico más frecuentemente detectado en aguas. Aproximadamente el 72% de la carbamacepina administrada por vía oral se adsorbe, mientras que el 28% no se modifica y se elimina por vía renal. Este medicamento ha sido propuesto por algunos autores [7] como marcador antropogénico por excelencia en el agua. Por lo general, la carbamacepina y sus metabolitos se vierten a las aguas residuales a través del sistema de alcantarillado. Recientes trabajos han determinado que la carbamacepina es bastante persistente y que las eficiencias de eliminación por las estaciones de depuración de aguas residuales (EDARs) siempre están por debajo del 10%.

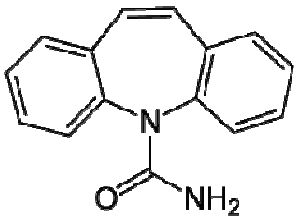

Fig. 2. Estructura química de la carbamacepina.

El **ketoprofeno** es un derivado del ácido fenil-propiónico [2-(3-benzoilfenil ácido)-propanoico]. La fórmula molecular es $C_{16}H_{14}O_3$. La estructura química se

puede observar en la Figura 3. Es un tipo de agente antiinflamatorio no esteroideo (AINE). Muestra actividad antiinflamatoria a altas dosis y analgésica a dosis bajas. Está indicado en el tratamiento de la artritis reumatoide, osteoartritis, espondilitis anquilosante, episodio agudo de gota, cuadros dolorosos asociados a la inflamación (dolor dental, traumatismos, dolor post-quirúrgico odontológico, etc.).

Ha sido detectado frecuentemente en efluentes de plantas de tratamiento de aguas residuales, aguas superficiales, aguas subterráneas y aguas potables [8,9]. Después de la ingesta de ketoprofeno, éste se metaboliza y posteriormente se excreta en la orina (más del 80% de la dosis ingerida) [10]. Se ha demostrado que la biodegradación de ketoprofeno es limitada en las EDAR. Los rendimientos de eliminación oscilan entre el 37% y el 90% [11,12]. Los resultados obtenidos por Quintana y col. [13] utilizando lodos activados en condiciones aerobias pusieron de manifiesto que el ketoprofeno era mineralizado sólo en parte por los microorganismos en las EDARs. Otros autores sugirieron que mediante la fototransformación directa y biodegradación, el ketoprofeno se eliminaba en el medio ambiente [9,14]. En cualquier caso, el ketoprofeno no se elimina por completo en la mayoría de las plantas de tratamiento de aguas residuales y se detecta tanto en los lodos como en los efluentes de depuradoras de aguas residuales [15].

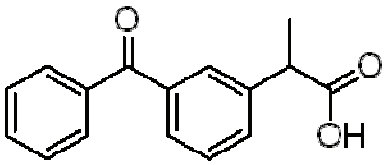

Fig. 3. Estructura química del ketoprofeno.

El **naproxeno** es un antiinflamatorio no esteroideo (AINE) de uso general, derivado del ácido propiónico [(S)-6-metoxi-α-metil-2-naftalenacético]. La fórmula molecular es $C_{14}H_{14}O_3$. La estructura química se puede observar en la Figura 4. Se emplea en el tratamiento del dolor leve a moderado, la fiebre, la inflamación y la rigidez provocados por afecciones como la osteoartritis, la artritis reumatoide, la artritis psoriásica, la espondilitis anquilosante, diversas lesiones, la tendinitis y la

bursitis, y en el tratamiento de la dismenorrea primaria y los calambres menstruales [16]. También se emplea en medicina veterinaria en cantidades considerables [17].

Debido a su amplio uso, por ser un medicamento sin necesidad de prescripción médica, se ha detectado en aguas superficiales, aguas subterráneas, aguas residuales e incluso en aguas potables [18,19]. La eliminación de naproxeno en EDAR presenta niveles bajos (40-66%) [20,21]. Por otra parte, Boyd y col. [22] observaron que el tratamiento de coagulación y sedimentación no fueron efectivos para la eliminación de naproxeno en las aguas superficiales.

Diversas pruebas de bioensayo han demostrado que el naproxeno produce una alta toxicidad crónica y los subproductos generados en la fotodegradación son más tóxicos que el propio producto de partida [23].

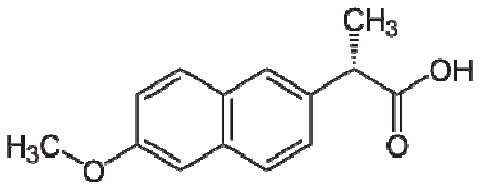

Fig. 4. Estructura química del naproxeno.

La **trimetoprima** es un antibiótico bacteriostático derivado de la trimetoxibenzilpirimidina ([2,4-diamino-5-(3',4',5'-trimethoxibenzilpirimidina]). La fórmula molecular es $C_{14}H_{18}N_4O_3$ y la estructura química se muestra en la Figura 5. Es uno de los antibióticos más importantes utilizados en la medicina humana y veterinaria en todo el mundo.

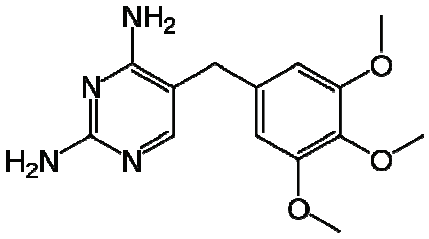

Figura 5. Estructura química de la trimetoprima.

Este antibiótico, pertenece a un grupo de agentes conocidos como inhibidores de la dihidrofolato reductasa [24-26]. Se utiliza principalmente en la profilaxis y en el tratamiento de infecciones urinarias, así como para la prevención y tratamiento de infecciones del sistema respiratorio y gastrointestinal en el ganado bovino, porcino y aves de corral [27].

B.3. Problemática ambiental de los productos farmacéuticos.

En 2011, la Organización Mundial de la Salud (OMS) publicó un informe acerca de los productos farmacéuticos presentes en el agua potable, los cuales generan riesgos en la salud humana. Además la entrada continua de estos fármacos en el medio ambiente puede representar un riesgo potencial para los organismos que viven en ambientes terrestres y acuáticos [28].

Un aspecto importante de los fármacos desde el punto de vista medioambiental, es que presentan una serie de características que les hace diferentes a los contaminantes químicos industriales convencionales:

- Las sustancias farmacológicamente activas incluyen compuestos formados por moléculas grandes y químicamente complejas.
- Son moléculas polares y tienen más de un grupo ionizable. El grado de ionización y sus propiedades dependen del pH de la solución.
- La persistencia en el medio ambiente es mayor de un año para fármacos como la eritromicina, ciclofosfamida, naproxeno, sulfametoxazol, etc., y de varios años para otros como el ácido clofíbrico, por lo que pueden acumularse alcanzando niveles biológicamente activos.
- Llegan al medio ambiente a través de su excreción y metabolización por el hombre y los animales.

Según las propiedades físico-químicas de los fármacos, sus metabolitos y productos de degradación, y las características de los suelos, estas sustancias pueden llegar a alcanzar las aguas subterráneas y contaminar los acuíferos o bien quedar

retenidas en el suelo y acumularse pudiendo afectar al ecosistema e incluso a los humanos a través de la cadena trófica.

Las concentraciones que se han encontrado en aguas superficiales (como consecuencia de una eliminación incompleta en las plantas de depuración de aguas) o en aguas subterráneas (debido a la escasa atenuación que experimentan algunos compuestos durante la filtración a través de suelos) se sitúan normalmente en el rango de $ng \cdot L^{-1}$ o $\mu g \cdot L^{-1}$, mientras que en suelos y sedimentos, en donde pueden persistir durante largos periodos de tiempo, alcanzan concentraciones de hasta $g \cdot Kg^{-1}$ [29]. Pero lo que ha despertado una mayor preocupación ha sido el hallazgo de algunos de ellos (como el ibuprofeno, el diclofenaco, la carbamacepina o el ácido clofíbrico) en aguas potables [30].

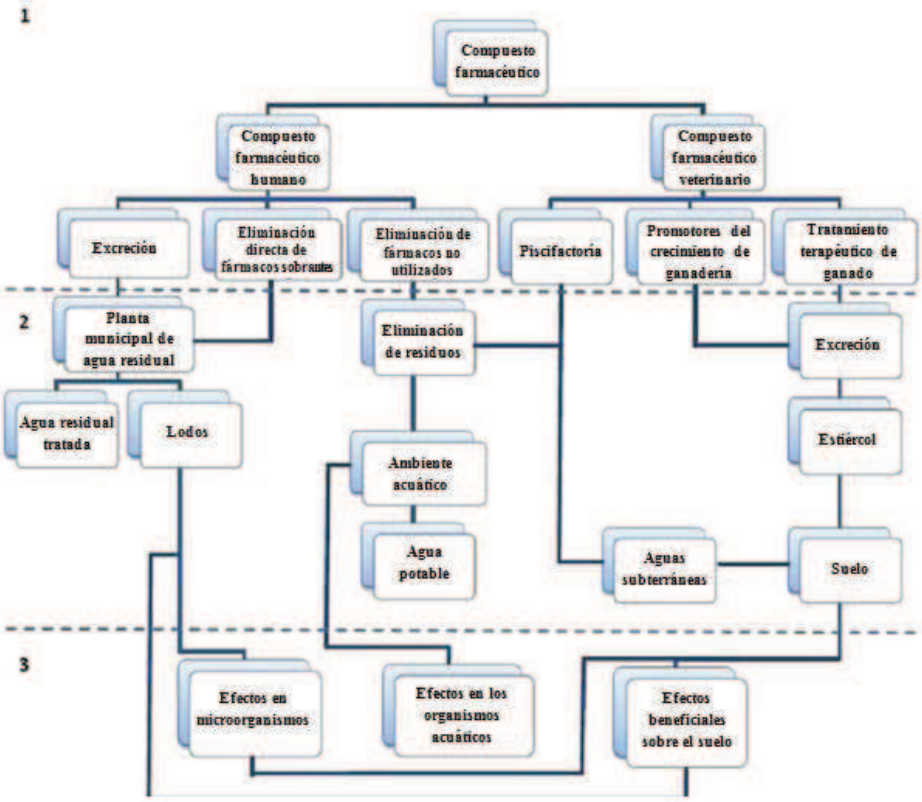

Figura 6. Presencia y efectos en el medio ambiente de residuos farmacéuticos (1-exposición, 2-destino, 3-efectos) (Adaptada de la referencia [31]).

Aunque el destino exacto y el efecto de estos compuestos en el medio ambiente no es fácil de predecir, las vías de exposición son tal como se esquematizan en la Figura 6 [31].

En muchos casos, las consecuencias de su presencia en el medio ambiente no están aún claras, pero en otros el riesgo parece evidente, y alarmante. Aunque hasta la fecha hay pocos estudios sobre los efectos directos de la presencia de estas sustancias en el medio ambiente, se han detectado ya algunos hechos y/o consecuencias que se describen más abajo:

- Ciertos problemas en algunas especies de peces pueden ser debidos a la presencia de medicamentos antidepresivos en el agua.
- Acumulación de componentes activos de medicamentos antidepresivos en el cerebro, el hígado y los músculos de tres tipos de peces diferentes que vivían en ríos a los que vertían efluentes de depuradoras.
- Alteraciones en el comportamiento y fisiología de los insectos, inhibición o estimulación del crecimiento en plantas acuáticas y algas, y desarrollo de bacterias resistentes, etc.
- El diclofenaco, aparte de afectar a los riñones en los mamíferos, se ha asociado (como consecuencia de su uso en veterinaria) con la desaparición de los buitres blancos en la India y Pakistán [32].
- El propanolol, que el equipo de investigación del Dr. Barceló ha detectado en múltiples ocasiones en España, tiene efectos sobre el zooplancton, así como sobre los organismos bentónicos [32].

Por otro lado, y aunque a corto plazo parece que no se pueden detectar efectos graves sobre la salud o sobre el medio ambiente, sí resultan probables:

- Efectos potencialmente acumulativos a medio o largo plazo pudiendo ocasionar cambios en el medio ambiente o daños en el hombre.
- Proliferación de microorganismos resistentes a los antibióticos.

- Combinación de diferentes metabolitos y compuestos biológicamente activos formando una especie de cóctel farmacológico, capaz de potenciar los efectos negativos en el hombre y en el medio ambiente.

Los medicamentos son excretados por el hombre sin metabolizar o en forma de metabolitos activos, habiéndose detectado en las aguas residuales, aguas superficiales y aguas subterráneas más de 50 sustancias farmacológicamente activas de diversos grupos. Entre ellos se encuentran los analgésicos, antibióticos, antiepilépticos, antidepresivos, antibióticos, antireumáticos, hipolipemiantes, hormonas esteroideas, etc. [33,34].

Aunque hasta el momento no hay demasiada información al respecto, parece ser que no todos los fármacos son totalmente eliminados de las aguas por medio de los tratamientos convencionales realizados en las estaciones depuradoras de aguas residuales (EDARs), existiendo además evidencias de que muchas de estas sustancias son poco o nada biodegradadas en el medio ambiente.

Dentro de las estaciones depuradoras de aguas residuales los fármacos pueden o bien degradarse y mineralizarse rápidamente, o bien pueden permanecer invariables. Los compuestos hidrofílicos resistentes a la degradación pueden permanecer disueltos en la fase acuosa o pueden adsorberse a los fangos. En los tratamientos primarios, algunos pueden ser eliminados por adsorción (ej. estradiol y agentes perfumantes), mientras que otros siguen permaneciendo en fase acuosa (ej. ibuprofeno, naproxeno, sulfametoxazol, iopromida, etc.) [20]. En el tratamiento biológico se han obtenido eliminaciones entre 30-75% para el caso de antiinflamatorios y antibióticos. En estudios realizados por Drewers y col. [35] con analgésicos, antilipemiantes y anticonvulsivos se ha demostrado que para todos estos fármacos excepto para los antiepilépticos, las plantas depuradoras que funcionaban con elevadas edades de fango mostraban concentraciones inferiores de analgésicos y antilipemiantes en sus efluentes en comparación con las depuradoras que operaban con edades de fango más bajas. Estos datos concuerdan con otros obtenidos en diversas investigaciones:

- El bezafibrato (10-97%) y el ibuprofeno (12-86%) se eliminan parcialmente en las EDAR, con rendimientos claramente dependientes de la edad del fango [7,36]. Ensayos a escala de laboratorio empleando SBR han demostrado que con tiempos de retención superiores a 4 días se observa una reducción de más del 90% de ibuprofeno y bezafibrato [36].
- Para el caso del diclofenaco, la reducción era independiente de la edad del fango [36].
- Para el caso de la carbamacepina, diversos autores han constatado que la carbamacepina no se elimina de forma significativa a su paso por las depuradoras [7,33,36,37].
- De los 4 analgésicos más comúnmente utilizados (paracetamol, ácido acetilsalicílico, ibuprofeno y diclofenaco) los tres primeros son fácilmente degradados en las depuradoras y sólo el diclofenaco tiene bajos rendimientos de eliminación [37].

Parece ser que entre el grupo de los antibióticos, las penicilinas se hidrolizan fácilmente en agua y las tetraciclinas precipitan fácilmente con cationes como el calcio acumulándose en los fangos [34]. La mayor parte de estas sustancias no son totalmente degradadas en las depuradoras de aguas residuales, por lo que son vertidas con los efluentes y acaban en las aguas superficiales y subterráneas [38].

En Alemania se han detectado valores de carbamacepina de hasta más de 1075 $ng \cdot L^{-1}$ en aguas superficiales. En análisis realizados en el río Ebro, los fármacos que se han detectado en mayor cantidad han sido los siguientes: ibuprofeno (60 $ng \cdot L^{-1}$), acetaminofen (42 $ng \cdot L^{-1}$), gemfibrozil (46 $ng \cdot L^{-1}$), carbamacepina (30 $ng \cdot L^{-1}$) y atenolol (72 $ng \cdot L^{-1}$) [39].

Además se ha observado que la coexistencia de productos farmacéuticos u otros productos químicos genera una mayor toxicidad. Se ha demostrado, por ejemplo, que la aparición combinada de diclofenaco, ibuprofeno, naproxeno y ácido acetilsalicílico produce un efecto sinérgico sobre la toxicidad del efluente [40].

C. MÉTODOS GENERALES DE TRATAMIENTO DE AGUAS.

Con el fin de adecuar las aguas tanto para su consumo (potabilización) como para su vertido (depuración), los efluentes se someten a procesos de tratamiento que eliminan contaminantes o elevan su calidad. Los avances en investigaciones acerca de ciertos agentes tóxicos y normas ambientales han hecho la actualización de técnicas de tratamiento más elaboradas y más eficaces encaminadas a eliminar contaminantes persistentes.

Los productos farmacéuticos presentes en el agua pueden eliminarse mediante procesos químicos, físicos y/o biológicos. Estas operaciones y procesos se utilizan conjuntamente en los sistemas de tratamiento ya que actualmente no existe un tratamiento individual que proporcione una barrera absoluta para dichos contaminantes, bajo condiciones de efectividad y economía.

Las **operaciones físicas** son métodos de tratamiento en los que predomina la acción de fuerzas físicas y se conocen como operaciones físicas unitarias. Fueron las primeras en ser aplicadas al tratamiento de aguas. Generalmente presentan bajo coste y conllevan poco impacto medioambiental. Estas tecnologías no destruyen el contaminante, sino que lo separan mediante técnicas como la extracción líquido-líquido, los procesos de membrana y la adsorción mediante resinas o carbón activado.

En los **procesos químicos,** hay que destacar la *oxidación química* para la eliminación o conversión de los contaminantes, que se consigue mediante la adición de productos químicos que actúan como oxidantes o catalizadores de la degradación gracias al desarrollo de ciertas reacciones químicas. La limitación más importante en la oxidación química, es la cinética del proceso, ya que resulta ser demasiado lenta en muchas ocasiones. Así, el desarrollo de las tecnologías de oxidación química para degradar contaminantes orgánicos en medio acuoso se basa en la introducción de uno o varios activadores de la reacción que actúan generando radicales intermedios muy reactivos, tales como los radicales hidroxilo (·OH). Dichos tratamientos combinados constituyen los denominados *Procesos de Oxidación Avanzada* (POAs), los cuales se basan principalmente en la generación *in situ* del radical hidroxilo que reacciona

rápidamente con la mayoría de los compuestos orgánicos, a excepción de los alcanos clorados [41]. Los principales procesos de generación de radicales hidroxilos son O_3/H_2O_2, reactivo de Fenton (Fe^{2+}/H_2O_2), O_3/UV, H_2O_2/UV, O_3/H_2O_2/UV, foto-Fenton, sistema Fenton-like y fotocatálisis (UV/TiO_2). Entre los POAs, los procesos de oxidación avanzada electroquímicos (POAEs) y, en particular, la oxidación anódica, y electro-Fenton, han demostrado ser técnicas muy eficaces a escala de laboratorio en la reducción de la contaminación de aguas.

Los procesos de tratamiento en los que la eliminación de los contaminantes se lleva a cabo gracias a la actividad biológica se conocen como **procesos biológicos.** Pueden ser divididos en aerobios o anaerobios, ambos son relativamente baratos y se emplean de forma frecuente en las plantas de tratamiento de aguas residuales para degradar compuestos orgánicos en general. La principal aplicación de los procesos biológicos es la eliminación de las sustancias orgánicas biodegradables presentes en el agua residual. Básicamente estas sustancias se convierten en gases, que se liberan a la atmósfera, y en tejido celular biológico, eliminable por sedimentación. No siempre se consigue eliminar en su totalidad productos farmacéuticos mediante estos procesos, sino que se obtienen productos de transformación modificados estructuralmente. Es por ello, que resulta interesante aplicar un pre-tratamiento al agua mediante procesos de oxidación química con el fin de generar intermedios de reacción más biodegradables que los compuestos de partida [42]. Mediante un adecuado control del medio, el agua residual se puede tratar biológicamente en la mayoría de los casos.

De manera tradicional, las aguas potables y residuales se han sometido a tratamientos distintos, en función de su naturaleza y del destino que se le vaya a dar. Así pues, las aguas potables suelen ingresar en las plantas de tratamiento ETAP (Estación de Tratamiento de Aguas Potables) y pasar por las siguientes etapas:

1. **Pretratamientos o tratamientos previos**: retirada de sólidos gruesos y de gran tamaño, así como aceites, grasas, arena y gravilla, que pueden ser separados del agua bruta con poco esfuerzo técnico mediante desbaste o tamizado.

2. **Tratamientos primarios:** todas las operaciones que se efectúan dentro de la planta de potabilización y que se basan en la separación física, encaminadas principalmente a la disminución considerable de toda la materia que no ha sido retirada por los pretratamientos. Se llevan a cabo para eliminar sólidos orgánicos en suspensión y especies coloidales, lo cual es necesario para el buen funcionamiento y mantenimiento de las unidades de tratamiento posteriores. Los tratamientos primarios son: coagulación-floculación, decantación, precipitación y flotación.

3. **Tratamientos terciarios:** aquellos que contemplan el acondicionamiento del agua mediante corrección química, es decir, con reactivos que posibilitan el cumplimiento de las normativas higienicosanitarias vigentes. Algunos de ellos son: neutralización, remineralización, reducción de oxígeno, inhibición de la corrosión y desinfección.

4. **Tratamientos especiales y/o avanzados:** vienen motivados por un deseo expreso de alta calidad en el agua de salida o bien porque el agua provenga de una fuente particularmente cargada de especies problemáticas, como metales pesados, pesticidas o agentes farmacéuticos. También pueden llevarse a cabo para incluir alguna propiedad deseable en el agua de consumo, como puede ser la fluoración para prevenir la caries. Entre estos tratamientos se encuentran todos los procesos de membrana, la adsorción, los procesos de intercambio iónico y los procesos de oxidación avanzada.

En el caso de las aguas residuales, cuya carga contaminante es muy superior, la línea de tratamiento de aguas se ve completada con una etapa intermedia denominada **tratamiento secundario**, compuesta por todas aquellas operaciones que implican el uso de reactores biológicos y organismos vivos en la depuración de las aguas. Las estaciones de depuración de aguas residuales (EDARs) incluyen normalmente dispositivos que propician la degradación de los compuestos más contaminantes por microorganismos aerobios o anaerobios, en distintas disposiciones tecnológicas

(biodiscos, lodos activados, reactores de contacto, etc.) seguidas de una etapa de decantación y sedimentación o filtración fina y microtamizado [43].

Como ya se ha comentado anteriormente, las plantas de tratamiento de aguas no están diseñadas para hacer frente a la eliminación de microcontaminantes altamente polares, como es el caso de los compuestos farmacéuticos. Éstos, en principio, deberían ser eliminados por adsorción en sólidos en suspensión o a través de la asociación a grasas y/o aceites durante la degradación aeróbica y anaeróbica, y por degradación química mediante procesos tales como la hidrólisis [44,45]. Sin embargo, un estudio reciente sobre la eliminación de una mezcla de productos farmacéuticos, mostró eficiencias de eliminación por debajo del 20% en las plantas depuradoras [46].

Teniendo en cuenta que las operaciones que se realizan en las estaciones depuradoras de aguas resultan insuficientes e ineficaces para la eliminación de estos contaminantes, y los posibles efectos adversos que provocan los fármacos originales y sus metabolitos en los organismos vivos, se requieren tecnologías más potentes y eficientes para su tratamiento.

Tras esta panorámica general de los diferentes tratamientos a que pueden ser sometidas las aguas (tanto naturales como residuales), en los siguientes apartados se describen, de forma más detallada, los fundamentos y características de aquellos tratamientos de adsorción, oxidación química y oxidación electroquímica que han sido empleados en la presente Tesis para la eliminación de los productos farmacéuticos seleccionados.

C.1. Procesos de Adsorción en aguas.

La adsorción es una operación de transferencia de materia mediante la cual se lleva a cabo la separación de uno o varios componentes de una mezcla fluida, gas o líquido, mediante un sólido adsorbente de distinta naturaleza y por consiguiente, ajeno a la misma. Es un fenómeno que tiene lugar en la interfase fluido/sólido. Cuando una fase fluida (disolución que contiene el soluto, adsorbato) se pone en contacto con un sólido (adsorbente), en el sistema heterogéneo actúan unas fuerzas que son las

responsables en último extremo de que ocurra el proceso de adsorción produciéndose una retención del componente transferible de la fase fluida.

El proceso de adsorción es espontáneo y, por tanto, tiene lugar con una disminución en la energía libre de adsorción. Las energías que contribuyen a la energía libre de adsorción se pueden agrupar en no electrostáticas y electrostáticas. Las interacciones no electrostáticas son siempre atractivas e incluyen las fuerzas de Van der Waals y las interacciones hidrófobas.

Un parámetro de especial importancia en el diseño de sistemas de eliminación de contaminantes mediante adsorción es la capacidad del adsorbente, la cual depende de muchos factores. En primer lugar se encuentran las propiedades del adsorbato, tales como su geometría, tamaño molecular, polaridad, hidrofobicidad, grupos funcionales que contiene y su solubilidad en agua. En segundo lugar se pueden citar las condiciones de la disolución, tales como su pH, temperatura, concentración del contaminante, fuerza iónica y solutos competitivos. Por último, se han de considerar las características del adsorbente, que incluyen el área superficial, la distribución de tamaños de poro o la distribución de grupos funcionales en la superficie. Los efectos habituales de algunos de estos factores son los siguientes [43]:

- *Temperatura:* En general, con el aumento de la temperatura se producen fenómenos que influyen en la adsorción. En algunos casos, este incremento de la movilidad molecular afecta positivamente al proceso, mientras que en otros sucede al contrario. No obstante, suele haber una correlación entre el incremento de temperatura y la variación en la capacidad del adsorbente.
- *Naturaleza del soluto:* Las sustancias no polares y de baja solubilidad en el agua suelen ser las que mejor se adsorben.
- *pH:* El efecto de la concentración de hidrogeniones de la disolución es, muchas veces, crucial para favorecer la adsorción de unas u otras especies. Las ácidas suelen adsorberse mejor a pH bajos, mientras que las básicas actúan al contrario.

La medida de la capacidad de los adsorbentes se suele medir según el parámetro q, que da una idea de cómo de eficaz es la adsorción. Se define según la Ecuación (1):

$$q(q_e) = \frac{(C_o - C_l(C_e)) \cdot V}{W} \tag{1}$$

siendo C_o (mg·L^{-1}) la concentración inicial de contaminante en disolución, C_l (C_e) (mg·L^{-1}) la concentración del contaminante a un tiempo dado (en el equilibrio), V (L) el volumen de la disolución, W (g) la masa de adsorbente y q (q_e) (mg·g^{-1}) la concentración de contaminante en fase sólida a un tiempo dado (en el equilibrio). Cuanto mayor es el valor de q, más eficiente es el adsorbente.

El proceso de adsorción presenta algunas ventajas con respecto a otras técnicas de separación, por ejemplo, la facilidad de automatización del proceso, la capacidad para trabajar a bajas concentraciones de adsorbato y unas necesidades de espacio asequibles. La principal desventaja de esta técnica es el elevado coste de operación, restringiéndose mucho el empleo de la misma.

C.1.1. Tipos de adsorción.

Se pueden definir dos tipos diferentes de adsorción según la naturaleza de la unión o atracción entre adsorbato y adsorbente: fisisorción y quimisorción.

La adsorción física o fisisorción es aquella que se produce a través de uniones de tipo físico, a través de fuerzas de Van der Waals. La molécula adsorbida no está fija en un lugar específico de la superficie, sino que se encuentra libre de trasladarse por el interior de la interfase. Esta adsorción se da a temperaturas bajas y, además, es un proceso reversible.

La adsorción química o quimisorción es aquella adsorción que se produce a través de uniones de tipo químico. En este caso las energías de adsorción son elevadas, del orden de las de un enlace químico, debido a que el adsorbato forma unos enlaces fuertes localizados en los centros activos del adsorbente. Se produce a temperaturas altas y es un proceso irreversible. En la mayoría de los casos se producen conjuntamente ambos tipos de adsorción, siendo bastante difícil distinguir una de la

otra. Siempre que se da la quimisorción se produce, en mayor o menor grado fisisorción. [47,48].

C.1.2. Cinética de adsorción.

La cinética de adsorción indica la cantidad de adsorbato que puede retener el adsorbente por unidad de tiempo. Con los datos obtenidos se puede tener una idea aproximada sobre el tiempo requerido para que se alcance el equilibrio de adsorción y es posible estimar el orden que sigue la cinética del proceso, así como estimar los valores de las constantes de velocidad.

Este proceso de adsorción se lleva a cabo a través de tres etapas en serie:

1. Difusión externa: difusión del adsorbato a través del seno de la disolución.
2. Difusión interna: difusión del adsorbato a través de los poros del adsorbente.
3. Adsorción: proceso de adsorción o retención del adsorbato en los centros activos del adsorbente.

Con objeto de estudiar este fenómeno se utilizaron tres modelos teóricos que permiten estimar el valor de ciertas variables para predecir la caída de concentración del contaminante con el tiempo, para ello se ajustan los datos experimentales a los modelos cinéticos de *pseudo-primer orden* (*Lagergren*), *pseudo-segundo orden* (*Ho*), *difusión intrapartícula*, *Bangham* y *Elovich*.

<u>*Modelos cinéticos de pseudo-primer y pseudo-segundo orden.*</u>

Los modelos de *pseudo-primer* y *pseudo-segundo orden* asumen que la adsorción es un proceso de reacción pseudo-químico y que la velocidad de adsorción se puede determinar, respectivamente, por las ecuaciones de pseudo-primer y pseudo-segundo orden (Ecuaciones (2) y (3)):

$$\frac{dq_t}{dt} = k_1 \cdot (q_e - q_t) \tag{2}$$

$$\frac{dq_t}{dt} = k_2 \cdot (q_e - q_t)^2 \tag{3}$$

donde q_e (mg·g^{-1}) es la capacidad del adsorbente en el equilibrio, q_t (mg·g^{-1}) es la capacidad de adsorbente a cada tiempo (min), y k_1 (min^{-1}) y k_2 (g·mg^{-1}·min^{-1}) son las constantes de pseudo-primer y pseudo-segundo orden, respectivamente.

Integrando las Ecuaciones (2) y (3) para la condición inicial $t= 0 \rightarrow q_t= 0,$ y reagrupando términos se llega a las Ecuaciones (4) y (5):

$$\log(q_e - q_t) = \log(q_e) - \frac{k_1}{2{,}303} \cdot t \tag{4}$$

$$\left(\frac{t}{q_t}\right) = \frac{1}{k_2 \cdot q_e^2} + \frac{1}{q_e} \cdot t \tag{5}$$

<u>*Modelo cinético de difusión intrapartícula.*</u>

Este modelo asume que la única etapa controlante es la difusión interna, lo cual suele cumplirse para disoluciones de compuestos puros. El modelo de difusión intrapartícula deriva de la segunda ley de Fick bajo dos suposiciones [49]:

- La difusividad intrapartícula, D, es constante.
- La afinidad del adsorbato por el adsorbente es pequeña en relación con la cantidad total de adsorbato en la disolución.

La Ecuación (6) es la que se obtiene para este modelo:

$$q_t = k_{id} \cdot t_e^{1/2} + C \tag{6}$$

donde k_{id} (mg·g^{-1}·min$^{-0,5}$) es la velocidad de difusión intrapartícula y C (mg·g^{-1}) es un parámetro relacionado con el espesor de la capa.

<u>*Modelo cinético de Bangham*</u>

El modelo teórico de *Bangham* asume que la velocidad de adsorción sólo depende de la difusión de poro. Si los datos experimentales se ajustan a este modelo, se puede decir que el principal factor que condiciona la cinética de adsorción es la difusión dentro de los poros del adsorbente.

El modelo viene determinado por la Ecuación (7):

$$\log\log\left(\frac{C_o}{C_o - q \cdot m}\right) = \log\left(\frac{k_b \cdot m}{2{,}303 \cdot V}\right) + a \cdot \log(t) \qquad (7)$$

<u>*Modelo cinético de Elovich*</u>

El modelo de *Elovich*, de aplicación general en procesos de quimisorción, supone que los sitios activos del adsorbente son heterogéneos, y por ello, exhiben diferentes energías de activación, basándose en un mecanismo de reacción de segundo orden para un proceso de reacción heterogénea [50].

Este modelo está representado por la Ecuación (8):

$$\frac{dq}{dt} = \alpha_E \cdot e^{-\beta_E \cdot q} \qquad (8)$$

donde α_E es la velocidad inicial de adsorción y β_E es la constante de desorción.

Si se integra entre los límites q= 0, t= 0 y q= q, t= t, la expresión resultante ya presenta forma lineal (Ecuación (9)):

$$q = \frac{1}{\beta_E} \cdot \ln(\alpha_E \cdot \beta_E) + \frac{1}{\beta_E} \cdot \ln t \qquad (9)$$

C.1.3. Equilibrio de adsorción.

La forma habitual de presentar los datos experimentales de adsorción obtenidos en condiciones de equilibrio es gráficamente como isoterma de adsorción. Se denomina isoterma de adsorción a la relación entre la cantidad de sustancia adsorbida por un adsorbente y la presión o concentración de equilibrio a una temperatura constante.

Hasta la fecha se han propuesto numerosas clasificaciones de las isotermas de adsorción según su forma. La propuesta por *Brunauer, Emett* y *Teller* (*BET*) incluye cinco formas diferentes de isoterma (ver Figura 7) [51].

A partir de la isoterma de adsorción se obtiene información acerca del proceso de adsorción. Para ello se estudia el ajuste de los resultados experimentales con los diferentes modelos teóricos existentes, y se pueden calcular los parámetros característicos de cada uno de ellos.

Las isotermas de *Langmuir* (1916) y *Freundlich* (1939) son los dos modelos más extensamente utilizados para describir la adsorción de un único componente. Además, existen otros modelos matemáticos más actuales y flexibles (hasta con tres variables ajustables) que intentan modelar de una forma más precisa los sistemas de adsorción en equilibrio. Entre ellos se encuentra el modelo de *Dubinin-Radushkevich*. Estos tres modelos son los que se utilizaron en esta investigación.

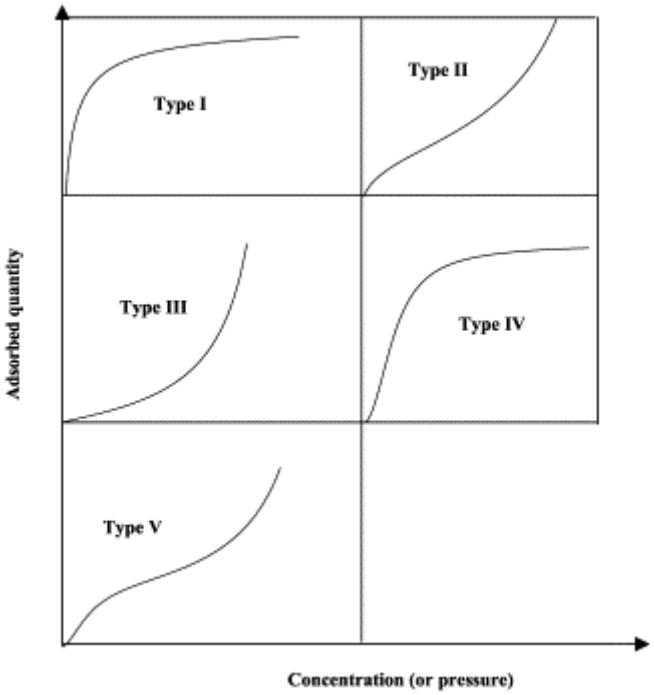

Figura 7. Representación esquemática de los cinco tipos de isotermas de adsorción. Clasificación de *BET.*

Modelo de Langmuir.

El modelo de *Langmuir* fue originalmente desarrollado para representar la adsorción de un gas sobre carbón activo. En este modelo la atracción entre las moléculas del adsorbato y la superficie del adsorbente se basa principalmente en fuerzas físicas (fuerzas electrostáticas o de Van der Waals) y no se tienen en cuenta las agrupaciones moleculares ni las variaciones de energía de la interacción con el material.

Para aplicar la isoterma de *Langmuir* hay que tener en cuenta las siguientes hipótesis [52]:

- La superficie de adsorción es uniforme.
- La adsorción de soluto por el adsorbente se produce sobre una monocapa.
- La energía de adsorción es constante y la afinidad de cada lugar de interacción por las moléculas de soluto es la misma.
- Las moléculas de soluto adsorbidas están localizadas y, por tanto, no se mueven sobre la superficie.

La expresión matemática de la ecuación de *Langmuir* es la siguiente (Ecuación (10)):

$$q_e = \frac{q^o_{\max} \cdot k_L \cdot C_e}{1 + k_L \cdot C_e} \tag{10}$$

siendo q_e (mg·g^{-1}) la capacidad del adsorbente en el equilibrio, q^o_{max} (mg·g^{-1}) la capacidad máxima de adsorción del adsorbente para un soluto dado, C_e (mg·L^{-1}) la concentración final de equilibrio del adsorbato en disolución, y k_L (L·g^{-1}) es la constante del modelo de *Langmuir*.

Modelo de Freundlich.

La isoterma de *Freundlich* tiene un origen empírico, y al igual que la isoterma de *Langmuir*, la adsorción es función de la concentración de equilibrio sin tener en cuenta la presencia de otras sustancias en disolución.

El modelo de *Freundlich* supone que la superficie del adsorbente es heterogénea y que las posiciones de adsorción tienen distintas afinidades, en primer lugar se ocuparían las posiciones de mayor afinidad y posteriormente el resto de posiciones [53]:

Para aplicar este modelo hay que tener en cuenta las siguientes hipótesis:

- No hay asociación de moléculas después de ser adsorbidas en la superficie del adsorbente.
- No hay quimisorción.

Por tanto, la isoterma de *Freundlich* será válida cuando la adsorción sea solamente un proceso físico y no haya un cambio en la configuración de las moléculas cuando han sido adsorbidas.

La ecuación empírica de *Freundlich* es la siguiente (Ecuación (11)):

$$q_e = k_F \cdot C_e^n \tag{11}$$

siendo q_e ($mg \cdot g^{-1}$) la capacidad del adsorbente en el equilibrio, C_e ($mg \cdot L^{-1}$) la concentración final de equilibrio del adsorbato en disolución, k_F ($L^{nF} \cdot mg^{-(nF-1)} \cdot g^{-1}$) la constante equilibrio de *Freundlich* y *n* una constante referida a la afinidad o energía de adsorción entre adsorbente y adsorbarto.

Modelo de Dubinin-Radushkevich.

El modelo de *Dubinin-Radushkevich* se fundamenta en la Teoría del potencial de Polanyi, y considera que el proceso de llenado de los microporos se produce de la misma forma que un líquido llena una botella, careciendo de sentido emplear el

término superficie específica. La ecuación de la isoterma [54] es la siguiente (Ecuación (12)):

$$q_e = q_m \exp\{-\beta \cdot \xi^2\} \tag{12}$$

siendo q_e la cantidad retenida de soluto por gramo de adsorbente ($mg \cdot g^{-1}$) en condiciones de equilibrio, q_m y β las constantes del modelo de *Dubinin–Radushkevich*, ($mg \cdot g^{-1}$) y ($mg^2 \cdot k^{-1} J^{-2}$), respectivamente, y ξ el potencial de Polanyi, que se calcula con la Ecuación (13).

$$\xi_D = R \cdot T \cdot \ln\left(1 + \frac{1}{C_{eq}}\right) \tag{13}$$

Operando sobre la Ecuación (12) se llega a la Ecuación (14):

$$\ln(C_{ads}) = \ln K_{DR} - \beta \cdot \xi^2 \tag{14}$$

siendo C_{ads} ($mol \cdot L^{-1} \cdot g^{-1}$) la capacidad del adsorbente por litro de disolución y K_{DR} es la cantidad máxima de compuesto adsorbida.

C.1.4. Adsorbentes poliméricos sintéticos.

Las resinas de adsorción o sintéticas se fundamentan en las bases de la adsorción física: adsorbente y adsorbato unidos mediante fuerzas de Van der Waals. Están formadas por polímeros y se diferencian entre sí en el tipo de matriz principalmente, ya que no poseen grupos funcionales. Algunas de las matrices más usuales son polímeros de estireno entrecruzado con divinilbenceno (SDVB), fenol formaldehído y éster acrílico. Entre ellas podemos encontrar las resinas sintéticas comerciales *Amberlite* y *Dowex Optipore*. Ente las resinas *Amberlite* cabe destacar las denominadas *XAD-4, XAD-761, XAD-1180N, XAD-1600N, XAD-18* y *XAD-7HP*. Dentro de las *Dowex* tienen importancia la *SD-2, L493, V493* y *V503*.

Las resinas *Amberlite XAD* tienen buenas propiedades físicas, como son elevada porosidad, gran área superficial y, desde el punto de vista químico, una homogénea estructura no iónica. Son buenos adsorbentes de compuestos sin carga. Además

presentan resistencia a todos los disolventes orgánicos de uso común, alta capacidad, alto rendimiento y alta estabilidad mecánica.

En este trabajo se empleó la resina *Amberlite XAD-7HP*. Se trata de una resina no iónica, constituida por polímeros acrílicos alifáticos de alta porosidad, que se utiliza para la inmovilización y la recuperación de péptidos, proteínas y compuestos de bajo peso molecular a partir de soluciones acuosas. Su gran área superficial puede adsorber y luego desorber un amplio grupo de compuestos, dependiendo del medio en el que se emplee. Se usa principalmente en el procesado de alimentos, bioprocesamiento y en la transformación farmacéutica.

En la Tabla 1 quedan reflejadas las principales características físico-químicas de la resina. En la Figura 8 se representa una imagen de la misma.

Tabla 1. Propiedades físicas y químicas de la resina *Amberlite XAD-7HP*.

Estructura de la matriz	Éster alifático
Forma física	Bolas blancas
Área superficial	$\geq$380 $m^2 \cdot g^{-1}$
Diámetro de poro	450 Å
Porosidad total	$\geq$ 0,50 $mL \cdot mL^{-1}$
Contenido en humedad	61-69 %
Tamaño de partícula	0,56-0,71 mm
Densidad aparente	655 $g \cdot L^{-1}$
Rango de pH	0-14
Limite de temperatura	80-100 ºC

Figura 8. Resina *Amberlite XAD-7HP.*

Estas resinas constituyen una buena alternativa al carbón activo como adsorbente, de ahí su interés actual. Por todo esto, se están llevando a cabo numerosas investigaciones con estos adsorbentes, ya que su uso no está aún muy extendido. En la literatura se han encontrado algunos trabajos que demuestran la bondad de éstas como adsorbentes de numerosos compuestos sin carga [55,56].

C.1.5. Adsorbentes naturales tanínicos.

Otro gran grupo de adsorbentes de gran interés debido a su sencillez instrumental, a su disponibilidad y a su amplia distribución geográfica son los llamados derivados tanínicos [43]. Estos productos aparecen a partir de los extractos de familias químicas polifenólicas de origen vegetal y son fruto de sencillas manipulaciones en laboratorio. Los taninos se modifican bien para generar coagulantes (cationización) o bien para producir adsorbentes (gelificación).

En el ámbito medioambiental, los taninos se encuentran presentes en cortezas, frutos, hojas, etc. de una enorme variedad de plantas. Tradicionalmente, las fuentes de taninos han sido la *Acacia mearnsii de Wild* (Acacia negra), la *Schinopsis balansae* (Quebracho colorado) y la *Caesalpinia spinosa* (Tara). Todas estas especies son de origen tropical, pero no es preciso acudir a plantas exóticas para encontrar taninos. Las familias vegetales del castaño (*Castanea*), de la encina y el roble (*Quercus ilex* o

robur) o del alcornoque (*Quercus suber*) son también fuentes primarias de taninos vegetales.

Los taninos son mayoritariamente compuestos polifenólicos de variable peso molecular (entre 500 y varios miles de Daltons). Existen dos tipos principales de taninos: hidrolizables y condensados. Éstos últimos son los más utilizados para la producción de adsorbentes (*tanigeles*).

Los *taninos condensados*. Se les conoce también como "proantocianidinas" debido a que pueden ser degradados en sus antocianidinas constituyentes tras un tratamiento con ácido fuerte. Constituyen más del 90% de la producción de taninos comerciales (alrededor de 200.000 toneladas al año). Son especialmente interesantes para la industria química porque presentan una alta reactividad a los aldehídos y, por tanto, constituyen una materia prima barata y disponible para la preparación de adhesivos, resinas y geles adsorbentes. Los taninos condensados se obtienen principalmente de los árboles: *Acacia mearnsii de Wild* (acacia negra o mimosa), *Schinopsis balansae* (quebracho colorado), familias de pinos *Pinus mediterranea, Pinus pinaster o Pinus radiata* y *Cupressus sempervivens* (ciprés). En la Figura 9 se muestran las fotografías de las fuentes de tanino utilizadas en este trabajo de investigación.

La Figura 10 representa la unidad estructural básica en los taninos condensados, que se forman a partir de la polimerización de flavonoides. Esta molécula se repite de 2 a 11 veces en los taninos originarios de la acacia o del quebracho, y presenta un grado de polimerización de entre 4 y 5. Esta unidad puede llegar a repetirse hasta 30 veces en el caso de los taninos del pino. Los centros nucleofílicos del anillo A tienden a ser más reactivos a la sustitución aromática (las flechas indican los lugares de ataque) que los lugares equivalentes del anillo B. Este hecho puede ser debido a la proximidad de sustituyentes hidroxilo que causan la activación general del anillo B con efectos diferentes a los producidos en el anillo A. Las estructuras de otros taninos condensados pueden variar, pero la base suele ser similar a los patrones de la Figura 10: resorcinol (anillo A) y pirogalol (anillo B).

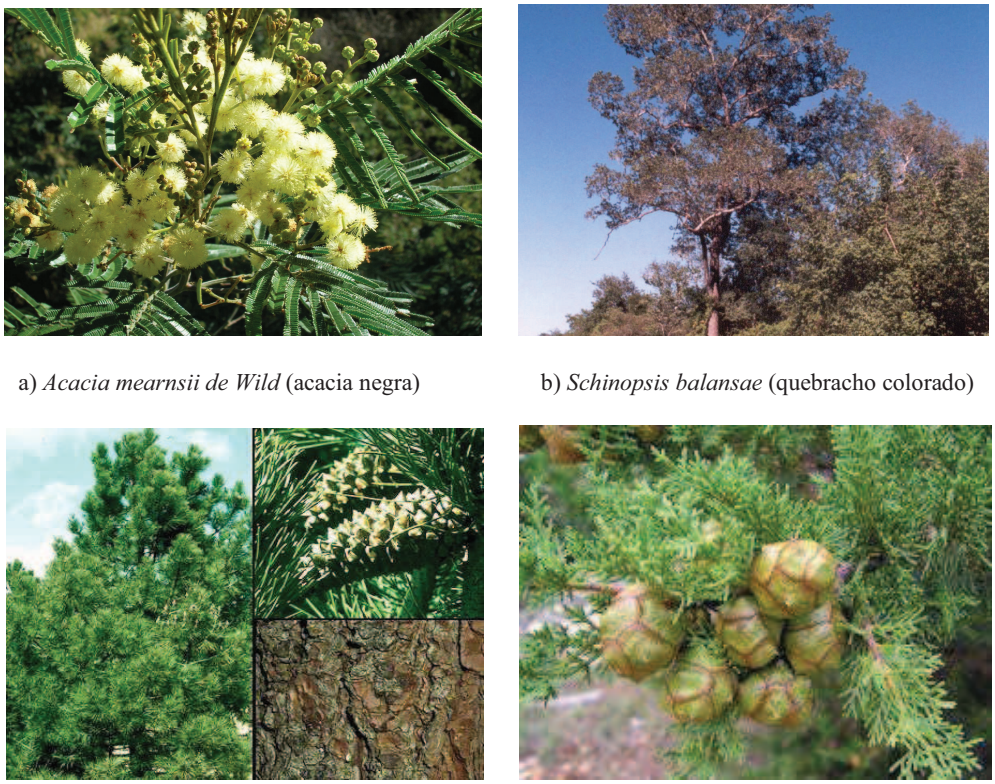

a) *Acacia mearnsii de Wild* (acacia negra)

b) *Schinopsis balansae* (quebracho colorado)

c) *Pinus pinaster* (pino)

d) *Cupressus sempervivens* (ciprés)

Figura 9. Plantas ricas en tanino empleadas en esta investigación.

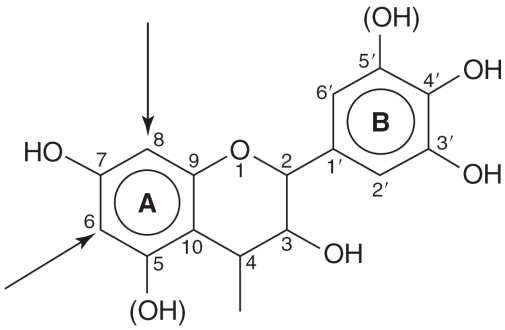

Figura 10. Unidad de Flavonoide constituyente de taninos condensados.

La complejidad química de los taninos y el hecho de que normalmente se extraen de matrices naturales no purificadas hacen que su aislamiento e identificación sea muy difícil de llevar a cabo, por lo que muchas veces sólo se puede estimar cuál es la disposición estructural más viable.

Los derivados tanínicos se pueden utilizar en el tratamiento de aguas como coagulante o como adsorbente. En este trabajo de investigación se lleva a cabo la adsorción de un compuesto farmacéutico, trimetoprima, en diferentes taninos condensados. Para su empleo como adsorbente, es necesaria la previa **gelificación** del tanino. Este procedimiento conlleva una inmovilización de los taninos en una matriz insoluble [57]. Las condiciones de gelificación descritas en estudios previos contemplan el uso de formaldehído (o algún otro aldehído) en medio ácido o básico. Las investigaciones de Nakano [58], Kim y Nakano [59] o Tondi y otros [60] son algunas muestras del interés que suscitan este tipo de procesos entre los científicos. Todos estos estudios asumen el medio básico de reacción, mientras que investigadores españoles [61, 62] han desarrollado algunas propuestas en medio ácido.

Las reacciones de gelificación (inmovilización) de taninos se pueden llevar a cabo a presión atmosférica, a temperatura moderada (40-90°) y sin catalizador [63]. Durante la reacción entre el tanino y el formaldehído, la masa de reacción adquiere un aspecto gelificado como consecuencia de la formación de un compuesto polimérico de mayor peso molecular que el tanino original e insoluble en agua. El mecanismo de reacción sugerido [43] consiste en una primera etapa de formación de un derivado con un grupo hidroximetileno (en el carbono C6 o C8, Figura 11) y una segunda etapa de condensación creando bien un puente metileno o bien un puente dimetilenéter (Figura 12). Cuando un extracto tanínico condensado se somete a la reacción de polimerización con formaldehído, el material resultante es un sólido de aspecto vítreo, al microscopio electrónico, que agrupa propiedades tanínicas interesantes (capacidades quelatantes o actividad electrostática superficial) en una matriz insoluble.

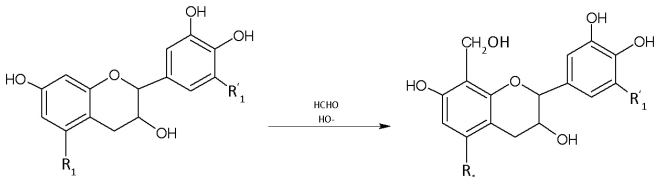

Figura 11. Mecanismo de reacción de un tanino condensado con formaldehído. Etapa 1.

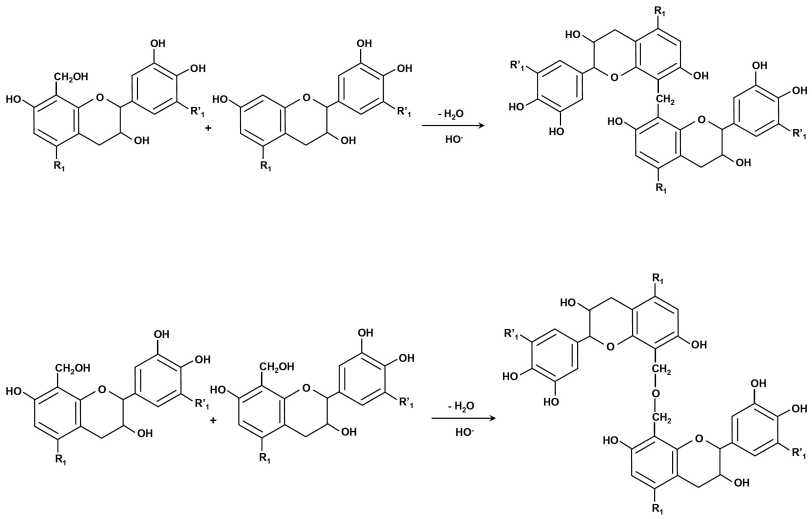

Figura 12. Mecanismo de reacción de un tanino condensado con formaldehído. Etapa 2.

La Figura 13 [43] muestra las modificaciones que se generan en la superficie microporosa de la materia tanínica. Tras la gelificación con formaldehído, esta formación microporosa se mantiene, sin embargo la estructura cristalina del tanino se pierde.

Estos *tanigeles* han resultado ser potentes adsorbentes de compuestos catiónicos en disolución y su utilización puede ser una alternativa real a productos ampliamente distribuidos, como son los carbones activados o las resinas de intercambio iónico en medidas depuradoras de efluentes contaminados. Se ha demostrado en otros trabajos que son adsorbentes efectivos en la eliminación de contaminación producida por metales, colorantes y compuestos fenólicos. Sin embargo, no se han encontrado trabajos previos en los que se utilicen estos adsorbentes naturales en la eliminación de compuestos farmacéuticos.

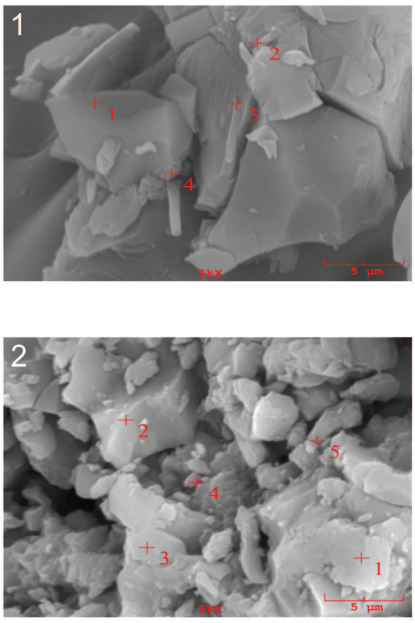

Figura 13. Microscopía electrónica del quebracho: 1) sin gelificar y 2) gelificado [43].

C.2. Tratamientos de Oxidación Química en aguas.

C.2.1. Procesos de Oxidación Avanzada.

Los Procesos de Oxidación Avanzada (POAs), son particularmente útiles para la eliminación de moléculas biológicamente tóxicas o no degradables, tales como compuestos aromáticos, colorantes, pesticidas y compuestos orgánicos volátiles presentes en aguas residuales [64-69]. Son procesos muy adecuados y eficaces para el tratamiento de compuestos farmacéuticos en aguas [70-72], aunque su aplicación a gran escala se limita y depende del coste de operación de los mismos. La reacción de destrucción implica diferentes agentes oxidantes que se generan *in situ* en el medio de reacción, como los radicales hidroxilo (·OH) y otras especies oxidantes fuertes (·O_2, HO_2· y ROO·). El radical hidroxilo, tiene un fuerte potencial de reducción estándar ($E_{\cdot OH/H2O}$= +2,8 V/SHE) [73,74], siendo el segundo agente oxidante más fuerte después del flúor, siendo capaz de eliminar compuestos especialmente recalcitrantes [75,76]. Los POAs son capaces de destruir las moléculas orgánicas a través de

hidroxilación o deshidrogenación y pueden mineralizar los compuestos orgánicos hasta CO_2 y H_2O [77,78].

Entre los oxidantes más utilizados en estos POAs, destacan la radiación UV, O_3 y H_2O_2, aunque también se pueden encontrar aplicaciones de H_2O_2 solo o en combinación con una sal de hierro, dando lugar a lo que se conoce como reactivo de Fenton. Una desventaja considerable de la mayoría de los agentes oxidantes y sus combinaciones es la necesidad de añadir un agente externo al medio de reacción. En estas situaciones, la eficacia de los procesos depende de la transferencia de materia gas-líquido o sólido-líquido, que en ocasiones puede ser la etapa controlante del proceso. Para evitar este problema, en los últimos años se han desarrollado nuevas técnicas de generación de radicales hidroxilo *in situ*, como son los métodos de tratamientos electroquímicos.

Por su utilización en el presente trabajo, se describen a continuación los siguientes POAs: Fe^{2+}/H_2O_2 (reactivo de Fenton), Fe^{3+}/H_2O_2 (reactivo de Fenton-like), O_3, UV/H_2O_2, y electro-oxidación (Proceso de Oxidación Avanzada Electroquímico).

C.2.1.1. Reactivo de Fenton y sistema Fenton-like.

La oxidación por el reactivo de Fenton es un proceso de oxidación homogéneo y se considera como una reacción de oxidación catalizada por metales, actuando el hierro como catalizador [79]. La principal desventaja del procedimiento es el bajo valor de pH requerido con el fin de evitar la precipitación del hierro [80].

El proceso se basa en la generación de radicales hidroxilo (·OH) a partir del reactivo de Fenton (Fe^{2+}/H_2O_2) a pH ácido (3-5). El Fe^{2+} actúa como catalizador homogéneo.

Los principales agentes oxidantes que origina el reactivo de Fenton son los que se exponen en las Ecuaciones (15) y (16), es decir, el radical hidroxilo y el radical hidroperóxido.

$$Fe^{2+} + H_2O_2 \rightarrow Fe^{3+} + OH^- + \cdot OH \qquad (15)$$

$$Fe^{3+} + H_2O_2 \rightarrow Fe^{2+} + \cdot OOH + H^+ \qquad (16)$$

Para que el procedimiento sea efectivo son necesarios los siguientes requisitos:

a) El pH del agua a tratar debe estar en el rango 3-5. Esto es debido a que a valores más elevados el hierro precipita como $Fe(OH)_3$ inactivando por tanto el sistema. Además, si el pH es elevado el peróxido de hidrógeno descompone hasta oxígeno.

b) Adición de la sal de Fe^{2+}, normalmente como $FeSO_4$, aunque se pueden añadir otras fuentes de Fe^{2+} o Fe^{3+}. En el caso de ser Fe^{3+}, el cual también es efectivo, se observa un pequeño retardo inicial de la reacción.

c) La adición de H_2O_2 debe ser muy lenta con objeto de evitar fenómenos de descomposición.

El ión Fe^{3+} puede reducirse por reacción con H_2O_2 y formar de nuevo ión Fe^{2+} y más radicales hidroxilo. Este segundo proceso se denomina Fenton-Like (Ecuación (16)).

La velocidad de reacción utilizando este sistema está generalmente limitada por la velocidad de generación de radicales ·OH, es decir, por la concentración de catalizador ferroso. Las proporciones Fe^{2+}: H_2O_2 típicas son 1:5-10 en peso, aunque los niveles de Fe^{2+} < 25-50 $mg \cdot L^{-1}$ pueden requerir un tiempo muy elevado de reacción (10-48 horas).

La presencia o adición de ciertas sustancias puede inhibir el proceso. En general, el proceso puede inhibirse por agentes quelatantes del ion ferroso/férrico, entre ellos: fosfatos, EDTA, formaldehído, y ácidos, como el ácido cítrico o el ácido oxálico, presentes en las aguas.

En muchos casos un substrato aparentemente refractario puede ser oxidado alterando las condiciones de peróxido de hidrógeno, temperatura, pH o concentración de catalizador.

En ausencia de sal ferrosa o férrica no existen evidencias de formación de radicales hidroxilo. Al aumentar la concentración de hierro, la velocidad de oxidación de compuestos orgánicos aumenta hasta un punto en el cual un aumento adicional de

dicha concentración de sal es ineficaz. Para la mayoría de las aplicaciones, no importa si se usa Fe^{2+} o Fe^{3+}, el ciclo catalizador comienza rápidamente si el peróxido de hidrógeno y el material orgánico están en concentración suficiente. Sin embargo, si se usan dosis bajas de oxidante (ej., < 10-25 $mg \cdot L^{-1}$ H_2O_2), es preferible el Fe^{2+}.

Cuando la dosis de H_2O_2 se aumenta, se obtiene una clara reducción de la materia orgánica, aunque puede producirse un cambio pequeño o inapreciable en la toxicidad. Una vez alcanzado un umbral mínimo, pequeños aumentos en la dosis de H_2O_2 ofrecen disminuciones claras en la toxicidad del efluente.

La velocidad de reacción con el reactivo de Fenton aumenta con la temperatura, con un efecto más pronunciado a temperaturas menores de 20 ºC. Sin embargo, cuando las temperaturas aumentan de 40-50 ºC, la eficacia del reactivo disminuye. Esto es debido a la descomposición acelerada de H_2O_2 en oxígeno y agua. Desde el punto de vista práctico, la mayor parte de las aplicaciones comerciales de este reactivo ocurren a temperaturas entre 20-40 ºC.

El pH óptimo de operación está comprendido entre 3 y 6. La ineficacia de un pH básico se atribuye a la transformación de las especies de hierro hidratadas hasta especies férricas coloidales. En esta última forma, el hierro descompone catalíticamente el peróxido de hidrógeno en oxígeno y agua, sin formar radicales hidroxilo. El sistema Fenton-Like es más sensible a la variación del pH que el reactivo de Fenton [81]. Este hecho se debe a la gran dependencia del Fe^{3+} a este parámetro. A pH menor que 2, tiene lugar la inhibición inicial entre el Fe^{3+} y el H_2O_2, y cuando el pH aumenta por encima de 3, se produce la precipitación del Fe^{3+}, ya que se forman oxihidróxidos amorfos ($Fe_2O_3 \cdot nH_2O$) que producen una disminución de la concentración de hierro en la disolución.

Las ventajas que presenta este proceso de oxidación son: el Fe^{2+} es abundante y no tóxico, el peróxido de hidrógeno es fácil de manejar y ambientalmente benigno, no se forman compuestos clorados como en otras técnicas oxidantes, no existen limitaciones de transferencia de materia por tratarse de un sistema homogéneo y el diseño de reactores para esta tecnología es bastante sencillo. Una ventaja adicional del proceso

Fenton, es la formación de complejos que promueven la coagulación de sólidos en suspensión después de las reacciones de oxidación [82].

Este proceso puede aplicarse a aguas residuales, lodos o suelos contaminados produciendo los siguientes efectos: 1) oxidación de contaminantes orgánicos, 2) reducción de la toxicidad, 3) reducción de la DQO, 4) reducción de la DBO_5 y 5) eliminación del olor y color.

El proceso de oxidación mediante reactivo de Fenton, se ha aplicado ampliamente para la oxidación de muchos tipos de fármacos, resultando una tecnología muy adecuada para la eliminación de estos contaminantes. Por este motivo, se considera que es uno de los pretratamientos más eficaces para la depuración de aguas residuales farmacéuticas debido a la gran capacidad de detoxificación y a la mejora de la biodegradabilidad [83,84].

En este trabajo de investigación los dos sistemas Fenton y Fenton-like se han aplicado de forma integrada. En la literatura se han encontrado estudios de estos dos procesos de manera separada pero nunca conjuntamente.

C.2.1.2. Ozono.

La ozonización de un agua es un proceso químico que tiene como objetivo principal oxidar la materia orgánica presente en la misma, así como reducir el contenido de microorganismos.

En la bibliografía se encuentra abundante información sobre reacciones químicas individuales entre ozono y compuestos orgánicos diversos, bien en fase homogénea por mezcla de disoluciones de ozono y compuestos orgánicos para evitar la influencia de la transferencia de materia, bien en fase heterogénea, en cuyo caso ha de tenerse en cuenta la etapa de transferencia de materia. El conjunto de estos estudios de ozonación de sustancias orgánicas individuales en medio acuoso ha puesto de manifiesto los mecanismos y vías de acción del ozono sobre la materia orgánica, que de forma resumida pueden describirse por el esquema mostrado en la Figura 14 [85].

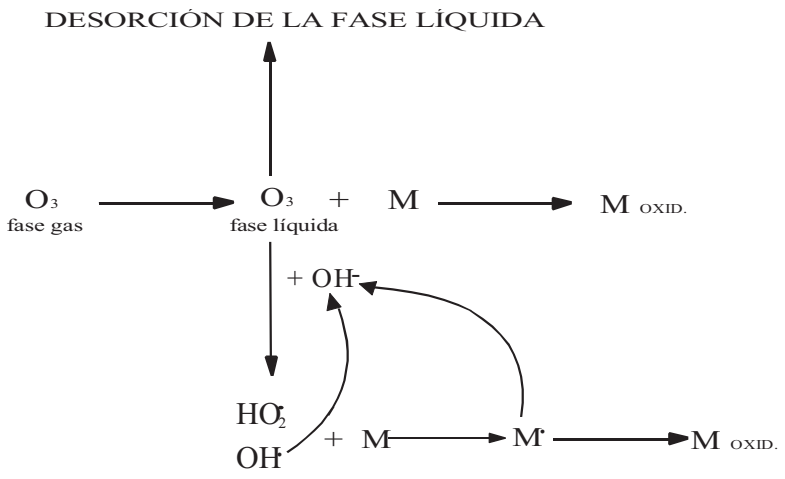

Figura 14. Mecanismo de acción del ozono sobre la materia orgánica (Adaptado de [85]).

De acuerdo con dicho esquema, durante la ozonación, parte del ozono disuelto reacciona directamente con la materia orgánica en disolución, siendo frecuentemente tales reacciones directas bastante lentas. Esto las hace altamente selectivas y en general son las reacciones más importantes a tener en cuenta en la ozonación de contaminantes de agua.

Por otra parte y de forma simultánea, una fracción importante del ozono descompone antes de reaccionar con los solutos y antes de desorberse. Esta descomposición está catalizada por los iones OH^- y por tanto tiene lugar más rápidamente y en mayor extensión con el incremento de pH, y conduce a la formación de varias especies muy reactivas y con marcado carácter oxidante, entre las que destacan los radicales hidroxilo (·OH) e hidroperóxido (HO_2·). Además esta descomposición puede asimismo ser adicionalmente acelerada por una reacción en cadena típicamente radicalaria en la cual los radicales producidos ·OH y HO_2· actúan como propagadores de la cadena. Adicionalmente, los radicales libres formados pueden reaccionar con la materia orgánica para dar otros radicales libres secundarios M· que, o bien también actúan como catalizadores de la descomposición de O_3, o bien conducen a la formación de compuestos finales oxidados.

De todas esas especies intermedias formadas, los radicales hidroxilo (·OH) juegan un papel primordial. Se encuentran entre los oxidantes más reactivos en agua puesto

que pueden oxidar fácilmente todos los tipos de compuestos orgánicos y muchos solutos inorgánicos mediante reacciones de tipo radicalario.

En segundo lugar en actividad oxidante se encuentran los radicales hidroperóxido ($HO_2^{\cdot}$), los cuales pueden disociarse a iones superóxidos y cuya presencia en la descomposición de ozono está también demostrada. Generalmente estas especies $HO_2\cdot$ son de más baja reactividad en la iniciación de oxidaciones que los radicales ·OH. Finalmente, existen otros radicales de menor actividad que pueden encontrarse asimismo en estas reacciones pero que por su menor importancia se omiten. En general, todos estos agentes formados durante la ozonación pueden considerarse oxidantes potenciales secundarios o terciarios, que contribuyen a los procesos de oxidación iniciados por ozono en agua.

En resumen, puede concluirse que la oxidación de la materia orgánica mediante ozono transcurre por dos vías fundamentales: unas reacciones directas por ozono y otras reacciones de tipo radicalario, principalmente por radicales ·OH [85]. En los sistemas heterogéneos, ha de considerarse además la resistencia a la transferencia de materia, la cual origina una velocidad global del proceso lógicamente menor que la velocidad correspondiente a las reacciones homogéneas. Pero una vez que el ozono está disuelto en la fase líquida, las dos vías de acción del mismo sobre la materia orgánica en la forma anteriormente expuesta para las reacciones homogéneas son igualmente aplicables en estas reacciones heterogéneas. Por tanto, el estudio cinético de estos sistemas heterogéneos no se puede realizar mediante las ecuaciones cinéticas convencionales, sino que resulta necesario la aplicación de diversas teorías que tengan en cuenta ambos aspectos: la transferencia de materia y la reacción química propiamente dicha.

Existen diferentes tipos de generación de ozono: por descarga eléctrica, fotoquímica y electroquímica, siendo la más empleada la descarga eléctrica de alto voltaje de aire u oxígeno.

La aplicación de ozono presenta una serie de ventajas:

1. Elimina de forma eficaz y controla los problemas de olor, sabor y color.

2. Es un poderoso oxidante y desinfectante, más efectivo que el dióxido de cloro y las cloraminas.
3. No forma subproductos halogenados, a no ser que haya presencia de bromuros.
4. Requiere una concentración y tiempo de contacto menor para su labor de desinfección.
5. Su efectividad no está influida por el pH.
6. La ventaja más notable es que aumenta la biodegradabilidad de los compuestos farmacéuticamente activos en agua cuando se aplica como un tratamiento previo [86].

Sin embargo, también presenta algunos inconvenientes a tener en cuenta:

1. Puede producir subproductos, como bromatos, aldehídos y ácidos.
2. Requiere gran cantidad de energía para su generación, así como equipos más costosos.
3. Es muy corrosivo y tóxico (puede formar óxido nítrico y ácido nítrico que causan la corrosión de los equipos).
4. Presenta baja solubilidad y es relativamente inestable en disolución acuosa. Desaparece con rapidez del agua, especialmente a altos valores de pH y temperatura.
5. Tiene que ser generado in situ.
6. Es altamente perjudicial para la salud humana, si el tiempo de exposición es elevado.
7. No es eficaz para la reducción de la toxicidad y la mineralización, excepto con la presencia de H_2O_2, lo que puede aumentar ligeramente la eliminación de carbono orgánico total (COT), pero no de toxicidad [87].

Entre los compuestos que provocan la estabilización o descomposición del ozono en agua pueden distinguirse:

- *Iniciadores*: inducen la formación del radical hidroxilo a partir de la molécula de ozono. Cabe destacar los cationes metálicos, radiación UV, OH^-, HO_2^-, etc.
- *Promotores*: aceleran las reacciones en cadena para la descomposición de ozono mediante la producción de radicales superóxido. Destacan los alcoholes primarios, el ión fosfato, el ácido fórmico, etc.
- *Inhibidores*: reaccionan con los radicales hidroxilo formando compuestos finales. Entre otros se pueden citar los carbonatos y bicarbonatos, el grupo alquilo y alcoholes terciarios como el terc-butanol.

En base a que el ozono es un oxidante muy potente, se utiliza cada vez más en el tratamiento de aguas. Se ha empleado en la purificación de aguas en la fase de pre-tratamiento, para la oxidación intermedia y la desinfección final. En el tratamiento de aguas residuales en la oxidación previa al tratamiento biológico y en el tratamiento de los lodos generados en los reactores biológicos, en el tratamiento de aguas de circuitos de refrigeración, desodorización de ambientes, etc.

Ha sido empleado tradicionalmente en el tratamiento de agua potable [88]. En otros trabajos [89,90] se observó que una dosis de ozono de 2 $mg \cdot L^{-1}$ era capaz de eliminar más del 80% de algunos fármacos, entre ellos trimetoprima, de un efluente del tratamiento secundario de una depuradora de aguas residuales. El estudio que realizó Adams y col. [91] mostró que la ozonización elimina más del 95% de varias sulfonamidas y trimetoprima de un agua de río en 1,3 minutos de tiempo de contacto con concentraciones de ozono de 7,1 $mg \cdot L^{-1}$. Durante la ozonación de aguas residuales, algunos fármacos, incluida trimetoprima, reaccionan predominantemente por vía directa con ozono, otros, son oxidados y transformados en gran medida por los radicales hidroxilo [92,93].

El ozono y/o radicales hidroxilo desactivan las propiedades bactericidas de los antibióticos mediante el ataque o la modificación de sus grupos funcionales

farmacéuticamente activos, por ejemplo, el anillo fenólico de la trimetoprima [93]. Se alcanzan eficacias elevadas de eliminación para compuestos con anillos aromáticos ricos en electrones, tales como hidroxilo, amino, acilamino, alcoxi y compuestos aromáticos de alquilo, así como compuestos con grupos aminos (ej. trimetoprima) y con grupos alquenos no aromáticos [94].

C.2.1.3. Sistemas UV y UV/H_2O_2.

El proceso de degradación de contaminantes mediante radiación UV [95] consiste en la utilización de la parte más energética del espectro solar como es la correspondiente al ultravioleta cercano (longitud de onda entre 200-400 nm) para producir una reacción de oxidación muy energética. Las longitudes de ondas de estas radiaciones dentro del espectro electromagnético corresponden a unas energías que varían de 30 a 140 $kcal \cdot mol^{-1}$, valores del orden de las energías de activación de numerosas reacciones químicas convencionales.

La irradiación directa conduce a la promoción de la molécula desde su estado fundamental a un estado singlete excitado. Tales estados excitados pueden sufrir, entre otros procesos, homólisis, heterólisis o fotoionización. En la mayoría de los casos, la ruptura homolítica produce radicales:

$$R\text{-}R + h\upsilon \rightarrow R\text{-}R^{*} \rightarrow 2R^{*} \qquad (17)$$

Estos radicales inician reacciones en cadena y producen productos finales de más bajo peso molecular. En presencia de oxígeno, son posibles reacciones adicionales de generación de radical superóxido:

$$R\text{-}R^{*} + O_2 \rightarrow R\text{-}R^{\cdot+} + O_2^{\cdot-} \qquad (18)$$

Aunque su poder oxidante no es muy alto, el radical superóxido puede degradar compuestos aromáticos sustituidos con alta absorción en el rango UV.

La degradación fotolítica puede ser directa o indirecta. En la fotólisis directa, el contaminante, en este caso el compuesto farmacéutico, absorbe un fotón produciendo la ruptura de la molécula. En el mecanismo de fotólisis indirecta, la materia orgánica disuelta que se encuentra en la matriz del agua es oxidada por fuertes agentes reactivos

que se generan, como por ejemplo oxígeno singlete ($^1O_2$), radicales hodroxilo (·OH), etc. [96,97]. En general, la degradación de un compuesto por radiación UV, se ve afectada por la absorción de energía UV y el rendimiento cuántico del compuesto. La energía absorbida por el compuesto a una determinada longitud de onda se mide mediante el coeficiente de extinción molar [98].

Las fuentes actuales de radiación más utilizadas son las lámparas de vapor de mercurio ya que cumplen las siguientes características: alta intensidad en la longitud de onda deseada, larga vida, dimensiones geométricas adecuadas para el proceso considerado, mínimo coste del equipo auxiliar necesario y facilidad de operación. A su vez, las lámparas de mercurio se subdividen en arcos de baja, media y alta presión. Las lámparas de mercurio de *baja presión* operan a temperatura ambiente con una presión de vapor 10^{-3} mmHg, suelen refrigerarse por aire y su vida media es de 9.500 a 12.000 horas. Las lámparas de mercurio de *media presión* operan alrededor de una atmósfera y su vida media es de 1.000 horas. Finalmente, las lámparas de mercurio de *alta presión*, quizás las más importantes desde el punto de vista industrial debido a su mayor potencia lumínica, operan a presiones de entre 2 y 110 atmósferas, la refrigeración es por aire o por agua y su duración es bastante más corta (100-200 horas).

El contenido de materia orgánica (COT, DQO), la dosis de radiación UV, el tiempo de contacto y la estructura química del compuesto, son factores importantes que rigen la eficiencia de eliminación de los compuestos farmacéuticos durante su fotólisis directa.

La radiación ultravioleta se ha utilizado ampliamente para el tratamiento de aguas y aguas residuales en todo el mundo y cada vez tiene más aplicaciones en este campo. Numerosos estudios demuestran que este tratamiento es eficaz para la eliminación de compuestos farmacéuticos encontrados en diferentes tipos de aguas superficiales [91,99,100]. Sin embargo, esta tecnología sólo es aplicable a las aguas que contienen compuestos fotosensibles y con bajas concentraciones de DQO (por ejemplo, río y agua potable) [101]. Por otra parte, los efluentes de estaciones depuradoras de aguas

residuales tienen compuestos orgánicos, los cuales pueden inhibir o mejorar el proceso [102]. En general, la fotólisis directa ha demostrado ser menos eficaz en la degradación de los compuestos farmacéuticos de aguas residuales y además requiere más energía [103] que, por ejemplo, la ozonización.

Por otro lado, numerosos autores han estudiado la fotólisis conjunta con peróxido de hidrógeno. El éxito de este proceso radica en la formación estequiométrica de radicales hidroxilo (·OH) a partir de la descomposición fotocatalítica de H_2O_2 (Ecuación (19)). La fotólisis de un compuesto orgánico en disolución acuosa catalizada por la presencia de peróxido de hidrógeno es un proceso muy complejo que, de forma resumida, se esquematiza en la Figura 15 [95], la cual muestra el mecanismo de reacciones más comúnmente aceptado para la misma [104].

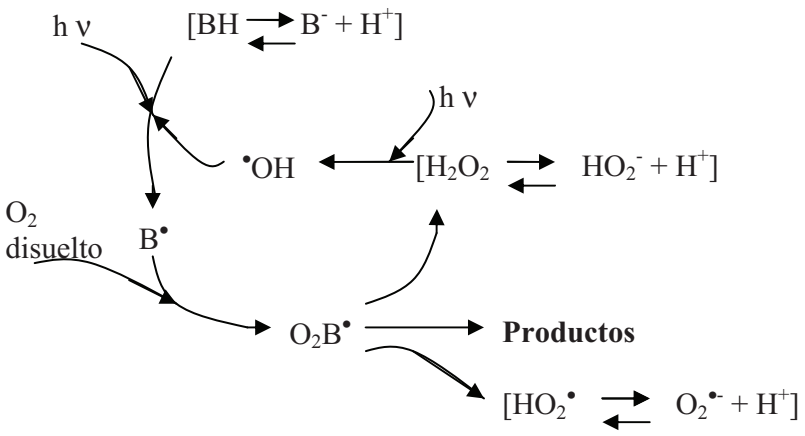

Figura 15. Mecanismo de reacción de la combinación UV/H_2O_2 sobre la materia orgánica [95].

Este mecanismo considera que en la primera etapa tiene lugar la degradación fotolítica de peróxido de hidrógeno que, mediante la escisión de una molécula del mismo, produce dos radicales libres hidroxilo por molécula descompuesta [105]:

$$H_2O_2 + h\upsilon \rightarrow 2\ \cdot OH \qquad (19)$$

El rendimiento cuántico de este proceso es muy elevado, formándose como máximo dos radicales hidroxilo por cuanto absorbido, e invariable con la longitud de onda aplicada [106].

Una vez formados estos radicales altamente reactivos, reaccionan a continuación con el compuesto orgánico mediante diferentes mecanismos: abstracción de un átomo de hidrógeno, adición a dobles enlaces C=C o transferencia de electrones, dependiendo de la naturaleza y grupos funcionales del compuesto orgánico. La vía de reacción más general es la abstracción de un átomo de hidrógeno y producción del consiguiente radical orgánico B·, que a su vez reacciona rápidamente con O_2 disuelto para formar el radical orgánico peróxido $O_2B\cdot$ [104]. Estos radicales orgánicos descomponen mediante reacciones bimoleculares dando lugar a los diferentes productos de degradación del compuesto de partida junto con otros subproductos tales como peróxido de hidrógeno, radicales hidroperóxido, formaldehído, etc [107].

Finalmente, las reacciones de dimerización de los propios radicales hidroxilo [108] y de los radicales hidroperóxido [109], conducen a la regeneración de peróxido de hidrógeno, el cual a su vez puede secuestrar radicales hidroxilo [110] y volver a formar radicales hidroperóxido:

$$2\ \cdot OH \rightarrow H_2O_2 \tag{20}$$

$$2\ HO_2\cdot \rightarrow H_2O_2 + O_2 \tag{21}$$

$$H_2O_2 + \cdot OH \rightarrow HO_2\cdot \tag{22}$$

Al mismo tiempo, hay que considerar los equilibrios de disociación del propio compuesto orgánico y de los diferentes intermedios formados, tales como peróxido de hidrógeno, radicales hidroperóxido, etc., que se muestran a continuación:

$$BH \rightleftharpoons B^- + H^+ \tag{23}$$

$$H_2O_2 \rightleftharpoons HO_2^- \tag{24}$$

$$HO_2\cdot \rightleftharpoons O_2^{\cdot -} + H^+ \tag{25}$$

En resumen, existe un ciclo de descomposición y formación simultánea de peróxido de hidrógeno cuyo resultado global dependerá de diversas variables, como la intensidad de la radiación ultravioleta, la temperatura, el pH y la naturaleza de los compuestos orgánicos.

Este tratamiento es considerado como uno de los procesos de oxidación avanzada más viable. Es preferible con respecto a la ozonización porque es menos sensible a la naturaleza y concentración de las especies contaminantes.

C.2.2. Procesos de Oxidación Avanzada Electroquímicos.

Entre los POAs, se encuentran los Procesos de Oxidación Avanzada Electroquímicos (POAEs), los cuales se han estudiado ampliamente durante la última década a escala de laboratorio. Algunos de estos estudios ya han sido publicados con perspectiva de aplicarlos en un futuro próximo en plantas piloto [111-114].

El uso de la electricidad para el tratamiento de aguas apareció por primera vez en 1889 [115]. Desde entonces, varias tecnologías electroquímicas se han aplicado con éxito en el tratamiento de aguas [116-118]. Entre ellas, podemos destacar la oxidación anódica, electro-Fenton, fotoelectro-Fenton y sonoelectro-Fenton [119].

En cuanto a la bibliografía, la mayoría de los estudios realizados que aplican POAEs se centran en la mineralización de un contaminante orgánico específico en agua ultra-pura y muy pocos prestan atención a la eliminación de un contaminante específico en matrices de agua más complejas, como las aguas residuales.

La electro-oxidación se puede definir como la técnica cuyo objetivo es la reducción del contenido en materia orgánica y compuestos de difícil eliminación mediante electrodos específicos. En la Figura 16 se muestra un esquema del proceso de electro-oxidación.

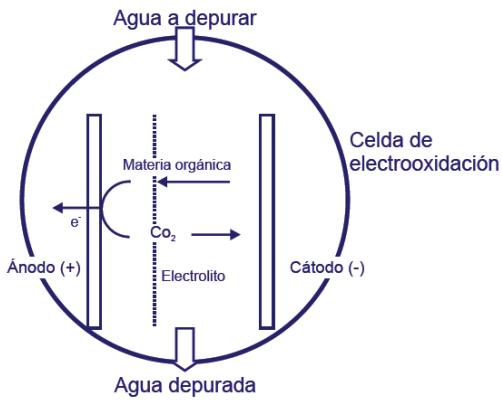

Figura 16. Detalle del fundamento teórico del proceso de Electro-oxidación.

La técnica electroquímica más comúnmente utilizada para el tratamiento de las aguas residuales es la oxidación electroquímica, llamada también oxidación anódica cuando se tratan disoluciones que no contienen cloruros. Este procedimiento implica la oxidación de los contaminantes en una celda electrolítica a través de las siguientes vías:

a) transferencia directa de electrones hacia el ánodo.

b) oxidación indirecta o mediada con especies oxidantes formadas a partir de la electrólisis del agua en el ánodo, por radicales ·OH fisisorbidos o por el "oxígeno activo" quimisorbido.

La existencia de estas especies permitió que se propusieran dos enfoques diferentes [113]:

1) *conversión electroquímica*, donde los compuestos orgánicos refractarios son transformados selectivamente en compuestos biodegradables, como ácidos carboxílicos, por el "oxígeno activo" quimisorbido.

2) *electroquímica de combustión*, donde los compuestos orgánicos se mineralizan por los radicales ·OH fisisorbidos.

La oxidación anódica es capaz de alcanzar la oxidación de los contaminantes del agua, ya sea por contacto directo o por procesos oxidativos que se originan en la

superficie del ánodo de la celda electroquímica, por lo que el proceso de oxidación no tiene que producirse necesariamente en el ánodo, pero sí iniciado en su superficie. Como consecuencia de ello, este tratamiento combina dos tipos principales de procesos [113]:

a) *Oxidación heterogénea de los contaminantes sobre la superficie del ánodo.* Este es un proceso complejo que consta de una serie de etapas simples: el transporte de los contaminantes a la superficie del electrodo, la adsorción del contaminante sobre la superficie, reacción electroquímica directa por transferencia de electrones, desorción de los productos y transporte de éstos al seno de la disolución.

b) *Oxidación homogénea de los contaminantes por oxidantes producidos en la superficie del ánodo a partir de los componentes del electrolito.* Estos oxidantes pueden ser producidos por la oxidación anódica heterogénea del agua o a partir de iones contenidos en el agua actuando en el seno de la disolución de la celda electrolítica. El oxidante más importante es el radical hidroxilo, que puede generarse por la oxidación del agua (Ecuación (26)) o por la oxidación del ión hidroxilo (Ecuación (27)):

$$H_2O \rightarrow \cdot OH_{ads} + H^+ + e^- \quad (26)$$

$$OH^- \rightarrow \cdot OH_{ads} + e^- \quad (27)$$

La generación de este radical permitió considerar la oxidación anódica como un POA. Debido a la capacidad de oxidación tan alta que tienen los radicales hidroxilo, éstos promueven la formación de otras muchas especies oxidantes (persulfatos, peroxofosfatos, ferratos, etc.) a partir de diferentes especies contenidas en las aguas [120]. Se ha demostrado que la presencia de estas especies tiene un efecto significativo en el aumento de la eficiencia de eliminación [121]. Los efectos sinérgicos de todos estos mecanismos pueden explicar las altas eficiencias obtenidas con esta tecnología en la eliminación de contaminantes y la alta mineralización alcanzada en comparación con otros POAs [122,123].

La Figura 17 muestra un breve esquema de los principales procesos que deben considerarse para comprender el proceso de oxidación anódica.

Dos puntos son de principal importancia en el proceso de oxidación anódica, el material del electrodo y el diseño de la celda electrolítica. El material del electrodo es importante puesto que puede influir significativamente en la oxidación directa de un contaminante orgánico dado y en la generación de oxidantes. En estos procesos es fundamental contar con materiales electródicos que tengan una elevada eficiencia en la eliminación-transformación de los compuestos orgánicos, así como una buena estabilidad en condiciones de polarización anódica y si es posible, un bajo coste de producción.

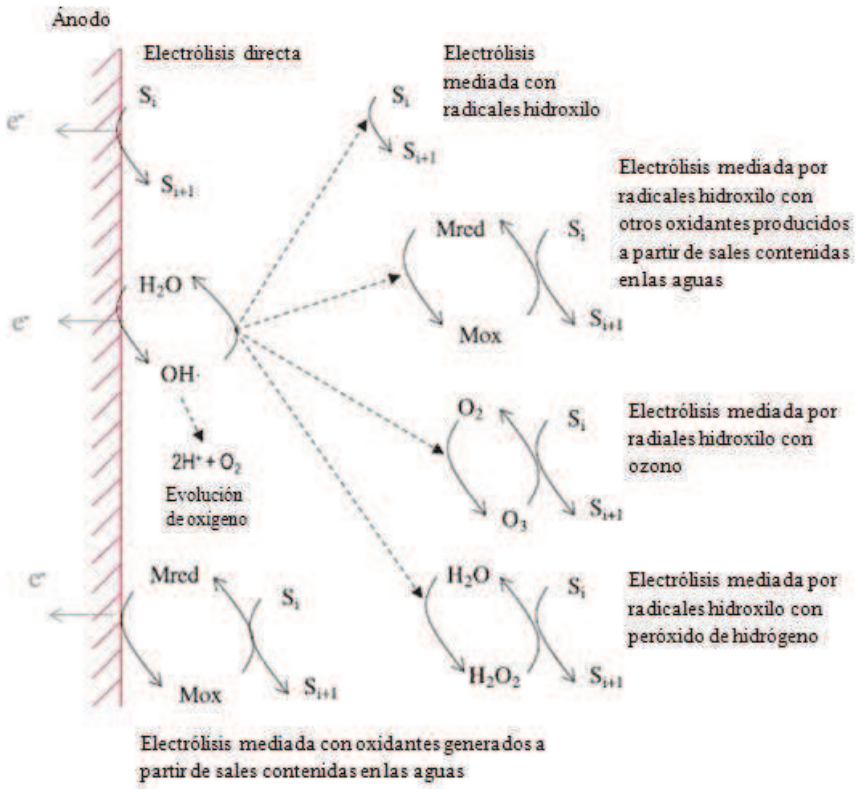

Figura 17. Descripción simple del mecanismo que ocurre durante la oxidación anódica de un contaminante. (Adaptada de la referencia [124]).

El diseño de la celda es también de especial interés, particularmente en el tratamiento de bajas concentraciones de contaminante, debido a que la cinética de estos procesos está controlada por la transferencia de materia. Un buen diseño mecánico, que promueva la turbulencia y que modifique factores que limiten la velocidad de oxidación, puede aumentar la eficiencia del proceso. Sin embargo, los estudios realizados de eliminación de compuestos farmacéuticos en aguas, sólo se han aplicado a nivel de laboratorio y por lo general, la optimización del diseño de la celda se requerirá cuando se trabaje a mayor escala, entonces es cuando se tendrá que mejorar el diseño del reactor [125]. En la actualidad, la mayoría de las celdas electroquímicas empleadas están formadas por un sólo compartimento y solamente se evalúa la influencia del material electródico. Sin duda, estos estudios a mayor escala serán de gran interés ya que ha sido completamente demostrada la aplicabilidad de esta tecnología a escala de laboratorio.

Con respecto al ánodo, su material es un punto clave de esta tecnología. En la bibliografía, según el material electródico, se describen dos comportamientos muy diferentes en la oxidación de contaminantes orgánicos [126]. Algunos materiales conducen a una potente oxidación del contaminante, formando CO_2 como producto final mayoritario y una pequeña cantidad de intermedios, mientras que otros materiales producen una menor oxidación y generan gran cantidad de subproductos de oxidación.

Aunque aún no están completamente claros los mecanismos que ocurren en los dos tipos de comportamientos, la interacción de los radicales hidroxilo formados durante el proceso electroquímico con la superficie del electrodo podría marcar las grandes diferencias entre ambos comportamientos. En el caso de tratamientos en los que se empleen materiales anódicos de alta eficiencia, los radicales hidroxilo no interactúan fuertemente con la superficie del electrodo y promueven la oxidación mediada de los compuestos orgánicos y la producción de otros oxidantes más estables. Comninellis [127] explica este comportamiento diferente por un modelo que asume la existencia de ánodos "no activos" y "activos”, respectivamente. En ambos tipos de ánodos, denotado como M, el agua se oxida dando lugar a la formación de radicales

hodroxilo fisisorbidos (M (·OH)) (Ecuación (28)). En el caso de ánodos "activos", este radical interactúa fuertemente con la superficie transformándose en "oxígeno activo" quimisorbido o superóxido MO (Ecuación (29)):

$$M+H_2O \rightarrow M(\cdot OH) + H^+ + e^- \quad (28)$$

$$M(\cdot OH) \rightarrow MO+ H^+ + e^- \quad (29)$$

$$MO + R \rightarrow M + RO \quad (30)$$

El par MO/M es un mediador en la conversión electroquímica de compuestos orgánicos (R), Ecuación (30). Por el contrario, la superficie de los ánodos "no activos" interactúan débilmente con las especies ·OH, por lo que estos radicales reaccionan directamente con los productos orgánicos hasta que se consigue la mineralización total. Estos radicales se encuentran fisisorbidos en sitios electroactivos del electrodo y éstos no sufren modificación durante la reacción de transferencia de electrones.

Los electrodos de grafito, otros con carbono sp^2, metálicos (Pt, Ti/Pt), electrodos de óxidos metálicos (IrO_2, RuO_2) y los de óxidos metálicos mixtos, se consideran como ánodos “activos” y se comportan como electrodos de baja eficiencia para la oxidación de compuestos orgánicos, generando una gran cantidad de compuestos intermedios. La mayoría de los compuestos aromáticos tratados con estos ánodos se degradan lentamente debido a la generación de ácidos carboxílicos que son difícilmente oxidables [128]. Se obtiene una pequeña mineralización y en algunos casos se generan polímeros, por lo que presentan pocas perspectivas de aplicación [129].

Algunos óxidos metálicos y óxidos metálicos mixtos (aquellos que contienen PbO_2 y/o SnO_2) y electrodos de diamante conductor, en particular, el **Diamante Dopado con Boro** (DDB), se consideran ánodos “no activos” y se comportan como electrodos de alta eficiencia para la oxidación de compuestos orgánicos. Éstos promueven la mineralización de los contaminantes, cuyo proceso está limitado sólo por el transporte de materia, y por lo general se consigue una mineralización prácticamente total del contaminante. Debido a ello, la oxidación anódica se puede

realizar a costes asequibles con tales electrodos, dependiendo principalmente de la potencia requerida para accionar el proceso electroquímico. No presenta los inconvenientes de los POAs comunes (formación de subproductos), considerándose por tanto una técnica muy útil [128,130,131]. Entre estos electrodos, los óxidos metálicos no son estables durante la inversión de la polaridad e incluso pueden degradarse durante el proceso. Por esta razón, sólo los electrodos de "diamante conductor" se están utilizando en esta técnica. Sin embargo, es importante tener en cuenta que el diamante conductor no es un material único, existen muchos tipos que presentan diferencias significativas y por tanto diferente comportamiento [132] dependiendo del sustrato, del compuesto dopante, del cociente sp^3/sp^2, etc. El ánodo de diamante dopado con boro es el electrodo conocido "no activo" más potente [113] considerándose el ánodo más adecuado para el tratamiento de compuestos orgánicos por oxidación anódica. En la Figura 18 se muestra una imagen de la superficie del DDB.

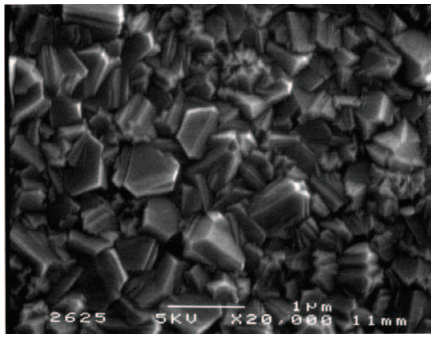

Figura 18. Microscopía electrónica de diamante dopado con boro.

Algunas de las características principales del diamante, como su elevada densidad atómica, dureza o inercia química lo convierten en un material de gran interés. El diamante natural es un aislante eléctrico, sin embargo, la introducción de algún átomo dopante en su estructura le confiere propiedades de conductor electrónico. Dependiendo de la cantidad de dopante puede comportarse como un semiconductor o como un semimetal. Debido a sus excepcionales cualidades, el diamante conductor se convierte en un material muy prometedor para su uso en aplicaciones electroquímicas. El dopante más utilizado es el boro que le confiere una semiconductividad tipo *p* a la

capa de diamante. Los depósitos de diamante se suelen realizar sobre un soporte, el cual tiene que cumplir simultáneamente tres importantes características: buena conductividad eléctrica, resistencia mecánica y que sea electroquímicamente inerte. Desde un punto de vista electroquímico, estos electrodos se caracterizan por tener un amplio rango de potencial donde el electrodo se comporta como idealmente polarizable. Los electrodos de diamante son muy resistentes a la corrosión electroquímica en condiciones extremas de polarización, tanto anódica como catódica. Debido a estas enormes ventajas que tiene con respecto a los demás materiales [133], el diamante dopado con boro es el más utilizado en la oxidación anódica y el único que se utiliza en este trabajo de investigación. La mayoría de los trabajos publicados se han centrado en este material o en la comparación del rendimiento del diamante con otros electrodos.

El grupo de investigación del Dr. Brillas fue el primero en aplicar la oxidación anódica con electrodos de DDB [134]. Se observó que la oxidación anódica de paracetamol con DDB era un método muy efectivo en medio acuoso. En este trabajo también se utilizó como material anódico el Pt, resultando que tenía un poder de oxidación mucho menor que el electrodo de diamante, y además conducía a una inferior mineralización del compuesto.

Otro interesante trabajo comparativo fue realizado por Murugananthan y col.[135] en el cual se estudió la oxidación anódica de ketoprofeno con electrodos de DDB y Pt. El ketoprofeno se oxidó por transferencia de electrones directa y la velocidad de oxidación aumentaba conforme lo hacía la densidad de corriente, sin embargo la mineralización disminuía, siendo ésta mayor a menor densidad de corriente. El mismo comportamiento fue observado por Brillas y col. [134,136] con paracetamol y diclofenaco. Esto nos indica que el proceso está controlado por fenómenos de transferencia de materia. En este estudio también se evaluó la influencia de la naturaleza del electrolito, observándose que la eliminación de carbono orgánico total (COT) era mucho mayor cuando se empleaban electrolitos que contenían sulfatos. Al comparar el rendimiento de ambos electrodos, como era de esperar, el DDB siempre era más eficaz que el Pt. Sin embargo, la velocidad inicial de mineralización fue

mayor con el Pt pero se formaban una mayor cantidad de compuestos refractarios intermedios. Otro trabajo realizado por Ciríaco y col. [138] consistió en la degradación de ibuprofeno con dos electrodos diferentes, DDB y Ti/Pt/PbO_2. La eficiencia de eliminación se encontró que era ligeramente mayor cuando se llevaba a cabo la oxidación anódica con DDB a baja densidad de corriente y similar para ambos ánodos a densidades de corriente mayores.

Por otro lado, también se ha sugerido la generación de diferentes oxidantes durante el proceso como ·OH heterogéneo (Ecuación (28)), H_2O_2, procedente de su dimerización (según Ecuación (31)) y O_3, por descomposición del agua en la superficie del ánodo (Ecuación (32)). Sin embargo, el ·OH fisisorbido es el oxidante más potente de todos.

$$2M(\cdot OH) \rightarrow 2MO + H_2O_2 \tag{31}$$

$$3H_2O_2 \rightarrow O_3 + 6H^+ + 6e^- \tag{32}$$

En otras investigaciones, se ha observado que cuando el agua contiene iones cloruro, se generan especies activas de cloro, Cl_2, HClO y/o ClO^- y ClO_2^- que pueden atacar a los compuestos orgánicos compitiendo con los otros oxidantes que se producen en el proceso de oxidación anódica [113]. También se pueden generar iones ClO_3^- e incluso transformarse en iones ClO_4^- [137,139]. Este procedimiento se llama *electro-oxidación con cloro activo* y se basa en la oxidación directa de los iones cloruros (Cl^-) en el ánodo para producir cloro soluble (según la Ecuación (33)), el cual se hidroliza rápidamente generando ácido hipocloroso e iones cloruro según la Ecuación (34):

$$2Cl^- \rightarrow Cl_2\,(aq) + 2e^- \tag{33}$$

$$Cl_2\,(aq) + H_2O \rightleftharpoons HClO + Cl^- + H^+ \tag{34}$$

El ácido hipoclorito está en equilibrio con el ácido hipocloroso a pK_a= 7,55, según la Ecuación (35):

$$HClO \rightleftharpoons ClO^- + H^+ \tag{35}$$

A partir de los equilibrios anteriores, se concluyó que la especie predominante hasta pH cercano a 3 es el Cl_2, en el rango de pH 3-8 predomina HClO y el ión ClO^- a pH superior a 8 [140]. La formación y la acumulación de cloroderivados tóxicos, trihalometanos, y cloraminas, supone un posible inconveniente de la electro-oxidación en presencia de cloro activo [141].

Otro aspecto importante de esta tecnología es el electrolito soporte que se emplee, el cual se ha demostrado que presenta una fuerte influencia en el proceso puesto que participa en los mecanismos de oxidación mediada.

El punto débil de las diferentes investigaciones que se han realizado hasta el momento es la alta concentración de los contaminantes que se han empleado, ya que se sitúan lejos de los niveles de concentración reales en un agua residual. Sin embargo, hay que tener en cuenta que no se centran en aplicaciones reales, sino en una evaluación preliminar de la tecnología.

Aunque se han realizado bastantes estudios de degradación oxidativa de productos farmacéuticos por POAs, pocos se han hecho en matrices de agua reales [142]. Con respecto a esto, hay un trabajo muy interesante en al cual se aplica la oxidación anódica con DDB con ósmosis inversa para la eliminación de 10 contaminantes emergentes (entre ellos, fármacos) en agua de EDAR [143]. Estos contaminantes fueron casi eliminados por completo, con porcentajes de eliminación superiores al 92% en todos los casos después de 2 horas de tratamiento.

Otro aspecto de especial interés, es el coste de operación de esta tecnología para futuras aplicaciones. Existe un estudio en el que se evalúa y compara los costes de operación de tres procesos: Fenton, ozonización y oxidación anódica, en varios tipos de aguas residuales [144]. Los resultados revelaron que la oxidación anódica supera claramente en eficacia a la ozonización y al reactivo de Fenton. Sin embargo, la oxidación por el reactivo de Fenton es el proceso más barato y la ozonización el más caro de los tres. Esto pone de manifiesto que la oxidación anódica podría competir en muchas aplicaciones a mayor escala con otras tecnologías más usuales.

En el tratamiento de efluentes mediante esta técnica, la tasa de degradación y la eficiencia de estos procesos dependen de parámetros experimentales tales como el pH, la temperatura, la agitación, la concentración del sustrato, la naturaleza del electrolito soporte y la densidad de corriente, y sus efectos deben ser estudiados para conseguir las mejores condiciones operativas del método.

De toda la información obtenida en los trabajos encontrados en bibliografía, se puede concluir que la oxidación anódica es una tecnología muy prometedora para la eliminación de compuestos farmacéuticos presentes en agua, particularmente cuando se utilizan electrodos de DDB.

D. JUSTIFICACIÓN Y OBJETIVOS DE ESTA INVESTIGACIÓN.

Este estudio forma parte de un amplio programa de investigación sobre la eliminación de contaminantes emergentes en aguas naturales y residuales mediante el empleo de técnicas físicas, químicas y biológicas, el cual presenta gran interés medioambiental que, durante los últimos años, se está desarrollando en Área de Ingeniería Química y Química Física de la Universidad de Extremadura (UEx).

El trabajo ha sido financiado por el Ministerio de Ciencia e Innovación a través de los Proyectos del plan Nacional CTQ 2007-60255, titulado “Aplicación de técnicas físicas y Procesos de Oxidación Avanzada a la degradación de productos farmacéuticos presentes en aguas”, y CTQ 2010-14823, titulado “Utilización de tecnologías avanzadas en aguas superficiales y tratadas para la eliminación de contaminantes resistentes a métodos convencionales”. También ha sido financiado por la Consejería de Ciencia y Tecnología de la Junta de Extremadura a través del Proyecto PRI-07A031, titulado “Aplicación de técnicas físicas y químicas a la eliminación de contaminantes preferentes en efluentes acuosos”. Es de destacar que parte de esta Tesis ha sido realizada en colaboración con el Departamento de Ingeniería Química de la Universidad de Castilla La Mancha (Ciudad Real, España).

En particular, la presente Tesis Doctoral tiene como *objetivo general* la degradación de varios compuestos farmacéuticos, comúnmente presentes en aguas, y seleccionados como modelo, aplicando procesos físicos, químicos y electroquímicos,

ya que se requiere la aplicación de métodos más severos que las técnicas de depuración actualmente implementadas en las estaciones de tratamiento de aguas potables y depuradoras de aguas residuales. Estos estudios se centran fundamentalmente en medir los niveles de eliminación alcanzados en los contaminantes estudiados, determinar la influencia de las diferentes variables operativas, así como las condiciones óptimas, en cada uno de los tratamientos aplicados. La importancia de estas determinaciones reside en que tales parámetros permiten llevar a cabo el diseño y la optimización de los dispositivos, equipos y reactores reales que se han de utilizar posteriormente en las plantas de tratamiento de aguas.

En este trabajo se decidió investigar la eliminación de los compuestos farmacéuticos siguientes: naproxeno, ketoprofeno, carbamacepina y trimetoprima. Los tratamientos seleccionados para llevar a cabo el presente estudio, tanto en agua ultra-pura como en diversas matrices acuosas reales, han sido los siguientes:

- Adsorción de los productos farmacéuticos mediante resinas poliméricas (*Amberlite XAD-7*) y derivados tanínicos (quebracho, pino, ciprés y acacia).
- Eliminación de los contaminantes elegidos y de materia orgánica (DQO y COT) mediante procesos de oxidación electroquímica, concretamente oxidación anódica con electrodos de diamante dopado con boro.
- Degradación de uno de los productos farmacéuticos seleccionado como modelo (carbamacepina) mediante procesos de oxidación química, empleando los sistemas oxidantes: ozono, UV/H_2O_2, Fe^{2+}/H_2O_2 (reactivo de Fenton), Fe^{3+}/H_2O_2 (reactivo Fenton like).

Los *objetivos específicos* fijados que permiten comprender con más detalle el alcance del trabajo, han sido los siguientes:

1. Estudio del proceso de adsorción sobre la resina *Amberlite XAD-7* de los cuatro compuestos farmacéuticos seleccionados de forma individual y en la mezcla. Estudio de la cinética y del equilibrio de adsorción mediante la

aplicación de diferentes modelos teóricos y establecimiento de la influencia de las condiciones de operación en este proceso.

2. Síntesis de adsorbentes de base tanínica y estudio de su eficacia en la adsorción de compuestos farmacéuticos. Determinación de la cinética y del equilibrio de adsorción mediante la aplicación de diferentes modelos teóricos y de las condiciones óptimas de trabajo, lo cual lleva a la selección del mejor extracto tanínico para la retirada de trimetoprima.
3. Aplicación del tratamiento de oxidación anódica con electrodos de diamante dopado con boro para la degradación de los contaminantes farmacéuticos seleccionados.
4. Estudio y comparación de la eficacia del proceso de electro-oxidación en la eliminación de carbamacepina en diferentes matrices de acuosas (ultra-pura, pantano, río, efluente EDAR).
5. Aplicación del tratamiento de oxidación anódica a un efluente residual de una industria farmacéutica. Estudio de la eliminación de materia orgánica mediante dos parámetros: DOQ y COT.
6. Estudio de diferentes procesos de oxidación: reactivo de Fenton y Fenton-like, ozono y UV/H_2O_2, en la eliminación de carbamacepina.
7. Estudio de la influencia de variables de todos los procesos aplicados.
8. Modelación teórica de todos los tratamientos y estudio de la interacción de variables mediante diseño de experimentos y análisis según la metodología de la superficie de respuesta.

E. BIBLIOGRAFÍA.

[1] Primer informe de las Naciones Unidas sobre el Desarrollo de los Recursos Hídricos en el Mundo. "Agua para todos, agua para la vida". Marzo **(2003)**.

[2] Segundo informe de las Naciones Unidas sobre el Desarrollo de los Recursos Hídricos en el Mundo. "El agua responsabilidad compartida". Marzo **(2006)**.

[3] Tercer informe de Naciones Unidas sobre el desarrollo de recursos hídricos del mundo. "El agua en un mundo en cambio". Marzo **(2009)**.

[4] Barceló, D.L.; López de Alda, M.J. "Contaminación y calidad química del agua: el problema de los contaminantes emergentes". Fundación Nueva Cultura del Agua. Panel científico-técnico de seguimiento de la política de aguas. Convenio Universidad de Sevilla-Ministerio de Medio Ambiente. Instituto de Investigaciones Químicas y Ambientales-CSIC (Barcelona).

[5] Petrovi´c, M.; González, S.; Barceló, D. "Analysis and removal of emerging contaminants in wastewater and drinking water". TRAC-Trends Anal. Chem. 22, 685 **(2003)**

[6] Cortacans, J.A.; Hernández, A.; Del Castillo, I.; Montes, E.; Hernández, A. "Presencia de fármacos en aguas residuales y eficacia de los procesos convencionales en su eliminación". III Congreso de Ingeniería Civil, Territorio y Medio Ambiente. Zaragoza, España, **(2006)**.

[7] Clara, M.; Strenn, B.; Kreuzinger, N. "Carbamazepine as a possible anthropogenic marker in the aquatic environment: Investigations on the behaviour of carbamazepine in wastewater treatment and during groundwater infiltration". Water Res. 38, 947 **(2004)**.

[8] Metcalfe, C.D.; Koenig, B.G.; Bennie, D.T.; Servos, M.; Ternes, T.A.; Hirsch, R. "Occurrence of neutral and acidic drugs in the effluents of Canadian sewage treatment plants". Environ. Toxicol. Chem. 22, 2872 **(2003)**.

[9] Tixier, C.; Singer, H.P.; Oellers, S.; Müller, S.R. "Occurrence and fate of carbamazepine, clofibric acid, diclofenac, ibuprofen, ketoprofen, and naproxen in surface waters". Environ. Sci. Technol. 37, 1061 **(2003)**.

[10] Skordi, E.; Wilson, I.D.; Lindon, J.C.; Nicholson, J.K. "Characterization and quantification of metabolites of racemic ketoprofen excreted in urine following oral administration to man by 1H NMR spectroscopy, directly coupled HPLC–MS and HPLC–NMR, and circular dichroism". Xenobiotica. 34, 1075 **(2004)**.

[11] Lindqvist, N.; Tuhkanen, T.; Kronberg, L. "Occurrence of acidic pharmaceuticals in raw and treated sewages and in receiving waters". Water Res. 39, 2219 **(2005)**.

[12] Santos, J.L.; Aparicio, I.; Alonso, E. "Occurrence and risk assessment of pharmaceutically active compounds in wastewater treatment plants. A case study: Seville city, Spain". Environ. Int. 33, 596 **(2007)**.

[13] Quintana, J.B.; Weiss, S.; Reemtsma, T. "Pathways and metabolites of microbial degradation of selected acidic pharmaceutical and their occurrence in municipal wastewater treated by a membrane bioreactor". Water Res. 39, 2564 **(2005)**.

[14] Matamoros, V.; Duhec, A.; Albaigés, J.; Bayona, J.M. "Photodegradation of carbamazepine, ibuprofen, ketoprofen and 17a-ethinylestradiol in fresh and Seawater". Water Air Soil Pollut. 196, 161 **(2009)**.

[15] Radjenovi´c, J.; Petrovi´c, M.; Barceló, D. "Fate and distribution of pharmaceuticals in wastewater and sewage sludge of the conventional activated sludge (CAS) and advanced membrane bioreactor (MBR) treatment". Water Res. 43, 831 **(2009)**.

[16] Boynton, C.S.; Dick, C.F.; Mayor, G.H. "NSAIDs: an overview". J. Clin. Pharmacol. 28, 512 **(1988)**.

[17] Loscher, W.; Ungemach, F.R.; Kroler, R. "Basics of Pharmacological Therapy of Domestic Animals". Verlag Paul Parey, Berlin, Hamburg **(1994)**.

[18] Benotti, M.J.; Trenholm, R.A.; Vanderford, B.J.; Holady, J.C.; Stanford, B.D.; Snyder, S.A. "Pharmaceuticals and endocrine disrupting compounds in U.S.drinking water". Environ. Sci. Technol. 43, 597 **(2009)**.

[19] Zhao, X.; Qu, J.; Liu, H.; Qiang, Z.; Liu, R.; Hu, C. "Photoelectrochemical degradation of anti-inflammatory pharmaceuticals at Bi2MoO6–boron-doped diamond hybrid electrode under visible light irradiation". Applied Catalysis B: Environmental. 91, 539 **(2009)**.

[20] Carballa, M.; Omil, F.; Lema, J.M.; Llompart, M.; Garcia-Jares, C.; Rodriguez, I.; Gomez, M.; Ternes, A. "Behavior of pharmaceuticals, cosmetics and hormones in a sewage treatment plant". Water Res. 38, 2918 **(2004)**.

[21] Nakada, N.; Tanishima, T.; Shinohara, H.; Kiri, K.; Takada, H. "Pharmaceutical chemicals and endocrine disrupters in municipal wastewater in Tokyo and their removal during activated sludge treatment". Water Res. 40, 3297 **(2006)**.

[22] Boyd, G.R.; Reemtsma, H.; Grimm, D.A.; Mitra, S. "Pharmaceuticals and personal care products (PPCPs) in surface and treated waters of Louisiana, USA and Ontario, Canada". Sci. Total Environ. 311, 135 **(2003)**.

[23] Isidori, M.; Lavorgna, M.; Nardelli, A.; Parrella, A.; Previtera, L.; Rubino, M. "Ecotoxicity of naproxen and its phototransformation products". Sci. Total Environ. 348, 93 **(2005)**.

[24] Bekci, Z.; Seki, Y.; Seki, Y.; Yurdakoc, M.K. "Equilibrium studies for trimethoprim adsorption on montmorillonite KSF". Hazard J. Mater. 133, 233 **(2006)**.

[25] Díaz-Cruz, M.S.; López de Alda, M.J.; Barceló, D. "Environmental behaviour and analysis of veterinary and human drugs in soils, sediments and sludge**".** Trends Anal. Chem. 22, 340 **(2003)**.

[26] Batt, A.L.; Aga, D.S. "Simultaneous analysis of multiple classes of antibiotics by ion trap LC/MS/MS for assessing surface water and groundwater contamination**".** Anal. Chem. 77, 2940 **(2005)**.

[27] De Paula, F.C.C.R.; de Pietro, A.C.; Cass, Q.B.J. **"**Simultaneous quantification of sulfamethoxazole and trimethoprim in whole egg samples by column-switching high-performance liquid chromatography using restricted access media column for on-line sample clean-up". Chromatogr. A. 1189, 221 **(2008)**.

[28] Sebastine, I.M.; Wakeman, R.J. "Consumption and environmental hazards of pharmaceutical substances in the UK". Process Saf. Environ. Prot. 81, 229 **(2003)**.

[29] Hernando, M.D.; Mezcua, M.; Fernandez-Alba, A.R.; Barcelo, D. "Environmental risk assessment of pharmaceutical residues in wastewater effluents, surface waters and sediments". Talanta. 69, 334 **(2006)**.

[30] Bedner, M.; Maccrehan, W.A. "Transformation of Acetaminophen by Chlorination Produces the Toxicants 1,4-Benzoquinone and N-Acetyl-p-benzoquinone Imine". Environ. Sci. Technol. 40, 516 **(2006)**.

[31] Halling-Sorensen, B.; Nors Nielsen, S.; Lanzky, P.F.; Ingerslev, F.; Holten Lutzhoft, H.C.; Jorgensen, S.E. "Occurrence, fate and effects of pharmaceutical substances in the environmental review". Chemosphere. 36, 357 **(1998)**.

[32] Fent, K.; Weston, A.A.; Caminada, D. "Ecotoxicology of human pharmaceuticals". Aquatic Toxicol. 76, 122 **(2006)**.

[33] Ternes, T.A. "Ocurrence of Drugs in German Sewage Treatment Plants and Rivers". Water Res. 32, 3245 **(1998)**.

[34] Daughton, C.G.; Ternes, T.A. "Pharmaceuticals and personal care products in the environment: agents of subtle change". Environ. Health Perspect. 107, 907 **(1999)**.

[35] Drewes, J.E.; Heberer, T.; Reddersen, K. "Fate of pharmaceuticals during indirect potable reuse". Water Sci. Technol. 46, 73 **(2002)**.

[36] Strenn, B.; Clara, M.; Gans, O.; Kreuzinger, N. "Carbamazepine, diclofenac, ibuprofen and bezafibrate-investigations on the behaviour of selected pharmaceuticals during wastewater treatment". Water Sci Technol. 50, 269 **(2004)**.

[37] Heberer, T. "Tracking persistent pharmaceutical residues from municipal sewage to drinking water". J. Hydrol. 266, 175 **(2002)**.

[38] Halling-Sorensen, B.; Nielsen, S.N.; Lanzky, P.F.; Ingerslev, F.; Lützhoft, H.C.H.; Jorgensen, S.E. "Ocurrence, Fate and Effects of Pharmaceutical Substances in the Environment-A Rewiew". Chremosphere. 36, 357 **(1998)**.

[39] Petrović, M.; Hernando, D.; Díaz-Cruz, S.; Barceló, D. "Liquid chromatography tandem mass spectrometry for the analysis of pharmaceutical residues in environmental samples: a review". J. Chromatogr. A. 1067, 1 **(2005)**.

[40] Cleuvers, M. "Mixture toxicity of the anti-inflammatory drugs diclofenac, ibuprofen, naproxen, and acetylsalicylic acid". Ecotoxicol. Environ. Saf. 59, 309 **(2004)**.

[41] Haag, W. R.; Yao, D. C. C. "Rate constants for reaction of hydroxyl radicals with several drinking water contaminants". Environ. Sci. Technol. 26, 1005 (**1992**).

[42] Scott, J.P.; Ollis, D.F. "Integration of chemical and biological oxidation processes for water treatment: review and recommendation". Environ. Prog. 14, 88 **(1995)**.

[43] Sánchez Martín, J. “Aplicación de productos naturales para el tratamiento de aguas. Empleo en países en desarrollo”. Tesis Doctoral **(2011)**.

[44] Sim, W.J.; Lee, J.W.; Lee, E.S.; Shin, S.K.; Hwang, S.R.; Oh, J.E. "Occurrence and distribution of pharmaceuticals in wastewater from households, livestock farms, hospitals and pharmaceutical manufactures". Chemosphere. 82, 179 **(2011)**.

[45] Williams, R.T. "Human Pharmaceuticals: Assessing the Impacts on Aquatic Ecosystems Society of Environmental Toxicology and Chemistry (SETAC)". USA (**2005**).

[46] Rosal, R.; Rodríguez, A.; Perdigón-Melón, J.A.; Petre, A.; García-Calvo, E.; Gómez, M.J.; Aguera, A.; Fernández-Alba, A.R. "Occurrence of emerging pollutants in urban wastewater and their removal through biological treatment followed by ozonation". Water Res. 44, 578 **(2010)**.

[47] Rassaei, L.; Sillanpaa, M.; Marken, F. "Modified carbón nanoparticle-chitosan film electrodes: Physisorption versus chemisorption". Electrochimica Acta. 53, 5732 **(2008)**.

[48] Xiong, W.; Peng, J.; Hu, Y. "Use or X-ray adsorption near edge structure (XANES) to identify physisorption and chemisorption of phosphate onto ferrihydrite modified diatomite". Journal of Colloid and interface science. 368, 528 **(2012)**.

[49] Yang, X.; Al-Duri, B. "Kinetic modeling of liquid-phase adsorption of reactive dyes on activated carbón". J. Colloid Interf. Sci. 37, 1061 **(2005)**.

[50] Pinzón- Bedoya, M. L.; Vera, L. E. "Modelamiento de la cinética de bioadsorción de Cr (III) usando cáscara de naranja". Redalyc. 160, 95 **(2009)**.

[51] Khalfaoui, M.; Knani, S.; Hachicha, M.A.; Ben Lamine, A. "New theorical expressions for the five adsorption type asotherms classified by BET based on statistical physics treatment". J. Colloid Interf. Sci. 263, 350 **(2003)**.

[52] Cooney, D. O. "Adsorption Design for Wastewater Treatment". Ed. Lewis Publishers, Boca Raton, (**1998)**.

[53] Ho, Y.S.; Porter, J.F.; McKay, G. "Equilibrium isotherm studies for the sorption of divalent metal ions onto peat: copper, nickel and lead single component systems". Water Air Soil Pollut. 141, 1 **(2002)**.

[54] Dubinin, M.M. "The potential theory of adsorption of gases and vapors for adsorbents with energetically non-uniform surface". Chem. Rev. 60, 235 **(1960)**.

[55] Lee, D.W.; Eum, C.H.; Lee, I.H.; Jeon, S.J. "Adsorption Behavior of 8-Hydroxyquinoline and Its Derivatives on Amberlite XAD Resins, and Adsorption of Metal Metal Ions by Using Chelating Agent-Impregnated Resins". Analytical Sciences. 4, 505 **(1988)**.

[56] Li, A.; Zhang, Q.; Chen, J.; Fei, Z.; Longa, C.; Li, W. "Adsorption of phenolic compounds on Amberlite XAD-4 and its acetylated derivative MX-4". React. Funct. Polym. 49, 225 **(2001)**.

[57] Pizzi, A. "Advanced Wood Adhesives Technology". Marcel Dekker, New York **(1994)**.

[58] Nakano, Y.; Takeshita, K.; Tsutsumi, T. "Adsorption mechanism of hexavalent chromium by redox within condensed-tannin gel". Water Res. 35, 496 **(2001)**.

[59] Kim, Y.H.; Nakano, Y. "Adsorption mechanism of palladium by redox within condensed-tannin gel". Water Res. 39, 1324 **(2005)**.

[60] Tondi, G.; Oo, C.W.; Pizzi, A.; Thevenon, M.F. "Metal absorption of tannin-based rigid foams". Ind. Crop. Prod. 29, 336 **(2009)**.

[61] Vázquez, G.; Antorrena, G.; González, J.; Doval, M.D. "Adsorption of heavy metal ions by chemically modified Pinus pinaster bark". Bioresour. technol. 48, 251 **(1994)**.

[62] Vázquez, G.; González-Álvarez, J.; Freire, S.; López-Lorenzo, M.; Antorrena, G. "Removal of cadmium and mercury ions from aqueous solution by sorption on treated Pinus pinaster bark: kinetics and isotherms". Bioresour. Technol. 82, 247 **(2002)**.

[63] Pizzi, A. "Natural phenolic adhesives I: Tannins". En: A. Pizzi and K.L. Mittal, (eds.), Handbook of Adhesive Technology, *2*nd edición, pages 573–588. Marcel Dekker, New York **(2003)**.

[64] Andreozzi, R.; Caprio, V.; Insola, A.; Marotta, R. "Advanced oxidation processes (AOP) for water purification and recovery". Catal. Today 53, 51 **(1999)**.

[65] Oturan, M.A.; Oturan, N.; Edelahi, M.C.; Podvorica, F.I.; Kacemi, K.E. "Oxidative degradation of herbicide diuron in aqueous medium by Fenton's reaction based advanced oxidation processes". Chem. Eng. J. 171, 127 **(2011)**.

[66] Borras, N.; Arias, C.; Oliver, R.; Brillas, E. "Mineralization of desmetryne by electrochemical advanced oxidation processes using a boron-doped diamond anode and an oxygen-diffusion cathode". Chemosphere. 85, 1167 **(2011)**.

[67] Rey, A.; Carbajo, J.; Adan, C.; Faraldos, M.; Bahamonde, A.; Casas, J.A.; Rodriguez, J.J. "Improved mineralization by combined advanced oxidation processes". Chem. Eng. J. 174, 134 **(2011)**.

[68] Biard, P.-F.; Couvert, A.; Renner, C.; Levasseur, J.-P. "Intensification of volatile organic compounds mass transfer in a compact scrubber using the O3/H2O2 advanced oxidation process: kinetic study and hydroxyl radical tracking". Chemosphere. 85, 1122 **(2011)**.

[69] Bouafia-Chergui, S.; Oturan, N.; Khalaf, H.; Oturan, M.A."Parametric study on the effect of the ratios [H2O2]/[Fe3+] and [H2O2]/[substrate] on the photo-Fenton degradation of cationic azo dye Basic Blue 41". J. Environ. Sci. Health, Part A 45, 622 **(2010)**.

[70] Isarain-Chavez, E.; Rodriguez, R.M.; Cabot, P.L.; Centellas, F.; Arias, C.; Garrido, J.A.; Brillas, E. "Degradation of pharmaceutical beta-blockers by electrochemical advanced oxidation processes using a flow plant with a solar compound parabolic collector". Water Res. 45, 4119 **(2011)**.

[71] Hussain, S.; Shaikh, S.; Farooqui, M. "COD reduction of waste water streams of active pharmaceutical ingredient – Atenolol manufacturing unit by advanced oxidation-Fenton process". J. of Saudi Chem. Soc. 17, 199 **(2013)**.

[72] Abdelmelek, S.B.; Greaves, J.; Ishida, K.P.; Cooper, W.J.; Song, W. "Removal of pharmaceutical and personal care products from reverse osmosis retentate using advanced oxidation processes". Environ. Sci. Technol. 45, 3665 **(2011)**.

[73] Ay, F.; Kargi, F. "Advanced oxidation of amoxicillin by Fenton's reagent treatment". J. Hazard. Mater. 179, 622 **(2010)**.

[74] Zazo, J.A.; Casas, J.A.; Mohedano, A.F.; Gilarranz, M.A.; Rodriguez, J.J. "Chemical pathway and kinetics of phenol oxidation by Fenton's reagent". Environ. Sci. Technol. 39, 9295 **(2005)**.

[75] Ternes, T.A.; Stuber, J.; Herrmann, N.; McDowell, D.; Ried, A.; Kampmann, M. Teiser, B. " Ozonation: a tool for removal of pharmaceuticals, contrast media and musk fragrances from wastewater". Water Res. 37, 1976 **(2003)**.

[76] Jeong, J.; Jung, J.; Cooper, W.J.; Song, W.H. "Degradation mechanisms and kinetic studies for the treatment of X-ray contrast media compounds by advanced oxidation/reduction processes". Water Res. 44, 4391 **(2010)**.

[77] Brillas, E.; Sires, I.; Oturan, M.A. "Electro-Fenton process and related electrochemical technologies based on Fenton's reaction chemistry". Chem. Rev. 109, 6570 **(2009)**.

[78] Almeida, L.C.; García-Segura, S.; Bocchi, N.; Brillas, E. "Solar photoelectro-Fenton degradation of paracetamol using a flow plant with a Pt/air-diffusion cell coupled with a compound parabolic collector: Process optimization by response surface methodology". Appl. Catal. B 103, 21 **(2011)**.

[79] Tekin, H., Bilkay, O., Ataberk, S.S., Balta, T.H., Ceribasi, I.H., Sanin, F.D. "Use of Fenton oxidation to improve the biodegradability of a pharmaceutical wastewater". J. Hazard. Mater. 136, 258 **(2006)**.

[80] Santos, A., Yustos, P., Rodríguez, S., Simón, E., García-Ochoa, F. "Abatement of phenolic mixtures by catalytic wet oxidation enhanced by Fenton's pretreatment: effect of H2O2 dosage and temperature". J. Hazard. Mater. 146, 595 **(2007)**.

[81] Pignatello, J.J. "Dark and photoassisted Fe^{3+} - catalyzed degradation of chlorophenoxy herbicides by hydrogen peroxide". Environ. Sci. Technol. 26, 944 **(1992)**.

[82] Kulik, N.; Trapido, M.; Goi, A.; Veressinina, Y.; Munter, Y. "Combined chemical treatment of pharmaceutical effluents from medical ointment production". Chemosphere. 70, 1525 **(2008)**.

[83] Sebastián, N.S.; Fernández, J.F.; Segura, X.F.; Ferrer, A.S. "Pre-oxidation of an extremely polluted industrial wastewater by the Fenton's reagent". J. Hazard. Mater. B 101, 315 **(2003)**.

[84] Badawy, M.I.; Wahaab, R.A.; El-Kalliny, A.S. "Fenton-biological treatment processes for the removal of some pharmaceuticals from industrial wastewater". J. Hazard. Mater. 15, 567 **(2009)**.

[85] Staehelin, J.; Hoigné, J. "Decomposition of ozone in water in the presence of organic solutes acting as promoters and inhibitors of radical chain reactions". Environ. Sci. Technol. 19, 1206 **(1985)**.

[86] Coelho, A.D.; Sans, C.; Aguera, A.; Gómez, M.J.; Esplugas, S.; Dezotti, M. "Effects of ozone pre-treatment on diclofenac: intermediates, biodegradability and toxicity assessment". Sci. Total Environ. 407, 3572 **(2009)**.

[87] Andreozzi, R.; Caprio, V.; Marotta, R.; Vogna, D. "Paracetamol oxidation from aqueous solutions by means of ozonation and H2O2/UV system". Water Res. 37, 993 **(2003)**.

[88] Litter, M.I. "Introduction to photochemical advanced oxidation processes for water treatment". Environmental Chemistry 2 (Pt. M), 325 **(2005)**.

[89] Hollender, J.; Zimmermann, S.G.; Koepke, S.; Krauss, M.; McArdell, C.S.; Ort, C.; Singer, H.; von Gunten, U.; Siegrist, H. "Elimination of organic micropollutants in a municipal wastewater treatment plant upgraded with a full-scale postozonation followed by sand filtration". Environ. Sci. Technol. 43, 7862 **(2009)**.

[90] Huber, M.M.; Gobel, A.; Joss, A.; Hermann, N.; Loffler, D.; McArdell, C.S.; Ried, A.; Siegrist, H.; Ternes, T.A.; von Gunten, U. "Oxidation of pharmaceuticals during ozonation of municipal wastewater effluents: a pilot study". Environ. Sci. Technol. 39, 4290 **(2005)**.

[91] Adams, C.; Asce, M.; Wang, Y.; Loftin, K.; Meyer, M. "Removal of antibiotics from surface and distilled water in conventional water treatment processes". J. Environ. Eng. 128, 253 **(2002)**.

[92] Dodd, M.C.; Buffle, M.; von Gunten, U. "Oxidation of antibiotic molecules by aqueous ozone: moiety-specific reaction kinetics and application to ozone-based wastewater treatment". Environ. Sci. Technol. 40, 1969 **(2006)**.

[93] Dodd, M.C.; Kohler, H.E.; von Gunten, U. "Oxidation of antibiotic compounds by ozone and hydroxyl radical: elimination of biological activity during aqueous ozonation processes". Environ. Sci. Technol. 43, 2498 **(2009)**.

[94] Dickenson, E.R.V.; Drewes, J.E.; Sedlak, D.L.; Wert, E.C.; Snyder, S.A. "Applying surrogates and indicators to assess removal efficiency of trace organic chemicals during chemical oxidation of wastewaters". Environ. Sci. Technol. 43, 6242 **(2009)**.

[95] Roldán, G. "Eliminación de compuestos farmacéuticos en aguas mediante procesos de oxidación avanzada y técnicas de filtración por membranas". Tesis Doctoral **(2011)**.

[96] Arnold, W.A.; McNeill, K.; Petrovi´c, M.; Barcelo´, D. "Transformation of Pharmaceuticals in the Environment: Photolysis and Other Abiotic Processes". Compr. Anal. Chem. 3, 361 **(2007)**.

[97] Fatta-Kassinos, D.; Vasquez, M.I.; Kümmerer, K. "Transformation products of pharmaceuticals in surface waters and wastewater formed during photolysis and advanced oxidation processes e degradation, elucidation of byproducts and assessment of their biological potency". Chemosphere. 85, 693 **(2011)**.

[98] Kim, I.; Yamashita, N.; Tanaka, H. "Performance of UV and UV/H2O2 processes for the removal of pharmaceuticals detected in secondary effluent of a sewage treatment plant in Japan". J. Hazard. Mater. 166, 1134 **(2009)**.

[99] Ryan, C.C.; Tan, D.T.; Arnold, W.A. "Direct and indirect photolysis of sulfamethoxazole and trimethoprim in wastewater treatment plant effluent". Water Res. 45, 1280 **(2011)**.

[100] Yuan, F.; Hu, C.; Hu, X.; Wie, D.; Chen, Y.; Qu, J. "Photodegradation and toxicity changes of antibiotics in UV and UV/H2O2 process". J. Hazard. Mater. 185, 1256 **(2011)**.

[101] Homem, V.; Santos, L. "Degradation and removal methods of antibiotics from aqueous matrices e a review". J. Environ. Manag. 92, 2304 **(2011)**.

[102] Jiao, S.; Zheng, S.; Yin, D.; Wang, L.; Chen, L. "Aqueous photolysis of tetracycline and toxicity of photocatalytic products to luminescent bacteria". Chemosphere. 73, 377 **(2008)**.

[103] Katsoyiannis, I.A.; Canonica, S.; Gunten, U. "Efficiency and energy requirements for the transformation of organic micropollutants by ozone, O3/H2O2 and UV/H2O2". Water Res. 45, 3811 **(2011)**.

[104] Legrini, O.; Oliveros, E.; Braun, A.M. "Photochemical processes for water treatment". Chem. Rev. 93, 671 **(1993)**.

[105] Baxendale, J. H.; Wilson, J.A. "The photolysis of hydrogen peroxide at high light intensities". Trans. Faraday Soc. 53, 344 **(1957)**.

[106] Gómez, L.; Urkiaga, A.; Gutiérrez, M.; De las Fuentes, L. "Fotooxidación de vertidos químicos". Ing. Química. 371, 211 **(2000)**.

[107] von Sonntag, C.; Schuchmann, H.P. "The Chemistry of free radicals: Peroxyl Radicals in aqueous solutions". Edited by Z. B. Alfassi **(1997).**

[108] Farhataziz, T.; Ross, A. B. "Selective specific rates of reactions of transients in water and aqueous solutions. III. Hydroxyl radical and Perhidroxyl radical and their radicals ions". Natl. Stand. Ref. Data Ser. 59 **(1977)**.

[109] Bielski, B. H. J.; Cabello, D. E.; Arudi, R. L.; Ross, A. B. "Pulse radiolysis study of the kinetics and mechanism of the reactions between manganese (II) complexes and perhydroxyl (HO_2)/hyperoxide (O_2^-) radicals. The phosphate complex and an overview". J. Phys. Chem. Ref. Data. 14, 1041 **(1985)**.

[110] Christensen, H.S.; Sehested, H.; Corfitzan, H. "Reactions of hydroxyl radicals with hydrogen peroxide at ambient and elevated temperatures". J. Phys. Chem. 86, 15 **(1982)**.

[111] Hammami, S.; Bellakhal, N.; Oturan, N.; Oturan, M.A.; Dachraoui, M. "Degradation of Acid Orange 7 by electrochemically generated ·OH radicals in acidic aqueous medium using a boron-doped diamond or platinum anode: a mechanistic study". Chemosphere. 73, 678 **(2008)**.

[112] Dirany, A.; Sires, I.; Oturan, N.; Oturan, M.A. "Electrochemical abatement of the antibiotic sulfamethoxazole from water". Chemosphere. 81, 594 **(2010)**.

[113] Panizza, M.; Cerisola, G. "Direct and mediated anodic oxidation of organic pollutants". Chem. Rev. 109, 6541 **(2009)**.

[114] Panizza, M.; Brillas, E.; Comninellis, C. "Application of boron-doped diamond electrodes for wastewater treatment". J. Environ. Eng. Manage 18, 139 **(2008)**.

[115] Guohua, C. "Electrochemical technologies in wastewater treatment". Sep. Purif. Technol. 38, 11 **(2004)**.

[116] Robinson, T.; McMullan, G.; Marchant, R.; Nigam, P. "Remediation of dyes in textile effluent: a critical review on current treatment technologies with a proposed alternative". Bioresour. Technol. 77, 247 **(2001)**.

[117] Martínez-Huitle, C.A.; Ferro, S. "Electrochemical oxidation of organic pollutants for the wastewater treatment: direct and indirect processes". Chem. Soc. Rev. 35, 1324 **(2006)**.

[118] Rajkumar, D.; Palanivelu, K. "Electrochemical treatment of industrial wastewater". J. Hazard. Mater. 113, 123 **(2004)**.

[119] Oturan, M.A.; Sires, I.; Oturan, N.; Perocheau, S.; Laborde, J.-L.; Trevin, S. "Sonoelectro-Fenton process: a novel hybrid technique for the destruction of organic pollutants in water". J. Electroanal. Chem. 624, 329 **(2008)**.

[120] Cañizares, P.; Sáez, C.; Sánchez-Carretero, A.; Rodrigo, M.A. "Synthesis of novel oxidants by electrochemical technology". J. Appl. Electrochem. 39, 2143 **(2009)**.

[121] Rodrigo, M.A.; Cañizares, P.; Sánchez-Carretero, A.; Sáez, C. "Use of conductive diamond electrochemical oxidation for wastewater treatment". Catal. Today 151, 173 **(2010)**.

[122] Cañizares, P.; Paz, R.; Sáez, C.; Rodrigo, M.A. "Electrochemical oxidation of wastewaters polluted with aromatics and heterocyclic compounds". J. Electrochem. Soc. 154, 165 **(2007)**.

[123] Cañizares, P.; Paz, R.; Sáez, C.; Rodrigo, M.A. "Electrochemical oxidation of alcohols and carboxylic acids with diamond anodes: a comparison with other advanced oxidation processes". Electrochim. Acta. 53, 2144 **(2008)**.

[124] Feng, L.; van Hullebusch, E.D.; Rodrigo, M.A.; Espósito, G.; Oturan. M.A. "Removal of residual anti-inflamatory and analgesic pharmaceuticals from aqueous systems by electrochemical advanced oxidation processes. A review". Chem. Eng. J. 228, 944 **(2013)**.

[125] Cañizares, P.; Lobato, J.; Paz, R.; Rodrigo, M.A.; Sáez, C. "Electrochemical oxidation of phenolic wastes with boron-doped diamond anodes". Water Res. 39, 2687 **(2005)**.

[126] Foti, G.; Gandini, D.; Comninellis, C.; Perret, A.; Haenni, W. "Oxidation of organics by intermediates of water discharge on IrO2 and synthetic diamond anodes". Electrochem. Solid-State Lett. 2, 228 **(1999)**.

[127] Comninellis, Ch. "Electrocatalysis in the electrochemical conversion/combustion of organic pollutants for waste water treatment". Electrochim. Acta. 39, 1857 **(1994)**.

[128] Waterston, K.; Wang, J.; Bejan, D.; Bunce, N. "Electrochemical waste water treatment: electrooxidation of acetaminophen". J. Appl. Electrochem. 36, 227 **(2006)**.

[129] Foti, G.; Gandini, D.; Comninellis, C.; Perret, A.; Haenni, W. "Oxidation of organicsby intermediates of water discharge on IrO2 and synthetic diamond anodes". Electrochem. Solid-State Lett. 2 , 228 **(1999)**.

[130] Andrade, L.S.; Tasso, T.T.; da Silva, D.L.; Rocha-Filho, R.C.; Bocchi, N.; Biaggio, S.R. "On the performances of lead dioxide and boron-doped diamond electrodes in the anodic oxidation of simulated wastewater containing the Reactive Orange 16 dye". Electrochim. Acta 54, 2024 **(2009)**.

[131] Song, S.; Fan, J.; He, Z.; Zhan, L.; Liu, Z.; Chen, J.; Xu, X. "Electrochemical degradation of azo dye C.I. Reactive Red 195 by anodic oxidation on Ti/SnO2– Sb/PbO2 electrodes". Electrochim. Acta 55, 3606 **(2010)**.

[132] Cañizares, P.; Sáez, C.; Sánchez-Carretero, A.; Rodrigo, M.A. "Influence of the characteristics of p-Si BDD anodes on the efficiency of peroxodiphosphate electrosynthesis process". Electrochem. Commun. 10, 602 **(2008)**.

[133] Panizza, M.; Kapalka, A.; Comninellis, C. "Oxidation of organic pollutants on BDD anodes using modulated current electrolysis". Electrochim. Acta 53, 2289 **(2008)**.

[134] Brillas, E.; Sires, I.; Arias, C.; Cabot, P.L.; Centellas, F.; Rodríguez, R.M.; Garrido, J.A. "Mineralization of paracetamol in aqueous medium by anodic oxidation with a boron-doped diamond electrode". Chemosphere. 58, 399 **(2005)**.

[135] Murugananthan, M.; Latha, S.S.; Bhaskar Raju, G.; Yoshihara, S. "Anodic oxidation of ketoprofen—an anti-inflammatory drug using boron doped diamond and platinum electrodes". J. Hazard. Mater. 180, 753 **(2010)**.

[136] Brillas, E.; García-Segura, S.; Skoumal, M.; Arias, C. "Electrochemical incineration of diclofenac in neutral aqueous medium by anodic oxidation using Pt and boron-doped diamond anodes". Chemosphere. 79, 605 **(2010)**.

[137] Sánchez-Carretero, A.; Sáez, C.; Cañizares, P.; Rodrigo, M.A. "Electrochemical production of perchlorates using conductive diamond electrolyses". Chem. Eng. J. 166, 710 **(2011)**.

[138] Ciriaco, L.; Anjo, C.; Correia, J.; Pacheco, M.J.; Lopes, A. "Electrochemical degradation of Ibuprofen on Ti/Pt/PbO2 and Si/BDD electrodes". Electrochim. Acta 54, 1464 **(2009)**.

[139] Rodrigo, M.A.; Canizares, P.; Buitron, C.; Sáez, C. "Electrochemical technologies for the regeneration of urban wastewaters". Electrochim. Acta 55, 8160 **(2010)**.

[140] Pérez, G.; Fernández-Alba, A.R.; Urtiaga, A.M.; Ortiz, I. "Electro-oxidation of reverse osmosis concentrates generated in tertiary water treatment". Water Res. 44, 2763 **(2010)**.

[141] Cañizares, P.; Paz, R.; Sáez, C.; Rodrigo, M.A. "Costs of the electrochemical oxidation of wastewaters: a comparison with ozonation and Fenton oxidation processes". J. Environ. Manage. 90, 410 **(2009)**.

[142] Bergmann, MEH.; Rollin, J.; Iourtchouk, T. "The occurrence of perchlorate during drinking water electrolysis using BDD anodes". Electrochim. Acta. 54, 2102 **(2009)**.

[143] Boxall, C.; Kelsall, G.H. "Hypochlorite electrogeneration. II. Thermodynamics and kinetic model of the anode reaction layer". Inst. Chem. Eng. Symp. Ser. 127, 59 **(1992)**.

[144] Martínez-Huitle, C.A.; Brillas, E. "Electrochemical alternatives for drinking water disinfection". Angew Chem. Int. Ed. 47, 1998 **(2008)**.

SEGUNDA PARTE

RESULTADOS Y DISCUSIÓN

RESULTADOS Y DISCUSIÓN

En esta segunda parte de la Tesis Doctoral, correspondiente a "Resultados y Discusión", se exponen y discuten de forma detallada los resultados obtenidos en el trabajo de investigación realizado, el cual tiene como objetivo global la eliminación de una selección de productos farmacéuticos presentes en diversas aguas mediante diferentes procesos: físico-químicos (adsorción), químicos (reactivo de Fenton y Fenton-like, ozonación, e irradiación UV en presencia de peróxido de hidrógeno) y electroquímicos (oxidación anódica). Esta sección está conformada por los artículos publicados en revistas científicas y resultantes de esta investigación.

En el **Capítulo 1** se estudió el proceso de adsorción de compuestos farmacéuticos presentes en aguas sobre resinas y *tanigeles*.

En primer lugar, el trabajo se centró en la evaluación de la cinética de adsorción de la carbamacepina, naproxeno y trimetoprima, en agua ultra-pura, sobre una resina polimérica comercial con excelentes propiedades fisicoquímicas de intercambio y adsorción, *Amberlite XAD-7*.

En el estudio cinético inicial se evaluó la influencia de diferentes parámetros de operación que afectan a la eficiencia del proceso. Además, los datos experimentales se ajustaron a diferentes modelos cinéticos para ver cuál de ellos simula el proceso real de manera más precisa. Las variables analizadas contemplaron un amplio margen de estudio, y fueron las siguientes: dosis de adsorbente, velocidad de agitación, pH, temperatura y concentración inicial del compuesto farmacéutico. Resultado de esta investigación se dedujo que el pH de la disolución es el factor que más influye en la eliminación de estos compuestos, con excepción de la carbamacepina, para la cual la adsorción resultó ser independiente del pH. Por otra parte, la dosis de adsorbente, presenta una influencia positiva sobre la eliminación de todos los contaminantes. La concentración inicial del fármaco y la temperatura de operación influyen de forma

moderada en la adsorción, mientras que la velocidad de agitación apenas afecta al proceso.

Para simular la cinética de adsorción, los datos experimentales obtenidos se ajustaron a cuatro modelos cinéticos teóricos: de *pseudo primer* y de *pseudo segundo orden*, de *difusión intrapartícula* y *Bangham.* Así, el modelo elegido para analizar la influencia de las condiciones de operación en la cinética de adsorción de los tres compuestos farmacéuticos fue el de *pseudo-segundo orden,* que proporcionó el mejor ajuste. A partir de este análisis se concluye una vez más que el pH es la variable que afecta de manera más significativa a la velocidad de adsorción. La temperatura y la velocidad de agitación, por su parte, también contribuyen de una forma más moderada a acelerar el proceso.

El porcentaje de eliminación alcanzado en las dos primeras horas de tratamiento (85% carbamacepina, 60% naproxeno, 70% trimetoprima) demuestra la alta eficacia del proceso de adsorción en la eliminación de estos compuestos orgánicos sobre la resina *Amberlite XAD-7*.

En segundo lugar, una vez estudiada la cinética, se procedió al estudio del equilibrio de adsorción de trimetoprima, carbamacepina, ketoprofeno, naproxeno, y de una mezcla de los cuatro fármacos sobre la misma resina (*Amberlite XAD-7*) en agua ultra-pura. Dichos experimentos, se llevaron a cabo en diferentes condiciones de pH (5-9), manteniendo constante la temperatura, la fuerza iónica del medio y la agitación. Los resultados obtenidos demostraron, de nuevo, que la adsorción de los fármacos es fuertemente dependiente del pH y que la influencia de este parámetro sobre la capacidad de adsorción es diferente para cada compuesto. Esta influencia es positiva en el caso de trimetoprima (fármaco de carácter básico), negativa para el naproxeno y ketoprofeno (fármacos ácidos), e indiferente en el caso de la carbamacepina (fármaco neutro).

La mayor capacidad de adsorción la presentó la carbamacepina, seguida de la trimetoprima. Los datos experimentales de equilibrio se ajustaron a los modelos de *Langmuir*, *Freundlich* y *Dubinin-Radushkevich*. Estos dos últimos modelos

proporcionaron el mejor ajuste. Los resultados obtenidos ponen de manifiesto la presencia de centros de adsorción energéticamente heterogéneos en todos los sistemas de adsorbente-soluto estudiados. La energía de adsorción media (E= 8,3-10,1 $kJ \cdot mol^{-1}$) obtenida por el modelo de *Dubinin-Radushkevich* indica que la adsorción es de tipo física.

En este mismo estudio también se observó el comportamiento de los contaminantes en la mezcla (adsorción competitiva) y cómo afectaba a cada uno de ellos la presencia del resto de compuestos. Comparando los parámetros de *Freundlich* para ambos sistemas (fármaco individual y en la mezcla) se concluyó que la capacidad de adsorción en la mezcla disminuye para los compuestos ácidos y neutros (ketoprofeno, naproxeno y carbamacepina) y que aumenta para el compuesto básico (trimetoprima). Esto puede ser explicado por la adsorción previa de las moléculas ácidas sobre la superficie de la resina, lo cual favorece la adsorción posterior de las moléculas básicas de trimetoprima, posiblemente por la formación de puentes de hidrógeno entre ambos tipos de moléculas. En función de lo observado, se puede decir que la presencia de fármacos con carácter ácido o neutro aumenta significativamente la capacidad de adsorción del adsorbente para fármacos básicos.

Por último, se realizaron experiencias para el estudio del equilibrio de adsorción en agua superficial (agua del río Guadiana) para los compuestos individuales y para la mezcla de los cuatro fármacos. Los resultados obtenidos no fueron muy satisfactorios debido a que el "ruido de fondo" que se observaba en los cromatogramas no permitía observar con nitidez el grado de eliminación de cada uno de los contaminantes.

De todo ello, podemos decir que esta resina demuestra tener una excelente capacidad para su aplicación como adsorbente de los compuestos farmacéuticos seleccionados, tanto de forma individual como en mezclas.

En tercer lugar, se sometieron a estudio adsorbentes naturales de base tanínica (*tanigeles*) para la eliminación de dichos compuestos farmacéuticos en agua ultra-pura. Una vez sintetizados para su empleo como adsorbentes mediante gelificación, se realizaron experimentos previos para comprobar la capacidad de adsorción de varios

tipos de *tanigeles* con carbamacepina, ketoprofeno, naproxeno y trimetoprima. De estas experiencias resultó que estos taninos gelificados sólo se comportan como adsorbentes eficaces para la retirada de trimetoprima, debido probablemente a la estructura iónica predominante. Este hecho puede ser atribuido a la presencia de dos grupos amino en la estructura molecular de este compuesto, los cuales pueden interaccionar con la superficie del *tanigel*. Así pues, en este apartado del Capítulo 1, se evaluó la capacidad de adsorción de varios *tanigeles* con trimetoprima en disolución acuosa. Hasta el momento, no hay trabajos previos que traten de la eliminación de fármacos con *tanigeles*. La publicación que se presenta es la primera que demuestra la aplicación de estos adsorbentes naturales en la retirada de compuestos farmacéuticos de aguas.

Los taninos se encuentran presentes en cortezas, frutos, hojas, etc. de una enorme variedad de plantas. Se seleccionaron cuatro extractos tanínicos cuyas fuentes fueron: *Acacia mearnsii de Wild* (Acacia), *Schinopsis balansae* (Quebracho colorado), *Pinus pinaster* (Pino) y *Cupressus sempervivens* (Ciprés) y dos aldehídos para el proceso de gelificación (formaldehído y acetaldehído). Este proceso de gelificación conlleva la inmovilización de las estructuras tanínicas y está suficientemente bien referido en bibliografía, si bien existen pocos precedentes en el estudio de la optimización del proceso de gelificación para la retirada de contaminantes de matrices acuosas. Por ello, para estudiar este procedimiento, se consideraron tres variables operativas: el extracto tanínico, el aldehído implicado y su concentración. El objetivo fue obtener un tipo de *tanigel* que maximizara la retirada de trimetoprima del agua.

La utilización de estrategias de base estadística, como el Diseño de Experimentos y su análisis según la metodología de la Superficie de Respuesta, permitió aislar y sintetizar el *tanigel* más eficiente, según la combinación más favorable de las tres variables de estudio. Los resultados mostraron que el mejor extracto tanínico para este fin fue el *Pinus pinaster* con formaldehído concentrado (PFC, según codificación de trabajo) y también se alcanzaron altos porcentajes de eliminación del contaminante con *Cupressus sempervivens* (CFC) y con *Schinopsis balansae* con formaldehído diluido (QFD).

Por otro lado, se analizó el proceso de retirada de trimetoprima con los óptimos de las tres categorías de *tanigeles*: PFC, CFC y QFD. Esta evaluación se llevó a cabo por un lado, mediante una modelización teórica del proceso de adsorción según hipótesis cinéticas tales como el modelo de primer orden (*Lagergen)*, segundo orden (H_0) y *Elovich*, y por otro lado, mediante una modelización teórica del proceso de adsorción en el equilibrio siguiendo los modelos de *Langmuir* y *Freundlich.*

Los datos obtenidos, tanto en los experimentos cinéticos como en los de equilibrio, se correlacionaron con los modelos y de acuerdo con los valores del estadístico r^2 de cada uno de ellos, todos los modelos explican el fenómeno de adsorción de un modo satisfactorio, puesto que el valor de r^2 es superior en todos los casos a 0,80. Análogamente, los modelos de equilibrio arrojaron buenos índices de correlación, esta vez superiores en todos los casos a 0,96.

Por tanto, se puede decir que los adsorbentes tanínicos estudiados son muy eficaces para el tratamiento de aguas contaminadas con trimetoprima, de manera que alcanzan incluso capacidades de adsorción por encima de 300 miligramos por gramo de adsorbente. En comparación con otros adsorbentes (resina *Amberlite XAD-7*, carbón activado, arcillas, etc.) su capacidad de adsorción es altamente competitiva y superior, en muchos casos, a la mostrada por adsorbentes comerciales ampliamente distribuidos.

Una vez estudiados los procesos físicos de adsorción, en el resto de la investigación se aplicaron procesos químicos y electroquímicos, concretamente Procesos de Oxidación Avanzada (POAs). Los siguientes capítulos 2, 3 y 4 están centrados en la oxidación de compuestos farmacéuticos mediante una técnica muy eficaz y novedosa denominada *electro-oxidación* utilizando electrodos de diamante dopado con boro (DDB).

Así pues, en el **Capítulo 2** se utilizó la técnica de electro-oxidación (oxidación anódica) con DDB para el tratamiento de los cuatro compuestos farmacéuticos seleccionados, de forma individual, en disolución acuosa. El objetivo principal fue la optimización del proceso mediante el estudio de las diferentes variables de operación

en el proceso, así como las posibles interacciones entre las mismas. Para ello, se llevó a cabo un diseño estadístico de experimentos (ortogonal y rotable) para cada fármaco. En todos los casos, las variables de operación estudiadas fueron: pH, intensidad de corriente, concentración de electrolito soporte (Na_2SO_4) y caudal de agua.

En referencia a la influencia de variables, para los cuatro fármacos puede generalizarse que la intensidad de corriente es el factor más influyente. Este hecho puede explicarse teniendo en cuenta que la generación de radicales hidroxilo, verdaderos agentes oxidantes del proceso, es totalmente dependiente de la intensidad de corriente. Sin embargo, a altos valores de intensidad de corriente, la elevada generación de burbujas de hidrógeno en el cátodo puede obstaculizar el proceso de oxidación en fase acuosa. La segunda variable más influyente es la dosis de electrolito soporte. La influencia de este factor es, en general, positiva y el valor máximo suele coincidir con la mayor concentración utilizada. Esto revela una respuesta creciente del sistema a medida que aumenta esta variable, de manera que el óptimo probablemente quede fuera del rango de trabajo. Esto se justifica teniendo en cuenta dos factores: un aumento en la concentración de electrolito favorece, por una parte, la conducción de la corriente en la solución, y por la otra la formación de especies oxidantes secundarias como peroxodisulfato. Para el caso del caudal de agua, en todos los casos, como era de esperar, influye negativamente ya que este parámetro es inversamente proporcional al tiempo de residencia de las moléculas en el reactor. El pH no demuestra una influencia importante sobre la eficacia del proceso, a la luz de los resultados obtenidos.

Para caracterizar completamente el proceso y optimizar la degradación de cada uno de los fármacos, se realizó el test ANOVA y se analizaron las superficies de respuesta y curvas de contorno para cada fármaco. En todos los casos se determinó un punto de operación óptimo en el cual siempre se alcanzó un nivel de degradación del 100 %. Dicho óptimo fue comprobado experimentalmente para cada compuesto.

Por otro lado, también se analizó la eficacia del proceso en la reducción de la demanda química de oxígeno (DQO) y el carbono orgánico total (COT), parámetros que indican el grado de contaminación y mineralización alcanzado. Una vez finalizado

el tratamiento con carbamacepina, la eliminación de DQO fue 45% y de COT 61%. En el caso del ketoprofeno, 38% y 85%, respectivamente. Para el naproxeno, los niveles de eliminación de DQO y COT fueron 43% y 38%, respectivamente. Y finalmente para la trimetoprima estos valores fueron 17% y 76%, respectivamente.

En función de los resultados satisfactorios obtenidos con esta técnica, se puede decir, que supone una opción muy interesante para la eliminación de este tipo de contaminantes en agua, debido fundamentalmente a su elevada eficacia sin necesidad de añadir reactivos y sin producir residuos peligrosos.

Aunque ya se ha indicado anteriormente que tres capítulos de este trabajo aplican la técnica de electro-oxidación, es importante aclarar que la instalación experimental empleada en el Capítulo 2 es diferente a la que se utiliza en el Capítulo 3 y 4. El depósito de la disolución, la celda electroquímica, la bomba peristáltica, la fuente de corriente, el tipo de refrigeración y hasta el modo de operar (continuo o discontinuo) son diferentes en ambas instalaciones. Los motivos que condujeron a este cambio de instalación fueron varios. Con respecto a la celda electroquímica utilizada en el Capítulo 2, ésta estaba diseñada para el tratamiento de aguas con una concentración de contaminante muy baja, con un electrodo de DDB muy pequeño y de capacidad volumétrica mínima. Tanto el ánodo como el cátodo eran de diamante dopado con boro y era necesario invertir la polarización en cada uno de los experimentos realizados con el objeto de que no se ensuciaran los electrodos. Además, los experimentos duraban muy poco tiempo debido a que se trabajaba en discontinuo, sin posibilidad de recircular la disolución. La refrigeración sólo se realizaba al principio del experimento puesto que la disolución se encontraba termostatizada en un tanque con camisa refrigerante. Las limitaciones de las técnicas analíticas empleadas y el hecho de que se tratara de una primera aproximación experimental a la eliminación de estos fármacos, justificaron un cambio en la escala de trabajo. Durante la estancia realizada en Ciudad Real, se utilizó otra instalación para llevar a cabo el tratamiento electroquímico de agua contaminada, la cual resultó mucho más adecuada para la investigación. Esta instalación es la que se emplea en los siguientes Capítulos 3 y 4, en la cual se opera en modo continuo y utiliza una celda electroquímica de mayor

tamaño, al igual que los electrodos (ánodo de diamante dopado con boro y cátodo de acero inoxidable).

Hasta este punto se han estudiado los niveles de eliminación alcanzados para los compuestos farmacéuticos elegidos como modelo. En una fase posterior, los diversos tratamientos de oxidación sólo se aplicaron a un compuesto farmacéutico, la carbamacepina. La carbamacepina fue elegida para continuar con esta investigación debido a que está considerado el compuesto farmacéutico más frecuentemente detectado en agua, incluso ha sido propuesto por algunos autores como marcador antropogénico. Además, se considera uno de los compuestos farmacéuticos más refractario presentando una gran resistencia a los métodos convencionales de tratamiento de aguas.

Conscientes del sesgo que supondría un estudio aislado de la eliminación de carbamacepina, esta investigación se completó con la realización de una evaluación pormenorizada de la eliminación de los cuatro compuestos de trabajo en mezcla y en diversas matrices acuosas reales (agua del pantano de Villar del Rey, agua del río Guadiana y efluente de salida de la EDAR de Badajoz) mediante POAs como el Reactivo de Fenton, UV/H_2O_2, Foto-Fenton, UV/TiO_2, UV/TiO_2/H_2O_2, los cuales aún no están discutidos y no se incluyen en la presente Tesis.

En el **Capítulo 3**, en primer lugar, se llevó a cabo la optimización del proceso de electro-degradación de carbamacepina mediante un diseño de experimentos con objeto de evaluar la influencia de dos variables importantes en el proceso electroquímico: la concentración inicial de compuesto y la intensidad de corriente. Aunque el estudio electroquímico de carbamacepina ya se ha realizado en el Capítulo 2, fue necesario volver a hacerlo en la nueva instalación experimental, para poder realizar análisis comparativos posteriores.

Todo el proceso fue modelado de acuerdo con una cinética de primer orden. Se eligió como variable objetivo la constante cinética aparente (k) y no el porcentaje de eliminación, es decir, la velocidad de degradación de la carbamacepina en cada uno de los experimentos que conforman el diseño. Esta variable vino definida de manera

autónoma según los resultados observados, de manera que se estima recoge fielmente el horizonte de estudio de la investigación.

El análisis gráfico y numérico de los resultados obtenidos indicó que las dos variables estudiadas son influyentes en el proceso, sin embargo la concentración inicial de compuesto es mucho más significativa que la intensidad de corriente. La concentración inicial ejerce un efecto negativo sobre la variable objetivo, mientras que la intensidad de corriente afecta positivamente. Las condiciones óptimas obtenidas por este procedimiento para alcanzar el mayor valor de k (0,72 min^{-1}), se consiguen a bajas concentraciones de contaminante e intensidades de corriente altas (3,4 A).

Posteriormente, con el fin de confirmar la viabilidad del proceso de degradación electroquímica, la carbamacepina se disolvió en tres matrices acuosas diferentes: agua del río Guadiana en su paso por Badajoz, agua del pantano de Villar del Rey (agua de entrada de la ETAP de Badajoz) y agua residual correspondiente al efluente del tratamiento secundario de la EDAR de Badajoz. Estas experiencias fueron llevadas a cabo en las condiciones óptimas obtenidas previamente en agua ultra-pura. La velocidad de eliminación de carbamacepina en agua milli-Q resultó ser menor que en las otras tres matrices acuosas. Esto indica que en el proceso intervienen otras especies químicas eléctricamente activas como es el cloro activo, el cual se considera el oxidante secundario que más se genera en los procesos de electro-oxidación (electro-oxidación indirecta o mediada con cloro). En el efluente de EDAR la eliminación ocurrió con mayor rapidez, seguida del agua de río y finalmente la que presentó la velocidad de eliminación más lenta fue la de pantano. Esta velocidad de degradación resultó estar directamente relacionada con la concentración de ión cloruro contenida en cada una de las muestras acuosas. Este efecto fue contrastado debidamente mediante la oxidación de disoluciones acuosas sintéticas del contaminante, con contenidos crecientes de ión cloruro.

En segundo lugar, se procedió al estudio de la optimización del proceso en sistemas con agua de pantano y con agua de EDAR, y se contrastaron los resultados con los obtenidos en agua ultra-pura. Las variables de estudio y operativa fueron las

mismas que en el caso anterior. Atendiendo a los resultados obtenidos, la concentración inicial de carbamacepina resulta ser el factor más influyente en agua milli-Q y en agua superficial, mientras que en el agua de EDAR la variable más significativa es la intensidad de corriente. Esto se atribuye al mayor contenido de materia orgánica en el agua de EDAR, lo cual convierte en menos selectivas las reacciones de oxidación, compitiendo la oxidación de carbamacepina con la de otras especies oxidables. En consecuencia la concentración de contaminante adquiere una influencia menor que la intensidad. En general, las dos variables siguen la misma tendencia en los tres casos aunque se observan diferencias significativas al comparar la influencia de cada variable por separado.

Una vez comprobada la gran eficiencia de esta técnica en la eliminación de compuestos farmacéuticos tanto en agua ultra-pura, como en aguas naturales y residuales, se evaluó la eficacia del proceso de electro-oxidación con DDB en el tratamiento de aguas con un elevado contenido en materia orgánica. Para ello se trató un efluente residual real de una industria farmacéutica de Ciudad Real. Este agua residual presentaba una DQO de 12.000 $mg \cdot L^{-1}$ y un contenido de COT de 3.200 $mg \cdot L^{-1}$. Dicho estudio fue realizado durante la estancia en Ciudad Real en el Departamento de Ingeniería Química de la UCLM, y es el que se aborda en el **Capítulo 4**. En este capítulo se optimizó el proceso electroquímico mediante un diseño de experimentos para determinar el significado estadístico de dos parámetros: la densidad de corriente y la velocidad de flujo.

En primer lugar, se estudió la contribución global de los parámetros operativos y la evolución del tiempo de residencia en la eliminación de DQO y COT. Para ello, en cada uno de los experimentos que presenta el diseño, se fue midiendo el contenido de estos parámetros a diferentes tiempos de tratamiento (entre 0 y 570 minutos). Se trataron los valores de eliminación de DQO y TOC, mediante estudio estadístico, para cada tiempo, de todos los experimentos que conforman el diseño factorial. Para cada uno de los tiempos se obtuvo una ecuación de regresión, la cual nos proporcionó información acerca de la contribución de las variables estudiadas. Mediante representación gráfica de cada una de las contribuciones, de la densidad de corriente,

del flujo y de la interacción de ambas, frente al tiempo, y a partir de la derivada de la contribución total, se dedujo un punto apropiado para realizar la modelización de la disminución de DQO a 98 minutos, mientras que para el caso del TOC éste resultó ser de 77 minutos. Se eligieron estos tiempos de tratamiento por ser donde se observaba la mayor influencia de los parámetros operativos. A tiempos superiores a 125-130 minutos, el sistema está totalmente controlado por el tiempo de residencia, y así, la densidad de corriente y el caudal dejan de ser factores influyentes.

En segundo lugar, se llevó a cabo la optimización del proceso a los tiempos elegidos. Resulta que la densidad de corriente es una variable estadísticamente significativa, ejerciendo un efecto positivo en la eliminación de los parámetros de interés, DQO y COT. Sin embargo, la velocidad de recirculación a través del reactor se comporta como una variable no significativa para la DQO, y poco significativa para el COT. Esto significa que el aumento de la velocidad del flujo no favorece el transporte de los contaminantes hasta la superficie del ánodo, como cabría esperar por disminución del tiempo de residencia en el reactor.

Una vez finalizado este apartado, se puede concluir que el proceso de electro-oxidación es capaz de lograr altos niveles de eliminación de materia orgánica en aguas residuales altamente contaminadas y en tiempos de tratamiento relativamente cortos.

Una vez aplicados los procesos electroquímicos, en los capítulos posteriores se discutió el estudio referido al empleo de procesos químicos de oxidación (reactivo de Fenton + Fenton-like, Ozono y UV/H_2O_2) para la eliminación de carbamacepina en disolución acuosa.

En el **Capítulo 5** se llevaron a cabo experimentos con el fin de conseguir la degradación de carbamacepina aplicando el sistema integrado Fenton + Fenton-like. Se empleó nuevamente un diseño factorial para optimizar el proceso, así como para estudiar las interacciones existentes entre las variables de estudio. Las variables de operación elegidas, de las que depende la eficiencia del proceso, fueron cuatro: el pH y las concentraciones iniciales de H_2O_2, de iones Fe^{2+} y Fe^{3+}. El nivel de eliminación de carbamacepina alcanzado a las 48 horas fue la variable respuesta u objetivo. Los

resultados obtenidos revelaron que el factor más influyente es la concentración inicial de H_2O_2, seguido de la concentración de Fe^{2+}, pH y finalmente la concentración de Fe^{3+}. Se alcanzó la degradación completa del compuesto farmacéutico en las condiciones óptimas obtenidas: $[H_2O_2]_0$= 1,39·10^{-4} mol·L^{-1}, $[Fe^{2+}]_0$= 1,25·10^{-5} mol·L^{-1}, $[Fe^{3+}]_0$= 1,68·10^{-5} mol·L^{-1} y pH= 3,52.

En este proceso integrado, el proceso Fenton es la vía de oxidación principal en el rango empleado de concentraciones de hierro. Sin embargo, esta vía de reacción alcanza una máxima eficacia para una relación molar de $[H_2O_2]/[Fe^{2+}]$= 11,1:1.

Por otro lado, el sistema Fenton-like se encuentra limitado a bajas concentraciones de hierro. Sin embargo, esta vía de reacción aumenta de manera constante con la concentración de hierro hasta alcanzar más del 50% de la reacción de Fenton.

En el **Capítulo 6** se exponen y se discuten los resultados obtenidos en la degradación de carbamacepina mediante ozono. El objetivo de este trabajo fue optimizar el proceso de degradación del compuesto orgánico a través de nuevas consideraciones como los aspectos económicos de costes operativos del proceso. Para ello se define una nueva variable objetivo "*X*", que no sólo incluía términos de eficacia en la eliminación del contaminante, sino también aspectos cinéticos que tienen que ver con la velocidad del proceso de ozonación. Se llevó a cabo un diseño de experimentos para analizar la influencia del caudal de aire, de la concentración de ozono a la entrada, y de la concentración inicial de carbamacepina, con el fin de encontrar valores óptimos para el proceso de degradación.

Los resultados obtenidos ponen de manifiesto que las tres variables ejercen un efecto positivo sobre la variable respuesta. La concentración de ozono en la corriente de entrada presenta una influencia muy significativa, seguida de la concentración inicial de compuesto. Sin embargo, el caudal de aire muestra una baja influencia en el proceso. El valor óptimo, es decir, la máxima eliminación de compuesto con costes mínimos, se obtuvo con un caudal de aire de 55 L·h^{-1}, una concentración de ozono en la corriente de entrada de 0,4 g·m^{-3} y una concentración inicial de carbamacepina de 18 mg·L^{-1}.

Para finalizar, en el **Capítulo 7**, se procedió al estudio de la fotodegradación de la carbamacepina en presencia de peróxido de hidrógeno (sistema UV/H_2O_2). Se llevó a cabo la optimización del proceso y se estudió la interacción de las variables de interés mediante un diseño estadístico de experimentos. Igualmente, se estableció la influencia de variables operativas tales como la concentración inicial de H_2O_2, el pH y la temperatura.

Los resultados indicaron que la concentración inicial de H_2O_2 es la variable que mayor influencia ejerce en el proceso. Esto sugiere que la degradación se lleva a cabo a través de un mecanismo de reacción radicalaria inducida por los radicales hidroxilo formados a partir de la fotólisis del peróxido. En cuanto a la temperatura, también ejerce un efecto notable, lo cual puede atribuirse al hecho de que el H_2O_2 tiende a descomponerse en oxígeno y agua al aumentar la temperatura. En lo que se refiere al pH, apenas tiene influencia en el proceso de fotodegradación del contaminante desde el punto de vista estadístico. Este hecho parece estar relacionado con el alto pK_a de la carbamacepina, lo que implica que esta molécula no sufre ninguna disociación apreciable a la largo del intervalo de pH de estudio. Así, con este sistema (UV/H_2O_2), en las condiciones óptimas de operación establecidas ($[H_2O_2]_0$= $0{,}38 \cdot 10^{-3}$ $mol \cdot L^{-1}$, pH= 1 y T= 35,6 ºC) la eliminación total de carbamacepina se alcanzó a los 10 minutos de tratamiento.

Capítulo 1:
ADSORPTION OF PHARMACEUTICALS

1.1. REMOVAL OF CARBAMAZEPINE, NAPROXEN AND TRIMETHOPRIM FROM WATER BY *AMBERLITE XAD-7*: A KINETIC STUDY

The adsorption kinetics of carbamazepine, naproxen and trimethoprim in aqueous solution by *Amberlite*^{TM} *XAD-7* has been studied. The influence of adsorbent dose (1-3 $g \cdot L^{-1}$), stirring rate (80-240 rpm), pH (2-9), temperature (20-60 °C) and initial concentration (25-75 ppm) on the adsorption kinetics has been analyzed. The removal efficiency in the first two hours reaches 85% for carbamazepine, 60% for naproxen and 70% for trimethoprim. The pH appears to be the most important factor conditioning the removal of these latter solutes, whereas carbamazepine adsorption seems to be independent of the pH of the adsorptive solution. Initial concentration and operation temperature moderately influence the adsorption process. Finally, stirring rate scarcely affects the process. The experimental data have been fitted to four kinetic models, namely pseudo-first and pseudo-second order, intra-particle diffusion and *Bangham's*. The model providing the best fit is the pseudo-second order one. Again, pH is the factor that affects the adsorption rate in a more remarkable manner although other parameters such as temperature and stirring rate also contribute to accelerate the removal of the solutes. Under the optimal operation conditions, *Amberlite*^{TM} *XAD-7* exhibits a promising ability for the removal of the pharmaceuticals under study.

Keywords: drug removal, kinetic modeling, pharmaceutically active compound, water pollution.

1.1.1. INTRODUCTION.

In the last few decades the presence of pharmaceutically-active compounds in the environment has become a serious concern since these chemicals constitute an important health risk for a wide range of organisms including human beings [1]. Many of these compounds do not exhibit an acute toxicity but have a noticeable cumulative long-term effect [2]. Many chemicals, and particularly pharmaceuticals, may reach

surface waters or even ground and drinking water. Frequently, human beings or animal's excrete these chemicals as such or in the form of active metabolites through urine or faeces. This makes it possible that these molecules reach the sewage system or the influent of wastewater treatment plants [3].

Additionally, pharmaceuticals may also entry into fresh bodies due to the disposal of agrochemicals, industrial by-products, medical treatment, etc. It is also worth noting that veterinary-pharmaceuticals may reach surface and ground waters via manure [4]. Recently, the development of new analytical methods has made it possible to confirm the occurrence of a number of pharmaceuticals in the aquatic environment [5-8].

Several research works have demonstrated the presence of this kind of pharmaceuticals in wastewater treatment plant effluents, rivers, lakes and, occasionally, in groundwater [9]. The removal of these chemicals has received a great deal of attention in the last few years [7]. Several methods have been tested with this purpose. The most significant treatment procedures are coagulation and sedimentation [10], biodegradation [11,12], electrocoagulation [13], phototransformation [14-16], chlorination [17] and ozonation [8,18,19]. A bibliographic revision reveals that adsorption has also been used as an alternative for the removal of naproxen and ketoprofen from water [11,20-24]. In this connection, organic sorbents are usually preferred to inorganic-based sorbents like silica gel because of their selectivity and their stability over a wide range of pH [25]. In comparison with classical adsorbents such as silica gels, alumina and activated carbons, macroporous polymeric adsorbents and, particularly, *Amberlites*^{TM} appear as an attractive alternative because of their wide range of pore structures and physico-chemical characteristics [26].

In this work, the adsorption of three pharmaceuticals, namely carbamazepine, naproxen and trimethoprim, in aqueous solution by *Amberlite*^{TM} *XAD-7* has been studied under a kinetic point of view. All of them are widely found in all kinds of polluted waters such as surface-, ground- and drinking-water as well as in wastewater treatment plants influents and effluents. The influence of different operational

parameters such as adsorbent dose, stirring rate, pH, temperature and initial concentration on the adsorption kinetics has been analyzed. Additionally, a kinetic modeling of the process has been performed and the experimental results have been fitted to four models, namely pseudo-first order, pseudo-second order, intra-particle diffusion and *Bangham's* models. The equilibrium aspects of the process have been previously reported by our research team [27].

1.1.2. MATERIALS AND METHODS.

1.1.2.1. Adsorbent and pharmaceuticals.

Resin *Amberlite*^{TM} *XAD-7*, an acrylic ester polymer exhibiting an intermediate value of polarity and a moderately hydrophilic behavior, was selected as the adsorbent. Its main physicochemical properties [28] are summarized in Table 1.1 *Amberlite*^{TM} *XAD-7* possess well-developed surface area and porosity. It is worth noting that a good sorbent must have specific physical properties such as high surface area, pore and particle sizes adapted to the analyte and density higher than that of water. Chemical properties such as hydrophilicity or chemical stability (towards solvents, acidic and basic solutions) must also be taken into account. Polymers in general and *Amberlites*^{TM} in particular have many advantages compared to silica gel as they can be used in a larger range of pH and do not contain interferential silanol groups [29].

Carbamazepine is the common name of the 5H-dibenzo[b,f]azepine-5-carboxamide (chemical formula, $C_{15}H_{12}N_2O$; CAS number, 298-46-4; pK_a= 13.4). Since the 1970 carbamazepine has been used to treat epileptic seizures, severe nerve pain (trigeminal neuralgia) as well as bipolar disorder. Naproxen is the accepted name of 2-(6-methoxynaphthalen-2-yl) propanoic acid (chemical formula, $C_{14}H_{14}O_3$; CAS number, 22204-53-1; pK_a= 4.2). Naproxen is a non-steroidal anti-inflammatory drug (NSAID) commonly used for the reduction of moderate to severe pain, fever, inflammation and stiffness. Finally, trimethoprim is the common name of 5-(3,4,5-trimethoxybenzyl)pyrimidine-2,4-diamine (chemical formula, $C_{14}H_{18}N_4O_3$; CAS number, 738-70-5; pK_a= 7.3). Trimethoprim is an antibiotic that has been commonly

used in the treatment of urinary tract infections. It is used in combination with other drugs to treat certain types of pneumonia. In combination with other drugs it is also used to treat certain types of pneumonia and "travellers" diarrhea.

All chemicals were of analytical grade and were purchased from Panreac (Spain). All the experiments were performed using ultrapure Milli-Q™ water as the aqueous matrix.

Table 1.1. Main physicochemical properties of the polymeric adsorbent *Amberlite XAD-7*.

Physical/chemical properties	
BET surface area ($m^2 \cdot g^{-1}$)	450
Particle size (mesh)	20-40
Average pore volume ($cm^3 \cdot g^{-1}$)	1.14
Average pore diameter (Å)	90
Total porosity ($cm^3 \cdot cm^{-3}$)	0.55
Polarity	intermediate
Structure	acrylic ester
Dipole moment	1.8
Dry/wet density ($g \cdot cm^{-3}$)	1.24/1.05
Vapor pressure (at 20 ºC)	17 mm Hg
Autoignition temp.	427 ºC
(*) pH_{PZC}	6.2

* pH value in which the electrical charge density of surface-resin is zero. Determined in this work.

1.1.2.2. Analytical method.

A UV-Vis spectrophotometric method reported elsewhere [27,30,31] was used. Ultrapure Milli-Q™ water was used as the reference.

Solutions of solute concentration ranging from 5 up to 50 mg·L^{-1} were used to determine the calibration curve for the different analytes (namely, carbamazepine, naproxen and trimethoprim).

1.1.2.3. Kinetic experiments.

In order to study the adsorption kinetics, fixed amounts of adsorbent and volumes of adsorptive solution (400 mL) of a given initial concentration were kept in contact under shaking and at constant temperature for a given period of time previously set. With the aim of checking the evolution of the adsorption process with time, the concentration of solute was analyzed as described in the previous section. The equilibrium time, t_e, may be defined as the minimum period of time that is necessary to keep the value of concentration unvaried (i.e., to reach the equilibrium concentration or C_e) [32].

The adsorbed amount (mg·g^{-1}) at a given time, t, was determined using a well-known mass balance Equation (1.1):

$$q_t = \frac{(C_0 - C_t) \cdot V}{W} \tag{1.1}$$

where q_t is the mass (mg) of solute that is adsorbed onto one gram of the adsorbent once a time, t, is elapsed; C_0 represents the concentration of pharmaceutical (mg·L^{-1}) initially present in solution; C_t is the concentration of such pharmaceutical (mg·L^{-1}) at a time, t; V represents the volume of solution (L) placed in each adsorption cell; and W is the mass of resin (g) kept in contact with the solution.

The removal efficiency, $X\%$ was determined according to the following Equation (1.2):

$$X\% = \frac{C_0 - C_e}{C_0} \cdot 100 \tag{1.2}$$

with C_e being the concentration of pharmaceutical in the solution (mg·L^{-1}) once the equilibration time is elapsed. Operational parameters such as adsorbent dose (1-3gL^{-1}), stirring rate (80-240 rpm), pH (2-9), temperature (20-60 ºC) and initial concentration

(25-75 mg·L^{-1}) were varied in order to design diverse series of experiments. In order to guarantee that pH was kept constant a commercial sodium hydroxide/phosphoric acid buffer solution (Panreac, Barcelona, Spain) was used. In all cases, experiments were performed in duplicate.

1.1.3. RESULTS AND DISCUSSION.

In this paper, the adsorption of carbamazepine, naproxen and trimethoprim by *Amberlite*^{TM} *XAD-7* has been studied from the kinetic standpoint.

Firstly, the influence of the operational parameters on the removal efficiency has been analyzed. Next, the adsorption process has been investigated by applying different kinetic models to the experimental data.

1.1.3.1. Influence of the operational parameters on the removal efficiency.

Influence of adsorbent dose and stirring rate.

Figure 1.1 depicts the removal efficiencies of carbamazepine, naproxen and trimethoprim when adsorbent dose (a) and stirring rate (b) are varied. The first point to be remarked is the fact that the removal efficiency of the drugs under analysis follows the trend carbamazepine > trimethoprim > naproxene. As expected, an increase in the adsorbent amount gives rise to a noticeable increase in the removal efficiency of all of the pharmaceuticals. Since the adsorption of the drugs is facilitated by the availability of larger surface area and sorption sites, it is readily understood that the number of available sorption sites increases by increasing adsorbent amount [6]. Consequently, an adsorbent dose of 3 g·L^{-1} was chosen for the remaining experiments. The individual fittings corresponding to all the experiments performed using different adsorbent doses for the three pharmaceuticals under study are depicted in Fig. S.1.1, Supporting Information.

On the other hand, Fig. 1.1(b) suggests that, in general, the stirring rate does not affect the removal efficiency. Stirring plays a significant role in many adsorption processes. In fact, it affects both the distribution of the solute in the bulk solution and the formation of the boundary layer [33]. An increase in stirring rate is expected to

reduce the film boundary layer around the particles and, consequently, the external film transfer coefficient rises thus increasing the removal efficiency [34]. Only in the case of trimethoprim there is a slight growth in the removal efficiency when the stirring rate increases.

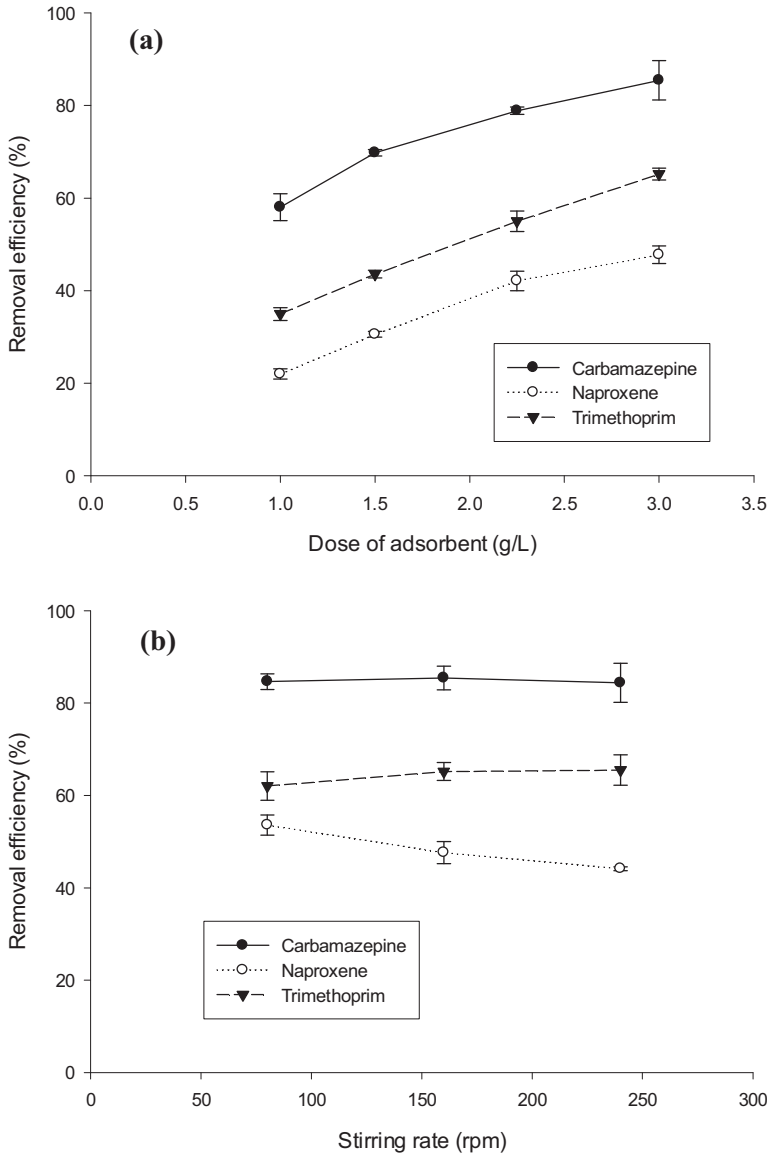

Fig. 1.1. Influence of adsorbent dose (a) and stirring rate (b) on the removal efficiency of carbamazepine, naproxen and trimethoprim. T= 20ºC. pH= 7. Initial concentration= 50 mg·L^{-1}.

For carbamazepine this parameter does not seem to exert any noticeable influence. This fact suggests that stirring at only 80 rpm is enough to minimize the bulk diffusion mass transfer coefficient. Hence, a further increase of the stirring rate does not cause any effect on the removal efficiency. Finally, for naproxen the removal efficiency appears to be disfavoured when the system is stirred in a faster manner, which is worth noting. Taking into account this later, an intermediate stirring rate equal to 160 rpm has been selected for all the remaining tests.

Figure S.1.2, Supporting Information, shows in detail all the fittings corresponding to the experiments performed at different stirring rates for each of the drugs.

Influence of pH.

Figure 1.2 illustrates the influence of pH (a) and temperature (b) on the removal efficiency of the three chemicals here studied. From the experimental data, shown in Fig. 1.2(a) as well as from those depicted in Fig. S.1.3, Supporting Information, it may be concluded that the pH of the adsorptive medium markedly conditions the removal efficiency of naproxen and trimethoprim in an opposite manner. Thus, as pH rises naproxen is less efficiently removed whereas larger amounts of trimethoprim are withdrawn from solutions at higher pH values. On the contrary, the removal efficiency of carbamazepine is scarcely affected by pH.

This parameter strongly conditions the adsorption process in general and the adsorption capacity in particular [33]. Changes in the pH affect the ionization degree and the solubility of the solute as well as the surface charge of the adsorbent [35]. This, in turn, influences the affinity of the solute towards an aliphatic resin such as *Amberlite*^{TM} *XAD-7*. Specific solute-sorbent interaction involving π-electrons on the sorbent surface may affect the adsorption of solutes onto polymeric resins [36,37]. Firstly, in the case of carbamazepine (a molecule with pK_a= 13.9), the compound remains neutral along the whole pH range here studied. Consequently, the main factor conditioning the binding of carbamazepine onto the *XAD-7* resin is the occurrence of non-electrostatic interactions. Probably, these interactions take place through hydrogen bonding between the oxygen groups of esters or by means of Van Der

Waals-forces [38]. Since the intensity of both kinds of interactions remains constant within the pH range here used, the removal of carbamazepine is scarcely affected by this parameter, as corroborated by the experimental data plotted in Fig. 1.2(a).

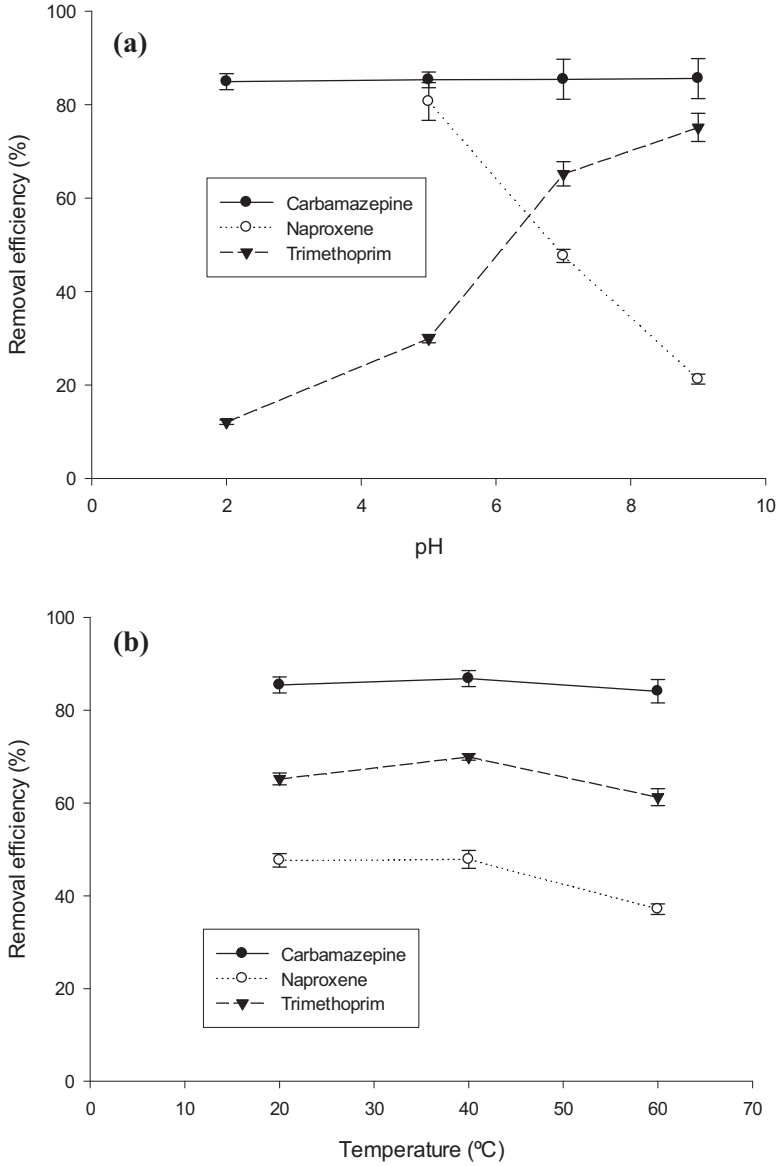

Fig. 1.2. Influence of pH (a) and temperature (b) on the removal efficiency of carbamazepine, naproxen and trimethoprim. Adsorbent dose= 3 $g \cdot L^{-1}$. Stirring rate= 160 rpm. Initial concentration= 50 $mg \cdot L^{-1}$.

On the contrary, the uptake of an acidic molecule such as naproxen on *XAD-7* is conditioned by electrostatic and/or by non-electrostatic interaction, depending on the pH of the adsorptive solution. Firstly, it must be kept in one's mind that naproxen is practically insoluble in water at low pH. Hence, data corresponding to pH 2 are not shown in Fig. 1.2(a). At pH < pK_a, naproxen is a neutral molecule. Under these circumstances, non-electrostatic interactions are responsible of the interaction between naproxen and the resin's surface. Hence, from the adsorption standpoint this chemical exhibits a behavior similar to that of carbamazepine. At pH > pK_a (e.g., pH 7 and 9), naproxen is negatively charged whereas the surface of resin (pH_{PZC}= 6.2) exhibits a progressively more negative charge. This leads to an electrostatic repulsion between the solute and the adsorbent. Consequently, adsorption of naproxen is handicapped and decreases markedly from 80% at pH 5 to approximately 20% at pH 9.

Finally, for trimethoprim (i.e., a basic drug), at pH < pK_a (e.g., at pH 5), the solute possess positive charge. At the same time, the surface of the resin gradually becomes more positively charged (remember that pH_{PZC}= 6.2). The latter leads to an electrostatic repulsion between them. Consequently, as can be seen in Fig. 1.2(a), at pH 5, trimethoprim molecules and XAD-7 surface groups are both positively charged, leading to a low value of removal efficiency. At pH 7 (i.e., pH ≈ pK_a) the protonation degree of trimethoprim is approximately equal to 50%. Hence, the adsorption of this drug is favoured. Finally, at pH 9 trimethoprim is a neutral molecule, which results in a more likely adsorption. Thus, the removal efficiency shows a remarkable increase, as corroborated from the experimental results.

Influence of temperature.

Usually, temperature noticeably influences the adsorption process due to its effect on two important factors such as the solubility of the drugs in water and the energy exchange that takes place during the process. In this case, however, temperature does not seem to affect the adsorption process in a noticeable manner. In all cases at higher temperatures the removal of drug decreases slightly. This suggests an exothermal nature of the adsorption. Nevertheless, this assertion should be

corroborated in the light of the adsorption equilibrium isotherms performed at different temperatures. The experimental data, shown in Fig. 1.2(b) and Fig. S.1.4, Supporting Information, reveal that an increase of temperature negatively influences the adsorption process. Thus, as temperature rises the removal efficiency tends to decrease. This fact suggests that, in general, as temperature rises, the interaction occurring between the solute and the active sites of the adsorbent becomes weaker, which is indicative of a physisorption process. Again, this should be corroborated by equilibrium experiments. Furthermore, as indicated above, an increase of temperature generally involves an increase of the solubility of the solute, thus favouring the solute–solvent interaction forces and consequently hindering its adsorption.

Influence of initial concentration.

Figures 1.3 and S.1.5, Supporting Information, illustrate the influence of the initial concentration of drug on the removal efficiency of carbamazepine, naproxen and trimethoprim.

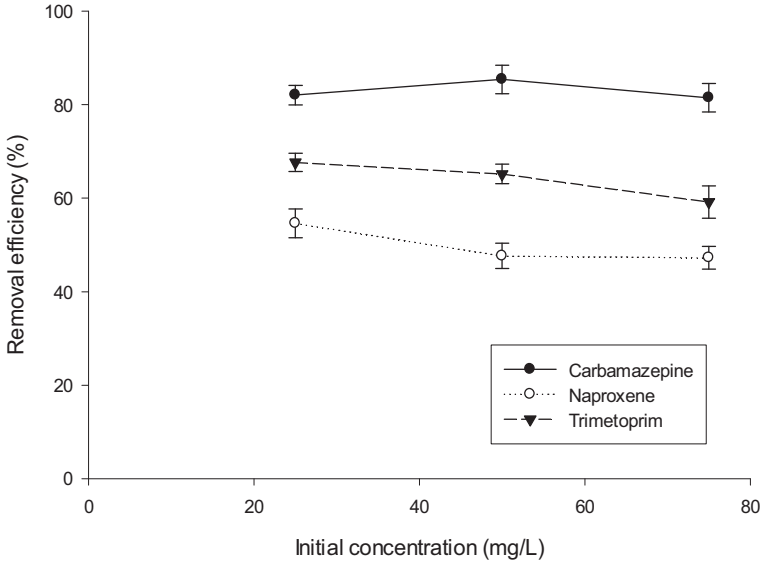

Fig. 1.3. Influence of initial concentration on the removal efficiency of carbamazepine, naproxen and trimethoprim. Adsorbent dose= 3 mg·L^{-1}. Temperature= 20 ºC. pH= 7. Stirring rate=160 rpm.

The initial concentration does not appear to exert a noticeable effect on the removal efficiency of the first two molecules. Only the removal of trimethoprim decreases to some extent as the initial concentration rises. This fact is somewhat surprising for this kind of molecules, since electrostatic interactions between the adsorbent surface and the chemicals should depend on the pollutant surface concentration [39]. Nevertheless, the results here obtained are similar to some previous observation reported in the literature (see [40] and references therein).

Maximum removable concentrations.

All the above exposed is numerically summarized in Table 1.2. In this table, the maximum concentrations in mg/L that are suitable to be removed by *Amberlite*^{TM} *XAD-7* under each of the experimental conditions here tested are shown.

Table 1.2. Maximum removable concentrations of carbamazepine, naproxen and trimethoprim adsorption under given operation conditions.

Adsorbent dose (g·L^{-1})	**Maximum removable concentration (mg·L^{-1})**		
	Carbamazepine	Naproxen	Trimethoprim
1	29.0	11.0	17.5
1.5	34.9	15.3	21.8
2.25	39.4	21.0	27.5
3	42.7	23.9	32.6
Stirring rate (rpm)	Carbamazepine	Naproxen	Trimethoprim
80	42.3	26.8	31.0
160	42.7	23.8	32.6
240	42.2	22.1	32.8
pH	Carbamazepine	Naproxen	Trimethoprim
2	42.5	-	6.0
5	42.7	40.3	15.0
7	42.7	23.8	32.6
9	42.8	10.6	37.6
Temperature (ºC)	Carbamazepine	Naproxen	Trimethoprim
20	42.7	23.8	32.6
40	43.4	23.9	35.0
60	42.0	18.5	30.6
Initial concentration (mg·L^{-1})	Carbamazepine	Naproxen	Trimethoprim
25	20.5	13.7	16.9
50	42.7	23.8	32.6
75	61.1	35.5	44.4

It is worth noting that according to the literature the concentration ranges of carbamazepine, naproxen and trimethoprim that have been reported in groundwater are comprised between 300–1100 ng·L^{-1} [41], 1300-5000 ng·L^{-1} [42] and 100-300 ng·L^{-1} [42], respectively. Hence, from the data shown in Table 1.2 it may be easily concluded that *Amberlite*^{TM} *XAD-7* is a promising adsorbent to be used in decontamination of waters potentially polluted by these compounds.

1.1.3.2. Kinetic modelling of the process.

Application of theoretical models.

In order to analyze in depth the adsorption process, the kinetic data here reported have been fitted to four commonly accepted kinetic models namely the pseudo-first order [43,44], pseudo-second order [45,46], intraparticle diffusion [47] and *Bangham* [48] models. Figure 1.4 depicts the fitting of the experimental data obtained under the selected conditions (i.e., adsorbent dose equal to 3 g·L^{-1}, 20 °C, pH 7, 160 rpm and initial concentration equal to 50 mg·L^{-1}) to the referred models.

The pseudo-first order equation, also known as *Lagergren* Equation, can be expressed as follows:

$$\frac{dq_t}{dt} = k_1(q_e - q_t) \tag{1.3}$$

where k_1 is the adsorption rate constant (s^{-1}), q_t denotes the mg of solute that is retained per mass unit of the adsorbent at a given time, t (mg·g^{-1}) and q_e is the value of q (mg·g^{-1}) reached once the equilibration time, t_e, is elapsed. Equation (1.3) may be integrated as:

$$\log(q_e - q_t) = \log q_e - \frac{k_1}{2.303}t \tag{1.4}$$

Consequently, if the kinetic data fit to the pseudo-first order model a plot of log $(q_e - q_t)$ versus t should give rise to a straight line. The slope and the intercept of this line can be easily used to determine the values of k_1 and q_e, respectively. Operating as described, the plots obtained by applying Eq. (1.4) to the experimental data are shown

in Fig. 1.4(a). The corresponding correlation coefficients (also included in Fig. 1.4(a)) reveal that the first-order kinetic model is able to fit reasonably well the kinetic data obtained for the three drugs under study ($R^2 > 0.97$ in all cases). On the other hand, Blanchard et al. [45] proposed in the 1980s the so called pseudo-second-order model. Approximately fifteen years later Ho and MacKay [46] published a modified equation that has been widely applied in the last years. The mathematical expression of this model is:

$$\frac{dq_t}{dt} = k_2\left(q_e - q_t\right) \tag{1.5}$$

where k_2 is the adsorption rate constant of pseudo-second order model ($g \cdot mg^{-1} \cdot min^{-1}$). The integrated form of Eq. (1.5) is:

$$\frac{1}{q_t} = \frac{1}{k_2 q_e^{\,2}} + \frac{1}{q_e} t \tag{1.6}$$

Analogously to the pseudo-first order model, from the slope and the intercept, respectively, of the *t/q* vs. *t* plots the values of q_e and k_2 can be calculated for the pseudo-second order kinetic model. Such *t/q* vs. *t* plots have been included in Fig. 1.4(b). The values of the correlation coefficients are also shown in this figure. It may be observed that this model provides an excellent fitting of the experimental data, all values of $R^2 > 0.995$. Therefore, it can be assumed that the pseudo-second order model describes the adsorption of the three drugs here studied in a more accurate manner.

In order to analyze if intra-particle diffusion is the main factor governing the adsorption kinetics of carbamazepine, naproxen and trimethoprim onto *Amberlite*^{TM} *XAD-7*, the model proposed by Weber and Morris [47] has been applied to the experimental data. It is well-known that a number of different factors may exert a noticeable influence on the adsorption kinetics. Among these factors, perhaps the most limiting one is diffusion [33]. The influence of intra-particle diffusion may be assessed by using the following relationship:

$$q_t = k_{id} t_e^{1/2} + C \tag{1.7}$$

where k_{id} is the intraparticle diffusion rate constant ($mg \cdot g^{-1} \cdot min^{-1/2}$) and C ($mg \cdot g^{-1}$) is a parameter related to the thickness of the boundary layer. In general, noticeable boundary layer effects are expectable if the value of C is high. In other words, if the q_t vs. $t^{1/2}$ plot provides a straight line passing through the origin (i.e., with a value of C≈0), then it may be assumed that the adsorption process is mostly controlled by intraparticle diffusion. On the contrary, if the q_t vs. $t^{1/2}$ plot exhibits more than one single linear plot, then it may be concluded that the adsorption process consists of two or more individual steps. This latter appears to be the case for the drugs under study in this work, as suggested by the shape of the plots shown in Fig. 1.4(c) as well as by the values of R^2.

Finally, the *Bangham's* equation makes it possible to analyze if the adsorption rate is only controlled by the pore diffusion step:

$$\log\log\left(\frac{C_0}{C_0 - qm}\right) = \log\left(\frac{k_b m}{2.303V}\right) + a\log t \tag{1.8}$$

where k_b represents the *Bangham's* rate constant.

If the *Bangham's* model is able to fit the experimental data in an adequate manner, it can be concluded that diffusion inside the pores of the adsorbent is the main factor that conditions the adsorption kinetics. Figure 1.4(d) suggests that this model is able to fit reasonably well the kinetic data of adsorption of the three drugs, particularly at the initial steps of the process. This means that pore diffusion exerts a noticeable influence on the adsorption process of carbamazepine, naproxen and trimethoprim by *XAD-7*.

Although, for the sake of brevity, in this section only the experiments performed under the optimal conditions have been reported, all the kinetic experiments (i.e., 13 experiments for each of the three drugs here studied) have been fitted to the four kinetic models, which yield a total of 156 fits. The fitting parameters corresponding to all of the experiments, as well as all of their respective q vs. t plots, are provided as "supplementary material". For further details, please see Tables S.1.1, S.1.2, S.1.3 and S.1.4, Supporting Information. Nevertheless, only the model providing the best fitting

(i.e., the pseudo-second order model) has been chosen to analyze the influence of the operation conditions on the adsorption kinetics of carbamazepine, naproxen and trimethoprim. This topic is discussed in the next section.

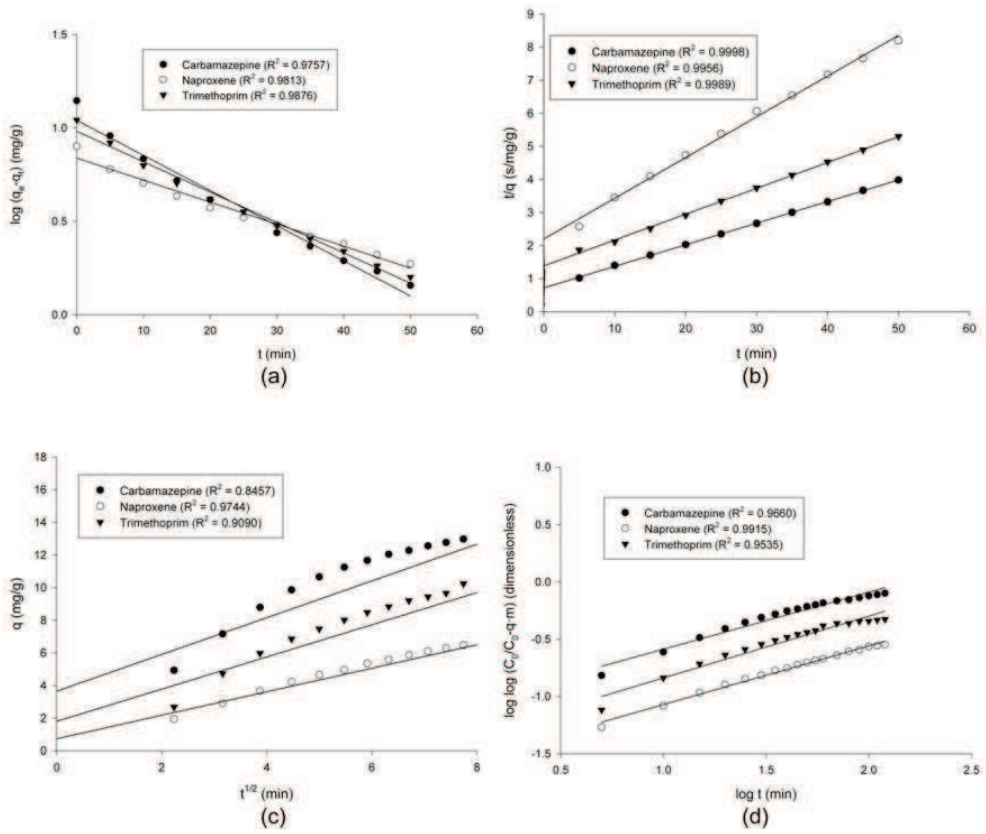

Fig. 1.4. Application of the pseudo-first order (a), pseudo-second order (b), intra-particle diffusion (c) and *Bangham's* (d) models to the adsorption kinetics of carbamazepine, naproxen and trimethoprim. Adsorbent dose= 3 g·L^{-1}. Temperature= 20 ºC. pH= 7. Stirring rate= 160 rpm. Initial concentration= 50 mg·L^{-1}.

1.1.3.3. Influence of the operational parameters on the adsorption rate.

The fitting parameters of the adsorption data to the pseudo-second order model are summarized in Table 1.2. These results corroborate that, as indicated in the previous section, this model fits the experimental data in an accurate manner the value of the correlation coefficient being in general above 0.99.

Influence of the adsorbent dose and stirring rate.

As a rule, an increase in the adsorbent dose from 1 to 3 $g \cdot L^{-1}$results in a remarkable acceleration of the adsorption process, as suggested by the growth of the values of the rate constant. The values of k_2 are 4.61, 1.97 and 1.46 times larger for carbamazepine, naproxen and trimethoprim, respectively. This fact confirms that the optimal adsorbent dose is 3 $g \cdot L^{-1}$, not only due to the increase in the removal efficiency (see Figure 1.1(a)) but also from the kinetic standpoint.

With respect to the influence of the stirring rate on the kinetics of the adsorption process, it may be observed that an increase in this parameter from 80 up to 240 rpm results in values of k_2 1.35, 2.63 and 1.92 times larger for carbamazepine, naproxen and trimethoprim, respectively. It is worth noting that the maximum increment in k_2 is observed for naproxen. A remarkable growth is found in the case of trimethoprim whereas the influence of stirring in the adsorption kinetics of carbamazepine is positive although rather limited. This is in good agreement with the plots shown in Figure 1.4(c). In fact, it may be observed that the experimental data corresponding to the adsorption of trimethoprim and, particularly, naproxen fit acceptably well to the intra-particle diffusion model, which suggests a noticeable influence of diffusion on the adsorption kinetics. Obviously, intra-particle diffusion is strongly conditioned by stirring and, hence, an increase in the stirring rate results in an acceleration of the adsorption process. On the contrary, the intra-particle diffusion model is not useful for modeling the adsorption kinetics of carbamazepine and the increase in k_2 is very discrete in this case. Furthermore, it may be observed that, in general, an increase of the stirring rate from 160 up to 240 rpm leads to very small differences in the rate constant corresponding to the adsorption of carbamazepine and trimethoprim. Thus, for comparative purpose, 160 rpm was selected as the optimal stirring rate for all the remaining experiments.

Influence of pH.

As indicated when discussing the influence of this parameter on the removal efficiency, pH is the most important factor conditioning the adsorption process. In

connection with the adsorption rate, pH does not exert any noticeable effect on the values of k_2 corresponding to carbamazepine.

On the contrary, an increase of pH from 5 up to 9 accelerates the removal process of naproxen by almost three times, whereas the same increment in pH makes the adsorption process of trimethoprim more than three times slower and almost six times if the value of k_2 calculated at pH= 2 is taken into consideration, which is worth noting. This, in turn, may be related with the removal efficiency of the different drugs. Thus, in the case of carbamazepine both the removal efficiency and the adsorption rate are very similar regardless what the pH is. On the contrary, naproxen is removed in a fast manner but only to a very limited extent. This latter gives rise to the availability of a large number of unoccupied active sites in the adsorbent's surface with a high tendency to adsorb solute molecules in a fast manner. Finally, large amounts of trimethoprim are removed from solution, which results in a slower adsorption rate probably due to the fact that most of the active sites on the adsorbent's surface are now occupied and the subsequent molecules of solute must be retained in less active sites probably forming a second -or successive molecular layer. This results in a lower value of the adsorption rate, k_2.

Given that, as exposed above, this parameter influences the adsorption rate and the removal efficiency too, in an opposite manner for the three drugs under study, a value of pH corresponding to the neutrality was chosen for the remaining experiments.

Influence of temperature.

From the results summarized in Table 1.3 it may be concluded that an increase in temperature tends to accelerate the adsorption process to a large extent (2.13, 2.95 and 2.79 times for carbamazepine, naproxen and trimethoprim, respectively). This may be attributable to the fact that higher temperatures favor the formation of the activated intermediate complex through which adsorption takes place. Additionally, the mass transfer rate of the solute is also strongly influenced by temperature [49].

Table 1.3. Fitting parameters of the experimental data of carbamazepine, naproxen and trimethoprim adsorption to the pseudo-second order equation. Influence of operation conditions.

Adsorbent dose ($g \cdot L^{-1}$)		**Carbamazepine**	**Naproxen**	**Trimethoprim**
1	q_e	31.95	13.03	18.13
	k_2	0.0013	0.0035	0.0030
	R^2	0.9989	0.9898	0.9954
1.5	q_e	25.43	11.36	15.66
	k_2	0.0020	0.0036	0.0037
	R^2	0.9982	0.9976	0.9968
2.25	q_e	19.64	10.75	12.66
	k_2	0.0031	0.0036	0.0042
	R^2	0.9999	0.9980	0.9955
3	q_e	15.31	8.12	12.80
	k_2	0.0060	0.0069	0.0044
	R^2	0.9998	0.9956	0.9989
Stirring rate (rpm)		**Carbamazepine**	**Naproxen**	**Trimethoprim**
80	q_e	15.62	9.81	13.47
	k_2	0.0046	0.0036	0.0025
	R^2	0.9999	0.9987	0.9842
160	q_e	15.31	8.12	12.80
	k_2	0.0060	0.0069	0.0044
	R^2	0.9998	0.9956	0.9989
240	q_e	14.78	7.70	11.44
	k_2	0.0062	0.0095	0.0048
	R^2	0.9998	0.9964	0.9980
pH		**Carbamazepine**	**Naproxen**	**Trimethoprim**
2	q_e	16.04	-	2.60
	k_2	0.0052	-	0.0327
	R^2	0.9997	-	0.9982
5	q_e	16.04	15.47	5.27
	k_2	0.0053	0.0048	0.0173
	R^2	0.9996	0.9992	0.9916
7	q_e	15.31	8.12	12.80
	k_2	0.0060	0.0069	0.0044
	R^2	0.9998	0.9956	0.9989
9	q_e	16.46	4.86	13.44
	k_2	0.0044	0.0127	0.0052
	R^2	0.9946	0.9965	0.9977
Temperature (ºC)		**Carbamazepine**	**Naproxen**	**Trimethoprim**
20	q_e	15.31	8.12	12.80
	k_2	0.0060	0.0069	0.0044
	R^2	0.9998	0.9956	0.9989
40	q_e	15.20	8.18	11.88
	k_2	0.0086	0.0095	0.0100
	R^2	0.9997	0.9976	0.9988
60	q_e	14.27	6.06	11.18
	k_2	0.0128	0.0204	0.0123
	R^2	1.0000	0.9994	0.9996
C_o (mg/L)		**Carbamazepine**	**Naproxen**	**Trimethoprim**
25	q_e	7.47	5.06	5.77
	k_2	0.0140	0.0113	0.0154
	R^2	0.9995	0.9979	0.9992
50	q_e	15.31	8.12	12.80
	k_2	0.0060	0.0069	0.0044
	R^2	0.9998	0.9956	0.9989
75	q_e	21.06	11.96	15.88
	k_2	0.0032	0.0050	0.0045
	R^2	0.9987	0.9991	0.9981

Thus, an increase in temperature results in a faster removal of the solute. This behavior has been previously reported by members of our research team [50-52] when describing the adsorption kinetics of organic and inorganic compounds in solution.

Influence of initial concentration.

The values of k_2 summarized in Table 1.3 suggest that, in all cases, as the initial concentration increases the adsorption process decelerates progressively. This finding is somewhat surprising since an increase in the value of the adsorption rate constant with increasing initial concentration would be expectable for a second order kinetics. However, in the pseudo-second order kinetic model and due to the assumptions made by Ho and MacKay [46] this is not necessarily so. In fact, a decrease in the adsorption rate with increasing initial concentration is repeatedly reported by these authors in a series of manuscripts published between 1998 and 2003 [53-59]. Nevertheless, the authors themselves do not provide a clear explanation to this empirical finding from a kinetic standpoint.

1.1.4. CONCLUSIONS.

The adsorption kinetics of three pharmaceuticals (namely, carbamazepine, naproxen and trimethoprim) in aqueous solution has been investigated. The influence of different parameters such as adsorbent dose, stirring rate, pH, temperature and initial concentration on the process has been analyzed. Four well-known theoretical models (i.e., the pseudo-first and pseudo-second order, the intra-particle diffusion and the *Bangham's* models) have been used in order to fit the experimental data. In general, the pseudo-second order model provides the best fit for the kinetic data. The experimental results reported in this work make it possible to draw the following conclusions.

- An increase in the adsorbent dose gives rise to a noticeable increase in the removal efficiency of all of the pharmaceuticals. However, this parameter affects the adsorption rate to a very limited extent.

- In general, the stirring rate does not affect the removal efficiency. On the contrary, an increase in the stirring rate results in a faster adsorption of trimethoprim and, particularly, naproxen, which is indicative of a noticeable influence of intra-particle diffusion in the adsorption kinetics of these pharmaceuticals. This assertion is corroborated by the good correlation obtained by applying the diffusive model to the experimental data.
- The pH of the adsorptive medium markedly conditions the removal efficiency and adsorption rate of naproxen and trimethoprim in an opposite manner. Thus, an increase in pH leads to noticeable decrease in the removal efficiency of naproxen, although the process is remarkably accelerated at high values of pH. On the contrary, at high pH trimethoprim is removed to a large extent but the process becomes noticeably slower as pH rises. The removal efficiency and adsorption rate of carbamazepine, on the contrary, are scarcely affected by changes in the pH of the adsorptive solution.
- Temperature does not seem to affect the removal efficiency of any of the pharmaceuticals under study in a noticeable manner. On the contrary, as temperature grows the adsorption process becomes faster, probably due to a positive influence of this parameter on the formation of the activated complex through which adsorption takes place.
- The initial concentration does not appear to exert a noticeable effect on the removal efficiency of the carbamazepine and naproxen. Only the removal of trimethoprim decreases to some extent as the initial concentration rises. Nevertheless, the values of the adsorption rate constants calculated by applying the pseudo-second order model to the experimental data decrease steadily in all cases as the initial concentration.

1.1.5. NOMENCLATURE.

For clearness, a list of all symbols used in this manuscript is presented below.

C Parameter of the intra-particle diffusion model related to the thickness of the boundary layer, $mg \cdot g^{-1}$.

C_e Concentration of solute in the solution once the equilibration time is elapsed, $mg \cdot L^{-1}$.

C_t Concentration of solute in the solution after a given time, $mg \cdot L^{-1}$.

C_0 Initial concentration of solute in the solution, $mg \cdot L^{-1}$.

k_{id} Intraparticle diffusion rate constant, $mg \cdot g^{-1} \cdot min^{-1/2}$.

k_1 Pseudo-first order adsorption rate constant, s^{-1}.

k_2 Pseudo-second order adsorption rate constant of model, $g \cdot mg^{-1} \cdot min^{-1}$.

q_e Amount of solute adsorbed at saturation, $mg \cdot g^{-1}$.

q_t Amount of solute retained per mass unit of the adsorbent at a given time, $mg \cdot g^{-1}$.

t Time, min.

t_e Equilibrium time, min.

V Volume of solution, L.

W Mass of adsorbent, g.

X Removal efficiency, %.

1.1.6. SUPPORTING INFORMATION.

Table S.1.1. Fitting parameters to the pseudo-first order model.

Adsorbent dose ($g \cdot L^{-1}$)		Carbamazepine	Naproxen	Trimethoprim
1	q_e	26.23	9.67	15.36
	k_1	0.0263	0.0313	0.0273
	R^2	0.9879	0.9659	0.9811
1.5	q_e	20.33	9.29	12.61
	k_1	0.0311	0.0272	0.0315
	R^2	0.9885	0.9914	0.9853
2.25	q_e	14.85	8.58	9.78
	k_1	0.0377	0.0275	0.0312
	R^2	0.9873	0.9906	0.9267
3	q_e	11.00	6.90	9.60
	k_1	0.0434	0.0272	0.0375
	R^2	0.9757	0.9813	0.9876
Stirring rate (rpm)		**Carbamazepine**	**Naproxen**	**Trimethoprim**
80	q_e	11.61	7.94	9.68
	k_1	0.0405	0.0285	0.0313
	R^2	0.9841	0.9886	0.9881
160	q_e	11.00	6.90	9.60
	k_1	0.0434	0.0272	0.0375
	R^2	0.9757	0.9813	0.9876
240	q_e	10.77	6.19	8.96
	k_1	0.0391	0.0315	0.0332
	R^2	0.9667	0.9781	0.9728
pH		**Carbamazepine**	**Naproxen**	**Trimethoprim**
2	q_e	11.60	-	1.86
	k_1	0.0433	-	0.0751
	R^2	0.9785	-	0.9885
5	q_e	11.56	11.41	3.99
	K_1	0.0418	0.0486	0.0381
	R^2	0.9725	0.9896	0.9778
7	q_e	11.00	6.90	9.60
	k_1	0.0434	0.0272	0.0375
	R^2	0.9757	0.9813	0.9876
9	q_e	11.74	4.54	10.42
	k_1	0.0439	0.0925	0.0342
	R^2	0.9781	0.9004	0.9757
Temperature (ºC)		**Carbamazepine**	**Naproxen**	**Trimethoprim**
20	q_e	11.00	6.90	9.60
	k_1	0.0434	0.0272	0.0375
	R^2	0.9757	0.9813	0.9876
40	q_e	10.11	6.37	8.52
	k_1	0.0484	0.0343	0.0368
	R^2	0.9638	0.9768	0.9512
60	q_e	8.55	4.24	7.47
	k_1	0.0508	0.0382	0.0538
	R^2	0.9428	0.9426	0.9779
Initial concentration ($mg \cdot L^{-1}$)		**Carbamazepine**	**Naproxen**	**Trimethoprim**
25	q_e	5.21	3.97	4.32
	k_1	0.0441	0.0338	0.0356
	R^2	0.9652	0.9883	0.9580
50	q_e	11.00	6.90	9.60
	k_1	0.0434	0.0272	0.0375
	R^2	0.9757	0.9813	0.9876
75	q_e	15.47	9.78	12.23
	k_1	0.0396	0.0293	0.0364
	R^2	0.9773	0.9759	0.9840

Table S.1.2. Fitting parameters to the pseudo-second order model.

Adsorbent dose ($g \cdot L^{-1}$)		Carbamazepine	Naproxen	Trimethoprim
1	q_e	31.95	13.03	18.13
	k_2	0.0013	0.0035	0.0030
	R^2	0.9989	0.9898	0.9954
1.5	q_e	25.43	11.36	15.66
	k_2	0.0020	0.0036	0.0037
	R^2	0.9982	0.9976	0.9968
2.25	q_e	19.64	10.75	12.66
	k_2	0.0031	0.0036	0.0042
	R^2	0.9999	0.9980	0.9955
3	q_e	15.31	8.12	12.80
	k_2	0.0060	0.0069	0.0044
	R^2	0.9998	0.9956	0.9989
Stirring rate (rpm)		**Carbamazepine**	**Naproxen**	**Trimethoprim**
80	q_e	15.62	9.81	13.47
	k_2	0.0046	0.0036	0.0025
	R^2	0.9999	0.9987	0.9842
160	q_e	15.31	8.12	12.80
	k_2	0.0060	0.0069	0.0044
	R^2	0.9998	0.9956	0.9989
240	q_e	14.78	7.70	11.44
	k_2	0.0062	0.0095	0.0048
	R^2	0.9998	0.9964	0.9980
pH		**Carbamazepine**	**Naproxen**	**Trimethoprim**
2	q_e	16.04	-	2.60
	k_2	0.0052	-	0.0327
	R^2	0.9997	-	0.9982
5	q_e	16.04	15.47	5.27
	k_2	0.0053	0.0048	0.0173
	R^2	0.9996	0.9992	0.9916
7	q_e	15.31	8.12	12.80
	k_2	0.0060	0.0069	0.0044
	R^2	0.9998	0.9956	0.9989
9	q_e	16.46	4.86	13.44
	k_2	0.0044	0.0127	0.0052
	R^2	0.9946	0.9965	0.9977
Temperature (ºC)		**Carbamazepine**	**Naproxen**	**Trimethoprim**
20	q_e	15.31	8.12	12.80
	k_2	0.0060	0.0069	0.0044
	R^2	0.9998	0.9956	0.9989
40	q_e	15.20	8.18	11.88
	k_2	0.0086	0.0095	0.0100
	R^2	0.9997	0.9976	0.9988
60	q_e	14.27	6.06	11.18
	k_2	0.0128	0.0204	0.0123
	R^2	1.0000	0.9994	0.9996
Initial concentration ($mg \cdot L^{-1}$)		**Carbamazepine**	**Naproxen**	**Trimethoprim**
25	q_e	7.47	5.06	5.77
	k_2	0.0140	0.0113	0.0154
	R^2	0.9995	0.9979	0.9992
50	q_e	15.31	8.12	12.80
	k_2	0.0060	0.0069	0.0044
	R^2	0.9998	0.9956	0.9989
75	q_e	21.06	11.96	15.88
	k_2	0.0032	0.0050	0.0045
	R^2	0.9987	0.9991	0.9981

Table S.1.3. Fitting parameters to the intra-particle diffusion model.

Adsorbent dose (g·L^{-1})		**Carbamazepine**	**Naproxen**	**Trimethoprim**
1	C	1.4587	3.9026	1.6824
	k_{id}	2.7088	0.4225	1.5764
	R^2	0.9796	0.1054	0.9729
1.5	C	2.6113	0.5518	1.9556
	k_{id}	2.0833	0.9605	1.2941
	R^2	0.9534	0.9779	0.9417
2.25	C	2.9923	0.5369	2.1960
	k_{id}	1.5100	0.8709	1.0556
	R^2	0.9094	0.9737	0.9171
3	C	3.6514	0.7360	1.8050
	k_{id}	1.1259	0.7200	0.9858
	R^2	0.8457	0.9744	0.9090
Stirring rate (rpm)		**Carbamazepine**	**Naproxen**	**Trimethoprim**
80	C	2.9810	0.6999	0.8606
	k_{id}	1.1783	0.8134	0.9716
	R^2	0.8821	0.9693	0.9482
160	C	3.6514	0.7360	1.8050
	k_{id}	1.1259	0.7200	0.9858
	R^2	0.8457	0.9744	0.9090
240	C	3.3210	1.1357	2.0424
	k_{id}	1.1426	0.6276	0.9364
	R^2	0.8747	0.9361	0.9231
pH		**Carbamazepine**	**Naproxen**	**Trimethoprim**
2	C	3.5688	-	0.6696
	k_{id}	1.1807	-	0.1739
	R^2	0.8533	-	0.7501
5	C	3.5708	3.2259	1.1776
	k_{id}	1.1925	1.1195	0.4091
	R^2	0.8548	0.8495	0.8940
7	C	3.6514	0.7360	1.8050
	k_{id}	1.1259	0.7200	0.9858
	R^2	0.8457	0.9744	0.9090
9	C	3.3620	1.0213	2.26
	k_{id}	1.1893	0.3117	1.0622
	R^2	0.8486	0.7644	0.9163
Temperature (ºC)		**Carbamazepine**	**Naproxen**	**Trimethoprim**
20	C	3.6514	0.7360	1.8050
	k_{id}	1.1259	0.7200	0.9858
	R^2	0.8457	0.9744	0.9090
40	C	4.7233	1.4827	3.2189
	k_{id}	1.0652	0.6628	0.9114
	R^2	0.7853	0.9194	0.8587
60	C	5.3600	1.6712	3.6066
	k_{id}	0.9447	0.4665	0.7784
	R^2	0.7173	0.8516	0.7749
Initial concentration (mg·L^{-1})		**Carbamazepine**	**Naproxen**	**Trimethoprim**
25	C	1.9733	0.6308	1.2168
	k_{id}	0.5460	0.4115	0.4483
	R^2	0.8252	0.9396	0.8789
50	C	3.6514	0.7360	1.8050
	k_{id}	1.1259	0.7200	0.9858
	R^2	0.8457	0.9744	0.9090
75	C	3.7764	1.4236	2.7975
	k_{id}	1.5869	1.0115	1.2520
	R^2	0.8829	0.9545	0.9103

Table S.1.4. Fitting parameters to the *Bangham's* model.

Adsorbent dose ($g \cdot L^{-1}$)		Carbamazepine	Naproxen	Trimethoprim
1	a	0.6116	0.5197	0.4799
	k_b	0.0202	0.0103	0.0187
	R^2	0.9875	0.9481	0.9873
1.5	a	0.5762	0.5396	0.4729
	k_b	0.0218	0.0082	0.0177
	R^2	0.9865	0.9809	0.9737
2.25	a	0.5648	0.5697	0.4617
	k_b	0.0202	0.0070	0.0175
	R^2	0.9728	0.9752	0.9547
3	a	0.4976	0.5115	0.5386
	k_b	0.0252	0.0080	0.0129
	R^2	0.9660	0.9915	0.9535
Stirring rate (rpm)		**Carbamazepine**	**Naproxen**	**Trimethoprim**
80	a	0.5542	0.5634	0.6320
	k_b	0.0576	0.0075	0.0220
	R^2	0.9732	0.9817	0.9548
160	a	0.4976	0.5115	0.5386
	k_b	0.0505	0.0080	0.0258
	R^2	0.9660	0.9915	0.9535
240	a	0.5135	0.4421	0.4734
	k_b	0.0305	0.0100	0.0218
	R^2	0.9791	0.9731	0.9817
pH		**Carbamazepine**	**Naproxen**	**Trimethoprim**
2	a	0.5374	-	0.2971
	k_b	0.0230	-	0.0052
	R^2	0.9691	-	0.8162
5	a	0.5479	0.5196	0.3300
	k_b	0.0224	0.0212	0.0107
	R^2	0.9685	0.9466	0.9749
7	a	0.4976	0.5115	0.5386
	k_b	0.0252	0.0080	0.0129
	R^2	0.9660	0.9915	0.9535
9	a	0.5656	0.3510	0.5206
	k_b	0.0200	0.0075	0.0165
	R^2	0.9428	0.8350	0.9776
Temperature (ºC)		**Carbamazepine**	**Naproxen**	**Trimethoprim**
20	a	0.4976	0.5115	0.5386
	k_b	0.0252	0.0080	0.0129
	R^2	0.9660	0.9915	0.9535
40	a	0.4277	0.4145	0.3877
	k_b	0.0372	0.0127	0.0272
	R^2	0.9598	0.9753	0.9806
60	a	0.3370	0.3069	0.3187
	k_b	0.0504	0.0149	0.0324
	R^2	0.9327	0.9543	0.9286
Initial concentration ($mg \cdot L^{-1}$)		**Carbamazepine**	**Naproxen**	**Trimethoprim**
25	a	0.4705	0.5053	0.4319
	k_b	0.0283	0.0107	0.0196
	R^2	0.9551	0.9747	0.9380
50	a	0.4976	0.5115	0.5386
	k_b	0.0252	0.0080	0.0129
	R^2	0.9660	0.9915	0.9535
75	a	0.5223	0.4830	0.4533
	k_b	0.0171	0.0088	0.0150
	R^2	0.9517	0.9784	0.9707

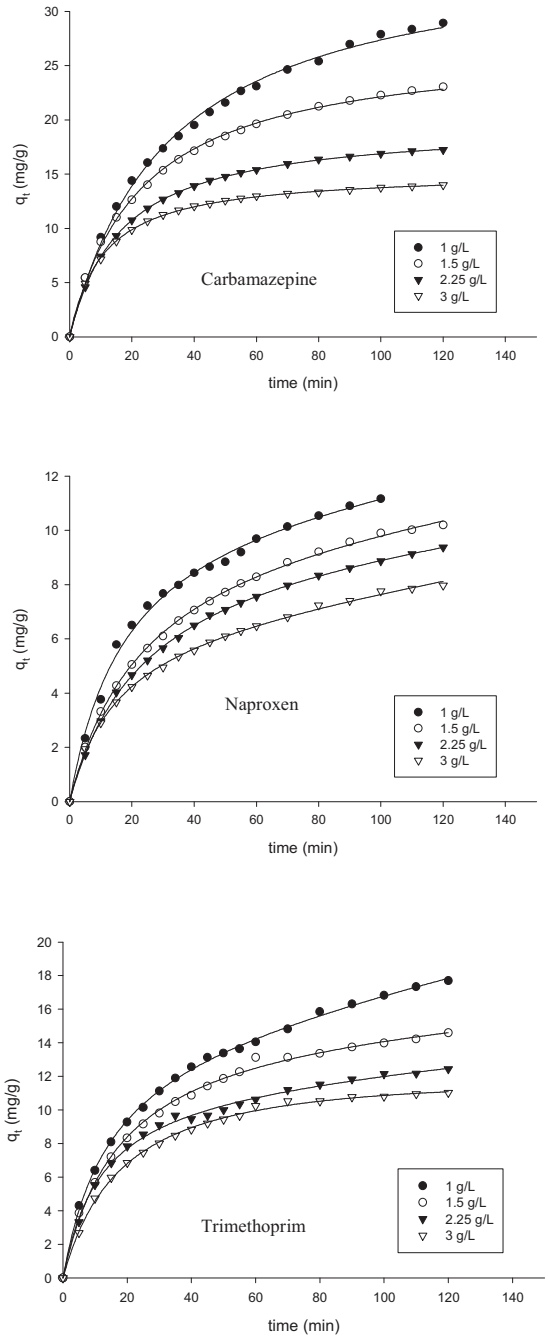

Fig. S.1.1. Influence of the adsorbent dose on the adsorption kinetics of carbamazepine, naproxen and trimethoprim. Stirring rate= 160 rpm. T= 20ºC. pH= 7. Initial concentration= 50 mg·L^{-1}.

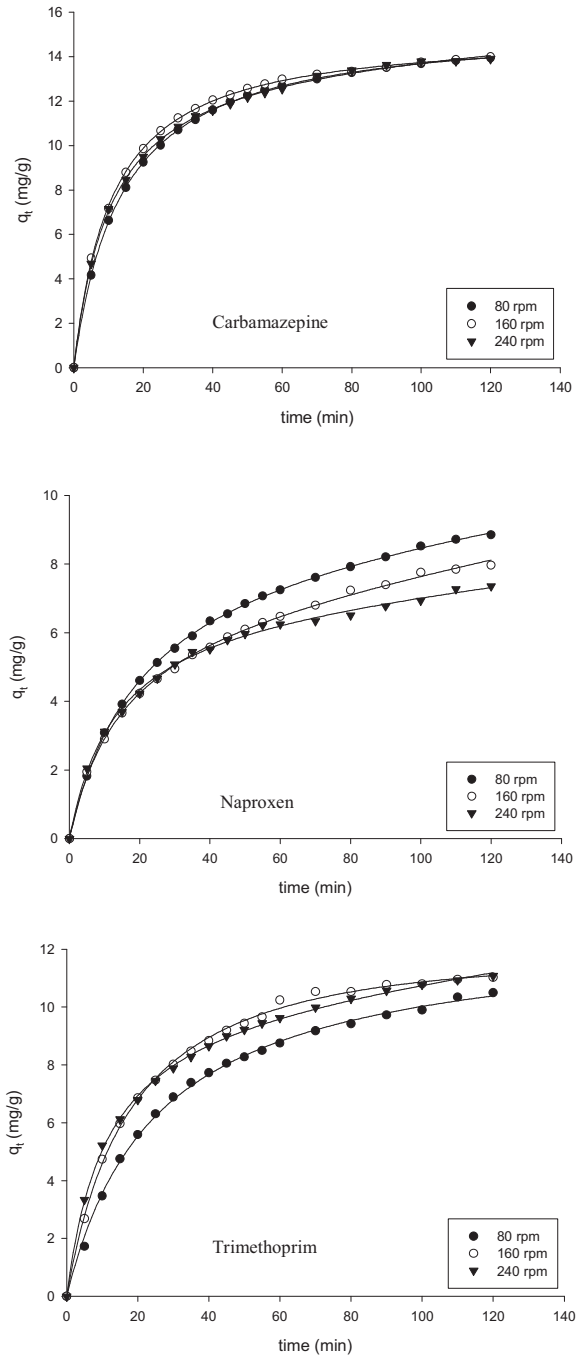

Fig. S.1.2. Influence of the stirring rate on the adsorption kinetics of carbamazepine, naproxen and trimethoprim. Adsorbent dose= 3 g·L^{-1}. T= 20ºC. pH= 7. Initial concentration= 50 mg·L^{-1}.

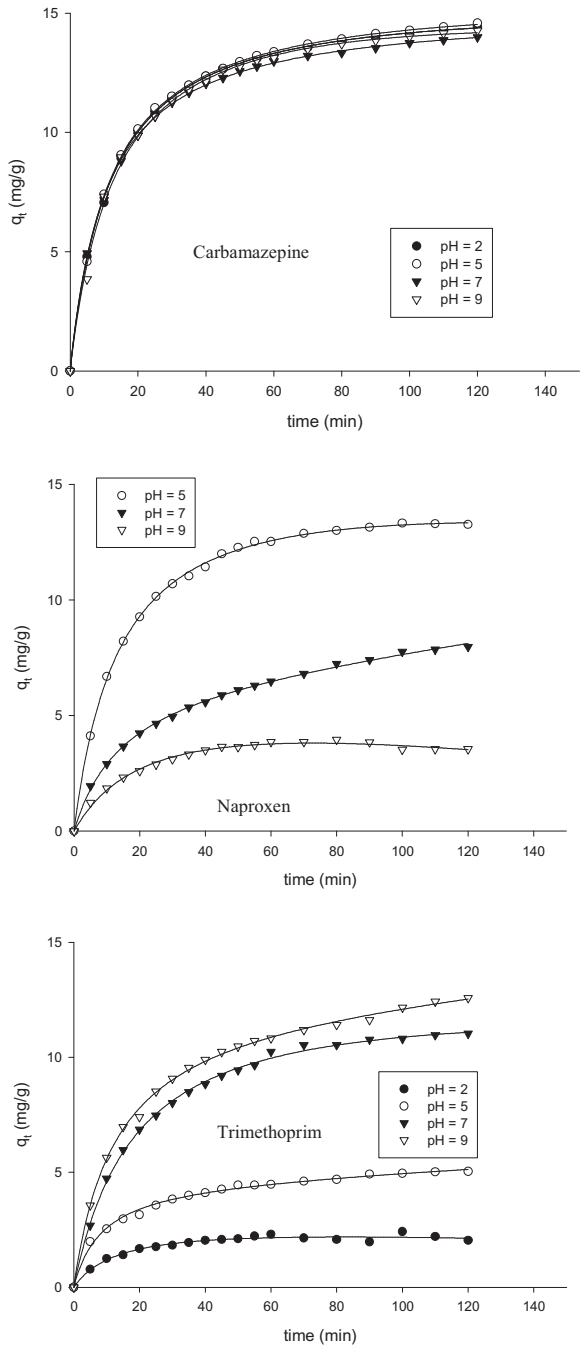

Fig. S.1.3. Influence of the pH on the adsorption kinetics of carbamazepine, naproxen and trimethoprim. Adsorbent dose= 3 g·L^{-1}. Stirring rate= 160 rpm. T= 20ºC. Initial concentration=50 mg·L^{-1}.

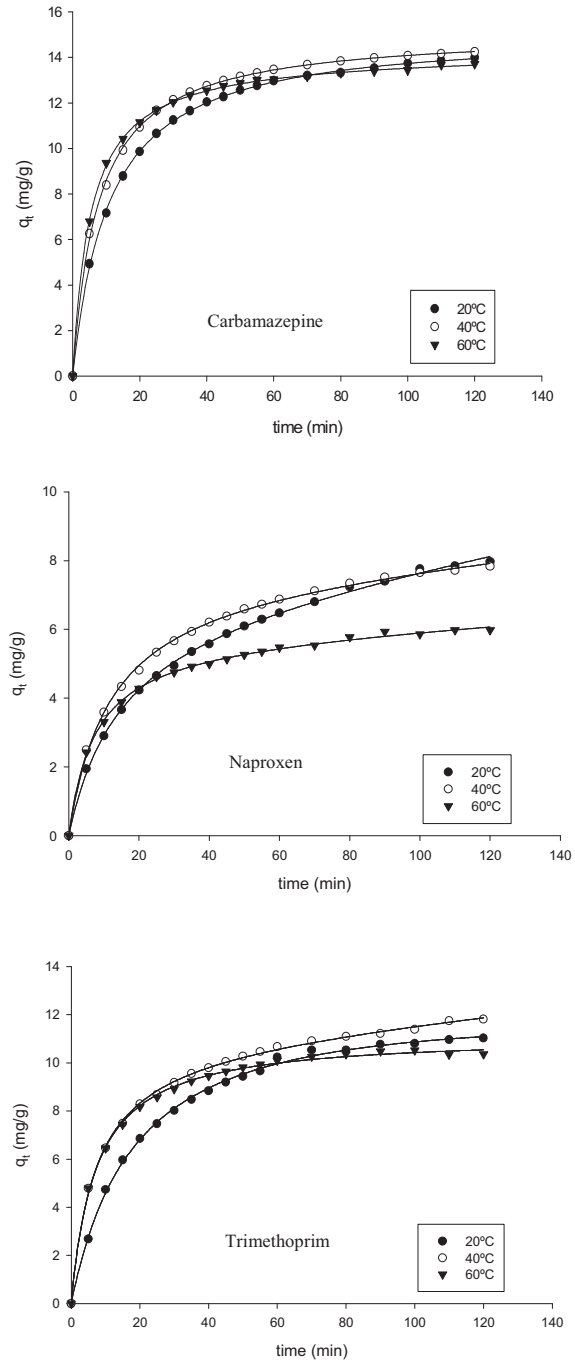

Fig. S.1.4. Influence of the temperature on the adsorption kinetics of carbamazepine, naproxen and trimethoprim. Adsorbent dose= 3 g·L^{-1}. Stirring rate= 160 rpm. pH= 7. Initial concentration= 50 mg·L^{-1}.

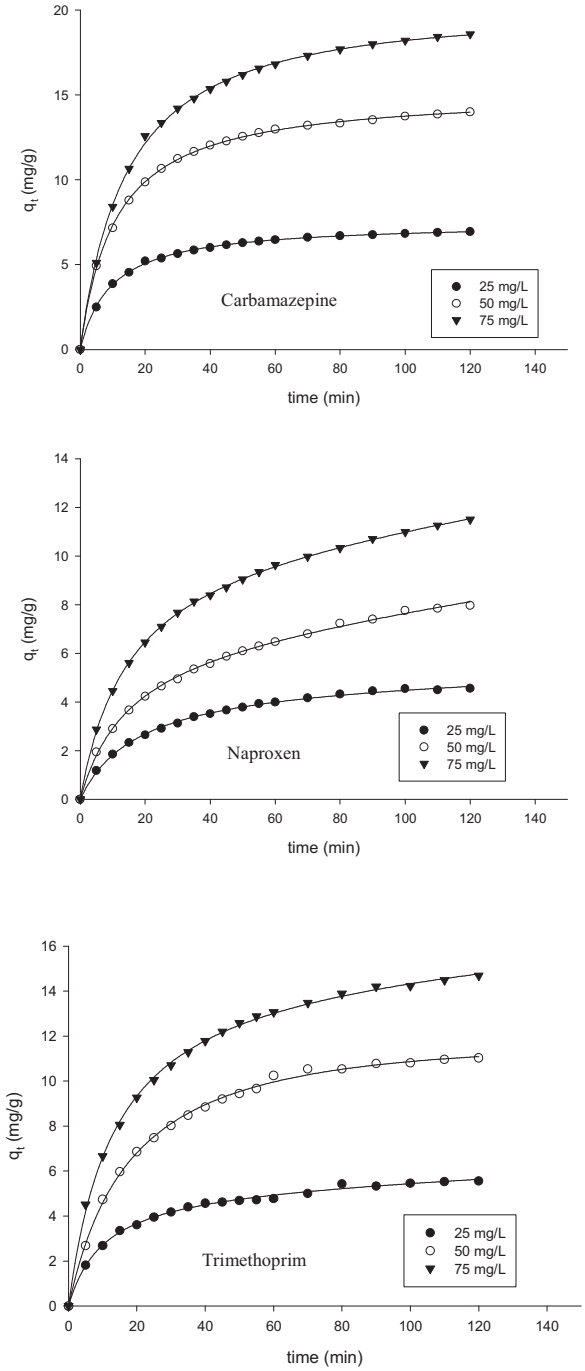

Fig. S.1.5. Influence of the temperature on the adsorption kinetics of carbamazepine, naproxen and trimethoprim. Adsorbent dose= $g \cdot L^{-1}$. Stirring rate= 160 rpm. pH= 7. Temperature= 20ºC.

1.1.7. REFERENCES.

[1] Kümmerer, K. (Ed.). "Pharmaceuticals in the environment sources, fate, effects and risks".Springer-Verlag, Berlin **(2001).**

[2] Wu, C.; Spongberg, A.L.; Witter, J.D.; Fang, M.; Ames, A.; Czajkowski, K.P. "Detection of pharmaceuticals and personal care products in agricultural soils receiving biosolids application". Clean Soil, Air, Water. 38, 230 **(2010).**

[3] Darlymple, O.K.; Yeh, D.H.; Trotz, M.A. "Removing pharmaceuticals and endocrine-disrupting compounds from wastewater by photocatalysis". J.Chem. Tech. Biotechnol. 82, 121 **(2007).**

[4] Khetan, S.K.; Collins, T.J. "Human pharmaceuticals in the aquatic environment: a challenge to green chemistry". Chem. Rev. 107, 2319 (**2007).**

[5] Mikami, E.; Goto, T.; Ohno, T.; Matsumoto, H.; Nishida, M. "Simultaneous analysis of naproxen, nabumetone and its major metabolite 6-methoxy-2-naphthylacetic acid in pharmaceuticals and human urine by high-performance liquid chromatography". J. Pharm. Biomed. Anal. 23, 917 **(2000).**

[6] Kocaoba, S. "Comparison of Amberlite IR 120 and dolomite's performances for removal of heavy metals". J. Hazard. Mater. 147, 488 (**2007)**

[7] Caliman, F.A.; Gavrilescu, M. "Pharmaceuticals, personal care products and endocrine disrupting agents in the environment. A review". Clean. 37, 277 **(2009).**

[8] Möder, M.; Braun, P.; Lange, F.; Schrader, S.; Lorenz, W. "Determination of endocrine disrupting compounds and acidic drugs in water by coupling of derivatization, gas chromatography and negative chemical ionization mass spectrometry". Clean**.** 35, 444 **(2007).**

[9] Quesada-Peñate, I.; Julcour-Lebigue, C.; Jáuregui-Haza, U.J.; Wilhelm, A.M.; Delmas, H. "Sonolysis of levodopa and paracetamol in aqueous solutions". Ultrasonics Sonochem. 16, 610 **(2009)**.

[10] Röhricht, M.; Krisam, J.; Weise, U.; Kraus, U.R.; Düring, R.A. "Elimination of carbamazepine, diclofenac and naproxen from treated wastewater by nanofiltration". Clean**.** 37, 638 **(2009)**.

[11] Hua, J.M.; An, P.L.; Winter, J.; Gallert, C. "Elimination of COD, microorganisms and pharmaceuticals from sewage by trickling through sandy soil below leaking sewers". Water Res. 37, 4395 **(2003)**.

[12] Kimura, K.; Hara, H.; Watanabe, Y. "Removal of pharmaceutical compounds by submerged membrane bioreactors (MBRs)". Desalination. 178, 135 **(2005)**.

[13] Martins, A.F.; Mallmann, C.A.; Arsand, D.R.; Mayer, F.M.; Brenner, C.G.B. "Occurrence of the antimicrobials sulfamethoxazole and trimethoprim in hospital effluent and study of their degradation products after electrocoagulation". Clean Soil, Air, Water**.** 39, 21 **(2011)**.

[14] Belgiorno, V.; Rizzo, L.; Fatta, D.; Della Rocca, C.; Lofrano, G.; Nikolaou, A.; Naddeo, V.; Meric, S. "Review on endocrine disrupting-emerging compounds in urban wastewater: occurrence and removal by photocatalysis and ultrasonic irradiation for wastewater reuse" Desalination. 215, 166 **(2007)**.

[15] Pereira, V.J.; Linden, K.G.; Weinberg, H.S. "Evaluation of UV irradiation for photolytic and oxidative degradation of pharmaceutical compounds in water". Water Res. 41, 4413 **(2007)**.

[16] Elmolla, E.S.; Chaudhuri, M. "Photocatalytic degradation of amoxicillin, ampicillin and cloxacillin antibiotics in aqueous solution using UV/TiO_2 and UV/H_2O_2/TiO_2 photocatalysis". Desalination. 252, 46 **(2010)**.

[17] Boyd, G.R.; Zhang, S.; Grimm, D.A. "Naproxen removal from water by chlorination and biofilm processes". Water Res. 39, 668 **(2005)**.

[18] Ternes, T.A.; Stüber, J.; Herrmann, N.; McDowell, D.; Ried, A.; Kampmann, M.; Teiser, B. "Ozonation: a tool for removal of pharmaceuticals, contrast media and musk fragrances from wastewater". Water Res. 37, 1976 **(2003)**.

[19] Babuna, F.G.; Camur, S.; Alaton, I.A.; Okay, O.; Iskender, G. "The application of ozonation for the detoxification and biodegradability improvement of a textile auxiliary: Naphtalene sulphonic acid". Desalination. 249, 682 **(2009)**.

[20] Bui, T.X.; Choi, H. "Adsorptive Removal of Selected Pharmaceuticals by Mesoporous Silica SBA-15". J. Hazard. Mater. 168, 602 **(2009)**.

[21] Önal, Y.; Akmil-Basar, C.; Sarici-Özdemir, C. "Elucidation of the naproxen sodium adsorption onto activated carbon prepared from waste apricot: Kinetic, equilibrium and thermodynamic characterization". J. Hazard. Mater. 148, 727 **(2007)**.

[22] Rivera-Jiménez, S.M.; Hernández-Maldonado, A.J. "Nickel(II) grafted MCM-41: A novel sorbent for the removal of Naproxen from water". Microporous Mesoporous Mater. 116, 246 **(2008)**.

[23] Urase, T.; Kikuta, T. "Separate estimation of adsorption and degradation of pharmaceutical substances and estrogens in the activated sludge process". Water Res. 39, 1289 **(2005)**.

[24] Yu, Z.; Peldszus, S.; Huck, P.M. "Adsorption characteristics of selected pharmaceuticals and an endocrine disrupting compound -Naproxen, carbamazepine and nonylphenol- on activated carbon". Water Res. 42, 2873 **(2008)**.

[25] Boussetta, S.; Branger, C.; Margaillan, A.; Boudenne, J.L.; Coulomb, B. "Salicylic acid and derivatives anchored on poly(styrene-co-divinylbenzene) resin and membrane via a diazo bridge: Synthesis, characterisation and application to metal extraction". React. Funct. Polym. 68, 775 **(2008)**.

[26] Li, A.; Zhang, Q.; Chen, J.; Fei, Z.; Longa, C.; Li, W. "Adsorption of phenolic compounds on Amberlite XAD-4 and its acetylated derivative MX-4". React. Funct. Polym. 49, 225 **(2001)**.

[27] Domínguez, J.R.; González, T.; Palo, P.; Cuerda-Correa, E.M. "Removal of common pharmaceuticals present in surface waters by Amberlite XAD-7 acrylic-ester-resin: Influence of pH and presence of other drugs". Desalination. 269, 231 **(2011)**.

[28] Rohm & Haas. "Datasheet of Amberlite^{TM} XAD-7HP Industrial Grade Polymeric Adsorbent". Philadelphia, USA **(2006)**.

[29] Bernard, J.; Branger, C.; Nguyen, T.L.A.; Denoyel, R.; Margaillan, A. "Synthesis and characterization of a polystyrenic resin functionalized by catechol: Application to retention of metal ions". React. Funct. Polym. 68, 1362 **(2008)**.

[30] González, T.; Domínguez, J.R.; Palo, P.; Sánchez-Martín, J.; Cuerda-Correa, E.M. "Development and optimization of the BDD-electrochemical oxidation of the antibiotic trimethoprim in aqueous solution". Desalination. 280, 197 **(2011**).

[31] Cuerda-Correa, E. M.; Domínguez-Vargas, J.R.; Olivares-Marín, F. J.; Beltrán de Heredia, J. "On the use of carbon blacks as potential low-cost adsorbents for the removal of non-steroidal anti-inflammatory drugs from river water". J. Hazard. Mater. 177, 1046 **(2010**).

[32] Domínguez-Vargas, J.R.; Navarro-Rodríguez, J.A.; Beltrán de Heredia, J.; Cuerda-Correa, E.M. "Removal of chlorophenols in aqueous solution by carbon black low-cost adsorbents. Equilibrium study and influence of operation conditions". J. Hazard. Mater. 169, 302 **(2009**).

[33] Crini, G.; Badot, P.M. "Application of chitosan, a natural aminopolysaccharide, for dye removal from aqueous solutions by adsorption processes using batch studies: A review of recent literature". Progress Polym. Sci. 33, 399 **(2008**).

[34] Nandi, B.K.; Goswami, A.; Purkait, M.K. "Removal of cationic dyes from aqueous solutions by kaolin: Kinetic and equilibrium studies". Appl. Clay Sci. 42, 583 **(2009)**.

[35] Noh, J.S.; Schwarz, J.A. "Stimation of the point of zero charge of simple oxides by mass titration". J. Colloid Interf. Sci. 130, 157 **(1989)**.

[36] Saikia, M.D.; Dutta, N.N. "Adsorption affinity of certain biomolecules onto polymeric resins: Effect of solute chemical nature." React. Funct. Polym. 68, 33 **(2008)**.

[37] Oshima, T.; Saisho, R.; Ohe, K.; Baba, Y.; Ohto, K. "Adsorption of amino acid derivatives on calixarene carboxylic acid impregnated resins". React. Funct. Polym. 69, 105 **(2009)**.

[38] de Ridder, D.J.; McConville, M.; Verliefde, A.R.D.; van der Aa, L.T.J.; Heijman, S.G.J.; Verberk, J.Q.J.C.; L. C . Rietveld, van Dijk, J.C. "Development of a predictive model to determine micropollutant removal using granular activated carbon". Drinking Water Engineering and Science Discussions. 2, 189 **(2009)**.

[39] Müller, G.; Radke, C.J.; Prausnitz, J.M. "Adsorption of weak organic electrolytes from dilute aqueous solution onto activated carbon. Singlesolute systems". J. Colloid Interf. Sci. 103, 466 **(1985)**.

[40] Rossner, A.; Snyder, S.A.; Knappe, D.R.U. "Removal of emerging contaminants of concern by alternative adsorbents". Water Res. 43, 3787 **(2009)**.

[41] Ziylan, A.; Ince, N.H. "The occurrence and fate of anti-inflammatory and analgesic pharmaceuticals in sewage and fresh water: Treatability by conventional and non-conventional processes". J. Hazard. Mater. 187, 24 **(2011).**

[42] Behera, S.K.; Kim, H.W.; Oh, J.E.; Park, H.S. "Occurrence and removal of antibiotics, hormones and several other pharmaceuticals in wastewater treatment plants of the largest industrial city of Korea". Sci. Tot. Environ. 409, 4351 **(2011)**.

[43] Lagergren, S. "Zur theorie der sogenannten adsorption gelöster stoffe Kungl. Svenska Vetenskapsakad. Handl". 24, 1 **(1898)**.

[44] Ho, Y.S.; McKay, G. "A comparison of chemisorption kinetic models applied to pollutant removal on various sorbents". Process Safety and Environmental Protection. 76, 332 **(1998)**.

[45] Blanchard, G.; Maunaye, M.; Martin, G. "Removal of heavy metals from waters by means of natural zeolites". Water Res. 18, 1501 **(1984)**.

[46] Ho, Y.S.; McKay, G. "A comparison of chemisorption kinetic models applied to pollutant removal on various sorbents". Trans IChemE. 76, 332 **(1998)**.

[47] Weber, W.J.; Morris, J.C. "Equilibria and capacities for adsorption on carbon". J. Sanit. Eng. Div. Proc. Am. Soc. Civ. Eng. 90, 79 **(1964)**.

[48] Bangham, D.H.; Burt, F.P. "The behaviour of gases in contact with glass surfaces". Proc. R. Soc. Lond. A. 105, 481 **(1924)**.

[49] Otero, M.; Grande, C.A.; Rodrigues, A.E. "Adsorption of salicylic acid onto polymeric adsorbents and activated charcoal". React. Funct. Polym. 60, 203 **(2004)**.

[50] Valenzuela-Calahorro, C.; Cuerda-Correa, E.; Navarrete-Guijosa, A.; Gonzalez Pradas, E. "Application of a single model to study the adsorption kinetics of prednisolone on six carbonaceous materials". J. Colloid Interf. Sci. 248, 33 **(2002)**.

[51] Valenzuela-Calahorro, C.; Navarrete-Guijosa, A.; Stitou, M.; Cuerda-Correa, E.M. "Retention of progesterone by four carbonaceous materials: study of the adsorption kinetics". Colloids Surf. A: Physicochem. Eng. Aspects. 224, 135 **(2003)**.

[52] Pardo-Botello, R.; Fernández-González, C.; Pinilla-Gil, E.; Cuerda-Correa, E.M.; Gómez-Serrano, V. "Adsorption kinetics of zinc in multicomponent ionic systems". J. Colloid Interf. Sci. 277, 292 **(2004)**.

[53] Ho, Y.S.; McKay, G. "Kinetic models for the sorption of dye from aqueous solution by wood". Trans IChemE. 76, 183 **(1998)**.

[54] Ho, Y.S.; McKay, G. "Sorption of dye from aqueous solution by peat". Chemical Engineering Journal. 70, 115 **(1998)**.

[55] Ho, Y.S.; McKay, G. "A two-stage batch sorption optimized design for dye removal to minimize contact time". Trans IChemE. 76, 313 **(1998)**.

[56] Ho, Y.S.; McKay, G. "A kinetic study of dye sorption by biosorbent waste product pith". Resources, Conservation and Recycling. 25, 171 **(1999)**.

[57] Ho, Y.S.; McKay, G. "Batch lead (II) removal from aqueous solution by peat: equilibrium and kinetics". Trans IChemE. 77, 165 **(1999)**.

[58] Ho, Y.S.; McKay, G. "The kinetics of sorption of divalent metal ions onto sphagnum moss peat". Water Research. 34, 735 **(2000)**.

[59] Ho, Y.S.; McKay, G. "Sorption of dyes and copper ions onto biosorbents". Process Biochemistry. 38, 1047 **(2003)**.

1.2. Removal of common Pharmaceuticals present in surface Waters by *Amberlite XAD-7* acrylic-ester-resin: Influence of pH and presence of other Drugs

Pharmaceutical products are often present in wastewater treatment effluents, rivers and lakes. A wide variety of drugs have been found in waterways of many countries, including analgesics, antibiotics and antiepileptics. The adsorption of four common pharmaceuticals present in surface-waters, trimethoprim (antibiotic), carbamazepine (antiepileptic), ketoprofen and naproxen (analgesics) onto *Amberlite XAD-7* (an acrylic ester resin) has been investigated. Adsorption experiments were carried out at different pH conditions and the experimental equilibrium data were fitted to the *Langmuir*, *Freundlich* and *Dubinin–Radushkevich* models. For the same experimental conditions (pH 7) the estimated adsorption capacities are from 97 $mg \cdot g^{-1}$ for carbamazepine > 54 $mg \cdot g^{-1}$ for trimethoprim > 45 $mg \cdot g^{-1}$ for ketoprofen ≈ 43 $mg \cdot g^{-1}$ for naproxen. The influence of adsorption pH was established for each compound. The investigation indicates that the mean sorption energy (E= 8.3-10.1 $kJ \cdot mol^{-1}$) characterizes a physical adsorption and the surface of the resin is energetically heterogeneous. On the other hand, the work studies the effect of the presence of other drugs in solution on the individual adsorption process. The comparison of *Freundlich*-parameters shows that the adsorption capacity decreases as expected for neutral and acidic drugs and increases for the case of trimethoprim (a basic drug).

Keywords: Amberlite XAD-7, pharmaceuticals, naproxen, ketoprofen, carbamazepine, trimethoprim.

1.2.1. INTRODUCTION.

Nowadays, pharmaceuticals have emerged as the major class of water pollutants, given their widespread usage and known biological effects. Antibiotics, antiepileptics and analgesics display "pseudo-persistence" [1,2]. Pharmaceuticals end up in surface waters and eventually in ground and drinking water after their excretion (in unmetabolized form or as active metabolites) from humans or animals via urine or faeces, through the sewage system and into the influent of wastewater treatment plants [3]. In addition to metabolic excretion, disposal of pharmaceuticals which are being used in agriculture, industry, medical treatment and common households also contributes to the entry of pharmaceuticals into fresh bodies. On the other hand, veterinary-pharmaceuticals contaminate directly soil via manure and surface and ground waters by runoff from fields [4].

In recent years and especially after the application of advanced measurement technologies [5] many pharmaceuticals have been identified and detected worldwide in the aquatic environment [6]. The presence of pharmaceuticals in various aqueous matrices (i.e. water and/or wastewater) has been repeatedly reported. Kummerer [7] reviewed the emission of drugs by hospitals. Al-Rifai et al. [8] and Gagné et al. [9] recently reported the occurrence of several pharmaceutically active products in municipal wastewater. Ternes [10] identified over 30 drugs in the influent of German Municipal Wastewater Treatment Plants (MWTP). Many of these active substances are persistent due to their ability to escape to conventional wastewater treatments and are thus becoming ubiquitous in the environment [11]. Antibiotics, non-steroidal anti-inflammatory drugs (NSAIDs), and anticonvulsants have been found in sewage treatment plant effluents around the world (China [12], Japan [13], Spain [14], and in the U.S. [15]). In particular, some antibiotics (trimethoprim), antiepileptics (carbamazepine) and analgesics (naproxen and ketoprofen), are neither degradable nor adsorbable on sewage sludge. There has been an increasing concern about the impact of these pharmaceuticals on public health and on the environment not only due to their

acute toxicity, but also to their genotoxicity, development of pathogen resistance and endocrine disruption [16].

Therefore, it is not surprising that research has recently focused on the application of non-biological processes for the elimination of pharmaceuticals in waters with emphasis on adsorption. Removal of pharmaceuticals by adsorption is one of the most promising techniques, due to its convenience once applied into current water treatment processes. So far, the removal of pharmaceuticals has been achieved by adsorption using activated carbon [17–19]. Although activated carbon displayed efficient removal for a number of pharmaceuticals, especially for hydrophobic compounds, inefficient removal for pharmaceuticals which are either electrically charged or hydrophilic has been observed. Furthermore, the working capacity of activated carbon greatly decreases in the presence of natural organic matter and the regeneration of these adsorbents is questionable. In this connection, polymeric adsorbents (PAs), namely synthetic resins (SRs), possess many striking features such as stable chemical structures, high porosity and surface areas, and large adsorption capacities. In particular, *Amberlite*^{TM} *XAD-7* acrylic-ester-resin exhibits good physical properties such as porosity, uniform pore size distribution, high surface area, and chemically homogeneous non-ionic structure. They have been shown to be good adsorbents for large amounts of uncharged compounds [20]. In this work, this resin was used to study the adsorption of four common drugs present in surface waters, trimethoprim (antibiotic), carbamazepine (antiepileptic) and naproxen and ketoprofen (analgesics).

1.2.2. MATERIALS AND METHODS.

1.2.2.1. Chemical and target compounds.

All reagents and solvents were of analytical reagent grade and were purchased from Panreac (Spain). The solution pHs were adjusted with sodium hydroxide/orthophosporic acid (0.01/0.01 mol·L^{-1}) buffer solution. Analytically pure carbamazepine (an antiepileptic), trimethoprim (antibiotic) and naproxen and ketoprofen (analgesics) were used to perform all the equilibrium experiments. All chemicals were provided by Sigma-Aldrich, Ltd (Tres Cantos, Madrid, Spain). The

molecular structure and some physicochemical properties of these pharmaceuticals are summarized in Table 1.4 [21].

Table 1.4. Molecular structure and main physicochemical properties of studied drugs.

Drug CAS number Molecular weight	Molecular structure	λ_{max} (nm)	ε x 10^2 ($L \cdot mg^{-1}$)	R^2	pK_a Log K_{OW}
Trimethoprim 738-70-5 290.32	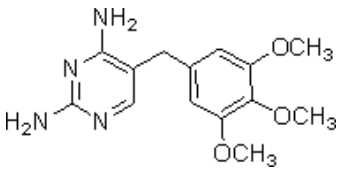	278	1.95	0.999	6.9 0.91
Carbamazepine 298-46-4 236.28	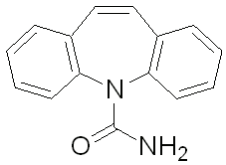	284	5.12	0.999	14.0 2.45
Ketoprofen 22071-15-4 254.29	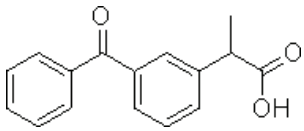	259	6.26	0.999	4.8 3.12
Naproxen 22204-53-1 230.27	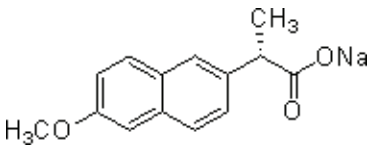	262	2.23	0.999	4.8 3.18

1.2.2.2. Polymeric adsorbent.

Aldrich Chemical resin [22] *Amberlite*^{TM} *XAD-7* was used in this work and its main physico-chemical properties are represented in Table 1.1. As can be seen, *Amberlite*^{TM} *XAD-7* resin has large surface area and average pore volume. *Amberlite*^{TM} *XAD-7* is an acrylic ester polymer of intermediate polarity and relatively hydrophilic character. In order to have a further knowledge regarding important aspects of the surface chemistry of the adsorbent, the pH of the point of zero charge (pH_{PZC}) has been determined according to a method previously described in the literature [23]. pH_{PZC} is considered as the pH at which the electric charge density of a given surface equals zero. In other words, it is the pH value at which a solid submerged in an electrolyte exhibits a surface net electric charge equal to zero. In order to determine this parameter, 50 mL of a 0.01 M NaCl solution was firstly placed in a series of teflonated test tubes. The pH was then adjusted to successive initial values between 2 and 12, by adding either HCl or NaOH and the resin (0.15 g) was added to the solution. The final pH, reached after 48 h, is measured and plotted against the initial pH. The pH at which the curve crosses the line pH(final)= pH(initial) is taken as the pH of the given adsorbent.

1.2.2.3. Determination of the equilibrium time.

First, batch adsorption of individual drugs was studied. In the equilibrium experiments, different amounts of adsorbent, ranging from 0.040 to 2.50 g, were placed into a series of 100 mL teflonated test tubes, fitted with Bakelite screw-on caps to avoid solvent losses by evaporation and interferences due to atmospheric carbon dioxide. Next, 90 mL of aqueous (ultrapure milli-Q^{TM} grade) solution of known concentration (50 $mg \cdot L^{-1}$) were added. Then, the tubes were mounted in thermostatic bath (Julabo SW-22) containing water and maintained under steady shaking (40 rpm). Different series of experiments were carried out by varying the pH of the solution (maintaining constant temperature, 20 ºC, ionic strength of solution, 0.01 M, and agitation, 40 rpm). In all cases a buffer solution constituted by sodium hydroxide and phosphoric acid was used in order to maintain pH and ionic strength constant. A

previous experiment was carried out with the aim of determining the equilibrium time. In all cases, a period of time equal to 15 days is long enough to ensure that equilibrium has been reached.

Next, batch adsorption of a mixture of the four drugs (carbamazepine, trimethoprim, naproxen and ketoprofen) was studied. In this case, 90 mL of solution of a mixture of the four pharmaceuticals (with 50 $mg \cdot L^{-1}$ of each compound) were added to teflonated test tubes. Adsorption isotherms were produced by varying the resin starting mass (between 0.04 and 2.50 g).

1.2.2.4. Analytical method.

The concentration of solute in the supernatant liquid after contacting the adsorptive solutions with the adsorbent was determined by means of an UV-Vis spectrophotometric method, with the aid of an Unicam Heλios γ UV-Vis spectrophotometer provided with a 1 cm optical pathway quartz cell. Ultrapure-milli-Q™ water (buffered at the desired pH) was used as the reference. Firstly, the optimal wavelength, λ_{max}, (i.e., that corresponding to the maximum absorbance) was determined for each of the drugs analyzed in this study. Next, different solutions of increasing solute concentration (comprised between 5 and 50 $mg \cdot L^{-1}$) were prepared, their absorbance being determined. By fitting the experimental measurements according to the Lambert-Beer law, the absorption coefficient, ε, of each solute was determined. Table 1.4 summarizes the values of λ_{max} and ε together with the regression coefficient corresponding to the analytical method of each of the solutes.

For the experiments carried out with the mixture of pharmaceuticals, the samples were analyzed by HPLC, using a Waters Chromatograph with a 996 Photodiode Array Detector and a Nova-Pak C18 column. A methanol/water/phosphoric acid mixture (15/84.4/0.6 vol.) was used as the mobile phase with a flow rate of 1 $mL \cdot min^{-1}$.

1.2.3. RESULTS AND DISCUSSION.

The adsorption equilibrium of four common pharmaceuticals (carbamazepine, trimethoprim, naproxen and ketoprofen) has been studied. In order to analyze the

influence of pH on the adsorption process, this parameter was modified within the range comprised between 5 and 9. All of these data were fitted to different mathematical expressions which describe adsorption equilibria. These equations correspond to the *Langmuir* (L), *Freundlich* (F), and *Dubinin–Radushkevich* (D-R) isotherm models [24–26].

1.2.3.1. Structure and surface chemistry of the adsorbent.

In general, *XAD* resins are nonpolar adsorbents generally used for adsorption of organic substances (hydrophobic compounds up to MW 20,000) from aqueous systems. In particular, to our knowledge, *XAD-7* is the only "moderately polar" *XAD* resin available nowadays. It has been used to remove a wide variety of pollutants from aqueous wastes, ground water and vapor streams [27].

Furthermore, FTIR analysis of the *XAD-7* resin [28] exhibits a band at 2972 cm^{-1} (strong, sharp) attributed to the stretching mode of aliphatic C-H group. In addition the absorption bands at 1468 and 1392 cm^{-1} are due to C-H deformation of CH_3. The absorption band at 1730 cm^{-1} corresponds to C=O stretching frequency. Two absorption bands at 1156 and 1265 cm^{-1} attributed to C-O stretching in ester are also observed. It also shows the presence of a broad band attributed to O-H stretching at 3476 cm^{-1} due to the presence of water.

The chemical structure of *Amberlite XAD-7* is shown in Figure 1.5. On the basis of the structure and the shape of the curve obtained in determining the point of zero charge of the resin (Figure 1.6), it may be concluded that the pH_{PZC} of the resin used as the adsorbent in the present work is around 6.3. Furthermore, Figure 1.6 suggests that surface charge obtained at intermediate values of operating pHs (5 and 7) should be very low. This latter is corroborated by the scarce deviation of the pH_e vs pH_o plot from the y= x plot at pH= 5 and pH= 7, which is indicative of the extremely low net charge that is present on the surface of the *XAD-7* resin here used.

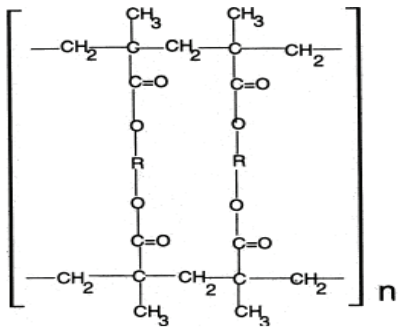

Fig. 1.5. Chemical structure of *Amberlite XAD-7* resin.

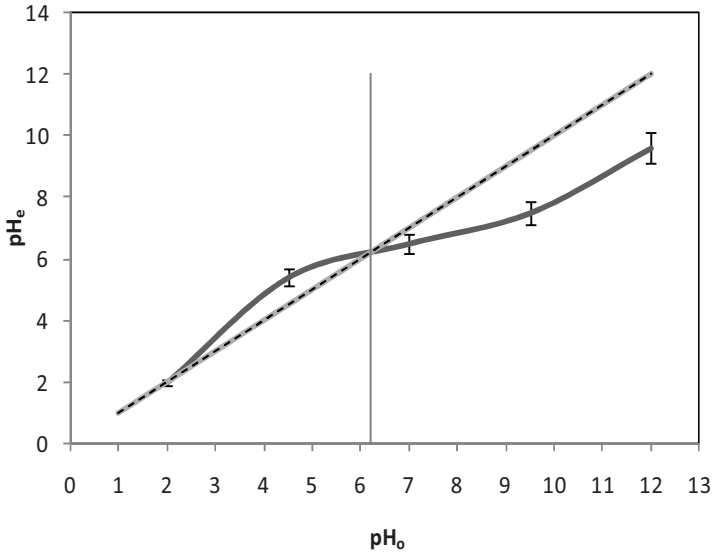

Fig. 1.6. Determination of the point of zero charge of the resin.

1.2.3.2. Equilibrium isotherms.

The equilibrium state may be described as the result of a dynamic adsorption-desorption process [29]. From the practical standpoint, this process is commonly represented in the form of the so-called adsorption isotherm that plots the amount of solute retained per mass unit of the solid adsorbent versus the equilibrium concentration of solute in the liquid phase at constant temperature. Thus, in order to plot the adsorption isotherm it is necessary to calculate the amount of solute retained

per mass unit of the adsorbent corresponding to each of the equilibrium concentrations experimentally determined.

The amount of solute retained per mass unit of the adsorbent was calculated according to the following Equation (1.9):

$$q = \frac{(C_0 - C_e)\cdot V}{W} \tag{1.9}$$

where q is the amount of solute retained per mass unit of the adsorbent ($mg\cdot g^{-1}$); C_0 is the initial concentration of solute in the solution ($mg\cdot L^{-1}$); Ce is the concentration of solute in the solution ($mg\cdot L^{-1}$) once the equilibration time is elapsed; V is the volume of solution (L) used in each experiment; and W is the mass of adsorbent (g) that has been kept in contact with the solution.

For thermodynamic consideration in terms of adsorption isotherms, experimental values were obtained for the individual adsorption of each drug on *XAD-7* and were plotted according to *Langmuir* (L), *Freundlich* (F), and *Dubinin–Radushkevich* (D-R) models.

The *Langmuir* model [24] was originally developed to represent physisorption on a set of well-defined localized adsorption sites having the same adsorption energy, independent of the surface coverage and with no interaction between adsorbed molecules. The familiar form of the *Langmuir* isotherm based on the kinetic consideration is expressed as:

$$q_e = \frac{q^0_{max}\cdot K_L\cdot C_e}{1 + K_L\cdot C_e} \tag{1.10}$$

where q_e is equal to the amount of drug adsorbed per gram of adsorbent, ($mg\cdot g^{-1}$); q^o_{max} is the maximum amount of solute adsorbed (mg) per gram of resin and this parameter is called the adsorption capacity, C_e is the equilibrium concentration of the drug in solution ($mg\cdot L^{-1}$), and K_L is the Langmuir constant ($L\cdot g^{-1}$) which is related to the equilibrium constant of adsorption process.

Fig. 1.7 shows the individual experimental data q_e vs C_e at pH 7, ionic strength 0.01 M, and temperature 20 ºC, for the different single systems; XAD-7/carbamazepine, XAD-7/trimethoprim, XAD-7/naproxen and XAD-7/ketoprofen. As can be seen, the adsorption efficacy ranking is as follows: carbamazepine > trimethoprim > naproxen ≈ ketoprofen. This could be due to the fact that, at pH 7, carbamazepine is in its neutral form. The same applies to trimethoprim, since this value of pH is nearly the same than it pK_a (i.e., 6.9). On the contrary, naproxen and ketoprofen are both deprotonated and thus negatively charged, as they are acidic drugs. Since the surface of the adsorbent is neutral, it is reasonable thinking that carbamazepine will be adsorbed in a more favorable manner than the remaining molecules.

In order to test the influence of pH on the adsorption process, different adsorption experiments were carried out using this resin as adsorbent at constant temperature (20ºC) and ionic strength (0.01 M). Table 1.5 shows the Langmuir parameters obtained for each compound at different pH values (5, 7 and 9). As can be seen, in the case of acid pharmaceuticals (ketoprofen and naproxen), it may be observed that, as pH increases, both parameters, the adsorption capacity of the monolayer (q_o^{max}) and the affinity of the solute towards the active sites of the adsorbent (K_L) decrease. In the case of carbamazepine, the values of q_o^{max} and K_L, fall within a narrow range, 94.3-98.6 $mg \cdot g^{-1}$ and 5.43-5.90 $L \cdot g^{-1}$, respectively. However, in the case of a basic drug as trimethoprim both parameters q_o^{max} and K_L increase when pH increases. In this case the values are comprised between 8.64 and 91.7 $mg \cdot g^{-1}$ for the adsorption capacity and 0.31-2.25 $L \cdot g^{-1}$ for K_L.

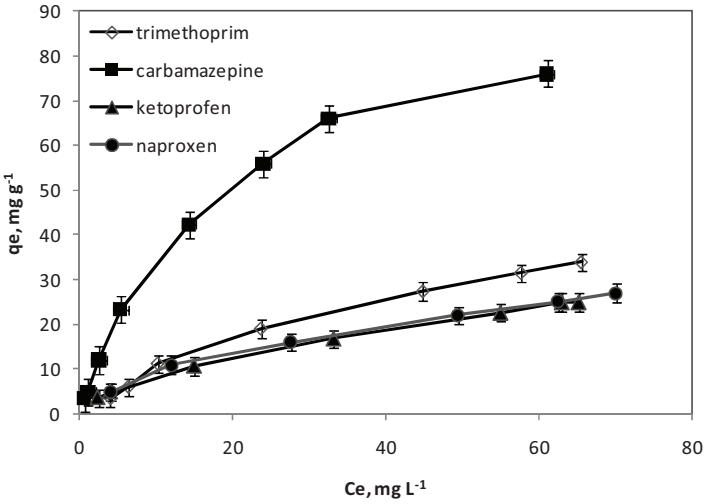

Fig. 1.7. Experimental results q_e vs C_e (pH 7, ionic strength 0.01 M and temperature 20 ºC) for the different single adsorption systems.

Table 1.5. *Langmuir* isotherm parameters of the *XAD-7* resin for the adsorption of the different drugs.

Pharmaceutical compounds	pH	q_o^{max} ($mg \cdot g^{-1}$)	k_L ($L \cdot g^{-1}$)	r^2
Trimethoprim	5	8.645	0.316	0.990
	7	54.35	1.300	0.979
	9	91.70	2.251	0.853
Carbamazepine	5	94.34	5.435	0.942
	7	97.09	5.794	0.984
	9	98.66	5.900	0.988
Ketoprofen	5	85.47	10.96	0.905
	7	45.25	1.129	0.792
	9	15.63	0.501	0.995
Naproxen	5	135.1	5.649	0.965
	7	43.67	1.242	0.991
	9	13.15	0.493	0.995

All *Langmuir* parameters shown in this table had a standard deviation less than ±5%.

On the other hand, the *Freundlich* isotherm [25], one of the more widely employed mathematical descriptions, usually fits the experimental data over a wide range of concentrations. This isotherm gives an empirical expression encompassing the surface heterogeneity and the exponential distribution of active sites and their energies. The *Freundlich* model is expressed as:

$$q_e = K_F \cdot C_e^n \tag{1.11}$$

where q_e and C_e have the same definitions as previously presented for the *Langmuir* isotherm, K_F is an empirical constant which provides an indication of the adsorption capacity of the adsorbent, and n indicates the energetic heterogeneity of adsorption sites and the intensity of adsorption.

Table 1.6 shows the *Freundlich* parameters obtained for each compound at different pH values (5, 7 and 9). As can be seen, the values obtained for the parameter "n" were below than 1 (between 0.55-0.82) in all of the XAD-7/drug systems, indicating favored adsorption. The "n" parameter of the *Freundlich* equation reveals the presence of energetically heterogeneous adsorption sites, but adsorption sites have a narrow energy distribution since its value is close to 1 in all cases. Moreover, the values obtained of K_F are quite different depending on pH. The evolution observed for the K_F constant with pH for all the drugs is similar to that obtained for the maximum adsorption capacity of the monolayer, q_o^{max}, in the *Langmuir* model. However, the values obtained for the regression coefficient "r^2" are higher than those obtained using the *Langmuir* model. These results suggest the presence of energetically heterogeneous adsorption sites in all of the adsorbent-solute systems studied.

Table 1.6. *Freundlich* isotherm parameters of the *XAD-7* resin for the adsorption of the different drugs.

Pharmaceutical compounds	pH	K_F ($L^n \cdot mg^{1-n} \cdot g^{-1}$)	n	r^2
Trimethoprim	5	0.69	0.547	0.969
	7	1.45	0.772	0.950
	9	2.53	0.822	0.983
Carbamazepine	5	4.73	0.818	0.982
	7	5.56	0.744	0.989
	9	6.14	0.729	0.992
Ketoprofen	5	7.88	0.755	0.959
	7	1.94	0.643	0.985
	9	0.91	0.615	0.991
Naproxen	5	6.64	0.757	0.989
	7	2.16	0.626	0.995
	9	0.95	0.574	0.988

All *Freundlich* parameters shown in this table had a standard deviation less than ±5%.

Finally, in order to distinguish between physical and chemical adsorption, the experimental data were applied to a *Dubinin–Radushkevich* (D-R) isotherm model [26]. In this model, the feature is the heterogeneity of energies over the surface. The linear form of D-R isotherm is given by:

$$\ln C_{ads} = \ln K_{D-R} - \beta\xi^2 \tag{1.12}$$

where C_{ads} is the amount of pharmaceutical adsorbed per unit mass of the XAD ($mol \cdot L^{-1} \cdot g^{-1}$), K_{DR} is the maximum amount of pharmaceutical adsorbed, and β is a constant with dimensions of energy and Polanyi potential ξ= RT ln[1 + (1/Ceq)], where R is a gas constant in $kJ \cdot K^{-1} \cdot mol^{-1}$ and T is the temperature in Kelvin. As can be seen in Table 1.7, the trend observed for the maximum adsorption capacity K_{DR} with pH, is similar to that obtained for the maximum capacity of monolayer, q_o^{max} of the *Langmuir* model, or the value of the constant K_F of *Freundlich* model. However, the values obtained for the regression coefficient "r^2" are higher than those obtained using the two previous models. The mean regression coefficient "r^2" obtained using the two heterogeneous-surface models, *Dubinin–Radushkevich* (r^2= 0.992) and

Freundlich (r^2= 0.985), can be compared with the value obtained using the *Langmuir* model, r^2= 0.948.

The D-R model considers the heterogeneity of energies over the surface. According to Saeed et al. [30] if the surface is considered heterogeneous and an approximation to a *Langmuir* isotherm is chosen as a local isotherm for all sites that are energetically equivalent then the quantity $\beta^{1/2}$ can be related to the mean sorption energy:

$$E = \frac{1}{\sqrt{-2\beta}} \tag{1.13}$$

which is the free energy of the transfer of one mol of solute from infinity to the surface of *Amberlite* resin. The numerical values of *E* calculated from Eq. (1.13) are in a narrow range between 8.28-10.1 kJ·mol^{-1} for all XAD-7/drug/pH systems. These values of energy characterize a physical adsorption process and are in accordance with the values obtained for other physical adsorption systems based on silica gel [31].

Table 1.7. *Dubinin-Radushkevich* isotherm parameters of the *XAD-7* resin for the adsorption of the different drugs.

Pharmaceutical compounds	pH	K_{DR} (mol·g^{-1})	β (kJ^2·mol^{-2})	E (kJ·mol^{-1})	r^2
Trimethoprim	5	0.0020	0.0049	10.10	0.974
	7	0.0121	0.0054	9.62	1.000
	9	0.0405	0.0066	8.70	0.987
Carbamazepine	5	0.0690	0.0064	8.84	0.990
	7	0.0500	0.0058	9.28	0.994
	9	0.0450	0.0055	9.53	0.997
Ketoprofen	5	0.0620	0.0056	9.45	0.969
	7	0.0091	0.0052	9.81	0.994
	9	0.0046	0.0055	9.53	0.994
Naproxen	5	0.1340	0.0073	8.28	0.993
	7	0.0127	0.0056	9.45	0.999
	9	0.0038	0.0052	9.81	0.992

All *Dubinin-Radushkevich* parameters shown in this table had a standard deviation less than ±5%.

The fact that the adsorption is mainly physical involves a certain degree of reversibility. This, however, represents an advantage since it allows recycling the adsorbent in an easier manner thus increasing its working life and palliating the relatively high cost of *Amberlite XAD-7*.

1.2.3.3. Effect of pH.

The removal efficiencies for the different drugs are shown in Fig. 1.8. This parameter has been calculated as follows:

$$X\% = \frac{(C_0 - C_e)}{C_0} \cdot 100 \qquad (1.14)$$

where X is the removal efficiency (%); C_0 is the initial concentration of solute in the solution ($mg \cdot L^{-1}$); and C_e is the concentration of solute in the solution ($mg \cdot L^{-1}$) once the equilibration time is elapsed.

As can be seen, as expected, adsorption of drugs is strongly dependent on pH. The experimental results displayed that, for carbamazepine, the removal efficiency is as high as 98% in the tested pH range. When pH was increased from 5 to 9, the removal of acidic pharmaceuticals (naproxen and ketoprofen) reduced gradually from 99% to 84%, while the removal of basic drug (trimethoprim) increased noticeably from 74% to 96%.

As indicated under section 1.2.3.1, the surface charge of the resin here used as the adsorbent is very low at least at intermediate values of operating pHs (5 and 7, see Fig. 1.6). As a consequence, it has been considered that this parameter is not the main factor governing the adsorption process. Furthermore, the chemical structure of *Amberlite XAD-7* (see Fig. 1.5) suggests that the presence of ionizable groups is very limited. Consequently, the following discussion is based on two factors, namely, the hydrophobicity of the drug (conditioned by the value of the octanol water partition coefficient, K_{ow}) and the ionization of the molecule (determined by the values of pH and pK_a). Both parameters, K_{ow} and pK_a, are taken into account for the calculation of log D.

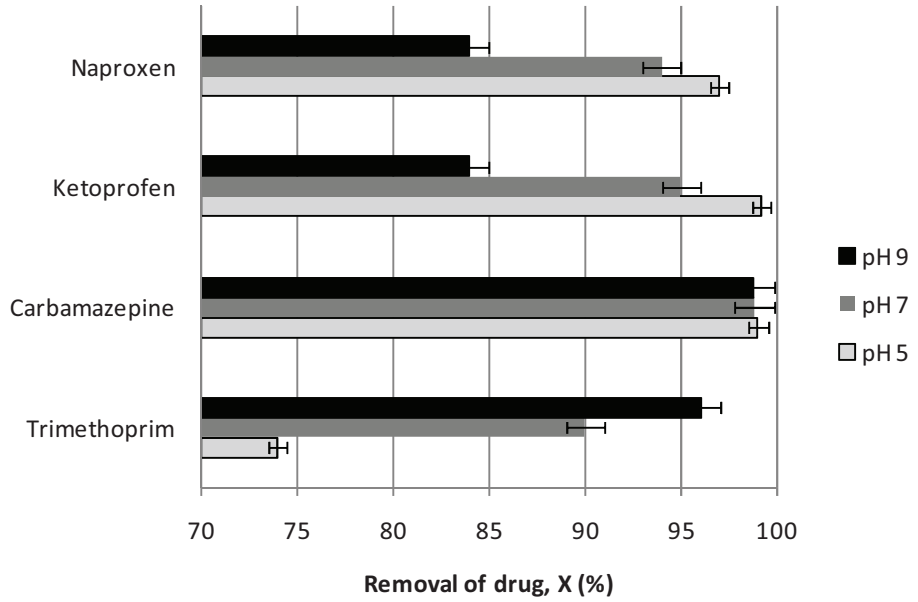

Fig. 1.8. Influence of pH on the removal efficiencies obtained for the different drugs (ionic strength 0.01 M and temperature 20 ºC).

Log D is a pH-dependent, modified octanol water partition coefficient and is relevant for solutes that are partly dissociated or protonated [32]. It can be calculated using Eq. (1.15) and (1.16). For acidic molecules Log D is determined as:

$$\text{Log D} = \text{Log K}_{ow} - \text{Log}\,(1 + 10^{(pH-pKa)}) \tag{1.15}$$

whereas for basic molecules Log D is:

$$\text{Log D} = \text{Log K}_{ow} - \text{Log}\,(1 + 10^{(pKa-pH)}) \tag{1.16}$$

Figure 1.9 shows the relationship existing between the maximum adsorbed amount (q^0_{max}) and Log D. It may be observed that, as a rule, as Log D increases the maximum adsorbed amount raises as well. This fact indicates that Log D is a valuable instrument to evaluate the adsorption capacity of the resin for the removal of different drugs (both, acidic and basic) in a wide range of operation pHs.

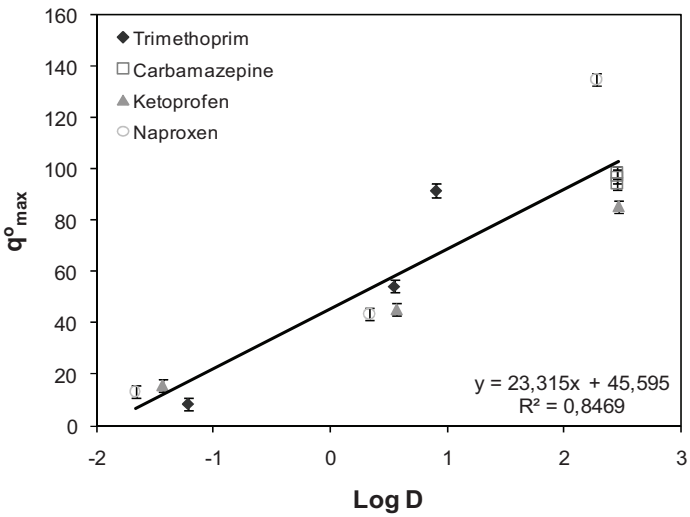

Fig. 1.9. Relationship existing between the maximum adsorbed amount of the drug (q^0max of *Langmuir* equation) and Log D.

The adsorption of pharmaceuticals onto *XAD-7* can be controlled by both non-electrostatic and electrostatic interaction. In the case of carbamazepine (pK_a= 14, see Table 1.4), a neutral compound in the tested pH range, its binding onto *XAD-7* is solely attributable to a non-electrostatic interaction involving hydrogen bonding, probably through the oxygen groups of esters, and Van der Waals interactions [33]. This can be seen in Fig. 1.10(a) Hydrogen bonding and Van der Waals interactions act with the same intensity along the whole range of pH studied. Meanwhile, uptake of acidic drugs (naproxen and ketoprofen) on *XAD-7* is attributed to both kinds of interaction, depending on solution pH. At pH below the pK_a, acidic drugs are neutral molecules, interacting with resin surface via non-electrostatic interaction and its behavior is similar to carbamazepine. When the pH is clearly above the pK_a of both drugs (pHs 7 and 9), acidic drugs have negative charge while surface of resin (pH_{PZC}= 6.2) gradually becomes more negatively charged, leading to an electrostatic repulsion between them. Consequently, adsorption of acidic pharmaceuticals dropped sharply (see Figs. 1.10(b) and 1.10(c)). Furthermore, when pH is around 9, acidic drug

molecules and surface groups on *XAD-7* completely become negatively charged, leading to no significant adsorption. However, in the case of a basic drug as trimethoprim, when the pH is below the pK_a (pH 5), basic drug has positive charge while surface of resin gradually becomes more positively charged (pH_{PZC}= 6.2), leading to an electrostatic repulsion between them. Consequently, as can be seen in Fig. 1.10(d) when pH is equal to 5, basic pharmaceutical molecules and XAD-7 surface groups become positively charged, leading to no significant adsorption. At pH 7, a pH value in the close vicinity of its pK_a, approximately 50% of the trimethoprim molecules are protonated and the adsorption of this drug increases. Finally, at pH 9 the molecule is completely neutral and the removal efficiency increases markedly.

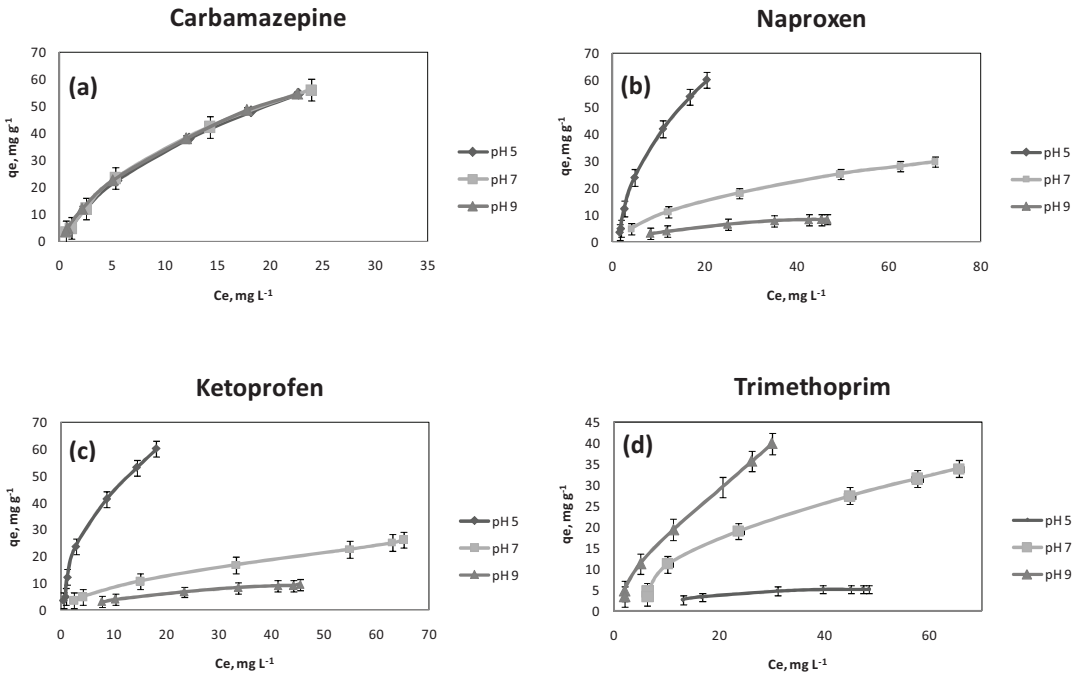

Fig. 1.10. Influence of pH on the adsorption isotherm of each drug (ionic strength 0.01 M and temperature 20 ºC). a) carbamazepine, b) naproxen, c) ketoprofen, d) trimethoprim.

1.2.3.4. Effect of other pharmaceuticals in solution. Competitive adsorption of the mixture.

In order to test the influence of the presence o other drugs in solution on the individual adsorption process, different adsorption experiments were carried out using a mixture of the four pharmaceuticals (ketoprofen, naproxen, trimethoprim and carbamazepine) in a 50 mg·L^{-1} concentration of each drug. The experiments were carried out at constant temperature (20 °C), pH 7 and ionic strength (0.01 M) for possible comparison with the individual systems.

Fig. 1.11 shows the experimental isotherm q_e vs C_e for the multi-component system (for each compound and for the total mass adsorbed). Fig. 1.12 compares the adsorption of the different drugs in both systems (individual or multi-component). As can be seen, in the case of acidic and neutral drugs (ketoprofen, naproxen and carbamazepine) the adsorption of the individual drugs decreases in the mixture.

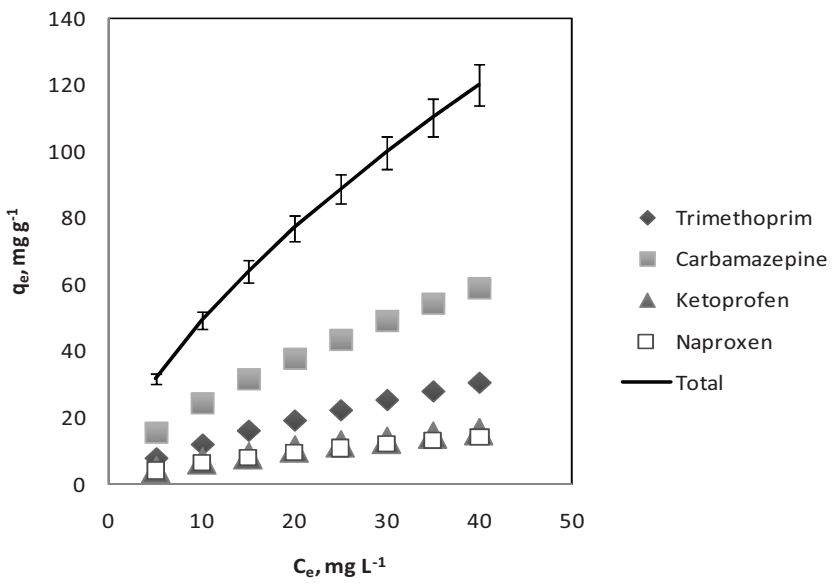

Fig. 1.11. Experimental isotherm q_e vs C_e for the multi-component system (pH 7, ionic strength 0.01 M and temperature 20 ºC).

However, in the case of the basic compound (trimethoprim) the presence of other adsorbed acid or neutral pharmaceuticals increase its adsorption. This fact may be explained taking into account the basicity of trimethoprim, the acidic character of naproxen and ketoprofen and the neutrality of the carbamazepine molecule. Thus, the previous adsorption of acidic molecules favours the subsequent adsorption of the basic molecule of trimethoprim, probably by involving the formation of hydrogen bonds between both types of molecules, as indicated above. As a consequence, the adsorption of the basic drug increases to a limited extent as shown in Fig. 1.12.

Table 1.6 compares the *Freundlich* parameters obtained for each compound in both systems (individual or multi-component) at pH 7, 20 ºC and ionic strength 0.01 M. In the mixture, the "n" parameter of the *Freundlich* equation reveals the presence of energetically heterogeneous adsorption sites, but adsorption sites have a narrow energy distribution since its values were close to 0.6.

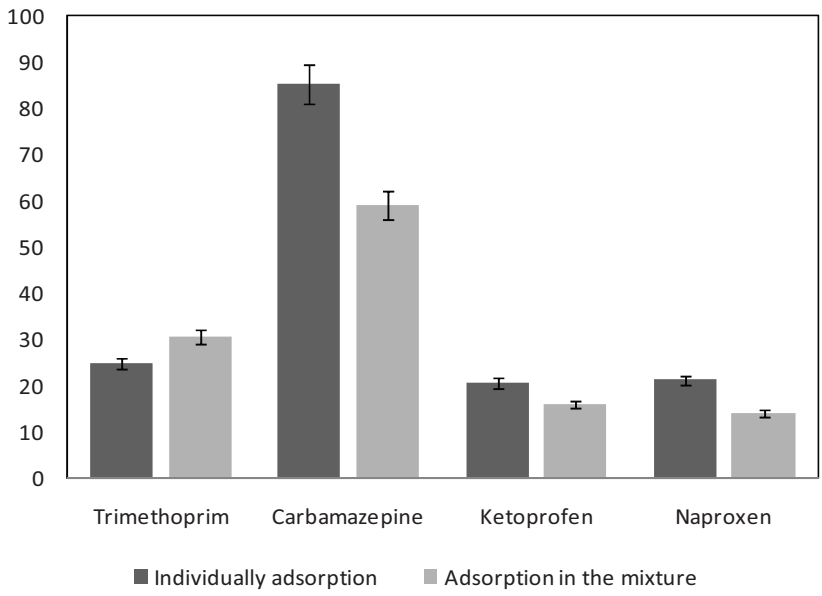

Fig. 1.12. Comparison of the adsorption of the different drugs in both systems (individual or multi-component). Equilibrium concentration in solution C_e= 40 mg·L^{-1}, pH 7, ionic strength 0.01 M and temperature 20 ºC.

In the case of carbamazepine, the values of "n" and K_F, oscillate in a narrow range, 0.74-0.64 and 5.56-5.53 $L^n \cdot mg^{1-n} \cdot g^{-1}$, for the indidual and multi-component system respectively. Taking into account the values of K_F, carbamazepine is probably the first adsorbed drug. For acid pharmaceuticals (ketoprofen and naproxen), it may be observed that the *Freundlich* constant K_F decreases as expected in a competitive adsorption model. However, the parameter "*n*" is unchanged by the presence of other drugs (remains around 0.6 for both systems). This implies a similar heterogeneity of the adsorbent surface and a similar intensity of adsorption. On the other hand, it is necessary to highlight the results obtained with the most basic drug (trimethoprim). In this case the value of K_F increases considerably (from 1.45 to 2.62 $L^n \cdot mg^{1-n} \cdot g^{-1}$) in the multi-component competitive adsorption. We can say that the presence of other adsorbed neutral or acidic drugs increases significantly the adsorption capacity of the adsorbent with respect to the basic drug. This result is unusual and surprising in competitive systems of this type.

Lastly, large quantities of drugs are adsorbed in the mixture, which is worth noting. Up to 130 mg of drug per gram of resin may be retained. This result can be compared with the results obtained in the individual adsorption of carbamazepine (see Figs. 1.11 and 1.12). These results manifest the capability of the resin in the multiple adsorption of drugs.

1.2.4. CONCLUSIONS.

From the results obtained in the present study the following conclusions may be drawn:

- The removal of four pharmaceuticals (namely, naproxen, ketoprofen, carbamazepine and trimethoprim) using *Amberlite XAD-7* acrylic ester resin has been investigated. The resin has demonstrated an excellent potential ability to be used as adsorbent in the removal process of the four drugs (individually and for the mixture).
- Adsorption of drugs is strongly dependent on pH. The influence of pH on the adsorption capacity is different for each compound. This influence is positive

in the case of trimethoprim (a basic drug), negative for naproxen and ketoprofen (acidic drugs), and indifferent in the case of carbamazepine (a neutral drug).

- The experimental equilibrium data were fitted to the *Langmuir* (L), *Freundlich* (F), and *Dubinin–Radushkevich* (D-R) models. These two latter models provide a very good fit for this resin (for all products and experimental conditions). The obtained results characterize the presence of energetically heterogeneous adsorption sites in all of the adsorbent-solute systems studied.
- The results derived from the *Dubinin–Radushkevich* model indicate that the mean sorption energy (E= 8.3-10.1 $kJ \cdot mol^{-1}$) characterizes a physical adsorption and the surface of the resin is energetically heterogeneous in a narrow range.
- With regard to the influence of other drugs in solution on the individual adsorption. The comparison of *Freundlich*-parameters for both systems shows that the adsorption capacity decreases as expected for neutral and acidic drugs. However, for the case of trimethoprim (a basic drug) its adsorption is favoured in the mixture.
- It is necessary to stand out the high quantities of drugs adsorbed in the mixture. Up to 130 mg of drug per gram of resin. These results manifest the kindness of the resin in the multiple adsorption of drugs.

1.2.5. REFERENCES

[1] Richardson, B.J.; Larn, P.K.S.; Martin, M. "Emerging chemicals of concern: pharmaceuticals and personal care products (PPCPs) in Asia, with particular reference to Southern China". Pollution Bulletin. 50, 913 **(2005)**.

[2] Hernando, M.D.; Mezcua, M.; Fernández-Alba, A.R.; Barceló, D. **"**Environmental risk assessment of pharmaceutical residues in wastewater effluents, surface waters and sediments". Talanta. 69, 334 **(2006)**.

[3] Darlymple, O.K.; Yeh, D.H.; Trotz, M.A. "Removing pharmaceuticals and endocrine-disrupting compounds from wastewater by photocatalysis". Journal of Chemical Technology and Biotechnology. 82, 121 **(2007)**.

[4] Khetan, S.K., Collins, T.J. "Human pharmaceuticals in the aquatic environment: a challenge to green chemistry". Chemical Reviews. 107, 2319 **(2007)**.

[5] Fatta, D.; Nikolaou, A.; Achilleos, A.; Meric, S. "Analytical methods for tracing pharmaceutical residues in water and wastewater". TrAC Trends Analytical Chemistry. 26, 515 **(2007)**.

[6] Hua, W.; Bennett, E.R.; Letcher, J.R. "Ozone treatment and the depletion of detectable pharmaceuticals and atrazine herbicide in drinking water sourced from the upper Detroit river, Ontario, Canada". Water Research. 40, 2259 **(2006)**.

[7] Kummerer, K. "Drugs in the environment: emission of drugs, diagnostic aids and disinfectants into wastewater by hospitals in relation to other sources. A review". Chemosphere. 45, 957 **(2001).**

[8] Al-Rifai, J.; Gabelish, C.; Schäfer, A. "Occurrence of pharmaceutically active and nonsteroidal estrogenic compounds in three different wastewater recycling schemes in Australia". Chemosphere. 69, 803 **(2007)**.

[9] Gagné, F.; Blaise, C.; André, C. "Occurrence of pharmaceutical products in a municipal effluent and toxicity to rainbow trout (Oncorhynchus mykiss) hepatocytes". Ecotoxicology Environmental Safety. 64, 329 **(2006)**.

[10] Ternes, T.A. "Occurrence of drugs in German sewage treatment plants and rivers". Water Research. 32, 3245 **(1998)**.

[11] Tauxe-Wuersch, A.; De Alencastro, L.F.; Grandjean, D.; Tarradellas, J. "Occurrence of several acidic drugs in sewage treatment plants in Switzerland and risk assessment". Water Research. 39, 1761 (2005).

[12] Gulkowska, A.; Leung, H.W.; So, M.K.; Taniyasu, S.; Yamashita, N.; Yeunq, L.W.Y.; Richardson, B.J.; Lei, A.P.; Giesy, J.P.; Lam, P.K.S. "Removal of antibiotics from wastewater by sewage treatment facilities in Hong Kong and Shenzhen (China)". Water Research. 42, 395 **(2008)**.

[13] Okuda, T.; Kobayashi, Y.; Nagao, R.; Yamashita, N.; Tanaka, H.; Tanaka, S.; Fujii, S.; Konishi, C.; Houwa, I. "Removal efficiency of 66 pharmaceuticals during wastewater treatment process in Japan". Water Science and Technology. 57, 65 **(2008)**.

[14] Gros, M.; Petrovic, M.; Barcelo, D. "Wastewater treatment plants as a pathway for aquatic contamination by pharmaceuticals in the Ebro river basin (northeast Spain)". Environmental Toxicology and Chemistry. 26, 1553 **(2007)**.

[15] Karthikeyan, K.G.; Meyer, M.T. "Occurrence of antibiotics in wastewater treatment facilities in Wisconsin (USA)". Science of the Total Environment. 361, 196 **(2006)**.

[16] Halling-Sorensen, B.; Nielsen, S.N.; Lanzky, P.F.; Ingerslev, F.; Lutzhoft, H.C.H.; Jorgensen, S.E. "Occurrence, fate and effects of pharmaceutical substances in the environment. A review". Chemosphere. 36, 357 **(1998)**.

[17] Ternes, T.A.; Meisenheimer, M.; McDowell, D.; Sacher, F.; Brauch, H.J.; Haist-Gulde, B.; Preuss, G.; Wilme, U.; Zulei-Seibert, N. "Removal of pharmaceuticals during drinking water treatment". Environmental Science & Technology. 36, 3855 **(2002)**.

[18] Westerhoff, P.; Yoon, Y.; Snyder, S.; Wert, E. "Fate of endocrine-disruptor, pharmaceutical, and personal care product chemicals during simulated drinkingwater treatment processes". Environmental Science & Technology. 39, 6649 **(2005)**.

[19] Vieno, N.M.; Harkki, H.; Tuhkanen, T.; Kronberg, L. "Occurrence of pharmaceuticals in river water and their elimination in a pilot-scale drinking water treatment plant". Environmental Science & Technology. 41, 5077 **(2007)**.

[20] Lee, D.W.; Eum, C.H.; Lee, I.H.; Jeon, S.J. "Adsorption Behavior of 8-Hydroxyquinoline and Its Derivatives on Amberlite XAD Resins, and Adsorption of Metal Metal Ions by Using Chelating Agent-Impregnated Resins". Analytical Sciences. 4, 505 **(1988)**.

[21] www.srcinc.com (last access October 13th, **2010**).

[22] Junior, A.F.S.; Korn, M.G.A.; Jaeger, H.V.; Silva, N.M.S.; Costa, A.C.S. "Determination of Mn, Cu and Zn in saline matrices by flame atomic absorption spectrometry after separation and preconcentration on Amberlite XAD-7 impregnated with Alizarin Red S". Química Nova. 25, 1086 **(2002)**.

[23] Lopez-Ramon, M.V.; Stoeckli, F.; Moreno-Castilla, C.; Carrasco-Marin, F. "On the characterization of acidic and basic surface sites on carbons by various techniques". Carbon. 37, 1215 **(1999)**.

[24] Langmuir, I. "The adsorption of gases on plane surfaces of glass, mica and platinum" Journal of the American Chemical Society. 40, 1361 **(1918)**.

[25] Freundlich, H. "Über die Adsorption in Lösungen, Zeitschrift für Physikalische Chemie". 57, 385-470 **(1906)**.

[26] Dubinin, M.M. ; Radushkevich, L.V. "Comptes Rendus de l'Académie des Sciences URSS". 55, 327 **(1947)**.

[27] Ciftci, H. ; Yalcin, H. ; Eren, E. ; Olcucu A. ; Sekerci, M. "Enrichment and determination of Ni^{2+} ions in water samples with a diamino-4-(4-nitro-phenylazo)-1H-pyrazole (PDANP) by using FAAS". Desalination. 256, 48 **(2010)**.

[28] Rohm & Haas. "Datasheet of AmberliteTM XAD7HP Industrial Grade Polymeric Adsorbent". Philadelphia, USA. **(2006)**.

[29] Valenzuela-Calahorro, C. ; Navarrete-Guijosa, A.; Stitou, M.; Cuerda-Correa, E.M. "A comparative study of the adsorption equilibrium of progesterone by a carbon black and a commercial activated carbon". Applied Surface Science. 253, 5274 **(2007)**.

[30] Saeed, M.M.; Hasany, S.M.; Ahmed, M. "Adsorption and thermodynamic characteristics of Hg(II)-SCN complex onto polyurethane foam". Talanta. 50, 625 **(1999)**.

[31] Antonio, P.; Iha, K.; Suárez-Iha, M.E.V. "Adsorption of di-2-pyridyl ketone salicyloylhydrazone on silica gel: characteristics and isotherms**".** Talanta. 64, 484 **(2004)**.

[32] de Ridder, D.J.; McConville, M.; Verliefde, A.R.D.; van der Aa, L.T.J.; Heijman, S.G.J.; Verberk, J.Q.J.C.; Rietveld, L.C.; van Dijk, J.C. "Development of a predictive model to determine micropollutant removal using granular activated carbon". Drinking Water Engineering and Science Discussions. 2 ,189 **(2009)**.

[33] Turku, I.; Sainio, T.; Paatero, E. "Thermodynamics of tetracycline adsorption on silica". Environmental Chemistry Letters. 5, 225 **(2007)**.

1.3. NATURAL ADSORBENTS DERIVED FROM TANNIN EXTRACTS FOR PHARMACEUTICAL REMOVAL IN WATER

Novel adsorbents can be synthesized through tannin gelation and they are effective agents for the removal of specific contaminants, for example the pharmaceutical species trimethoprim. The current paper presents an optimization process for obtaining the best adsorbent from four tannin feedstock: *Acacia mearnsii* de Wild, *Schinopsis balansae*, *Cupressus sempervivens* and *Pinus pinaster* bark extract. The cross-linking was undergone with formaldehyde and acetaldehyde; hence the type of aldehyde and its concentration in the gelation mixture were considered operative variables as well as the tannin source. The best categories resulted to be *Cupressus sempervivens* and *Pinus pinaster* with formaldehyde (3.68 mmol pure formaldehyde per g of of tannin extract) and *Schinopsis balansae* with diluted formaldehyde (1 mmol of pure formaldehyde per g of tannin extract). Tannin-derived rigid gels were very effective adsorbents for the removal of this dangerous pharmaceutical: trimethoprim, with maximum adsorption capacities even higher than 300 mg of trimethoprim per g of adsorbent.

Keywords: tannins, trimethoprim, pharmaceutical pollution, natural adsorbents, gelation.

1.3.1. INTRODUCTION.

Pharmaceutical products have become one of the main emerging pollution sources nowadays [1,2]. Their presence in the environment is now a well contrasted fact and they are found almost everywhere in aqueous solution under certain safe limit [3]. The refractory nature of these kind of chemicals and their usage all along the world in large amount [4] have made the scientific community realize this new problem in water treatment is already a real menace. Among all the chemical families related to pharmaceuticals, antibiotics is one of the most relevant types, which are one of the most ubiquitous environmental contaminants [5]. Apart from many others noxious effects, the presence (and uncontrolled disposal) of antibiotics may also accelerate the

development of antibiotic resistance genes and bacteria, which shade health risks to humans and animals [6].

Trimethoprim (TMP) [2,4-diamino-5-(3',4',5'-trimethoxybenzylpyrimidine)] (molecular formula $C_{14}H_{18}N_4O_3$, molecular weight 290.32, CAS Number 738-70-5, pK_a= 7.2) is the model compound in this work. Its chemical structure is presented in Figure 1.13 TMP is one of the most important antibiotics (synthetic antibiotics) used in human and veterinary medicine worldwide acting as an inhibitor in the chemotherapy treatment due to its antifolate effect by interaction with dihydrofolate coenzymes [7-9]. TMP is mainly used in the prophylaxis and treatment of urinary tract infections, as well as for prevention and treatment of respiratory or gastro-intestinal tract infections in cattle, swine and poultry [10].

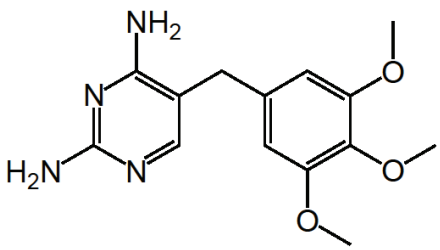

Fig. 1.13. Trimethoprim chemical structure.

In the context of pollution remediation, natural raw materials are an interesting potential source of low-cost adsorbents [11-13]. One class of such materials is that of the *tannins*, a term which covers many families of chemical compounds. Their name comes from their traditional use in tanning animal skins for the production of leather [14], and today they are also widely used in tannin-modified adhesive formulations [15], as adsorbents for pollution control of industrial effluents [16], and as flocculants. Their natural origin is as secondary metabolites of plants [17], occurring in the bark, fruit, leaves, etc. While *Acacia* and *Schinopsis* bark constitute the principal source of tannins for the leather industry, the bark of other, non-tropical trees such as *Quercus ilex*, *Q. suber*, *Q. robur*, *Castanea* sp., and *Pinus* sp. can also be tannin-rich.

Tannin gelation has been widely reported as a procedure that makes tannins insoluble [18] keeping properties available, such as metal chelation. The material resulting from this gelation (sometimes called *tannin rigid resin*) is non-flammable and undeformable [19-21]. Gelation of tannins has been widely described in the scientific literature and in patents. The experimental conditions for gelation may involve the use of formaldehyde or other aldehyde in a basic or acid medium. One may find examples of basic gelation in the scientific literature [22-24], and in patents such as US patent 5,158,711 [25], and acid gelation is described by other workers [16,26].

The chemical bases of the tannin gelation are widely reported [27]. Formaldehyde and other aldehydes react with tannins to induce polymerization through methylene bridge linkages at reactive positions on the tannin flavonoid molecules. The reactive position of the rings depends on the type of tannin, but mainly involves the upper terminal flavonoid units. For example, the A-rings of *Acacia mearnsii* and *Quebracho* tannins show reactivity towards formaldehyde comparable to that of resorcinol. However, aspects such as size and shape make the tannin molecules lose mobility or flexibility at relatively low level of condensation, so that the available reactive sites are too far apart for further methylene bridge formation. The result may be incomplete polymerization and therefore poor material properties. It is needed to search for constitutional differences between several tannin extracts in order to predict the gelated product. E.g., among condensed tannins from mimosa bark (*Acacia mearnsii*) the main polyphenolic pattern is represented by flavonoid analogues based on resorcinol A-rings and pyrogallol B-rings (Figure 1.14). This is similar in the case of *Quebracho* bark extract, but no phloroglucinol A-ring pattern exists in the first or in the second type. However, the A-rings in the tannin molecule posses only the phloroglucinol type of structure, much more reactive towards formaldehyde than resorcinol-type counterpart. A probable mechanism of this gelation process is presented for condensed tannins in Figure 1.15.

According to the electrophilic aromatic substitution theory, hydroxyl groups are activating substituents in ortho and para positions. Therefore, the carbons 6 and 8 in

the A ring can be positions where the molecule of formaldehyde could react to give a CH_2OH group (Figure 1.15, Reaction 1). Subsequently, this new intermediate product can be condensed with a tannin molecule (Reaction 2a) or by self-condensation (Reaction 2b). These new polymerized species have likewise ortho positions with respect to hydroxyl groups, marked by arrows in Figure 1.15. In these positions can again take place the attack of formaldehyde and subsequent condensation of the CH_2OH group, continuing the polymerization chain.

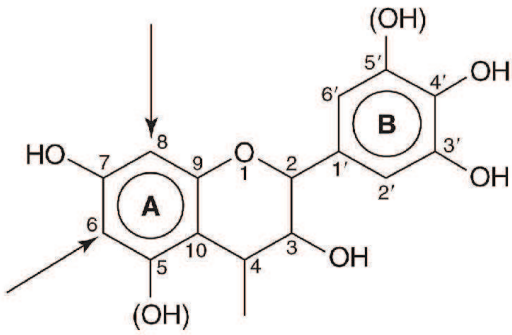

Fig. 1.14. Probable flavonoid constitutional unit in condensed tannins.

Gelation has been reported to be an effective way to remove various pollutants from wastewater because tannin gels are solids with a known negative charged surface [19] and consequently cationic pollutants are expected to be removed by adsorption processes in aqueous solution once the gelation has insolubilized the tannin matrix. One finds many references to metal removal or recovery by means of these novel adsorbents: for example, Pb^{2+}, Cu^{2+}, and Zn^{2+} are described as adsorbing onto *Valonia* tannin resin with an average effectiveness of 100 $mg \cdot g^{-1}$, 25 $mg \cdot g^{-1}$, and 20 $mg \cdot g^{-1}$, respectively [28], and the removal of other metals has been also reported, such as Cr^{6+} and Pd^{2+} [22,23]. Other previous investigations also pointed out their utility in removing dyes [29] or phenols [30].

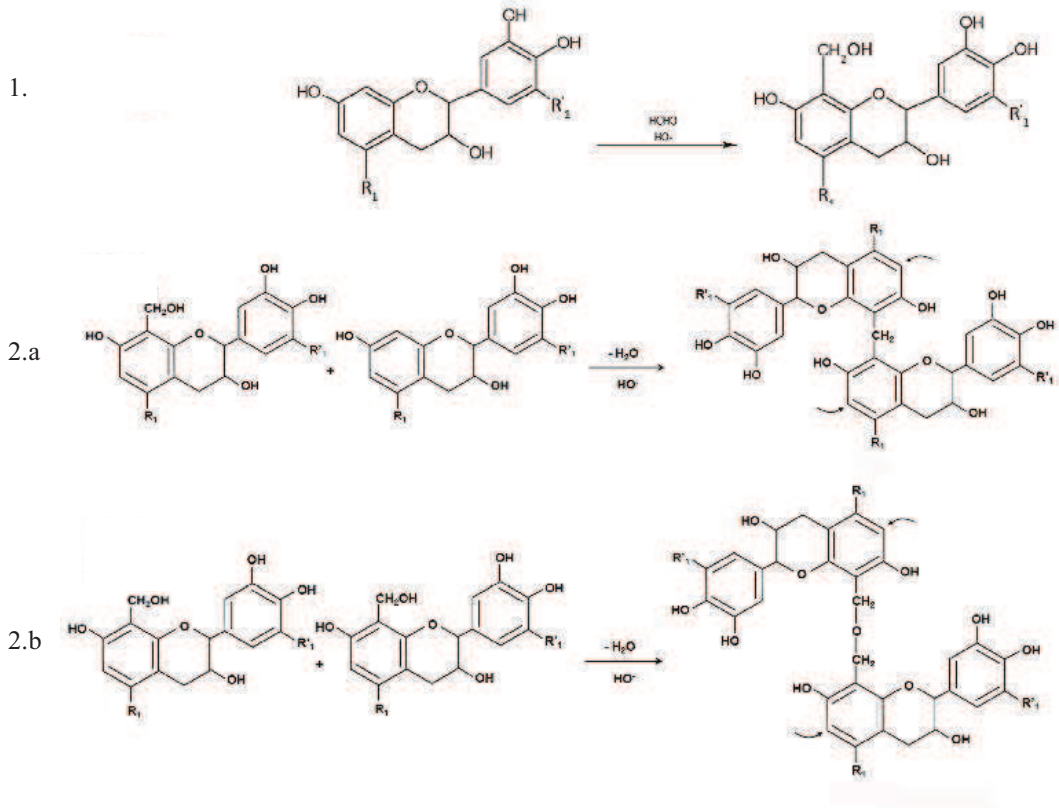

Fig. 1.15. Probable generic gelification mechanism between condensed tannin and formaldehyde. 1) First step: Hydroxy methylation; 2.a) Second step: Methylene bridge immovilization; 2.b.) Methylene ether bridge immovilization.

As far as we know, no previous works were found in pharmaceutical removal by tannin gels. Although adsorption is a well known process for removing these kinds of pollutants [31] and tannin gels were prepared previously in several works [27,29] natural tannin gels were never used with this scope. This article is focused on the evaluation of the ability of different tannin gels in removing trimethoprim from aqueous solutions. The influence of three significant variables in the gelation process is evaluated under a statistical point of view: tannin extract, type of aldehyde and its dose. Many ways of gelifying tannins were studied in the recent past, but no optimization was considered under a statistical point of view. With this scope, we have selected four tannin feedstocks (*Acacia mearnsii*, *Schinopsis balansae*, *Pinus*

pinaster and *Cupressus sempervivens*), two aldehyde (formaldehyde and acetaldehyde) and two aldehyde doses. This procedure will lead us to select the most adequate combination in order to synthesize the best tannin gel for trimethoprim adsorption.

1.3.2. MATERIALS AND METHODS.

1.3.2.1. Tannin extracts.

Tannin extracts were obtained from two main sources:

(1) Commercially available tannin extracts, such as *Acacia mearnsii* de Wild (Weibull black) and *Schinopsis balansae* (Quebracho colorado) were supplied by TANAC (Brazil). They were products involved in the leather treatment and they are presented as powder.

(2) Lab-extracted tannins, such as *Pinus pinaster* (Pine) and *Cupressus sempervivens* (Cypress). They are extracted according to the following procedure [32]: 100 g of bark were milled in a cutting mill (RETSCH, SM 2000 model) and they were put in 600 mL of tap water. Then 5 g of NaOH (PANREAC) were added and the mixture was stirred in magnetic stirrer at 90 ^{o}C for 1 h. Solids were separated by filtration and liquid fraction was dried in oven (65 ^{o}C) overnight. The resultant was considered the *tannin extract*.

1.3.2.2. Tannin gels preparation.

Tannin gels were prepared according to the basis of our previous paper [29]. Five g of tannin extract were dissolved in 32 mL of NaOH (PANREAC) 0.125 $mol{\cdot}L^{-1}$ and 30 mL of distilled water at 80°C. When mixture was homogeneous, certain amount of aldehyde was added and reaction was kept at the same temperature for 8 hours until polymerization was considered completed. The relative amounts of aldehyde were measured as mmol of pure formaldehyde or acetaldehyde per g of tannin extract. Then, the apparent gummy product was lead to complete evaporation of water remain and dried in oven (65 ^{o}C) overnight. After drying, tannin rigid gels were

crushed and sieved to produce 38-53 μm diameter particles. They were washed successively with distilled water and HNO_3 0.01 mol·L^{-1} (PANREAC) to remove unreacted sodium hydroxide. Finally, the adsorbent was dried again in oven. Differences are found between this preparation way and the description made by Yurtsever and Sengil [33], mainly concerning the amount of formaldehyde. Our studies [34,35] established the working range for aldehyde dosage.

1.3.2.3. Trimethoprim stock solution.

TMP was provided by Sigma-Aldrich Spain of the highest purity available (>98% TLC). TMP stock solution was prepared with high purity water obtained from a Millipore Milli-Q system. TMP concentration present in each sample was determined by HPLC in a Waters Chromatograph equipped with a 996 Photodiode Array Detector and a Waters Nova-Pak C18 Column (5 μm 150×3.9 mm). It displayed a well defined peak for TMP at a retention time of 4.9 min at 277 nm. For these analyses, samples of 100 μL were injected into the chromatograph and a 30:70 (v/v) methanol/water (10^{-2} M orthophosphoric acid) mixture was passed at a flow rate of 1 mL·min^{-1} as mobile phase.

1.3.2.4. General adsorption test.

In order to test the ability of each tannin gel in the removal of TMP, a standard protocol of adsorption was developed. Samples of aqueous solutions with the corresponding pollutant were put into 100 mL flask under strict thermal control (20 ºC) and pH 7 in distilled water (no salt addition). A fixed amount of tannin gel was added to each flask (20 mg) with different volumes of contaminated aqueous solutions. Preliminary data were obtained in previous researching stages (data not shown) and they supported the equilibrium period of two weeks. Magnetic stirring was applied and the concentrations of the model compound before and after the trial were determined.

1.3.2.5. Statistical procedure.

Design of experiments was carried out by using *SPSS 15.0 for Windows* [36]. Two replicates of each tannin gel combination were synthesized, and each one was tested twice. The bases of the statistical method are found in the interaction of variables. Briefly, it can be summarized as follows:

(1) Up to thirteen different combinations regarding three variables (tannin extract, aldehyde type and aldehyde dosage) were attempted. The feasible combinations were just nine of them; the rest did not gelify (Table 1.8).

(2) As long as it is not possible to test every combination since there are some of them that did not drive to a solid product, the whole system was considered as a *categorical design*, that is, no different variables are observed but nine different categories can be put into relationship, so an optimum point should be obtained.

(3) Inside this hypothesis, the two replicates of each product must be compared in order to establish if significative differences can be observed. If no, then one can work under the assumption that each replicate is indistinguishable from the other, so four tests of each tannin gel on the adsorption of each model compound are taken into account.

(4) Categorical box-and-whisker plot of the whole system can be established, so an optimum appears.

1.3.2.6. Physical characterization of tannin gels.

In order to characterize the main adsorbent aspect of the tannin gels, porosimetry and scanning electron microscopy were carried out. For the porosimetry study, a Quantachrome PoreMaster apparatus was used. The BET surface area was determined with an AUTOSORB AS-1. SEM images were taken using Field Emission Gun (mod. HITACHI S-4800) microscopy. Samples were pre-treated with chrome sputtering.

Table 1.8. Gelification Experiments.

Tanin extract	Formaldehyde ($mmol \cdot g^{-1}$)	Acetaldehyde ($mmol \cdot g^{-1}$)	Does it gelify?	Symbol
Cypress	1	0	No	
Cypress	3.68	0	Yes	CFC
Quebracho	1	0	Yes	QFD
Quebracho	3.68	0	Yes	QFC
Quebracho	0	1.30	No	
Quebracho	0	4.85	No	
Pine	3.68	0	Yes	PFC
Pine	1	0	Yes	PFD
Pine	0	4.85	No	
Weibull black	1	0	Yes	WFD
Weibull black	3.68	0	Yes	WFC
Weibull black	0	1.30	No	
Weibull black	0	4.85	yes	WAC

1.3.3. RESULTS AND DISCUSSION.

The usual way of evaluating the efficacy of the adsorption processes implies the q capacity. It is defined according the Eq. (1.17):

$$q = \frac{(C_o - C_1) \cdot V}{W} \tag{1.17}$$

where C_0 is initial pollutant concentration, ($mg \cdot L^{-1}$), C_l is equilibrium pollutant concentration in bulk solution, ($mg \cdot L^{-1}$), V is the volume of solution, (L), and W is

adsorbent mass (g). q capacity allows the evaluation of the efficiency of the removal: The higher q, the more efficient the adsorbent is.

The adsorption process in these kinds of adsorbents usually follows responds to chemisorption patterns according to previous works [37-38]. It involves chemical reaction between the active centers in the adsorbate and the ones placed onto the adsorbent surface. This is consistent with the experimental results we have obtained regarding the low kinetics and the stability of the adsorption mechanism, which seems to be irreversible.

1.3.3.1. Preliminary gelation procedure.

Table 1.8 gives the main data of the experimental planification. Three qualitative variables were considered: tannin extract, type of aldehyde and dosage of this last one. Bearing in mind this general framework, not all the possible combinations drove to a satisfactory gelation product. It is clear that acetaldehyde presents a weak polymerization action if compared with formaldehyde: all acetaldehyde combination but WAC resulted unfeasible. This can be due to the specific structure of the aldehyde, two carbon atoms make a longer molecule that surely present less reactivity in the crosslinking process. The large majority of the authors performed this process only with formadehyde [39,19] although the possibility of using other aldehydes is referenced since long time ago [18]. The reactivity level of acetaldehyde drives to the need of a large amount of tannin extract from Weibull black (in addition, the most tannin-rich extract [17]) and a high aldehyde ratio (4.85 $mmol \cdot g^{-1}$) for producing WAC.

Regarding the gelation through formaldehyde polymerization, all the possible combinations are feasible and solid *tannin gels* are produced, but significative differences are observed between them in terms of efficiency in the TMP removal. When dealing with natural raw materials, such as these tannin extracts, the intrinsic composition of each product may differ due to the purification process (if any) or to the extraction method and it is very difficult and expensive isolating tannins chemically pure [40]. The polymerization of tannins with this aldehyde is previously

referred in similar works [29,41-43], but no quantitative studies were carried out regarding the aldehyde-tannin ratio.

1.3.3.2. Indistinguishable observation.

Following the statistical procedure one must check the reproducibility of the synthesis that is the scope of replicating each tannin gel twice. If ANOVA test gives a p-value above 0.05, no difference can be observed between the two replicates, so they are indistinguishable. Significativity level was stated at 0.05, so 95% of confidence is obtained in statistical conclusions. ANOVA tests includes two main variables in this step: *Tannin*, which means the specific extract and *Replicate*, the current replicate (first or second one). Actually, the ANOVA test shows p-values equal to 0.18 for *Replicate* variable, 0.63 for intersection *Tannin×Replicate* and 0 for *Tannin*. This presents the efficient inclusion of the *Tannin* variable in the general statistical model and the indistinguishability of the replicates. Statistical corrected r^2 value reaches 0.91. Consequently, both replicates can be considered as part of a sole experiment with up to four tests and the model is consistent. A graphical representation of this situation is presented in Figure 1.16.

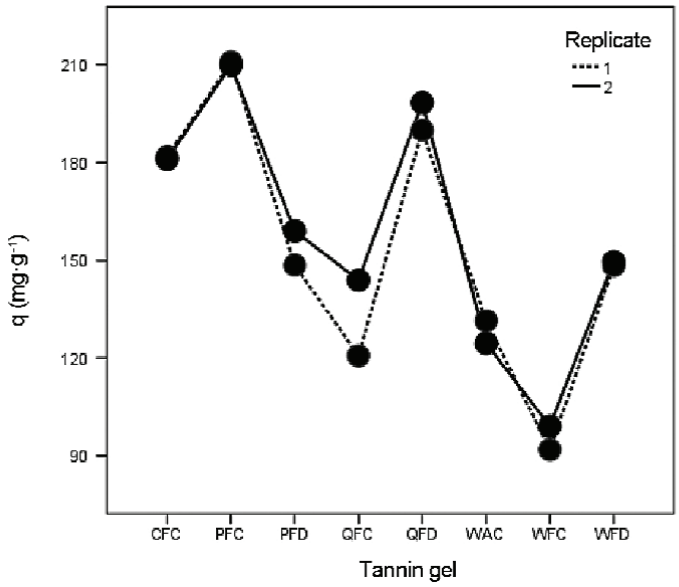

Fig. 1.16. Comparison of the two replicates of each combination tannin-aldehyde.

1.3.3.3. Optimal adsorbents.

The particular analysis of the target variable can lead to the identification of several combinations that seem to work better regarding the removal of the studied contaminant agents. The specific graphic plot is presented in Supporting Information (Box-and-Whisker plot, Fig. S.1.6)). Moreover, homogeneous subsets in Tukey's test for multiple comparison gives the idea of functional groups regarding the elimination of TMP (Table S.1.5 in Supporting Information).

Feasible combinations are divided into five different groups according to the general consideration of significativity level. The statistical p-value of Tukey multiple comparison test is the numerical criteria for classify the eight adsorbent products. Group 4 and 5 include the best adsorbents, this is, the optimal categories. CFC, QFD and PFC are presented as the best adsorbents within the two last groups. There is no statistical difference between CFC and QFD (p-value equal to 0.68, above 0.05) and between QFD and PFC (p-value of 0.40). However, the best adsorbent is this last one, with an average q capacity of 210.4 $mg \cdot g^{-1}$.

1.3.3.4. Physical characterization of tannin gels.

Subsequently, the characterization of the three optimal *tannin gel* and a fourth one (WFC, for including a sample of each tannin extract) was carried out. Three main determinations were made on the representative samples of each different tannin sources: SEM, BET surface area and porosimetry studies (histogram of pore size). The bulk density of these *tannin gels* are quite similar amongst them all, with a mean value of 1.43 $g \cdot cm^{-3}$ inside the range of 1.35-1.58. As a matter of fact, just comparative studies can be made in order to explain the slow kinetics and the high adsorbent q capacity. Firstly, a graphical approach to the nature of the rigid gels was carried out with the SEM images that are shown in Supporting information (Fig. S.1.7). Significant differences are presented in each case. The four *tannin gels* are quite similar in their macroscopic structure and appearance (rigid and non-porous aspect). However, PFC seemed to be rather different in its mechanical properties; it is more brittle. This means the polymerization was carried out in a different way with *Pinus*

pinaster and in the rest of the tannin resins, surely due to the polyphenolic nature of the tannin extracts.

BET surface area was determined for the four types of adsorbents. The specific values of this parameter were 6 $m^2 \cdot g^{-1}$ for WFC, 5 $m^2 \cdot g^{-1}$ for PFC, and 2 $m^2 \cdot g^{-1}$ for both CFC and QFC. These are very low surface values if compared with the normal BET surfaces areas that are obtained with other natural raw materials, e.g. such as *Moringa oleifera* [44] or activated carbon from coconut husk [45]. Regarding other similar materials, such as the classical resorcinol-formaldehyde resins or *xerogels*, the BET surface area that these *tannin gels* presented were significantly lower [46,47]. These differences may be due to the absence of catalyst [48] and in the fact that natural raw materials included a large amount of impurities that difficults the pore development [49]. Similar works, such as those presented by Sengil and Özacar [28,43] and Yurtsever and Sengil [33] also confirmed our results. In these works, *tannin gels* were obtained from valonia, mimosa (*Acacia*) and quebracho tannin extracts in a very similar way. BET surface area of these materials were 11.7, 13 and 0.82 $m^2 \cdot g^{-1}$ respectively. Further studies must be carried out in order to increase the BET surface area by means of gasification or other procedures, as some relevant authors have recently proposed [50,51].

Finally, the pore size distribution was determined and these results are also presented in Figure S.1.8 in Supporting information. These graphics show the normalized pore volume linked to the pore diameter. According to the general classification of pores, microporosity appears when pores are narrower than 2 nm, mesopores are within the range of 2-50 nm and macropores are wider than 50 nm. Pore distribution for the four products reveals just a small mesoporosity, since the majority of the pore volume (in the end of the histogram) corresponds to the void spaces between granules. This is the typical histogram for a nonporous material, as these adsorbents seem to be.

1.3.3.5. Adsorption characterization of the optimal categories.

The three optimal categories (PFC, QFD and CFC) were studied in their adsorption performance. Two main aspects were included at this point: adsorption kinetics of TMP and equilibrium theoretical modelization.

Kinetics of TMP removal.

In a first approach, one must observe the shape of the representative curve (adsorption capacity versus time). Three curves can be drawn for each CFC, QFD and PFC. As an example the one that belongs to CFC is presented in Figure 1.17 and the rest of them are presented in Supporting Material (Fig. S.1.9. and Fig. S.1.10). It is clear that the adsorption process is performed in two different stages: one fast adsorption (during the first 10 hours) where the large majority of the pollutant is adsorbed onto the *tannin gel*; and a second one more slowly, that lasts for the rest of the experimental period.

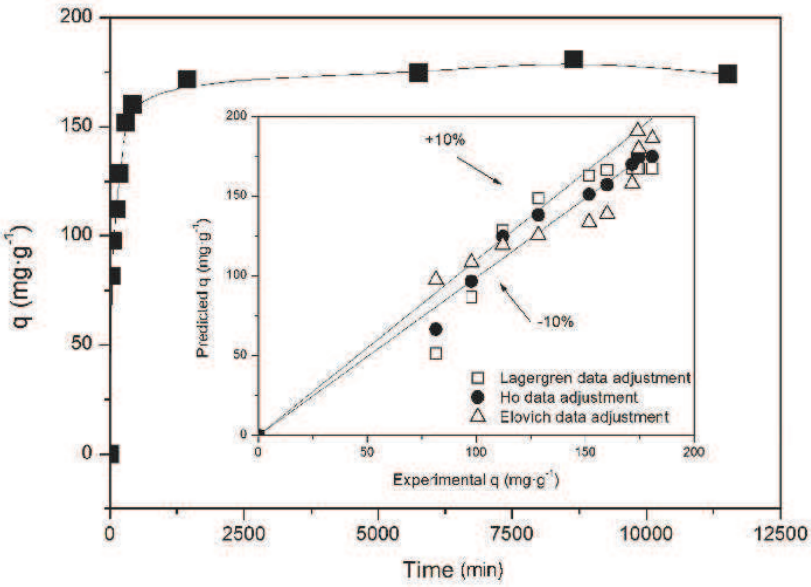

Fig. 1.17. Kinetics of TMP adsorption onto CFC. Secondary graphic: predicted vs. experimental capacity, filled symbols for best fit model.

The first rapid increase of q can be attributed to the free non-porous surface, which is almost the total of the BET area. The slow diffusion through the small mesoporosity (as presented in Supporting Material) should be responsible of the final increase of q during the last part of the adsorption process.

Three theoretical models have been considered for explaining the adsorption phenomenon: *Lagergren* pseudo-first order [52]; H_o pseudo-second order [53] and *Elovich* model [54].

Pseudo-first order: Lagergren model.

The *Lagergren* Eq. [1.18] is one of the most widely used adsorption rate equations for the adsorption of solute from a liquid solution. The modified first order kinetic model of *Lagergren* may be represented by the following Equation (1.18):

$$\frac{dq}{dt} = k_1 \cdot (q_e - q) \tag{1.18}$$

where q is the adsorption capacity defined according to Eq. (1.17), (mg of pollutant·(g of adsorbent)$^{-1}$); k_l is the first order *Lagergren* constant, (min^{-1}); q_e is the equilibrium q capacity, (mg of pollutant·(g of adsorbent)$^{-1}$); and t is the contact time, (min).

Integrating this equation with the boundary conditions t= 0 to t= ∞ and consequently q= 0 to q= q_e, gives Eq. (1.19):

$$q = q_e - q_e \cdot e^{-k_l \cdot t} \tag{1.19}$$

which can be used in a nonlinear adjustment in order to determine q_e and k_l .

Pseudo-second order: Ho model.

The second order kinetic model is expressed as Eq. (1.20):

$$\frac{dq}{dt} = k_h \cdot (q_e - q)^2 \tag{1.20}$$

Rearranging the variables and taking into account similar boundary conditions as in Eq. (1.18), second order model can be represented by the Eq. (1.21):

$$q = \frac{t}{\frac{1}{h} + \frac{t}{q_e}} \tag{1.21}$$

where h is the initial adsorption rate, defined as Eq. (1.22):

$$h = k_h \cdot q_e^{\ 2} \tag{1.22}$$

and k_h is the second order constant ($g \cdot mg^{-1} \cdot min^{-1}$).

<u>*Elovich model.*</u>

The *Elovich* model is presented by the Eq. (1.23):

$$\frac{dq}{dt} = \alpha \cdot e^{-\beta \cdot q} \tag{1.23}$$

where α is the initial adsorption rate ($mg \cdot g^{-1} \cdot min^{-1}$), and β is the desorption constant, ($g \cdot mg^{-1}$).

Integrating within the boundary conditions $q = 0$, $t = 0$ and $q = q_e$, $t = \infty$, expresion (1.23) yields to the linear form (Eq. (1.24)):

$$q = \frac{1}{\beta_E} \cdot \ln(\alpha_E \cdot \beta_E) + \frac{1}{\beta_E} \cdot \ln t \tag{1.24}$$

The applications of these three models have been carried out by a non-linear adjustment and results are presented in Figure 1.17 and in the Supporting Material. As can be appreciated, the three of them fit reasonably well to the experimental situations, so regression coefficient r^2 may be considered in order to discriminate the goodness of each data fit. Table 1.9 refers these data about the specific parameters and r^2. In addition, each figure presents the best fit through filled symbols.

According to r^2 values of each model, the three models explain rather well the adsorption process, since r^2 values are high enough.

Bearing in mind these kinetic data, further experiments were carried out for the duration of 15 days in total to guarantee the chemical equilibrium was achieved. This is the main challenge to work on because it is needed to obtain tannin gels with higher reactivity to the adsorbates and faster kinetics therefore. There are already several approaches [50] but it is still the objective for further studies.

Table 1.9. Kinetics Parameters[a].

Tannin adsorbent	Lagergren	Ho	Elovich
CFC	q_e=167.2; k_l=1.22·10^{-2}; r^2=0.93	q_e=175.5; h=3.58 k_h=1.59·10^{-5}; r^2=0.98	α_E=269.6; β_E=6.42·10^{-2}; r^2=0.85
QFD	q_e=193.0; k_l=6.77·10^{-3}; r^2=0.99	q_e=203.4; h=2.03 k_h=4.91·10^{-5}; r^2=0.98	α_E=18.96; β_E=4.42·10^{-2}; r^2=0.79
PFC	q_e=188.6; k_l=2.24·10^{-3}; r^2=0.95	q_e=204.2; h=0.76 k_h=1.86·10^{-5}; r^2=0.98	α_E=2.64; β_E=3.22·10^{-2}; r^2=0.99

[a]Units in text.

Equilibrium studies and theoretical model.

In order to characterize even more the adsorption phenomenon, a theoretical model which explains the TMP removal by the action of these adsorbents must be performed. For this scope, the Langmuir model was used. Experiments were carried out at 20 ºC and pH 7 for at least two weeks, in order to complete the adsorption process and reach equilibrium.

Langmuir and *Freundlich* adsorption models were considered in the present work. The first assumes that the molecules striking the surface have a given probability of adsorbing. Molecules already adsorbed similary have a given probability of desorbing. At equilibrium, equal numbers of molecules desorb and adsorb at any time. The probabilities are related to the strenght of the interaction between the adsorbent

surface and the adsorbate [55]. By means of Eq. (1.25) is possible to confirm the suitability of this model to the experimental data, although several different adsorption processes can parallely occur.

$$q = q_{\max} \frac{C_l}{b + C_l} \tag{1.25}$$

where q_{max} is the asymptotic value of the adsorption capacity ($mg \cdot g^{-1}$), and b is the *Langmuir* adsorption constant ($mg \cdot L^{-1}$).

Another theoretical hypothesis is *Freundlich* model, which was derived from empirical data [56] and assumes that q capacity is a power function of the equilibrium TMP concentration (C_l). That is what Eq. (1.26) express:

$$q = k_f \cdot C_l^{\,n_f} \tag{1.26}$$

where n_f is the *Freundlich* adsorption order (dimensionless) and k_f is the *Freundlich* adsorption constant ($[L^{nf}] \cdot g^{-1} \cdot [mg^{nf\,-1}]$).

Presenting linearized expression of both models is quite normal and it gives the goodness of the data fit, but non linear adjustment is preferred in order to the reliability of the parameters in any case [57]. Figure 1.18 depicts the adsorption isotherms for pollutant removal. Experimental points are placed onto the predicted path for *Langmuir* and *Freundlich* adsorption hypotheses, according to a very high regression level.

Attending to the r^2 values in Table 1.10, which are relative to the accuracy of the non linear regression, both models fit rather well since these values are always above 0.95. Moreover, there is no analytical criteria for selecting one model or other because the average r^2 are almost the same (0.97) in both cases. However, at a first glance, the three isotherms present the typical shape of L-class in the specific classification made by Giles [58]: a concave initial region followed by a saturation zone in the last part of the curve. This is usual in those systems where the adsorption becomes more difficult as the pollutant concentration increases and leads to a final equilibrium asymptote. Table 1.10 also shows the rest of the regression parameters, such as q_{max} and b for

Langmuir model. As can be seen, PTG presents a quite higher capacity inside the working range.

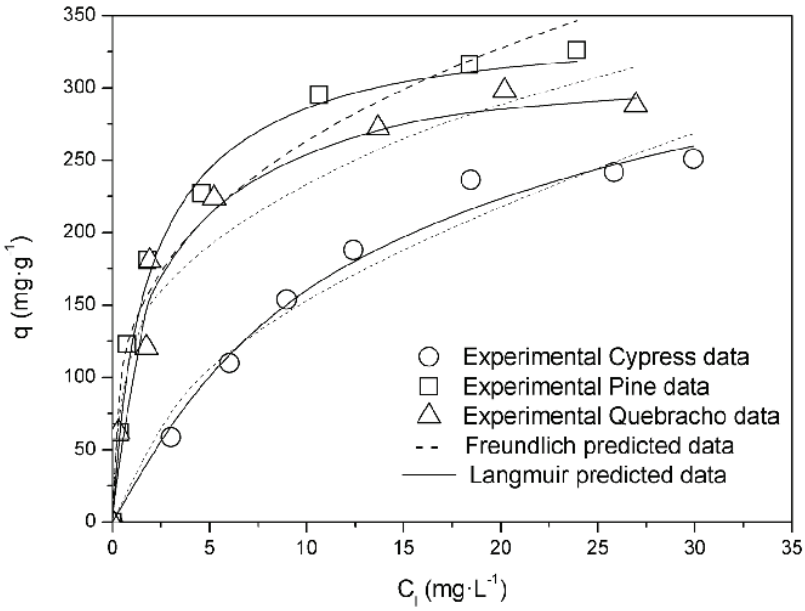

Fig. 1.18. Equilibrium studies on TMP adsorption onto the three optimal tannin gel.

Maximum adsorption capacity gives us an idea of how efficient is certain material if compared with other ones. There are several interesting previous works on the removal of TMP with other adsorbents. Table 1.11 shows some of them that reported adsorption capacities. If compared with the final values in Table 1.10, one can realize that the efficiencies obtained with *tannin gels* are significantly higher than the capacities obtained with other different materials, such as activated carbon, clays or synthetic polyacrylamide resins. The referenced works presented maximum adsorption capacities between 5 and 257 $mg \cdot g^{-1}$ in the best possible conditions, therefore the comparison with our own results is consistent. The current work obtained a very competitive adsorption capacity (over 370 $mg \cdot g^{-1}$ in the case of CFC), which is higher than the rest of data. *Pinus tannin gel* is also very interesting, with a maximum adsorption capacity over 340 $mg \cdot g^{-1}$.

Table 1.10. Theorical Models Nonlinear Fitting Parameters[a].

Model	Tannin gel	Parameter values	r^2
Langmuir	CFC	q_{max}=373.6; b=13.1	0.98
	QFD	q_{max}=313.4; b=1.90	0.96
	PFC	q_{max}=340.1; b=1.63	0.98
Freundlich	CFC	k_f=47.6; n_f=0.51	0.97
	QFD	k_f=135.8; n_f=0.29	0.98
	PFC	k_f=126.3; n_f=0.27	0.97

[a]Units in text.

Table 1.11. Comparison with Other Adsorbents.

Adsorbent	Maximum adsorption capacity ($mg \cdot g^{-1}$)	Reference
Aluminum-derived clay Al-KSF	5	59
Aluminum-derived clay Al-K10	18	59
Shyntetic resin Amberlite XAD-7	45	60
Montmorillonite clay KSF	50	7
Activated powdered carbon	257	61
Cypress tannin gel	373	This work

Tannin gels were previously tested in other own papers and they presented there promising capacities [35,37,38]. This research confirms the feasibility of these adsorbents in the removal of modern and recalcitrant pharmaceutical pollutants.

1.3.4. CONCLUSIONS.

Natural raw materials, such as tannin-derived gels, should be studied as a source of novel adsorbent agents, in order to obtain new cheaper remediation processes for wastewater. Considering up to four tannin types and two combinations of aldehyde compounds, a factorial design has pointed out the best tannin extract for this scope was *Pinus pinaster* with concentrated formaldehyde. *Cypress sempervivens* and *Schinopsis balansae* also presented high adsorbent products. These tannin gels are able to retain between 313 and 370 $mg \cdot g^{-1}$, according to a *Langmuir* general adsorption behaviour. Further studies must be developed in order to characterize and optimize even more these kinds of adsorbent.

1.3.5. SUPPORTING INFORMATION.

1.3.5.1. Statistical assessment.

Table S.1.5. Turkey´s homogeneous group.

	Turkey´s subgroup				
Tannin adsorbent	**1**	**2**	**3**	**4**	**5**
WFC	95.5				
WAC		128.0			
QFC		132.3	132.3		
WFD		149.0	149.0		
PFD			153.7		
CFC				181.4	
QFD				194.2	194.2
PFC					210.4
Significativity	1	0.13	0.12	0.68	0.40

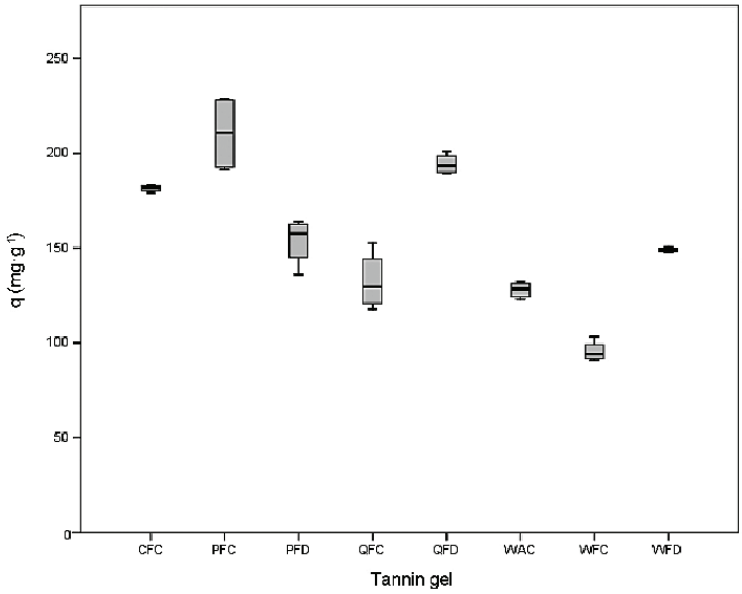

Fig. S.1.6. Box-and-whisker plot for the eight products in adsorption treatment of Trimethoprim.

1.3.5.2. Physical characterization of tannin gels.

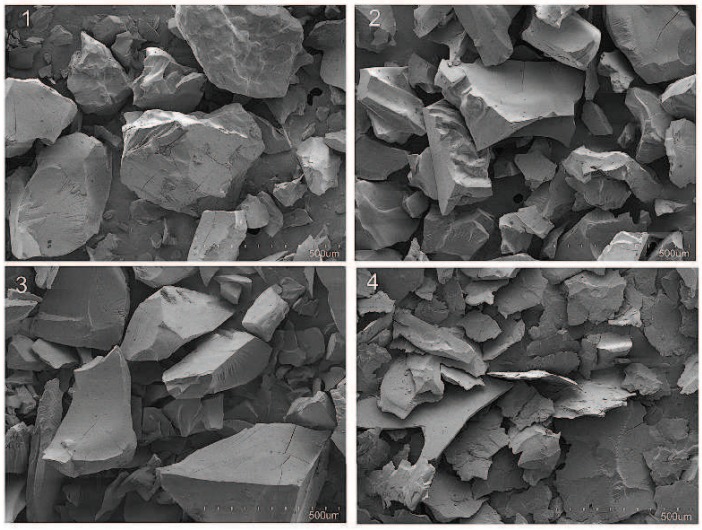

Fig. S.1.7. SEM images of 1) CFC, 2) QFD, 3) WFC and 4) PFC. The specific conditions of these photographs were Vacc.= 1 kV; Mag.= x100 and working distance= 15 mm.

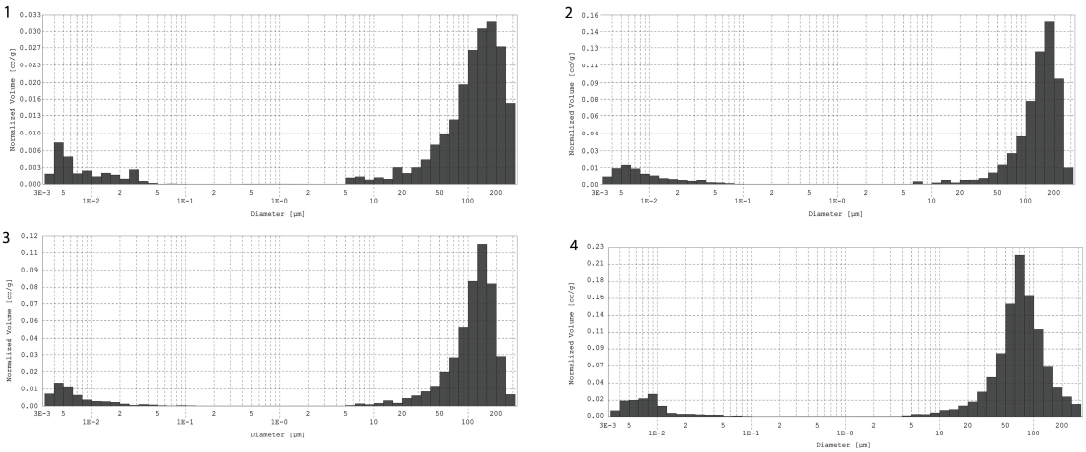

Fig. S.1.8. Normalized pore histogram of 1) CFC, 2) QFD, 3) WFC and 4) PFC.

1.3.5.3. Kinetics of Quebracho and Pine.

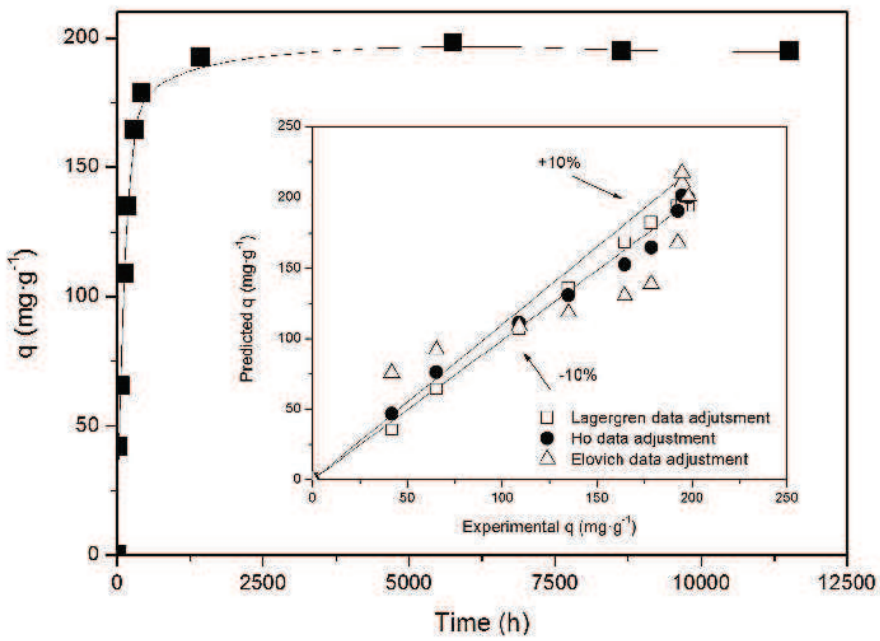

Fig. S.1.9. Kinetics of TMP adsorption onto QFD. Secondary graphic: predicted vs. experimental capacity, filled symbols for best fit model.

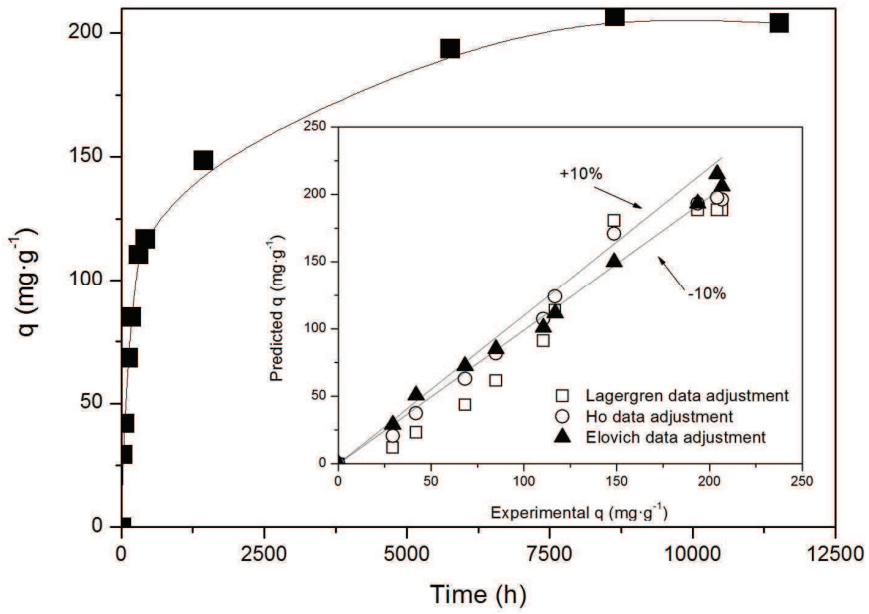

Fig. S.1.10. Kinetic of TMP adsorption onto PFC. Secondary graphic: predicted vs. experimental capacity, filled symbols for best fit model.

1.3.6. REFERENCES

[1] Kümmerer, K. "Antibiotics in the aquatic environment - A review - Part I". Chemosphere. 75, 417 **(2009)**.

[2] Kümmerer, K. "Antibiotics in the aquatic environment - A review - Part II". Chemosphere. 75, 435 **(2009)**.

[3] Velagaleti, R.; Burns, P.K.; Gill, M.; Prothro, J. "Impact of current good manufacturing practices and emission regulations and guidances on the discharge of pharmaceutical chemicals into the environment from manufacturing, use, and disposal". Environmental Health Perspectives. 110, 213 **(2002)**.

[4] Holm, J.V.; Ruegge, K.; Bjerg, P.L.; Christensen, T.H. "Occurrence and distribution of pharmaceutical organic compounds in the groundwater downgradient of a landfill (Grindsted, Denmark)". Environmental Science and Technology. 29, 1415 **(1995)**.

[5] Real, F.J.; Benítez, F.J.; Acero, J.L.; Sagasti, J.J.P.; Casas, F. "Kinetics of the chemical oxidation of the pharmaceuticals primidone, ketoprofen and diatrizoate in ultrapure and natural waters". Industrial & Engineering Chemistry Research. 48, 3380 **(2010)**.

[6] Kemper, N. "Veterinary antibiotics in the aquatic and terrestrial environment". Ecological Indicators. 8, 1 **(2008)**.

[7] Bekçi, Z.; Seki, Y.; Yurdakoç, M.K. "Equilibrium studies for trimethoprim desorption on montmorillonite KSF". Journal of Hazardous Materials. 133, 233 **(2006)**.

[8] Diaz-Cruz, M.S.; Lopez de Alda, M.J.; Barcelo, D. "Environmental behavior and analysis of veterinary and human drugs in soils, sediments and sludge". Trends in Analytical Chemistry. 22, 340 **(2003)**.

[9] Batt, A.L.; Aga, D.S. "Simultaneous analysis of multiple classes of antibiotics by ion trap LC/MS/MS for assessing surface water and groundwater contamination". Analytical Chemistry. 77, 2940 **(2005)**.

[10] De Paula, F.C.C.R.; De Pietro, A.C.; Cass, Q.B.J. "Simultaneous quantification of sulfamethoxazole and trimethoprim in whole egg samples by column-switching high-performance liquid chromatography using restricted access media column for on-line sample clean-up". Journal of Chromathography A. 1189, 221 **(2008)**.

[11] Altenor, S.; Carene, B.; Emmanuel, E.; Lambert, J.; Ehrhardt, J.J.; Gaspard, S. "Adsorption studies of methylene blue and phenol onto *vetiver* roots activated carbon prepared by chemical activation". Journal of Hazardous Materials. 165, 1029 **(2009)**.

[12] Demirbas, A. "Heavy metal adsorption onto agro-based waste materials: A review". Journal of Hazardous Materials. 157, **(2008)**.

[13] Pavan, F.A.; Mazzocato, A.C.; Gushikem, Y. "Removal of methylene blue dye from aqueous solutions by adsorption using yellow passion fruit peel as adsorbent". Bioresource Technology. 99, 3162 **(2008)**.

[14] Covington, A.D. "Modern tanning chemistry". Chemical Society Reviews. 26, 111 **(1997)**.

[15] López-Suevos, F.; Riedl, B. "Effects of *pinus pinaster* bark extracts content on the cure properties of tannin-adhesives and on bonding of exterior grade MDF". Journal of Adhesion Science and Technology. 17, 1507 **(2003)**.

[16] Vázquez, G.; González-Álvarez, J.; Freire, S.; López-Lorenzo, M.; Antorrena, G. "Removal of cadmium and mercury ions from aqueous solution by sorption on treated *Pinus pinaster* bark: kinetics and isotherms". Bioresource Technology. 82, 247 **(2002)**.

[17] Schofield, P.; Mbugua, D. M.; Pell, A.N. "Analysis of condensed tannins: A review". Animal Feed Science and Technology. 91, 21 **(2001)**.

[18] Pizzi, A. "Advanced Wood Adhesives Technology". Marcel Dekker, New York. **(1994)**.

[19] Tondi, G.; Zhao, W.; Pizzi, A.; Du, G.; Fierro, V., Celzard, A. "Tannin-based rigid foams: A survey of chemical and physical properties". Bioresource Technology. 100, 5162 **(2009)**.

[20] Zhao, W.; Fierro, V.; Pizzi, A.; Du, G.; Celzard, A. "Effect of composition and processing parameters on the characteristics of tannin-based rigid foams. Part II: Physical properties". Materials Chemistry and Physics. 123, 210 **(2010)**.

[21] Ping, L.; Brosse, N.; Chrusciel, L.; Navarrete, P.; Pizzi, A. "Extraction of condensed tannins from grape pomace for use as wood adhesives". Industrial Crops and Products. 33, 253 **(2011)**.

[22] Nakano, Y.; Takeshita, K.; Tsutsumi, T. "Adsorption mechanism of hexavalent chromium by redox within condensed-tannin gel". Water Research. 35, 496 **(2001)**.

[23] Kim, Y-H; Nakano. Y. "Adsorption mechanism of palladium by redox within condensed-tannin gel". Water Research. 39, 1324 **(2005)**.

[24] Tondi, G.; Oo, C.W.; Pizzi, A.; Thevenon, M.F. "Metal absorption of tannin-based rigid foams". Industrial Crops and Products. 29, 336 **(2009)**.

[25] Shirato, W.; Kamei, Y. "Insoluble tannin preparation process, waste treatment process and adsorption process using tannin". US patent 5. 158, 711 **(1992)**.

[26] Vázquez, G.; Antorrena, G.; González, J.; Doval, M. D. "Adsorption of heavy metal ions by chemically modified *Pinus pinaster* bark". Bioresource technology. 48, 251 **(1994)**.

[27] Pizzi, A. "Tannins: major sources, properties and applications". In Belgacem M. and Galdini, A., editors, Monomers, Polymers and Composites from Renewable Sources. Elsevier, Amsterdam. **(2008)**.

[28] Sengil, I.A., Özacar, M. "Competitive biosorption of Pb^{2+}, Cu^{2+} and Zn^{2+} ions from aqueous solutions onto valonia tannin resin". Journal of Hazardous Materials. 166, 1488, **(2009)**.

[29] Sánchez-Martín, J.; González-Velasco, M.; Beltrán-Heredia, J.; Gragera-Carvajal, J.; Salguero-Fernández, J. "Novel tannin-based adsorbent in removing cationic dye (methylene blue) from aqueous solution". Kinetic and equilibrium studies. Journal of Hazardous Materials. 174, 9 **(2010)**.

[30] Vázquez, G.; Alonso, R.; Freire, S.; González-Álvarez, J.; Antorrena, G. "Uptake of phenol from aqueous solutions by adsorption in a *Pinus pinaster* bark packed bed". Journal of Hazardous Materials. 133, 61 **(2006)**.

[31] Stackelberg, P.E.; Gibs, J.; Furlong, E.T.; Meyer, M.T.; Zaugg, S.D.; Lippincott, R.L. "Efficiency of conventional drinking-water-treatment processes in removal of pharmaceuticals and other organic compounds". Science of the Total Environment. 377, 255 **(2007)**.

[32] Vázquez, G.; González-Álvarez, J.; Freire, S.; López-Suevos, F.; Antorrena, G. "Characteristics of *Pinus pinaster* bark extracts obtained under various extraction conditions". European Journal of Wood and Wood Products. 59, 451 **(2001)**.

[33] Yurtsever, M.; Sengil, I.A. "Biosorption of Pb (II) ions by modified quebracho tannin resin". Journal of Hazardous Materials. 163, 58 **(2009)**.

[34] Beltrán-Heredia, J.; Sánchez-Martín, J.; Carmona-Murillo, C. "Adsorbents from *Schinopsis balansa*: Optimisation of significant variables". Industrial Crops and Products. 33, 409 **(2011)**.

[35] Sánchez-Martín, J.; Beltrán-Heredia, J.; Gibello-Sánchez, P. "Adsorbent biopolymers from tannin extracts for water treatment". Chemical Engineering Journal. 168, 1241 **(2011)**.

[36] SPSS Inc. SPSS 14.0 Developer's guide. Chicago, Illinois **(2005)**.

[37] Beltrán-Heredia, J.; Sánchez-Martín, J.; Gragera-Carvajal, J. "*Caesalpinia spinosa* and *Castanea sativa* tannins: a new source of biopolymers with adsorbent capacity. Preliminary assesment on cationic dye removal". Industrial Crops and Products. 34, 1238 **(2011)**.

[38] Sánchez-Martín, J.; González-Velasco, M.; Beltrán-Heredia, J. "Adsorbent derived from *Pinus pinaster* tannin for cationic surfactant removal". Journal of Wood Chemistry and Technology. In press, corrected proof **(2011)**.

[39] Morisada, S.; Kim, Y-H.; Ogata, T.; Marutani, Y.; Nakano, Y. "Improved adsorption behaviors of amine-modified tannin gel for palladium and platinum ions in acidic chloride solutions". Industrial & Engineering Chemistry Research. 50, 1875 **(2011)**.

[40] Galvez Garro, J.M.; Riedl, B.; Conner, A.H. "Analytical studies on tara tannins". Holzforschung. 51, 235 **(1997)**.

[41] Meikleham, N. E.; Pizzi, A. "Acid and alkali catalyzed tannin-based rigid foams". Journal of Applied Polymer Science. 53, 1547 **(1994)**.

[42] Pizzi, A. "Natural phenolic adhesives I: Tannin". In Pizzi, A. and Mittal, K.L., editors, Handbook of Adhesive Technology, 2nd edition. 573. Marcel Dekker, New York **(2003)**.

[43] Sengil, I.A.; Özacar, M. "Biosorption of Cu(II) from aqueous solutions by mimosa tannin gel". Journal of Hazardous Materials. 157, 277 **(2008)**.

[44] Pollard, S.J.T.; Thompson, F.E.; McConnachie, G.L. "Microporous carbons from *Moringa oleifera* husks for water purification in less developed countries". Water Research. 29, 337 **(1995)**.

[45] Tan, I.A.W.; Ahmad, A.L.; Hameed, B. H. "Adsorption of basic dye on high-surface- area activated carbon prepared from coconut husk: Equilibrium, kinetic and thermodynamic studies". Journal of Hazardous Materials. 154, 337 **(2008)**.

[46] Kocklenberg, R.; Mathieu, B.; Blacher, S.; Pirard, R.; Pirard, J.P.; Sobry, R.; Van den Bossche, G. "Texture control of freeze-dried resorcinol-formaldehyde gels". Journal of Non-Crystalline Solids. 225, 8 **(1998)**.

[47] Job, N.; Panariello, F.; Marien, J.; Crine, M.; Pirard, J.P.; L´eonard, A. "Synthesis optimization of organic xerogels produced from convective air-drying of resorcinol-formaldehyde gels". Journal of Non-Crystalline Solids. 352, 24 **(2006)**.

[48] Tamon, H.; Ishizaka, H. "Influence of gelation temperature and catalysts on the mesoporous structure of resorcinol-formaldehyde aerogels". Journal of Colloid and Interface Science. 223, 305 **(2000)**.

[49] Lee, W-J; Lan, W-C. "Properties of resorcinol-tannin-formaldehyde copolymer resins prepared from the bark extracts of taiwan acacia and china fir". Bioresource Technology. 97, 257 **(2006)**.

[50] Tondi, G.; Pizzi, A.; Delmotte, L.; Parmentier, J.; Gadiou, R. "Chemical activation of tannin-furanic carbon foams". Industrial Crops and Products. 31, 327 **(2010)**.

[51] Zhao, W.; Pizzi, A.; Fierro, V.; Du, G.; Celzard, A. "Effect of composition and processing parameters on the characteristics of tannin-based rigid foams. Part I: Cell structure". Materials Chemistry and Physics. 122, 175 **(2010)**.

[52] Lagergren, S. "Zur theorie der sogenannten adsorption geloster stoffe". Kungliga Svenska Vetenskapsakademiens, Handlingar. Band. 24, 1, **(1898)**.

[53] Ho, Y.S.; McKay, G. "The kinetics of sorption of basic dyes from aqueous solutions by sphagnum moss peat". Canadian Journal of Chemical Engineering. 76, 822 **(1998)**.

[54] Aroua, M.K.; Leong, S.P.P.; Teo, L.Y.; Yin, C.Y.; Daud, W.M.A.W. "Real-time determination of adsorption of lead (II) onto palm shell-based activated carbon using ion selective electrode". Bioresource Technology. 99, 5786 **(2008)**.

[55] Langmuir, I. "The constitution and fundamental properties of solids and liquids. Part I. Solids". Journal of American Chemical Society. 38, 2221 **(1916)**.

[56] Freundlich, H. "Uber die adsorption in losungen". Z. Phys. Chem. 57, 385. **(1906)**.

[57] Kumar, K.V.; Porkodi, K.; Rocha, F. "Isotherms and thermodynamics by linear and non-linear regression analysis for the sorption of methylene blue onto activated carbon: Comparison of various error functions". Journal of Hazardous Materials. 151, 794 **(2008)**.

[58] Giles, A.P.; D'Silva, C.H.; Easton, I.A. "A general treatment and classification of the solute adsorption isotherm. Part II. Experimental interpretation". Journal of Colloid and Interface Science. 47, 766 **(1974)**.

[59] Molu, Z.B.; Yurdako¸ K. "Preparation and characterization of aluminum pillared K10 and KSF for adsorption of trimethoprim". Microporous and Mesoporous Materials. 127, 50 **(2010).**

[60] Domínguez, J.R.; González, T.; Palo, P.; Cuerda-Correa, E.M. "Removal of common pharmaceuticals present in surface waters by Amberlite XAD-7 acrylic-ester-resin: Influence of pH and presence of other drugs". Desalination. 269, 231 **(2011)**.

[61] Kim, S.H.; Shon, H.K.; Ngo, H.H. "Adsorption characteristics of antibiotics trimethoprim on powdered and granular activated carbon". Journal of Industrial and Engineering Chemistry. 16, 344 **(2010)**.

Capítulo 2:
ELECTROCHEMICAL OXIDATION OF MODEL COMPOUNDS

2.1. ELECTROCHEMICAL ADVANCED OXIDATION OF CARBAMAZEPINE ON BORON-DOPED DIAMOND ANODES. INFLUENCE OF OPERATING VARIABLES

A wide variety of drugs have been found in wastewater treatment effluents, rivers and lakes, including analgesics, antibiotics and antiepileptics. Electrochemical advanced oxidation processes are promising technologies to treat low contents of toxic and biorefractory pollutants in water. Anodic oxidation of carbamazepine, the most frequently detected drug in water bodies, was carried out using boron-doped diamond (BDD) anodes at galvanostatic mode. In order to optimize the process and study the interaction between the four modified variables (pH, current, concentration of supporting electrolyte Na_2SO_4, and solution flow rate) a design of experiments procedure has been carried out. The influence of these four variables has been evaluated. The influence of current was the greatest in studied variables, the second one was the salt concentration, and the third one was the flow rate. ANOVA test reported significant for 5 of the 14 involved variables and Response Surface Methodology technique used to optimize carbamazepine degradation. An optimum carbamazepine degradation of 100% was found at pH 9, flow rate equal to 1.25 $cm^3 \cdot min^{-1}$, and current density equal to 190 $mA \cdot cm^{-2}$ using a supporting electrolyte concentration equal to 0.48 $mol \cdot L^{-1}$.

Keywords: electrochemical advanced oxidation processes, electro-oxidation, anodic oxidation, boron-doped diamond electrodes, pharmaceuticals, carbamazepine.

2.1.1. INTRODUCTION.

In recent years, the presence of emerging pollutants such as pharmaceuticals and personal care products (PPCPs) in the environment has received much attention [1,2]. The worldwide average per capita consumption of pharmaceutical compounds (PCs)

per year is estimated to be about 15 g and in industrialized countries the value is expected to be between 50 and 150 g [3]. The advances in analytical chemistry have allowed the detection of a large variety of PCs and metabolites including analgesics, anti-inflammatories, antimicrobials, antiepileptics, beta-blockers, estrogens and lipid regulators as emerging pollutants in waters has been recently documented [4-7]. After their consumption and excretion, these compounds and their metabolites reach sewage systems, where they are barely reduced. Consequently, they are released into the environment either by the receiving waters of the sewage treatment plants. If the PCs are not effectively removed from the water and wastewater treatment plants, they are unintentionally consumed by humans. To avoid the potential adverse health effects of these pollutants on living beings, research efforts are underway to develop efficient oxidation techniques for achieving their total removal.

In this context, carbamazepine is the most frequently detected PC in water bodies thus far. This drug is used for the treatment of seizure disorders, for relief of neuralgia, and for a wide variety of mental disorders. Approximately 72% of orally administered carbamazepine is absorbed, while 28% is unchanged and subsequently discharged through the faeces. This drug has been proposed by some authors [8] as an anthropogenic marker in water bodies. Table 2.1 present the main physicochemical properties and the annual consumed volumes of carbamazepine in some countries [9-17].

Usually, carbamazepine and their metabolites are flushed with wastewater to the wastewater treatment plants (WWTPs) through the sewage system. Investigations found that carbamazepine is persistent and its removal efficiencies by the WWTPs are mostly below 10%. In the classification scheme for pharmaceutical biodegradation, the removal status of carbamazepine is classified as ‘‘no removal” [18].

These facts make Advanced Oxidation Processes (AOP) [19-21] chemical, photochemical, photocatalytic, and electrochemical methods, as possible candidates for the removal of this pharmaceutical pollutant. They are promising environmentally

friendly technologies for the treatment of wastewaters containing low contents of toxic and biorefractory pollutants [22]. Among them, electrochemical advanced oxidation

Table 2.1. Main physico-chemical properties of carbamazepine and annual consumed volumes of in some countries.

		Reference
Structure	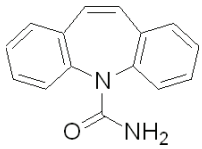	
Formula	$C_{15}H_{12}N_2O$	
CAS number	298-46-4	
Molecular Weight	236.27 g mol^{-1}	
Usage	Analgesic and Antiepileptic	
Water solubility	17.7 mg L^{-1} (25 ºC)	SRC [9]
LogP (octanol–water)	2.45	SRC [9]
Henry's Law Constant	1.09×10^{-5} Pa m^3 mol^{-1} (25 ºC)	SRC [9]
pK_a	Neutral	Hoover [10]
Elimination half-life	25-65 h	Wishart et al. [11]
Excretion	72% of oral dosage excreted in urine and 28% in faeces	RxList [11]
Dosage	Usually 800–1200 mg daily.	Sosiak and Hebben [13]
Annual consumed volume in Germany (in 1999)	87 tons	BLAC [14]
Annual consumed volume in France (in 2001)	40 tons	Ferrari et al. [15]
Annual consumed volume in England (in 2001)	40 tons	Jones et al. [16]
Annual consumed volume in USA (in 2000)	43 tons	Thacker [17]

Processes (EAOPs) [23-26] are very attractive for water and wastewater decontamination due to their low cost and high effectiveness, without needing addition of toxic chemical reagents and without producing dangerous wastes.

Among these EAOP, anodic oxidation (AO) [27] is the most effective technique. It consists in the destruction of pollutants in an electrolytic cell under the action of hydroxyl radicals formed as intermediate from water oxidation at the surface of the anode [28,29]:

$$M + H_2O \rightarrow M(\cdot OH) + H^+ + e^- \qquad (2.1)$$

where M(·OH) denotes the hydroxyl radical adsorbed on the anode M or remaining near its surface. Recently, AO has attracted great attention for wastewater treatment due to the manufacture of a new anode material. The use of a boron-doped diamond (BDD) thin-film anode brings technologically important characteristics such as an inert surface with low adsorption properties, remarkable corrosion stability and wide potential windows in aqueous medium [30,31]. These properties confer to the BDD-anode a much greater O_2 overvoltage than a conventional anode such as Pt, allowing the production of a higher amount of reactive M(·OH) from Equation (2.1). This material is considered the best "non-active" anode, the material interacts so weakly with the ·OH radicals which allows the direct reaction of organics with M(·OH) to give fully oxidized reaction products such as CO_2 as follows:

$$\alpha\, M(\cdot OH) + R \rightarrow \alpha\, M + m\, CO_2 + n\, H_2O + x\, H^+ + y\, e^- \qquad (2.2)$$

where R is an organic compound with *m* carbon atoms and without any heteroatom, which needs $\alpha = (2m + n)$ oxygen atoms to be totally mineralized to CO_2. Different authors have shown that several pollutants have been completely mineralized by AO with BDD-anodes, whereas the use of a Pt-anode under comparable conditions leads to weak decontamination because of the formation of carboxylic acids that are hardly ever oxidized with this material [32-36].

When BDD-anode is used, other weaker oxidizing species like peroxodisulphate, (if sodium sulphate is used as supporting electrolyte, as in this investigation) can also be competitively formed with reactive oxygen species (see Eq. (2.3)):

$$2SO_4^{2-} \rightarrow S_2O_8^{2-} + 2e^- \qquad (2.3)$$

This work presents the results obtained from the BDD-AO of carbamazepine. The design of experiments (DOE) was used to study the influence of the different operating variables: pH (in the range 1-9), current density (J from 0 to 320 $mA \cdot cm^{-2}$), supporting electrolyte concentration (SEC), Na_2SO_4 in the range 0-0.5 $mol \cdot L^{-1}$, and solution flow rate (Q_v) between 1.25-10.80 $cm^3 \cdot min^{-1}$. Response Surface Methodology (RSM) technique was used to optimize carbamazepine degradation (X_C, %). So, the objective of the present study was to analyze the influence of the different operating variables and to find out the optimum values for this decontamination process.

2.1.2. MATERIALS AND METHODS.

2.1.2.1. Chemicals.

Carbamazepine was provided by Sigma–Aldrich, Spain, of the highest purity available (> 98%). Carbamazepine stock solution ($2.11 \cdot 10^{-4}$ $mol \cdot L^{-1}$) was prepared with high purity water obtained from a Millipore Milli-Q® system. All reagents and solvents were of analytical reagent grade and were purchased from Panreac (Spain). The solution pH values were adjusted with sodium hydroxide and orthophosphoric acid (0.01/0.01 $mol \cdot L^{-1}$) buffer solution. The supporting electrolyte used in this investigation, Na_2SO_4, was provided by Panreac in analytical purity grade

2.1.2.2. Electrolytic cell and power supply.

Electrochemical experiments were carried out using an electrochemical module based on Adamant electrodes (Adamant Technologies, CSEM SA, Switzerland). This module consists in a single compartment two-electrode cell in conjunction with a controlled DC Power Supply FA-665 (Promax, Ltd., Spain). The electrodes consist in a boron-doped diamond (BDD) coating deposit (3 μm, 100-150 mΩ·cm) on a silicon plate (p-silicon, 100 mΩ·cm, 2 mm thick). The electrode surface

area was 12.5 cm^2 with a gap of 0.1 cm. This implies a reactor volume of 1.25 cm^3. This reactor was equipped with a water inlet and outlet. Two adaptable copper current feeding electrodes allow efficient electrical connections with 4 mm diameter connectors. The Adamant electrodes are connected with the current-feeding electrode using a silver paste.

2.1.2.3. Degradation experiments.

Electro-oxidation experiments were conducted at galvanostatic mode. The initial concentration of carbamazepine for all experiments was $2.11 \cdot 10^{-4}$ $mol \cdot L^{-1}$. A thermo regulated water bath was used to maintain a constant temperature (25 ± 0.1 ˚C). The cell potential was remained constant during the galvanostatic electrolysis indicates that electrode activity is not affected. Figure 2.1 shows a general scheme of the experimental installation used in this work. The experimental installation can vary the flow rate between 0-10 $cm^3 \cdot min^{-1}$ and the current density between 0-320 $mA \cdot cm^{-2}$.

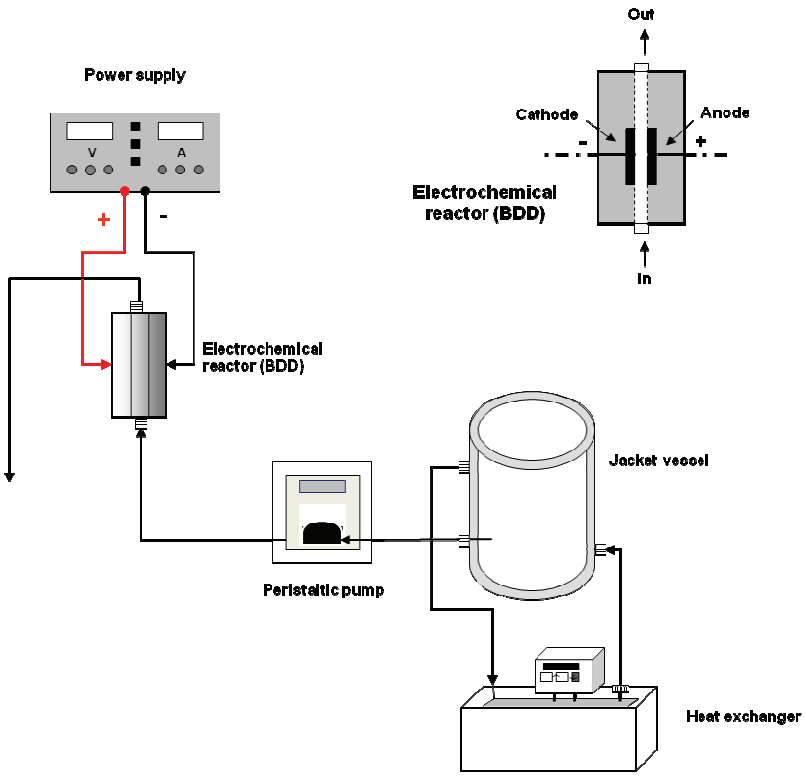

Fig. 2.1. Sketch of electrochemical installation.

2.1.2.4. Analytical methods.

The carbamazepine concentration present in each sample was determined by HPLC in a Waters chromatograph equipped with a 996 photodiode array detector and a Waters Nova-Pak C18 Column (5 μm 150×3.9mm). It displayed a well defined peak for carbamazepine at a retention time (t_r) of 5.21 min at 286 nm. For these analyses, samples of 50 μL were injected into the chromatograph and a 60:40 (v/v) methanol/water (10^{-2} M orthophosphoric acid) mixture was passed at a flow rate of 1 $mL \cdot min^{-1}$ as mobile phase.

Total Organic Carbon content (TOC) was determined by using a Lange TOC cuvette test (Hach Lange Ltd., Spain), using a shaker TOC-X5, where the open digestion cuvette is inserted during 5 minutes. The range of concentrations selected was 3–30 $mg \cdot L^{-1}$. For COD determination the Lange COD cuvette test method was used. The range of concentrations selected was 15–150 mg $(O_2) \cdot L^{-1}$. For both analyses a thermostat Lange LT 200 and a Hach Lange Xion Σ-500 photometer were used.

2.1.2.5. Mathematical and statistical procedures.

The data of section 2.1.3.1 was statistically analyzed by using StatGraphics® Plus 5.1. A factorial central composite orthogonal and rotatable (CCORD) design was used with 12 replicates of central point, so the total number of experiments was 36.

2.1.3. RESULTS AND DISCUSSION.

2.1.3.1. Experimental design. Surface response methodology.

The one factor at a time approach is the traditional way to study the influence of several operation variables (factors) on a parameter (response). However, this classical method involves a large number of experiments, and some important conclusions on the interaction among factors can be missed. An efficient way to solve this problem is the (DOE). It offers a better alternative to study the effect of variables and their responses with minimum number of experiments [37].

The DOE is a common methodology used to improve industrial and economical production processes [38-40]. Therefore, this methodology can be a useful tool to examine the influence of operating conditions on electrochemical oxidation of pollutants and to determine the optimum conditions using RSM (response surface methodology). Using RSM, the aggregate mix proportions can be arrived with minimum number of experiments without the need for studying all possible combination experiments. StatGraphichs software provides a useful and powerful mathematical and statistical tool in order to develop the experimental planning and to analyze the results, searching for conclusions.

In this methodology, the data obtained must be analyzed in a statistical manner, using regression, in order to determine if there exist a relationship between the factors and the response variables investigated. The test factors were coded according to Eq. (2.4):

$$x_i = \frac{X_i - X_i^X}{\Delta X_i} \tag{2.4}$$

where, x_i is the coded value of the ith independent variable, X_i is the natural value of the ith independent variable, X_i^X the natural value of the ith independent variable at the center point, and ΔX_i is the value of step change.

Each response Y can be represented by a mathematical equation that correlates the response surface.

$$Y = b_o + \sum_{j=1} b_j x_j + \sum_{i,j=1} b_{ij} x_i x_j + \sum_{j=1} b_{jj} x_j^2 \tag{2.5}$$

where Y is the predicted response, b_0 is the offset term, b_j the linear effect, b_{ij} is the first-order interaction effect and b_{jj} is the squared effect, and k is the number of independent variables.

In this work, Central Composite Orthogonal and Rotatable Design (CCORD) was selected, which is one of the most popular classes of second-order design. It involves the use of a two–level factorial design with 2^k points combined with $2k$ axial points

and *n* center runs, *k* being the number of factors. *N*, the total number of experiments with *k* factor is obtained according to Eq (2.6):

$$N = 2^k + 2 \cdot k + n \tag{2.6}$$

where *n* was equal to 12 and the axial distance was 2 in order to guarantee an orthogonal and rotatable design.

To evaluate the influence of pH, current (*I*), supporting electrolyte concentration (*SEC*), and flow rate (Q_v) and their concomitant effects on the effectiveness of BDD-electrochemical oxidation of carbamazepine in aqueous solution, different levels were set for this process. This selection has considered previous studies (data not shown). Table 2.2 shows these operating levels.

Table 2.2. Selected operating levels for the DOE.

Level	pH	Q_v ($cm^3 \cdot min^{-1}$)	I (A)	SEC ($mol \cdot L^{-1}$)
low level (-1)	3	3.64	1	0.125
central	5	6.03	2	0.250
high level (+1)	7	8.42	3	0.375

The specific study involves a range of 1-9 in pH, 1.25-10.80 $cm^3 \cdot min^{-1}$ in flow rate, 0-4 A in current, and 0–0.5 $mol \cdot L^{-1}$ in the concentration of supporting electrolyte. Consequently, a step is equal to 2 in pH, 2.39 $cm^3 \cdot min^{-1}$, 1 A, and 0.125 $mol \cdot L^{-1}$; the central value is equal to pH 5, Q_V= 6.03 $cm^3 \cdot min^{-1}$, I= 2A, and SEC= 0.250 $mol \cdot L^{-1}$. As the target variable, carbamazepine removal has been evaluated for each experiment. Table 2.3 shows the experimental planning in DOE, and obtained response for each experiment.

Table 2.3. Experimental Planning in DOE and Obtained Response for Each Experiment.

Run	Coded pH	Coded Q_v	Coded I	Coded SEC	X_C (%)
1	1	1	-1	-1	41.7
2	1	-1	-1	1	84.6
3	-1	-1	-1	-1	62.9
4	1	-1	1	-1	84.9
5	-1	1	-1	1	73.2
6	0	0	0	-2	57.7
7	0	-2	0	0	94.8
8	1	-1	1	1	97.8
9	0	0	-2	0	0.0
10	-1	-1	1	1	96.8
11	-1	1	1	-1	73.2
12	0	0	0	0	77.3
13	1	1	1	-1	72.3
14	0	0	0	0	77.4
15	-1	1	-1	-1	45.1
16	0	0	0	0	79.3
17	0	0	0	0	81.5
18	0	0	0	2	97.0
19	2	0	0	0	86.7
20	0	0	0	0	79.4
21	1	-1	-1	-1	55.2
22	1	1	-1	1	66.5
23	0	0	0	0	77.1
24	-1	-1	-1	1	85.7
25	0	0	0	0	80.1
26	0	0	0	0	83.4
27	-1	-1	1	-1	85.3
28	0	2	0	0	68.5
29	0	0	2	0	90.7
30	0	0	0	0	80.3
31	-1	1	1	1	90.2
32	0	0	0	0	77.9
33	0	0	0	0	81.0
34	0	0	0	0	77.7
35	-2	0	0	0	93.1
36	1	1	1	1	99.2

2.1.3.2. Anova report.

In a first approach, we should reference the ANOVA analysis that shows us the significance of the different parameters. Table 2.4 gives all of the data of this statistical analysis. According to the RSM, fourteen factors are considered and five of them have a *p*-value below 0.05 (limit of significance), so they are statistically significant. This means that the model used to represent the behaviour of the interactive factors is consistent. Also, the mean absolute error (MAE) of the residuals was very low and equal to 3.355.

Table 2.4. ANOVA Analysis.

Factor	Sum of squares	Degrees of freedom	F-ratio	p-values
A: coded pH	22.04	1	0.58	0.4500
B: coded Q_v	868.8	1	22.81	0.0001
C: coded I	5587.6	1	146.70	0.0000
D: codec SEC	2646.0	1	69.47	0.0000
AA	296.87	1	7.79	0.0109
AB	2.40	1	0.06	0.8041
AC	47.61	1	1.25	0.2762
AD	13.32	1	0.35	0.5606
BB	30.94	1	0.81	0.3776
BC	64.0	1	1.68	0.2089
BD	25.50	1	0.67	0.4224
CC	2095.2	1	55.01	0.0000
CD	84.64	1	2.22	0.1509
DD	0.269	1	0.01	0.9338
Total error	799.8	21		

Non-linear polynomial regression is carried out taking into account Eq. (2.5). In this sense, this regression is the following expression (Eq. (2.7)):

$$X_C = 79.28 - 0.958 \cdot A - 6.02 \cdot B + 15.26 \cdot C + 10.5 \cdot D + 3.04 \cdot A^2 + \\ + 0.387 \cdot AB + 1.725 \cdot AC + 0.912 \cdot AD + 0.983 \cdot B^2 + 2 \cdot BC + 1.262 \cdot BD - \\ - 8.09 \cdot C^2 - 2.3CD - 0.092 \cdot D^2 \quad (2.7)$$

where the values of A (pH), B (flow rate, Q_v), C (current, I) and D (Na_2SO_4 concentration of SEC) should be coded according to Eq. [2.4]. The values of carbamazepine removal, X_C, are given in %. The adjusted correlation factor r^2 is equal to 0.89. Adjusted correlation r^2 is used instead of nonadjusted r^2 since the first includes the effect of number of degrees of freedom. This regression leads to an optimum X_C (100%) at pH equal to 9, operating with a flow rate of 1.25 $cm^3 \cdot min^{-1}$ (retention time equal to 0.988 min), current density J= 190 $mA \cdot cm^{-2}$ and a salt concentration of 0.49 $mol \cdot L^{-1}$.

The ANOVA test also gives us the value of Durbin–Watson statistic, which has a value equal to 1.46, with a p-value of 0.066. As this p-value is higher than 0.05, there are no evidence of correlation in the residuals series. This means the random order of experiments has been effective in order to avoid any systematic error. Figure 2.2 (Residual correlation: X_C experimental - X_C calculated) is the graphical representation of this aspect.

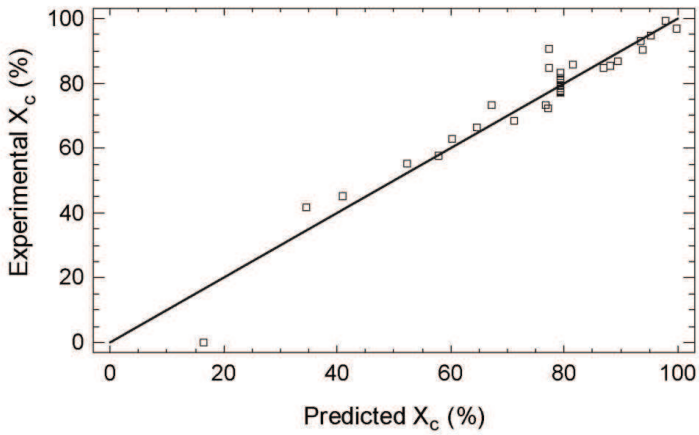

Fig. 2.2. Residual correlation: X_C experimental – X_C calculated by model.

2.1.3.3. Significant variables.

Modelization is made on the basis of fourteen factors which correspond to Eq.(2.7). A graphical expression of the ANOVA test results may be the Pareto graphic (Figure 2.3). Bars represent the standardized effects of each involved factor, considering them as the pH, current (I), supporting electrolyte concentration (SEC), the flow rate (Q_v), and combinations of all them. Filled bars are a graphical representation of negative-affecting factors, such as pH, flow rate, the combination of I-SEC, and the squared of current and SEC. That means that these factors appear in the Eq. (2.7) behind a negative sign. On the other hand, nonfilled bars represent positive-affecting factors, such as I, SEC, the squared of Q_v and pH, and the combination of Q_v-I, pH-SEC, pH-Q_v, pH-I, and Q_v-SEC. The vertical rule stands near to 2 and has to do with the level of significance of the ANOVA test, which is equal to 95% of confidence. Factors above this rule (as B, C, D, AA and CC) are inside the significance region, while the rest of them are not statistically significant. The Pareto graphic also gives us an idea of how factors influence the final response X_C. Positive bars indicate that by varying the variable, X_C increases. Negative bars indicate the contrary. It can be shown that as the rate of flow level rises, X_C decreases, and as current or salt concentration rises, X_C increases.

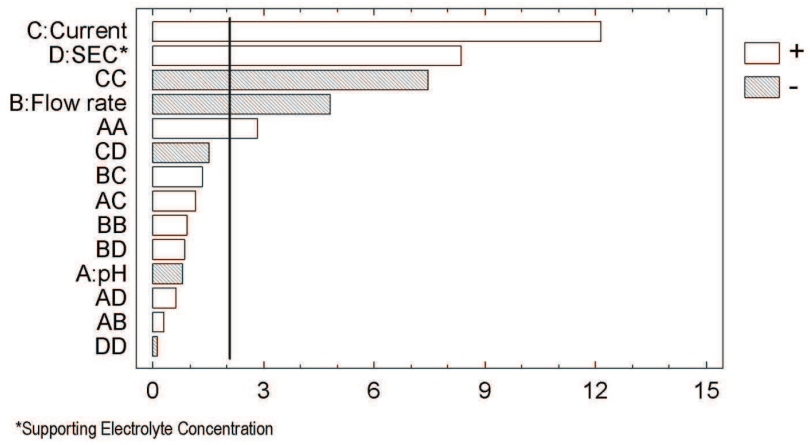

Fig. 2.3. Pareto graphic: standarized effects.

2.1.3.4. Main variables.

The evaluation of the CCORD model leads also to the study of the main effects of the involved variables. This can be observed in Figure 2.4. Four curves are drawn representing the effect of varying each variable while the other ones keep constant.

Current tends to present a maximum: in the end part of the curve (region of +1), SEC presents a linear positive-affecting tendency, while Q_v presents a linear negative-tendency. The fourth one, pH, presents a minimum in the middle-end part of the curve.

As can be seen the influence of current was the greatest in studied variables (this effect is due to an increase in the hydroxyl radicals generation from water oxidation, see Eq. (2.2)), the second one was the supporting electrolyte concentration (due to the generation of other oxidizing species like peroxodisulphate, see Eq. (2.3)), and the third one was the flow rate (because it modifies the residence time of molecules in the reactor). However, the influence of pH is very soft, because the molecule of carbamazepine is not ionizable.

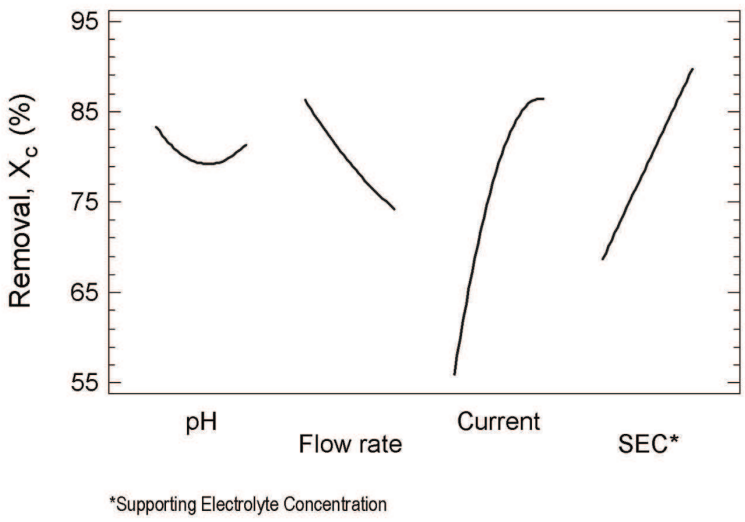

Fig. 2.4. Main effects of flow rate, pH, dosage of Na_2SO_4, and current.

2.1.3.5. Interaction between variables.

Figure 2.5 shows the interaction between each two of the four variables studied. Each pair of curves represents the evolution of X_C by varying one variable in the extremes of the CCORD model, that is, with its pair variable equal to +1 (upper value) and equal to −1 (low value). Parallel lines mean there is no interaction between them, crossing lines indicate the contrary. The level of interaction of one variable on the other is represented between these two situations. As the curves, for the pairs of variables AB, present a parallel behaviour, it may be assumed that there is not interaction, and the modification of one of the variables does not affect to the other one. When the pairs AC, AD, BC, BD and CD are observed in this Figure 2.5, the fact that interaction appears between this variables is evident. As the curves do not present a parallel behaviour, it may be assumed that there is interaction, and the modification of one of the variables affects the other one. The crossing occurs outside the region of the CCORD model.

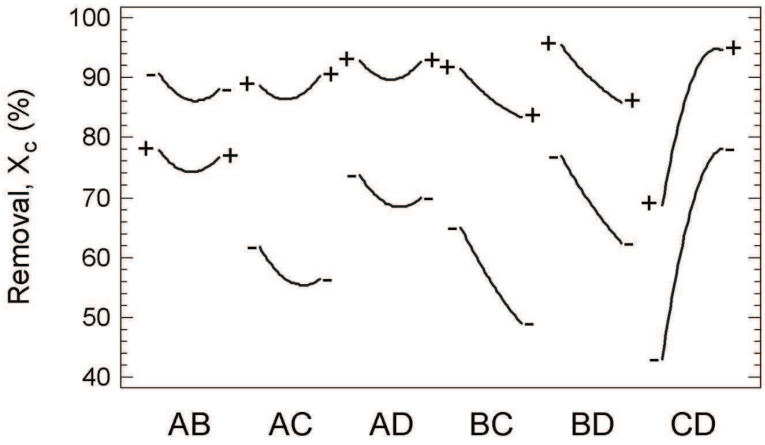

Fig. 2.5. Interaction graphic for flow rate, pH, dosage of Na_2SO_4, and current.

2.1.3.6. Response surface and contour plots.

The surface graphic is the most important graphical representation in the RSM (Figures 2.6(a) and 2.6(b)). It plots Eq. (2.7) and allows an evaluation from a qualitative point of view of how the behaviour of the whole system is studied. As it

can be appreciated in Figure 2.6(b), pH does not affect this level, and Q_v affects slightly. On the other hand, the response is a nearly plain surface as there is no interaction between variables inside the studied region.

a)

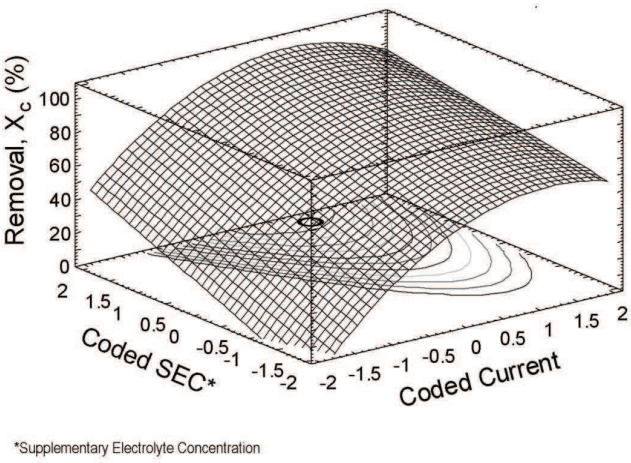

b)

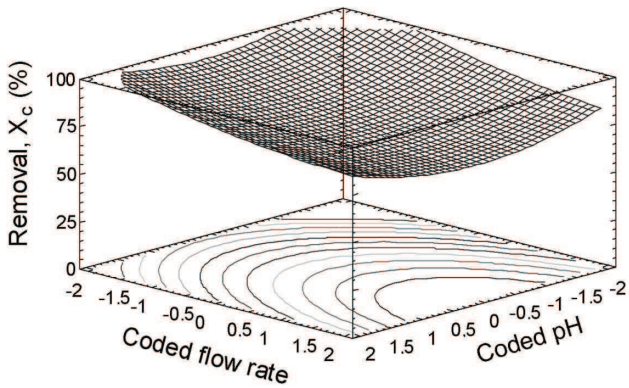

Fig. 2.6. Response surfaces: a) Current-SEC; b) pH-Q_v.

As it can be been in Figure 2.6(a), the response is a quite convex surface inside the studied region, and a maximum is apparent in the middle-start region of coded I (+0.37) of the studied region. The contour plot, which is drawn in the same Figure 2.6(a), is more clearly in order to identify the maximum point (it appears as a black

circle). Quantitatively, a statistical analysis of the model yields to an optimum in the point +1.99 for pH, -2 for Q_V, +0.37 for I and +1.91 for SEC, which is equivalent to pH= 9, Q_v= 1.25 $cm^3 \cdot min^{-1}$ (a retention time equal to 0.98 min), 2.37 A (current density, J= 190 $mA \cdot cm^{-2}$) and 0.48 $mol \cdot L^{-1}$ of salt.

As three of the four factors are inside the significant region of the model (that is, three of them are statistically significant as their *p*-values are under 0.05), this optimum may be considered as statistically different from other near points. The maximum value of X_C is equal to 100 % of removal of carbamazepine.

2.1.3.7. Experimental confirmation of the maximum.

An experiment was carried out in optimal conditions (pH= 9 Q_v= 1.25 $cm^3 \cdot min^{-1}$, J= 190 $mA \cdot cm^{-2}$ and SEC= 0.48 $mol \cdot L^{-1}$), in order to determine the reached removals of carbamazepine, TOC, and COD. Table 2.5 shows the obtained results for the experiment carried out in these optimal conditions. As can be seen, the removals of carbamazepine, COD, and TOC are equal to 100%, 59.4%, and 61%, respectively.

Table 2.5. Obtained experimental results for Carbamazepine electro-oxidation in optimum conditions.

X_C (%)	COD_o ($mg \cdot L^{-1}$)	TOC_o ($mg \cdot L^{-1}$)	X_{COD} (%)	X_{TOC} (%)
100	108	39.6	45	61

2.1.3.8. Physical meaning to the results of the DOE.

Figure 2.4 shows four curves representing the effect of varying each variable (into region -1 to +1) while the other ones are keet constant. As can be seen the influence of current was the greatest in studied variables. This may be explained by Eq. (2.1). The hydroxyl radical generation is due to the current. However, current tends to present an optimum in the end part of the curve. From the results of the DOE, we can conclude that above a certain value of current density (J equal to 190 $mA \cdot cm^{-2}$)

the drug removal rate does not increase with current. In this sense, the high generation of hydrogen bubbles at the cathode can hinder the oxidation process in aqueous phase.

The second more important variable studied was the supporting electrolyte concentration. The influence of this parameter was positive into studied region (-1 to +1). This can be justified taking into account two factors. An increase in the concentration of salt favours, on the one hand, the conduction of current in solution, and on the other, radical formation of oxidizing species like peroxodisulphate (see Eq. (2.3)). Therefore, the model predicts an optimum value outside this range (for +1.91).

The obtained result for the flow rate was expected if we consider that this parameter is inversely proportional to the residence time of molecules into reactor. The pH does not present significant influence. This fact can be explained taking into account that this drug is not ionizable in this pH range. Therefore, the model predicts an optimal value outside the studied region (for +1.99).

2.1.4. CONCLUSIONS.

Boron-doped-diamond anodic oxidation of carbamazepine in aqueous solution was studied. An orthogonal, rotatable factorial central composite design of experiments was carried out. It showed that the influence of current density was the greatest in studied variables, the second one was the supporting electrolyte concentration, the third one the flow rate. On the other hand, pH does not present significant influence inside the region of the model. ANOVA test reported significant for five of the fourteen involved variables and Response Surface Methodology technique was used to optimize carbamazepine degradation. An optimum carbamazepine degradation of 100% was found at pH 9, flow rate equal to 1.25 $cm^3 \cdot min^{-1}$, current density equal to 190 $mA \cdot cm^{-2}$ using a supporting electrolyte concentration equal to 0.48 $mol \cdot L^{-1}$.

2.1.5. REFERENCES.

[1] Radjenovic´, J.; Petrovic´, M.; Barceló, D. “Analysis of pharmaceuticals in wastewater and removal using a membrane bioreactor”. Anal. Bioanal. Chem. 387, 1365 **(2007)**.

[2] Radjenovic´, J.; Jelic´, A.; Petrovic´, M.; Barceló, D. "Determination of pharmaceuticals in sewage sludge by pressurized liquid extraction (PLE) coupled to liquid chromatography-tandem mass spectrometry (LC–MS/MS)". Anal. Bioanal. Chem. 393, 1685 **(2009)**.

[3] Alder, A.C.; Bruchet, A.; Carballa, M.; Clara, M.; Joss, A.; Löffler, D.; McArdell, C.S.; Miksch, K.; Omil, F.; Tuhkanen, T.; Ternes, T.A. "Consumption and Occurrence. In: Ternes, T.A., Joss, A. (Eds.), Human Pharmaceuticals, Hormones and Fragrances. The Challenge of Micropollutants in Urban Water Management". IWA Publishing. **(2006)**.

[4] Bound, J.P.; Voulvoulis, N. "Pharmaceuticals in the aquatic environment. A comparison of risk assessment strategies".Chemosphere. 56, 1143 **(2004)**.

[5] Tauxe-Wuersch, A.; De Alencastro, L.F.; Grandjean, D.; Tarradellas, J. "Occurrence of several acidic drugs in sewage treatment plants in Switzerland and risk assessment". Water Res. 39, 1761 **(2005)**.

[6] Emblidge, J.P.; Delorenzo, M.E. "Preliminary risk assessment of the lipid-regulating pharmaceutical clofibric acid, for three estuarine species". Environ. Res**.** 100, 216 **(2006)**.

[7] Farre, M.; Ferrer, I.; Ginebreda, A.; Figueras, M.; Olivella, L.; Tirapu, L.; Vilanova, M.; Barcelo, D. "Determination of drugs in surface water and wastewater samples by liquid chromatography-mass spectrometry: methods and preliminary results including toxicity studies with Vibrio fischeri". Journal of Chromatography A. 938, 187 **(2001)**.

[8] Clara, M.; Strenn, B.; Kreuzinger, N. "Carbamazepine as a possible anthropogenic marker in the aquatic environment: investigations on the behaviour of carbamazepine in wastewater treatment and during groundwater infiltration". Water Res. 38, 947 **(2004)**.

[9] SRC, PhysProp Database. http://www.syrres.com/esc/physdemo.htm **(2006)**.

[10] Hoover, J.E. carbamazepine. In: Troy, D. (Ed.), Remington: The Science and Practice of Pharmacy; Lippincott Williams & Wilkins: Philadelphia. **(2005)**.

[11] Wishart, D.S.; Knox, C.; Guo, A.C.; Shrivastava, S.; Hassanali, M.; Stothard, P.; Chang, Z.; Woolsey, J. "DrugBank: a comprehensive resource for in silico drug discovery and exploration". Nucleic Acids Res. 34, 668 **(2006)**.

[12] RxList. The Internet Drug Index. http://www.rxlist.com **(2006)**.

[13] Sosiak, A.; Hebben, T. "A preliminary survey of pharmaceuticals and endocrine disrupting compounds in treated municipal wastewaters and receiving rivers of Alberta". Alberta Environ: Edmonton **(2005)**.

[14] BLAC, Arzneimittel in der Umwelt Auswertung der Untersuchungsergebnisse. http://www.blak-uis.de/servlet/is/2146/P-2c.pdf **(2003)**.

[15] Ferrari, B.; Paxéus, N.; Giudice, R.L.; Pollio, A.; Garric, J. Ecotoxicological impact of pharmaceuticals found in treated wastewaters: study of carbamazepine, clofibric acid, and diclofenac. Ecotox. Environ. Safe. 55, 359 **(2003)**.

[16] Jones, O.A.H.; Voulvoulis, N.; Lester, J.N. "Aquatic environmental assessment of the top 25 English prescription pharmaceuticals". Water Res. 36, 5013 **(2002)**.

[17] Thacker, P.D. "Pharmaceutical data eludes environmental researchers". Environ. Sci. Technol. 39, 193 **(2005)**.

[18] Joss, A.; Zabaczynski, S.; Göbel, A.; Hoffmann, B.; Löffler, D.; McArdell, C.S.; Ternes, T.A.; Thomsen, A.; Siegrist, H. "Biological degradation of pharmaceuticals in municipal wastewater treatment: proposing a classification scheme". Water Res. **2006**, 40, 1686.

[19] Zwiener, C.; Frimmel, F.H. "Oxidative treatment of pharmaceuticals in water". Water Res. 34, 1881 **(2000)**.

[20] Pérez-Estrada, L.A.; Malato, S.; Gernjak, W.; Agüera, A.; Thurman, E.M.; Ferrer, I.; Fernández-Alba, A.R. "Photo-Fenton degradation of Diclofenac: Identification of main intermediates and degradation pathway". Environ. Sci. Technol. 39, 8300 **(2005)**.

[21] Sharma, V.K.; Mishra, S.K. "Ferrate (VI) oxidation of ibuprofen: A kinetic study". Environ. Chem. Lett. 3, 182 **(2006)**.

[22] Tarr, M. (Ed.). "Chemical Degradation Methods for Wastes and Pollutants. Environmental and Industrial Applications". Marcel-Dekker, New York **(2003)**.

[23] Bensalah, N.; Quiroz Alfaro, M.A.;. Martínez-Huitle, C.A. "Electrochemical treatment of synthetic wastewaters containing Alphazurine A dye". Chem. Eng. J. 149, 348 **(2009)**.

[24] Güven, G.; Perendeci, A.; Tanyolaç, A. "Electrochemical treatment of simulated beet sugar factory wastewater". Chem. Eng. J. 151, 149 **(2009)**.

[25] Basha A.; C.; Chithra, E.; Sripriyalakshmi, N.K. "Electro-degradation and biological oxidation of non-biodegradable organic contaminants". Chem. Eng. J. 149, 25 **(2009)**.

[26] Brillas, E.; Sirés, I.; Oturan, M.A. "Electro-Fenton process and related electrochemical technologies based on Fenton's reaction chemistry". Chem. Rev. 109, 6570 **(2009)**.

[27] Panizza, M.; Cerisola, G. "Direct and mediated anodic oxidation of organic pollutants". Chem. Rev. 109, 6541 **(2009)**.

[28] Marselli, B.; García-Gomez, J.; Michaud, P.A.; Rodrigo, M.A.; Comninellis, Ch. "Electrogeneration of hydroxyl radicals on boron-doped diamond electrodes". J. Electrochem. Soc. 150, 79 **(2003)**.

[29] Panizza, M.; Cerisola, G. "Application of diamond electrodes to electrochemical processes". Electrochim. Acta. 51, 191 **(2005)**.

[30] Brillas, E., Calpe, J.C., Casado, J. "Mineralization of 2,4-D by advanced electrochemical oxidation processes". Water Res. 34, 2253 **(2000)**.

[31] Martínez-Huitle, C.A.; Ferro, S. "Electrochemical oxidation of organic pollutants for the wastewater treatment: direct and indirect processes". Chem. Soc. Rev. 35, 1324 **(2006)**.

[32] Brillas, E.; Sirés, I.; Arias, C.; Cabot, P.L.; Centellas, F.; Rodríguez, R.M.; Garrido, J.A. "Mineralization of paracetamol in aqueous medium by anodic oxidation with a boron-doped diamond electrode". Chemosphere. 58, 399 **(2005)**.

[33] Cañizares, P.; Lobato, J.; Paz, R.; Rodrigo, M.A.; Sáez, C. "Electrochemical oxidation of phenolic wastes with boron-doped diamond anodes". Water Res. 39, 2687 **(2005)**.

[34] Boulbaba, L.; Nasr, B.; Abdellatif, G. "Electrochemical oxidation of benzoic acid derivatives on boron doped diamond: voltammetric study and galvanostatic electrolyses". Chem. Eng. Technol. 29, 944 **(2006)**.

[35] Flox, C.; Ammar, S.; Arias, C.; Brillas, E.; Vargas-Zavala, A.V.; Abdelhedi, R.. "Electro-Fenton and photoelectro-Fenton degradation of indigo carmine in acidic aqueous medium". Appl. Catal. B Environ. 67, 93 **(2006)**.

[36] Sirés, I.; Centellas, F.; Garrido, J.A.; Rodríguez, R.M.; Arias, C.; Cabot, P.L.; Brillas, E. "Mineralization of clofibric acid by electrochemical advanced oxidation processes using a

borondoped diamond anode and Fe^{2+} and UVA light as catalysts". Appl. Catal. B Environ. 72, 373 **(2007)**.

[37] Montgomery, D.C. Design and Analysis of Experiments (5th ed.), John Wiley and Sons, New York **(2001)**.

[38] Milani, A.S.; Wang, H.; Frey, D.D.; Abeyaratne, R.C. "Evaluating three DOE methodologies: optimization of a composite laminate under fabrication error". Qual. Eng. 21, 96 **(2009)**.

[39] Bhatia, S.; Othman, Z.; Ahmad, A.L. "Pretreatment of palm oil mill effluent (POME) using *Moringa oleifera* seeds as natural coagulant". J. Hazard. Mater. 145, 120 **(2007)**.

[40] Sabio, E.; Zamora, F.; Gañán, J.; González-García, C.M.; González, J.F. "Adsorption of *p*-nitrophenol on activated carbon fixed-bed". Water Res. 40, 3053 **(2006)**.

2.2. ANODIC OXIDATION OF KETOPROFEN ON BORON-DOPED DIAMOND (BDD) ELECTRODES. ROLE OF OPERATIVE PARAMETERS

Electrochemical oxidation is a promising technology to treatment of bio-refractory compounds. Anodic oxidation of ketoprofen, a representative endocrine disrupting chemical, was carried out using boron-doped diamond (BDD) electrodes at galvanostatic mode. A design of experiments procedure has been carried out in order to optimize the process and study the interaction between the studied variables: pH, current (I), supporting electrolyte concentration, Na_2SO_4, and solution flow rate (Q_v). The influence of current was the greatest in studied variables, the second one was the salt concentration and the third one was the flow rate. The fourth one, pH, does not present significant influence inside the region of the central composite orthogonal and rotatable design. ANOVA test reported significant for four of the fourteen involved variables. An optimum ketoprofen degradation, X_K, of 100% was found at pH 3.99, Q_v= 1.42 $cm^3 \cdot min^{-1}$, current density equal to 235 $mA \cdot cm^{-2}$ and a supporting electrolyte concentration equal to 0.5 $mol \cdot L^{-1}$.

Keywords: electrochemical advanced oxidation processes, electro-oxidation, anodic oxidation, boron-doped diamond electrodes, pharmaceuticals, ketoprofen.

2.2.1. INTRODUCTION.

Pharmaceuticals compounds (PCs) have emerged as a novel class of pollutants because of their potential adverse impacts on human health and the environment even at trace levels. Of special concerns are those that have been found to be resistant in water and wastewater treatment processes [1-3]. In these concerns nonsteroidal anti-inflammatory drugs (NSAID) are paid more attention to environmental scientists due to their large consumption in terms of thousands of tons annually for therapeutic purposes; as anti-inflammatory, analgesic or antipyretic.

Ketoprofen (2-(3-benzoylphenyl)-propanoic acid), chemical formula $C_{16}H_{14}O_3$ molecular formula (see Figure 2.7) and CAS number 22071-15-4 is a type of NSAID

extensively used as non-prescription drug, which has been frequently detected in wastewater treatment plant (WWTP) effluent, surface water, groundwater, and drinking water [4,5]. After intake of ketoprofen in humans, it is primarily metabolized by acyl glucuronidation and subsequently excreted in the urine for more than 80% of the given doses [6]. Once glucuronide conjugates reached wastewater treatment plants (WWTPs), they can be cleaved by enzymatic processes releasing ketoprofen. Several studies have demonstrated that biodegradation of ketoprofen in WWTP was limited. The removal efficiencies of ketoprofen in WWTPs were reported by several authors, ranging from 37% to almost 100% [7,8]. Results obtained by Quintana et al. [9] using activated sludge in aerobic conditions indicated that ketoprofen (in a concentration of 20 $mg \cdot L^{-1}$) was partially mineralized as a sole source of carbon and energy by microorganisms in WWTPs. Other authors suggested direct phototransformation and biodegradation as the main elimination processes of ketoprofen in the environment [5,10]. In any case, ketoprofen is not completely removed in most of sewage treatment plants and it is detected in both sewage sludge and effluent from WWTPs [11].

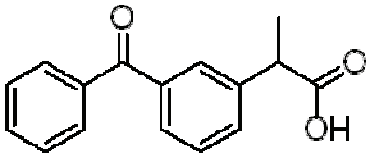

Fig. 2.7. Molecular formula of ketoprofen.

These facts have stimulated recent research for different processes for removing these types of compounds, namely Advanced Oxidation Processes (AOP) [12-14] and Electrochemical Advanced Oxidation Processes (EAOPs) [15-17]. The degradation of ibuprofen solution at pH 3.0 has been comparatively studied by different EAOPs like electro-Fenton, UVA photoelectro-Fenton and solar photoelectro-Fenton at constant current density [18]. Paracetamol solutions at pH 3.0 have been efficiently mineralized by environmentally clean electrochemical methods such as electro-Fenton and photoelectro-Fenton processes [19,20]. The mineralization of clofibric acid solutions by indirect electro-Fenton was carried out by Sirés et al. [21]. On the other hand, the direct anodic oxidation of 17-β-estradiol on boron-doped diamond anodes using

cathodes of Pt has been carried out by Murugananthan et al. [22]. However, research studies based on the design of experiments to analyze the influence of the different variables were not found.

In this context, anodic oxidation (AO) is an interesting EAOP based on chemical reaction with electrogenerated species from water discharge at the anode such as physically adsorbed ‘‘active oxygen’’ (physisorbed hydroxyl radical (·OH)) or chemisorbed ‘‘active oxygen’’ (oxygen in the form of a higher metal oxide (MO)). The proposed model assumes that the initial reaction in the anode (denoted as M) corresponds to the oxidation of water molecules leading to the formation of physisorbed hydroxyl radicals (M(·OH) see Eq. (2.1).

Both the electrochemical and chemical reactivity of heterogeneous M(·OH) are dependent on the nature of the electrode material. Usually, the surface of active anodes interacts strongly with ·OH and then, a so-called higher oxide (MO) may be formed following Eq. (2.8). This may occur when higher oxidation states are available for a metal oxide anode.

$$M(\cdot OH) \rightarrow MO + H^{+} + e^{-} \tag{2.8}$$

For the case of boron-doped diamond (BDD) electrodes, these new materials have received great attention, because they possess several technologically important characteristics including an inert surface with low adsorption properties, remarkable corrosion stability even in strongly acidic media and extremely high O_2 evolution overvoltage [23,24]. This material is considered the best “non-active” anode, the material interacts so weakly with ·OH radicals that allows the direct reaction of organics with M(·OH) to give fully oxidized reaction products such as CO_2 (see Eq.(2.2)).

This reaction also competes with the side reactions of M(·OH) such as direct oxidation to O_2 from reaction (2.9) or indirect consumption through dimerization to hydrogen peroxide by reaction (2.10):

$$2\,M(\cdot OH) \rightarrow 2M + O_2 + 2H^{+} + 2e^{-} \tag{2.9}$$

$$2\ M(\cdot OH) \rightarrow 2M + H_2O_2 \qquad (2.10)$$

These reactive oxygen species such as heterogeneous (·OH), H_2O_2, and O_2 are generated, although physisorbed (·OH) is the strongest oxidant of organics. This species, however, has so short lifetime that only acts while direct current is supplied to the anode. When BDD is used, other oxidizing species like peroxodisulphate, (if Na_2SO_4 is used as supporting electrolyte, as in this investigation) can also be competitively formed with reactive oxygen species (see Eq. (2.3)).

In this context, EAOP in general, and AO in particular, have attracted wide attention as one of the environmental-friendly technologies in wastewater treatment. Other advantages of AO include high efficiency in organic degradation, simple structure and easy control [25]. AO of various refractory pollutants have been extensively studied, such as phenol [26], nitrophenols [27], dyes [28,29] and surfactants [30].

In this work, we present the results obtained from the BDD-AO of ketoprofen. The design of experiments was used to study the effect of pH (in the range 3-11), current intensity (J= 0-320 $mA \cdot cm^{-2}$), supporting electrolyte concentration (SEC), Na_2SO_4 in the range 0.05-0.50 $mol \cdot L^{-1}$, and solution flow rate (Q_v) between 1.42 and 8.34 $cm^3 \cdot min^{-1}$. Response Surface Methodology (RSM) technique was used to optimize ketoprofen degradation (X_K, %), after AO treatment (against four input process variables). So, the objective of the present study is to find out the optimum values of the process.

2.2.2. MATERIALS AND METHODS.

2.2.2.1. Chemicals.

Ketoprofen was provided by Sigma–Aldrich Spain of the highest purity available (>98%). Ketoprofen stock solution ($1.96 \cdot 10^{-4}$ $mol \cdot L^{-1}$) was prepared with high purity water obtained from a Millipore Milli-Q® system. All reagents and solvents were of analytical reagent grade and were purchased from Panreac (Spain). The solution pHs were adjusted with sodium hydroxide and orthophosphoric acid

(0.01/0.01 mol·L^{-1}) buffer solution. The supporting electrolyte used in this investigation, Na_2SO_4, was provided by Panreac in analytical purity grade.

2.2.2.2. Electrolytic cell and power supply.

Electro-oxidation experiments were conducted at galvanostatic mode. The initial concentration of ketoprofen for all experiments was $1.96 \cdot 10^{-4}$ mol·L^{-1}. A thermo-regulated water bath was used to maintain a constant temperature (25±0.1 ˚C). The cell potential was remained constant during the galvanostatic electrolysis, indicates that electrode activity is not affected. Figure 2.1 shows a general scheme of the experimental installation used in this work. Experimental installation can vary the flow rate between 0 and 10 cm^3 ·min^{-1} and the current density between 0 and 320 mA·cm^{-2}.

2.2.2.3. Degradation experiments.

Electro-oxidation experiments were conducted at galvanostatic mode. The initial concentration of ketoprofen for all experiments was $1.96 \cdot 10^{-4}$ mol·L^{-1}. A thermo-regulated water bath was used to maintain a constant temperature (25±0.1 ˚C). The cell potential was remained constant during the galvanostatic electrolysis, indicates that electrode activity is not affected. Figure 2.1 shows a general scheme of the experimental installation used in this work. Experimental installation can vary the flow rate between 0 and 10 cm^3 ·min^{-1} and the current density between 0 and 320 mA·cm^{-2}.

2.2.2.4. Analytical methods.

Ketoprofen concentration present in each sample was determined by HPLC in a Waters Chromatograph equipped with a 996 Photodiode Array Detector and a Waters Nova-Pak C18 Column (5 µm 150 mm×3.9 mm). It displayed a well defined peak for ketoprofen at a retention time (t_r) of 4.1 min at 261 nm. For these analyses, samples of 50 µL were injected into the chromatograph and a 60:40 (v/v) methanol/water (10^{-2} M orthophosphoric acid) mixture was passed at a flow rate of 1 mL·min^{-1} as mobile phase.

Total Organic Carbon content (TOC) was determined by using a Lange TOC® cuvette test (Hach Lange Ltd., Spain), using a shaker TOC-X5, where the open digestion cuvette is inserted during five minutes. The range of concentrations selected was 3–30 $mg \cdot L^{-1}$. For COD determination the Lange COD® cuvette test method was used. The range of concentrations selected was 15–150 mg $(O_2) \cdot L^{-1}$. For both analyses a thermostat Lange LT 200 and a Hach Lange Xion Σ-500 photometer were used.

2.2.2.5. Mathematical and statistical procedures.

Section 2.2.3.1 was statistically analyzed by using StatGraphics® Plus for Windows 5.1. A factorial central composite orthogonal and rotatable design (CCORD) was used with twelve replicates of central point, so the total number of experiments was 36.

2.2.3. RESULTS AND DISCUSSION.

2.2.3.1. Design of experiments. Response surface methodology.

The one factor at a time approach is the traditional way to study the influence of several operation variables (factors) on a parameter (response). However, this classical method involves a large number of experiments and some important conclusions on the interaction among factors can be missed. An efficient way to solve this problem is the design of experiments (DOE). It offers a better alternative to study the effect of variables and their responses with minimum number of experiments [31]. DOE is a common methodology in order to improve industrial and economical production processes [32-34]. Therefore, this methodology can be a useful tool to examine the influence of operative parameters on AO of different pollutants, and to determine the optimum conditions using response surface methodology (RSM).

Using RSM, the aggregate mix proportions can be arrived with minimum number of experiments without the need for studying all possible combination experiments. StatGraphichs® software provides a useful and powerful mathematical and statistical tool in order to develop the experimental planning and to analyse the results, searching for conclusions. In this methodology, the data obtained must be analyzed in a

statistically manner, using regression, in order to determine if there exist a relationship between the factors and the response variables investigated. The test factors were coded according to Eq. (2.4) and each response *Y* can be represented by a mathematical equation that correlates the response surface (see Eq. (2.5)).

For this work, Central Composite Orthogonal and Rotatable Design (CCORD) was selected, which is one of the most popular classes of second-order design. It involves the use of a two–level factorial design with 2^k points combined with 2*k* axial points and *n* center runs, *k* being the number of factors. *N*, total number of experiments with *k* factor is obtained according to Eq. (2.6).

Table 2.6 shows the variables design with their high (+1), low (-1) and center point values. On the other hand, Table 2.7 shows the experimental planning in DOE, and obtained response in each experiment we have carried out (removal of ketoprofen in percentage, X_K %).

Table 2.6. Variables design. Operating levels.

pH			Q_v ($cm^3 min^{-1}$)			I (A)			SEC ($mol \cdot L^{-1}$)		
Low level (-1)	**High level (+1)**	**Center point**	**Low level (-1)**	**High level (+1)**	**Center point**	**Low level (-1)**	**High level (+1)**	**Center point**	**Low level (-1)**	**High level (+1)**	**Center point**
5	9	7	3.15	6.61	4.88	1	3	2	0.163	0.388	0.275

Table 2.7. Experimental planning in DOE and obtained response in each experiment.

Run	Real pH	Real Q_v ($cm^3 \cdot min^{-1}$)	Real I (A)	Real SEC ($mol \cdot L^{-1}$)	X_K (%)
1	9	6.61	1	0.163	39
2	9	3.15	1	0.388	75
3	5	3.15	1	0.163	50
4	9	3.15	3	0.163	75
5	5	6.61	1	0.388	67
6	7	4.88	2	0.050	50
7	7	1.42	2	0.275	86
8	9	3.15	3	0.388	87
9	7	4.88	0	0.275	0
10	5	3.15	3	0.388	95
11	5	6.61	3	0.163	60
12	7	4.88	2	0.275	69
13	9	6.61	3	0.163	60
14	7	4.88	2	0.275	73
15	5	6.61	1	0.163	35
16	7	4.88	2	0.275	71
17	7	4.88	2	0.275	74
18	7	4.88	2	0.500	85
19	11	4.88	2	0.275	65
20	7	4.88	2	0.275	71
21	9	3.15	1	0.163	47
22	9	6.61	1	0.388	59
23	7	4.88	2	0.275	69
24	5	3.15	1	0.388	68
25	7	4.88	2	0.275	68
26	7	4.88	2	0.275	69
27	5	3.15	3	0.163	72
28	7	8.34	2	0.275	57
29	7	4.88	4	0.275	80
30	7	4.88	2	0.275	66
31	5	6.61	3	0.388	72
32	7	4.88	2	0.275	70
33	7	4.88	2	0.275	58
34	7	4.88	2	0.275	64
35	3	4.88	2	0.275	63
36	9	6.61	3	0.388	78

2.1.3.2. Anova test.

In a first approach, we should refer the ANOVA analysis that shows us the significance of the different operative parameters. According to the RSM, fourteen factors are considered and four of them have a p-value below 0.05 (limit of significance) (see Table 2.8), so they are statistically significant. This means that the model used to represent the behaviour of the interactive factors is consistent. Also, the mean absolute error (MAE) is obtained and resulted be equal to 3.9.

Table 2.8. ANOVA Analysis.

Factor	Sum of squares	Degrees of freedom	F-ratio	p-values
A: coded pH	2.04	1	0.04	0.83
B: coded Q_v	1008	1	21.67	0.00
C: coded I	4218	1	90.62	0.00
D: codec SEC	2250	1	48.34	0.00
AA	7.54	1	0.16	0.69
AB	0.49	1	0.01	0.92
AC	0.06	1	0.00	0.97
AD	7.02	1	0.15	0.70
BB	64.03	1	1.38	0.25
BC	29.16	1	0.63	0.44
BD	0.04	1	0.00	0.97
CC	1346	1	28.91	0.00
CD	60.06	1	1.29	0.27
DD	5.84	1	0.13	0.73
Total error	997.6	21		

Non-linear polynomial regression is carried out taking into account Eq. (2.5). In this sense, this regression is the following expression (Eq. (2.11)):

$$\begin{aligned} X_{\kappa} &= 68.56 + 0.292\cdot A - 6.48\cdot B + 13.26\cdot C + 9.68\cdot D - 0.485\cdot A^2 + \\ &+ 0.175\cdot AB - 0.0625\cdot AC - 0.663\cdot AD + 1.41\cdot B^2 - 1.35\cdot BC - 0.05\cdot BD - \\ &- 6.48\cdot C^2 - 1.94\cdot CD - 0.427\cdot D^2 \end{aligned} \tag{2.11}$$

where the values of *A* (pH), *B* (flow rate, Q_v), *C* (current, I) and *D* (Na_2SO_4, SEC) should be coded according to Eq. (2.4). The values of ketoprofen removal, X_K, are given in %. The correlation factor r^2 is equal to 0.90 and the "adjusted correlation factor" R^2 (this includes the effect of number of degrees of freedom) is equal to 0.84. This regression leads to an optimum X_K (100%) at pH equal to 3.99, operating with a flow rate of 1.42 $cm^3 \cdot min^{-1}$ (retention time equal to 0.88 min), with a current density of 235 $mA \cdot cm^{-2}$ and a salt concentration of 0.5 $mol \cdot L^{-1}$.

ANOVA test also gives us the value of Durbin–Watson statistic, which has a value equal to 1.77, with a p-value of 0.30. As this p-value is higher than 0.05, there are no evidence of correlation in the residuals series. This means the random order of experiments has been effective in order to avoid any systematic error.

For each experiment, the difference between experimental X_K and calculated X_K (according to Eq. (2.11)) is represented in Figure 2.8 versus the specific run number. As no correlation can be appreciated (residuals are located in a random order to both the sides of the 0 axis), the randomization of the design is fully working and no accumulation of experimental error is observed.

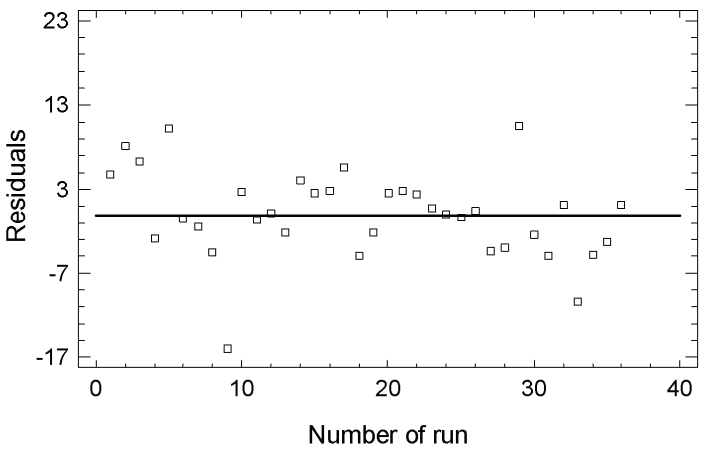

Fig. 2.8. Residuals vs. run number.

2.2.3.3. Significant variables.

Modelization is made on the basis of fourteen factors which correspond to Eq.(2.11). A graphical expression of the ANOVA test results may be the Pareto graphic (Figure 2.9). Bars represent the standardized effects of each involved factor, considering them as the pH, current (I), supporting electrolyte concentration (SEC), the flow rate (Q_v) and combinations of all them. Filled bars are a graphical representation of negative-affecting factors, such as flow rate, the squared of current and pH, the combination of I-SEC, Q_v-I, pH-SEC, pH-I and Q_v-SEC. That means that these factors appear in the expression (2.11) behind a negative sign. On the other hand, unfilled bars represent positive-affecting factors, such as I, SEC, pH, the squared of Q_v and SEC, and the combination of pH-Q_v, pH–I. The vertical rule stands near to 2 and has to do with the signification level of ANOVA test, which is equal to 95% of confidence. Factors above this rule (as B, C, D and CC) are inside the significance region, while the rest of them are not statistically significant. The Pareto graphic also gives us an idea of how factors influence on the final response X_K.

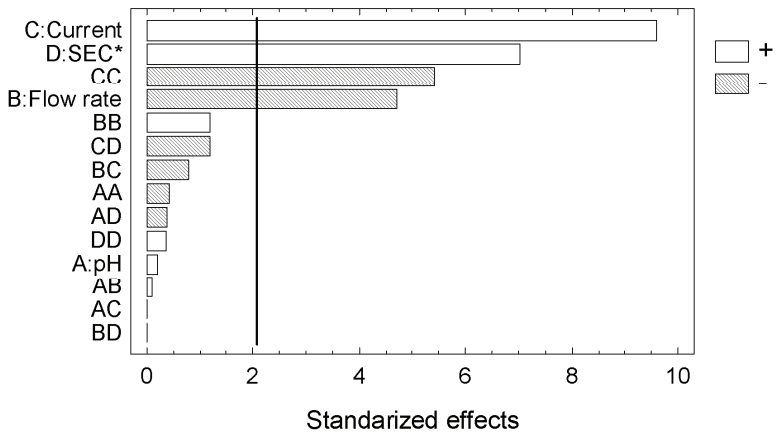

Fig. 2.9. Pareto graphic: standarized effects.

2.2.3.4. Main variables.

The evaluation of the CCORD model leads also to the study of the main effects of the involved variables. This can be observed in Figure 2.10. Four curves are

drawn representing the effect of varying each variable while the other ones keep constant. Current tends to present an optimum in the end part of the curve (region of +1), SEC presents a linear positive-affecting tendency, while Q_v presents a linear negative-tendency. The fourth one, pH, does not present significant influence. This will be clearly appreciated in the response surface and in the optimum point. As can be seen the influence of current was the greatest in studied variables, the second one was the supporting electrolyte concentration and the third one was the flow rate.

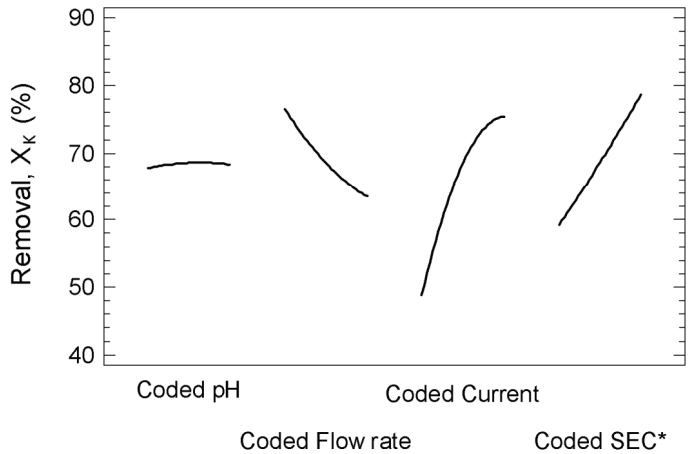

Fig. 2.10. Main effects of flow rate, pH, dosage of Na_2SO_4, and current.

2.2.3.5. Operating parameters interaction.

Figure 2.11 shows the interaction between each two of the four variables studied. Each pair of curves represents the evolution of X_K by varying one variable in the extremes of the CCORD model, that is, with its pair variable equal to 1 (upper value) and equal to −1 (low value). Parallel lines mean there is no interaction between them, crossing lines indicate the contrary. The level of interaction of one variable on the other is represented between these two situations As the curves, for the pairs of variables AB, AC, BC and BD, present a parallel behaviour, it may be assumed that there is not interaction, and the modification of one of the variables does not affect to the other one. When the pairs AD and CD are observed in Figure 2.11, the fact that interaction appears between these variables is evident. As the curves do not present a

parallel behaviour, it may be assumed that there is interaction, and the modification of one of the variables affects to the other one. The crossing occurs outside the region of the CCORD model.

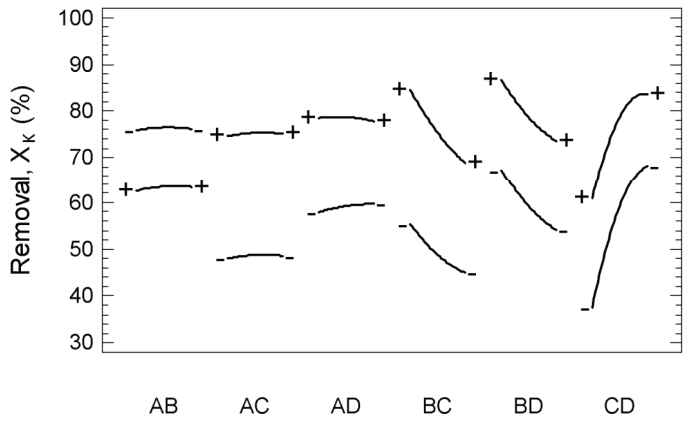

Fig. 2.11. Interaction graphic for flow rate, pH, dosage of Na_2SO_4, and current.

2.2.3.6. Response surface and contour plots.

The surface graphic is the most important graphical representation in the RSM (see Figures 2.12 and 2.13). It plots Eq. (2.11) and allows to evaluate from a qualitative point of view how is the behaviour of the whole studied system. As it can be appreciated in Figure 2.12, the response is a quite convex surface and a maximum is apparent in the final region of coded I (+1) of the studied region. Numerical coordinates of this point are -1.5 for pH, -1.99 for Q_v, +0.90 for I and +2 for SEC. This is outside drawn region, so the contour plot does not include it.

On the other hand, in Figure 2.13, the response is a quite plain surface as there is no interaction between variables inside the studied region. The strong influence of Q_v is represented by the inclined plane where the slope is primarily due to the variation of Q_v, while pH affects this level only slightly.

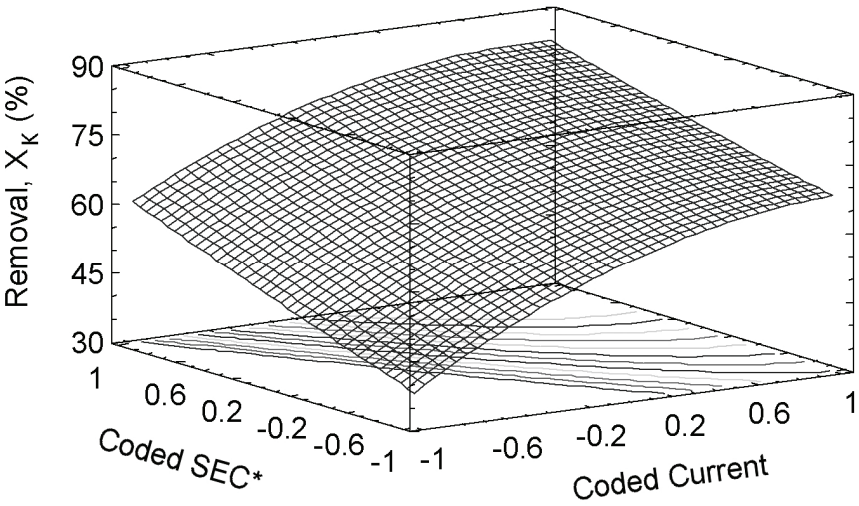

Fig. 2.12. Response surface: current-SEC.

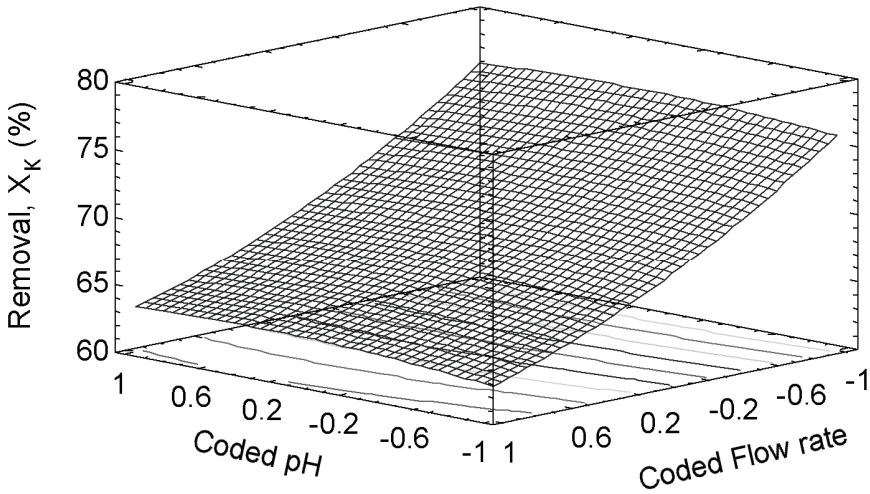

Fig. 2.13. Response surface: pH-Q_v.

The contour plot, which is drawn in Figure 2.14, is more clearly in order to identify the maximum point. Quantitatively, a statistical analysis of the model yields to an optimum in the point -1.5 for pH, -1.99 for Q_V, +0.90 for I and +2 for SEC, which is equivalent to pH= 3.99, Q_v= 1.42 $cm^3 \cdot min^{-1}$ (retention time equal to 0.88

min), 2.937 A (equivalent to a current intensity, J, equal to 235 mA·cm^{-2}) and a SEC equal to 0.5 mol·L^{-1} of salt. As three of the four factors are inside the significant region of the model (that is, three of them are statistically significant as their p-values are under 0.05), this optimum may be considered as statistically different from other near points. Maximum value of X_K (equal to 100 % of degradation) is predicted by the model in these conditions.

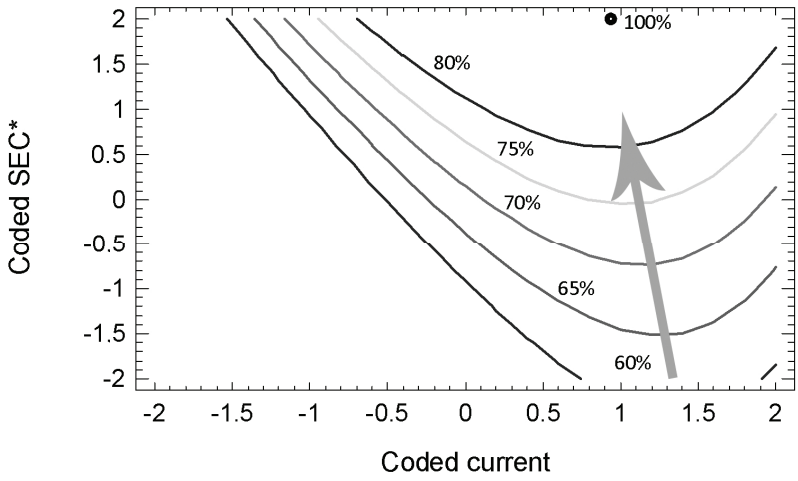

Fig. 2.14. Contour plot of the response surface: current-SEC.

2.2.3.7. Experimental confirmation of the maximum.

An experiment was carried out in optimal conditions (pH= 3.99, Q_v= 1.42 cm^3·min^{-1}, J= 235 mA·cm^{-2} and SEC= 0.5 moL^{-1}), in order to determine the reached removals of ketoprofen (X_K) and chemical oxygen demand (X_{COD}). Table 2.9 shows the obtained results for the experiment carried out in these optimal conditions. As can be seen, in these conditions, the reductions of ketoprofen and COD result to be equal to 100% and 38% respectively.

Table 2.9. Obtained experimental results for carbamazepine electro-oxidation in optimum conditions.

[ketoprofen]$_o$ (mg·L^{-1})	X_K (%)	COD$_o$ (mg·L^{-1})	X_{COD} (%)
50	100	116	38

2.2.3.8. Physical meaning to the results of the DOE.

As can be seen in Figure 2.10, the influence of current was the greatest in studied variables. This may be explained by Eq. (2.1). The hydroxyl radical generation is due to the current. However, current tends to present an optimum in the end part of the curve (region of +1). From the results of the DOE, we can conclude that above a certain value of current density (J= 235 $mA \cdot cm^{-2}$) the radical production does not increase with current. Radical production reaches a saturation value, and an increase in current intensity is negative.

The second more important variable studied was the supporting electrolyte concentration. The influence of this parameter was positive in all the range. There is not an optimum value for this parameter. This can be justified taking into account two factors. An increase in the concentration of salt favours, on the one hand, the conduction of current in solution, and on the other, radical formation of oxidizing species like peroxodisulphate (see Eq. (2.3)).

The obtained result for the flow rate was expected if we consider that this parameter is inversely proportional to the residence time of molecules into reactor. The pH does not present significant influence, although there is an optimal value. This pH value should be adequate to support both, the reaction of the anode (favored at basic pH) and the cathode reaction (favored at acid pH). Furthermore, in the optimal conditions (pH 3.99) the drug remains protonated being more reactive to hydroxyl radicals.

2.2.4. CONCLUSIONS.

Boron-doped diamond anodic oxidation of ketoprofen in aqueous solution was studied. DOE was used to study the effect of pH (in the range 3-11), current intensity (J= 0-320 $mA \cdot cm^{-2}$), supporting electrolyte concentration (Na_2SO_4) in the range 0.05-0.5 $mol \cdot L^{-1}$, and solution flow rate (Q_v) between 1.42-8.34 $cm^3 \cdot min^{-1}$. Response Surface Methodology technique was used to optimize ketoprofen degradation (X_K, %). So, the objective of the present study was to study the influence of operative

parameters and to find out the optimum experimental conditions for this oxidation technology.

An orthogonal, rotatable factorial central composite design of experiments was carried out. It showed that the influence of current intensity was the greatest in studied variables, the second one was the supporting electrolyte concentration and the third one the flow rate. The influence of pH was very soft. Anova test reported significance for four variables (current, SEC, flow rate and the squared of current) of the fourteen involved. An optimum oxidation point was found at pH= 3.99, Q_v= 1.42 $cm^3 \cdot min^{-1}$, J=235 $mA \cdot cm^{-2}$ using a SEC= 0.5 moL^{-1}.

2.2.5. REFERENCES.

[1] Kosjek, T.; Heath, E.; Kompare, B. "Removal of pharmaceutical residues in a pilot wastewater treatment plant". Anal. Bioanal. Chem. 387, 1379 **(2007)**.

[2] Glassmeyer, S.T.; Furlong, E.T.; Kolpin, D.W.; Cahill, J.D.; Zaugg, S.D.; Werner, S.L.; Meyer, M.T.; Kryak, D.D. "Transport of chemical and microbial contaminants from known wastewater discharges: potential for use as indicators of human fecal contamination". Environ. Sci. Technol. 39, 5157 **(2005)**.

[3] Paxeus, N. "Removal of selected non-steroidal anti-inflamatory drugs (NSAIDs), gemfibrozil, carbamazepine, b-blockers, trimethoprim and triclosan in conventional wastewater treatment plants in five EU countries and their discharge to the aquatic environment". Water Sci. Technol. 50, 253 **(2004)**.

[4] Metcalfe, C.D.; Koenig, B.G.; Bennie, D.T.; Servos, M.; Ternes, T.A.; Hirsch, R. "Occurrence of neutral and acidic drugs in the effluents of Canadian sewage treatment plants". Environ. Toxicol. Chem. 22, 2872 **(2003)**.

[5] Tixier, C.; Singer, H.P.; Oellers, S.; Müller, S.R. "Occurrence and fate of carbamazepine, clofibric acid, diclofenac, ibuprofen, ketoprofen, and naproxen in surface waters". Environ. Sci. Technol. 37, 1061 **(2003)**.

[6] Skordi, E.; Wilson, I.D.; Lindon, J.C.; Nicholson, J.K. "Characterization and quantification of metabolites of racemic ketoprofen excreted in urine following oral administration to man by

1H NMR spectroscopy, directly coupled HPLC–MS and HPLC–NMR, and circular dichroism". Xenobiotica. 34, 1075 **(2004)**.

[7] Lindqvist, N.; Tuhkanen, T.; Kronberg, L. "Occurrence of acidic pharmaceuticals in raw and treated sewages and in receiving waters". Water Res. 39, 2219 **(2005)**.

[8] Santos, J.L.; Aparicio, I.; Alonso, E. "Occurrence and risk assessment of pharmaceutically active compounds in wastewater treatment plants. A case study: Seville city, Spain". Environ. Int. 33, 596 **(2007)**.

[9] Quintana, J.B.; Weiss, S.; Reemtsma, T. "Pathways and metabolites of microbial degradation of selected acidic pharmaceutical and their occurrence in municipal wastewater treated by a membrane bioreactor". Water Res. 39, 2564 **(2005)**.

[10] Matamoros, V.; Duhec, A.; Albaigés, J.; Bayona, J.M. "Photodegradation of carbamazepine, ibuprofen, ketoprofen and 17a-ethinylestradiol in fresh and seawater". Water Air Soil Pollut. 196, 161 **(2009)**.

[11] Radjenovic´, J.; Petrovic´, M.; Barceló, D. "Fate and distribution of pharmaceuticals in wastewater and sewage sludge of the conventional activated sludge (CAS) and advanced membrane bioreactor (MBR) treatment". Water Res. 43, 831 **(2009)**.

[12] Zwiener, C.; Frimmel, F.H. "Oxidative treatment of pharmaceuticals in water". Water Res. 34, 1881 **(2000)**.

[13] Pérez-Estrada, L.A.; Malato, S.; Gernjak, W.; Agüera, A.; Thurman, E.M.; Ferrer, I.; Fernández-Alba, A.R. "Photo-Fenton degradation of Diclofenac: Identification of main intermediates and degradation pathway". Environ. Sci. Technol. 39, 8300 **(2005)**.

[14] Sharma, V.K.; Mishra, S.K. "Ferrate (VI) oxidation of ibuprofen: A kinetic study". Environ. Chem. Lett. 3, 182 **(2006)**.

[15] Bensalah, N.; Quiroz Alfaro, M.A.; Martínez-Huitle, C.A. "Electrochemical treatment of synthetic wastewaters containing Alphazurine A dye". Chem. Eng. J. 149, 348 **(2009)**.

[16] Güven, G.; Perendeci, A.; A. Tanyolaç. "Electrochemical treatment of simulated beet sugar factory wastewater". Chemical Engineering Journal. 151, 149 **(2009)**.

[17] Ahmed Basha, C.; Chithra, E.; Sripriyalakshmi, N.K. "Electro-degradation and biological oxidation of non-biodegradable organic contaminants". Chem. Eng. J. 149, 25 **(2009)**.

[18] Skoumal, M.; Rodríguez, R.M.; Cabot, P.L.; Centellas, F.; Garrido, J.A.; Arias, C.; Brillas, E. "Electro-Fenton, UVA photoelectro-Fenton and solar photoelectro-Fenton degradation of the drug ibuprofen in acid aqueous medium using platinum and boron-doped diamond anodes". Electrochim. Acta. 54, 2077 **(2009)**.

[19] Sirés, I.; Arias, C.; Cabot, P.L.; Centellas, F.; Rodríguez, R.M.; Garrido, J.A.; Brillas, E. "Paracetamol mineralization by advanced electrochemical oxidation processes for wastewater treatment". Environ. Chem. 1, 26 **(2004)**.

[20] Brillas, E.; Sirés, I.; Oturan, M.A. "Electro-Fenton Process and Related Electrochemical Technologies Based on Fenton's Reaction Chemistry". Chem. Rev. 109, 6570 **(2009)**.

[21] Sirés, I.; Centellas, F.; Garrido, J. A.; Rodríguez, R. M.; Arias, C.; Cabot, P.-L.; Brillas, E. "Mineralization of clofibric acid by electrochemical advanced oxidation processes using a boron-doped diamond anode and Fe^{2+} and UVA light as catalysts". Applied Catalysis B: Environmental. 72, 373 **(2007)**.

[22] Murugananthan, M.; Yoshihara, S.; Rakuma, T.; Uehara, N.; Shirakashi, T. "Electrochemical degradation of 17[beta]-estradiol (E2) at boron-doped diamond (Si/BDD) thin film electrode". Electrochimica Acta. 52, 3242 **(2007)**.

[23] Panizza, M.; Cerisola, G. "Application of diamond electrodes to electrochemical processes". Electrochim. Acta. 51, 191 **(2005)**.

[24] Martínez-Huitle, C.A.; Ferro, S. "Electrochemical oxidation of organic pollutants for the wastewater treatment: direct and indirect processes". Chem. Soc. Rev. 35, 1324 **(2006)**.

[25] Juttner, K.; Galla, U.; Schmieder, H. "Electrochemical approaches to environmental problems in the process industry". Electrochim. Acta. 45, 2575 **(2000)**.

[26] Feng, Y.J.; Li, X.Y. "Electro-catalytic oxidation of phenol on several metal-oxide electrodes in aqueous solution". Water Res. 37, 2399 **(2003)**.

[27] Cañizares, P.; Saez, C.; Lobato, J.; Rodrigo, M.A. "Electrochemical treatment of 4-nitrophenol-containing aqueous wastes using boron-doped diamond anodes". Ind. Eng. Chem. Res. 43, 1944 **(2004)**.

[28] Chen, X.M.; Chen, G.H.; Yue, P.L. "Anodic oxidation of dyes at novel Ti/B-diamondelectrodes". Chem. Eng. Sci. 58, 995 **(2003)**.

[29] Chen, X.M.; Chen, G.H.; Yue, P.L. "Anodic oxidation of dyes at novel Ti/B-diamond electrodes". Chem. Eng. Sci. 58, 995 **(2003)**.

[30] Panizza, M.; Cerisola, G. "Application of diamond electrodes to electrochemical processes". Electrochim. Acta. 51, 191 **(2005)**.

[31] Montgomery, D.C. "Design and Analysis of Experiments". Fifth ed., John Wiley and Sons, New York **(2001)**.

[32] Milani, A.S.; Wang, H.; Frey, D.D.; Abeyaratne, R.C. "Evaluating three DOE methodologies: optimization of a composite laminate under fabrication error". Qual. Eng. 21, 96 **(2009)**.

[33] Bhatia, S.; Othman, Z.; Ahmad, A.L. "Pretreatment of palm oil mill effluent (POME) using Moringa oleifera seeds as natural coagulant". J. Hazard. Mater. 145, 120 **(2007)**.

[34] Sabio, E.; Zamora, F.; Ganán, J.; González-García, C.M.; González, J.F. "Adsorption of p-nitrophenol on activated carbon fixed-bed". Water Res. 40, 3053 **(2006)**.

2.3. CONDUCTIVE-DIAMOND ELECTROCHEMICAL ADVANCED OXIDATION OF NAPROXEN IN AQUEOUS SOLUTION: OPTIMIZING THE PROCESS

Electrochemical advanced oxidation treatment using boron-doped diamond (BDD) electrodes is a promising technology to treat small amounts of toxic and biorefractory pollutants in water. This process has been tested on the degradation of naproxen, a common pollutant drug present in surface waters. To optimize the process a series of experiments have been designed to study the interaction between four variables: pH (over the range 5-11); current (0-320 $mA \cdot cm^{-2}$); supporting Na_2SO_4 electrolyte concentration (0-0.375 $mol \cdot L^{-1}$); and solution flow rate (Q_v) between 3.64 and 10.8 $cm^3 \cdot min^{-1}$. Among these variables the influence of current was the greatest, the second was the salt concentration, the third flow rate, and the fourth pH. An ANOVA test reported significance for seven of the fourteen variables involved and the degradation of naproxen was optimized using response surface methodology. Optimum conditions for naproxen removal (100%) were found to be pH= 10.70, Q_v= 4.10 $cm^3 \cdot min^{-1}$, current density= 194 $mA \cdot cm^{-2}$ using a supporting electrolyte concentration of 0.392 $mol \cdot L^{-1}$.

Keywords: electrochemical advanced oxidation, Boron-doped diamond electrodes, pharmaceuticals, naproxen.

2.3.1. INTRODUCTION.

In the last few decades the presence and fate of pharmaceuticals and personal care products (PPCPs) have received considerable attention [1-3]. Monitoring of PPCP residues has been conducted in raw and treated sewage, surface waters, ground waters, and drinking waters. More than 100 pharmaceuticals have been detected in municipal sewage and surface water samples [4-6]. These pharmaceuticals end up in surface waters and eventually in ground and drinking water after their excretion (in unmetabolized form or as active metabolites) from humans or animals via urine or faeces, through the sewage system and into the influent of wastewater treatment plants [7]. In this context, non-steroidal anti-inflammatory drugs (NSAIDs) are a wide non-

chemically related group of compounds that are also called "aspirin-like drugs" for sharing similar therapeutic actions. Within the most widely prescribed and recognized drugs, Naproxen is well-established NSAID, exhibiting anti-inflammatory, analgesic, antithrombotic and antipyretic properties, and recently it has been detected in engineered and natural aquatic environments [8,9].

Naproxen [(S)-6-methoxy-α-methyl-2-naphthalene acetic acid], $C_{14}H_{14}O_3$, CAS number 22204-53-1, is a NSAID drug widely used. Due to its extensive use as non-prescription drug, naproxen has been detected in surface water, groundwater, wastewater and even in drinking water [10-12]. The discharge from wastewater treatment plants (WWTPs), which contains pharmaceuticals that were not completely removed during the treatment process, is recognized as an important source of pharmaceuticals in the environment. The removal of naproxen in WWTPs obtain lower degradation levels (40–66%) [13,14]. On the other hand, Boyd et al. [15] observed that coagulation and sedimentation were not effective drinking water treatment processes for removal of naproxen in natural surface waters.

Therefore, it is not surprising that research has recently focussed on the application of Advanced Oxidation Processes (AOPs) for the elimination of pharmaceuticals in waters with emphasis on Electrochemical Advanced Oxidation Processes (EAOPs). Between these techniques, Anodic Oxidation (AO) consists in the oxidation of pollutants in an electrolytic cell by: (i) Direct anodic oxidation (or direct electron transfer to the anode), which yields very poor decontamination. (ii) Chemical reaction with electrogenerated species from water discharge at the anode such as physically adsorbed ''active oxygen'' (physisorbed hydroxyl radical (·OH)) or chemisorbed ''active oxygen'' (oxygen in the lattice of a metal oxide (MO) anode). The action of these oxidizing species leads to total or partial decontamination, respectively.

In this context, AO has attracted wide attention as one of the environmental-friendly technologies in wastewater treatment processes. Other advantages of electrochemical oxidation include high efficiency in organic degradation, simple

structure and easy control [16]. AO of various refractory drugs have been extensively studied; Ciriaco et al. [17] have carried out the electrochemical degradation of ibuprofen on Ti/Pt/PbO_2 and Si/BDD electrodes. Also, Brillas et al. have mineralized diclofenac [18], clofibric acid [19], salicylic acid [20] and paracetamol [21] by different EAOPs. However, the high energy consumption of electrochemical oxidation limited its industrial application. It is well known that the current efficiency of an AO system strongly depends on anode material. In this sense, the development of new anode materials as boron-doped diamond (BDD) has attracted more attention recently, because it has several important technologically properties [22,23]: an extremely wide potential window, corrosion stability in very aggressive media, an inert surface with low adsorption, a strong tendency to resist deactivation, and the robust oxidation capacity. The BDD anode is the best non-active electrode, then being proposed as the preferable anode for treating organics by AO. Thanks to the electrogeneration of hydroxyl radical as mediated oxidant (·OH), AO is considered an EAOP (Electrochemical Advanced Oxidation Process). Furthermore, when BDD is used, other weaker oxidizing species like peroxodisulphate (if supporting electrolyte is a sulphate) can also be competitively formed from the anodic material.

In this work, we present the results obtained from the BDD-AO of naproxen. The design of experiments was used to study the effect of pH (over the range 5-11), current (0-320 $mA \cdot cm^{-2}$), supporting electrolyte concentration (SEC), Na_2SO_4 over the range 0-0.375 $mol \cdot L^{-1}$, and solution flow rate (Q_v) between 3.64 and 10.8 $cm^3 \cdot min^{-1}$. Response Surface Methodology (RSM) technique was used to optimize naproxen degradation (X_N, %), after AO treatment (against the four input process variables). So, the objective of the present study is to optimize the process variables studied.

2.3.2. MATERIALS AND METHODS.

2.3.2.1. Chemicals.

All reagents and solvents were of analytical reagent grade and were purchased from Panreac (Spain). The solution pH was adjusted with sodium hydroxide and

orthophosphoric acid (0.01/0.01 mol·L^{-1}) buffer solution. The supporting electrolyte used in this investigation, SO_4Na_2, was provided by Panreac in analytical purity grade.

Naproxen was provided by Sigma–Aldrich (Spain) of the highest purity available. Initial naproxen solution (2,11·10^{-4} mol·L^{-1}) was prepared with high purity water obtained from a Millipore Milli-Q® system (Millipore Iberica S.A., Spain) and the pH was adjusted using the buffer solution.

2.3.2.2. Electrolytic system.

Electrochemical experiments were carried out using an electrochemical module based on Adamant®-Electrodes (Adamant Technologies, CSEM SA, Switzerland). This module consists in a single compartment two-electrode cell in conjunction with a controlled DC Power Supply FA-665 (Promax, Ltd., Spain). The electrodes consist in a boron-doped diamond (BDD) coating deposit (3 µm, 100-150 mΩ·cm) on a silicon plate (p-silicon, 100 mΩ·cm, 2mm thick). The electrode surface area was 12.5 cm^2 with a gap of 0.1 cm. This implies a reactor volume of 1.25 cm^3. The cell is equipped with a water inlet and outlet. A thermo-regulated water bath was used to maintain a constant temperature (25 ºC). Two adaptable copper current feed electrodes allow efficient electrical connections with 4 mm diameter connectors. The Adamant® Electrodes are connected with the current feed electrode using a silver paste. Figure 2.1 shows a general scheme of the experimental installation used in this work.

Degradation experiments were conducted in a galvanostatic mode. The cell potential was remained constant during the galvanostatic electrolysis, indicating that electrode activity is not affected. The flow rate can vary between 0 and 10.8 cm^{3}min^{-1}. The current density was varied between 0 and 320 mA·cm^{-2}.

2.3.2.3. Analytical methods.

Naproxen concentration in each sample was determined by HPLC using a Waters Chromatograph (provided by Waters Cromatografía, S.A., Spain) equipped with a 996 Photodiode Array Detector and a Waters Nova-Pak C18 Column (5 µm

150×3.9mm). The chromatogram displayed a well defined peak for naproxen at a retention time (t_r) of 4.6 min at 263 nm. For these analyses, samples of 50 μL were injected into the chromatograph and a 60:40 (v/v) methanol/water (10^{-2} mol·L^{-1} orthophosphoric acid) mixture at a flow rate of 1 mL·min^{-1} as the mobile phase.

Total Organic Carbon content (TOC) was determined using a Lange TOC® cuvette test (Hach Lange Ltd., Spain), in a shaker TOC-X5, where the open digestion cuvette is inserted for five minutes. The range of concentrations selected was 3–30 mg·L^{-1}. For COD determination the Lange COD® cuvette test method was used. The range of concentrations selected was 15–150 mg (O_2)·L^{-1}. For both analyses a thermostat Lange LT 200 and a Hach Lange Xion$^{\Sigma}$-500 photometer were used.

2.3.2.4. Mathematical and statistical procedures.

The experimental results were analyzed statistically using StatGraphics® Plus for Windows 5.1. A factorial central composite orthogonal and rotatable design was used with twelve replicates of central point, so the total number of experiments was 36.

2.3.3. RESULTS AND DISCUSSION.

2.3.3.1. Experimental design. Surface response methodology.

The approach varying one factor at a time is the traditional way to study the influence of several operating variables (factors) on a parameter (response). However, this classical method involves a large number of experiments and some important conclusions on the interaction among factors can be missed. An efficient way to solve this problem is the design of experiments (DOE) procedure. It offers a better alternative to study the effect of variables and their responses with a minimum number of experiments [24].

DOE is a common methodology to improve industrial and economical production processes [25-27]. Therefore, this methodology can be useful to examine the influence of operating conditions on electrochemical oxidation of pollutants, and to determine the optimum conditions using response surface methodology (RSM). Using RSM, the

aggregate mix proportions can be obtained with a minimum number of experiments without the need for studying all possible combinations. Furthermore, StatGraphichs® software provides a useful and powerful mathematical and statistical tool to develop the experimental planning and to analyse the results, searching for conclusions. In this methodology, the data obtained must be analyzed in a statistically manner, using regression, to determine if a relationship exists between the factors and the response variables investigated. The test factors were coded according to Eq. (2.4) and each response Y can be represented by a mathematical equation (Eq. (2.5) that correlates the response surface.

In this work, Central Composite Design (CCD) was selected; which is one of the most popular classes of second-order design. It involves the use of a two–level factorial design with 2^k points combined with $2k$ axial points and n center runs, k being the number of factors. N, total number of experiments with k factor is obtained according to Eq (2.6).

In Table 2.10 the design of experiments with coded variables is shown. On the other hand, Table 2.11 shows the experimental planning in DOE, and the response obtained in each experiment we have carried out (removal of the drug in percentage, X_N,%).

Table 2.10. Design of experiments. Coded variables.

Run	Coded pH	Coded Q_v	Coded I	Coded SEC
1	1	1	-1	-1
2	1	-1	-1	1
3	-1	-1	-1	-1
4	1	-1	1	-1
5	-1	1	-1	1
6	0	0	0	-2
7	0	-2	0	0
8	1	-1	1	1
9	0	0	-2	0
10	-1	-1	1	1
11	-1	1	1	-1
12	0	0	0	0
13	1	1	1	-1
14	0	0	0	0
15	-1	1	-1	-1
16	0	0	0	0
17	0	0	0	0
18	0	0	0	2
19	2	0	0	0
20	0	0	0	0
21	1	-1	-1	-1
22	1	1	-1	1
23	0	0	0	0
24	-1	-1	-1	1
25	0	0	0	0
26	0	0	0	0
27	-1	-1	1	-1
28	0	2	0	0
29	0	0	2	0
30	0	0	0	0
31	-1	1	1	1
32	0	0	0	0
33	0	0	0	0
34	0	0	0	0
35	-2	0	0	0
36	1	1	1	1

Table 2.11. Experimental planning of DOE and obtained response in each experiment (X_N).

Run	Real pH	Real Q_v ($cm^3 \cdot min^{-1}$)	Real I (A)	Real SEC ($mol \cdot L^{-1}$)	X_N (%)
1	11	8.416	1	0.125	28.2
2	11	3.642	1	0.375	88.0
3	7	3.642	1	0.125	41.9
4	11	3.642	3	0.125	79.4
5	7	8.416	1	0.375	42.3
6	9	6.029	2	0.000	38.1
7	9	1.255	2	0.250	97.7
8	11	3.642	3	0.375	98.6
9	9	6.029	0	0.250	0.00
10	7	3.642	3	0.375	99.4
11	7	8.416	3	0.125	67.6
12	9	6.029	2	0.250	91.8
13	11	8.416	3	0.125	80.9
14	9	6.029	2	0.250	90.7
15	7	8.416	1	0.125	32.7
16	9	6.029	2	0.250	94.2
17	9	6.029	2	0.250	91.1
18	9	6.029	2	0.500	99.7
19	13	6.029	2	0.250	95.4
20	9	6.029	2	0.250	92.3
21	11	3.642	1	0.125	60.8
22	11	8.416	1	0.375	78.7
23	9	6.029	2	0.250	94.8
24	7	3.642	1	0.375	78.7
25	9	6.029	2	0.250	91.9
26	9	6.029	2	0.250	92.7
27	7	3.642	3	0.125	79.6
28	9	10.803	2	0.250	78.7
29	9	6.029	4	0.250	96.0
30	9	6.029	2	0.250	91.2
31	7	8.416	3	0.375	99.5
32	9	6.029	2	0.250	95.3
33	9	6.029	2	0.250	96.4
34	9	6.029	2	0.250	95.2
35	5	6.029	2	0.250	71.5
36	11	8.416	3	0.375	99.9

2.3.3.2. Anova report.

In a first approach, we should mention the ANOVA analysis that shows us the significance of the different parameters. According to the RSM, fourteen factors are considered and seven of them have a *p*-value below 0.05 (significance limit) (see Table 2.12), so they are statistically significant. This means that the model used to represent the behaviour of the interactive factors is consistent.

Table 2.12. ANOVA results.

Factor	Sum of squares	Degrees of freedom	F-ratio	p-values $\times 10^2$
A: coded pH	606.0	1	13.8	0.13
B: coded Q_v	754.9	1	17.2	0.05
C: coded I	8273	1	188	0.00
D: codec SEC*	4738	1	108	0.00
AA	184.3	1	4.2	5.34
AB	21.25	1	0.5	49.5
AC	140.4	1	3.2	8.84
AD	19.85	1	0.5	50.9
BB	47.05	1	1.1	31.3
BC	384.2	1	8.7	0.76
BD	4.05	1	0.1	76.6
CC	4059	1	92.3	0.00
CD	73.10	1	1.7	21.1
DD	1166	1	27	0.00
Total error	923.7	21		

* Supporting electrolyte concentration of Na_2SO_4.

Non-linear polynomic regression is carried out taking into account Eq. (2.5). In this sense, the following expression describes this regression (Eq. (2.12)):

$$\begin{aligned} X_N &= 93.13 + 5.03 \cdot A - 5.61 \cdot B + 18.57 \cdot C + 14.05 \cdot D - 2.4 \cdot A^2 + \\ &+ 1.15 \cdot AB - 2.96 \cdot AC + 1.11 \cdot AD - 1.21 \cdot B^2 + 4.9 \cdot BC + 0.5 \cdot BD - \\ &- 11.26 \cdot C^2 - 2.14 \cdot CD - 6.04 \cdot D^2 \end{aligned} \tag{2.12}$$

where the values of A (pH), B (flow rate, Q_v), C (current, I) and D (Na_2SO_4 concentration, SEC) should be coded according to Eq. (2.4). The values of naproxen removal, X_N, are given in %. The adjusted correlation factor r^2 is equal to 0.93. Adjusted correlation r^2 is used instead of non-adjusted r^2 since the first includes the effect of number of degrees of freedom. This regression leads to an optimum X_N(100%) at pH equal to 10.70, operating with a flow rate of 4.10 $cm^3 \cdot min^{-1}$ (retention time into reactor equal to 0.305 min), current density of 194 $mA \cdot cm^{-2}$ and a salt concentration of 0.392 $mol \cdot L^{-1}$.

The ANOVA test also gives us the value of Durbin–Watson statistic, which has a value of 1.45, with a *p*-value of 0.062. As this *p*-value is higher than 0.05, there is no evidence of correlation in the residuals series. This means the random order of experiments has been effective in avoiding any systematic error. Figure 2.15 (residual correlation: X_N experimental - X_N calculated) is the graphical representation of this aspect. Moreover, for each experiment, the difference between experimental X_N and calculated X_N (according to Eq. (2.12)) was represented versus the specific run number. As no correlation was shown (residuals are located in a random order to both the sides of the 0 axis), the randomization of the design is fully working and no accumulation of experimental error was observed.

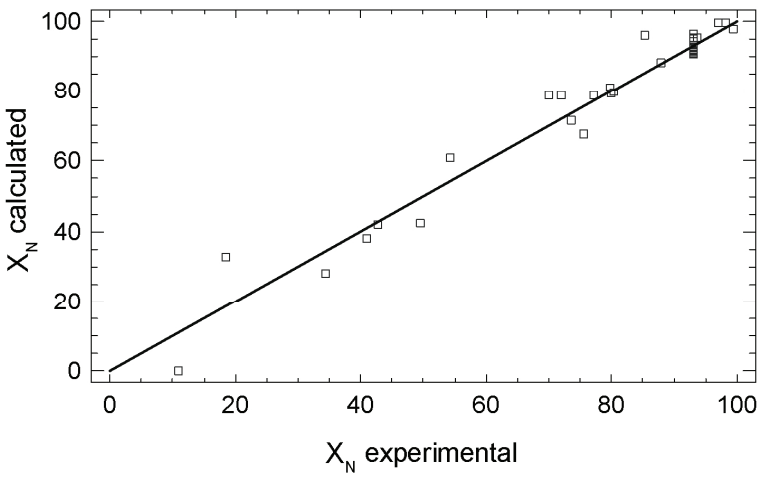

Fig. 2.15. Residual correlation: X_N experimental - X_N calculated.

2.3.3.3. Significant variables.

Modelling was made on the basis of fourteen factors which correspond to Eq.(2.12). A graphical expression of the ANOVA test results may be the Pareto graph (Figure 2.16). Bars represent the standardized effects of each factor involved, with filled bars representing positive-affect factors, such as, SEC, pH and the combination of Q_v–I, pH-Q_v, pH-SEC and SEC-Q_v. Non-filled bars are a graphical representation of negative-affecting factors, such as flow rate, the combination of pH-current and current-SEC, and all squared factors. This means that these factors appear in Eq.(2.12) behind a negative sign. On the other hand, the vertical rule stands near to 2 and has to do with the signification level of ANOVA test, which is equal to 95% confidence. Factors above this rule (such as A, B, C, D, CC, DD and BC) are inside the significant region, while the rest have no significance in the final response. The Pareto graph also gives us an idea of how factors influence the final response X_N. Positive bars indicate that by varying the variable the value of X_N increases. Negative bars indicate the contrary. As can be shown, as the rate flow level raises X_N decreases and as current, pH and salt concentration raises X_N increases.

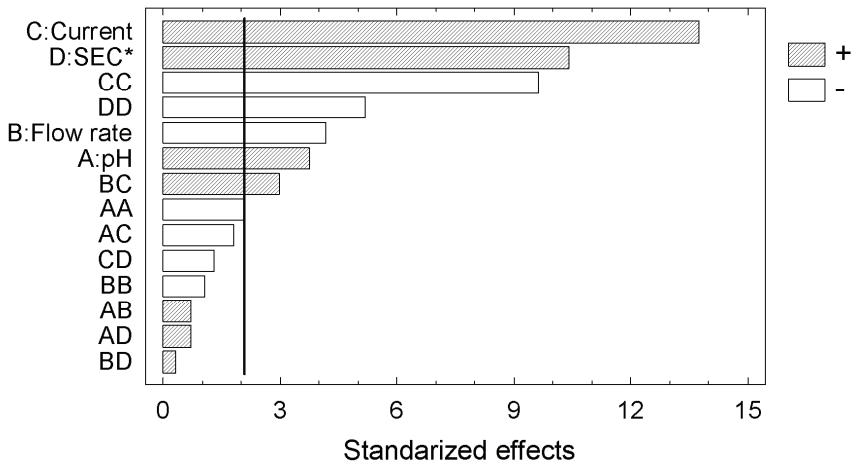

*Supporting electrolyte concentration

Fig. 2.16. Pareto graphic: standarized effects.

2.3.3.4. Main variables.

The evaluation of the CCD model leads also to the study of the main effects of the variables involved. This can be observed in Figure 2.17. Four curves are drawn representing the effect of varying each variable while the others are kept constant. Each curve shows a maximum: in the end of the curve in the case of pH, current and SEC, and in the first part of the curve in the case of flow rate. This will be clearly appreciated in the response surface and in the optimum point.

As can be seen for the variables studied the influence of current was the greatest, second was the concentration of supporting electrolyte, third was the rate flow and the fourth the pH.

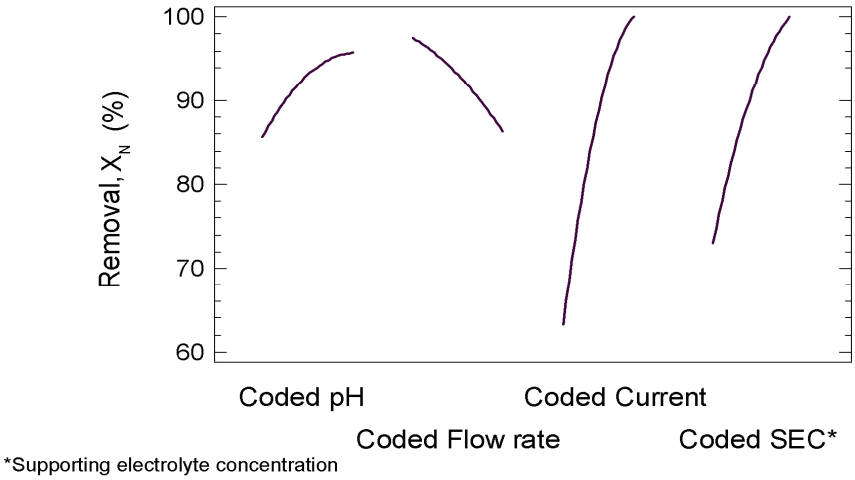

Fig. 2.17. Main effects: pH, flow rate, current and dosage of SEC.

2.3.3.5. Interaction between variables.

Figure 2.18 shows the interaction between each pair of the four variables studied. The fact that interaction appears between each pair of variables AC, AD, BC and CD is evident in the Figure 2.18. Each pair of curves represents the evolution of X_N by varying one variable in the extremes of the CCD model, that is, with its pair variable equal to +1 (upper value) and equal to −1 (low value). As the curves do not present parallel behaviour, it may be assumed that there is interaction, and the modification of one of the variables affects to the other. When the pairs of variables

AB and BD are observed, in the same Figure 2.18, their curves present parallel behaviour, so it may be assumed that there is no interaction and the modification of one of the variables does not affect to the other.

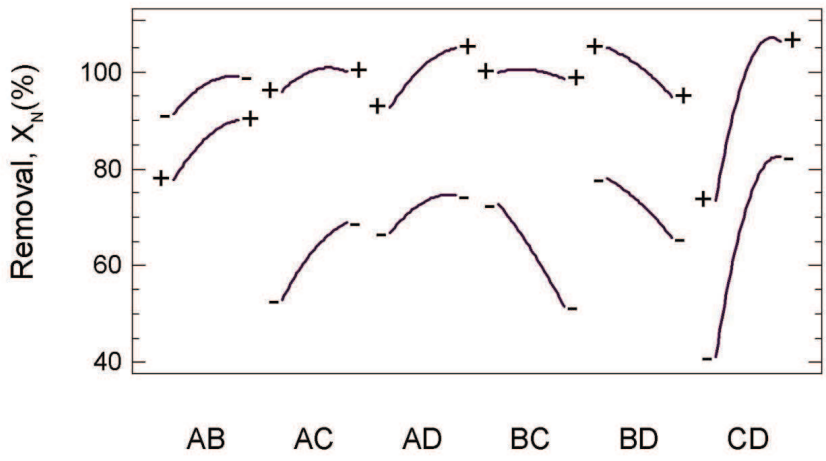

Fig. 2.18. Interaction graphic for flow rate, pH, dosage of Na_2SO_4 and current.

2.3.3.6. Response surfaces and contour plots.

The surface graphic is the most important graphical representation in the RSM (Figures 2.19(a) and 2.19(b)). This plots Eq. (2.12) and allows the evaluation from a qualitative point of view of the behaviour of the whole system studied. As can be appreciated, the response is a convex surface inside the studied region. The four variables have similar influence on the target variable X_N and an optimum value is obtained, that is a maximum.

The contour plot, Figure 2.20, (a) and (b), identifies the maximum almost more clearly. It appears in the negative part of the coded rate flow values, in the positive part of the coded pH and salt concentration, and around the centre of the current. Quantitatively, a statistical analysis of the model yields an optimum in the point +0.85 for pH , −0.81 for Q_V, +0.42 for current and +1.13 for SEC, which is equivalent to pH= 10.70, Q_v= 4.10 $cm^3 \cdot min^{-1}$ (retention time in the reactor equal to 0.305 min), 2.43 A (current density, J, equal to 194 $mA \cdot cm^{-2}$) and 0.392 $mol \cdot L^{-1}$ of salt. As the four

factors are inside the significant region of the model (that is, all them are statistically significant with *p*-values under 0.05), this optimum may be considered statistically different from other near points. The maximum value of X_N is 100 % degradation of naproxen.

a)

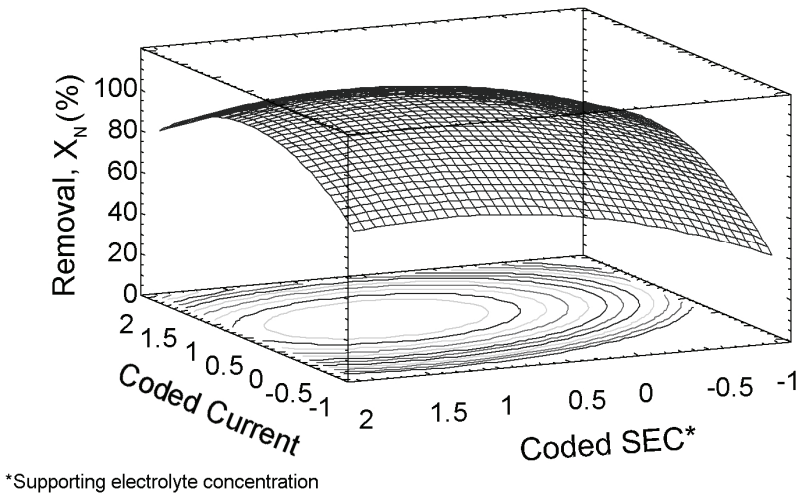

b)

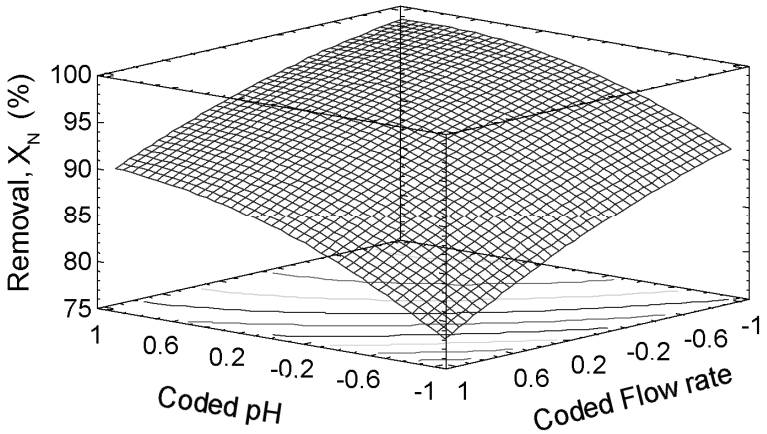

Fig. 2.19. Contour plot of the response surface: current-SEC.

a)

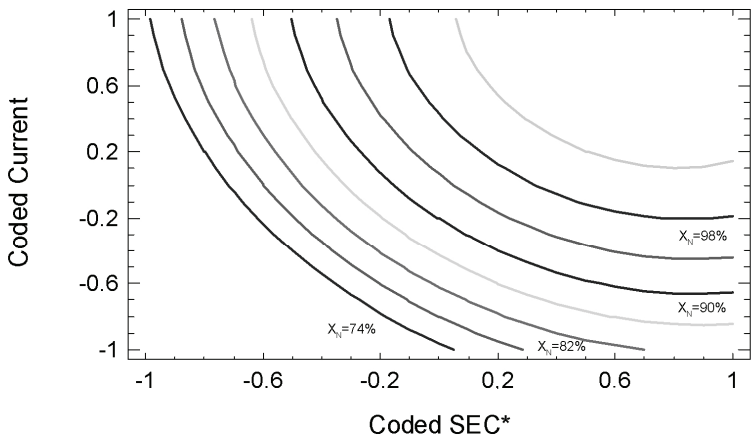

*Supporting electrolyte concentration

b)

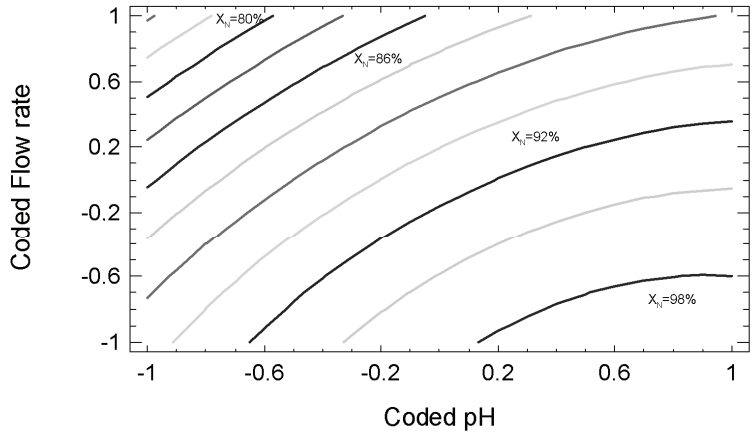

Fig. 2.20. Contour plot of the response surface: current-SEC.

The physical meaning to the results of the DOE can be justified as follows. As can be seen, the influence of current was the greatest of the variables studied. This may be explained by Eq. (2.1) indicating that the generation of hydroxyl radicals is due to the current. However, current tends to indicate an optimum in the last part of the curve. From the results of the DOE, we can conclude that above a certain value of current density (J equal to 194 $mA \cdot cm^{-2}$) the drug removal rate does not increase with current.

Suggesting that the high generation of hydrogen bubbles at the cathode can hinder the oxidation process in the aqueous phase.

The second most important variable was the supporting electrolyte concentration. The influence of this parameter was positive in studied region (-1 to +1). This can be justified by taking into account two factors: an increase in the concentration of salt favours, on the one hand, the conduction of current in solution; and on the other, formation of oxidizing species like peroxodisulphate (see Eq. (2.3)). Therefore, the model predicts an optimum value outside this range (for +1.13).

The result obtained for the flow rate was expected if we consider that this parameter is inversely proportional to the residence time of molecules into reactor. However, there is an optimum value in the initial part of the curve (for -0.81). This implies that a residence time above 0.305 min can have a negative effect on drug removal. This can be explained taking into account the competitive oxidation of the drug with other generated oxidation-products. On the other hand, the pH indicates an optimal value of +0.85. This pH value should be adequate to support both reactions, the more important anode reaction (favoured at basic pH) and the cathode reaction (favoured at acid pH).

2.3.3.7. Results obtained in optimum conditions.

An experiment was carried out under optimal conditions (pH= 10.70, Q_v= 4.10 $cm^3 \cdot min^{-1}$, J= 194 $mA \cdot cm^{-2}$ and SEC= 0.392 $mol \cdot L^{-1}$), to determine the removal of naproxen; TOC and COD obtained. Under such conditions, the reductions of naproxen, COD and TOC were 100%, 35.5% and 38%, respectively.

2.3.4. CONCLUSIONS.

The boron-doped diamond anodic electrochemical oxidation of naproxen in aqueous solution was studied. Design of experiments procedure was used to study the effect of pH (range 5-11), current density (J= 0-320 $mA \cdot cm^{-2}$), supporting electrolyte concentration Na_2SO_4 (range 0-0.375 $mol \cdot L^{-1}$), and solution flow rate (Q_v) between 3.64 and 0.8 $cm^3 \cdot min^{-1}$. Response surface methodology was used to optimize naproxen

degradation (X_N, %). The object of the present study was to find the optimum experimental conditions for this oxidation process.

An orthogonal, rotatable factorial central composite design of experiments was carried out. It showed that the influence of current density was the greatest of the studied variables, second was the supporting electrolyte concentration, third flow rate and fourth pH (the Anova test reported significance for seven of the fourteen variables involved). An optimum oxidation point was found at pH= 10.70, Q_v= 4.10 $cm^3 \cdot min^{-1}$ (which indicates a retention time in the reactor of 0.305 min), current density J= 194 $mA \cdot cm^{-2}$ using a supporting electrolyte concentration of 0.392 $mol \cdot L^{-1}$.

2.3.5. REFERENCES.

[1] Kolpin, DW.; Furlong, ET.; Meyer, MT.; Thurman, EM.; Zaugg, SD.; Barber, LB.; Buxton, HT. "Pharmaceuticals, hormones, and other organic wastewater contaminants in US streams, 1999–2000: a national reconnaissance". Environ. Sci. Technol. 36, 1202 **(2002)**.

[2] Boxall, ABA.; Kolpin, DW.; Halling-Sørensen, B.; Tolls, J. "Are veterinary medicines causing environmental risks?". Environ. Sci. Technol. 37, 286A **(2003)**.

[3] Snyder, SA.; Westerhoff, P.; Yoon, Y.; Sedlak, DL. "Pharmaceuticals, personal care products, and endocrine disruptors in water: implication for the water industry". Environ. Eng. Sci. 20, 449 **(2003)**.

[4] Ellis, JB. "Pharmaceutical and personal care products (PPCPs) in urban receiving waters". Environ. Poll. 144, 189 **(2006)**.

[5] Yu, JT.; Bouwer, EJ.; Coelhan, M. "Occurrence and biodegradability studies of selected pharmaceuticals and personal care products in sewage effluent, Agricultural". Water Management. 86, 72 **(2006)**.

[6] Al-Rifai, JH.; Gabelish, CL.; Schäfer, AI. "Occurrence of pharmaceutically active and non-steroidal estrogenic compounds in three different wastewater recycling schemes in Australia". Chemosphere. 69, 803 **(2007)**.

[7] Darlymple, OK.; Yeh, DH.; Trotz, MA. "Removing pharmaceuticals and endocrine-disrupting compounds from wastewater by photocatalysis". J. Chem.. Tech.. Biotechnol. 82, 121 **(2007)**.

[8] Metcalfe, CD.; Koenig, BG.; Bennie, DT.; Servos, M.; Ternes, TA.; Hirsch, R. "Occurrence of neutral and acidic drugs in the effluents of Canadian sewage treatment plants". Environ. Toxicology & Chemistry. 22, 2872 **(2003).**

[9] Boyd, GR.; Palmeri, JM.; Zhang, S.; Grimm, DA. "Pharmaceuticals and personal care products (PPCPs) and endocrine disrupting chemicals (EDCs) in stormwater canals and Bayou St. John in New Orleans, Louisiana, USA". Science of the Total Environment. 333, 137 **(2004)**.

[10] Benotti, MJ.; Trenholm, RA.; Vanderford, BJ.; Holady, JC.; Stanford, BD.; Snyder, SA. "Pharmaceuticals and endocrine disrupting compounds in U.S.drinking water". Environ. Sci. Technol. 43, 597 **(2009)**.

[11] Zhao, JL.;, Ying, GG.; Wang, L.; Yang, JF.; Yang, XB.; Yang, LH.; Li, X. "Determination of phenolic endocrine disrupting chemicals and acidic pharmaceuticals in surface water of the Pearl Rivers in South China by gas chromatography–negative chemical ionization–mass spectrometry". Science of the Total Environment . 407, 962 **(2009a)**.

[12] Zhao, X.; Qu, J.; Liu, H.; Qiang, Z.; Liu, R.; Hu, C. "Photoelectrochemical degradation of anti-inflammatory pharmaceuticals at Bi2MoO6–boron-doped diamond hybrid electrode under visible light irradiation". Applied Catalysis B: Environmental. 91, 539 **(2009b)**.

[13] Carballa, M.; Omil, F.; Lema, JM.; Llompart, M.; Garcia-Jares, C.; Rodríguez, I.; Gomez, M.; Ternes, A. "Behavior of pharmaceuticals, cosmetics and hormones in a sewage treatment plant". Wat. Res. 38, 2918 **(2004)**.

[14] Nakada, N.; Tanishima, T.; Shinohara, H.; Kiri, K.; Takada, H. "Pharmaceutical chemicals and endocrine disrupters in municipal wastewater in Tokyo and their removal during activated sludge treatment". Wat. Res. 40, 3297 **(2006)**.

[15] Boyd, GR.; Reemtsma, H.; Grimm, DA.; Mitra, S. "Pharmaceuticals and personal care products (PPCPs) in surface and treated waters of Louisiana, USA and Ontario, Canada". Sci. of he Total Environment. 311, 135 **(2003)**.

[16] Juttner, K.; Galla, U.; Schmieder, H. "Electrochemical approaches to environmental problems in the process industry". Electrochimica Acta. 45, 2575 **(2000)**.

[17] Ciríaco, L.; Anjo, C.; Correia, J.; Pacheco, MJ.; Lopes, A. "Electrochemical degradation of Ibuprofen on Ti/Pt/PbO2 and Si/BDD electrodes". Electrochimica Acta. 54, 1464 **(2009)**.

[18] Brillas, E.; Garcia-Segura, S.; Skoumal, M.; Arias, C. "Electrochemical incineration of diclofenac in neutral aqueous medium by anodic oxidation using Pt and boron-doped diamond anodes". Chemosphere. 79, 605 **(2010)**.

[19] Sirés, I.; Cabot, PL.; Centellas, F.; Garrido, JA.; Rodríguez, RM.; Arias, C.; Brillas, E. "Electrochemical degradation of clofibric acid in water by anodic oxidation: Comparative study with platinum and boron-doped diamond electrodes". Electrochimica Acta. 52, 75 **(2006)**.

[20] Guinea, E.; Arias, C.; Cabot, PL.; Garrido, JA.; Rodríguez, RM.; Centellas, F.; Brillas, E. "Mineralization of salicylic acid in acidic aqueous medium by electrochemical advanced oxidation processes using platinum and boron-doped diamond as anode and cathodically generated hydrogen peroxide". Wat. Res. 42, 511 **(2008)**.

[21] Brillas, E.; Sirés, I.; Arias, C.; Cabot, PL.; Centellas, F.; Rodríguez, RM.; Garrido, JA. "Mineralization of paracetamol in aqueous medium by anodic oxidation with a boron-doped diamond electrode". Chemosphere. 58, 399 **(2005)**.

[22] Panizza, M.; Cerisola, G. "Application of diamond electrodes to electrochemical processes". Electrochimica Acta. 51, 191 **(2005)**.

[23] Zhu, XP.; Tong, MP.; Shi, SY.; Zhao, HZ.; Ni, JR. "Essential explanation of the strong mineralization performance of boron-doped diamond electrodes". Environ. Sci. Technol. 42, 4914 **(2008)**.

[24] Montgomery, DC. "Design and Analysis of Experiments", 5th ed. John Wiley and Sons, New York **(2001)**.

[25] Milani AS, H.; Wang, H.; Frey, DD.; Abeyaratne, RC. "Evaluating three DOE methodologies: optimization of a composite laminate under fabrication error". Quality Engineering. 21, 96 **(2009)**.

[26] Bhatia, S.; Othman, Z.; Ahmad, AL. "Pretreatment of palm oil mill effluent (POME) using Moringa oleifera seeds as natural coagulant". J. Hazard. Mater. 145, 120 **(2007)**.

[27] Sabio, E.; Zamora, F.; Ganán, J.; González-García, CM.; González, JF. "Adsorption of p-nitrophenol on activated carbon fixed-bed". Wat. Res. 40, 3053 **(2006)**.

2.4. DEVELOPMENT AND OPTIMIZATION OF THE BDD-ELECTROCHEMICAL OXIDATION OF THE ANTIBIOTIC TRIMETHOPRIM IN AQUEOUS SOLUTION

The occurrence of antibiotics in the aquatic environment has led to an increasing concern about the potential environmental risks and the maintenance and spread of antibacterial resistance among microorganisms. Electrochemical oxidation processes are promising technologies to treat low contents of toxic and biorefractory pollutants in water. Anodic oxidation of trimethoprim, the most frequently detected antibiotic in surface waters, was carried out using boron-doped diamond electrodes at galvanostatic mode. A statistical design of experiments has been used to study the influence of the different operating variables: pH (in the range 3-11), current intensity (from 0 to 320 $mA \cdot cm^{-2}$), supporting electrolyte concentration Na_2SO_4 in the range 0-0.5 $mol \cdot L^{-1}$, and solution flow rate between 1.25 and 10.80 $cm^3 \cdot min^{-1}$. Response Surface Methodology technique was used to optimize trimethoprim degradation. Current intensity resulted to be the main variable influencing trimethoprim degradation, followed by salt concentration and pH. ANOVA test reported significance for five of the fourteen involved variables. An optimum trimethoprim degradation of 100% was found at pH 3, under a flow rate equal to 1.25 $cm^3 \cdot min^{-1}$, and with a current density equal to 207 $mA \cdot cm^{-2}$, using a supporting electrolyte concentration equal to 0.49 $mol \cdot L^{-1}$.
Keywords: electrochemical advanced oxidation processes, electro-oxidation, anodic oxidation, boron-doped diamond electrodes, pharmaceuticals, trimethoprim.

2.4.1. INTRODUCTION.

Considering the wide variety and different applications of antibiotics and the ever increasing tendency to use antibiotics, it is no surprise that these drugs are among the most ubiquitous environmental contaminants [1,2]. The occurrence of antibiotics in the aquatic environment has led to an increasing concern about the potential environmental risks as well as about the maintenance and spread of antibacterial resistance among microorganisms. Development of antibiotic resistance of bacteria was demonstrated in surface and groundwater affected by the sewage treatment plant

effluent [3]. Whether antibiotics transported in the environment from human and livestock sources lead to increased antibiotic resistant bacteria or have deleterious effects on water quality is an important but largely unresolved issue. The use of antibiotics may also accelerate the development of antibiotic resistance genes and bacteria, which shade health risks to humans and animals [4].

The main source of antibiotics in the environment is the excretion of incompletely metabolized drugs by humans and animals. Other sources may include the disposal of unused antibiotics and waste from pharmaceutical manufacturing processes [5]. Residential care facilities and hospitals are known contributors of antibiotics to municipal wastewater [6]. Other contributors to surface and groundwater are effluent from wastewater treatment plants [6] and industrial facilities (including pharmaceutical plants), and surface run-off from concentrated animal feeding operations [1].

Recently, scientists have raised concerns about pharmaceutical residues detected in surface waters and wastewaters and their potential to cause adverse effects in humans and aquatic species [7,8]. Wastewater typically contains any number of medications and antibiotics that people have either used or discarded. Many of these chemical compounds remain biologically active. And some of them, especially antibiotics, stimulate the development of antibiotic resistant bacteria.

Recent studies have confirmed the presence of low levels of pharmaceuticals in estuaries, rivers, streams, and ground water as well as in sediments [9,10]. The ecological effects of these contaminants in coastal waters are largely unknown. However, there is growing evidence that some of these chemicals may have negative effects on reproduction in aquatic species or stimulate the development of antibiotic resistant bacteria.

Trimethoprim (TMP) [2,4-diamino-5-(3′,4′,5′-trimethoxybenzylpyrimidine)] (molecular formula $C_{14}H_{18}N_4O_3$, molecular weight 290.32, CAS Number 738-70-5, pKa= 7.2) is a very good antifolate drug. It selectively inhibits the bacterial form of the dihydrofolate reductase enzyme [11,12]. TMP is among the most important

synthetic antibiotics used worldwide in human and veterinary medicine acting as an inhibitor in the chemotherapy treatment due to its antifolate effect by interaction with dihydrofolate coenzymes [13-15]. TMP is mainly used in the prophylaxis and treatment of urinary tract infections, as well as for prevention and treatment of respiratory or gastro-intestinal tract infections in cattle, swine and poultry [16].

In light of these facts, advanced drinking and wastewater treatment options should be considered for the removal of these drugs. Between these options, Electrochemical Advanced Oxidation Processes (EAOPs) [17-19] are very attractive for water and wastewater decontamination due to their low cost and high effectiveness, without needing addition of toxic chemical reagents and without producing dangerous wastes. Among EAOP, Anodic Oxidation (AO) is the most effective technique. It consists in the destruction of pollutants in an electrolytic cell under the action of hydroxyl radicals formed as intermediate from water oxidation at the surface of the anode [20,21].

Recently, AO has attracted great attention for wastewater treatment due to manufacture of a new anode material. The use of a boron-doped diamond (BDD) thin-film anode brings technologically important characteristics such as an inert surface with low adsorption properties, remarkable corrosion stability and a wide potential window in aqueous medium [22,23]. These properties confer to the BDD-anode a much greater O_2 overvoltage than a conventional anode such as Pt, allowing the production of larger amounts of highly reactive M(·OH) product from Equation (2.1). This material is considered the best "non-active" anode. The material interacts so weakly with ·OH radicals that allows the direct reaction of organics with M(·OH) to give fully oxidized reaction products such as CO_2 as follows:

$$42\ M(\cdot OH) + C_{14}H_{18}N_4O_3 \rightarrow 42M + 14CO_2 + 9H_2O + 4NO_2 \qquad (2.13)$$

Different authors have shown that several pollutants have been completely mineralized by AO with BDD-anodes, whereas the use of a Pt-anode under comparable conditions leads to weak decontamination because of the formation of carboxylic acids that are hardly ever oxidized with this material [24-28].

When BDD-anode is used, other weaker oxidizing species like peroxodisulphate, (if sodium sulfate is used as supporting electrolyte, as in this work) can also be competitively formed with reactive oxygen species (see Eq. (2.3)):

This investigation presents the results obtained from the BDD-AO of TMP. A statistical design of experiments (DOE) was used to study the influence of the different operating variables: pH (in the range 3-11), current intensity (J from 0 to 320 $mA \cdot cm^{-2}$), supporting electrolyte concentration (SEC), Na_2SO_4 in the range 0-0.5 $mol \cdot L^{-1}$, and solution flow rate (Q_v) between 1.25 and 10.80 $cm^3 \cdot min^{-1}$. Response Surface Methodology (RSM) technique was used to optimize TMP degradation (X_T,%). So, the objective of the present study was to analyze the influence of the different operating variables and find out the optimum values for this decontamination process.

2.4.2. MATERIALS AND METHODS.

2.4.2.1. Experimental procedures.

TMP of the highest purity available (>98% TLC) was provided by Sigma–Aldrich Spain. TMP stock solution was prepared with high purity water obtained from a Millipore Milli-Q® system. All reagents and solvents were of analytical grade and were purchased from Panreac (Spain). The solution pH was adjusted with sodium hydroxide and orthophosphoric acid (0.01/0.01 $mol \cdot L^{-1}$) buffer solution. The supporting electrolyte used in this investigation, Na_2SO_4, was provided by Panreac in analytical purity grade.

A detailed description of the experimental procedure in terms of electrolytic cell, power supply and degradation experiments have been provided in a previous paper [29].

The initial concentration of TMP for all experiments was $1.72 \cdot 10^{-4}$ $mol \cdot L^{-1}$ and temperatures was kept constant at 25 ± 0.1ºC. TMP concentration was determined in all cases by HPLC with the aid of a Waters Chromatograph equipped with a 996 Photodiode Array Detector and a Waters Nova-Pak C18 Column (5 µm 150×3.9mm).

It displayed a well defined peak for TMP at a retention time (t_r) of 2.42 min at 277 nm. For these analyses, samples of 50 µl were injected into the chromatograph and a 30:70 (v/v) methanol/water (10^{-2} M orthophosphoric acid) mixture was passed at a flow rate of 1 $mL \cdot min^{-1}$ as mobile phase.

Total Organic Carbon content (TOC) was determined as described elsewhere [29].

2.4.2.2. Mathematical and statistical procedures.

Typically, the one-factor-at-a-time approach has been used to study the influence of several operation variables (factors) on a parameter (response). Nevertheless, this classical methodology involves a large number of experiments and some important conclusions on the interaction among factors can be missed. To avoid these important disadvantages, statistical design of experiment (DOE) offers an efficient alternative since it offers the possibility of analyzing the effect of variables and their responses minimizing the number of experiments [30].

In the present study, a routine DOE previously optimized by our research group [29] has been used. StatGraphics® software provides a useful and powerful mathematical and statistical tool in order to develop the experimental planning, to analyse the results and to draw conclusions on a rigorous basis. StatGraphics® Plus was used to design and analyze the experimental results. A factorial central composite orthogonal and rotatable (CCORD) design was used with twelve replicates of the central experiment. This design involves the use of a two–level factorial design with 2^k points combined with $2k$ axial points and n replicates of the central experiment, k being the number of factors. N, the total number of experiments with k factors is obtained according to Eq. (2.6).

In this study k was equal to four and n, as indicated above, was considered to be twelve. The axial distance was 2 in order to guarantee an orthogonal and rotatable design. Hence, according to Eq. (2.6), the total number of experiments resulted to be 36.

To evaluate the influence of pH, I, SEC and Q_v and their concomitant effects on the effectiveness of the BDD electrochemical oxidation of TMP, different levels were set for this pharmaceutical. The selection of such levels was performed in antecedence (data not shown). Table 2.13 summarizes the operating levels used in the present study.

Table 2.13. Operating levels.

pH		Q_v ($cm^3 \cdot min^{-1}$)		I (A)		SEC ($mol \cdot L^{-1}$)	
Low level (-1)	**High level (+1)**	**Low level (-1)**	**High level (+1)**	**Low level (-1)**	**High level (+1)**	**Low level (-1)**	**High level (+1)**
5	9	3.64	8.42	1	3	0.125	0.375

Additionally to the operating levels indicated in Table 2.13, in order to guaranty the rotatability of the design, a set of experiments with coded values of variables equal to ±2 was performed. Hence, this specific study involves a range of 3-11 in pH, 1.25 - 10.80 $cm^3 \cdot min^{-1}$ in flow rate, 0-4 A in current and 0–0.5 M in the concentration of supporting electrolyte. Table 2.14 shows the experimental planning in DOE, and the response obtained in each of the experiments performed in this study.

Table 2.14. Experimental planning in DOE and obtained response in each experiment.

Run	Coded pH	Coded Q_v	Coded I	Coded SEC	X_T (%)
1	1	1	-1	-1	83.8
2	1	-1	-1	1	99.8
3	-1	-1	-1	-1	62.7
4	1	-1	1	-1	99.8
5	-1	1	-1	1	68.2
6	0	0	0	-2	69.7
7	0	-2	0	0	99.9
8	1	-1	1	1	100
9	0	0	-2	0	0.00
10	-1	-1	1	1	100
11	-1	1	1	-1	89.6
12	0	0	0	0	98.9
13	1	1	1	-1	99.7
14	0	0	0	0	98.5
15	-1	1	-1	-1	50.5
16	0	0	0	0	98.8
17	0	0	0	0	99.5
18	0	0	0	2	100
19	2	0	0	0	99.5
20	0	0	0	0	99.3
21	1	-1	-1	-1	64.4
22	1	1	-1	1	94.9
23	0	0	0	0	97.9
24	-1	-1	-1	1	93.3
25	0	0	0	0	97.8
26	0	0	0	0	98.8
27	-1	-1	1	-1	96.6
28	0	2	0	0	92.8
29	0	0	2	0	99.8
30	0	0	0	0	98.9
31	-1	1	1	1	99.4
32	0	0	0	0	98.7
33	0	0	0	0	98.0
34	0	0	0	0	98.8
35	-2	0	0	0	82.7
36	1	1	1	1	99.6

2.4.3. RESULTS AND DISCUSSION.

As indicated above, Table 2.14 shows the experimental planning in DOE as well as the response obtained in each experiment in terms of removal efficiency of TMP (X_T).

2.4.3.1. Numerical analyses. Anova report.

The ANOVA analysis reports on the significance of the different parameters. The results of the ANOVA tests are summarized in Table 2.15. According to the RSM, fourteen factors have been considered and only five of them exhibit a *p*-value below a limit of significance of 0.05, so they are statistically significant. This latter confirms the consistency of the model used to represent the behavior of the interactive factors.

Table 2.15. ANOVA results.

Factor	Sum of squares	Degrees of freedom	F-ratio	p-values $\times 10^2$
A: coded pH	553.9	1	6.95	0.0154
B: coded Q_v	84.75	1	1.06	0.3142
C: coded I	5602	1	70.2	0.0000
D: codec SEC*	1185	1	14.8	0.0009
AA	15.82	1	0.20	0.6605
AB	216.8	1	2.72	0.1140
AC	187.0	1	2.35	0.1405
AD	13.87	1	0.17	0.6808
BB	11.88	1	0.15	0.7033
BC	13.51	1	0.17	0.6848
BD	60.45	1	0.76	0.3937
CC	3874	1	48.6	0.0000
CD	415.1	1	5.21	0.0330
DD	164.2	1	2.06	0.1659
Total error	1674	21		

* Supporting electrolyte concentration of Na_2SO_4.

Non-linear polynomial regression was carried out and the following expression was obtained:

$$\begin{aligned} X_T &= 98.64 + 4.80 \cdot A - 1.88 \cdot B + 15.28 \cdot C + 7.03 \cdot D - 0.703 \cdot A^2 + \\ &+ 3.68 \cdot AB - 3.42 \cdot AC - 0.93 \cdot AD + 0.61 \cdot B^2 + 0.92 \cdot BC - 1.94 \cdot BD - \\ &- 11 \cdot C^2 - 5.09 \cdot CD - 2.26 \cdot D^2 \end{aligned} \tag{2.14}$$

where the values of A (pH), B (flow rate, Q_v), C (current intensity, I) and D (Na_2SO_4 concentration) should be coded. The values of TMP removal, X_T, are given in %. The correlation factor r^2 is equal to 0.88. This regression predicts an optimum X_T equal to 100% at pH equal to 3, operating under a flow rate of 1.25 $cm^3 \cdot min^{-1}$ (retention time equal to 0.996 min), current intensity equal to 2.59 A (i.e., equivalent to a current density of 207 $mA \cdot cm^{-2}$ provided that the electrode surface is 12.5 cm^2) and a salt concentration equal to 0.493 $mol \cdot L^{-1}$. For each experiment, the difference between experimental X_T and calculated X_T (according to Eq. (2.14)) is represented in Figure 2.21 versus the specific run number. It may be easily concluded from Figure 2.21 that residuals are located in a random order at both the sides of the 0 axis. This fact suggests that no correlation can be appreciated and, hence, the randomization of the design is fully effective and no accumulation of experimental error is observed.

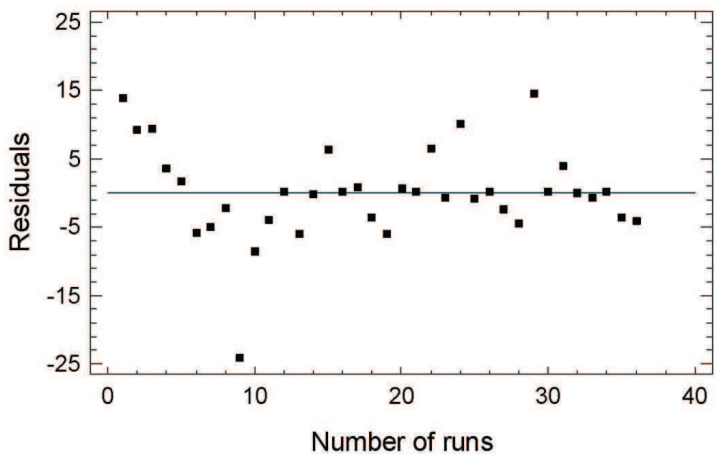

Fig. 2.21. Residual versus run number.

2.4.3.2. Graphical analyses and significance of variables.

The modelization of results was made on the basis of the fourteen factors indicated in Eq. (2.14). The Pareto plot (Figure 2.22) is considered as a graphical expression of the ANOVA test. In this kind of plots, bars represent the standardized effects of each of the factors involved in the analysis, considering them as the pH, current (I), supporting electrolyte concentration (SEC), flow rate (Q_v) and combinations of all them. Nonfilled bars are a graphical representation of negative-affecting factors. In this case the Pareto plot indicates that flow rate, the squared of current, pH and SEC, and the combinations of I-SEC, pH-SEC, pH-I and Q_v-SEC affect in a negative manner the removal efficiency of TMP. The mathematical expression of the negative influence of these factors is the fact that all of them appear in expression (2.14) behind a negative sign (-). On the contrary, filled bars within the Pareto plot represent positive-affecting factors. In this case I, SEC, pH, the squared of Q_v, and the combination of pH-Q_v and Q_v-I exert a positive effect on the removal efficiency of TMP, X_T. It is worth noting that a vertical rule stands near to 2 in the Pareto plot. In this connection it must be born in one's mind that this rule is closely related to the signification level of ANOVA test, which has been fixed in a 95% of confidence. Accordingly, bars overcoming the vertical rule in the Pareto plot must be considered as inside the significance region (i.e., factors A, C, D, CC and CD). On the contrary, bars located behind the vertical rule are not statistically significant (i.e., B, AA, BB, DD, AB, AC, AD, BC and BD). The Pareto plot also provides interesting information on how factors influence the final response, X_T. Positive, filled, bars indicate that an increase in a given variable makes X_T increase too. Negative, nonfilled, bars indicate exactly the opposite. Hence, as an example, it may be observed that as rate flow level raises the value of X_T decreases whereas if current intensity and salt concentration rise, X_T increases as well.

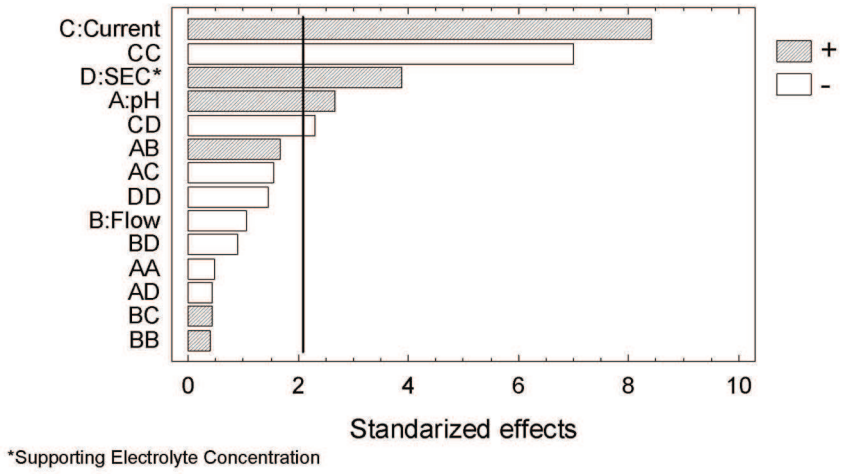

Fig. 2.22. Pareto graphic: standarized effects.

2.4.3.3. Influence of variables. Possible interactions.

The use of a CCORD model makes it also possible to analyze the main effects of the involved variables. In particular, the influence of single variables can be observed in Figure 2.23 (a). In this figure four plots have been drawn representing the effect of varying each of the variables while the other ones are kept constant. It may be easily observed that current intensity, SEC and pH exhibit a quasi-linear positive-affecting tendency, whereas Q_v presents a slightly linear negative-tendency, which suggests a scarcely negative influence of this latter variable. Current intensity appears to be the variable exerting a more remarkable effect on the removal efficiency of TMP, followed by the supporting electrolyte concentration (SEC) and pH. These results are in accordance with those depicted in the Pareto plot (Figure 2.22). However, the fact that the optimal point is set in the lowest pH level (-2.00 in coded values) may be somewhat surprising. This may be attributable to the occurrence of an interaction involving pH and flow rate as well as to the fact that the squared pH factor (A^2) exhibits a negative sign in Eq. (2.14). As a consequence of this specific circumstance, the optimal point is located at a negative value of pH. Finally, the influence of the fourth variable (flow rate) resulted to be not significant.

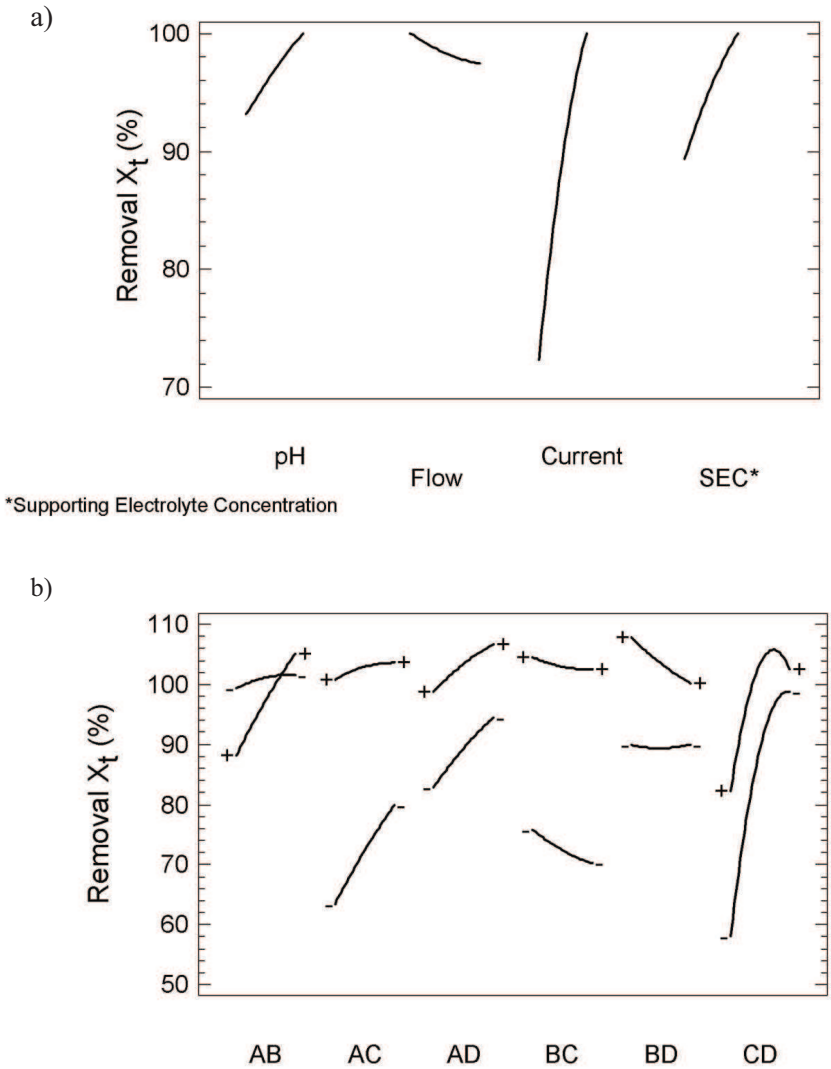

Fig. 2.23. Single effects (a) and interactions (b) of flow rate, pH dosage of Na_2SO_4 and current density.

Figure 2.23 (b) shows the interaction between each two of the four variables studied. Each pair of curves represents the evolution of X_T by varying one variable in the extremes of the CCORD model, that is, with its pair variable equal to 1 (upper value) and equal to −1 (low value). If parallel lines are obtained it may be concluded

that there is no interaction between the variables under study. The occurrence of crossing lines indicates the opposite. The level of interaction of one variable with the other is represented as an intermediate between these two situations.

According to this latter, no interaction may be assumed in the case of the pairs of variables AD, as the curves exhibit a parallel behavior. Hence, the modification of one of the variables does not significantly affect the other one. In contrast, for the pairs of variables AB the corresponding lines clearly intersect as shown in Figure 2.23 (b). Hence, the interaction between pH (A) and flow rate (B) is evident. An intermediate situation is observed in the case of the pairs AC, BC, BD and CD, where plots cannot be considered as parallel but they do not intersect, either. Since these plots do not exhibit a parallel behavior, it may be assumed that there is interaction, and consequently the modification of one of the variables affects the other one. However, it must be assumed that the intersection takes place outside the region analyzed in this particular CCORD model.

2.4.3.4. Response surface and contour plot.

The surface plot is a graphical representation that allows evaluating the behavior of the whole system under analysis from a qualitative point of view. It is perhaps the most important graphical representation in the response surface methodology approach.

Figure 2.24 represents the surface plot corresponding to Eq. (2.14). This figure clearly shows that the response surface plot is a quite convex surface within the whole studied region. Additionally, a maximum is apparent in the positive middle region of the coded I (+0.59). Figure 2.24 also includes the contour plot.

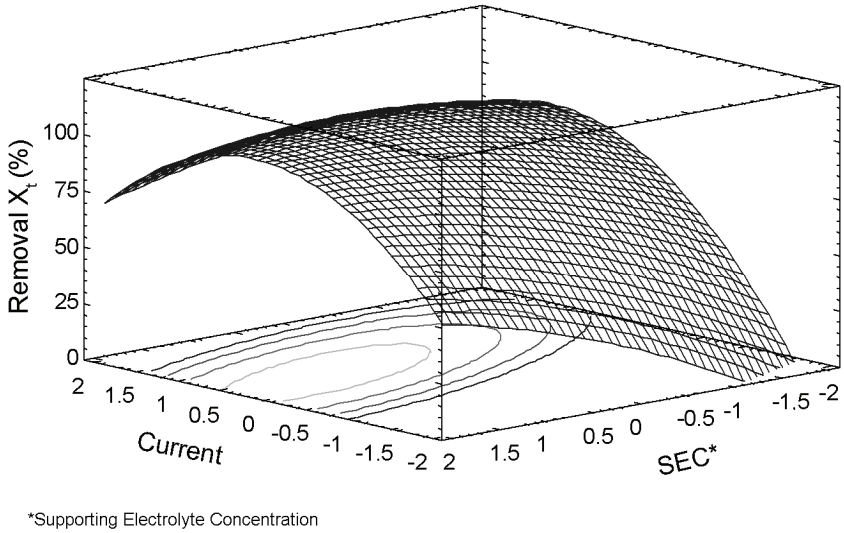

Fig. 2.24. Response surface and contour plot model CCORD: current-SEC.

From a quantitative point of view, a statistical analysis of the model yields to an optimum at the coded values equal to -2 for pH, -2 for Q_V, +0.59 for I and +1.94 for SEC, which is equivalent to pH= 3, flow rate Q_v= 1.25 $cm^3 \cdot min^{-1}$ (retention time equal to 0.996 min), current intensity I= 2.59 A (current density, J, equal to 207 $mA \cdot cm^{-2}$) and supporting electrolyte concentration SEC= 0.493 $mol \cdot L^{-1}$ of Na_2SO_4.

Given the fact that three of the four factors under study are inside the significant region of the model (that is, all three of them are statistically significant as their *p*-values are under 0.05), this optimum may be considered as statistically different from other close points. Under the optimal conditions a maximum value of TMP removal, X_T, equal to 100 % is predicted by the model. In order to corroborate this assertion, an experiment was performed under the optimal conditions provided by the model (i.e., pH= 3, Q_v= 1.25 $cm^3 \cdot min^{-1}$, J= 207 $mA \cdot cm^{-2}$ and SEC= 0.493 $mol \cdot L^{-1}$). The results obtained for TMP removal, COD and TOC, were 100%, 20.1% and 50.9%, respectively.

2.4.3.5. Rationalization of the results.

As indicated above, current intensity is the most important variable influencing the removal of TMP. This fact may be explained taking into consideration Eq. (2.1). According to this equation, the generation of the very reactive hydroxyl radical is remarkably influenced by the current intensity. However, Figure 2.23 (a) suggests that current tends to present an optimum. Thus, it may be concluded that above a certain value of current density (in this case J= 207 $mA \cdot cm^{-2}$) the TMP removal efficiency does not increase with current. In this sense, the generation of large amounts of hydrogen bubbles at the cathode may result in the hindering of the oxidation process in aqueous phase.

The second most important variable influencing the TMP removal was the supporting electrolyte concentration. The influence of this parameter is positive within the whole interval here studied. This fact may be justified by taking into account two factors. Firstly, an increase in the concentration of salt favors the electrical conductivity in solution. Secondly, the formation of such an oxidizing species like peroxodisulphate (see Eq. (2.3)) is also favored by the increase of SO_4^{2-} ions in solution. As a consequence, the model predicts an optimum value outside this range (for +1.94).

The fact that flow rate exerts a negative influence on the removal efficiency of TMP was expectable since the larger the flow rate, the shorter is the residence time of TMP molecules inside the reactor.

Finally, for pH, the optimum point is set in the lowest pH level (-2.00 in coded values). This fact is attributable to the protonation of amino groups of TMP, hence increasing their reactivity towards the highly nucleophilic hydroxyl radicals.

2.4.4. CONCLUSIONS.

Electrochemical Advanced Oxidation of trimethoprim on Boron-Doped Diamond Electrodes in aqueous solution has been studied. In order to establish the influence of operating variables, an orthogonal, rotatable factorial central composite statistical

design of experiments was performed. The results obtained clearly show that current intensity is the variable exerting the most remarkable influence on the removal efficiency of trimethoprim, followed by the supporting electrolyte concentration and pH. On the other hand, the fourth variable, flow rate, does not appear to exert a significant influence within the region of the CCORD model. The use of the ANOVA test reported significance for five of the fourteen variables involved. The model predicted an optimum oxidation point at pH= 3, Q_v= 1.25 $cm^3 \cdot min^{-1}$ (retention time equal 0.996 min), J= 207 $mA \cdot cm^{-2}$, using a SEC= 0.493 $mol \cdot L^{-1}$. These optimal conditions were confirmed experimentally and a value of X_T= 100% was achieved.

2.4.5. REFERENCES.

[1] Hirsch, R.; Ternes, T.; Haberer, K.; Kratz, K.L. "Occurrence of antibiotics in the aquatic environment". Science of the Total Environment. 225, 109 **(1999)**.

[2] Harwood, V.J.; Whitlock, J.; Withington, V. "Classification of antibiotic resistance patterns of indicator bacteria by discriminant analysis: Use in predicting the source of fecal contamination in subtropical waters". Applied and Environmental. Microbiology. 66, 3698 **(2000)**.

[3] Halling-Sorensen, B.; Nielsen, S.N.; Lanzky, P.F.; Ingerslev, F.; Holten Liitzhofl, H.C.; Jorgensen, S.E. "Occurrence, fate and effects of pharmaceutical substances in the environment-A review". Chemosphere. 36, 357 **(1998)**.

[4] Kemper, N. "Veterinary antibiotics in the aquatic and terrestrial environment". Ecological Indicators. 8, 1 **(2008)**.

[5] Kathryn, D.B.; Jerzy, K.; Bruce, T.; Timothy, H.C.; Douglas, B.M. "Occurrence of antibiotics in hospital, residential, and dairy effluent, municipal wastewater, and the Rio Grande in New Mexico". Science of the Total Environment. 366, 772 **(2005)**.

[6] Alder, A.C.; McArdell, C.S.; Golet, E.M.; Molnar, E.M.; Kuch, H.M.; Giger, W. "Environmental exposure of antibacterial agents in hospital and municipal wastewater and river water in Switzerlan". Proceedings of 3rd International Conference on Pharmaceuticals and Endocrine Disrupting Chemicals in Water. Minneapolis, 236, March **(2003)**.

[7] Ouattara, L.; Chowdhry, M.M.; Comninellis, C. "Electrochemical treatment of industrial wastewater". New Diamond and Frontier Carbon Technology. 14, 239 **(2004)**.

[8] Mascia, M.; Vacca, A.; Polcaro, A.M.; Palmas, S.; Ruiz, J.R.; Da Pozzo, A. "Electrochemical treatment of phenolic waters in presence of chloride with boron-doped diamond (BDD) anodes: Experimental study and mathematical model". Journal of Hazardous Materials. 174, 314 **(2010)**.

[9] Cañizares, P.; Paz, R.; Lobato, J.; Sáez, C.; Rodrigo, M.A. "Electrochemical treatment of the effluent of a fine chemical manufacturing plant". Journal of Hazardous Materials. 138, 173 **(2006)**.

[10] Scialdone, O.; Galia, A.; Guarisco, C.; Randazzo, S.; Filardo, G. "Electrochemical incineration of oxalic acid at boron doped diamond anodes: Role of operative parameters". Electrochimica Acta. 53, 2095 **(2008)**.

[11] Hitching, G.H.; Kuyper, L.F.; Baccananari, D.P. in: Sandler, M., Smith, H.J. (Eds). "Design of Enzyme Inhibitors as Drugs". Oxford University Press. NY, 343 **(1998)**.

[12] Raj, S.B.; Stanley, N.; Muthiah, P.T.; Bocelli, G.; Ollá, R.; Cantoni, A. "Crystal Engineering of Organic Salts: Hydrogen-Bonded Supramolecular Motifs in Trimethoprim Sorbate Dihydrate and Trimethoprim. o-Nitrobenzoate". Crystal Growth & Design. 4, 567 **(2003)**.

[13] Bekçi, Z.; Seki, Y.; Yurdakoç, M.K. "Equilibrium studies for trimethoprim dsorption on montmorillonite KSF". Journal of. Hazardous Materials. 133, 233 **(2006)**.

[14] Diaz-Cruz, M.S.; Lopez de Alda, M.J.; Barcelo, D. "Environmental behavior and analysis of veterinary and human drugs in soils, sediments and sludge". Trends in Analytical Chemistry. 22, 340 **(2003)**.

[15] Batt, A.L.; Aga, D.S. "Simultaneous analysis of multiple classes of antibiotics by ion trap LC/MS/MS for assessing surface water and groundwater contamination". Analytical Chemistry 77, 2940 **(2005)**.

[16] De Paula, F.C.C.R.; de Pietro, A.C.; Cass, Q.B.J. "Simultaneous quantification of sulfamethoxazole and trimethoprim in whole egg samples by column-switching high-performance liquid chromatography using restricted access media column for on-line sample clean-up". Journal of. Chromatography A. 1189, 221 **(2008)**.

[17] Bensalah, N.; Quiroz Alfaro, M.A.; Martínez-Huitle, C.A. "Electrochemical treatment of synthetic wastewaters containing Alphazurine A dye". Chemical Engineering Journal. 149, 348 **(2009)**.

[18] Güven, G.; Perendeci, A.; Tanyolaç, A. "Electrochemical treatment of simulated beet sugar factory wastewater". Chemical Engineering Journal. 151, 149 **(2009)**.

[19] Ahmed Basha, C.; Chithra, E.; Sripriyalakshmi, N.K. "Electro-degradation and biological oxidation of non-biodegradable organic contaminants". Chemical Engineering Journal. 149, 25 **(2009)**.

[20] Marselli, B.; García-Gomez, J.; Michaud, P.A.; Rodrigo, M.A.; Comninellis, Ch. "Electrogeneration of hydroxyl radicals on boron-doped diamond electrodes". Journal of the Electrochemical Society. 150, D79 **(2003)**.

[21] Panizza, M.; Cerisola, G. "Application of diamond electrodes to electrochemical processes". Electrochimica Acta. 51, 191 **(2005)**.

[22] Brillas, E.; Calpe, J.C.; Casado, J. "Mineralization of 2,4-D by advanced electrochemical oxidation processes". Water Research. 34, 2253 **(2000)**.

[23] Martínez-Huitle, C.A.; Ferro, S. "Electrochemical oxidation of organic pollutants for the wastewater treatment: direct and indirect processes". Chemical Society Reviews. 35, 1324 **(2006)**.

[24] Brillas, E.; Sirés, I.; Arias, C.; Cabot, P.L.; Centellas, F.; Rodríguez, R.M.; Garrido, J.A. "Mineralization of paracetamol in aqueous medium by anodic oxidation with a boron-doped diamond electrode". Chemosphere. 58, 399 **(2005)**.

[25] Cañizares, P.; Lobato, J.; Paz, R.; Rodrigo, M.A.; Sáez, C. "Electrochemical oxidation of phenolic wastes with boron-doped diamond anodes". Water Research. 39, 2687 **(2005)**.

[26] Boulbaba, L.; Nasr, B. Abdellatif, G. "Electrochemical oxidation of benzoic acid derivatives on boron doped diamond: voltammetric study and galvanostatic electrolyses". Chemical Engineering & Technology. 29, 944 **(2006)**.

[27] Flox, C.; Ammar, S.; Arias, C.; Brillas, E.; Vargas-Zavala, A.V.; Abdelhedi, R. "Electro-Fenton and photoelectro-Fenton degradation of indigo carmine in acidic aqueous medium". Applied Catalysis B: Environmental. 67, 93 **(2006)**.

[28] Sirés, I.; Centellas, F.; Garrido, J.A.; Rodríguez, R.M.; Arias, C.; Cabot, P.L.; Brillas, E. "Mineralization of clofibric acid by electrochemical advanced oxidation processes using a borondoped diamond anode and Fe^{2+} and UVA light as catalysts". Applied Catalysis B: Environmental. 72, 373 **(2007)**.

[29] Domínguez, J.R.; González, T.; Palo, P.; Sánchez-Martín, J. "Anodic oxidation of ketoprofen on boron-doped diamond (BDD) electrodes". Role of operative parameters, Chemical Engineering Journal. 162, 1012 **(2010)**.

Capítulo 3:
ELECTROCHEMICAL DEGRADATION OF CARBAMAZEPINE. EFFECTS OF WATER MATRICES

3.1. ELECTROCHEMICAL DEGRADATION OF CARBAMAZEPINE IN AQUEOUS SOLUTIONS. OPTIMIZATION OF KINETIC ASPECTS BY DESIGN OF EXPERIMENTS

Electrodegradation of simulated pharmaceutical wastewaters was performed and optimized. To this end, carbamazepine was used as model compound and a design of experiments was planned for evaluating the influence of two main variables in the electrochemical process: initial carbamazepine concentration (in logarithm terms) and the current intensity. Target variable was an apparent first-order kinetic constant (*k*). Interaction of variables was confirmed and an optimum *k* constant of 0.72 min^{-1} was obtained. This value corresponds to a design corner, so the higher the initial pollution, the fastest the pollutant removal is. Carbamazepine was also removed from real wastewater matrices, such as urban wastewater sample or surface lake water.

Keywords: Electrodegradation, pharmaceuticals, design of experiments, carbamazepine, wastewater treatment.

3.1.1. INTRODUCTION.

Large amounts of pharmaceutical compounds are used to human and animal disease. The worldwide average per capita consumption of pharmaceutical compounds per year is estimated to be about 15 g and in industrialized countries the value is expected to be between 50 and 150 g [1]. After their consumption, most of them are excreted by bodies, and enter sewage treatment plants. Other sources may include the disposal of unused antibiotics and waste from pharmaceutical manufacturing processes [2].

The most representative pharmaceuticals detected in urban wastewaters are anti-inflammatory drugs, anticonvulsants, antibiotics and antihypertensives [3]. However,

some of them are not completely eliminated by conventional wastewater treatments [4,5], and has been detected in aquatic environments worldwide, like drinking waters [6-9] and surface waters [10,11].

Due to this problem, there is an increasing interest in reliable technologies for their removal. Electrooxidation is finding its application in wastewater treatment in combination with other technologies such as chemical, photochemical and photocatalytic methods [12-15]. Electrooxidation is effective in degrading the refractory pollutants on the surface of a few electrodes, among them the diamond film electrodes, used in this work. It should be noted its excellent chemical and electrochemical properties, its main remarkable characteristic is its high overpotential for water electrolysis allowing the generation of large amounts of hydroxyl radicals [16-18]. The hydroxyl radical is a very powerful oxidant (E^0= 2.80 V) and it seems to be directly involved in the oxidation mechanisms that occur on diamond surfaces [19-21].

In this context, investigations found that the pharmaceutical used in this work, carbamazepine (common name of the 5H-dibenzo[b,f]azepine-5-carboxamide; Chemical Formula, $C_{15}H_{12}N_2O$; CAS Number, 298-46-4; pK_a13.4), is persistent and its removal efficiencies by the wastewater treatment plants are mostly below 10%. The removal status of Carbamazepine is classified as ‘‘no removal” in the classification scheme for pharmaceutical biodegradation [22].

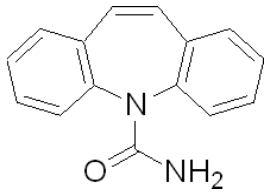

Figure 3.1. Chemical structure of carbamazepine.

Carbamazepine is used for the treatment of seizure disorders, for relief of neuralgia, and for a wide variety of mental disorders. This drug is the most frequently detected in water/wastewater thus far. Approximately 72% of orally administered carbamazepine is absorbed, while 28% is unchanged and subsequently waters reach

through faeces and urine [22]. So, this pharmaceutical compound has been proposed by some authors [23] as an anthropogenic marker in waters.

The main aim of this paper is to optimize the electrochemical degradation process of carbamazepine polluted wastewaters. To this end, we have selected two operating variables: the initial pollutant concentration (measured as *logC*) and the current intensity in the electrochemical cell. Moreover, since many experiments should reach the total pollutant elimination in a reasonably short period, we have focused our attention not in the total CBZ removal (this undoubtedly depends on the initial concentration) but in the chemical degradation rate of each sample. This is represented as "*k*" constant in the kinetic model we have proposed in section 3.1.2.6.

3.1.2. MATERIALS AND METHODS.

3.1.2.1. Chemicals.

All reagents and solvents were of analytical reagent grade and were purchased from Panreac (Spain). Carbamazepine (analytical grade, >98%) purity) was supplied by Sigma-Aldrich (Spain). Anhydrous sodium sulphate of analytical grade used in this investigation as supporting electrolyte was provided by Panreac in analytical purity grade. All solutions were prepared with high-purity water obtained from a Millipore Milli-Q system. HPLC-grade methanol was purchased from Sigma-Aldrich (Spain). Phosphoric acid (85% purity) was obtained from Sigma-Aldrich (Spain).

3.1.2.2. Water matrices.

In the second group of experiments, carbamazepine was dissolved into three different water matrices, in order to confirm the feasibility of electrochemical degradation process of this compound not only in simulated lab water. They were a secondary effluents from municipal wastewater treatment plant (WWTP) and surface water from river and lake. All they were located in Badajoz, Spain. The main quality parameters (pH, total organic carbon content (TOC), chemical oxygen demand (COD) and UV absorbance) of these water systems are compiled in Table 3.1.

Table 3.1. Quality parameters of the used water matrices.

Water matrices	Lab sample (Milli-Q)	Lake	River	WWTP
pH	6.9	7.1	8.1	8.3
TOC ($mg \cdot L^{-1}$)	≤ 0.05	6.7	6.1	14.6
COD ($mg \cdot L^{-1}$)	-	18.2	16.2	32.2
A_{254} (cm^{-1})	-	0.187	0.119	0.245
Conductivity ($\mu S \cdot cm^{-1}$)	0.056	8	55	58
Alkalinity ($mg \cdot L^{-1}$ $CaCO_3$)	-	3	22	32
Chloride ($mg \cdot L^{-1}$)	0.001	25	76	70

3.1.2.3. Analytical procedures.

The concentrations of carbamazepine present in each sample quantified by high performance liquid chromatography (HPLC) in a Waters Chromatograph equipped with 996 Photodiode Array Detector and a Waters Nova-Pack C18 column (5 µm 150 mm x 3.9 mm). The detection wavelength used to detect Carbamazepine was 286 nm. A sample volume of 100 µL was injected in each run. Mobile phase were aqueous solution of 10^{-2} $mol \cdot L^{-1}$ orthophosphoric acid and methanol. The entire flow rate used 1 $mL \cdot min^{-1}$. Carbamazepine peak is defined at a retention time of 5.34 min. The chromatographic method was isocratic. It held the mobile phase composition 60:40 (v/v) mixture of methanol/aqueous solution, respectively. The total organic carbon (TOC) of the initial and electrolyzed solutions was determined with a TOC analyzer (multi N/C 3100 Analytikjena).

3.1.2.4. Electrochemical cells.

The electrochemical oxidation trials of CBZ were carried out in a single compartment electrochemical flow cell working under a batch-operation model (Figure 3.2). A conductive-diamond electrode (p- Si- boron-doped diamond) was used as anode and stainless steel (AISI 304) as cathode. Both electrodes were circular (100 mm diameter) with a geometric area of 78 cm^2 and an electrode gap of 9 mm. Boron-

doped diamond (BDD) films were provided by Adamant Technologies (Neuchatel, Switzerland) and synthesized by the hot filament chemical vapour deposition technique (HFCVD) on single-crystal-p-type Si <100>; waters (0.1 Ωcm, Siltronix). The boron content of the electrodes was 500 ppm and the sp^3/sp^2 ratio was 194.

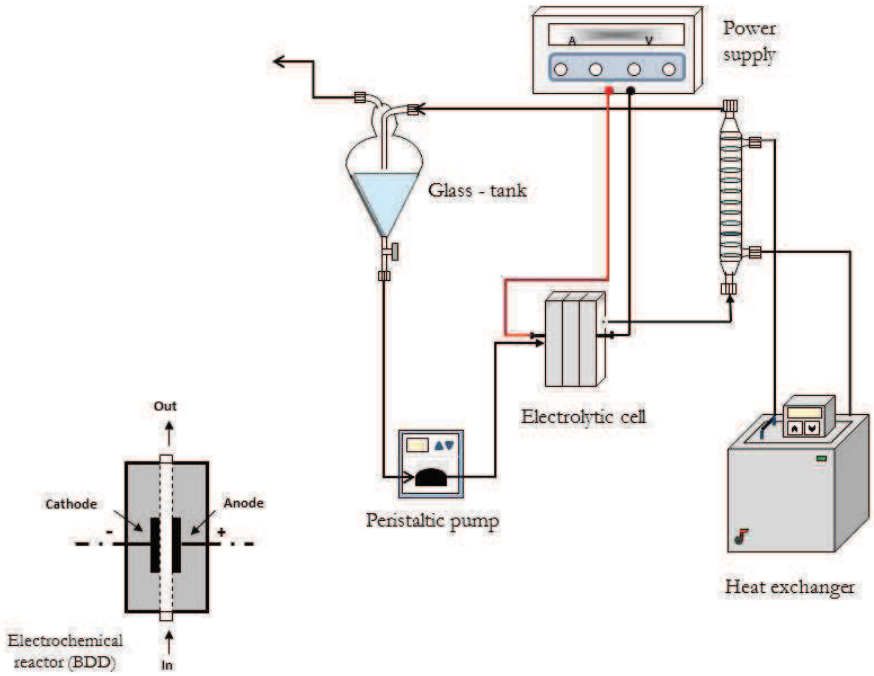

Figure 3.2. Experimental installation of the electrochemical system. On the left corner: Detail of the electrochemical cell.

3.1.2.5. Experimental procedures.

Bench-scale electrolyses of 600 cm^3 of wastewater were carried out under galvanostatic condition. The concentration of CBZ was ranged from 0.1 to 62.3 mgL^{-1} according to the corresponding codification in the Design of Experiments (section 3.1.2.5). Sodium sulphate (7,100 $mg \cdot L^{-1}$ Na_2SO_4) was used as supporting electrolyte. The current density was varied between 7.5 and 43.8 $mA \cdot cm^2$. The cell potential remained constant during each electrolysis, indicating that electrode activity was not

affected, that conductive-diamond layers did not undergo appreciable deterioration or passivation. The electrode was polarized for 10 min in a 5000 $mg \cdot L^{-1}$ Na_2SO_4 (pH 2) solution at 30 $mA \cdot cm^{-2}$ to remove any kind of impurity from its surface. The wastewater was stored in a glass tank and circulated through the electrolytic cell by means of a centrifugal pump operating at a flow rate of 0.25 $L \cdot min^{-1}$. A thermo-regulated water bath was used to maintain the temperature at 20º C in all cases. Figure 3.2 shows a general scheme of the experimental installation used in this work and a detail of the electrochemical cell.

3.1.2.6. Mathematical and statistical procedures.

The experimental results were statistically analyzed by using StatGraphics Plus [24]. A factorial central composite orthogonal and rotatable (CCORD) design was used with 8 replicates of central point, so the total number of experiments was 16. CCORD is one of the most popular classes of second-order design. It involves the use of a two-level factorial design with 2^z points combined with $2z$ axial points and n center runs, z being the number of factors. N, total number of experiments, with z factor is obtained according to Eq. (3.1):

$$N = 2z + 2z + n \tag{3.1}$$

where n is considered to be 8 and the axial distance is $2^{0.5}$ in order to guarantee an orthogonal and rotatable design. This kind of design was previously used in many own papers [25,26] and is consequently well described elsewhere.

Kinetic data adjustments were carried out by using SPSS 14.0 for Windows (SPSS Inc., 2005) according to non-linear multiparametric procedures. These are known to be more reliable and accurate than linear ones [27].

3.1.3. RESULTS AND DISCUSSION.

As we have clearly stated out before, the scope of this research is to evaluate the influence of several operating variables in the general electrodegradation process of a CBZ effluent. First of all, one must define a target variable that should include not

only the final contaminant concentration, but also the kinetic considerations about the entire electrochemical process.

Since the elimination of CBZ seems to follow an exponential pattern, we propose the following expression to model the electrochemical degradation of a pharmaceutical compound, as we did previously [28]. It is presented in Eq. (3.2):

$$C = C_o \cdot e^{-kt} \tag{3.2}$$

This is apparent first-order concentration decay in a batch reactor. *k* variable gives us an idea of how fast is this decay and therefore how fast CBZ is being removed from the aqueous effluent by electrooxidation.

The entire list of experiments, as well as the initial and final results in terms of pollutant removal and kinetic adjustments, is presented in Table 3.2. As can be shown, a wide operational range is achieved by using the variable codification and including the logarithm expression of C (pollutant concentration). So we are able to enlarge the experimental region according to the Design of Experiments principles.

Table 3.2. Experimental plan and results in Design of Experiments. Units in Nomenclature.

Experiment	log C*	j*	Real C	Real j	Adjusted *k* (min^{-1})	r^2
1	-1	-1	0.24	1	0.110	0.997
2	1.41	0	62.26	2	0.010	0.999
3	0	0	2.40	2.0	0.068	0.998
4	-1	1	0.24	3.0	0.551	0.946
5	0	0	2.40	2.0	0.073	0.997
6	0	-1.41	2.40	0.6	0.017	0.998
7	1	1	23.99	3.0	0.018	0.989
8	0	0	2.40	2.0	0.100	0.993
9	0	0	2.40	2.0	0.073	0.997
10	0	0	2.40	2.0	0.077	0.999
11	0	0	2.40	2.0	0.077	0.999
12	0	0	2.40	2.0	0.077	0.999
13	0	1.41	2.40	3.4	0.131	0.999
14	0	0	2.40	2.0	0.077	0.999
15	-1.41	0	0.09	2.0	0.323	0.940
16	1	-1	23.99	1.0	0.008	0.991

* Coded values

3.1.3.1. Analytical results.

It is well known the first group of analysis must deal with the ANOVA test [29]. The basis of this statistical tool is the data adjustment to a polynomial function under the form of Eq. (3.3):

$$Y = b_o + \sum_{j=1} b_j x_j + \sum_{i,j=1} b_{ij} x_i x_j + \sum_{j=1} b_{jj} x_j^2 \qquad (3.3)$$

where Y is the predicted response, b_0 the offset term, b_j the linear effect, b_{ij} the first-order interaction effect and b_{jj} is the squared effect and k is the number of independent variables. One can assume the value of the abovementioned terms are in direct relationship with the concomitant importance of each factor.

ANOVA statistical test gives us a real and accurate idea of how precise is the data adjustment, according to the non-linear least squares method [27]. The result is, therefore, the global evaluation of the entire system and mainly the consideration of the variables as influent or not in the final response [30]. Table 3.3 presents the statistical summary of this test. As can be shown, the ANOVA test is fully reliable since p-value of one variable at least is under 0.05 (significativity limit). In fact, just BB factor (squared expression of *j*, current intensity) is not significant.

Table 3.3. ANOVA statistical summary.

Factor	Squares sum	F-Ratio	p-Value
A: logC	0.145	68.9	0
B: j	0.045	22.2	0.0008
AA	0.026	12.4	0.0055
AB	0.046	22	0.0008
BB	0.0009	0.46	0.5132
Corrected Total Error	0.286		

Other analytical aspects of this statistical test are r^2 and Durbin-Watson factor. The first of them is equal to 0.88 (adjusted for 15 freedom degrees) and the second one is equal to 1.68. Durbin-Watson statistical presents, on the other hand, a p-value equal to

0.27; that is higher than 0.05 and there is no autocorrelation evidences in the error distribution. The randomization of the experimental data was effective and the whole design is reliable therefore [31]. This is analytically confirmed by Figure 3.3, the representation of residuals along the experimental plan (number of run, X-axis).

Since no pattern can be observed from Figure 3.3, no autocorrelation can be intuited and hence randomization of the entire study is correct.

Eq. (3.3) presents the specific form of Eq. (3.4) when the adjustment is carried out:

$$k = 0.077 - 0.13\log C + 0.07\,j + 0.057(\log C)^2 - 0.107\,j\log C + 0.011\,j^2 \quad (3.4)$$

As is commonly accepted, variables behind a minus sign represent negative-affecting factors, whereas plus sign identifies the positive-affecting variables. It is remarkable that the offset is quite low (0.077) if we compared it with the optimum maximum *k* level (0.72, section 3.1.3.3). This means the operative factors are really influent in the final response of the system. These results are graphically confirmed by means of several complementary tests and representations.

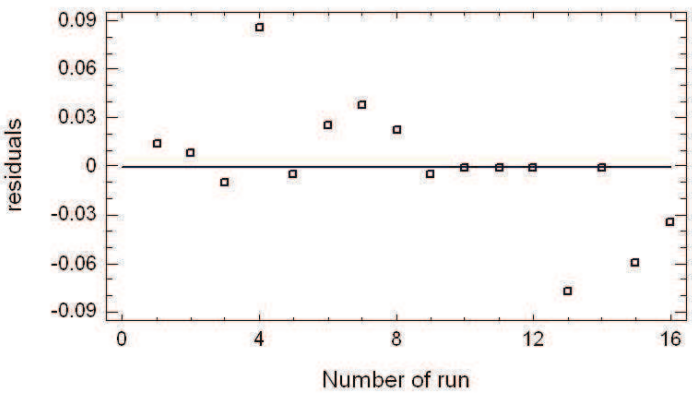

Figure 3.3. Residuals' random distribution.

3.1.3.2. Graphical results.

Graphically, the adjustment of Eq. (3.4) to the entire system can be studied under three complementary evaluations: Pareto graphic, main effects and interactions. The Response Surface Graphic is the final representation of the system, where a curved surface identifies the predicted responses.

Pareto graphic is a representation of each variable's influence in the final response. In this case, this target is the *k* constant of the kinetic model Eq. (3.2). *Pareto* results are given in Figure 3.4.

Figure 3.4 presents graphically what was analytically analyzed in Eq. (3.4). As can be seen, the length of each bar is in direct relationship with the influence of each variable, and the most influent one is A (*logC*). Positive-affecting variables are here represented by void bars, whereas filled ones represent negative-affecting factors. Individually, the two studied variables (A and B) presents opposite effects. This is evident when attention is focused on the representation of main effects (Fig. 3.5).

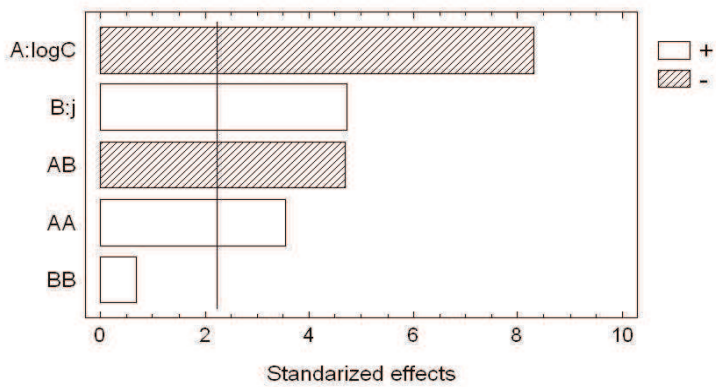

Figure 3.4. Pareto graphic.

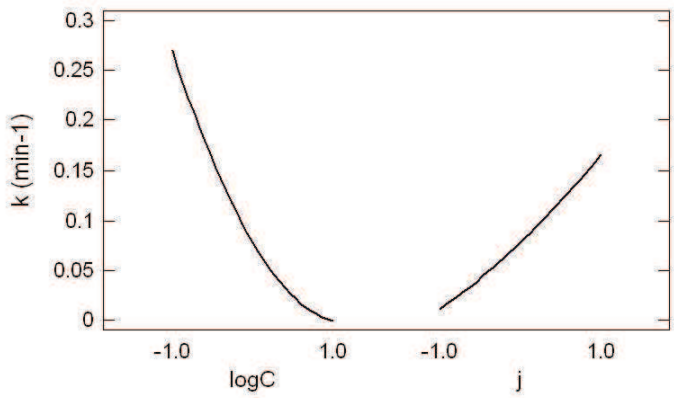

Figure 3.5. Main effects

Figure 3.5 presents the evolution of the system when only one of the studied factors is varied, while the other one is kept constant. As can be observed, both factors are influent, although *logC* is much more significant than *j*. In Pareto graphic (Fig. 3.4) this is represented by the standarized bars, here one must observe the slope of the curve.

However, either Fig. 3.4 or Fig. 3.5 shows the real interaction of both operative studied factors. Bar representing AB in Pareto graphic shows this in fact exists, but a more accurate representation is given by Figure 3.6, which is called specifically Interaction Graphic:

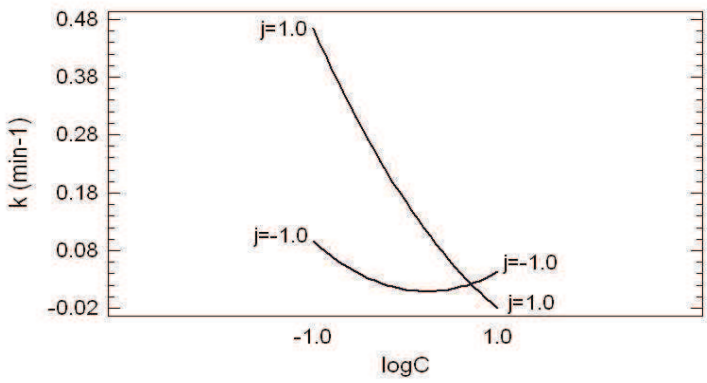

Figure 3.6. Interaction Graphic

The interaction between both variables is evident since the representative curves of each factor are clearly crossed near the end of the operative area for factor *A* (*logC*). This point remarks a new tendency in the system once it is trespassed: low *j* levels are required after this point, while higher ones give better responses before.

Finally, a global evaluation of the system can be carried out by drawing the specific Response Surface. This is represented in Figure 3.7. A concave curve is depicted, with a rapid elevation of the response as *logC* tends to be lower and *j* higher. Consequently, the optimum combination of both variables is placed out of the working area, but we can assume this best point corresponds with the exact point of (-1.44, 1). This will be discussed in section 3.1.3.3.

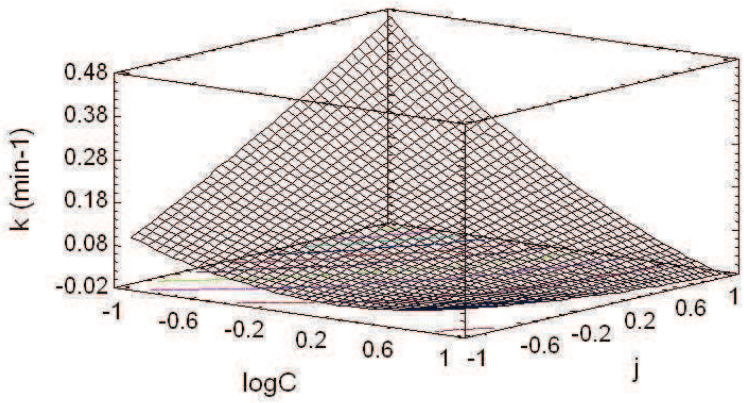

Figure 3.7. Response Surface

3.1.3.3. Optimal experimental conditions.

The best combination of both studied factors corresponds to the maximum *j* and minimum *logC*. This is experimentally 0.09 mg·L^{-1} and 3.4 A. When operating under these conditions, *k* reaches a maximum value of 0.72 min^{-1}, what is experimentally confirmed. This means up to 50% of CBZ removal is obtained after just 1 minute of electrochemical treatment.

The optimal conditions lead us to recommend low pollutant concentrations (what is usually presented in real wastewater effluents) and relevant current intensities. By this procedure, energy costs would tend to be lower.

3.1.3.4. Other water matrixes.

In order to confirm the feasibility of this process not only in simulated lab water, several trials were carried out in real water matrixes, urban wastewater effluents and surface free water. These experiments were performed a high current intensity (2.8 A) and an initial pollutant concentration of 24 $mg \cdot L^{-1}$. The results in terms of CBZ concentration and they are graphically presented in Figure 3.8.

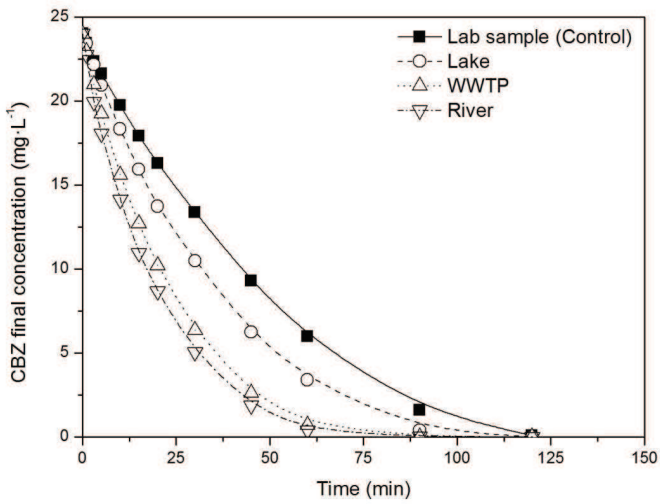

Figure 3.8. CBZ decay by electrodegradation in four different samples: simulated lab wastewater, real water samples from a lake, a river and a wastewater treatment plant.

As can be shown, significant differences are appreciated between the four water matrixes. The rate of the CBZ degradation is slowest in the lab sample (solid line in Figure 3.8) whereas the electrodegradation in WWTP and river samples significantly higher. The k values of each curve (with r^2 above 0.98 in every case) were 0.022, 0.029, 0.045 and 0.053 for lab simulated wastewater, lake, WWTP and river effluent respectively. The entire process is therefore influenced by the presence of other

chemical species electrically active. In this sense, this fact can be explained taking into account the chloride concentration of the different water samples (see Table 3.1). Active chlorine is the most traditional secondary oxidant generated in EO processes. Chlorine-mediated electrolysis has been reported in the oxidation of a wide range of model pollutants [32,33,34]. Indeed, oxygen transfer to organic molecules can be attained either on the electrode surface (chloro or oxychloro radicals) or in the bulk of the solution, through long-lifetime oxidants (chlorine, hypochlorous acid, or hypochlorite) anodically produced, according to the following reactions:

$$2Cl^- \rightarrow Cl_2 + 2e- \quad (3.4)$$

$$Cl_2 + H_2O \rightarrow HOCl + H^+ + Cl^- \quad (3.5)$$

$$HOCl \rightarrow H^+ + OCl^- \quad (3.6)$$

An explanation of the mediating role of chloride ions have been proposed by De Battisti [35,36]. They extended the diagram for electrochemical oxygen transfer reactions proposed by Comninellis [37] to the cases where oxygen transfer is carried out by adsorbed oxychloro species. The presence of chloride ions seems to inhibit oxygen-evolution reaction, causing an increase in anode potential and, therefore, a higher reactivity of adsorbed chloride-oxychloride radicals.

3.1.4. CONCLUSIONS.

Electrodegradation of carbamazepine is a real, feasible process for treating wastewater. Pollutant concentration can be reduced down to non-dangerous quantities by the application of a boron-doped diamond electrocell. The entire process can be modeled according to a first-order reaction kinetic and chemical reaction rate (k) can be used as a target variable for optimizing the procedure. Optimum combination of carbamazepine and electric current (j) was discovered to be at 0.09 $mg \cdot L^{-1}$ and 3.4 A, where k reached a maximum value of 0.72 min^{-1}. This wastewater treatment was also feasible, even with more effectiveness, in different water matrixes, such as river, lake or urban wastewater samples. This fact can be explained taking into account the chloride concentration of the different water samples

3.1.5. REFERENCES.

[1] Alder, A.C.; Bruchet, A.; Carballa, M.; Clara, M.; Joss, A.; Löffler, D.; McArdell, C.S.; Miksch, K.; Omil, F.; Tuhkanen, T.; Ternes, T.A. Consumption and Occurrence. In: Ternes, T.A., Joss, A. (Eds.), Human Pharmaceuticals, Hormones and Fragrances. The Challenge of Micropollutants in Urban Water Management. IWA Publishing **(2006)**.

[2] Kathryn, D.B.; Jerzy, K.; Bruce, T.; Timothy, H.C.; Douglas, B.M. "Occurrence of antibiotics in hospital, residential, and dairy effluent, municipal wastewater, and the Rio Grande in New Mexico". Science of the Total Environment. 366, 772 **(2005)**.

[3] Suárez, S.; Carballa, M.; Omil, F.; Lema, J. "How are pharmaceutical and personal care products (PPCPs) removed from urban wastewaters?". Reviews in Environmental Science and. Biotechnology. 7, 125 **(2008)**.

[4] Daughton, C.G.; Ternes, T.A. "Pharmaceuticals and personal care products in the environment: agents of subtle change?". Environmental Health Perspectives. 107, 907 **(1999)**.

[5] Clara, M.; Kreuzinger, N.; Strenn, B.; Gans, O.; Kroiss, H. "The solids retention time – a suitable design parameter to evaluate the capacity of wastewater treatment plants to remove micropollutants". Water Research. 39, 97 **(2005)**.

[6] Ternes, T.A.; Meisenheimer, M.; McDowell, D.; Sacher, F.; Brauch, H.J.; Gulde, B.H.; Preuss, G.; Wilme, U.; Seibert, N.Z. Removal of pharmaceuticals during drinking water treatment. Environmental Science & Technology. 36, 3855 **(2002)**.

[7] Jones, O.A. ; Lester, J.N. ; Voulvoulis, N. "Pharmaceuticals: a threat to drinking water?". Trends in Biotechnology. 23, 163 **(2005)**.

[8] Snyder, S.A.; Wert, E.; Lei, H.D.; Westerhoff, P.; Yoon, Y. "Removal of EDCs and Pharmaceuticals in Drinking and Reuse Treatment Processes". American Water Works Association Research Foundation (AWWARF). Denver, Colorado **(2007)**.

[9] Benotti, M.J.; Trenholm, R.A.; Vanderford, B.J.; Holady, J.C.; Stanford, B.D.; Snyder, S.A. Pharmaceuticals and endocrine disrupting compounds in U.S. drinking water. Environmental Science & Technology, 43, 597 603 **(2009)**.

[10] Heberer, T.; Dunnbier, U.; Reilich, C.; Stan, H.J. "Detection of drugs and drug metabolites in ground water samples of a drinking water treatment plant. Fresenius Environmental Bulletin, 6, 438 **(1977)**.

[11] Mompelat, S.; Lebot, B.; Thomas, O. "Occurrence and fate of pharmaceutical products and by-products, from resource to drinking water". Environment International. 35, 803 **(2009)**.

[12] Benítez, F.J.; Real, F.J.; Acero, J.L.; Roldán, G. "Removal of selected pharmaceuticals in waters by photochemical processes. Journal of Chemical Technology and Biotechnology". 84, 1186 **(2009)**.

[13] Vilhunen, S.; Vilve, M.; Vepsäläinen, M.; Sillanpää, M. "Removal of organic matter from a variety of water matrices by UV photolysis and UV/H_2O_2 method". Journal of. Hazardous. Materials. 179, 776 **(2010)**.

[14] Benítez, F.J.; Acero, J.L.; Real, F.J.; Roldán, G.; Casas, F. "Comparison of different chemical oxidation treatments for the removal of selected pharmaceuticals in water matrices". Chemical Engineering Journal. 168, 1149 **(2011)**.

[15] Kusic, H.; Koprivanac, N.; Bozic, A.L. "Treatment of chlorophenols in water matrix by UV/ferrioxalate system: Part I. Key process parameter evaluation by response surface methodology". Desalination. 279, 258 **(2011)**.

[16] Hupert, M.; Muck, A.; Wang, J.; Stotter, J.; Cvackova, Z.; Haymond, S.; Show, Y.; Swain, G. "Conductive diamond thin-films in electrochemistry". Diamond and Related Materials. 12, 1940 **(2003)**.

[17] Marselli, B.; García-Gómez, J.; Michaud, P.A.; Rodrigo, M.A.; Comninellis, Ch. "Electrogeneration of hydroxyl radicals on boron-doped diamond electrodes". Journal of The Electrochemical Society. 150, 79 **(2003)**.

[18] Chen, G. "Electrochemical technologies in wastewater treatment". Separation and Purification Technology. 38, 11 **(2004)**.

[19] Brillas, E.; Calpe, J.C.; Casado, J. "Mineralization of 2,4-D by advanced electrochemical oxidation processes". Water Research. 34, 2253 **(2000)**.

[20] Panizza, M.; Cerisola, G. "Application of diamond electrodes to electrochemical processes". Electrochimica. Acta. 51, 191 **(2005)**.

[21] Martínez-Huitle, C.A.; Ferro, S. "Electrochemical oxidation of organic pollutants for the wastewater treatment: direct and indirect processes". Chemical Society Reviews. 35, 1324 **(2006)**.

[22] RxList. The Internet Drug Index. http://www.rxlist.com **(2006)**.

[23] Clara, M.; Strenn, B.; Kreuzinger, N. "Carbamazepine as a possible anthropogenic marker in the aquatic environment: investigations on the behaviour of carbamazepine in wastewater treatment and during groundwater infiltration". Water Research. 38, 947 **(2004)**.

[24] StatPoint Technologies Inc. StatGraphics Centurion XVI User Manual. Virginia, USA **(2009)**.

[25] Beltrán-Heredia, J.; Sánchez-Martín, J.; Solera-Hernández, C. "Removal of sodium dodecyl benzene sulfonate from water by means of a new tannin-based coagulant: Optimization studies through design of experiments". Chem. Eng. J. 153, 56 **(2009)**.

[26] Beltrán-Heredia, J.; Sánchez-Martín, J.; Frutos-Blanco, G. "Schinopsis balansae tannin-based flocculant in removing sodium dodecylbenzene sulfonate". Sep. Pur. Technol. 67, 292 **(2009).**

[27] Kumar, V ; Porkodi, K ; Rocha, F. "Isotherms and thermodynamics by linear and non-linear regression analysis for the sorption of methylene blue onto activated carbon. Comparison of various error functions". J Hazard. Mater. 141, 794 **(2008)**.

[28] Domínguez, J.R.; González, T.; Palo, P.; Sánchez-Martín, J.; Rodrigo M.A.; Sáez, C. "Conductive-diamond electrochemical oxidation of a pharmaceutical effluent with high COD. Kinetics and optimization of the process by RSM". Env. Eng. and Manag. Journal. Accepted for publication **(2012)**.

[29] Beltrán-Heredia, J.; Sánchez-Martín, J.; Delgado-Regalado, A.; Jurado-Bustos, C. "Removal of Alizarin Violet 3R (anthraquinonic dye) from aqueous solutions by natural coagulants". J. Hazar. Mater. 170, 43 **(2009)**.

[30] Beltrán-Heredia, J.; Palo, P.; Sánchez-Martín, J.; Domínguez, J.R.; González, T. "Natural Adsorbents Derived from Tannin Extracts for Pharmaceutical Removal in Water". Industrial and Eng. Chemistry Research. 51, 50 **(2012)**.

[31] Montgomery, D.C. "Design and Analysis of Experiments". 7th edition. John Wiley and Sons **(2009)**.

[32] Malpass, G.R.P.; Miwa, D. W.; Machado, S. A. S.; Olivi, P.; Motheo, A.J. "Oxidation of the pesticide atrazine at DSA® electrodes". J. Journal of. Hazardous. Materials. 137, 565 **(2006)**.

[33] Panizza, M.; Delucchi, M.; Cerisola, G. "Electrochemical degradation of anionic surfactants". Journal of Applied Electrochemistry. 35, 357 **(2005)**.

[34] Panizza, M.; Barbucci, A.; Ricotti, R.; Cerisola, G. "Electrochemical degradation of. Methylene Blue". Separation and Purification Technology. 54, 382 **(2007)**.

[35] Bonfatti, F.; De Battisti, A.; Ferro, S.; Lodi, G.; Osti, S. "Anodic mineralization of organic substrates in chloride-containing aqueous media". Electrochimica Acta. 46, 305 **(2000a)**.

[36] Bonfatti, F.; Ferro, S.; Lavezzo, F.; Malacarne, M.; Lodi, G.; De Battisti, A. "Electrochemical Incineration of Glucose as a Model Organic Substrate. II. Role of Active Chlorine Mediation". Journal of Electrochemical Society. 147, 592 **(2000b)**.

[37] Comninellis, C. "Electrocatalysis in the electrochemical conversion/combustion of organic pollutants for waste water treatment". Electrochimica Acta. 39, 1857 **(1994)**.

3.2. FEASIBILITY OF ELECTROCHEMICAL DEGRADATION OF PHARMACEUTICAL POLLUTANTS IN DIFFERENT AQUEOUS MATRICES. OPTIMIZING THE SYSTEM

Electrochemical degradation of different effluents polluted with carbamazepine, a well-known refractory pharmaceutical contaminant, was addressed in this paper. Ultrapure water (Milli-Q technology), surface water from a lake and urban wastewater were the considered matrixes for evaluating the feasibility of electro-oxidation. A different design of experiments was planned for each aqueous medium, taking as operative variables the initial carbamazepine concentration and the electric current intensity. Although the optimum combination of both variables follows the same tendency in the three cases, significant differences are observed regarding the comparative influence of each variable.

Keywords: Electro-oxidation, pharmaceuticals, Design of Experiments, Carbamazepine, Wastewater treatment.

3.2.1. INTRODUCTION.

Hundreds of tons of pharmaceutical compounds (PCs) are estimated to be produced and consumed annually in developed countries [1,2]. The presence of pharmaceutical compounds has been routinely detected in different aquatic environments, like natural waters [3], wastewater secondary effluents [4] and drinking waters [5]. The occurrence of these pollutants into these aquatic systems is attributed to their incomplete removal by conventional wastewater treatment plants (WWTPs) [6,7].

In this context, carbamazepine (CBZ) (5H-dibenzo[b,f]azepine-5-carboxamide; Chemical Formula, $C_{15}H_{12}N_2O$; CAS Number, 298-46-4; pK_a= 13.4) is persistent and its removal efficiencies by WWTPs are mostly below 10%. For this reason, carbamazepine is classified as ‘‘no removal” in the classification scheme for pharmaceutical biodegradation [8]. Furthermore, this drug is the most frequently detected in water/wastewater thus far. Approximately 30% of orally administered

carbamazepine is unchanged and subsequently waters reach through faeces and urine [8]. So, this pharmaceutical compound has been proposed by some authors [9] as the anthropogenic marker for excellence.

On the other hand, advanced oxidation processes (AOPs) and more specifically electrochemical oxidation processes (EOPs), which are based in the generation of hydroxyl radicals (·OH) on the surface of electrodes, have attracted great interest for the degradation of refractory and/or hazardous organic micropollutants in water systems. In this sense, electro-oxidation technology (EO) is finding its application in water and wastewater treatment [10-12]. Electro-oxidation is effective in degrading refractory pollutants on the surface of electrodes, among them the diamond film electrodes, used in this work. It should be noted its excellent chemical and electrochemical properties, its main remarkable characteristic is its high overpotential for water electrolysis allowing the generation of large amounts of hydroxyl radicals [13-15]. The hydroxyl radical is a very powerful oxidant (E^0= +2.80 V) and it seems to be directly involved in the oxidation mechanisms that occur on diamond surfaces [16-18].

The main aim of this paper was to optimize the electrochemical degradation process of carbamazepine polluted wastewaters in different water matrices. To this end, we have selected two operating variables: the initial pollutant concentration (measured as *logC*) and the electrical current intensity in the electrochemical cell. Experimental trials were performed on simulated wastewater sample (lab-made solution), a surface water sample collected from a local lake and urban wastewater effluent from a local Wastewater Treatment Plant (WWTP). Each matrix was considered a different design of experiments and the results were contrasted for evaluating the feasibility of this electrochemical process in different experimental conditions.

3.2.2. MATERIALS AND METHODS.

3.2.2.1. Chemicals.

All reagents and solvents were of analytical reagent grade and were purchased from Panreac (Spain). Carbamazepine (analytical grade, > 98%) purity) was supplied by Sigma-Aldrich (Spain). Anhydrous sodium sulphate of analytical grade used in this investigation as supporting electrolyte was provided by Panreac in analytical purity grade. All solutions were prepared with high-purity water obtained from a Millipore Milli-Q system. HPLC-grade methanol was purchased from Sigma-Aldrich (Spain). Phosphoric acid (85% purity) was obtained from Sigma-Aldrich (Spain).

3.2.2.2. Analytical procedures.

The concentrations of carbamazepine present in each sample quantified by high performance liquid chromatography (HPLC) in a Waters Chromatograph equipped with 996 Photodiode Array Detector and a Waters Nova-Pack C18 column (5 µm 150 mm x 3.9 mm). The detection wavelength used to detect carbamazepine was 286 nm. A sample volume of 100 µL was injected in each run. Mobile phase were aqueous solution of 10^{-2} mol·L^{-1} orthophosphoric acid and methanol. The entire flow rate used was 1 mL·min^{-1}. Carbamazepine peak is defined at a retention time of 5.34 min. The chromatographic method was isocratic. It held the mobile phase composition 60:40 (v/v) mixture of methanol/aqueous solution, respectively. The total organic carbon (TOC) of the initial and electrolyzed solutions was determined with a TOC analyzer (multi N/C 3100 Analytikjena).

3.2.2.3. Electrochemical cells.

The electrochemical oxidation trials of CBZ were carried out in a single compartment electrochemical flow cell working under a batch-operation model (Figure 3.2). A conductive-diamond electrode (p- Si- boron-doped diamond) was used as anode and stainless steel (AISI 304) as cathode. Both electrodes were circular (100 mm diameter) with a geometric area of 78 cm^2 and an electrode gap of 9 mm. Boron-doped diamond (BDD) films were provided by Adamant Technologies (Neuchatel,

Switzerland) and synthesized by the hot filament chemical vapour deposition technique (HFCVD) on single-crystal-p-type Si <100>; waters (0.1 Ωcm, Siltronix). The boron content of the electrodes was 500 ppm and the sp^3/sp^2 ratio was 194.

3.2.2.4. Water samples.

Ultrapure water (Milli-Q technology), surface water from a lake and urban wastewater were the considered matrixes for evaluating the feasibility of electro-oxidation of carbamazepine. Table 3.4 shows the main physico-chemical properties of these matrixes.

Table 3.4. Quality parameters of the used water matrices.

Water matrices	Milli-Q water	Lake	WWTP
pH	6.9	7.1	8.3
TOC ($mg \cdot L^{-1}$)	≤ 0.05	6.7	14.6
COD ($mg \cdot L^{-1}$)	-	18.2	32.2
A_{254} (cm^{-1})	-	0.187	0.245
Conductivity (µS)	0.056	8	58
Alkalinity ($mg \cdot L^{-1}$ $CaCO_3$)	-	3	32
Chloride ($mg \cdot L^{-1}$)	0.001	25	70

3.2.2.5. Experimental procedure.

Bench-scale electrolyses of 600 cm^3 of wastewater were carried out under galvanostatic conditions. The concentration of CBZ was ranged from 0.1 to 62.3 $mg \cdot L^{-1}$ according to the corresponding codification in the Design of Experiments (see Table 3.5). Sodium sulphate (7100 $mg \cdot L^{-1}$ Na_2SO_4) was used as supporting electrolyte. The current density was varied between 7.5 and 43.8 $mA \cdot cm^2$. The cell potential remained constant during each experiment, indicating that electrode activity was not affected, that conductive-diamond layers did not undergo appreciable deterioration or passivation. The electrode was polarized for 10 min in a 5000 $mg \cdot dm^{-3}$ Na_2SO_4 (pH 2) solution at 30 $mA \cdot cm^{-2}$ to remove any kind of impurity from its surface. The

wastewater was stored in a glass tank and circulated through the electrolytic cell by means of a centrifugal pump operating at a flow rate of 0.25 $L \cdot min^{-1}$. A thermo-regulated water bath was used to maintain the temperature at 20º C in all cases. Figure 3.2 shows a general scheme of the experimental installation used in this work and a detail of the electrochemical cell.

Table 3.5. Working range for Design of Experiments

Factor	Upper limit (+1)	Lower limit (-1)	Center (0)
Current intensity (*j*)	3 A	1 A	2 A
Initial CBZ concentration (*logC*)	24 $mg \cdot L^{-1}$	0.24 $mg \cdot L^{-1}$	2.40 $mg \cdot L^{-1}$

3.2.2.6. Mathematical and statistical procedures.

The experimental results were statistically analyzed by using StatGraphics Plus [19]. A factorial central composite orthogonal and rotatable (CCORD) design was used with 8 replicates of central point, so the total number of experiments was 16. CCORD is one of the most popular classes of second-order design. It involves the use of a two-level factorial design with 2^z points combined with $2z$ axial points and n center runs, z being the number of factors. N, total number of experiments, with z factor is obtained according to Eq. (3.1).

This kind of design was previously used in many own papers [20,21] and is consequently well described elsewhere.

Kinetic data adjustments were carried out by using SPSS 14.0 for Windows (SPSS Inc., 2005) according to non-linear multiparametric procedures. These are known to be more reliable and accurate than linear ones [22].

3.2.3. RESULTS AND DISCUSSION.

As we have clearly stated out before, the scope of this research is to evaluate the influence of several operating variables in the general electrodegradation process of a CBZ effluent in different aqueous matrixes. First of all, one must define a target

variable that should include not only the final contaminant concentration, but also the kinetic considerations about the entire electrochemical process.

According to previous similar studies [23] we propose the expression to model the electrochemical degradation of a pharmaceutical compound (Eq. (3.2)).

This is an apparent first-order concentration decay in a batch reactor. *k* variable gives us an idea of how fast is this decay and therefore how fast CBZ is being removed from the aqueous effluent by electrooxidation.

The entire list of experiments is presented in Table 3.6. As can be shown, a wide operational range is achieved by using the variable codification and including the logarithm expression of C (pollutant concentration). So we are able to enlarge the experimental region according to the Design of Experiments principles.

Table 3.6. Experimental plan and results in Design of Experiments.

			MilliQ	**Surface**	**WWTP**	
Experiment	**log C***	**j***		**k (min^{-1})**		**Average r^2**
1	-1	-1	0.110	0.291	0.074	0.963
2	1.41	0	0.010	0.012	0.019	0.999
3	0	0	0,068	0.091	0.105	0.984
4	-1	1	0,551	0.394	0.172	0.949
5	0	0	0,073	0.088	0.110	0.993
6	0	-1.41	0,017	0.037	0.033	0.993
7	1	1	0,018	0.022	0.046	0.982
8	0	0	0,100	0.087	0.102	0.991
9	0	0	0,073	0.094	0.112	0.994
10	0	0	0,077	0.110	0.107	0.993
11	0	0	0,077	0.061	0.107	0.988
12	0	0	0,077	0.089	0.107	0.994
13	0	1.41	0,131	0.055	0.172	0.969
14	0	0	0,077	0.087	0.107	0.994
15	-1.41	0	0,323	0.500	0.111	0.960
16	1	-1	0,008	0.012	0.017	0.991

* Coded values

3.2.3.1. Analytical results.

It is well known that the first group of analysis must deal with the ANOVA test [24]. The basis of this statistical tool is the data adjustment to a polynomial function under the form of Eq. (3.3). One can assume the value of the abovementioned terms are in direct relationship with the concomitant importance of each factor.

ANOVA statistical test gives us a real and accurate idea of how precise is the data adjustment, according to the non-linear least squares method [25]. The result is, therefore, the global evaluation of the entire system and mainly the consideration of the variables as influent or not in the final response [26].

Table 3.7 presents the statistical summary of this test for the three aqueous matrixes. As can be shown, the ANOVA test is fully reliable since p-value of one variable at least is under 0.05 (significativity limit) in every case. Moreover, only one variable (BB, squared expression of *j*) is not significant in two of the three cases. When compared the three water matrixes, trials performed on surface water present a higher influence of the two operating factors and their corresponding interactions surprisingly.

Table 3.7. ANOVA statistical summary.

Factor	Milli-Q	Surface	WWTP
		p-value	
A: logC	0	0	0
B: j	0.0008	0.0355	0
AA	0.0055	0	0.0001
AB	0.0008	0.0437	0.0082
BB	0.5132	0.0778	0.3137
Corrected Total Error	0.2867	0.3012	0.0318
Adjusted r^2	0.89	0.98	0.95
Durbin-Watson (p-value)	1.68 (0.27)	9.93 (0.32)	1.25 (0.06)

Other analytical aspects of this statistical test are r^2 and Durbin-Watson factor. The first of them is always kept above 0.89, that means the correlation of the system is relevant and the modelation of the phenomenon (according to Eq. (3.3)) is significant. On the other hand, Durbin-Watson factor helps us to confirm the actual randomization of the experiments. The corresponding p-values (0.27, 0.32 and 0.06) are above 0.05, the signification limit. Therefore, there are no autocorrelation evidences in the error distribution. The randomization of the experimental data were effective and the designs were reliable therefore.

Eq. (3.3) presents the specific form of Eq. (3.5), (3.6) and (3.7) for Milli-Q, Surface and WWTP samples once the adjustment were carried out:

$$k = 0.077 - 0.13\log C + 0.07j + 0.057(\log C)^2 - 0.107j\log C + 0.011j^2 \quad (3.5)$$

$$k = 0.088 - 0.16\log C + 0.017j + 0.091(\log C)^2 - 0.023\log C + 0.014j^2 \quad (3.6)$$

$$k = 0.107 - 0.039\log C + 0.04j + 0.022(\log C)^2 - 0.017\log C + 0.004j^2 \quad (3.7)$$

As is commonly accepted, variables behind a minus sign represent negative-affecting factors, whereas plus sign identifies the positive-affecting variables. It is remarkable that the offset is quite low in every case, if compared with optimum value of k (0.72 min^{-1} for Milli-Q water samples, 0.20 min^{-1} for WWTP samples and 0.55 min^{-1} for surface water). This means the operative factors are really influent in the final response of the system. These results are graphically confirmed by means of several complementary tests and representations.

3.2.3.2. Graphical results.

Graphically, the adjustment of Eq. (3.5), (3.6) and (3.7) to each entire system can be studied under three complementary evaluations: Pareto graphic, main effects and interactions. The Response Surface Graphic is the final representation of the system, where a curved surface identifies the predicted responses.

Pareto graphic is a representation of each variable's influence in the final response. In this case, this target is the *k* constant of the kinetic model (Eq. (3.2)). *Pareto* results for each system are given in Figure 3.9.

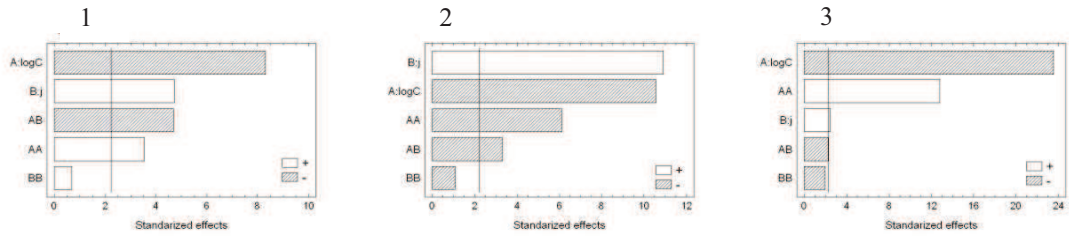

Figure 3.9. Pareto graphics for 1) Milli-Q water; 2) WWTP samples; 3) Surface water.

Each subfigure presents the influence of every variable alone (A,B) or in combination between them (AA, BB and AB). The length of each bar is in direct relationship with the influence of each variable and positive-affecting variables are here represented by void bars, whereas filled ones represent negative-affecting factors. The most interesting aspect of these graphics is the fact that we can compare how every factor tends to change its influence as the aqueous matrix is different. At a first glance, it is remarkable that four of the five involved factors are considered as statistically significant (bars trespass the significativity limit represented by the vertical rule). Initial pollutant concentration is the most influent one in system 1 and 3 (Milli-Q and Surface water) whereas in WWTP sample this first position corresponds to current intensity (j).

The main difference between first and third case and the second one is the fact that organic content is exponentially increase in WWTP water sample, mainly due to the high number of organic diluted species. In this case, the influence of current intensity gains the first position in Pareto analysis because the oxidation reactions should be less selective and consequently pollutant concentration factor acquires a secondary role. As can be expected, for all cases log C is a negative factor, as well as *j* is positive.

Another remarkable difference is the absolute value of the influence of *logC* in the third case, that is, surface lake water. As can be seen, the final value of this bar reaches almost 24 (standarized effect) whereas the rest of influent bars are around 10. This means the influence of such effect is relatively the most important in this case, perhaps due to the increase of polar species (Cl^-, PO_4^{3-}, SO_4^{2-}) rather than organic non-polar ones in the second case.

In fact, Figure 3.10 presents graphically what was analytically analyzed in Eqs. (3.5), (3.6) and (3.7). Globally, both direct variables (A,B) present opposite effects. This is evident when attention is focused on the representation of the main effects (Fig. 3.10):

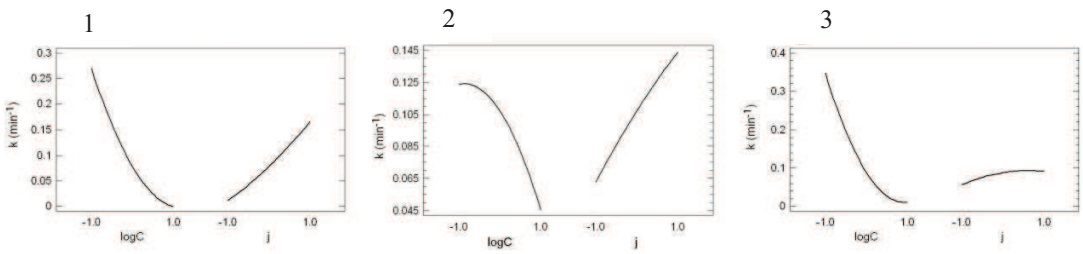

Figure 3.10. Main effects for 1) Milli-Q water; 2) WWTP samples; 3) Surface water.

Figure 3.10 presents the evolution of each system when only one of the studied factors is varied, while the other one is kept constant. As can be observed, both factors are influent in the three cases, being the relevance of *logC* similar in Milli-Q and surface water. In agreement with precedent Pareto analysis, main effects are comparable for *logC* and j only in the first two cases. The third one (surface lake water) presents a higher influence of *logC* if compared with j, as it was correspondingly explained before. However, the role of current intensity (*j*) is less influent in the case of surface water (3) and WWTPs sample (2), whereas is more relevant in the system 1 (Milli-Q). In Pareto graphic (Fig. 3.9) this is represented by the standarized bars, here one must observe the slope of the curve.

This change in the influence of *j* has to do with the probable competence of CBZ oxidation with other oxidizable species. Milli-Q sample is free from other interaction

species, whereas the rest of aqueous matrixes do present a wide variety of them, so (j) is less influent in the specific elimination of such pollutant.

However the said, neither Fig. 3.9 nor Fig. 3.10 shows the real interaction of both operative studied factors. Bar representing AB in Pareto graphic shows this in fact exists, but a more accurate representation is given by Figure 3.11, which is called specifically Interaction Graphic:

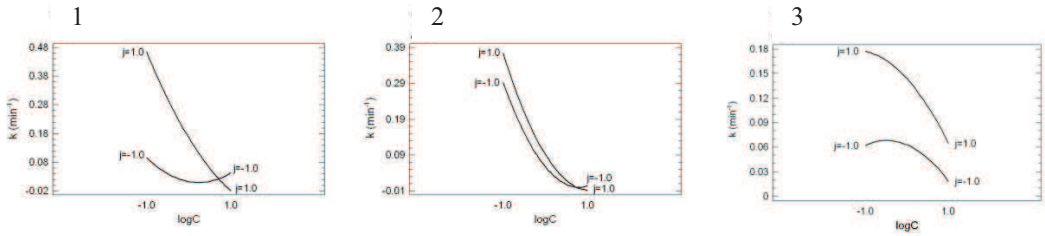

Figure 3.11. Interaction Graphic for 1) Milli-Q water; 2) Surface water; 3) WWTP samples.

As can be easily observed, a tendency is presented from Figure 3.11: Milli-Q water matrix produces a clear interaction between both variables since the curves are crossed. When talking about surface water and WWTP water, this interaction is lower because the two lines are significantly more parallel. This is a logical consequence of the organic molecules increase, more oxidizable competences.

Finally, a global evaluation of each system can be carried out by drawing the specific Response Surface. These are represented in Figure 3.12. It is remarkable that the shape of the surface changes from systems with less organic or inorganic species interference (subfigures 1 and 3) presented a concave shape, whereas a concave one is presented in subfigure 2 (WWTP). This, again, should have to do with the increasing influence of *j* (electric current intensity). Although the evolution of the response is different, in the three cases a rapid elevation of the response is presented as *logC* tends to be lower and *j* higher. Consequently, the optimum combination of both variables is placed out of the working area, but we can assume this best point corresponds with the exact point of (-1.44,1.44) in the three systems. This will be discussed in section 3.2.3.3.

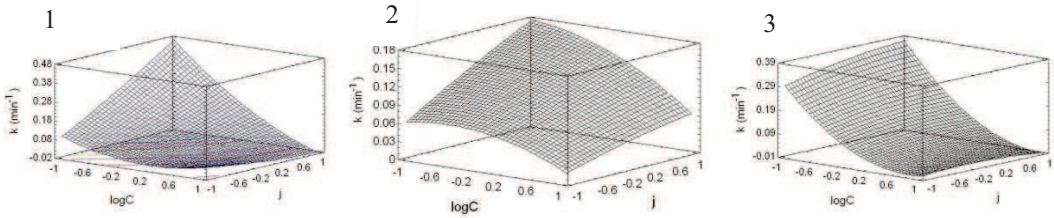

Figure 3.12. Response Surface for 1) Milli-Q water; 2) WWTP samples; 3) Surface water.

3.2.3.3. Optimal experimental conditions.

The best combination of both studied factors corresponds to the maximum *j* and minimum *logC*. This is experimentally 0.09 mg·L^{-1} and 3.4 A in every case. When operating under these conditions, *k* reaches a maximum value of 0.72 min^{-1} for Milli-Q water, 0.20 for WWTP sample and 0.55 min^{-1} for surface water. These values were experimentally confirmed and this is another proof of the selectivity decrease of the process, as other species appear in disolution. This means, E.g., up to 50% of CBZ removal is obtained after just 1 minute of electrochemical treatment, in the first case.

The optimal conditions lead us to recommend low pollutant concentrations (what is usually presented in real wastewater effluents) and relevant current intensities. By these procedures, energy costs would tend to be lower.

3.2.4. CONCLUSIONS.

Electrodegradation of carbamazepine is a real, feasible process for treating wastewater in several aqueous matrixes. We have addressed the reduction of such pollutant in three different media: ultrapure water (Milli-Q), surface water from a lake and effluents from an urban wastewater treatment plant.

Pollutant concentration can be reduced down to non-dangerous quantities by the application of a boron-doped diamond electrocell. The entire process can be modeled according to a first-order reaction kinetic and chemical reaction rate (*k*) can be used as a target variable for optimizing the procedure in the three effluents. Optimum combination of carbamazepine and electric current (*j*) was discovered to be at 0.09

$mg \cdot L^{-1}$ and 3.4 A, where *k* reached a maximum value of 0.72 min^{-1} in the case of MilliQ water, 0.20 for WWTP sample and 0.55 min^{-1} for surface water.

3.2.5. NOMENCLATURE.

b_0 Variable Offset term in DOE.

b_j Variable Linear effect in DOE.

b_{ij} Variable First-order interaction effect in DOE.

b_{jj} Variable Squared effect in DOE.

C_0 Pollutant initial concentration, $mg \cdot L^{-1}$.

C Pollutant concentration, $mg \cdot L^{-1}$.

J Electrical current intensity, A.

K Kinetic constant in pollutant decay model, min^{-1}.

n Number of center runs in DOE.

N Final number of experiments in DOE.

s Number of independent variables in DOE.

Y Variable Predicted response in DOE.

z Number of factors in DOE.

3.2.6. REFERENCES.

[1] Scheytt, T.J.; Mersmann, P.; Heberer, T. "Mobility of pharmaceuticals carbamazepine, diclofenac, ibuprofen, and propyphenazone in miscible-displacement experiments". Journal of Contaminant Hydrology. 83, 53 **(2006)**.

[2] Polar, J.A. "The fate of pharmaceuticals after wastewater treatment". Florida Water Resources Journal. 6, 26 (**2007**).

[3] Mompelat, S.; Lebot, B.; Thomas, O. "Occurrence and fate of pharmaceutical products and by-products, from resource to drinking water". Environ. Int. 35, 803 **(2009)**.

[4] Martínez-Bueno, M.J.; Aguera, A.; Gómez, M.J.; Hernando, M.D.; García-Reyes, J.F.; Fernández-Alba, A.R. "Application of LC/quadrupole-linear ion trap mass spectrometry and time of flight mass spectrometry to the determination of pharmaceuticals and related contaminants in wastewater". Anal. Chem. 79, 9372 **(2007)**.

[5] Benotti, M.J.; Trenholm, R.A.; Vanderford, B.J.; Holady, J.C.; Stanford, B.D.; Snyder, S.A. "Pharmaceuticals and endocrine disrupting compounds in U.S. drinking water". Environ. Sci. Technol. 43, 597 **(2009)**.

[6] Daughton, C.G.; Ternes, T.A. "Pharmaceuticals and personal care products in the environment: agents of subtle change?". Environ. Health Persp. 107, 907 **(1999)**.

[7] Clara, M.; Kreuzinger, N.; Strenn, B.; Gans, O.; Kroiss, H. "The solids retention time –a suitable design parameter to evaluate the capacity of wastewater treatment plants to remove micropollutants". Water Res. 39, 97 **(2005)**.

[8] RxList. The Internet Drug Index. http://www.rxlist.com **(2006)**.

[9] Clara, M.; Strenn, B.; Kreuzinger, N. "Carbamazepine as a possible anthropogenic marker in the aquatic environment: investigations on the behavior of carbamazepine in wastewater treatment and during groundwater infiltration". Water Res. 38, 947 **(2004)**.

[10] González, T.; Domínguez, J.R.; Palo, P.; Sánchez-Martín, J. "Development and Optimization of the BDD-Electrochemical Oxidation of the Antibiotic Trimethoprim in Aqueous Solution". Desalination, 280, 197 **(2011)**.

[11] Domínguez, J.R.; González, T.; Palo, P.; Sánchez-Martín, J.; Rodrigo, M. A.; Sáez, C. "Electrochemical Degradation of a Real Pharmaceutical Effluent". Water Air Soil Pollut. 223, 2685 (**2012)**.

[12] Domínguez, J.R.; González, T.; Palo, P.; Sánchez-Martín, J. "Electrochemical Advanced Oxidation of Carbamazepine on Boron-Doped Diamond Anodes. Influence of Operating Variables". Industrial and Engineering Chemistry Research. 49, 8353 (**2010)**.

[13] Hupert, M.; Muck, A.; Wang, J.; Stotter, J.; Cvackova, Z.; Haymond, S.; Show, Y.; Swain, G. "Conductive diamond thin-films in electrochemistry". Diam. Relat. Mater. 12, 1940 (**2003)**.

[14] Chen, G. "Electrochemical technologies in wastewater treatment". Sep. Purif. Technol. 38, 11 **(2004)**.

[15] Marselli, B.; García-Gomez, J.; Michaud, P.A.; Rodrigo, M.A.; Comninellis, Ch. "Electrogeneration of hydroxyl radicals on boron-doped diamond electrodes". J. Electrochem. Soc. 150, 79 **(2003)**.

[16] Panizza, M.; Cerisola, G. "Application of diamond electrodes to electrochemical processes". Electrochim. Acta 51, 191 **(2005)**.

[17] Brillas, E.; Calpe, J.C.; Casado, J. "Mineralization of 2,4-D by advanced electrochemical oxidation processes". Water Res. 34, 2253 **(2000)**.

[18] Martínez-Huitle, C.A.; Ferro, S. "Electrochemical oxidation of organic pollutants for the wastewater treatment: direct and indirect processes". Chem. Soc. Rev. 35, 1324 **(2006)**.

[19] StatPoint Technologies Inc. StatGraphics Centurion XVI User Manual. Virginia, USA **(2009)**.

[20] Beltrán-Heredia, J.; Sánchez-Martín, J.; Solera-Hernández, C. "Removal of sodium dodecyl benzene sulfonate from water by means of a new tannin-based coagulant: Optimization studies through design of experiments". Chem. Eng. J. 153, 56 **(2009)**.

[21] Beltrán-Heredia, J.; Sánchez-Martín, J.; Frutos-Blanco, G. "Schinopsis balansae tannin-based flocculant in removing sodium dodecylbenzene sulfonate". Sep. Pur. Technol. 67, 292 **(2009).**

[22] Kumar, V ; Porkodi, K ; Rocha, F. "Isotherms and thermodynamics by linear and non-linear regression analysis for the sorption of methylene blue onto activated carbon. Comparison of various error functions". J Hazard. Mater. 141, 794 **(2008)**.

[23] Domínguez, J.R.; González, T.; Palo, P.; Sánchez-Martín, J.; Rodrigo M.A.; Sáez, C. "Conductive-diamond electrochemical oxidation of a pharmaceutical effluent with high COD. Kinetics and optimization of the process by RSM". Env. Eng. and Manag. Journal. Accepted for publication **(2012)**.

[24] J. Beltrán-Heredia, J. Sánchez-Martín, A. Delgado-Regalado, C. Jurado-Bustos. "Removal of Alizarin Violet 3R (anthraquinonic dye) from aqueous solutions by natural coagulants". J. Hazar. Mater. 170, 43 **(2009)**.

[25] Beltrán-Heredia, J.; Palo, P.; Sánchez-Martín, J.; Domínguez, J.R.; González, T. "Natural Adsorbents Derived from Tannin Extracts for Pharmaceutical Removal in Water". Industrial and Eng. Chemistry Research. 51, 50 **(2012)**.

[26] Montgomery, D.C. Design and Analysis of Experiments. 7th edition. John Wiley and Sons, **(2009)**.

Capítulo 4:
ELECTRO-OXIDATION OF AN INDUSTRIAL PHARMACEUTICAL EFFLUENT

4.1. CONDUCTIVE-DIAMOND ELECTROCHEMICAL OXIDATION OF A PHARMACEUTICAL EFFLUENT WITH HIGH COD. KINETICS AND OPTIMIZATION OF THE PROCESS BY RSM

Conductive-diamond electrochemical oxidation processes are promising technologies for treating biorefractory industrial wastes with organic loads below 20000 $mg \cdot L^{-1}$. In this work, electrochemical oxidation of a real industrial pharmaceutical wastewater with conductive-diamond anodes has been studied. The electrolyses were carried out in discontinuous operation mode under galvanostatic conditions, using a bench-scale plant equipped with a single compartment electrochemical flow cell. For optimizing the process and studying the interaction between the operating conditions, different experiments were performed by modifying the current density (from 25 to 180 $mA \cdot cm^{-2}$) and recirculation flow rate (from 105 to 565 $mL \cdot min^{-1}$) with residence times between 0 and 570 minutes. The corresponding contribution of these two operative parameters on COD removal and its evolution versus residence time was studied. A time of 98 minutes was obtained in order to evaluate the highest influence of operative parameters. For this time, the current density was found to have a considerable positive effect, while the flow rate proved to be a statistically insignificant variable. ANOVA test reported significance for three of the five involved variables and Response Surface Methodology technique was used to optimize COD removal.

Keywords: anodic oxidation; boron-doped diamond electrodes; conductive-diamond electrochemical oxidation; pharmaceuticals; wastewater.

4.1.1. INTRODUCTION.

In the last few decades the presence of pharmaceutically-active compounds in the

Pharmaceutical Industrial Wastewaters (PIW) are emerging pollution sources due to the high demand of medicines in modern life. These contaminant effluents are characterized by their complex intrinsic nature since they consists of a large variety of raw materials. Moreover, pharmaceuticals are produced through very advanced chemical processes, so wastes from these types of industries are refractory to traditional wastewater treatment and present high biopersistance in the environment. Usually, pharmaceutical plants operate in batch mode and the effluents generally contain small quantities of reaction intermediates and products and large amounts of the dissolvent used to recover the raw materials. PIW include a huge variety of biorefractory organic compounds that resist conventional treatment techniques. In addition to its potential toxicity, these biorefractive compounds are not completely removed by biological treatment and physical and/or chemical additional treatments are needed to improve the quality and biodegradability of wastewater [1-3].

Therefore, it is not surprising that scientists have recently focused their research activities directly towards the application of non-biological processes for the destruction of pharmaceuticals in waters. In recent years, only few papers have engaged on the treatment of these kinds of current wastes, and they have been focused mainly on the study of ozonation [4], Fenton [5], electro-Fenton [6] and photochemical AOP [7], but not on conductive-diamond electrochemical oxidation processes. Recently, conductive-diamond electrochemical oxidation has been widely studied with synthetic industrial wastes at lab and bench-scale plants [8-18], but unfortunately only few papers have focused the electrochemical treatment of current aqueous wastes [19].

Electro-oxidation has been widely investigated for wastewater treatment with electrodes made of several different materials such as graphite, Pt, TiO_2, SnO_2, IrO_2, RuO_2, PbO_2 and several Ti-based alloys. In recent years, a new type of electrode material, namely boron-doped diamond (BDD) has received growing attention for pollutants oxidation since it exhibits significant chemical and electrochemical stability, good conductivity as well as it increase rates of effluent mineralization with very high current efficiencies [15, 20-23]. The BDD anode is the best non-active

electrode and consequently it is proposed as the preferable anode for treating organic pollutants by anodic oxidation. Moreover, it has been demonstrated that hydroxyl radicals are formed during the conductive diamond electrochemical oxidation of aqueous wastes [17,23], and this fact allowed classifying this technology as an advanced oxidation process (AOP).

Energy is needed for electro-oxidation and it is considered the first cost in the application of such treatment process. It is the source for radical production, so the longer the reactor is working, the more expensive the treatment results because the amount of electricity is higher. Obviously, and many previous works have already pointed out this aspect [24], it is clear that long residence times indefectibly drive to the mineralization of the pollutants, but the treatment cost raises up critically [11,10]. This is the reason one must evaluate theses parameters for proposing a realistic use of electro-oxidation.

Our previous work [24] showed interesting results in the field of TOC reduction. However, COD considerations were put out from that study.

According to the recent results, the efficiency of this novel technology is very high, and it only seems to be limited by the transport of pollutants to the anodic surface. For this reason, we chose the recirculation flow rate as one operating variable. Other variables such as temperature, pH or conductivity could be included in further studies. So, the aim of this work was to study the electrochemical oxidation of a pharmaceutical effluent over a BDD anode regarding the effect of two operating conditions such as current density (J) and recirculation flow rate (Q_v) at various residence times. A factorial design methodology was adopted for determining the statistical significance of each parameter, taking the removal of COD as the target variable.

4.1.2. MATERIALS AND METHODS.

4.1.2.1. Wastewater effluent.

A real pharmaceutical industry plant was selected for sample collecting. It was placed in Ciudad Real (Spain). PIW usually presents a more or less constant composition, although some variations can appear. The main chemical characteristics are showed in Table 4.1.

It is evident that the organic load is high enough (1200 $mg \cdot dm^{-3}$ of COD) and the ratio TOC/COD is around 0.27. The main organic compounds are aromatic and aliphatic and some solvents such as methanol and ethanol are included as well. The usual addition of chloride ions can be the responsible of such conductivity levels.

Table 4.1. Characteristics of the pharmaceutical industry wastewater (PIW).

Parameter	Value
COD ($mg \cdot L^{-1}$)	12000
TOC ($mg \cdot L^{-1}$)	3200
Conductivity ($mS \cdot cm^{-1}$)	37
pH	8.5
Total solids ($mg \cdot L^{-1}$)	5000
Composition	Aromatic and aliphatic compounds, ethanol, methanol

4.1.2.2. Electrochemical degradation experiments.

A single compartment cell was used for the electrochemical oxidation trials. These were carried out in batch operation mode [20]. The specific experimental conditions were presented elsewhere [24] and they involved diamond-based anode and stainless steel (AISI 304) as cathode. The reactor was composed of a glass recipient of 0.6 L and the maximum flow rate of the treating wastewater was 565 $mL \cdot min^{-1}$ by using a centrifugal pump. The whole system was thermally controlled by a Digiterm 100 bath (Selecta, Barcelona) at 20 ºC.

Boron-doped diamond (BDD) films were provided by CSEM (Switzerland) and synthesized by the hot filament chemical vapor deposition technique (HF CVD) on single-crystal p-type Si (100) wafers (0.1 Ω cm, Siltronix). The temperature range of the filament was 2440–2560 °C and that of the substrate was 830 °C. The reactive gas was methane in excess hydrogen (1% CH_4 in H_2) whereas the dopant gas was trimethylboron with a concentration of 3 $mg \cdot dm^{-3}$. The gas mixture was supplied to the reaction chamber at a flow rate of 5 $dm^3 \cdot min^{-1}$, giving a growth rate of 0.24 $\mu m \cdot h^{-1}$ for the diamond layer. The resulting diamond film thickness was about 1 μm. This HF CVD process produces columnar, random texture and polycrystalline films with an average resistivity of 0.01 Ω cm. Some extra information should be included in further studies in order to complete the comprehension of the oxidation process, such as cyclic voltammetry [24].

4.1.2.3. Analytical methods.

Chemical Oxygen Demand (COD) was determined using a thermoreactor (Velp Cientifica) and a HACH 200 direct reading spectrophotometer analyzer. Measurements of pH and conductivity were carried out with an InoLab WTW pH-meter and a GLP 31 Crison conductimeter, respectively.

4.1.2.4. Mathematical and statistical procedures.

Section 4.1.3 was statistically analyzed by using StatGraphics® Plus 5.1. A factorial central composite orthogonal and rotatable (CCORD) design was used with eight replicates of central point, so the total number of experiments was 16. CCORD is one of the most popular classes of second-order design and it is widely used in previous works [24]. For analyzing the growing contributions of each parameter in the electro-oxidation process, kinetic considerations were made.

4.1.2.5. Kinetics.

The CCORD gave us a specific experimental planning where kinetics was not included in the first approach. The offset term in the Design of Experiments was correspondingly assigned to *Residence time* variable, which was not initially evaluated

in the CCORD. Hence, this offset term can be compared to the contributions of each variable and kinetics can be evaluated.

4.1.3. RESULTS AND DISCUSSION.

The selected variables to work on were the inlet recirculation flow rate (Q_v), and the current density (J). It is evident that *time* variable must be considered if one wants to present some results about kinetics. This *time* variable is actually the *residence period*. Since we are working with a real effluent wastewater, this parameter should be included in the offset term as no specific variable is involved in CCORD.

Target variable should be COD removal and the concomitant effects of Q_v and J on the effectiveness of the electrochemical degradation were evaluated by setting up two different levels for this effluent. Table 4.2 shows these operating levels.

Table 4.2. Characteristics of the pharmaceutical industry wastewater (PIW).

Current density ($mA \cdot cm^{-2}$)			Recirculation flow rate ($mL \cdot min^{-1}$)		
Low level (-1)	**High level (+1)**	**Center point**	**Low level (-1)**	**High level (+1)**	**Center point**
48.2	156.9	102.6	172.1	497.3	334.7

4.1.3.1. Growing contributions. Kinetic considerations of the CCORD.

In the manner we have arranged CCORD, it does not allow evaluating the influence of time variable since it works with the final results of a certain number of experiments. However, the importance of such variable is relevant taking into account the oxidation process is not in continuous regime [13]. The first election one must make is the residence time for statistically significant conclusions: a very short period will drive to almost null COD removal; on the contrary a too long residence time will reduce the influence of the others variables (flow rate and coded density).

Taking this aspect into account, the experimental plan was defined by including the evaluation of the individual contribution of each variable separately at different periods, so the kinetics of the process can be clearly observed. The Design of

Experiments is a common methodology that can easily improve the performing of industrial production [26,27,28]. Therefore, it can be a useful tool to examine the influence of operating conditions on electrochemical oxidation of pollutants, and to determine the optimum conditions using RSM (response surface methodology). Using RSM, the aggregate mix proportions can be arrived with minimum number of experiments without the need for studying all possible combination experiments.

Although the exact procedure for this methodology was previously presented in many works [24], a brief summary of the main concepts must be included here in order to facilitate the understanding of this relatively-new optimization process. Firstly, the data must be coded according to Eq. (4.1):

$$x_i = \frac{X_i - X_i^X}{\Delta X_i} \tag{4.1}$$

where, x_i is the coded value of the *i*th independent variable, X_i the natural value of the *i*th independent variable, X_i^X the natural value of the *i*th independent variable at the center point, and ΔX_i is the value of step change.

Each response Y can be represented by a mathematical equation that correlates the response surface.

$$Y = b_o + \sum_{j=1}^{k} b_j x_j + \sum_{\substack{i=1, j=1 \\ i \neq j}}^{k} b_{ij} x_i x_j + \sum_{j=1}^{k} b_{jj} x_j^2 \tag{4.2}$$

where Y is the predicted response, b_0 the offset term, b_j the linear effect, b_{ij} the first-order interaction effect and b_{jj} is the squared effect and k is the number of independent variables. One can assume the value of the abovementioned terms are in direct relationship with the concomitant importance of each factor. Hence, b_0 should be identified with all the non-considered aspects of the process, mainly residence time.

As it is referred above, COD data were taken from each experiment during an experimental period of 0-450 minutes and the evolution of each contribution factor in Eq. (4.2) was plot on Fig. 4.1.

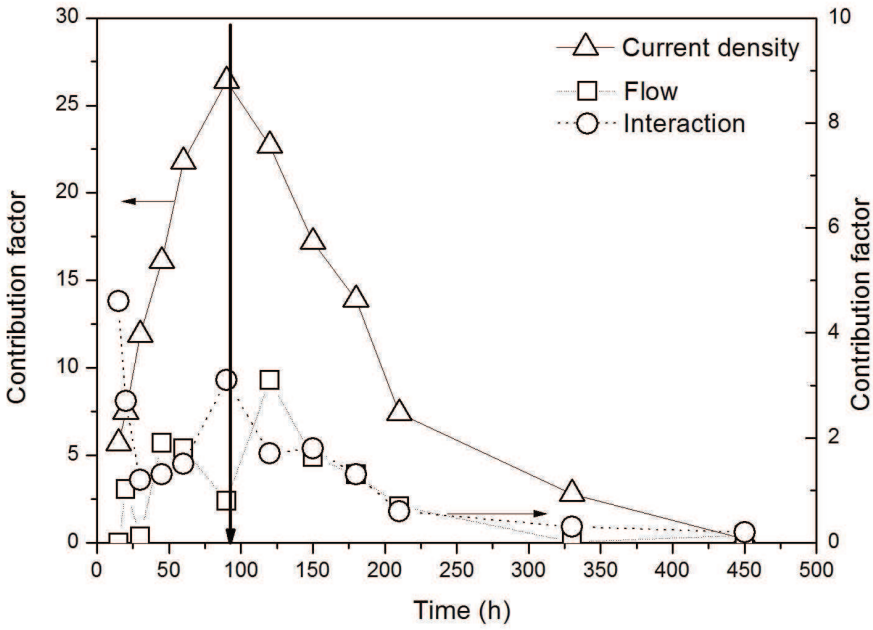

Fig. 4.1. Individual contributions of concomitant individual influence factors.

As it is clearly depicted, two levels are presented regarding the studied variables. On one hand, the contribution factor of J is much higher than the ones linked to Q_v and to Q_v-J (interaction), which have to be read on the right axis. However, the three terms appeared in Eq. (4.3) after a positive sign, so they are additive to the response variable (COD removal). In this sense, it is possible to assume the local maximum of the three curves appear around 100 minutes, although it is not an analytical conclusion, but a descriptive one. For confirming this, a sum of the three individual contributions can be presented together with the offset (Fig. 4.2).

The optimum point can be observed from Fig. 4.2, where the sum of the contributions (squared points) clearly shows the null derivative (continuous and solid line) at exactly 98 minutes. On the other hand, the growing influence of the offset term (linked to the residence period) reaches a maximum near 130 minutes. According to this, one can establish that once this period is trespassed, the study of the individual influence of the operative parameters is not interesting because the system is totally ruled by the residence time and almost 100% of COD removal is obtained.

Consequently, shady interval in Fig. 4.2 represents the constrained range where the optimization study on inlet recirculation flow rate or current density is feasible. Hence, we have focused our optimum residence time at 98 minutes in order to evaluate the highest influence of the operative parameters.

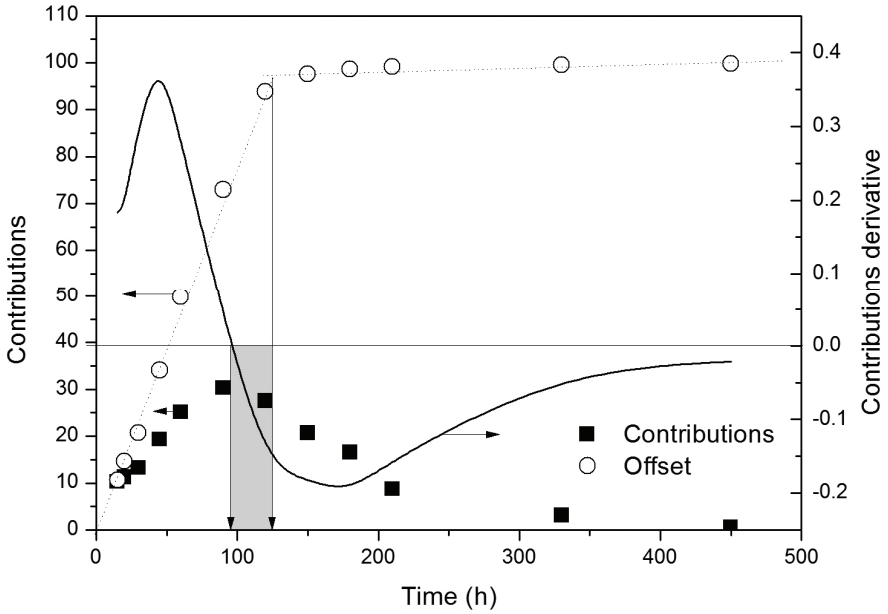

Fig. 4.2. Global contribution of operative parameters and evolution of the offset in the COD removal modelization.

4.1.3.2. Experimental design. Surface response methodology.

It is known that the classical method, one factor at a time, is not able to study the influence of every factor on a response in a concomitant way. That is, unless a huge number of experiments are carried out, the information we obtain through such methodology is scarce. So, the design of experiment (DOE) is an efficient way to solve this problem. It offers a better alternative to study the effect of variables and their responses with minimum number of experiments [29].

The specific working coded range (-1 to +1) involves 48-156 $mA \cdot cm^{-2}$ (regarding J) and 172-497 $mL \cdot min^{-1}$ (regarding Q_v). Consequently, one step is equal to 54 for current intensity and 163 for flow rate. $2^{0.5}$ was set as axial distance in this design, so it

was used for setting out the corresponding experimental points. Table 4.3 shows the final design of experiments and the obtained response for a residence time of 98 min.

Table 4.3. Experimental planning in DOE and obtained response at 98 min of residence time.

Run	Coded J	Coded Q_v	COD removal X (%)
1	1	-1	90.5
2	0	0	72.0
3	0	1.41421	74.5
4	0	0	71.9
5	-1.41421	0	24.9
6	0	0	70.6
7	-1	-1	39.8
8	-1	1	35.3
9	1.41421	0	93.6
10	0	-1.41421	72.3
11	0	0	72.6
12	0	0	78.1
13	0	0	73.0
14	0	0	73.0
15	0	0	73.0
16	1	1	98.5

4.1.3.3. Numerical Analyses and ANOVA report.

ANOVA analysis is the first test where one can find the significance of the different parameters. Five factors are considered inside the DOE and only three of them present a *p*-value below 0.05 (limit of significance), so they are statistically significant. This means that the model used to represent the behaviour of the interactive factors is consistent and the ANOVA test has statistical sense. Non-linear polynomial regression is carried out taking into account Eq. (4.2). In this sense, this regression is the following expression (Eq. (4.3)):

$$X\ (\%) = 73.02 + 26.38 \cdot J + 0.82 \cdot Q_v - 6.96 \cdot J^2 + 3.12 \cdot J \cdot Q_v + 0.11 \cdot Q_v^{\ 2} \qquad (4.3)$$

where the values of J (current density) and Q_v (recirculation flow rate) should be coded according to Eq. [4.2]. The values of COD removal, X, are given in %. The adjusted correlation factor r^2 is equal to 0.98 and the Durbin-Watson statistical is above 5%, so no autocorrelation evidences are presented and the randomization of the whole system was correct. This is graphically confirmed in Fig. 4.3, where the residuals do not follow any specific pattern. No correlation can be appreciated (residuals are located in a random order to both the sides of the 0 axis), the randomization of the design is fully working and no accumulation of experimental error is observed.

The goodness of the model data is given by the value of the adjusted correlation factor, which is above 0.98.

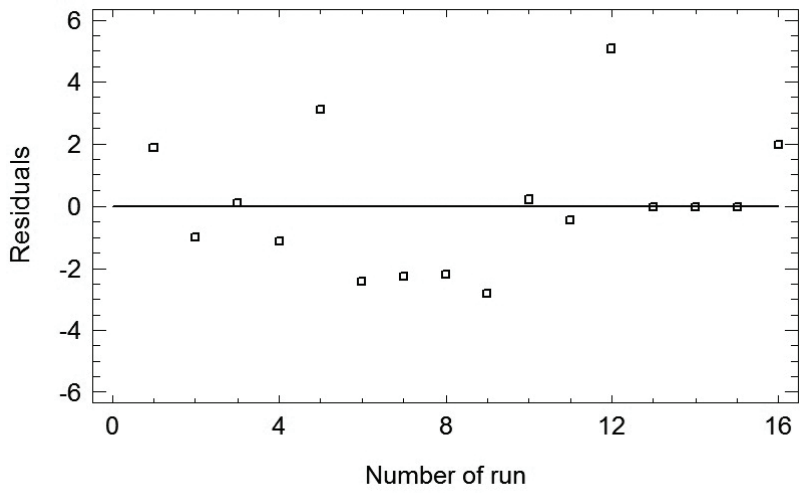

Fig. 4.3 Residuals in random manner.

4.1.3.4. Graphical analyses. Significant variables.

Eq. (4.3) allows us to carry out the data modelization. A graphical expression of the ANOVA test results may be the Pareto graphic (Fig. 4.4). Bars represent the standardized effects of each involved factor and combinations of all them. Nonfilled bars are a graphical representation of negative-affecting factors, such as the squared

current density. That means that this factor appears in the Equation (4.4) behind a negative sign. On the other hand, filled bars represent positive- affecting factors, the rest of them. The vertical rule stands near to 2 and has to do with the signification level of ANOVA test, which is equal to 95% of confidence. Bars trespassing the vertical rule are inside significant region, while bars behind it are not statistically significant. The Pareto graphic also gives us an idea of how factors influence on the final response X (COD removal percentage). Positive bars indicate that by varying the variable X increases. Negative bars indicate the contrary. As can be shown, the increase of both factors leads to an increase in the response, but the influence of current density (J) is much more relevant.

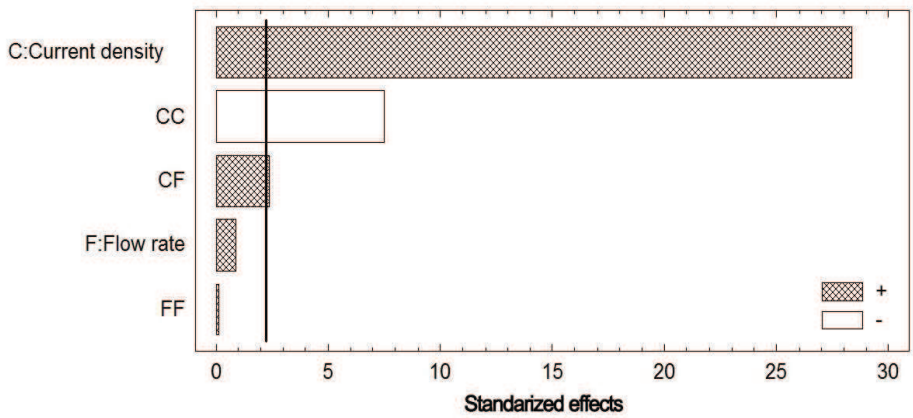

Fig. 4.4. Pareto graphic for standardized effects.

4.1.3.5. Influence of single variables.

One of the best features of the Design of Experiments is the fact that one can study the main effects of the involved variables individually. This can be observed in Fig. 4.5. Two curves are drawn representing the effect of varying each variable while the other ones keep constant. As it is clearly shown, the effect of the current density (J) is positive and its influence on the COD removal is rapidly increased. This may be explained by taking into account that hydroxyl radical generation on BDD anode is due to the current.

On the other hand, the influence of the recirculation flow rate (Q_v) is quasi-linear, that is, the response is independent from this variable. This is the graphical representation of a non-significant variable. These obtained results show that an increase in the recirculation flow rate does not favour the transport of pollutants to the anodic surface.

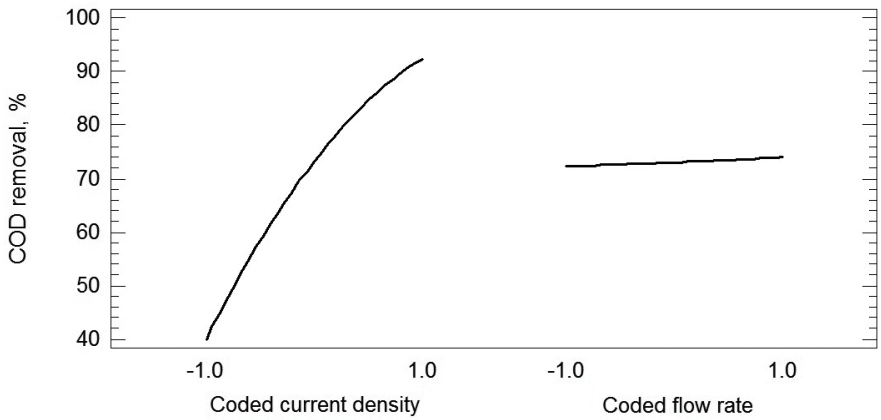

Fig. 4.5. Main effects.

4.1.3.6. Interaction between variables.

Moreover, attending to Fig. 4.6 the interaction between each two of the four variables can be studied. Each curve is a representation of the evolution of the COD percentage removal by varying one variable in the extremes of the experimental model, that is, with its pair variable equal to +1 (upper value) and equal to −1 (low value). Parallel lines mean there is no interaction between them, crossing lines indicate the contrary. The level of interaction of one variable on the other is represented between these two situations.

The fact that interaction appears between the two studied variables is evident from this graphic because the two curves are clearly crossed, so it may be assumed that the modification of one of the variables affects to the behaviour of the other one and, consequently, the final response.

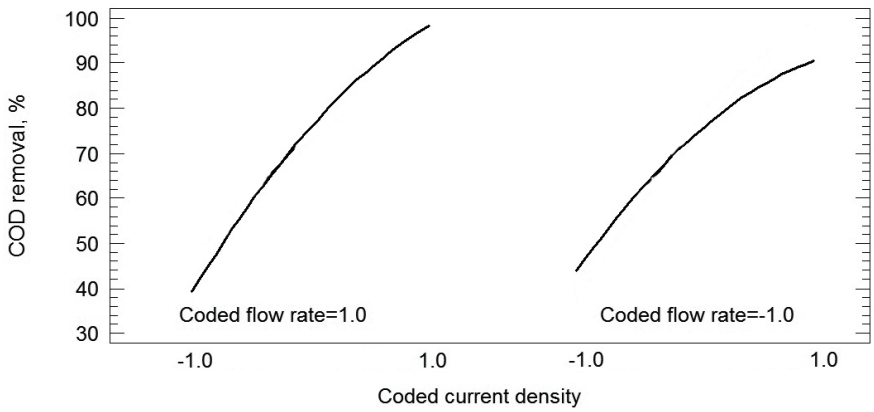

Fig. 4.6. Interaction graphic.

4.1.3.7. Response surface and contour plot.

For the final evaluation of the whole system in a holistic view, the surface graphic is the most important graphical representation in the RSM. It plots Eq. (4.3) and allows evaluating from a qualitative point of view. As Fig. 4.7 depicts, the response is a quite convex surface inside the studied region, and a clear tendency of growing COD removal is presented as current density (J) increases. On the other hand, recirculation flow rate (Q_v) presents its low influence on the final response, since almost parallel contour lines are plot below the surface.

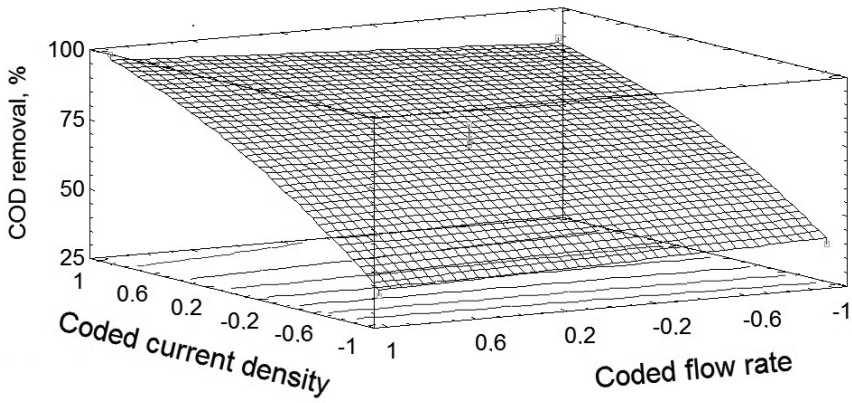

Fig. 4.7. Response Surface graphic for the studied variables.

This behaviour is typical in stable systems. As can be appreciated, the final response is almost dependent on one of the two variables in a non-linear relationship, due to the significance of the squared term in Eq. (4.3).

4.1.4. CONCLUSIONS.

The conclusions drawn from this study can be summarized as follows:

- Electrochemical oxidation over BDD electrodes is a relative innovative process in industrial wastewater treatment. In this view, an effluent from pharmaceutical industry was chosen to be treated electrochemically with emphasis given on the effect of two operating conditions, such as current density and recirculation flow rate, with various reaction residence times. In general, the process was able to achieve satisfactory levels of COD removal at short treatment times.
- To evaluate the importance of both parameters on treatment efficiency, an orthogonal, rotatable factorial central composite design of experiments was carried out, taking the removal of COD as the target variable.
- From kinetic considerations, residence times above 130 minutes, the system is totally ruled by residence time. The highest influence of operative parameters has been determined at a residence time of 98 minutes.
- Of the two parameters tested, current density positively affected COD removal at a statistically significant level, while recirculation flow rate resulted be a non-significant variable.

4.1.5. NOMENCLATURE.

List of symbols:

J Current density, $mA \cdot cm^{-2}$.

Q_v Flow rate, $mL \cdot min^{-1}$.

N Total number of experiments in DOE.

n Number of center replications in DOE.

k Number of factors in DOE.

x_i Coded value of the ith independent variable in DOE.

X_i Natural value of the ith independent variable in DOE.

X_i^X Natural value of the ith independent variable at the center point ΔX_i non Value of step change in DOE.

Y Percentage removal in response surface methodology, %.

b_0 Offset term in RSM.

b_j Linear effect in RSM.

b_{ij} First-order interaction effect in RSM.

b_{jj} Squared effect in RSM.

4.1.6. REFERENCES.

[1] Bai, J.; Xu, H.; Zhang, Y.; Peng, Z.; Xu, G. "Combined industrial and domestic wastewater by periodic allocating water hybrid hydrolysis acidification reactor followed by SBR". Biochem. Engin. J. 70, 115 **(2013)**.

[2] Mareci, I.; Matei, F.; Bocanu, C.; Aelenei, N. "Contributions of electrochemical oxidation of CN^- ions study". Environ. Engineer. Manag. J. 2, 357 **(2003)**.

[3] Barrera-Díaz, C.; Linares-Hernández, I.; Roa-Morales, G.; Bilyeu, B.; Balderas-Hernández, P. "Removal of biorefractory compounds in industrial wastewater by chemical and electrochemical pretreatments". Ind. Eng. Chem. Res. 48, 1253 **(2009)**.

[4] Balcioglu, I.A.; Otker, M. "Treatment of pharmaceutical wastewater containing antibiotics by O_3 and O_3/H_2O_2 processes". Chemosphere. 50, 85 **(2003).**

[5] Sebastian, N.S.; Figuls, J.; Font, X.; Sanchez, A. "Preoxidation of an extremely polluted industrial wastewater by the Fenton's reagent". J. Hazard. Mater. 101, 315 **(2003)**.

[6] Saghafinia, M.S.; Emadian, S.M.; Vossoughi, M. "Performances evaluation of photo-Fenton and Sonolysis for the treatment of Penicillin G formulation effluent". Procedia Environ. Sci. 8, 202 **(2011)**.

[7] Balcioglu, I.A.; Alaton, I.A.; Otker, M.; Bahar, R.; Bakar, N.; Ikiz, M. "Application of advanced oxidation processes to different industrial wastewaters". J. Environ. Sci. Health Part A. 38, 1587 **(2003).**

[8] Domínguez, J.R.; González, T.; Palo, P., Sánchez-Martin, J. "Anodic oxidation of ketoprofen on boron-doped diamond (BDD) electrodes. Role of operative parameters". Chem. Eng. J. 162, 1012 **(2010)**.

[9] Domínguez, J.R.; González, T.; Palo, P.; Sánchez-Martin, J. "Electrochemical advanced oxidation of carbamazepine on boron-doped diamond anodes. Influence of Operating Variables". Ind. Eng. Chem. Res. 49, 8353 **(2010)**.

[10] González, T.; Domínguez, J.R.; Palo, P.; Sánchez-Martin, J. "Conductive-Diamond Electrochemical Advanced Oxidation of Naproxen in Aqueous Solution: Optimizing the Process". J. Chem. Technol. Biotechnol. 86, 121 **(2011)**.

[11] Cañizares, P.; Sáez, C.; Lobato, J.; Rodrigo, M.A. "Electrochemical treatment of 4-nitrophenol-containing aqueous wastes using boron-doped diamond anodes". Ind. Eng. Chem. Res. 4, 1944 **(2004)**.

[12] Cañizares, P.; Sáez, C.; Lobato, J.; Rodrigo, M.A. "Electrochemical oxidation of polyhidroxibenzenes on BDD anodes". Ind. Eng. Res. 43, 6629 **(2004)**.

[13] Cañizares, P.; Diaz, M.; Domínguez, J.A.; Lobato, J.; Rodrigo, M.A. "Electrochemical treatment of diluted cyanide aqueous wastes". J. Chem. Technol. Biotechnol. 80, 565 **(2005)**.

[14] Cañizares, P.; Lobato, J.; Paz, R.; Rodrigo, M.A.; Sáez, C. "Electrochemical oxidation of phenolic compound wastes with BDD anodes". Water Res. 39, 2687 **(2005)**.

[15] Cañizares, P.; Sáez, C.; Lobato, J.; Rodrigo, M.A. "Detoxification of synthetic industrial wastewaters using electrochemical oxidation with boron doped diamond anodes". J. Chem. Technol. Biotechnol. 81, 352 **(2006)**.

[16] Brillas, E.; Boye, B.; Sires, I.; Garrido, J.A.; Rodríguez, R.M.; Arias, C.; Cabot, P.L.; Comninellis, Ch. "Electrochemical destruction of chlorophenoxy herbicides by anodic

oxidation and electro-Fenton using a boron-doped diamond electrode". Electrochim. Acta. 49, 4487 **(2004)**.

[17] Marselli, B.; García-Gomez, J.; Michaud, P.A.; Rodrigo, M.A.; Comninellis, Ch. "Electrogeneration of hydroxyl radicals on boron-doped diamond electrodes". J. Electrochem. Soc. 150, 79 **(2003)**.

[18] de Lucas, A.; Cañizares, P.; Rodrigo, M.A.; García-Gomez, J. "Electrochemical Treatment of Aqueous Phenol Wastes: A preliminary Economical Outlook in Waste Management and the Environment". WIT Press. 161, Southampon **(2002)**.

[19] Rodrigo, M.A.; Cañizares, P.; Sánchez-Carretero, A.; Sáez, C. "Use of conductive-diamond electrochemical oxidation for wastewater treatment". Catal. Today. 151, 173 **(2010)**.

[20] Cañizares, P.; Lobato, J.; Paz, R.; Rodrigo, M.A.; Sáez, C. "Advanced oxidation processes for the treatment of olive-oil mills wastewater". Chemosphere. 67, 832 **(2007)**.

[21] Martínez-Huitle, C.A.; Brillas, E. "Decontamination of wastewaters containing synthetic organic dyes by electrochemical methods. A general review ". Appl. Catal. B. 87, 105 **(2009)**.

[22] Martínez-Huitle, C.A. ; Quiroz, M.A. "Diamond electrode: recent environmental applications". J. Environ. Eng. Manag. 18, 155 **(2008)**.

[23] Panizza, M.; Cerisola, G. "Application of diamond electrodes to electrochemical processes". Electrochim. Acta, 51, 191 **(2005)**.

[24] Domínguez, J.R.; González, T.; Palo, P.; Sánchez-Martín, J.; Rodrigo, M.A.; Sáez, C. "Electrochemical degradation of a real pharmaceutical effluent". Water, Air & Soil Pollut. 223, 2685 **(2012)**.

[25] Zhu, X.; Ni, J.; Lai, P. "Advanced treatment of biologically pretreated coking wastewater by electrochemical oxidation using boron-doped diamond electrodes". Water Res. 4, 4347 **(2009)**.

[26] Milani, A.S.; Wang, H., Frey, D.D.; Abeyaratne, R.C. "Evaluating three DOE methodologies: optimization of a composite laminate under fabrication error". Qual. Eng. 21, 96 **(2009)**.

[27] Deligiorgis, A.; Xekoukoulotakis, N.P.; Diamadopoulos, E.; Mantzavinos, D. "Electrochemical oxidation of table olive processing wastewater over boron-doped diamond electrodes: Treatment optimization by factorial design". Water Res. 42, 1229 **(2008)**.

[28] Bhatia, S.; Othman, Z.; Ahmad, A.L. "Pretreatment of palm oil mill effluent (POME) using Moringa oleifera seeds as natural coagulant". J. Hazard. Mater. 145, 120 **(2007).**

[29] Montgomery, D.C. "Design and Analysis of Experiments". John Wiley and Sons. New York **(2001)**.

4.2. ELECTROCHEMICAL DEGRADATION OF A REAL PHARMACEUTICAL EFFLUENT

In this work, the electrochemical treatment of an effluent from pharmaceutical industry with boron-doped diamond electrodes was investigated. The electrolyses were carried out in a discontinuous operation mode under galvanostatic conditions, using a bench-scale plant equipped with a single compartment electrochemical flow cell The effect of operating conditions, such as current density (from 25.7 to 179.4 $mA \cdot cm^2$) and flow rate (from 104.8 to 564.7 $cm^3 \cdot min^{-1}$), at residence times between 0 and 570 minutes, was studied. Design of experiments was used for optimizing the process. The global contribution of operative parameters and evolution of the residence time in TOC removal was studied and a time of 77 minutes was obtained in order to evaluate the highest influence of the operative parameters. For this time, ANOVA test reported significance for four of the five involved variables. The current density was found to have a considerable positive effect on TOC removal, whereas the flow rate was found to have a moderate negative effect on target variable.

Keywords: electrochemical advanced oxidation processes, electro-oxidation, anodic oxidation, boron-doped diamond electrodes, pharmaceuticals.

4.2.1. INTRODUCTION.

Pharmaceutical and drugs are some of the most relevant emerging pollutants nowadays. Their noxious and dangerous presences in the aquatic environment make researchers focus their attention to these new contaminants. Drugs enter into the environment through excretion and metabolism of both humans and animals since the consumption of pharmaceuticals is high enough in modern life [1]. The usual way of environmental disposal should be the excretion under the form of glucuronide or sulfate conjugates, such as a metabolite, or a mixture of many metabolites. In general, drugs in the body are metabolized by different mechanisms (oxidation, reduction, hydrolysis, conjugation, etc.) and then excreted in the form of derivatives more polar and soluble in water, which have a reduced pharmacological activity compared to the original compound. For example, carbamazepine is metabolized in the human body

and is excreted only 2-3% of the administered dose in their original form. The painkiller diclofenac 1% is excreted as such and 60% as glucuronides. Lipid lowering bezafibrate is being excreted from the administered dose, 50% as glucuronide and 20% in its original form [2]. After the treatments carried out in the sewage treatment stations some compounds still remaining in the aqueous phase (eg. ibuprofen, naproxen, sulfamethoxazole, iopromide, etc.) [3].

European countries are currently worried about the presence of pharmaceuticals in their surface waters, mainly due to the effect these compounds present to humanlife [4]. For example, in Germany, carbamazepine detected values up to more than 1075 $ng \cdot L^{-1}$ in river waters. In tests carried out on the river Ebro (Spain), the drugs were found in greater amounts were as follows with the average values indicated of ibuprofen (60 $ng \cdot L^{-1}$), acetaminophen (42 $ng \cdot L^{-1}$), gemfibrozil (46 $ng \cdot L^{-1}$), carbamazepine (30 $ng \cdot L^{-1}$) and atenolol (72 $ng \cdot L^{-1}$) [5].

Advanced Oxidation Processes (AOP) [6,7,8] are feasible methods for combating this emerging pollution. They are promising environmentally friendly technologies for the treatment of wastewaters containing low contents of toxic and biorefractory pollutants [9]. Among them, Electrochemical Advanced Oxidation Processes (EAOPs) [10-12] are very attractive for water and wastewater decontamination due to their low cost and high effectiveness, without needing the addition of toxic chemical reagents and without producing dangerous wastes.

Anodic Oxidation (AO) is the most effective technique in this group of EAOP. It involves the destruction of pollutants in an electrolytic cell under the action of hydroxyl radicals formed as intermediate from water oxidation at the surface of the anode [13,14]. The use of a boron-doped diamond (BDD) thin-film anode brings technologically important characteristics such as an inert surface with low adsorption properties, remarkable corrosion stability and wide potential windows in aqueous medium [15,16].

Although the electrochemical oxidation over BDD electrodes of several classes of organic pollutants has been studied extensively [17,18], process application for

industrial effluent treatment is limited, and appears as a very promising answer to solve the environmental problem generated by the discharge of these pharmaceutically polluted effluents.

The traditional installations of electrooxidation present a main source of costs: electricity. In terms of water treatment, these economical considerations are linked to the residence time in the reactor: the longer the wastewater is kept inside it, the more expensive is the whole treatment due to the higher amount of electricity involved in the process. However, it is well known electrooxidation is effective if a period long enough is established [19]. The evaluation of this parameter is therefore mandatory in order to optimize the treatment process under an economical point of view.

The present work aims to study the electrochemical oxidation of a pharmaceutical effluent with a BDD anode regarding the effect of two operating conditions such as current density and flow rate at various residence times. A factorial design methodology was adopted to determine the statistical significance of each parameter as well as optimal treatment conditions. Kinetics are also determined according to the evaluation of the offset contribution. Since we are working with real pharmaceutical wastewater effluent, it should be very difficult to modelate the purification system by considering the removal of specific chemical species. Moreover, this speciation should be not very accurate or consistent since the composition of the effluent may vary qualitatively during the study. Instead, we focused our attention on an objective variable which should be representative of such kind of dangerous pollutants. That is the Total Organic Carbon (TOC), which was the target variable during the experiments.

4.2.2. MATERIALS AND METHODS.

4.2.2.1. Effluent.

The effluent used in this study was taken from a pharmaceutical industry plant in Ciudad Real (Spain). Although the concentration and proportion of pollutants contained in PIW can vary, the average composition and characteristics of the effluent almost does not fluctuate. Its main characteristics are summarized in Table 4.1. It is

mainly composed of organics (aromatic and aliphatic compounds) and solvents such as methanol and ethanol. Its organic load is around 12000 $mg \cdot dm^{-3}$ of COD and the ratio TOC/COD is around 0.27. Moreover, its high conductivity can be explained in terms of a very high concentration of chloride ions.

4.2.2.2. Electrochemical degradation experiments.

Electrochemical oxidation trials were carried out in a single compartment electrochemical flow-cell working under a batch operation mode [20]. Diamond-based material was used as anode and stainless steel (AISI 304) as cathode. Both electrodes were circular of 100 mm diameter with a geometric area of 78 cm^2 and an electrode gap of 9 mm. The wastewater was stored in a glass tank (0.6 dm^3) and circulated through the electrolytic cell by means of a centrifugal pump operating at a maximum flow rate of 565 $cm^3 \cdot min^{-1}$. A heat exchanger coupled with a controlled thermostatic bath (Digiterm 100, JP Selecta, Barcelona, Spain) was used to maintain the temperature at 20 ºC in all cases.

Boron-doped diamond (BDD) films were provided by CSEM (Switzerland) and synthesized by the hot filament chemical vapour deposition technique (HF CVD) on single-crystal p-type Si (100) wafers (0.1 Ω cm, Siltronix). The temperature range of the filament was 2440–2560 °C and that of the substrate was 830 °C. The reactive gas was methane in excess hydrogen (1% CH_4 in H_2) whereas the dopant gas was trimethylboron with a concentration of 3 $mg \cdot dm^{-3}$. The gas mixture was supplied to the reaction chamber at a flow rate of 5 $dm^3 min^{-1}$, giving a growth rate of 0.24 $\mu m \cdot h^{-1}$ for the diamond layer. The resulting diamond film thickness was about 1 μm. This HF CVD process produces columnar, random texture and polycrystalline films with an average resistivity of 0.01 Ω cm.

4.2.2.3. Analytical methods.

TOC Analysis

The carbon concentration was monitored using a Shimadzu TOC-5050 analyzer. Section 4.2.3 was statistically analyzed by using StatGraphics® Plus [21]. A

factorial central composite orthogonal and rotatable (CCORD) design was used with eight replicates of central point, so the total number of experiments was 16. CCORD is one of the most popular classes of second-order design. It involves the use of a two–level factorial design with 2^k points combined with $2k$ axial points and n center runs, k being the number of factors. N, total number of experiments with k factor is obtained according to Equation (4.4):

$$N = 2^k + 2 \cdot k + n \tag{4.4}$$

where n is considered to be eight and the axial distance is $2^{0.5}$ in order to guarantee an orthogonal and rotatable design. For analyzing the growing contributions of each parameter in the electrooxidation process, kinetic considerations were taken into account.

4.2.2.4. Kinetics.

Once the Design of Experiments selected, samples of the treated effluent were collected at equal intervals of time. The contributions of each variable were therefore evaluated under the statistical perspective of CCORD and the offset term was assigned to *residence time* variable (out of the design).

4.2.3. RESULTS AND DISCUSSION.

According to previous studies and scientific references [22], the selected variables to work on were the current density (J) and the inlet flow rate (Q_V). Obviously, when talking about kinetics one must consider the *time* variable, that is, the residence period. Since we are working with a real effluent wastewater, this parameter should be included in the offset term (see below). Target variable, according to this, should be TOC removal. Consequently, to evaluate the influence of J and Q_V and their concomitant effects on the effectiveness of the electrochemical degradation, different levels were set for this pharmaceutical effluent. This selection was considered according to previous studies (data not shown). Table 4.4 shows these experimental planning.

Table 4.4. Experimental planning in the design of experiments.

Run	Coded J	Coded Q_v	Real J ($mA \cdot cm^{-2}$)	Real Q_v ($cm^3 \cdot min^{-1}$)
1	1	-1	156.9	172.1
2	0	0	102.6	334.7
3	0	1.41421	102.6	564.7
4	0	0	102.6	334.7
5	-1.41421	0	25.7	334.7
6	0	0	102.6	334.7
7	-1	-1	48.2	172.1
8	-1	1	48.2	497.3
9	1.41421	0	179.4	334.7
10	0	-1.41421	102.6	104.8
11	0	0	102.6	334.7
12	0	0	102.6	334.7
13	0	0	102.6	334.7
14	0	0	102.6	334.7
15	0	0	102.6	334.7
16	1	1	156.9	497.3

4.2.3.1. Growing contributions. Kinetic considerations of the CCORD.

Design of experiments does not allow evaluating the influence of time variable since it works with the final results of a certain number of experiments. However, the importance of such variable is high taking into account the process is not in continuous regime but in batch-scale one. The first election one must make is the residence time for statistically significant conclusions: a very short period will drive to almost null TOC removal; on the contrary a too long residence time will reduce the influence of the others variables (flow rate and coded density).

Fortunately, the experimental method was planned in order to evaluate the individual contribution of each variable separately at different periods (so kinetics of

the degradation process can be observed). In this scenario, the design of experiments is a common methodology in order to improve industrial and economical production processes [23-25]. Therefore, this methodology can be a useful tool to examine the influence of operating conditions on electrochemical oxidation of pollutants, and to determine the optimum conditions using RSM (response surface methodology). Using RSM, the aggregate mix proportions can be arrived with minimum number of experiments without the need for studying all possible combination experiments.

In this methodology, the data obtained must be analyzed in a statistically manner, using regression, in order to determine if there exist a relationship between the factors and the response variables investigated. The test factors were coded according to Eq. (4.1). Each response *Y* can be represented by a mathematical equation that correlates the response surface (see Eq. (4.2)).

As referred above, TOC data were taken from each experiment during a experimental period of 0-450 minutes and the evolution of each contribution factor in Eq. (4.2) was plot on Figure 4.8.

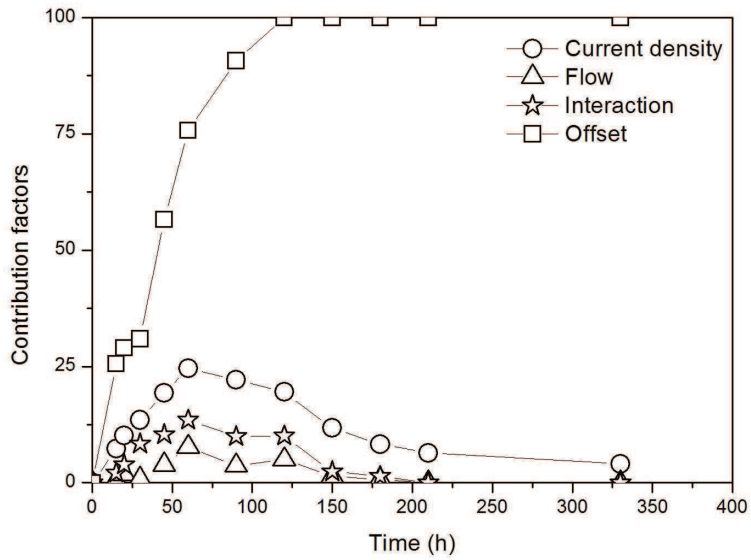

Figure 4.8. Individual contributions of concomitant individual influence factors.

As it is clearly depict, two levels are presented regarding the studied variables. On one hand, the contribution factor for the offset is much higher than the rest of contributions (current density, flow rate and the interaction between both of them). The considerations about the offset term should be taken into account later. At a first glance, it is possible to assume the local maximum of the three curves appear around 60 minutes regarding the form of the three curves, although it is not an analytical conclusion, but a descriptive one. A mathematical confirmation of this should be presented, and to this end, the sum of the three individual contributions can be presented together with the offset contribution (Figure 4.9).

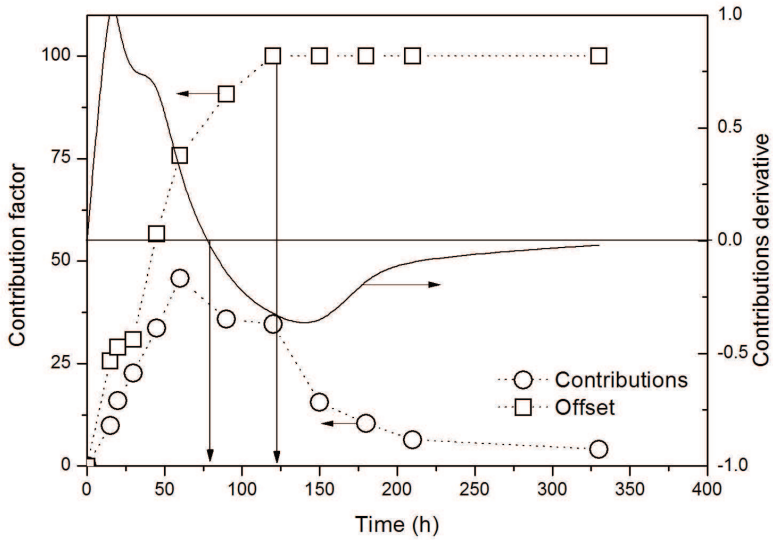

Figure 4.9. Global contribution of operative parameters and evolution of the offset in the TOC removal modelization.

Figure 4.9 clearly shows that the sum of the contributions (rounded points) presents an optimum near 75 minutes and this fact is confirmed by the null value of the derivative curve (continuous and solid line). This exactly points the local maximum at 77 minutes. On the other hand, the growing influence of the offset term (linked to the residence period) reaches a maximum near 125 minutes. This means that once this period is trespassed, the study of the individual influence of the operative

parameters is not interesting, since the system is totally ruled by the residence time and almost 100% of TOC removal is obtained. Consequently, shady interval in Figure 4.9 represents the constrained range, outside from it the optimization study on inlet flow rate or current density has no sense. Hence, we have focused our residence time at 77 minutes in order to evaluate the highest influence of the operative parameters.

4.2.3.2. Experimental design. Surface response methodology.

The classical method, one factor at a time approach, to study the influence of several operation variables (factors) on a parameter (response) involves a large number of experiments and some important conclusions on the interaction among factors can be missed. So, the design of experiment (DOE) is an efficient way to solve this problem. It offers a better alternative to study the effect of variables and their responses with minimum number of experiments [26,27], as said before.

The specific working range involves 48.2-156 $mA \cdot cm^{-2}$ (regarding J) and 172.1-497.3 $mL \cdot min^{-1}$ (regarding Q_V). Consequently, one step is equal to 53.9 for current intensity and 162.6 for flow rate. $2^{0.5}$ is set as axial distance in this design, so it was used for setting out the corresponding experimental points.

4.2.3.3. Numerical analyses and ANOVA report.

In a first approach, we should refer the ANOVA analysis that shows us the significance of the different parameters. Supplementary Data (Table S.4.1) gives all of the data of this statistical analysis. According to the RSM, five factors are considered and four of them have a *p*-value below 0.05 (limit of significance), so they are statistically significant. This means that the model used to represent the behaviour of the interactive factors is consistent.

Nonlinear polynomial regression is carried out taking into account Eq. (4.2). In this sense, this regression is the following expression Eq. (4.5):

$$X\ (\%) = 75.72 + 24.63J - 7.66Q_V - 6.68 \cdot J^2 + 13.5 \cdot JQ_V - 2.35Q_V^{\ 2} \qquad (4.5)$$

where the values of J and Q_V should be coded according Eq.(4.1). The values of TOC removal, *X*, are given in %. The adjusted correlation factor r^2 is equal to 0.89 and no autocorrelation evidences are presented. Graphically, this effective randomization of the experimental runs is presented in Figure 4.10, where the residuals do not follow any specific pattern. No correlation can be appreciated (residuals are located in a random order to both the sides of the 0 axis), the randomization of the design is fully working and no accumulation of experimental error is observed. Moreover, a numerical measure of this randomization is the Durbin-Watson statistic (DW). It presents the correlation hypothesis and the p-value linked to this statistic confirms or refuse the randomization. Since DW is equal to 2.84 (which corresponds to a p-value equal to 0.94) there is no evidence of auto-correlation and randomization was fully working.

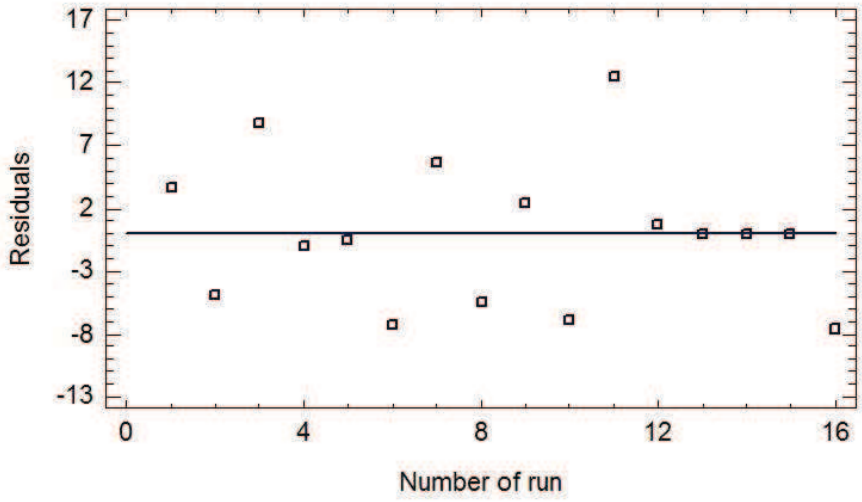

Figure 4.10. Residuals in random manner.

For each experiment, the difference between experimental and predicted *X* is presented in Figure 4.11. This is the graphical expression of adjusted correlation factor, which is above 0.98.

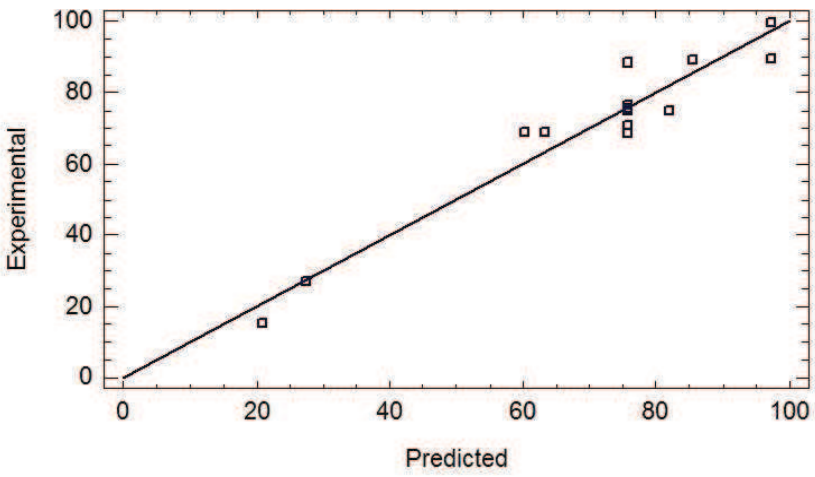

Figure 4.11. Predicted vs experimental removal TOC percentage.

4.2.3.4. Graphical analyses. Significant variables.

Modelization is made on the basis of five factors which correspond to the terms involved in Equation (4.5). A graphical expression of the ANOVA test results may be the Pareto graphic (Figure 4.12). Bars represent the standardized effects of each involved factor and combinations of all them. Filled bars are a graphical representation of negative-affecting factors, such as the squared current density. That means that this factor appears in the expression (4.5) behind a negative sign. On the other hand, nonfilled bars represent positive-affecting factors, the rest of them. The vertical rule stands near to 2 and has to do with the signification level of ANOVA test, which is equal to 95% of confidence. Bars trespassing the vertical rule are inside significant region, while bars behind it are not statistically significant. The Pareto graphic also gives us an idea of how factors influence on the final response *X* (TOC percentage removal). Positive bars indicate that by varying the variable *X* increases. Negative bars indicate the contrary. As can be shown, the increase of both factors leads to an increase in the response, but the influence of current density (A) is much more relevant.

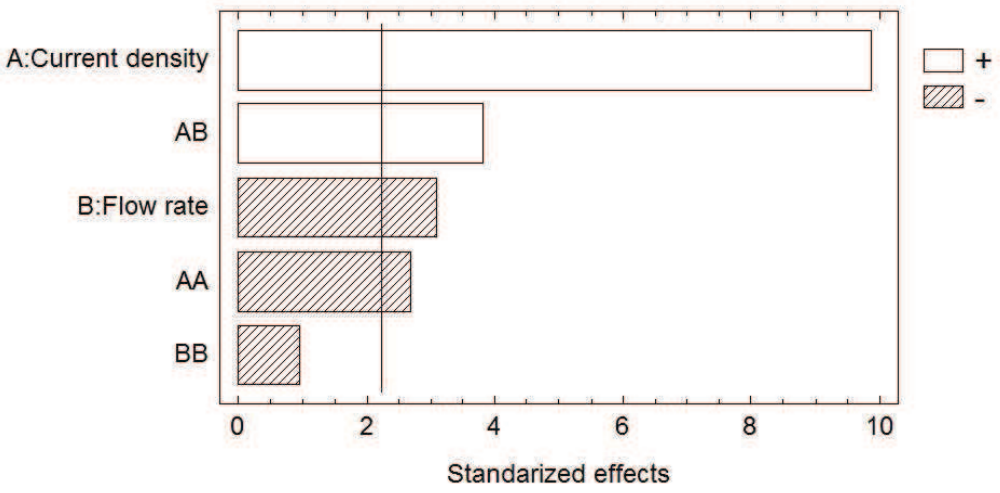

Figure 4.12. Pareto graphic for standardized effects.

4.2.3.5. Influence of single variables.

The evaluation of the model leads also to the study of the main effects of the involved variables. This can be observed in Figure 4.13. Two curves are drawn representing the effect of varying each variable while the other ones keep constant. As it is clearly shown, the effect of the current density is positive and its influence on the TOC removal is rapidly increased. On the other hand, the influence of the flow rate is less relevant and on the contrary: by increasing it the final response becomes lower.

4.2.3.6. Interaction between variables.

Figure 4.14 shows the interaction between each two of the four variables studied. Each curve is a representation of the evolution of the TOC percentage removal by varying one variable in the extremes of the experimental model, that is, with its pair variable equal to +1 (upper value) and equal to −1 (low value). Parallel lines mean there is no interaction between them, crossing lines indicate the contrary. The level of interaction of one variable on the other is represented between these two situations.

The fact that interaction appears between the two studied variables is evident from this graphic. The two curves are clearly crossed, so it may be assumed that the modification of one of the variables affects to the behaviour of the other one and, consequently, the final response.

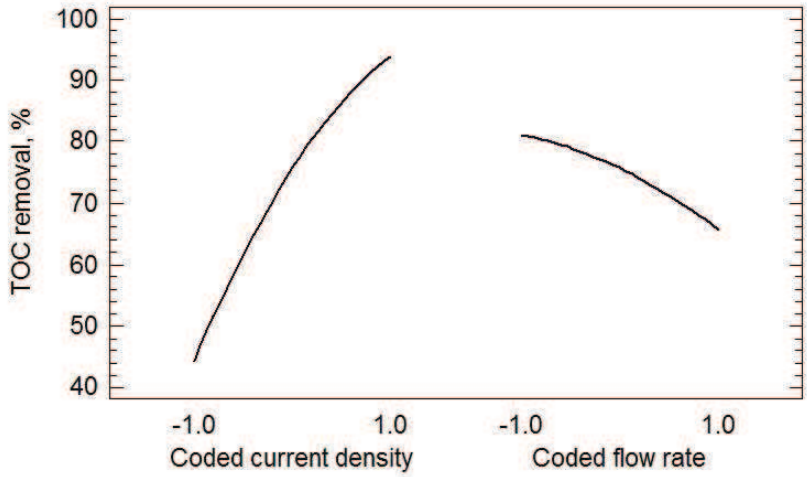

Figure 4.13. Main effects of single variables.

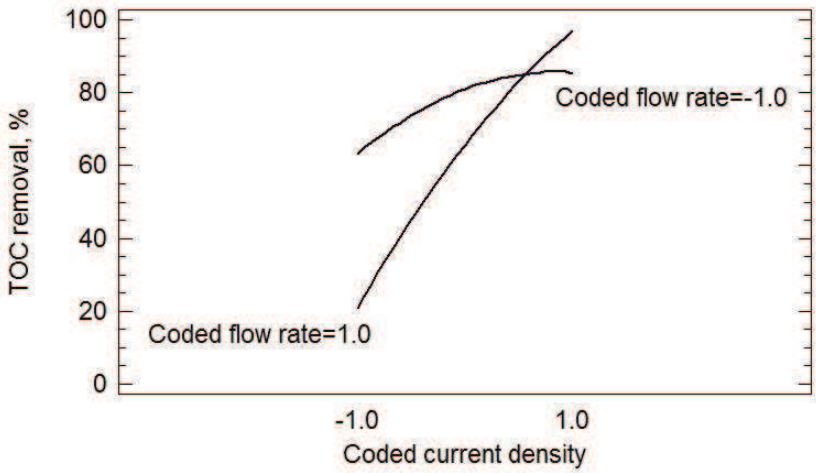

Figure 4.14. Interaction graphic.

4.2.3.7. Response surface and contour plot.

The surface graphic is the most important graphical representation in the RSM. It plots Eq. (4.5) and allows evaluating from a qualitative point of view how the behaviour of the whole studied system is.

As Figure 4.15 depicts, the response is a quite convex surface inside the studied region, and a clear tendency of growing TOC removal is presented as current density increases. On the other hand, flow rate presents its low influence on the final response, if compared to current density.

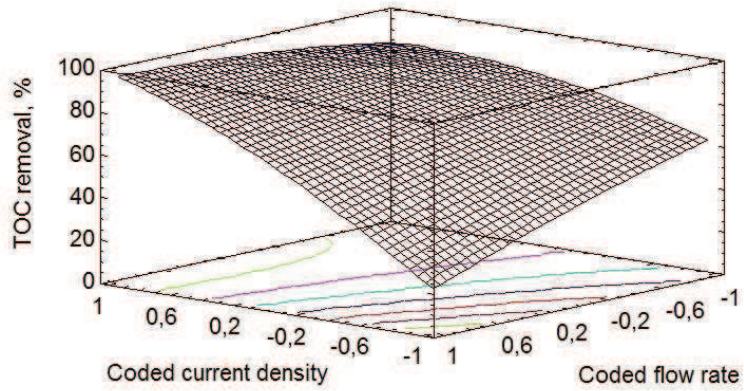

Figure 4.15. Main effects. Response surface.

This behaviour is typical in stable systems. As can be appreciated, the final response is almost dependent on both variables in a non-linear relationship, due to the significance of the interaction term in Eq. (4.5).

4.2.4. CONCLUSIONS.

Pharmaceutical effluents are completely reactive to electrochemical oxidation with BDD electrode. This relative innovative process is fully working depending on the residence time, so the optimization of this variable is needed for minimizing

energetic consumption. In general, the process was capable of achieving satisfactory levels of TOC removal at short treatment times.

Periods longer than 125 minutes make the system be totally ruled by residence time, so the operative parameters such as current density and flow rate are relevant at an optimum residence time of 77 minutes. Amongst these two test parameters, current density was found to have a great positive influence on TOC removal, while the flow was found to have a moderate negative influence on the target variable. With adequate combinations of both variables almost 100% of TOC content can be removed.

4.2.5. SUPPLEMENTARY DATA.

Table S.4.1. ANOVA results.

Factor	Sum of squares	Degrees of freedom	F-ratio	p-values
A: Coded current density	5568.11	1	802.60	0.00
B: Coded recirculation flow rate	5.46	1	0.79	0.39
AA	387.81	1	55.90	0.00
AB	39.06	1	5.63	0.04
BB	0.10	1	0.01	0.91
Total error	69.37	10		

4.2.6. REFERENCES.

[1] Domènech, X.; Ribera, M.; Peral, J. "Assessment of pharmaceuticals fate in a model environment". Water, Air & Soil Pollution. 218, 413 **(2011)**.

[2] Scharf, S.; Gans, O.; Sattelberger, R. "Arzneimittelwirkstoffe inm Zu-und Ablauf von Kläranlagen". Umweltbundesamt Wien. Report UBA-BE-201 **(2002)**.

[3] Carballa, M.; Omil, F., Lema, J.M.; Llompart, M.; Garcia-Jares, C.; Rodriguez, I.; Gomez, M.; Ternes, A. "Behavior of pharmaceuticals, cosmetics and hormones in a sewage treatment plant". Water Research. 38, 2918 **(2004)**.

[4] Ragugnetti, M.; Adams, M.; Guimarães, A.; Sponchiado, G.; Carvalho-Vasconcellos, E.; Rivas-Oliveira, C. "Ibuprofen genotoxicity in aquatic environment: an experimental model using Oreochromis niloticus". Water, Air & Soil Pollution, 218, 361 **(2011)**.

[5] Petrović, M.; Hernando, D.; Díaz-Cruz, S.; Barceló, D. "Liquid chromatography tandem mass spectrometry for the analysis of pharmaceutical residues in environmental samples: a review". Journal of Chromatography A. 1067, 1 **(2005)**.

[6] Zwiener, C; Frimmel, F.H. "Oxidative treatment of pharmaceuticals in water". Water Research. 34, 1881 **(2000)**.

[7] Pérez-Estrada, L.A.; Malato, S.; Gernjak, W.; Agüera, A.; Thurman, E.M.; Ferrer, I.; Fernández-Alba, A.R. "Photo-Fenton degradation of Diclofenac: Identification of main intermediates and degradation pathway". Environmental Science Technology, 39, 8300 **(2005)**.

[8] Sharma, V.K; Mishra, S.K. "Ferrate (VI) oxidation of Ibuprofen: A kinetic study". Environmental Chemical Letters. 3, 182 **(2006)**.

[9] Tarr, M. editor. "Chemical Degradation Methods for Wastes and Pollutants". Environmental and Industrial Applications. Marcel-Dekker, New York **(2003)**.

[10] Bensalah, N.; Quiroz Alfaro, M.A.; Martínez-Huitle, C.A. "Electrochemical treatment of synthetic wastewaters containing Alphazurine A dye". Chemical Engineering Journal. 149, 348 **(2009)**.

[11] Güven, G., Perendeci, A.; Tanyolaç, A. "Chemical treatment of simulated beet sugar factory wastewater". Chemical Engineering Journal. 151, 149 **(2009)**.

[12] Ahmed Basha, C.; Chithra, E.; Sripriyalakshmi, N.K. "Electro-degradation and biological oxidation of non-biodegradable organic contaminants". Chemical Engineering Journal. 149, 25 **(2009)**.

[13] Marselli, B.; García-Gomez, J.; Michaud, P.A.; Rodrigo, M.A.; Comninellis, Ch. "Electrogeneration of hydroxyl radicals on boron-doped diamond electrodes". J. Electrochem. Soc. 150, 79 **(2003)**.

[14] Panizza, M.; Cerisola, G. "Application of diamond electrodes to electrochemical processes". Electrochimica Acta. 51, 191 **(2005)**.

[15] Brillas, E.; Calpe, J.C.; Casado, J. "Mineralization of 2,4-D by advanced electrochemical oxidation processes". Water Research. 34, 2253 **(2000)**.

[16] Martínez-Huitle, C.A.; Ferro, S. "Electrochemical oxidation of organic pollutants for the wastewater treatment: direct and indirect processes". Chemical Society Reviews. 35, 1324 **(2006)**.

[17] Chen, G. "Electrochemical technologies in wastewater treatment". Separation and Purification Technology. 38 (1), 11 **(2004)**.

[18] Chen, X.; Gao, F.; Chen, G. "Comparison of Ti/BDD and Ti/SnO2–Sb2O5 electrodes for pollutant oxidation". Journal of Applied Electrochemistry. 35 (2), 185 **(2005)**.

[19] Rajkumar, D.; Palanivelu, K. "Electrochemical treatment of industrial wastewater". Journal of Hazardous Materials. 113 (1-3), 123 **(2004)**.

[20] Cañizares, P.; Lobato, J.; Paz, R.; Rodrigo, M.A.; Sáez, C. "Electrochemical oxidation of phenolic compound wastes with BDD anodes". Water Res. 39, 2687 **(2005)**.

[21] StatPoint Technologies Inc. StatGraphics Centurion XVI User Manual. Virginia, USA, **(2009)**.

[22] González, T.; Domínguez, J.R.; Palo, P.; Sánchez-Martín, J.; Cuerda-Correa, E. "Development and optimization of the BDD-electrochemical oxidation of the antibiotic trimethoprim in aqueous solution". Desalination. 280, 197 **(2011)**.

[23] Milani, A.S.; Wang, H.; Frey, D.D.; Abeyaratne, R.C. "Evaluating three DOE methodologies: optimization of a composite laminate under fabrication error". Quality Engineering. 21, 96 **(2009)**.

[24] Bhatia, S.; Othman, Z.; Ahmad, A.L. "Pretreatment of palm oil mill effluent (POME) using Moringa oleifera seeds as natural coagulant". Journal of Hazardous Materials. 145, 120 **(2007)**.

[25] Deligiorgis, A.; Xekoukoulotakis, N.P.; Diamadopoulos, E.; Mantzavinos, D. "Electrochemical oxidation of table olive processing wastewater over boron-doped diamond electrodes: Treatment optimization by factorial design". Water Research. 42, 1229 **(2008)**.

[26] Montgomery, D.C. "Design and Analysis of Experiments" (5th ed.). John Wiley and Sons. New York **(2001)**.

[27] Lazic, Z.R. "Design of experiments in chemical engineering". A practical guide. Wiley-VCH. Weinheim **(2004)**.

Capítulo 5:
FENTON OXIDATION PROCESS OF CARBAMAZEPINE

FENTON + FENTON-LIKE INTEGRATED PROCESS FOR CARBAMAZEPINE DEGRADATION: OPTIMIZING THE SYSTEM

A factorial central composite orthogonal and rotatable design was employed to optimize the carbamazepine degradation using an integrated Fenton + Fenton-like oxidation process. The pH and the initial concentrations of hydrogen peroxide and ferrous and ferric ions were considered as the variables for the process optimization. A design of experiments procedure has been carried out in order to optimize the process as well as to study the interactions existing between the four variables under study. The initial concentration of hydrogen peroxide was found to be the most important variable conditioning the removal efficiency, followed by ferrous ion concentration, pH, and, finally, ferric ion concentration. The ANOVA test reported significance for 5 of the 14 involved variables. The response surface methodology technique was used to optimize carbamazepine degradation. Under optimal conditions (hydrogen peroxide concentration= $1.39 \cdot 10^{-4}$ mol·L^{-1}, ferrous ion concentration= $1.25 \cdot 10^{-5}$ mol·L^{-1}, ferric ion concentration= $1.68 \cdot 10^{-5}$ mol·L^{-1}, and pH= 3.52) total carbamazepine degradation was achieved.

Keywords: Fenton's reagent, Fenton-like, advanced oxidation processes, pharmaceuticals, carbamazepine.

5.1. INTRODUCTION.

In recent years, the presence of pharmaceutical compounds (PCs) in the aquatic environment has been of growing interest [1-3]. These "emerging contaminants" are important because many of them are not degraded under the typical biological treatments applied in the wastewater treatment plants (WWTPs). More than 100 PCs have been detected in municipal sewage and surface water samples [4-6]. These PCs

end up in surface waters and eventually in ground and drinking water after their excretion (in unmetabolized form or as active metabolites) from humans or animals via urine or faeces, through the sewage system and into the influent of WWTPs [7]. In this sense, carbamazepine (CBZ) is the most frequently detected PC in water bodies thus far. This drug is used for the treatment of seizure disorders, for relief of neuralgia, and for a wide variety of mental disorders. Approximately 72% of orally administered CBZ is absorbed, while 28% is unchanged and subsequently discharged through the faeces. This drug has been proposed by some authors [8] as an anthropogenic marker in water bodies. Table 5.1 presents the main physicochemical properties of CBZ [9-14]. Usually, CBZ and their metabolites are flushed with wastewater to the WWTPs through the sewage system. Recent research works [9] have reported that CBZ is persistent and its removal efficiencies by the WWTPs are mostly below 10%. According to these authors, CBZ has been detected in WWTP effluents, surface waters, groundwater, and occasionally in drinking water worldwide (Europe, America, and Asia) although its concentrations are significantly different among countries. In the classification scheme for PCs biodegradation, the removal status of CBZ is classified as “no removal” [15].

In this context, advanced oxidation processes (AOPs) represent a good choice for treatment of hazardous nonbiodegradable pollutants. These processes are based on the generation of very reactive species such as hydroxyl radicals (·OH) which degrade a broad range of organic pollutants quickly and nonselectively. Among these AOPs, Fenton and Fenton-like processes are promising technologies, due to their high performance and simplicity of technology, low cost, and low toxicity of the reagents [16,17]. The oxidation with Fenton’s reagent is based on the hydrogen peroxide decomposition in acidic medium, catalyzed by ferrous ion. This process involves several parallel and consecutive reactions:

$$H_2O_2 + Fe^{2+} \rightarrow \cdot OH + OH^- + Fe^{3+} \quad (5.1)$$

$$\cdot OH + RH \rightarrow R\cdot + H_2O \quad (5.2)$$

$$R\cdot + Fe^{3+} \rightarrow R^{+} + Fe^{2+} \quad (5.3)$$

$$Fe^{2+} + \cdot OH \rightarrow Fe^{3+} + OH^{-} \quad (5.4)$$

$$\cdot OH + H_2O_2 \rightarrow HO_2\cdot + H_2O \quad (5.5)$$

On the other hand, ferric ions can react to produce ferrous ions. The reaction of hydrogen peroxide with ferric ions is referred to as a Fenton-like reaction:

$$Fe^{3+} + H_2O_2 \rightarrow FeOOH^{2+} + H^{+} \quad (5.6)$$

$$FeOOH^{2+} \rightarrow HO_2\cdot + Fe^{2+} \quad (5.7)$$

$$H_2O_2 + Fe^{2+} \rightarrow \cdot OH + OH^{-} + Fe^{3+} \quad (5.8)$$

$$\cdot OH + RH \rightarrow R\cdot + H_2O \quad (5.9)$$

These two processes, namely Fenton [17] and Fenton-like [18] have always been studied separately by researchers. The novelty of this work was to integrate both processes, and then optimize the resulting integrated process (Fenton+Fenton-like). To the best of the authors' knowledge, this kind of integrated processes has not been reported to the date. The authors could not found in literature studies on this integrated process. The efficiency of this integrated process depends on several variables, mainly pH and concentrations of hydrogen peroxide, ferrous and ferric ion. In order to achieve high performances, these experimental conditions must be optimized. Most of the published studies are based on the single-factor-at-a-time approach, considering the effect of each variable independently and keeping all other conditions constant. Therefore, possible interactions between variables and their potential effects on the process response are not taken into account. With the purpose of overcoming this disadvantage, the application of experimental design (DOE) becomes essential. This statistical approach allows a multivariate analysis, using a minimum number of experiments [19,20].

Table 5.1. Main physico-chemical properties of carbamazepine and annual consumed volumes of in some countries.

		Reference
Structure	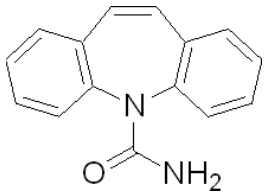	
Formula	$C_{15}H_{12}N_2O$	
CAS number	298-46-4	
Molecular Weight	236.27 $g \cdot mol^{-1}$	
Usage	Analgesic and Antiepileptic	
Water solubility	17.7 $mg \cdot L^{-1}$ (25 ºC)	[9]
LogP (octanol–water)	2.45	[9]
Henry's Law Constant	1.09×10^{-5} Pa $m^3 \cdot mol^{-1}$ (25 ºC)	[9]
pK_a	Neutral	[10]
Elimination half-life	25-65 h	[11]
Excretion	72% of oral dosage excreted in urine and 28% in faeces	[12]
Dosage	Usually 800–1200 mg daily.	[13]

5.2. MATERIALS AND METHODS.

5.2.1. Chemicals.

CBZ was provided by Sigma-Aldrich (Spain) of the highest purity available. Initial CBZ solution ($2.11 \cdot 10^{-5}$ mol·L^{-1}) was prepared with high purity water obtained from a Millipore Milli-Q system. Since the phosphate ions act as a scavenger toward the hydroxyl radicals, it was not possible to use a conventional phosphate buffer. Hence, pH was adjusted using a perchloric acid/perchlorate buffer solution. Hydrogen peroxide (33% w/v), iron (III) sulphate, and iron (II) sulphate heptahydrate were obtained from Merck, all of them of analytical grade.

5.2.2. Experimental procedure.

All experiments were performed in a batch thermostatic reactor with 250 mL of capacity. Uniform mixing was provided using a magnetic stirrer and a thermostatic bath was used in order to keep the temperature constant (25±0.5 ºC for all experiments). For each of the experiments, the reactor was filled with 150 mL of CBZ aqueous solution ($2.11 \cdot 10^{-5}$ mol·L^{-1}). Then the pH was adjusted using the perchloric acid/perchlorate buffer solution and the required amount of iron (II) and/or iron (III) sulphate was added to the reactor. Finally, the reaction began with the addition of a certain quantity of H_2O_2.

A series of preliminary kinetic experiments, not shown for the sake of brevity, was performed in order to determine the equilibration time. The oxidation reaction was quenched with sodium bisulphite at preset time intervals. These experiments demonstrated that equilibration was reached within the first 24-36 h. Hence, an experimental time equal to 48 h was used along the experimental work.

5.2.3. Analytical method.

CBZ concentration present in each sample was determined at 48 h of reaction by HPLC in a Waters chromatograph equipped with a 996 photodiode array detector and a Waters Nova-Pak C18 column (5 μm, 150×3.9 mm^2). A well-defined peak for CBZ at a retention time (t_r) of 5.21 min at 286 nm was obtained. Samples of 50 μL

were injected into the chromatograph and a 60:40 (v/v) methanol/water (10^{-2} M orthophosphoric acid) mixture was used as the mobile phase under a flow rate of 1 $mL \cdot min^{-1}$.

5.2.4. Design of Experiments (DOE).

DOE is a useful tool to verify the effects of different variables and of their interactions on the process response within a certain range and with a minimum number of experiences. The application of RSM allowed then establishment of a mathematical relationship between dependent and independent variables and the process optimization. Therefore, experimental data were fitted to a polynomial equation as follows [21,22].

$$Y = b_o + \sum_{j=1} b_j x_j + \sum_{i,j=1} b_{ij} x_i x_j + \sum_{j=1} b_{jj} x_j^2 \qquad (5.10)$$

where Y is the predicted response, b_0 is the offset term, b_j is the linear effect, b_{ij} is the first-order interaction effect, b_{jj} is the squared effect, and k is the number of independent variables. For this work, one of the most popular classes of second-order design, namely CCORD, was selected. It involves the use of a two-level factorial design with 2^k points combined with $2k$ axial points and n center runs, k being the number of factors. The total number of experiments given a k factor, N, is obtained according to:

$$N = 2^k + 2 \cdot k + n \qquad (5.11)$$

where n is considered to be 12 and the axial distance is 2 in order to guarantee an orthogonal and rotatable design. To convert the natural variables into dimensionless codified values it is necessary to use the following equation:

$$x_i = \frac{X_i - X_i^X}{\Delta X_i} \qquad (5.12)$$

where x_i is the coded value of the ith independent variable, X_i the natural value of the ith independent variable, X_i^X the natural value of the ith independent variable at the

center point, and ΔX_i is the value of step change. Table 5.2 shows the operating levels of the DOE. On the other hand, Table 5.3 shows the experimental planning in DOE and obtained response in each experiment (removal of CBZ in percentage, X_{CBZ}, %).

To perform this study, a factorial central composite orthogonal and rotatable design (CCORD) was used with 12 replicates of central point, so that the total number of experiments was 36. Values of the independent variables and their variation limits were determined based on preliminary runs and literature. The experimental results were statistically analyzed by using Stat-Graphics Centurion XV software, and the statistical validation was achieved by ANOVA test at 95% confidence. The obtained drug removal at 48 h was considered as the response. The effect of initial concentrations of H_2O_2, Fe^{2+}, Fe^{3+}, and pH were assessed applying response surface methodology (RSM).

The 12 replications of the center (0,0,0,0) point were performed in the order shown in Table 5.3 in order to ensure randomization. Randomization is strongly recommended to prevent external lurking variables (such as changes in the process overtime) to bias the results.

Table 5.2. Operating levels of the DOE.

pH			$[H_2O_2]$ x 10^5 (mol·L^{-1})			$[Fe^{2+}]$ x 10^5 (mol·L^{-1})			$[Fe^{3+}]$ x 10^5 (mol·L^{-1})		
Lower level (-2)	**Upper level (+2)**	**Center Point (0)**	**Lower level (-2)**	**Upper level (+2)**	**Center Point (0)**	**Lower Level (-2)**	**Upper level (+2)**	**Center Point (0)**	**Lower level (-2)**	**Upper level (+2)**	**Center Point (0)**
2.5	4.5	3.5	0	16.8	8.4	0	1.68	0.84	0	1.68	0.84

Table 5.3. Operating levels of the DOE.

Run	Coded pH	Coded [H_2O_2]	Coded [Fe^{2+}]	Coded [Fe^{3+}]	X_{CBZ} (%)
1	1	1	-1	-1	71.7
2	1	-1	-1	1	59.3
3	-1	-1	-1	-1	42.3
4	1	-1	1	-1	56.5
5	-1	1	-1	1	80.2
6	0	0	0	-2	79.7
7	0	-2	0	0	0.0
8	1	-1	1	1	67.1
9	0	0	-2	0	46.1
10	-1	-1	1	1	66.4
11	-1	1	1	-1	86.8
12	0	0	0	0	82.4
13	1	1	1	-1	96.6
14	0	0	0	0	86.2
15	-1	1	-1	-1	67.5
16	0	0	0	0	87.2
17	0	0	0	0	85.6
18	0	0	0	2	90.3
19	2	0	0	0	63.8
20	0	0	0	0	89.2
21	1	-1	-1	-1	64.1
22	1	1	-1	1	92.8
23	0	0	0	0	91.3
24	-1	-1	-1	1	51.1
25	0	0	0	0	85.6
26	0	0	0	0	88.9
27	-1	-1	1	-1	71.2
28	0	2	0	0	99.3
29	0	0	2	0	92.3
30	0	0	0	0	86.4
31	-1	1	1	1	95.5
32	0	0	0	0	91.2
33	0	0	0	0	93.6
34	0	0	0	0	90.9
35	-2	0	0	0	63.4
36	1	1	1	1	98.5

5.3. RESULTS AND DISCUSSION.

5.3.1. Preliminary runs.

In Fenton and Fenton-like processes the production of ·OH radicals depends on several factors such as pH or initial concentrations of H_2O_2, Fe^{2+}, and Fe^{3+}. Some preliminary runs were performed to achieve a suitable initial H_2O_2 concentration and pH range. The literature review also constituted a starting point to set ranges for Fe^{2+} and Fe^{3+} initial concentrations [21,23-32].

Effect of the initial H_2O_2 concentration.

According to the experimental results, the initial H_2O_2 concentration appears to be the most important variable governing CBZ removal. The results shown in Figure 5.1 demonstrated that within the range comprised between 0 and $1.7 \cdot 10^{-4}$ $mol \cdot L^{-1}$, the degradation of CBZ was significantly improved. All experiments were conducted with the presence of Fe^{2+} and the iron concentration was in all cases 10 times lower than that of H_2O_2. In the same figure it is possible to observe that for higher H_2O_2 concentrations ($>1.7 \cdot 10^{-4}$ $mol \cdot L^{-1}$), the performance of the oxidation reaction remains nearly unchanged. This fact can be explained by taking into account the inhibitory effect of H_2O_2. An increase in H_2O_2 concentration may promote radicals scavenging (see Eq. (5.5)) and the subsequent formation of a new radical ($HO_2\cdot$), with an oxidation potential considerably smaller than that of ·OH.

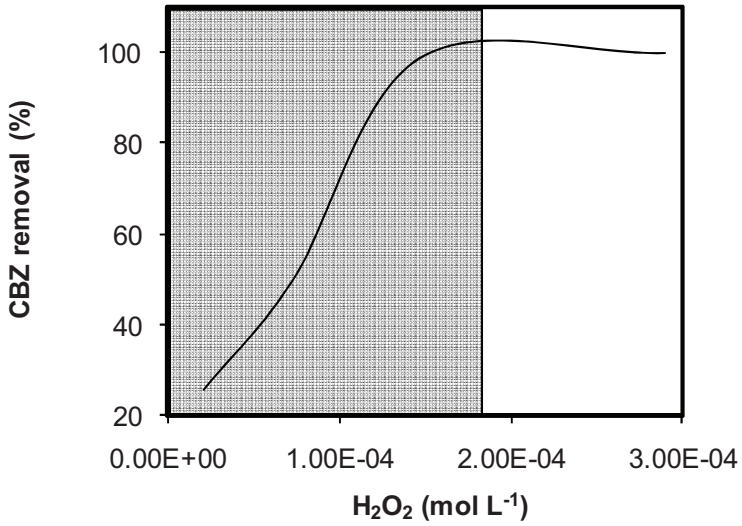

Figure 5.1. Influence of hydrogen peroxide initial concentration on CBZ removal. $[H_2O_2]_0/[Fe^{2+}]_0$=10:1, pH= 3.5, T= 25 ºC.

Effect of the pH

Equations [5.1], [5.4], [5.6], and [5.9] clearly point out that pH value affects the generation and destruction of hydroxyl radicals. In this work, different pH values comprised within the range 2.5-4.5 were tested. Figure 5.2 shows that the maximum degradation rate was reached for pH values of 3.5-4. Oliveira et al. [29] have demonstrated that for pH values below 3 the Fenton's reaction is severely affected, causing the reduction of hydroxyl radicals in solution. Besides, due to the formation of oxonium ions, hydrogen peroxide is chemically more stable at low pH values, thus decreasing its reactivity toward ferrous ion. Furthermore, at pH 1-2 an inhibition in the formation of hydroxyl radicals occurs, due to H^+ ions scavenging [24]. With regard to the Fenton-like reactions, some authors also suggest that at low pH the amount of soluble Fe^{3+} decreases, thus inhibiting the formation of ·OH radicals. Nevertheless, for pH values above 4.5 precipitation of iron hydroxides takes place, hence inhibiting both the regeneration of the active species Fe^{2+} and the formation of hydroxyl radicals [25].

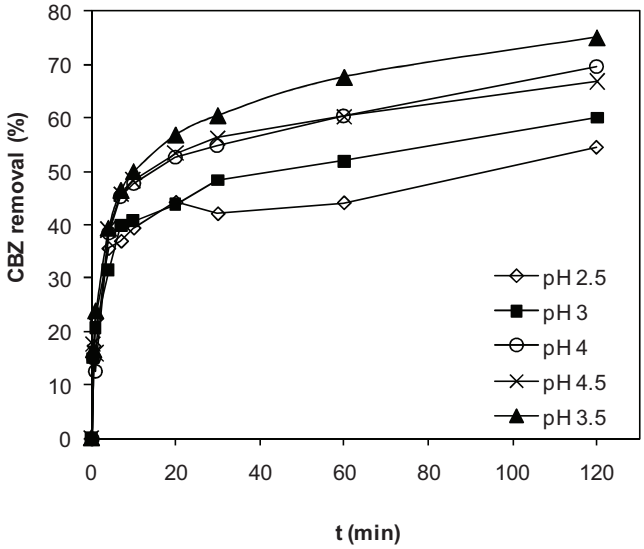

Figure 5.2. Influence of pH on the oxidation process. $[H_2O_2]_0/[Fe^{2+}]_0/[Fe^{3+}]_0$= 10:1:1, T=25ºC.

Effect of the Iron Concentration.

In this research work on the Fenton + Fenton-like integrated process, ferrous and ferric ion concentrations have also been considered as independent variables in the DOE. The Fe^{2+} ion acts in the decomposition of hydrogen peroxide as a catalytic agent (see Eq. (5.1)) and the Fe^{3+} ion is the responsible element for the regeneration of Fe^{2+} (see Eq. (5.7) and Eq. (5.8)).

On the other hand, several researchers have investigated the optimal $[H_2O_2]_0$:$[Fe^{n+}]_0$ molar ratio for Fenton and Fenton-like processes. Tang and Huang [24] deduce a theoretical expression to calculate this optimal molar ratio. Taking into consideration the values of the rate constants reported by Walling [18] and Dorfman and Adams [32], respectively, the authors deduced an optimal molar ratio of 10.5:1. In another work, Elmolla and Chaudhuri [23] optimized the Fenton process for treatment of amoxicillin, ampicillin, and cloxacillin antibiotics using a molar ratio equal to 10:1. On the other hand, Beltran de Heredia et al. evaluated Fenton oxidation for the removal of organic matter from cork processing wastewater [25-27] and table olive washing wastewater [28]. In both studies the elimination of organic matter was maximized using a molar ratio of $[H_2O_2]_0/[Fe^{2+}]_0$ equal to 10:1. Consequently, the

central point of the DOE (coded value: 0,0,0,0) was selected using this optimal ratio. Hence, the central points of the DOE correspond to $[H_2O_2]_0$= 8.4×10^{-5} mol·L^{-1}, $[Fe^{2+}]_0$= 8.4×10^{-6} mol·L^{-1}, $[Fe^{3+}]_0$= 8.4 ×10^{-6} mol·L^{-1}, and pH= 3.5.

5.3.2. Analysis of the experimental results.

Numerical analysis.

The ANOVA analysis provides the significance of the different parameters. The values of the ANOVA test results are summarized in Table 5.4. According to the RSM, 14 factors are considered. It is worth noting that five of them exhibit a p-value below 0.05 (significance limit), which indicate that such factors are statistically significant at 95% of confidence.

Table 5.4. ANOVA results**.**

Factor	Sum of squares	Degrees of freedom	F-ratio	p-values
A: Coded pH	89.70	1	1.29	0.27
B: Coded $[H_2O_2]_0$	7011	1	100	0.00
C: Coded $[Fe^{2+}]_0$	1700	1	24.4	0.00
D: Coded $[Fe^{3+}]_0$	236.9	1	3.40	0.08
AA	843.2	1	12.1	0.00
AB	11.60	1	0.17	0.69
AC	144.0	1	2.07	0.16
AD	0.705	1	0.01	0.92
BB	2378	1	34.1	0.00
BC	27.01	1	0.39	0.54
BD	74.80	1	1.07	0.31
CC	446.0	1	6.40	0.02
CD	28.60	1	0.41	0.53
DD	1.501	1	0.02	0.88
Total error	1462	21		

A nonlinear polynomial regression was carried out taking into account Eq. (5.10), and the following expression was obtained accordingly:

$$X_{CBZ}(\%) = 88.21 + 17.09 \cdot H_2O_2 + 8.42 \cdot Fe^{2+} + 3.15 \cdot Fe^{3+} + 1.93 \cdot pH - 5.13 \cdot pH^2 + \\ +0.85 \cdot pH \cdot H_2O_2 - 3.00 \cdot pH \cdot Fe^{2+} + 0.21 \cdot pH \cdot Fe^{3+} - 8.62 \cdot H_2O_2{}^2 + \\ 1.30 \cdot H_2O_2 \cdot Fe^{2+} + 2.16 \cdot H_2O_2 \cdot Fe^{3+} - 3.73 \cdot Fe^{2+2} - 1.34 \cdot Fe^{2+} \cdot Fe^{3+} \\ +0.22 \cdot Fe^{3+2} \tag{5.13}$$

This equation reveals that the concentrations of hydrogen peroxide, Fe^{2+} ions, and Fe^{3+} ions as well as the pH are preceded by a positive (+) sign and, hence, all of them exert a positive effect on the removal of CBZ. In other words, an increase in these parameters results in a more effective removal of the pollutant. The same applies to the combinations of (i) pH and hydrogen peroxide concentration; (ii) pH and Fe^{3+} ion concentration; (iii) hydrogen peroxide and Fe^{2+} ion concentrations; (iv) hydrogen peroxide and Fe^{3+} ion concentrations; and (v) the squared Fe^{3+} ion concentration.

On the contrary, the remaining factors exhibit a negative (-) sign in Eq. (5.12), which is indicative of a negative influence of these factors on the removal of the target molecule. Thus, an increase in each of these factors tends to hinder CBZ removal from solution. According to Eq. (5.12), the factors negatively influencing carbamazepine removal are (i) the squared pH; (ii) the combination of pH and Fe^{2+} ion concentration; (iii) the squared hydrogen peroxide concentration; (iv) the squared Fe^{2+} ion concentration; and (v) the combination of Fe^{2+} and Fe^{3+} ions concentration.

The obtained correlation factor r^2 was equal to 0.90. This regression leads to an optimum X_{CBZ} (100%) at pH equal to 3.52, using a hydrogen peroxide concentration equal to $1.39 \cdot 10^{-4}$ mol·L^{-1}, a ferrous ion concentration of $1.25 \cdot 10^{-5}$ mol·L^{-1} and a ferric ion concentration equal to $1.68 \cdot 10^{-5}$ mol·L^{-1}.

The ANOVA test also provides the value of the Durbin-Watson statistic, which has a value equal to 2.03, with a p-value of 0.465. As this p-value is higher than 0.05, there is no evidence of correlation in the residuals series. This means that the random order of experiments has been effective in order to avoid any systematic error. Moreover, for each experiment, Figure 5.3 represents the observed X_{CBZ} versus the calculated X_{CBZ} (according to Eq. (5.12)). A good correlation between both parameters

may be observed. This implies that the randomization of the design has been properly planned and performed, so that accumulation of experimental error may be discarded.

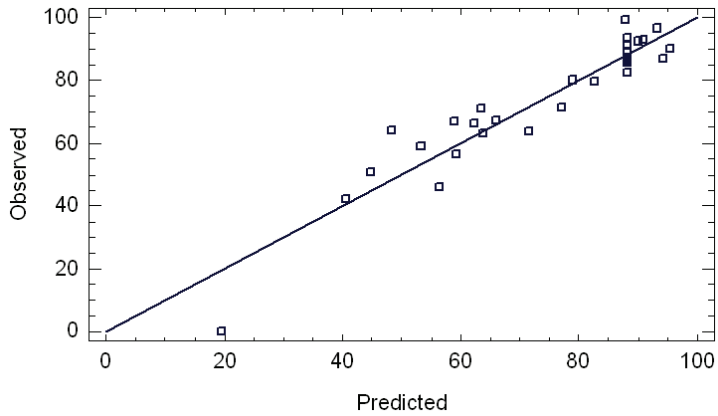

Figure 5.3. Observed X_{CBZ} versus calculated X_{CBZ} according to Eq. (5.12).

Graphical analysis.

Modelization was made on the basis of 14 factors which correspond to Eq. (5.11). The so-called Pareto plot (see Figure 5.4) is a graphical expression of the ANOVA test results. Bars represent the standardized effects of each involved factor, considering them as the initial concentrations of H_2O_2, Fe^{2+}, Fe^{3+}, and pH, and combinations of all of them. Filled bars are a graphical representation of positively affecting factors. Hence, the Pareto plot confirms that, as revealed by Eq. (5.12), factors such as H_2O_2 concentration, Fe^{2+} concentration, Fe^{3+} concentration, pH, the combination of H_2O_2-Fe^{3+}, H_2O_2-Fe^{2+}, pH-H_2O_2, pH-Fe^{3+}, and the squared of Fe^{3+} exert a positive influence on the CBZ removal. On the other hand, nonfilled bars represent negatively affecting factors, such as the squared of H_2O_2, pH, and Fe^{2+}, and the combinations of pH-Fe^{2+}, and Fe^{2+}-Fe^{3+}. All of them exert a negative influence on the CBZ removal as previously suggested by Eq. (5.12). The vertical rule stands close to 2 and is related with the signification level of ANOVA test, which is equal to 95% of confidence. Factors above this rule (e.g., B, C, AA, BB, and CC) are within the significant region, while the remaining ones do not have a significant influence in the final response. The Pareto plot also provides an idea on how factors influence the final

response, X_{CBZ}. Positive bars indicate that by varying a given variable the value of X_{CBZ} increases. Negative bars indicate the contrary.

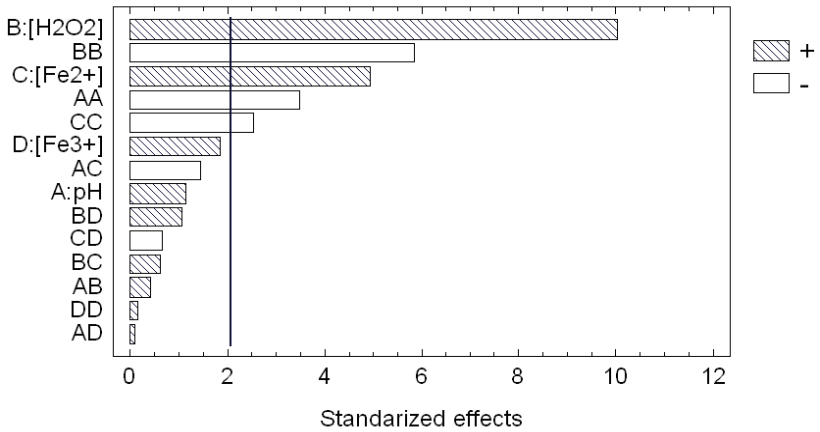

Figure 5.4. Pareto plot: standardized effects.

The evaluation of the CCORD model leads also to the study of the main effects of the involved variables. This can be observed in Figure 5.5. Four curves are drawn representing the effect of varying each variable (from -2 up to +2) while the other ones are kept constant and equal to the central value (0). A maximum is shown in the final part of the curve in the case of H_2O_2 and Fe^{2+} initial concentrations, as well as in the middle part of the plot for pH. On the contrary, Fe^{3+} concentration shows a positive influence along the whole operation interval but no optimum point may be observed. This will be clearly appreciated in the response surface and contour plot figures.

Figure 5.5 also illustrates that initial H_2O_2 concentration is the main factor governing the CBZ removal, followed by Fe^{2+} initial concentration. It is worth noting that both factors constitute the conventional Fenton's reagent. Finally, pH and initial Fe^{3+} concentration, which constitute the Fenton-like process, influence X_{CBZ} in a more limited manner.

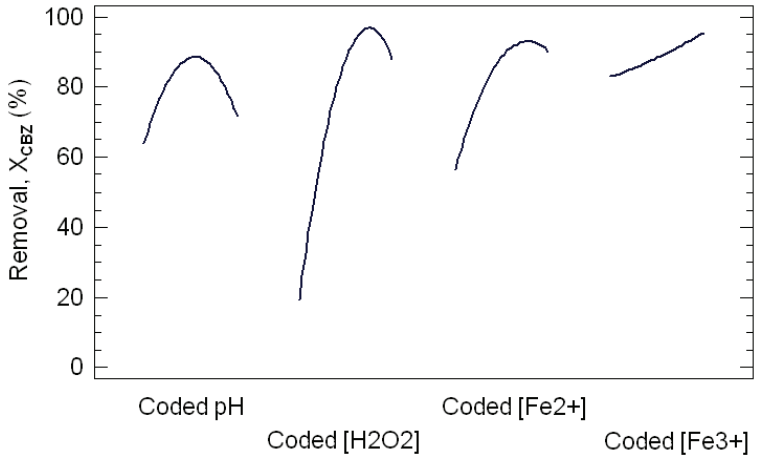

Figure 5.5. Main effects of pH, H_2O_2, Fe^{2+} and Fe^{3+}.

With regard to the interaction between variables, Figure 5.6 shows the interaction between each two of the four variables studied. Each pair of curves represents the evolution of X_{CBZ} by varying one variable in the extremes of the CCORD model, that is, with its pair variable equal to +2 (upper plot) and equal to -2 (lower plot). The fact that the curves do not present a parallel behaviour involves that interaction occurs and the modification of one of the variables affects the other one. Accordingly, from Figure 5.6 it may be concluded that interaction appears between the pairs of variables AC, BC, BD (more clearly), and CD. On the contrary, the curves corresponding to the pairs of variables AB and AD in Figure 5.6 exhibit a parallel behaviour. Thus, it may be assumed that no interaction takes place in these cases and the modification of one of the variables does not affect the other one.

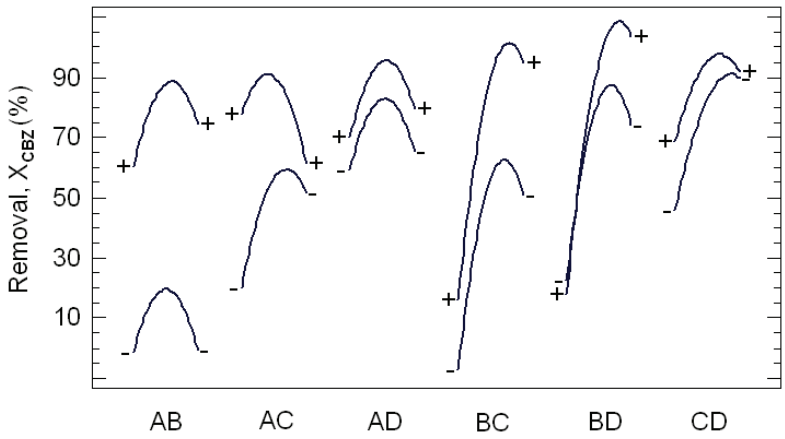

Figure 5.6. Interaction plot for pH, H_2O_2, Fe^{2+} and Fe^{3+}.

Response surfaces and contour plots.

The surface plot is the most important graphical representation in the RSM (see Figure 5.7 a-c). It represents Eq. (5.13) and allows evaluating the behaviour of the whole system under study from a qualitative point of view. As it can be appreciated, within this region the studied response is represented by a convex surface. Three of the four variables (namely, $[H_2O_2]_0$, $[Fe^{2+}]_0$, and pH) suppose a similar affection on the target variable X_{CBZ} and an optimum, represented by a maximum in the surface plot, is obtained. The contour plots, which are depicted in Figure 4.8 a-c, are also very useful to identify the optimal operation conditions. The maximum appears in the positive side of coded H_2O_2 and Fe^{2+} concentrations, as well as in the middle zone of coded pH, very close to zero. Quantitatively, a statistical analysis of the model yields optimal coded values of +0.05 for pH, +1.32 for H_2O_2 initial concentration, +0.98 for Fe^{2+} concentration, and +2.00 for Fe^{3+}. Such values, once decoded, are equivalent to pH= 3.52, $[H_2O_2]_0$= $1.39\cdot10^{-4}$ mol·L^{-1}, $[Fe^{2+}]_0$= $1.25\cdot10^{-5}$ mol·L^{-1}, and a $[Fe^{3+}]_0$= $1.68\cdot10^{-5}$ mol·L^{-1}. As can be seen, three factors are inside the region of the model. Furthermore, since their p-values are in all cases below 0.05, they are statistically significant. Consequently, this optimum set of values may be considered as statistically different from other near points. Moreover, the DOE and RSM analyses predict that, at least

theoretically, using the optimum set of values a maximum removal efficiency of CBZ equal to 100% should be obtained.

a)

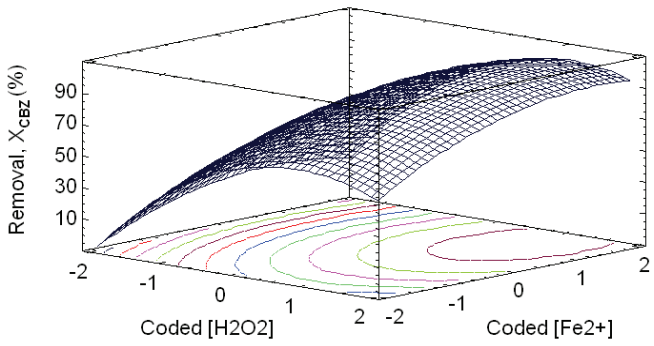

b)

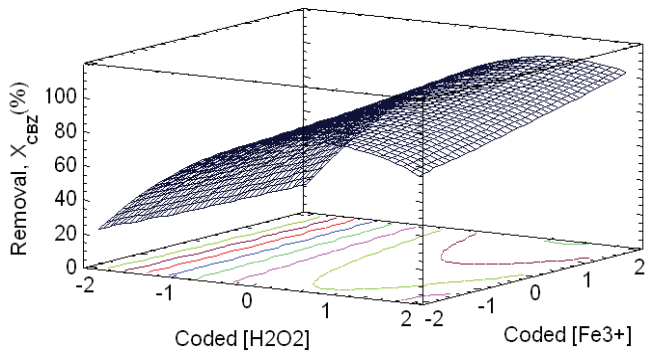

c)

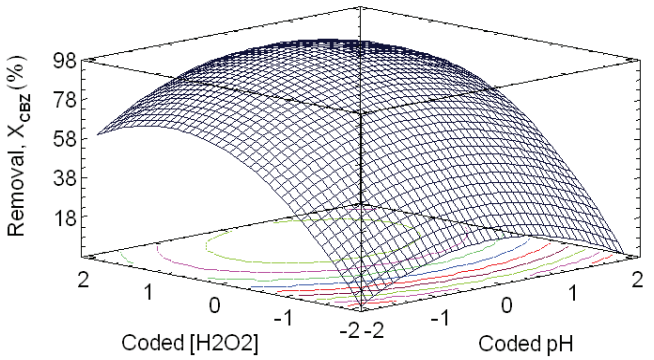

Figure 5.7. Response surfaces: a) coded H_2O_2-Fe^{2+}; b) coded H_2O_2-Fe^{3+}; c) coded H_2O_2-pH.

a)

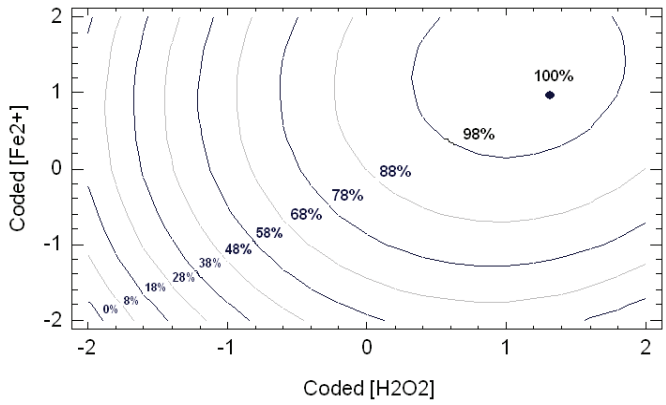

b)

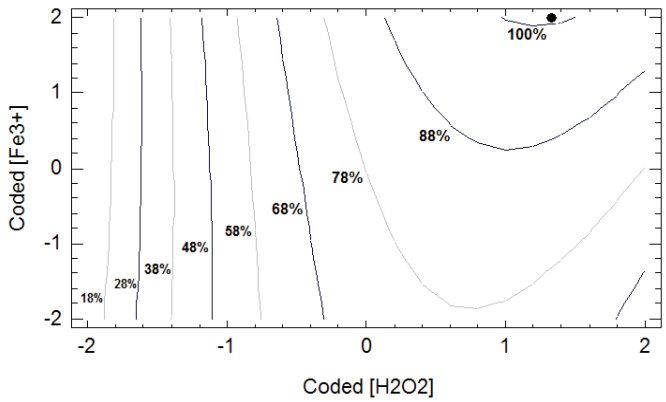

c)

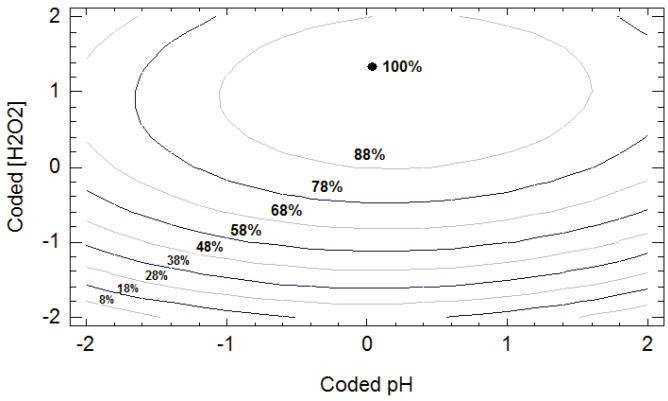

Figure 5.8. Contour plots: a) coded H_2O_2-Fe^{2+}; b) coded H_2O_2-Fe^{3+}; c) coded H_2O_2-pH.

5.3.3. Interpretation of results.

Influence of variables.

As indicated before, H_2O_2 initial concentration appears to be the most influential of the studied variables. This may be explained taking into consideration Eq. (5.1) and Eq. (5.6). The hydroxyl radical generation is due to the hydrogen peroxide decomposition. This decomposition may be catalyzed by Fe^{2+} (Fenton process) or Fe^{3+} (Fenton-like process). However, the hydrogen peroxide concentration exhibits an optimum in the final part of the curve, that is, at a coded value equal to +1.32, which is equivalent to $[H_2O_2]_0$= $1.39 \cdot 10^{-4}$ $mol \cdot L^{-1}$. This optimum can be explained taking into account that an increase of the H_2O_2 concentration may promote radicals scavenging (see Eq. (5.5)) and the formation of another radical ($HO_2\cdot$), which has an oxidation potential considerably smaller than ·OH [21].

The second variable in importance was found to be ferrous ion concentration (i.e., an essential constituent of the Fenton's reagent). The statistical analysis of the model yielded to an optimum at a coded value equal to +0.98, which corresponds to $[Fe^{2+}]_0$= $1.25 \cdot 10^{-5}$ $mol \cdot L^{-1}$. As can be deduced, under these conditions the molar ratio is $[H_2O_2]_0/[Fe^{2+}]_0$= 11.1:1. This result can be compared with the values of 10.5:1 (theoretically deduced by Tang and Huang [23]), and 10:1 (experimentally obtained by Elmolla and Chaudhuri [23]; and Beltran de Heredia et al. [25-28]). This optimal value can be justified taking into account the "scavenging" effect of iron (see Eq. (5.4)).

With respect to the influence of pH, several researchers have proposed an optimal pH between 2.5 and 4 for Fenton and Fenton-like processes [17,20,21,23]. Values of pH above 4.5 can invalidate the oxidation system due to the ferric hydroxide precipitation. Also, as it may be easily inferred from Eqs. (5.1), (5.4), (5.6) and (5.8) pH plays an important role in this kind of reactions. In this case, the deduced optimum value for this integrated process (Fenton + Fenton-like) was equal to 3.52.

With regard to the influence of the ferric ion concentration (part of the Fenton-like process), the influence of this parameter was positive within the whole experimental

range (from -2 up to +2). This can be justified taking into account two factors. First, the important rule of this ion in the formation of hydroperoxide radicals ($HO_2\cdot$) as revealed by Eqs. (5.6) and (5.7). And second, the importance of this ion for the regeneration of Fe^{2+} as indicated by Eqs. (5.3) and (5.6).

Importance of Fenton and Fenton-like Reaction Pathways.

Figure 5.9 shows the influence of iron concentration (coded Fe^{2+} or Fe^{3+} concentration) depending on the considered system, Fenton or Fenton-like, on the drug removal. To calculate the influence of Fenton or Fenton-like processes, the factors of Eq. (5.12) including Fe^{2+} and Fe^{3+} initial concentrations were considered separately. Hence, the former were applied to evaluate the Fenton process whereas the latter were used to estimate the Fenton-like contribution. In both cases, optimal values for pH and hydrogen peroxide concentration were used.

Figure 5.9 clearly shows that the Fenton process is the main oxidation process within the whole experimental range. However, this reaction pathway leads to a maximum for a coded value of +1.32. On the other hand, the Fenton-like reaction represents a limited reaction pathway at low ferric concentrations, its influence increasing steadily until it comes to represent over 50% of the Fenton pathway. More details on the reaction pathways involved in this kind of processes have been reported previously by our research group [33-35].

5.3.4. Experimental confirmation of the model predictions.

An experiment was carried out under optimal conditions (i.e., pH= 3.52, $[H_2O_2]_0$= $1.39\cdot10^{-4}$ mol·L^{-1}, $[Fe^{2+}]_0$= $1.25\cdot10^{-5}$ mol·L^{-1} and a $[Fe^{3+}]_0$= $1.68\cdot10^{-5}$ mol·L^{-1}), in order to determine the removal of carbamazepine. As expected, under these experimental conditions the removal of CBZ reached the predicted value of 100%. This experimental result corroborates the appropriateness of the DOE and RSM strategies performed in the present study.

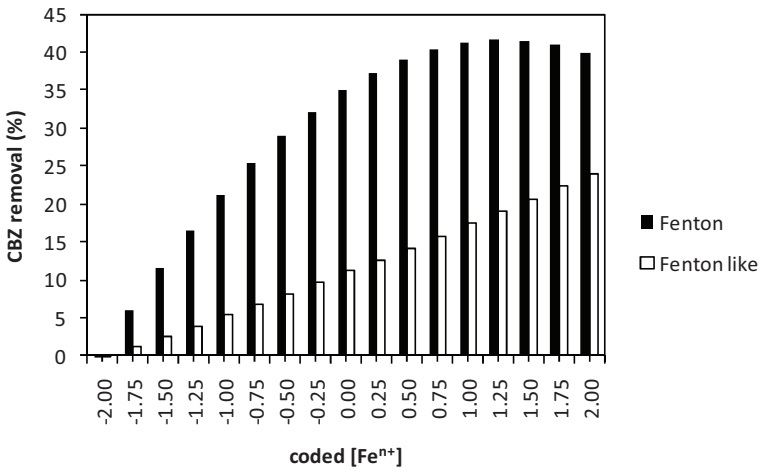

Figure 5.9. Carbamazepine removal by Fenton and Fenton-like process.

5.4. CONCLUSIONS.

Fenton + Fenton-like oxidation of carbamazepine in aqueous solution was carried out. The variables considered for the process optimization were pH and hydrogen peroxide, Fe^{2+} and Fe^{3+} initial concentrations. An orthogonal, rotatable, factorial and central composite design of experiments was carried out in order to optimize the process. The main findings of this investigation were as follows:

(i) The initial concentration of hydrogen peroxide is the most influential of the studied variables, followed by ferrous ion concentration, pH, and, finally, ferric ion concentration.

(ii) The ANOVA test reported significance for 5 of the 14 involved factors. A nonlinear polynomic regression was proposed to calculate the final drug removal. The obtained correlation factor r^2 was equal to 0.90.

(iii) Response surface methodology technique was used to optimize carbamazepine degradation. Under optimal conditions (hydrogen peroxide concentration= $1.39 \cdot 10^{-4}$ mol·L^{-1}, ferrous ion concentration= $1.25 \cdot 10^{-5}$ mol·L^{-1}, ferric ion concentration= $1.68 \cdot 10^{-5}$ mol·L^{-1}, and pH= 3.52) it was possible to achieve total carbamazepine degradation.

(iv) In this integrated process, Fenton's reaction is the main oxidation pathway within the whole range of iron concentrations. However, this reaction pathway reaches a maximum for a molar ratio $[H_2O_2]_0/[Fe^{2+}]_0$= 11.1:1. On the other hand, the Fenton-like reaction represents a limited reaction pathway at low ferric concentrations. Nevertheless, this reaction pathway increases steadily in importance with ferric concentration until reaching over 50% of the Fenton reaction pathway.

5.5. REFERENCES.

[1] Kolpin, D.; Furlong, E.; Meyer, M.; Thurman, E.; Zaugg, S.; Barber, L.; Buxton, H. "Pharmaceuticals, hormones, and other organic wastewater contaminants in US streams 1999-2000: A national reconnaissance". Environ. Sci. Technol. 36, 1202 **(2002)**.

[2] Boxall, A.; Kolpin, D.; Halling-Sørensen, B.; Tolls, J. "Are veterinary medicines causing environmental risks?". Environ. Sci. Technol. 37, 286 **(2003)**.

[3] Snyder, S.; Westerhoff, P.; Yoon, Y.; Sedlak, D. "Pharmaceuticals, personal care products, and endocrine disruptors in water: Implication for the water industry". Environ. Eng. Sci. 20, 449 **(2003)**.

[4] Ellis, J. "Pharmaceutical and personal care products (PPCPs) in urban receiving waters". Environ. Pollut. 144, 188 **(2006)**.

[5] Yu, J.; Bouwer, E.; Coelhan, M. "Occurrence and biodegradability studies of selected pharmaceuticals and personal care products in sewage effluent". Agric. Water Manage. 86, 72 **(2006)**.

[6] Al-Rifai, J.; Gabelish, C.; Scheafer, A. "Occurrence of pharmaceutically active and non-steroidal estrogenic compounds in three different wastewater recycling schemes in Australia". Chemosphere. 69, 803 **(2007)**.

[7] Darlymple, O.; Yeh, D.; Trotz, M. "Removing pharmaceuticals and endocrine-disrupting compounds from wastewater by photocatalysis". J. Chem. Tech. Biotechnol. 82, 121 **(2007)**.

[8] Clara, M.; Strenn, B.; Kreuzinger, N. "Carbamazepine as a possible anthropogenic marker in the aquatic environment: Investigations on the behaviour of carbamazepine in wastewater treatment and during groundwater infiltration". Water Res. 38, 947 **(2004)**.

[9] Zhang, Y.; Geissen, S.; Gal, C. "Carbamazepine and diclofenac: Removal in wastewater treatment plants and occurrence in water bodies". Chemosphere. 73, 1151 **(2008)**.

[10] PhysProp Database. http://www.syrres.com/esc/physdemo.htm.

[11] Remington: The Science and Practice of Pharmacy; Lippincott Williams & Wilkins: Philadelphia **(2005)**.

[12] Wishart, D.; Knox, C.; Guo, A.; Shrivastava, S.; Hassanali, M.; Stothard, P.; Chang, Z.; Woolsey, J. "DrugBank: A comprehensive resource for in silico drug discovery and exploration". Nucleic Acids Res. 34, 668 **(2006)**.

[13] The Internet Drug Index. http://www.rxlist.com.

[14] Sosiak, A.; Hebben, T. "A Preliminary Survey of Pharmaceuticals and Endocrine Disrupting Compounds in Treated Municipal Wastewaters and Receiving Rivers of Alberta". Alberta Environ: Edmonton, Canada **(2005)**.

[15] Joss, A.; Zabaczynski, S.; G€obel, A.; Hoffmann, B.; Leoffler, D.; McArdell, C.; Ternes, T.; Thomsen, A.; Siegrist, H. "Biological degradation of pharmaceuticals in municipal wastewater treatment: Proposing a classification scheme". Water Res. 40, 1686 **(2006)**.

[16] Lee, H.; Shoda, M. "Removal of COD and color from livestock wastewater by Fenton method". J. Hazard. Mater. 153, 1314 **(2008)**.

[17] Wang, S. "A comparative study of Fenton and Fenton-like reaction kinetics in decolourisation of wastewater". Dyes Pigm. 76, 714 **(2008)**.

[18] Walling, C. "Fenton's reagent revisited". Acc. Chem. Res. 8, 125 **(1975)**.

[19] Pignatello, J. "Dark and photoassisted Fe^{3+}-catalyzed degradation of chlorophenoxy herbicides by hydrogen peroxide". Environ. Sci. Technol. 26, 944 **(1992)**.

[20] Arslan-Alaton, I.; Dogruel, S. "Pre-treatment of penicillin formulation effluent by advanced oxidation processes". J. Hazard. Mater. 112, 105 **(2004)**.

[21] Arslan-Alaton, I.; Tureli, G.; Olmez-Hanci, T. "Treatment of azo dye production wastewaters using Photo-Fenton like advanced oxidation processes: Optimization by response surface methodology". J. Photochem. Photobiol. 202, 142 **(2009)**.

[22] Rodrigues, C.; Madeira, L.; Boaventura, R. "Optimization of the azo dye Procion Red-H-EXL degradation by Fenton's reagent using experimental design". J. Hazard. Mater. 164, 987 **(2009)**.

[23] Elmolla, E.; Chaudhuri, M. "Optimization of Fenton process for treatment of amoxicillin, ampicillin and cloxacillin antibiotics in aqueous solution". J. Hazard. Mater. 170, 666 **(2009)**.

[24] Tang, W.; Huang, C. "2,4-dichlorophenol oxidation kinetics by Fenton's reagent". Environ. Technol. 17, 1371 **(1996)**.

[25] Beltrán de Heredia, J.; Domínguez, J.; López, R. "Treatment of cork process wastewater by a successive chemical-physical method". J. Agr. Food Chem. 52, 4501 **(2004)**.

[26] Beltrán de Heredia, J.; Domínguez, J.R.; López, R. "Fenton reagent advanced oxidation of cork processing wastewater: kinetics and stoichiometry". J. Chem. Technol. Biotechnol. 79, 407 (2004).

[27] Peres, J.; Beltrán de Heredia, J.; Domínguez, J.R. "Integrated Fenton's reagent coagulation/flocculation process for the treatment of cork processing wastewaters". J. Hazard. Mater. 107, 115 **(2004)**.

[28] Beltrán de Heredia, J.; Domínguez, J.R. "Aplicación del reactivo de Fenton para la depuración de las aguas residuales de la industria productora de aceituna de mesa". Tecnol. Agua. 21, 50 **(2001)**.

[29] Oliveira, R.; Almeida, M.; Santos, L.; Madeira, L. "Experimental design of 2,4-dichlorophenol oxidation by Fenton's reaction". Ind. Eng. Chem. Res. 45, 1266 **(2006)**.

[30] Lucas, M.; Peres, J. "Decolorization of the azo dye Reactive Black 5 by Fenton and photo-Fenton oxidation". Dyes Pigm. 71, 236 **(2006)**.

[31] El-Desoky, H.; Ghoneim, M.; El-Sheikh, R.; Zidan, N. "Oxidation of Levafix CA reactive azo-dyes in industrial wastewater of textiledyeing by electrogenerated Fenton's reagent". J. Hazard. Mater. 175, 858 **(2010)**.

[32] Dorfman, L.; Adams, G. "Reactivity of the Hydroxyl Radical in Aqueous Solutions". NSRDS-NBS: Washington DC, **(1973)**.

[33] Beltrán De Heredia, J.; Torregrosa, J.; Domínguez, J.R.; Peres, J. "Kinetic model for phenolic compound oxidation by Fenton's reagent". Chemosphere. 45, 85 **(2001)**.

[34] Domínguez, J.R.; Peres, J.; Beltrán-Heredia, J. "Phenolic acids ozonation: QSAR analysis and pH influence on the selectivity of ozone". J. Adv. Oxidation Technol. 12, 249 **(2009)**.

[35] Peres, J.; Domínguez, J.R.; Beltrán-Heredia, J. "Reaction of phenolic acids with Fentongenerated hydroxyl radicals: Hammett correlation". Desalination. 252, 167 **(2010)**.

Capítulo 6:
OZONATION OF CARMAZEPINE
OZONATION OF A CARMAZEPINE EFFLUENT. DESIGNING THE OPERATIONAL PARAMETERS UNDER ECONOMIC CONSIDERATIONS

Ozonation of water effluent polluted with carbamazepine (CBZ), an ubiquitous and refractory pharmaceutical contaminant, has been addressed. This paper aims to optimize the remediation process through novel considerations, such as economical aspects of operational costs. To this end, firstly we have defined an efficiency variable which included not only global efficacy terms (pollutant removal) but also kinetic aspects, which has to do with the ozonation chemical rate. This target variable was involved in a Design of Experiments that optimized air flow, ozone concentration and pollutant initial content. An optimum was obtained at 55 $L \cdot h^{-1}$, 0.4 $g \cdot m^3$ and 18 $mg \cdot L^{-1}$ respectively.

Keywords: AOPs, operational costs optimization, design of experiments, pharmaceutical removal wastewater treatment

6.1. INTRODUCTION.

Ozonation is one of the methods that gives better results in the degradation of organic species at low concentrations. In general, it is often preferred to chlorination for the removal of organic pollutants present in water effluents due to its higher oxidation potential than that of chlorine. In addition, chlorination has been linked to the formation of organohalogen compounds in general, and trihalomethanes in particular, whereas ozonation does not leave by-products that need to be removed [1]. Due to its interest, the role of ozonation and its related oxidation processes in treating several organic substances, which are frequently present in industrial effluents and wastewaters, has been examined by different authors [2,3].

Oxidation reactions by ozone in water are generally rather complex. In water, not all ozone in solution reacts, but only a part of it, which attacks the organic solutes.

Another part may decompose before reaction. Such decompositions are catalysed by hydroxide ions generating highly reactive secondary oxidants, such as ·OH radicals [4]. These radicals and their reaction products can additionally accelerate the decomposition of ozone as it is known since long time ago [5]. Therefore, radical type chain reactions may occur concurrently through direct reaction mechanism of ozone with organic compounds. Because of this advantages, this decontamination process is widely used in treating a long list of wastewater either alone [6] or in combination with other treatment methods [7,8].

On the other hand, in recent years, the presence of emerging pollutants such as pharmaceuticals compounds (PCs) in the environment has received much attention [9,10]. The average per capita consumption of PCs per year in industrialized countries is estimated to be about 50-150 g [11]. The quantification and detection of a large variety of PCs, including analgesics, anti-inflammatories, antimicrobials, antiepileptics, beta-blockers, estrogens, and lipid regulators in waters have been recently documented [12-16]. After their consumption and excretion, these compounds and their metabolites reach sewage systems, where they are barely reduced. Consequently, they are released into the environment either by the receiving waters of the sewage treatment plants. If the PCs are not effectively removed from the water and wastewater treatment plants, they are unintentionally consumed by humans.

In this context, carbamazepine (CBZ) is the most frequently detected PC in water bodies thus far. This drug is used for the treatment of seizure disorders, for relief of neuralgia, and for a wide variety of mental disorders. Approximately 30% of orally administered CBZ is unchanged and subsequently discharged through the feces. This drug has been proposed by some authors as an anthropogenic marker in water bodies. So, CBZ is flushed with wastewater to the wastewater treatment plants (WWTPs) through the sewage system. Investigations found that carbamazepine is persistent, and its removal efficiencies by the WWTPs are mostly below 10%. In the classification scheme for pharmaceutical biodegradation, the removal status of CBZ is classified as “no removal” [17].

These facts make ozonation process a possible candidate for the removal of this pharmaceutical pollutant in water. It is a promising environmentally friendly technology for the treatment of wastewaters containing low contents of PCs in water.

This work presents the results obtained from the ozonation of a carbamazepine effluent. The design of experiments (DOE) was used to study the influence of the different operating variables: ozone flow, carbamazepine concentration and ozone concentration in water. Response surface methodology (RSM) technique was used to optimize economic costs for carbamazepine degradation, which are linked to X variable. So, the objective of the present study was to analyze the influence of the different operating variables and to find out the optimum values for this decontamination process (Table 6.1).

Table 6.1. Experimental planning in DOE.

Experiment	Flow ($L \cdot h^{-1}$)	Ozone concentration ($g \cdot m^{3}$)	Carbamazepine concentration ($mg \cdot L^{-1}$)
1	14.8	0.7	6
2	44.8	0.7	6
3	29.8	1.2	11
4	29.8	1.2	11
5	14.8	1.7	16
6	44.8	0.7	16
7	29.8	0.4	11
8	4.5	1.2	11
9	29.8	2.0	11
10	29.8	1.2	11
11	14.8	0.7	16
12	29.8	1.2	11
13	29.8	1.2	11
14	44.8	1.7	6
15	14.8	1.7	6
16	29.8	1.2	11
17	29.8	1.2	11
18	29.8	1.2	20
19	44.8	1.7	16
20	55.1	1.2	11
21	29.8	1.2	2
22	29.8	1.2	11
23	29.8	1.2	11

6.2. MATERIALS AND METHODS.

6.2.1. Experimental installation.

Experiments were carried out in a semi-continuous agitated glass reactor submerged in a thermostatic bath to keep the temperature at the desired value within ±0.2 ^{o}C. The reactor had four inlets at the top for sampling, bubbling the gas feed, venting and measuring the temperature. Ozone was produced from an oxygen stream in an ozone generator (Sander Ozonisator mod. 501, Germany), and the ozone-oxygen mixture could be sent to the reactor or to an ozone analyzer (Anseros mod. GM, Germany). For every experiment conducted, the reactor was filled with 300 cm^3 of CBZ aqueous solution.

In each ozonation experiment CBZ was dissolved in the aqueous solution with the adjusted initial concentration. During the experiments, samples were taken out periodically to determine the remaining CBZ concentration in the solution.

6.2.2. Reagents.

Carbamazepine was purchased to Sigma-Aldrich (Spain) in analitycal purity grade. Pollutant stock solution (20 $mg \cdot L^{-1}$) was prepared with high purity Milli-Q water. In order to guarantee pH stability, the solution was adjusted with sodium hydroxide and orthophosphoric acid buffer solution.

6.2.3. Analysis

Carbamazepine concentration was analitically determined by HPLC in a Waters chromatograph equipped with a 996 photodiode array detector and a Waters Nova-Pak C18 column (5μm 150×3.9 mm). Carbamazepine peak is defined at a retention time of 5.21 min at 286 nm. Samples (50 μL) were sequentially injected into the chromatograph and a 60:40 (v/v) mixture of methanol/aqueous solution respectively was used as mobile phase. This aqueous solution was of 10^{-2} $mol \cdot L^{-1}$ ortophosphoric acid. The entire flow rate was 1 $mL \cdot min^{-1}$.

6.2.4. Mathematical and statistical methods.

Non linear data adjustments were carried out by using SPSS 14.0 for Windows [18]. Statistics regarding Design of Experiments (DOE) and Response Surface Methodology (RSM) were performed by StatGraphics Centurion XVI for Windows [19]. A factorial central composite orthogonal and rotatable design was used with 9 central replicates and 23 total experiments.

6.3. RESULTS AND DISCUSSION.

This investigation is focused on the optimization of a well known advanced oxidation process, such as ozonation, according to two new aspects: on the one hand the applicability of this technique to the degradation of carbamazepine, a dangerous and emerging pharmaceutical pollutant; on the other hand a new objective variable was presented, where economic and kinetic considerations, together with those related with the overall efficiency, are merged. The optimization was carried out according to the Design of Experiments protocol, and results were analyzed following the Response Surface Methodology. Results are therefore reliable for the further implementation at pilot plant scale.

6.3.1. Kinetics.

The experimental series included up to 23 ozonation trials in different conditions. Depending on them, the reaction went faster or slower, and many operational factors affect to this process. At regular time laps, samples of the experimental polluted solution were collected and analyzed. The carbamazepine decay is specific for each experiment, depending on the initial concentration, ozone concentration and flow (the three variables involved in the Design of Experiments). According to this, Figure 6.1 presents the evolution of five experiments, given as an example.

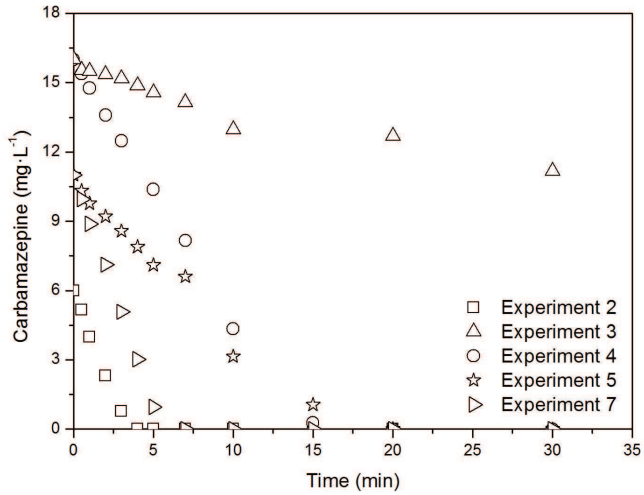

Fig. 6.1. Some experiments on the carbamazepine decay. Experiment labeling according to Table 6.1

Each experiment gives us a significative number of experimental points that can be easily modelled according to an apparent first-order chemical reaction. This should be the significance of Equation (6.1):

$$-\frac{dC}{dt} = kC \tag{6.1}$$

where the chemical reaction rate is given by the decomposition of carbamazepine. Integrating Eq. (6.1) within the boundary conditions (t= 0, t= t; C= C_0 , C= C) yields to Eq. (6.2):

$$C = C_o \cdot e^{-kt} \tag{6.2}$$

that actually fits to the experimental data. Each series can be adjusted following a non linear least-squared data adjustment for obtaining the representative kinetic constant (that is, *k*), which gives us the idea of the chemical reaction rate. Non linear adjustments do not require homocedasticity in the data population, so the reliability of the model constants is higher [20,21]. Table 6.2 presents the results of these adjustments. As can be easily appreciated, the theoretical model predicts rather well the behavior of the entire system, since the large majority of r^2 correlation factors is

above 0.9. The variation in k values is representative of the chemical reaction rate and this is the first parameter one must consider in order to propose a holistic variable which would include this chemical rate, the effective pollutant removal and the economical costs.

6.3.2. Designing a target variable.

The evaluation of this advanced oxidation process under economical perspectives leads us to consider two types of variables:

1. *Positive variables*, hence those that should be as high as possible. This is the case of chemical rate (which can be represented by k) and the process global efficiency (the difference between initial and final carbamazepine concentration).

2. *Negative variables*, those that must be kept at low levels. These are the economic costs.

According to simplicity and following some previous references [22], we have selected an economical model that considers only the direct costs. Therefore, this variable includes electric energy (given by the power of the ozonizator) and the cost of the air (we are working with compressed industrial air). We have not included the equipments amortization or the personnel salaries. Further studies could include other instrumental dispositions that should modify the target variable. E.g. researchers could implement an air compression stage for working directly with environmental free air. This would reduce the reagents cost although would include other equipments.

Target variable (named X) is therefore the function presented in Eq. (6.3):

$$X = \frac{k\left(C_o - C_f\right)}{\left(E + A\right)} \tag{6.3}$$

X is the objective variable we have selected for optimizing the whole system according to the corresponding Design of Experiments and its interpretation under the Response Surface Methodology. It is remarkable that this target variable is made on

Table 6.2. Least squared adjustment for each experimental series in kinetic model.

Experiment	k (min^{-1})	r^2
1	0.031	0.981
2	0.040	0.991
3	0.154	0.963
4	0.155	0.969
5	0.117	0.963
6	0.013	0.902
7	0.106	0.962
8	0.045	0.959
9	0.308	0.968
10	0.100	0.970
11	0.005	0.857
12	0.125	0.965
13	0.130	0.856
14	0.701	0.975
15	0.176	0.956
16	0.140	0.969
17	0.130	0.885
18	0.089	0.965
19	0.347	0.969
20	0.217	0.971
21	0.588	0.953
22	0.130	0.964
23	0.150	0.955

the basis of technological and economical consideration. *X* involved not only pollutant global removal percentages, but also the kinetic aspects of the reaction rate. The three dimensions of the efficiency (kinetic, global removal and economic costs) draw a reliable objective variable for evaluating the performance of the entire system.

6.3.3. Design of experiments.

Design of experiments is a well known technique for optimizing the response of a given system with a minimum number of significative trials. We have previously presented this methodology in many scientific papers, most of them regarding to chemical engineering: advanced oxidation [23], adsorption [24] or coagulation [25]. Briefly, this procedure involves the codification of the experimental variables, the adequate planification of the trials according to the rotatable and orthogonal conditions and the proper interpretation of the results following the Response Surface Methodology. Table 6.3 presents the coded and real values of the experimental variables.

Table 6.3. Coded and real values of experimental variables in DOE.

Variable	Coded level	
	+1	**-1**
Flow ($L \cdot h^{-1}$)	44.9	14.8
Ozone concentration ($g \cdot m^{-3}$)	1.7	0.7
Carbamazepine initial concentration ($mg \cdot L^{-1}$)	16	6

The correct interpretation of this DOE according to RSM should drive to a characteristically polynomial equation such as Eq. (6.4) presents:

$$X = b_o + \sum_{j=1} b_j x_j + \sum_{i \neq j, i=1} b_{ij} x_i x_j + \sum_{j=1} b_{jj} x_j^2 \qquad (6.4)$$

In the particular current case, the response target variable is given by Eq. (6.3) and must be maximize by varying the three studied variables simultaneously. The multiple analysis of this non linear adjustment will give us the numerical conclusions (ANOVA report) and the graphical interpretation of the phenomenon.

One of the main influent aspects when planning a DOE is the selection of the working range. If we choose a very wide range (involving any of the operating variables) it is possible we are not able to appreciate an optimum. On the other hand, if we select a very narrow segment, the virtual optimum point could lay out of our scope. For adjusting an adequate working range, preliminary experiments in *one-variable-at-time* methodology must be carried out. These will focus the interesting working area, although the results of this experimental series are not shown.

6.3.4. Anova report.

Every statistical consideration must be begun with an analytical study. This is the case of the general ANOVA report, where one can find the reliability levels of the entire design [26]. Since our target variable X is defined by Eq. (6.3), the optimization process involves either kinetic and efficiency considerations. The three operating variables presented in Table 6.3 are analyzed in ANOVA report according to their corresponding significance inside the experimental design. So, just the first of them (flow) is out of significance region (p-value over 0.05), whereas ozone concentration, pollutant content and four interactions between variables should be considered for the proper explanation of the whole system. Table 6.4 presents the specific sum of squares, f-ratio and p-value for each response category.

Adjusted r^2 correlation factor (which gives the idea of experimental-predicted data adjustment) is of 0.77, high enough for considering this model as a reliable one. Moreover, the randomization of the experiments was effective since Durbin-Watson statistic is equal to 2.18, with a corresponding p-value of 0.33; far away from the significance level of 0.05. This means there is no autocorrelation in the error series and therefore the experimental design was adequately built. Graphically, this is also presented in Figure 6.2. Subfigure 6.2.1 presents the correlation between experimental

and predicted data. These points fit rather well to the perfect diagonal which would represent a r^2 of 1; subfigure 6.2.2 is instead the random disposition of errors. This graph presents error measures that are randomly located around 0 level. Since no pattern is observed, the experimental methodology was correctly performed.

Table 6.4. ANOVA report statistical summary.

Parameter	Sum of squares	F Ratio	P Value
F: Flow	1,493	4.24	0.06
O: Ozone concentration	14,828	42.1	0
C: Carbamazepine concentration	2,010	5.71	0.03
FF	356	1.01	0.33
FA	1,541	4.38	0.05
FC	1,863	5.29	0.03
OD	3,307	9.39	0
CO	4,282	12.16	0
CC	7.09	0.02	0.88
Total error	4,578		

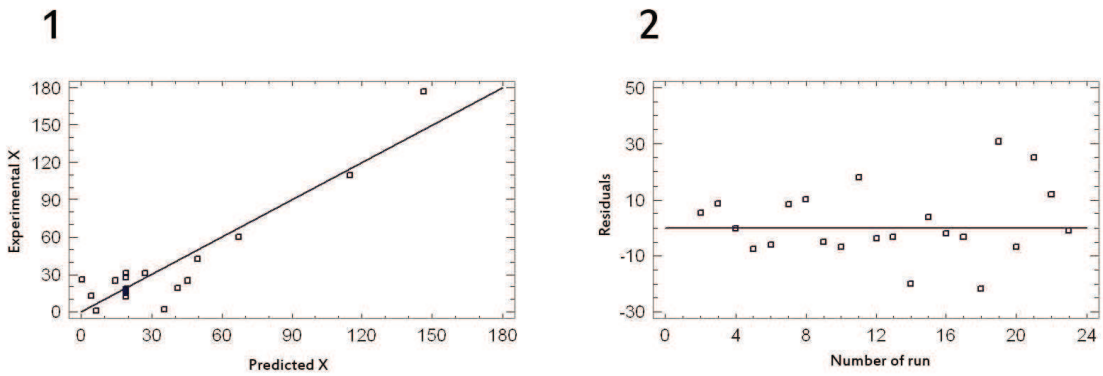

Fig. 6.2. Graphical aspects from ANOVA report. 1. Correlation between experimental and predicted values of *X* (units in Nomenclature); 2. Randomly disposition of residuals.

6.3.5. Significant graphics.

PARETO: The analytical data from ANOVA report can be easily translated into significant graphs. Therefore, a very useful way of visualizing if operating variables are inside the region of significance or not is the Pareto representation (Figure 6.3). As many other previous papers presented [25,27], Pareto graphic presents the standarized effects in a bar figure. The longer the bar, the more influent the effect is; moreover negative and positive effects can be concomitant in the same graphic. Figure 6.3 presents the positive effect of every factor and the significance of each one. Bars trespassing the vertical rule near 2 represent significant variables.

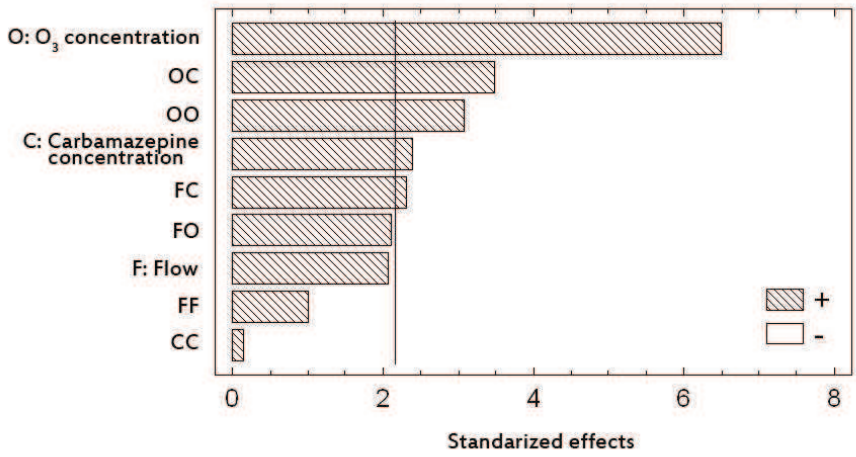

Fig. 6.3. PARETO graphic for studied operating variables.

Interaction between variables: No quantitative levels of interaction between factors can be observed from PARETO graphic. However, this is one of the main scopes of Design of Experiments: evaluating how variables affect one to each other and the three of them onto the target variable *X* [28]. To this end, the interaction between these parameters can be presented in Figure 6.4.

As can be seen, it is graphically confirmed the relationship between *Ozone concentration* (O) and *Carbamazepine concentration* (C) presents interaction, as well as in the case of *Flow* (F) and (C). Nevertheless, (O) and (F) are out from the

interaction zone, although both parameters tend to this crossing since their respective lines are not parallel.

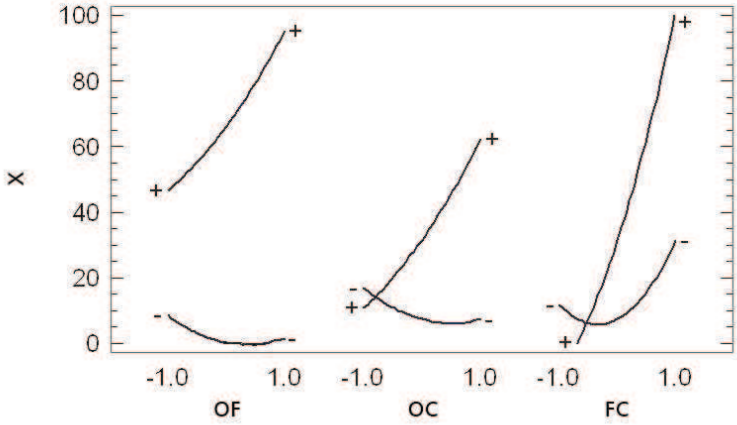

Fig. 6.4. Interaction factors. *X* units in Nomenclature, coded values of variables.

Main effects: The evaluation of the influence of each parameter should isolate the magnitude of each effect separately. This is the scope of the Main effects analysis, what is presented in Figure 6.5. As can be clearly observed, the efficiency of the system (represented under the *X* variable) tends to grow faster when we vary the ozone concentration, while it rises in a less marked slope if we only modify the flow or the initial pollutant concentration.

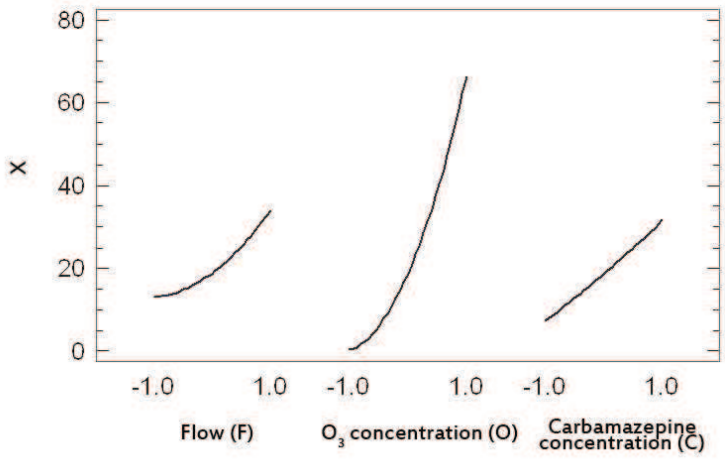

Fig. 6.5. Main effects. *X* units in Nomenclature, coded values of variables.

Response surface: The statistical analysis of this system should drive us to the determination of an optimum combination of the three variables according to the target *X*. In fact, this optimum value for each variable is given by Table 6.5 and it is experimentally confirmed.

Table 6.5. Optimum combination of the three studied variables.

Variable	Coded value	Real value
Flow	1.68	55 $L \cdot h^{-1}$
O_3 concentration	1.68	0.4 $g \cdot m^{-3}$
Carbamazepine concentration	1.38	18 $mg \cdot L^{-1}$

Equation (6.4) acquires the specific form of Eq. (6.5) once the corresponding correlating coefficients are included:

$$X = 18.80 + 10.45F + 32.95O + 12.13C + 4.73C^2 + 13.88FO + 15.26FC + 14.42O^2 + 23.13OC + 0.66C^2 \quad (6.5)$$

The graphical representation of Eq. (6.5) is given by Figure 6.6. Since three variables are involved, one of them must be adjusted. This is the case of *C*, *carbamazepine concentration*. Consequently, Figure 6.6 shows the evolution of the other two variables when optimum value of *C* is adjusted (that is, 1.38 in coded level, 18 $mg \cdot L^{-1}$). From this figure is more than evident that the response grows rapidly as ozone concentration tends to increase, whereas the flow variable presents a lower influence.

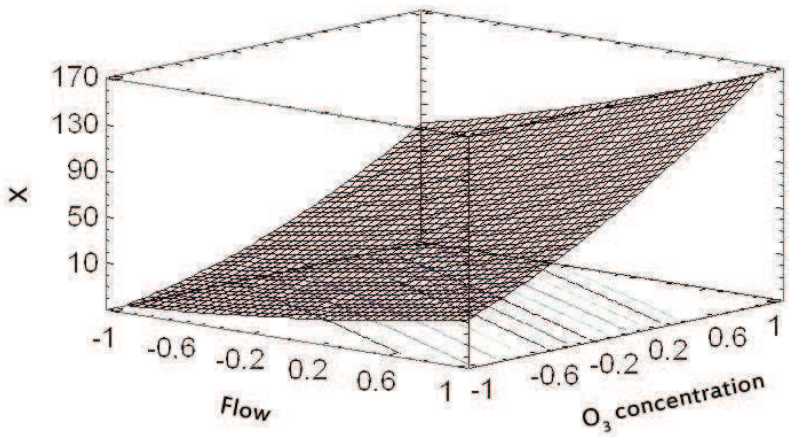

Fig. 6.6. Response surface. *C* adjusted to 1.38, *X* units in Nomenclature, coded values of variables.

6.4. CONCLUSIONS.

Ozonation as an advanced oxidation process is a feasible and reliable process for eliminating pharmaceutical compounds from water and wastewater effluents. Specifically, economical considerations on the oxidation of carbamazepine present an optimum value (that is, maximum pollutant removal with minimum costs) at an intermediate initial contaminant concentration and high ozone-rich air flow and ozone concentration. This recommended combination gives an optimum in terms of economic costs, kinetic rate and pollutant elimination. Further studies should include the suggested variable X (kinetic rate, pollutant removal and economic costs) in the proper considerations on water and wastewater treatment.

6.5. NOMENCLATURE.

C Carbamazepine instant concentration, $mg \cdot L^{-1}$.

C_0 Carbamazepine initial concentration, $mg \cdot L^{-1}$.

C_f Carbamazepine final concentration, $mg \cdot L^{-1}$.

k Apparent kinetic constant, min^{-1}.

t Time, min.

E Energy cost, $e \cdot min^{-1}$.

A Air cost, $e \cdot min^{-1}$.

X Efficiency variable, $mg \cdot L^{-1} \cdot e^{-1}$.

6.6. REFERENCES.

[1] Beltrán-Heredia, J.; Torregrosa, J.; Domínguez, J.R.; Peres, J.A. "Kinetics of the reaction between ozone and phenolic acids present in agro-industrial wastewaters". Water Research. 35, 1077 **(2001)**.

[2] Beltrán-Heredia, J.; Torregrosa, J.; Domínguez, J.R.; García, J. "Treatment of black-olive wastewaters by ozonation and aerobic biological degradation". Water Research. 34, 3515 **(2000)**.

[3] Benítez, J.; Beltrán-Heredia, J.; Peres, J.A., Domínguez, J.R. "Kinetics of p-hydroxybenzoic acid photodecomposition and ozonation in a batch reactor". Journal of Hazardous Materials, 73, 161 **(2000)**.

[4] Masten, S.; Davies, S.H.R. "The use of ozonization to degrade organic contaminants in wastewaters". Environmental Science Technology. 28, 180 **(1994)**.

[5] Staehelin, J.; Hoigne, J. "Decomposition of ozone in the presence of organic solutes acting as promoters and inhibitors of radical chain reactions". Environmental Science Technology. 19, 1206 **(1985)**.

[6] Machado, E.; de Sales Dambros, V.; Kist, L.; Alcayaga, E.; Tedesco, S.; Moro, C. "Use of ozonization for the treatment of dye wastewaters containing Rhodamine B in the agate industry". Water, Air, & Soil Pollution. 223, 1753 **(2012)**.

[7] García-Peña, E.; Zarate-Segura, P.; Guerra-Blanco, P.; Poznyak, T.; Chairez, I. "Enhanced phenol and chlorinated phenols removal by combining ozonation and biodegradation". Water, Air, & Soil Pollution. 223, 4047 **(2012)**.

[8] Uslu, M.; Rahman, M.; Jasim, S.; Yanful, E.; Biswas, N. "Evaluation of the reactivity of organic pollutants during O_3 /H_2O_2 process". Water, Air, & Soil Pollution. 223, 3173 **(2012)**.

[9] Radjenovic, J.; Jelic, A.; Petrovic, M.; Barceló, D. "Determination of pharmaceuticals in sewage sludge by pressurized liquid extraction (PLE) coupled to liquid chromatography-tandem mass spectrometry (LC-MS/MS)". Analytical and Bioanalytical Chemistry. 393, 1685 **(2009)**.

[10] Radjenovic, J.; Petrovic, M. and Barceló, D. "Analysis of pharmaceuticals in wastewater and removal using a membrane bioreactor". Analytical and Bioanalytical Chemistry. 387, 1365 **(2007)**.

[11] Alder, A.; Bruchet, A.; Carballa, M.; Clara, M.; Joss, A.; Loffler, D.; McArdell, S.S.; Miksch, K.; Omil, F.; Tuhkanen, T.; Ternes, T.A. "Consumption and Occurrence. In Human Pharmaceuticals, Hormones and Fragrances. The Challenge of Micropollutants in Urban Water Management". IWA Publishing, London, UK **(2006)**.

[12] Bound, J.P.; Voulvoulis, N. "Pharmaceuticals in the aquatic environments. A comparison of risk assessment strategies". Chemosphere. 56, 1143 **(2004)**.

[13] Tauxe-Wuersch, A.; Alencastro, L.F. De; Grandjean, D.; Tarradellas, J. "Occurrence of several acidic drugs in sewage treatment plants in Switzerland and risk assessment". Water Research, 39, 1761 **(2005)**.

[14] Emblidge, J.P.; Delorenzo, M.E. "Preliminary risk assessment of the lipid-regulating pharmaceutical clofibric acid, for three estuarine species". Environmental Research. 100, 216 **(2006)**.

[15] Farré, M.; Ferrer, I.; Ginebreda, A.; Figueras, M.; Olivella, L.; Tirapu, L.; Vilanova, M.; Barceló, D. "Determination of drugs in surface water and wastewater samples by liquid chromatography–mass spectrometry: methods and preliminary results including toxicity studies with Vibrio fischeri". Journal of Chromatography A. 938, 187 **(2001)**.

[16] Clara, M.; Strenn, B.; Kreuzinger, N. "Carbamazepine as a possible anthropogenic marker in the aquatic environment: investigations on the behaviour of Carbamazepine in wastewater treatment and during groundwater infiltration". Water Research. 38, 947 **(2004)**.

[17] Joss, A.; Zabczynski, S.; Góbel, A.; Hoffmann, B.; L´'offler, D.; McArdell, C.S.; Ternes, T.A.; Thomsen, A.; Siegrist, H. "Biological degradation of pharmaceuticals in municipal wastewater treatment: Proposing a classification scheme". Water Research. 40, 1686 **(2006)**.

[18] SPSS Inc. SPSS 14.0 Developer's guide. Chicago, Illinois **(2005)**.

[19] StatPoint Technologies Inc. StatGraphics Centurion XVI User Manual. Virginia, USA. **(2009)**.

[20] Kumar, V.; Sivanesan, S. "Pseudo second order kinetics and pseudo isotherms for malachite green onto activated carbon: Comparison of linear and non-linear regression methods". Journal of Hazardous Materials. 136, 721 **(2006)**.

[21] Kumar, V.; Porkodi, K.; Rocha, F. "Isotherms and thermodynamics by linear and non-linear regression analysis for the sorption of methylene blue onto activated carbon: Comparison of various error functions". Journal of Hazardous Materials. 151, 794 **(2008)**.

[22] Real, F.J.; Benítez, F.J.; Acero, J.L.; Roldán, G. "Combined chemical oxidation and membrane filtration techniques applied to the removal of some selected pharmaceuticals from water systems". Journal of Environmental Science and Health A. 47, 522 **(2012)**.

[23] Domínguez, J.R.; González, T.; Palo, P.; Sánchez-Martín, J. "Electrochemical advanced oxidation of carbamazepine on boron-doped diamond anodes. Influence of operating variables". Industrial & Engineering Chemistry Research. 49, 8353 **(2010)**.

[24] Beltrán-Heredia, J.; Sánchez-Martín, J.; Carmona-Murillo, C. "Adsorbents from *Schinopsis balansae*: Optimisation of significant variables". Industrial Crops and Products. 33, 409 **(2011)**.

[25] Beltrán-Heredia, J.; Sánchez-Martín, J.; Jiménez-Giles, M. "Tannin-based coagulants in the depuration of textile wastewater effluents: elimination of anthraquinonic dyes". Water, Air, and Soil Pollution. 222, 53 **(2011)**.

[26] Montgomery, D.C. "Design and Analysis of Experiments". 5th ed. John Wiley and Sons, New York **(2001)**.

[27] Beltrán-Heredia, J.; Sánchez-Martín, J.; Martín-García, L. "Multiparameter quantitative optimization in the synthesis of a novel coagulant derived from tannin extracts for water treatment". Water, Air, & Soil Pollution. 223, 2277 **(2011)**.

[28] Beltrán-Heredia, J.; Sánchez-Martín, J.; Solera-Hernández, C. "Removal of sodium dodecyl benzene sulfonate from water by means of a new tannin-based coagulant: optimization studies through design of experiment". Chemical Engineering Journal. 153, 56 **(2009)**.

Capítulo 7:
PHOTOOXIDATION OF CARBAMAZEPINE BY UV IRRADIATION IN THE PRESENCE OF HYDROGEN PEROXIDE

ADVANCED PHOTOCHEMICAL OXIDATION OF CARBAMAZEPINE IN AQUEOUS SOLUTION. OPTIMIZING THE SYSTEM

The combination of UV radiation with hydrogen peroxide has been widely used for the photodegradation of pollutants in aqueous solutions. Statistical design of experiments is a powerful tool to optimize this kind of processes. Initial hydrogen peroxide concentration, pH and temperature were considered as the variables for the process optimization. The interactions existing between these three variables were analyzed. Initial concentration of hydrogen peroxide resulted to be the most important variable conditioning the removal efficiency, followed by temperature, while pH shows a non-significant positive influence along the whole operation interval. ANOVA test reported significance for five of the nine involved variables. Response Surface Methodology technique was used to optimize carbamazepine degradation. Under optimal conditions (hydrogen peroxide concentration= $0.38 \cdot 10^{-3}$ mol·L^{-1}, pH= 1 and temperature= 35.6 ºC) total carbamazepine degradation was achieved at 10 min of reaction time.

Keywords: Combined UV/H_2O_2, advanced oxidation processes, pharmaceuticals, carbamazepine.

7.1. INTRODUCTION.

Advanced oxidation processes (AOPs) may be defined as all those processes (or combinations of processes) such as ozone, UV radiation, hydrogen peroxide, etc, that involve *in situ* generation of highly reactive species such as hydroxyl radicals (·OH) [1]. Hydroxyl radical is powerful oxidizing specie that exhibits an oxidation potential of 2.80 V [2]. Hence, it has received a great deal of attention in the field of AOPs.

Important advantages of hydroxyl radicals with respect to many other oxidants are its scarce selectivity [3], which results in a wider range of potential target pollutants, and enhanced reaction rate [4]. Furthermore, hydroxyl radicals can attack organic molecules by abstracting a hydrogen atom, adding hydroxyl groups, or transferring electrons [5]. In fact, hydroxyl radical may react with a wide variety of potentially harmful chemicals giving rise to intermediate products with less complexity and toxicity.

AOPs neither transfer pollutants from one phase to another (as in chemical precipitation, adsorption and volatilization) nor produce massive amounts of hazardous sludge (as in activated sludge processes) [6]. This constitutes an important advantage over many other processes and, hence, AOPs may be considered as "*environmental-friendly*".

From a methodological standpoint, AOPs aimed to the treatment of water and wastewater may be divided into two main groups, namely non-photochemical and photochemical processes. Among the first group, ozonation [7], Fenton [8], Fenton-like [9], photo-Fenton [10,11], electro-Fenton [12], electrochemical oxidation [13], supercritical water oxidation [14], microwaves [15], wet-air oxidation [16] and pulsed plasma processes [17] are to be mentioned. The most important photochemical processes include UV-oxidation [18] and all its variants (e.g., UV/H_2O_2, UV/O_3 or UV/H_2O_2/O_3), photo-Fenton processes [19], photocatalysis [20] and sonophotocatalysis [21].

Ultraviolet (UV)-based AOPs have been found to be very effective in the removal of organic pollutants [22]. Strong oxidizing species, principally hydroxyl radicals, are generated from ozone or hydrogen peroxide in the presence of UV light [23]. The elimination of organic compounds occurs through at least two mechanisms: direct photolysis and hydroxyl radical attack [24]. Comparing direct photolysis and radical attack it is worth noting that the latter is advantageous from the energy consumption standpoint [25]. Another important aspect of H_2O_2/UV process is that, under the

appropriate conditions, the organic carbon can be completely mineralized into CO_2 without introducing any secondary pollution.

On the other hand, in recent years the presence of pharmaceutical compounds (PCs) in the aquatic environment has been of growing interest [23,26]. Carbamazepine (CBZ) is the common name of the 5H-dibenzo[b,f]azepine-5-carboxamide (Chemical Formula, $C_{15}H_{12}N_2O$; CAS Number, 298-46-4; pK_a= 13.4). Since the 1970s CBZ has been used to treat epileptic seizures, severe nerve pain (trigeminal neuralgia) as well as bipolar disorder. Approximately 72% of orally administered CBZ is absorbed, while 28% is unchanged and subsequently discharged through the faeces. CBZ is the most frequently detected pharmaceutical compound in water bodies thus far. This drug has been proposed by some authors as an anthropogenic marker in water bodies [27]. Usually, CBZ and their metabolites are flushed with wastewater to the wastewater treatment plants (WWTPs) through the sewage system. Frequently, conventional treatment processes cannot remove recalcitrant pollutants. Hence, it is necessary to introduce additional advanced treatment technologies in those areas where a persistent pollution problem has been found [28]. Recent research works have reported that CBZ is persistent and its removal efficiencies by the WWTPs are mostly below 10%. In the classification scheme for PCs biodegradation, the removal status of CBZ is classified as "*no removal*" [29].

This work presents the results obtained from the photodegradation with hydrogen peroxide of CBZ. The application of statistical design of experiments (DOE) in this kind of studies is extremely helpful. This statistical approach allows a multivariate analysis, using a minimum number of experiments [30]. DOE was used to study the influence of the different operating variables: hydrogen peroxide initial concentration (from 0 to $0.5 \cdot 10^{-3}$ $mol \cdot L^{-1}$), pH (in the range 1-9), and solution temperature (T) between 10 and 50 ºC. Response Surface Methodology (RSM) technique was used to optimize CBZ removal (X_{CBZ}, %).

7.2. MATERIALS AND METHODS.

7.2.1. Chemicals.

CBZ was provided by Sigma-Aldrich (Spain) of the highest purity available. Initial CBZ solution ($2.11 \cdot 10^{-5}$ mol·L^{-1}) was prepared with high purity water obtained from a Millipore Milli-Q™ system and pH was adjusted using a perchloric acid/sodium perchlorate buffer solution to avoid the scavenging effect of the conventional phosphate buffer. Hydrogen peroxide (33% w/v, analytical grade) was obtained from Merck.

7.2.2. Analytical methods.

CBZ concentration present in each sample was determined by HPLC in a Waters Chromatograph equipped with a 996 Photodiode Array Detector and a Waters Nova-Pak C-18 Column (5 μm 150x3.9 mm). A well defined peak for CBZ at a retention time of 5.21 min at 286 nm was obtained. Samples of 50 μL were injected into the chromatograph and a 60:40 (v/v) methanol/water mixture was used as the mobile phase under a flow rate of 1 mL·min^{-1}.

Total Organic Carbon content (TOC) was determined by using a TOC Analyzer-Analytik Jena multi N/C™ 3100, which combines catalytic high-temperature combustion, VITA™, Focus Radiation NDIR- Detector™, as well as flow injection with intelligent rinsing technology for particle-containing samples.

For COD determination the Lange-COD™ cuvette test method was used. The range of concentrations selected was 5-60 mg $O_2 \cdot L^{-1}$. For both analyses a thermostat Lange LT-200™ and a Hach Lange Xion Σ-500™ photometer were used.

7.2.3. Design of experiments (DOE).

A commonly-used way to approach scientific research work is approximating the response with a single variable or a set of assumed independent variables, by implementing the "*One Factor at a Time*" (OFAT) approach. The OFAT approach, which is sometimes conflated with the *scientific method*, implicitly assumes a lack of

statistical interaction of variables and relies on the intuition as well as the practical and theoretical knowledge of the experimenter. The simplicity of the analysis of data from OFAT experiments ignores the fact that for many problems, the central assumption of absence of statistical interaction is not appropriate [31]. On the contrary, for some variables both, individual and interactive effects may be involved. Particularly, in the H_2O_2/UV process, several variables (e.g., H_2O_2 initial concentration, UV-light intensity, pH, temperature, etc...) may exert an important influence on the removal efficiency [32]. Even more, such variables may interact with each other. As a consequence, the task of optimizing the process is far from being easy and direct.

In contrast, statistical design of experiments (DOE) aims to acknowledging the statistical interaction of variables, and utilizes statistics as an objective way of drawing conclusions in the presence of errors, noise, and unknown variables.

In order to perform this study, a factorial central composite orthogonal and rotatable design (CCORD) was used with nine replicates of central point, so that the total number of experiments was 23. Values of the independent variables and their variation limits were determined based on preliminary runs and literature. The experimental results were statistically analyzed by using *StatGraphics*^{TM} *Centurion XV* software and the statistical validation was achieved by ANOVA test at 95% confidence. The obtained drug removal at 10 min was considered as the response. The effect of initial concentration of H_2O_2, pH and temperature were assessed by applying response surface methodology (RSM).

RSM consists of a group of mathematical and statistical techniques that are based on the fit of empirical models to the experimental data obtained in relation to experimental design. With such an aim, linear or square polynomial functions are employed to describe the system studied and, consequently, to explore (modeling and displacing) experimental conditions until its optimization [33]. The use of RSM makes it possible to overcome the shortcoming of the classical or empirical methods such as OFAT method, which is a time-consuming process and unable of searching the global optimal condition especially if interactions between independent variables occur.

DOE is a useful tool to verify the effects of different variables and of their interactions on the process response within a certain range and with a minimum number of experiences. Additionally, RSM has proven to be a reliable statistical tool in the investigation of photocatalytic processes [34]. The application of RSM permitted to establish a mathematical relationship between dependent and independent variables and the process optimization. Therefore, experimental data were fitted to a polynomial equation as follows [35].

$$Y = b_o + \sum_{j=1} b_j x_j + \sum_{i,j=1} b_{ij} x_i x_j + \sum_{j=1} b_{jj} x_j^2 \tag{7.1}$$

where Y is the predicted response, b_0 the offset term, b_j the linear effect, b_{ij} the first-order interaction effect, b_{jj} is the squared effect and k is the number of independent variables. In this work, one of the most popular classes of second-order design, namely CCORD was selected. It involves the use of a two-level factorial design with 2^k points combined with $2k$ axial points and n center runs, k being the number of factors. The total number of experiments given a k factor, N, is obtained according to e Eq. (7.2):

$$N = 2^k + 2 \cdot k + n \tag{7.2}$$

where n is considered to be nine and the axial distance is 1.681 in order to guarantee an orthogonal and rotatable design. To convert the natural variables into dimensionless codified values it is necessary to use Eq. (7.3):

$$x_i = \frac{X_i - X_i^{X}}{\Delta X_i} \tag{7.3}$$

where, x_i is the coded value of the *ith* independent variable, X_i the natural value of the *i-th* independent variable, X^X and ΔX_i is the value of step change.

7.2.4. Experimental procedure.

All experiments were performed in a cylindrical glass reactor described in detail elsewhere [25]. Basically, the reactor is equipped with a radiation lamp in axial

position and a quartz sleeve which houses the lamp. This is a Hanau TNN 15/32^{TM} low pressure mercury lamp, which emits a monochromatic radiation at 254 nm. The photodegradation experiments were performed by bubbling air into the reaction liquid, in order to maintain stirred the whole solution. An external jacket surrounding the reactor maintained the selected temperature in each experiment.

For each of the experiments conducted the reactor was filled with 350 cm^3 of buffered aqueous solutions with the selected initial H_2O_2 concentration. Once the process started (when the lamp was connected) samples were taken at regular times (in preliminary runs) and at 10 minutes (in DOE) to evaluate the remaining concentration of CBZ. On the other hand, for the experiment carried out under optimal conditions, samples were taken at different times to determine the removals of CBZ, COD and TOC achieved.

7.3. RESULTS AND DISCUSSION.

7.3.1. Preliminary runs.

In these processes the production of ·OH radicals depends on several factors such as pH, temperature and initial concentration of H_2O_2. Some preliminary runs were performed to achieve a range of suitable initial H_2O_2 concentration. According to the experimental results, the initial H_2O_2 concentration appears to be an important variable governing CBZ removal. The results shown in Figure 7.1 demonstrated that within the range comprised between $0.05 \cdot 10^{-3}$ and 10^{-3} $mol \cdot L^{-1}$ the degradation of CBZ was significantly improved. The role of the hydrogen peroxide in the process when combined with UV radiation is clearly pointed out by the experiments represented in this Figure. As can be observed, its presence enhances the oxidation, and an increase in its concentration leads to an increase in the degradation. Also, a previous experiment was conducted with UV alone, and no oxidation was obtained.

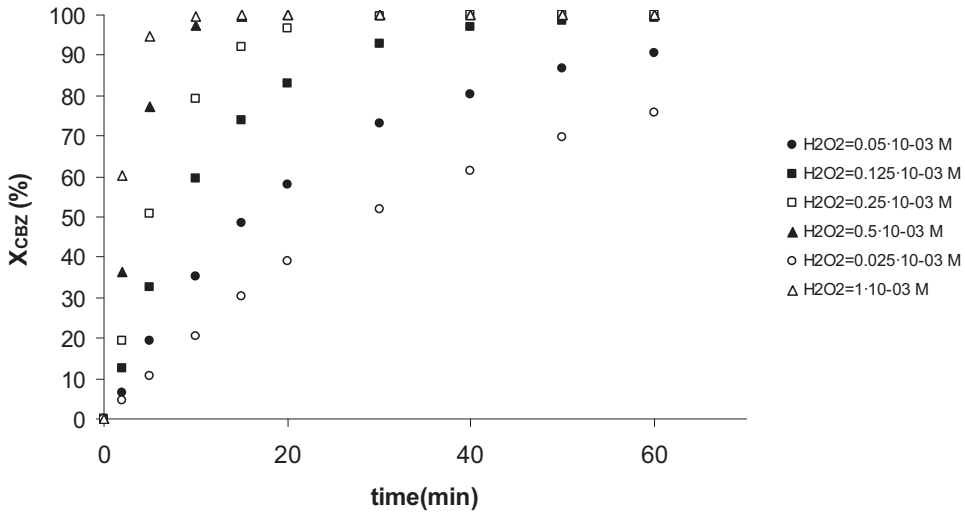

Fig. 7.1. Preliminary runs. Effect of the initial H_2O_2 concentration.

7.3.2. Experimental design and data analysis.

As indicated above, DOE is a useful tool to verify the effects of different variables and their interactions on the process response within a certain range and with a minimum number of experiments. According to the preliminary runs and taking into account the literature review previously performed [36,37] the pH, temperature and initial H_2O_2 concentration ranges were selected. Table 6.1 shows the operating levels of the DOE. On the other hand, Table 7.2 summarizes the experimental planning in the DOE and the obtained response in each experiment (i.e., removal of CBZ in percent, X_{CBZ}, %).

Table 7.1. Variables design. Operating levels.

pH			$[H_20_2]$ (mol·L^{-1})			T (ºC)		
Low level (-1)	High level (+1)	Center point	Low level (-1)	High level (+1)	Center point	Low level (-1)	High level (+1)	Center point
2.6	7.4	5	$1.0\cdot10^{-4}$	$4.0\cdot10^{-4}$	$2.5\cdot10^{-4}$	18.1	41.9	30

Table 7.2. Experimental planning in DOE and obtained response in each experiment.

Run	Coded pH	Coded [H_2O_2]	Coded T	X_{CBZ} (%)
1	0	0	0	91.0
2	0	0	0	92.5
3	0	0	0	91.3
4	-1.68	0	0	90.2
5	-1	1	1	97.5
6	-1	-1	-1	40.6
7	0	0	1.68	93.9
8	0	0	0	91.6
9	0	0	0	91.3
10	-1	-1	1	66.2
11	0	0	0	92.2
12	1	1	1	98.9
13	0	0	0	94.5
14	0	-1.68	0	7.7
15	1	-1	-1	47.4
16	1.68	0	0	90.9
17	1	1	-1	89.8
18	1	-1	1	72.6
19	0	0	0	91.9
20	0	0	-1.68	62.2
21	0	1.68	0	99.2
22	0	0	0	91.9
23	-1	1	-1	91.7

Numerical analysis

The values of the ANOVA test results are summarized in Table 7.3. According to the RSM, nine factors are considered. It is worth noting that five of them exhibit a p-value below 0.05 (significance limit), which indicate that such factors exert a statistically significant effect on the response variable, X_{CBZ} at 95% of confidence.

Table 7.3. ANOVA results.

Factor	Sum of squares	Degrees of freedom	*F* -ratio	*p*-values
A:Coded $[H_2O_2]_0$	6810.88	1	323.87	0.0000
B:Coded pH	14.1012	1	0.67	0.4276
C:Coded T	1037.14	1	49.32	0.0000
A	2720.59	1	129.37	0.0000
A	23.4613	1	1.12	0.3101
A	161.101	1	7.66	0.0160
B	0.01596	1	0.00	0.9784
B	1.05125	1	0.05	0.8266
C	305.904	1	14.55	0.0021
Total error	273.388	13	21.0298	

Non-linear polynomial regression was carried out and the following expression was obtained accordingly:

$$X_{CBZ}(\%) = 91.96 + 22.33 \cdot H_2O_2 + 1.023 \cdot pH + 8.73 \cdot T - 13.07 \cdot H_2O_2^{\,2} \\ -1.71 \cdot H_2O_2 \cdot pH - 4.49 \cdot H_2O_2 \cdot T + 0.044 \cdot pH^2 + 0.378 pH \cdot T - 4.38 \cdot T^2 \quad (7.4)$$

An excellent correlation factor r^2 equal to 0.96 was obtained. This regression leads to an optimum X_{CBZ} (equal to 100%) at values of pH equal to 1, temperature equal to 35.6 ºC and hydrogen peroxide concentration equal to $0.38 \cdot 10^{-3}$ mol·L^{-1}. For each experiment, the difference between experimental X_{CBZ} and calculated X_{CBZ} according to Eq. (7.4) is represented in Figure 7.2 (a) versus the specific run number. No correlation can be appreciated since residuals are located in a random order to both

sides of the 0 axis. Hence, it may be concluded that the randomization of the design is fully working and no accumulation of experimental error is observed.

Also, for each experiment Figure 7.2 (b) represents the observed X_{CBZ} versus the values of X_{CBZ} calculated according to Eq. (7.4). A good correlation between both parameters may be observed. This latter also corroborates that the randomization of the design has been properly planned and performed, so that accumulation of experimental error may be discarded.

a)

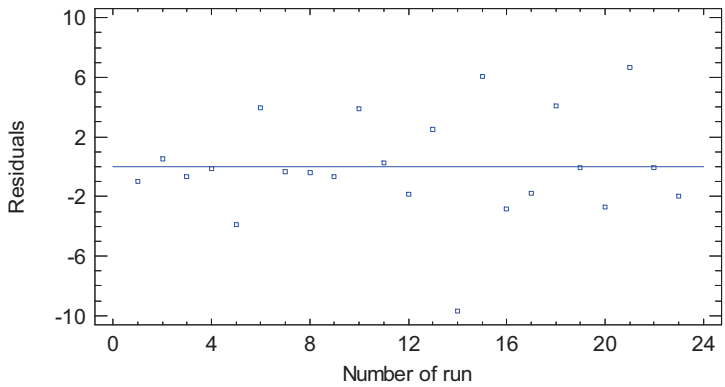

b)

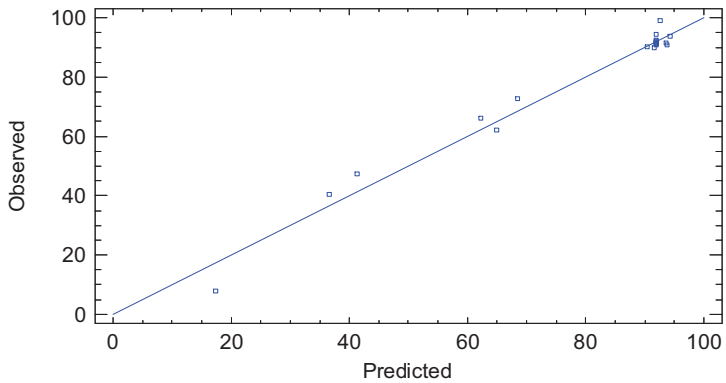

Fig. 7.2. Residuals versus run number (a) and observed vs. predicted X_{CBZ} correlation (b).

Graphical analysis

Modelization was made on the basis of fourteen factors which correspond to Eq. (7.4). The so-called Pareto plot (see Figure 7.3, left) is a graphical expression of the ANOVA test results. Bars represent the standardized effects of each involved factor, considering them as the initial concentration of H_2O_2, pH and temperature and combinations of all them. Grey bars are a graphical representation of positively-affecting factors, such as H_2O_2 concentration, pH, T, the combination of pH-T and the squared pH. This means that these factors appear in Eq. (7.4) behind a positive sign. On the other hand, blue bars represent negatively-affecting factors, such as the squares of H_2O_2 and T, and the combinations of H_2O_2-pH and H_2O_2-T. It may be observed that these factors appear in Eq. (7.4) behind a negative sign. The vertical rule that stands close to 2 is related with the signification level of ANOVA test, which is equal to 95% of confidence. Factors reaching this rule (e.g., A, C, AA, CC and AC) are within the significant region, while the remaining ones have no significance in the final response. The Pareto plot also provides an idea on how factors influence the final response, X_{CBZ}. Positive (grey) bars indicate that by varying a given variable the value of X_{CBZ} increases. Negative (blue) bars indicate the opposite.

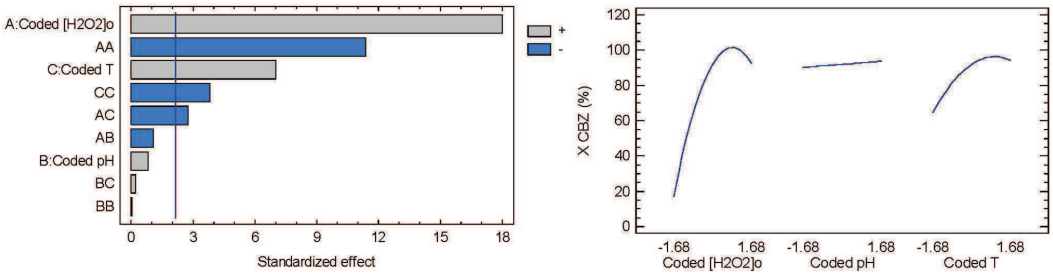

Fig. 7.3. Pareto plot of standardized effects (left) and main effects plot of initial H_2O_2 concentration, pH and temperature (right).

The application of the CCORD model also makes it possible to analyze the main effects of the involved variables. Such effects can be observed in Figure 7.3 (right). Three curves are drawn representing the effect of varying each variable (from -1.68 up to +1.68) while the other ones are kept constant in their respective central values. A

maximum is shown in the final part of the curve in the case of H_2O_2 initial concentration and temperature. On the contrary, pH shows an insignificant positive influence along the whole operation interval. This will be clearly appreciated in the response surface and contour plot figures that will be discussed below. Figure 7.3 (right) also illustrates that initial H_2O_2 concentration is the main factor governing the CBZ removal, followed by temperature.

With regard to the interaction between variables, Figure 7.4 shows the interaction between each two of the three variables studied. Each pair of curves represents the evolution of X_{CBZ} by varying one variable in the extremes of the CCORD model, that is, with its pair variable equal to +1.68 (upper plot) and equal to -1.68 (lower plot). The fact that the curves do not present a parallel behavior involves that interaction occurs and the modification of one of the variables affects the other one. Accordingly, from Figure 7.4 it may be concluded that interaction clearly appears between the pairs of variables AB and AC. On the contrary, the curves corresponding to the pair of variables BC in Figure 7.4 exhibit almost parallel behavior. Thus, it may be assumed that no interaction takes place in this case and the modification of one of the variables does not affect the other one.

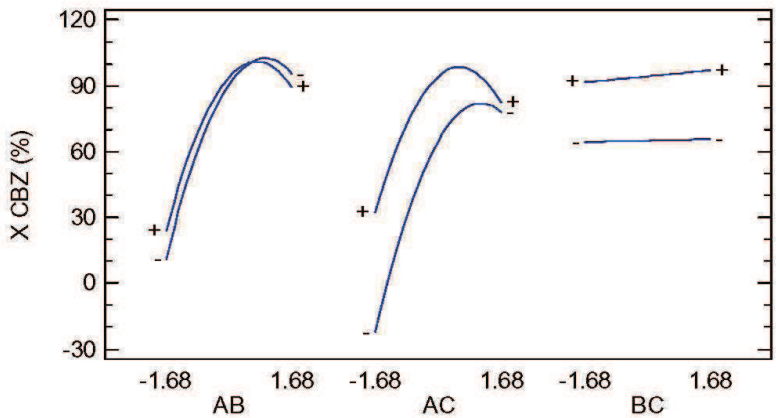

Fig. 7.4. Interaction graphic for initial H_2O_2 concentration, pH and temperature.

Response surfaces and contour plots

The surface plot is the most important graphical representation in the RSM (see Figure 7.5). It constitutes a graphical representation of Eq. (7.4) and makes it possible to evaluate the behavior of the whole system under study from a qualitative point of view. As it can be appreciated, within the region here studied response is represented by a convex surface. One of the three variables (namely, $[H_2O_2]_0$) supposes the most important affection on the target variable X_{CBZ} and an optimum, represented by a maximum in the surface plot, is obtained. The variable T presents an intermediate influence, while pH appears to affect X_{CBZ} in a very limited manner.

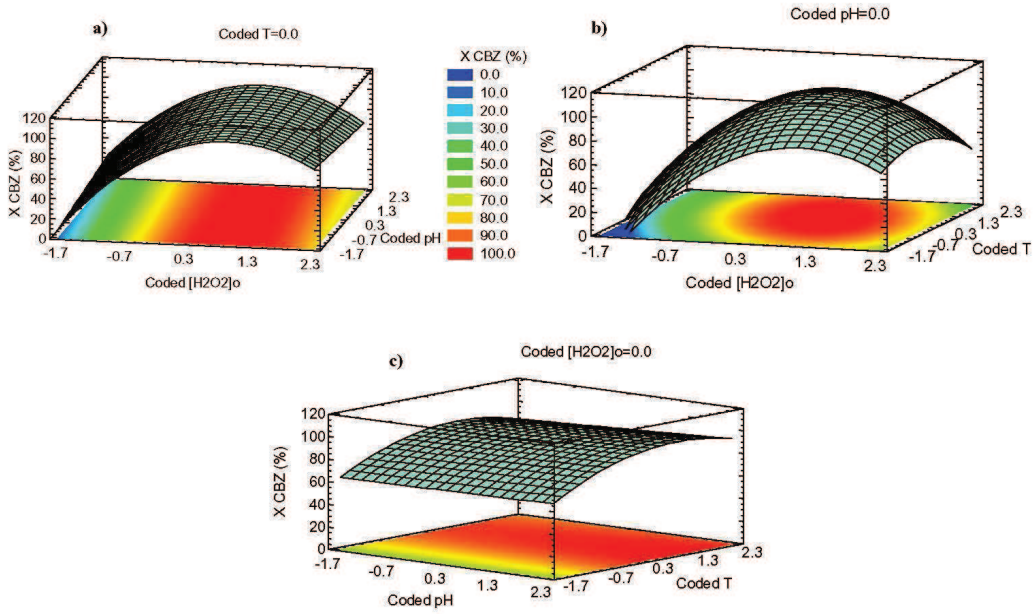

Fig. 7.5. Response surfaces, a) $[H_2O_2]_0$-pH; b) $[H_2O_2]_0$-T; c) pH-T.

The contour plots, which are depicted in the same Figure 7.5 below the surface plot, are also very useful in order to identify the optimal operation conditions. The maximum (i.e., X_{CBZ}= 100%) appears in the positive side of coded H_2O_2 concentration and T, as well as in the negative zone of coded pH. Quantitatively, a statistical analysis of the model yields optimal coded values of +0.88 for H_2O_2 initial

concentration, -1.68 for pH and +0.47 for T. Such values, once decoded, are equivalent to $[H_2O_2]_0$= 0.38·10^{-3} mol·L^{-1}, pH= 1 and T= 35.6 ºC. In Figure 7.5 a) and c) it may also be appreciated the scarce influence of pH on this process.

As two of the three factors are inside the significant region of the model (that is, two of them are statistically significant as their *p*-values are under 0.05), this optimum may be considered as statistically different from other near points. It is worth noting that a maximum value of X_{CBZ} equal to 100% of CBZ removal can be reached, at least theoretically.

Experimental confirmation of the theoretical maximum

In order to test if the theoretical maximum predicted by the model is achieved in practice, an experiment was carried out under the optimal conditions (i.e., $[H_2O_2]_0$=0.38·10^{-3} mol·L^{-1} and T= 35.6 ºC), X_{CBZ}, TOC and COD being determined as indicated above. According to the DOE analysis, the effect of pH is not significant. Hence, the experiment was carried out at pH= 7. Table 7.4 summarizes the obtained results for the experiment carried out under optimal conditions. It may be concluded that, after 10 min of reaction time, the removal of CBZ resulted to be equal to 100% as predicted by the model. On the other hand, in the same Table the evolution of COD and TOC within the time interval comprised between 10 and 120 min can be appreciated. Once elapsed this time, the values of COD and TOC resulted to be equal to 43% and 58%, respectively.

This experimental result corroborates the appropriateness of the DOE and RSM strategies performed in the present study.

Table 7.4. Results of the experiment performed under optimal conditions.

Time (min)	X_{CBZ} (%)	X_{COD} (%)	X_{TOC} (%)
10	100	3	7
30	100	13	30
60	100	30	43
90	100	40	52
120	100	43	58

Influence of variables

As indicated above, H_2O_2 initial concentration appears to exert the most significant influence among all the studied variables. In fact, data summarized in Table 6.2 show a dramatic fall in X_{CBZ} for run number 14 (X_{CBZ}= 7.7%). In this particular experiment, the coded value of $[H_2O_2]_0$ is -1.68, which corresponds to a total absence of hydrogen peroxide in solution. This fact is consistent with other previously published results. For instance, Vogna et al. [38] compared direct photolysis of carbamazepine during UV/H_2O_2 and UV treatment and found that direct photolysis of carbamazepine was negligible in the absence of H_2O_2. This fact may be explained taking into account that the hydroxyl radical generation is due to the hydrogen peroxide decomposition. In this connection, it must be born in mind that CBZ is considerably soluble at the investigated concentrations in water and non-volatile, (e.g. Henry's law constant is $4.73 \cdot 10^{-12}$ atm·m^3·mol^{-1}) [39]. Hence, hydroxyl radical-induced reactions are likely to be the main pharmaceutical degradation mechanism [40]. As a consequence, the UV-photolytic degradation without oxidant is scarcely relevant as indicated by Sichel et al [41]. The same results have been reported in the literature [36,37,42].

However, according to the DOE here applied the hydrogen peroxide concentration exhibits an optimum in the final part of the curve i.e., at a coded value equal to +0.88, which is equivalent to $[H_2O_2]_0$= $0.38 \cdot 10^{-3}$ mol·L^{-1}. This optimum can be explained taking into account that an increase of H_2O_2 concentration may promote radicals scavenging [43]. The scavenging process (Eq. (7.5)) results in the formation of another radical ($HO_2\cdot$), which has an oxidation potential considerably smaller than HO· [30]. Particularly, Naddeo et al. [40] have reported that in air-saturated media oxygen atoms are formed through molecular oxygen dissociation (Eq. (7.6)). Under such conditions hydroperoxyl radical may also be formed through the reaction of molecular oxygen with hydrogen atoms (Eq. (7.7)). Finally, $HO_2\cdot$ can also dimerize to regenerate H_2O_2 (Eq. (7.8)):

$$H_2O_2 + \cdot O \rightarrow HO\cdot \qquad (7.5)$$

$$O_2 \rightarrow O\cdot + O\cdot \quad (7.6)$$

$$O_2 + H\cdot \rightarrow HO_2\cdot \quad (7.7)$$

$$HO_2\cdot + HO_2\cdot \rightarrow H_2O_2 + O_2 \quad (7.8)$$

The second variable in importance was found to be temperature. The statistical analysis of the model yielded to an optimum at a coded value equal to +0.47, which corresponds to T= 35.6 ºC. The influence of temperature on the removal of CBZ by advanced oxidation processes and, particularly, by UV/H_2O_2 photooxidation has been scarcely studied. Other researchers have reported an increase in both, the removal rate [44] and the removal efficiency [44,45] as the operation temperature rises. Nevertheless, when increasing the operation temperature it must be taken into account the fact that hydrogen peroxide tends to decompose into oxygen and water [25], which would negatively affect the effectiveness of the removal process. Thus, an operation temperature of 35.6 ºC is compatible simultaneously with the speeding up of the oxidation process as well as with an adequate thermal stability of hydrogen peroxide towards its decomposition into oxygen and water, which justifies the occurrence of an optimum for such a value of temperature.

With respect to the non-significant influence of pH, several researchers have obtained similar results with other organic products [46]. In the present work, although the model indicates that this variable lacks of statistical significance an optimum value was obtained at a coded pH equal to -1.68. In the case of CBZ Vogna et al. [38] demonstrated that degradation by UV/H_2O_2 treatment was not affected by changing the pH of the solution in the range of 2.0-8.0. Klamerth et al [47] also reported the scarce effect of pH on the removal of CBZ from MWTP effluents. This is an important advantage of the UV/H_2O_2 advanced oxidation process with respect to other commonly-used procedures as, for instance, photo-Fenton. In this latter process it has been demonstrated that it is necessary to operate at a pH below 3 (typically pH= 2.8, as the most powerful UV-Vis light absorbing Fe-aqua complexes are formed at this pH) because Fe (III) hydroxides tend to precipitate at higher pH [48]. It has also been

reported in the literature [45] that excessive amounts of free radical scavengers may be formed in the presence of high alkalinity, thus difficulting the removal of pollutants.

On the other hand, it must be taken into account that the CBZ molecule exhibits a pK_a as high as 13.9 [49]. Hence, this molecule does not suffer any appreciable dissociation along the whole pH interval, which also justifies the scarce influence of this variable.

7.4. CONCLUSIONS.

From the results obtained in the present study the following conclusions may be drawn:

• A factorial central composite orthogonal and rotatable design of experiments has been used to analyze the influence of the operating conditions on the photooxidation of Carbamazepine by UV irradiation in the presence of hydrogen peroxide. H_2O_2 initial concentration exerts the most significant influence among all the studied variables. This suggests that the degradation takes place through a hydroxyl radical-induced mechanism.

• Temperature also exerts a noticeable effect on CBZ degradation, which is attributable to the fact that hydrogen peroxide tends to decompose into oxygen and water as temperature rises.

• The pH exerts a non-significant effect on the degradation of CBZ from the statistical standpoint. This appears to be related to the high pK_a of CBZ, which involves that this molecule does not suffer any appreciable dissociation along the whole pH interval.

7.5. REFERENCES.

[1] Acero, J.L.; Benítez, F.; Beltrán de Heredia, J.; Leal, A. "Chemical treatment of cork-processing wastewaters for potential reuse". J. Chem. Technol. Biotechnol. 79, 1065 **(2004)**.

[2] CRC handbook of chemistry and physics: a ready-reference book of chemical and physical data, CRC Press, Boca Raton, FL **(2012)**.

[3] Mendez-Díaz, J.; Sánchez-Polo, M.; Rivera-Utrilla, J.; Canonica, S.; Von Gunten, U. "Advanced oxidation of the surfactant SDBS by means of hydroxyl and sulphate radicals". Chem. Eng. J. 163, 300 **(2010)**.

[4] Matilainen, A.; Sillanpä, A. "Removal of natural organic matter from drinking water by advanced oxidation processes". Chemosphere. 80, 351 **(2010)**.

[5] López, A.; Bozzi, A.; Mascolo, G.; Kiwi, J. "Kinetic investigation on UV and UV/H_2O_2 degradations of pharmaceutical intermediates in aqueous solution". J. Photochem. Photobiol. A 156, 121 **(2003)**.

[6] Ince, N.; Apikyan, I. "Combination of activated carbon adsorption with light-enhanced chemical oxidation via hydrogen peroxide". Water Res. 34, 4169 **(2000)**.

[7] Ikehata, K.; Naghashkar, NJ.; Ei-Din, M G. "Degradation of aqueous pharmaceuticals by ozonation and advanced oxidation processes: A review". Ozone Sci. Eng. 28, 353 **(2006)**.

[8] Bautista, P.; Mohedano, A.; Casas, J.; Zazo, J.; Rodríguez, J. "An overview of the application of fenton oxidation to industrial wastewaters treatment". J. Chem. Technol. Biotechnol. 83, 1323 **(2008)**.

[9] Zhang, Y.Y.; He, C.; Sharma, VK.; Li, XZ.; Tian, SH,; Xiong, Y. "A new reactor coupling heterogeneous fenton-like catalytic oxidation with membrane separation for degradation of organic pollutants". J. Chem. Technol. Biotechnol. 86, 1488 **(2011)**.

[10] Pérez-Moya, M.; Mansilla, H.; Graells, M. "A practical parametrical characterization of the fenton and the photo-fentonsulfamethazine treatment using semi-empirical modeling". J. Chem. Technol. Biotechnol. 86, 826 **(2011)**.

[11] Andreozzi, R.; Caprio, V.; Marotta, R. "Oxidation of benzothiazole,2-mercaptobenzothiazole and 2-hydroxybenzothiazole in aqueous solution by means of H_2O_2/UV or photoassisted fenton systems". J. Chem. Technol. Biotechnol. 76, 196 **(2001)**.

[12] Ma, X.; Zhou, M. "A comparative study of azo dye decolorizationby electro-fenton in two common electrolytes". J. Chem. Technol. Biotechnol. 84, 1544 **(2009)**.

[13] Panizza, M.; Cerisola, G. "Electrochemical oxidation as a final treatment of synthetic tannery wastewater". Environ. Sci. Technol. 38, 5470 **(2004)**.

[14] Loppinet-Serani, A.; Aymonier, C.; Cansell, F. "Supercritical water for environmental technologies". J.Chem. Technol. Biotechnol. 85, 583 **(2010)**.

[15] Serpone, N.; Horikoshi, S.; Emeline, A. "Microwaves in advanced oxidation processes for environmental applications. A brief review". J. Photochem. Photobiol. 11, 114 **(2010)**.

[16] Kim, KH.; Ihm, SH. "Heterogeneous catalytic wet air oxidation of refractory organic pollutants in industrial wastewaters: A review". J. Hazard. Mater. 186, 16 **(2011)**.

[17] Chang, J. "Thermal plasma solid waste and water treatments: A critical review". Int. J. Plasma Environ. Sci. Technol. 3, 67 **(2009)**.

[18] Vilhunen, S.; Sillanpää, M. "Recent developments in photochemical and chemical AOPs in water treatment: A mini-review". Rev. Environ. Sci. Biotechnol. 9, 323 **(2010)**.

[19] Umar, M.; Aziz, H.; Yusoff, M. "Trends in the use of Fenton, electro-Fenton and photo-Fenton for the treatment of landfill leachate". Waste Manage. 30, 2113 **(2010)**.

[20] Di Paola, A.; García-López, E.; Marcì, G.; Palmisano, L. "A survey of photocatalytic materials for environmental remediation". J. Hazard. Mater. 211, 3 **(2012)**.

[21] Adewuyi, Y. "Sonochemistry in environmental remediation. Combinative and hybrid sonophotochemical oxidation processes for the treatment of pollutants in water". Environ. Sci. Technol. 39, 3409 **(2005)**.

[22] Deng, Y. "Advanced oxidation processes (AOPs) for reduction of organic pollutants in landfill leachate: A review". Int. J. Environ. Waste Management. 4, 366 **(2009)**.

[23] Kurniawan, T.; Lo, WH. "Chan G. Radicals-catalyzed oxidation reactions for degradation of recalcitrant compounds from landfill leachate". Chem. Eng. J. 125, 35 **(2006)**.

[24] Anglada, A.; Rivero, M.; Ortiz, I.; Urtiaga, A. "Effect of dye auxiliaries on the kinetics of advanced oxidation UV/H_2O_2 of acid orange 7 (AO7)". J. Chem. Technol. Biotechnol. 83, 1339 **(2008)**.

[25] Beltrán-Heredia, J.; Torregrosa, J.; Domínguez, J. R.; Peres, J. "Kinetics of the oxidation of p-hydroxybenzoic acid by the H_2O_2/UV system". Ind. Eng. Chem. Res. 40, 3104 **(2001)**.

[26] Snyder, S.; Westerhoff, P.; Yoon, Y.; Sedlak, D. "Pharmaceuticals, personal care products, and endocrine disruptors in water: implication for the water industry". Environ. Sci. Technol. 37, 286 **(2003)**.

[27] Clara, M.; Strenn, B.; Kreuzinger, N. "Carbamazepine as a possible anthropogenic marker in the aquatic environment: Investigations on the behaviour of carbamazepine in wastewater treatment and during groundwater infiltration". Water Res. 38, 947 **(2004)**.

[28] Benítez, F.; Real, F.; Acero, J.L.; Roldán, G. "Removal of selected pharmaceuticals in waters by photochemical processes". J. Chem. Technol. Biotechnol. 84, 1186 **(2009)**.

[29] Joss, A.; Zabczynski, S.; Göbel, A.; Hoffmann, B.; Loffler, D.; McArdell, C.; Ternes, T,.; Thomsen, A.; Siegrist, H. "Biological degradation of pharmaceuticals in municipal wastewater treatment: Proposing a classification scheme". Water Res. 40, 1686 **(2006)**.

[30] Arslan-Alaton, I.; Tureli, G.; Olmez-Hanci, T. "Treatment of azo dye production wastewaters using photo-Fenton-like advanced oxidation processes: Optimization by response surface methodology". J. Photochem. Photobiol. 202, 142 **(2009)**.

[31] Riter, LS.; Vitek, O.; Gooding, KM.; Hodge, BD. "Julian R.K Jr. Statistical design of experiments as a tool in mass spectrometry". J. Mass Spectrom. 40, 565 **(2005)**.

[32] Arslan-Alaton, I.; Akin, A.; Olmez-Hanci, T. "An optimization and modeling approach for H_2O_2/UV-C oxidation of a commercial non-ionic textile surfactant using central composite design". J. Chem. Technol. Biotechnol. 85, 493 **(2010)**.

[33] Bezerra, M.; Santelli, R.; Oliveira, E.; Villar, L.; Escaleira, L. "Response surface methodology (RSM) as a tool for optimization in analytical chemistry". Talanta 76, 965 **(2008)**.

[34] Betianu, C.; Caliman, F.; Gavrilescu, M.; Cretescu, I.; Cojocaru, C.; Poulios, I. "Response surface methodology applied for orange II photocatalytic degradation in TiO_2 aqueous suspensions". J. Chem. Technol. Biotechnol. 83, 1454 **(2008)**.

[35] Domínguez, J.R.; González, T.; Palo, P.; Cuerda-Correa, E. "Fenton + Fenton- like integrated process for carbamazepine degradation: Optimizing the system". Ind. Eng. Chem. Res. 51, 2531 **(2012)**.

[36] Rosario-Ortiz, F.; Wert, E.; Snyder, S. "Evaluation of UV/H_2O_2 treatment for the oxidation of pharmaceuticals in wastewater". Water Res. 44, 1440 **(2010)**.

[37] Kim, I.; Yamashita, N.; Tanaka, H. "Photodegradation of pharmaceuticals and personal care products during UV and UV/H_2O_2 treatments". Chemosphere. 77, 518 **(2009)**.

[38] Vogna, D.; Marotta, R.; Andreozzi, R.; Napolitano, A.; d'Ischia, M. "Kinetic and chemical assessment of the UV/H_2O_2 treatment of antiepileptic drug carbamazepine". Chemosphere. 54, 497 **(2004)**.

[39] Zhang, Y.; Geissen, SU.; Gal, C. "Carbamazepine and diclofenac: Removal in wastewater treatment plants and occurrence in water bodies". Chemosphere. 73, 1151 **(2008)**.

[40] Naddeo, V.; Eric, S.; Kassinos, D.; Belgiorno, V.; Guida, M. "Fate of pharmaceuticals in contaminated urban wastewater effluent under ultrasonic irradiation". Water Res. 43, 4019 **(2009)**.

[41] Sichel, C.; Garcia, C.; Andre, K. "Feasibility studies: UV/chlorine advanced oxidation treatment for the removal of emerging contaminants". Water Res. 45, 6371 **(2011)**.

[42] Im, JK.; Cho, IH.; Kim, SK.; Zoh, KD. "Optimization of carbamazepine removal in O_3/UV/H_2O_2 system using a response surface methodology with central composite design". Desalination. 285, 306 **(2012)**.

[43] Achilleos, A.; Hapeshi, E.; Xekoukoulotakis, N.; Mantzavinos, D.; Fatta-Kassinos, D. "Factors affecting diclofenac decomposition in water by UV-A/TiO_2 photocatalysis". Chem. Eng. J. 161, 53 **(2010)**.

[44] Mandal, T.; Maity, S.; Dasgupta, D.; Datta, D. "Advanced oxidation process and biotreatment: Their roles in combined industrial wastewater treatment". Desalination. 250, 87 **(2010)**.

[45] Monteagudo, J.; Rodriguez, L.; Villasenor, J. "Advanced oxidation processes for destruction of cyanide from thermoelectric power station waste waters". J. Chem. Technol. Biotechnol. 79, 117 **(2004)**.

[46] Benítez, F.; Beltrán-Heredia, J.; González, T.; Real, F. "Photooxidation of carbofuran by a polychromatic UV irradiation without and with hydrogen peroxide". Ind. Eng. Chem. Res. 34, 4099 **(1995)**.

[47] Klamerth, N.; Rizzo, L.; Malato, S.; Maldonado, M.; Aguëra, A.; Fernández-Alba, A. "Degradation of fifteen emerging contaminants at μg L−1initial concentrations by mild solar photo-Fenton in MWTP effluents". Water Res. 44, 545 **(2010)**.

[48] Klamerth, N.; Malato, S.; Aguëra, A.; Fernández-Alba, A.; Mailhot, G. "Treatment of municipal wastewater treatment plant effluents with modified photo-Fenton as a tertiary

treatment for the degradation of micro pollutants and disinfection". Environ. Sci. Technol. 46, 2885 **(2012)**.

[49] Jones, O.; Voulvoulis, N.; Lester, J. "Aquatic environmental assessment of the top 25 English prescription pharmaceuticals". Water Res. 36, 5013 **(2002)**.

TERCERA PARTE

CONCLUSIONES

CONCLUSIONES

De los resultados obtenidos en la presente Tesis Doctoral se pueden extraer las siguientes conclusiones finales:

Con respecto al Proceso de Adsorción:

- En la adsorción de los diferentes compuestos farmacéuticos estudiados (ketoprofeno, naproxeno, carbamacepina y trimetoprima) sobre la resina polimérica *Amberlite XAD-7* se obtuvieron muy buenos resultados tanto al tratar los compuestos individuales como formando parte de mezclas. De todos ellos, la carbamacepina es el contaminante que mejor se adsorbe.

- En el estudio cinético de la adsorción sobre resina, los datos experimentales se ajustaron a cuatro modelos teóricos, resultando ser el modelo de *pseudo-segundo orden* el que mejor simula el proceso. Con respecto al estudio del equilibrio de adsorción, los datos presentaron un buen ajuste al modelo de *Freundlich* y *Dubinin-Radushkevich.* Esto pone de manifiesto la presencia de sitios de adsorción enérgicamente heterogéneos en la superficie de la resina. La energía de adsorción media obtenida por el modelo de *Dubinin* (E= 8,3-10,1 $kJ \cdot mol^{-1}$) indica que la adsorción es física.

- En el estudio de la influencia de los diferentes parámetros (pH, concentración de adsorbente e inicial del fármaco, velocidad de agitación y temperatura) que intervienen en el proceso de adsorción de los fármacos seleccionados sobre la resina, se observó que el pH es la variable más influyente, excepto para carbamacepina. Esta influencia sobre la capacidad de adsorción es diferente para cada compuesto dependiendo de su naturaleza ácida, básica o neutra.

- En la comparación de los parámetros de *Freundlich* de los dos sistemas ensayados (fármaco individual y en mezcla) se concluyó que la capacidad de

adsorción en la mezcla disminuía para los compuestos ácidos y neutros (ketoprofeno, naproxeno y carbamacepina) y aumentaba para el compuesto básico (trimetoprima).

- En el empleo de adsorbentes naturales tanínicos, sintetizados previamente mediante gelificación, éstos mostraron una elevada eficacia de adsorción de trimetoprima. Diferentes *tanigeles* (extractos del pino, ciprés, acacia y quebracho) fueron testados con este compuesto para confirmar su capacidad de adsorción, establecer la influencia de variables del proceso de gelificación (tipo de extracto, aldehído empleado y su dosis), estudiar su comportamiento cinético y determinar las isotermas de equilibrio. Los resultados demostraron que el mejor extracto tanínico para este fin es el *Pinus pinaster* (pino) y *Cupressus sempervivens* (ciprés) con formaldehído concentrado, y *Schinopsis balansae* (quebracho) con formaldehido diluido. Así mismo, se puso de manifiesto una aceptable correlación en los ensayos de equilibrio (r^2 superior a 0,96 en todos los casos) y una capacidad máxima de adsorción alrededor de 370 $mg \cdot g^{-1}$ según el modelo de *Langmuir*. Estos datos declaran que la capacidad de adsorción de los *tanigeles*, en comparación con otros adsorbentes, como *Amberlite XAD-7*, es mucho más elevada para la retirada de trimetoprima.

Con respecto al Proceso de Oxidación Anódica con Diamante Dopado con Boro:

- La técnica de electro-oxidación con electrodo DDB resultó ser una opción muy interesante para la eliminación de los cuatro compuestos farmacéuticos seleccionados, debido fundamentalmente a su elevada eficacia y a la no producción de residuos peligrosos.

- Los resultados del diseño de experimentos llevado a cabo para cada uno de los compuestos elegidos con objeto de optimizar algunos de los parámetros que intervienen en el proceso (pH, intensidad de corriente, concentración de electrolito soporte y caudal de agua) indicaron que la intensidad de corriente es el factor más influyente en la eliminación de los productos farmacéuticos,

seguida de la dosis de electrolito soporte. Para todos los casos, se determinó un punto de operación óptimo en el cual se obtuvo un nivel de degradación del 100% del contaminante, alcanzándose elevados niveles de mineralización.

- En la comparación del proceso de oxidación anódica de carbamacepina en diferentes matrices acuosas (ultra-pura, pantano, río y efluente secundario EDAR) realizada desde un punto de vista cinético, las condiciones óptimas obtenidas para alcanzar el mayor valor de la *constante cinética de primer orden (k)* se consiguieron a bajas concentraciones de contaminante y elevadas intensidades de corriente. La eficacia del tratamiento se ve claramente influida por las matrices acuosas empleadas, observándose un incremento en la velocidad de degradación del contaminante cuanto mayor es el nivel de contaminación de las mismas y de su contenido en iones cloruro. Estos resultados indican la existencia de una segunda vía de oxidación indirecta o mediada por cloro. Así mismo, en el caso de las aguas menos contaminadas, la concentración inicial de carbamacepina resulta ser el factor más influyente, mientras que en el efluente de EDAR es la intensidad de corriente.

- El proceso de oxidación anódica es capaz de lograr altos niveles de eliminación de materia orgánica en aguas residuales altamente contaminadas y en tiempos de tratamiento relativamente cortos. En la optimización del proceso de depuración de un efluente residual de una industria farmacéutica, cuyo objetivo fue la eliminación de DQO y COT, se desarrolló un diseño de experimentos a diferentes tiempos, en los cuales la contribución de las variables de estudio fueron máximas. Referente a la influencia de variables, la densidad de corriente afecta de forma significativa y positivamente a la eliminación de las variables de estudio, mientras que la velocidad del flujo no presenta influencia significativa, por lo que puede deducirse que no favorece el transporte del contaminante a la superficie anódica.

Con respecto a los otros Procesos de Oxidación Avanzada aplicados:

- En el sistema integrado Fenton + Fenton-like, se observó que el proceso de Fenton fue la vía de oxidación principal de carbamacepina. Esta ruta predominante alcanzó un máximo para una relación molar de $[H_2O_2]_0/[Fe^{2+}]_0$= 11:1. El sistema Fenton-like se encuentra limitado a bajas concentraciones de hierro (III), sin embargo, esta vía de reacción aumenta de manera constante con la concentración de estos iones metálicos hasta llegar a un 50% de la vía Fenton. Con respecto al análisis de la influencia de variables en este proceso, mediante diseño de experimentos, se probó que la variable más influyente es la concentración inicial de H_2O_2, seguida de la concentración inicial de Fe^{2+}, pH y finalmente la concentración inicial de Fe^{3+}. Se alcanzó la degradación completa del compuesto farmacéutico en las condiciones óptimas: $[H_2O_2]_0$= 1,39·10^{-4} mol·L^{-1}, $[Fe^{2+}]_0$= 1,25·10^{-5} mol·L^{-1}, $[Fe^{3+}]_0$= 1,68·10^{-5} mol·L^{-1} y pH= 3,52.

- En la ozonación de carbamacepina, el estudio del proceso se realizó sobre una nueva variable objetivo que incluía términos de eficacia en la eliminación del contaminante y aspectos cinéticos. En la optimización de los parámetros que intervienen en el proceso, los resultados del diseño experimental indicaron que la concentración inicial de ozono es la variable más influyente, seguida de la concentración inicial de carbamazepina. Por el contrario, el caudal de aire a la entrada del reactor no presenta un efecto significativo en la variable respuesta. El valor óptimo, es decir, la máxima eliminación de compuesto con costes mínimos, se obtuvo con un caudal de aire de 55 L·h^{-1}, una concentración inicial de ozono de 0,4 g·m^{-3} y una concentración inicial de carbamacepina de 18 mg·L^{-1}.

- En la fotodegradación de carbamacepina en presencia de H_2O_2, se demostró que la oxidación del contaminante ocurre a través de un mecanismo radicalario, ya que la concentración inicial de H_2O_2 es la variable que mayor influencia ejerce en la eliminación del compuesto. La temperatura también

afecta al proceso significativamente, sin embargo el pH apenas tiene influencia en la degradación debido al elevado valor de pK_a de la carbamacepina. La eliminación total del fármaco se alcanzó a los 10 minutos de tratamiento en las condiciones óptimas establecidas: $[H_2O_2]_0$= $0{,}38 \cdot 10^{-3}$ $mol \cdot L^{-1}$, pH= 1 y T= 35,6 ºC.

En resumen, se puede concluir que los Procesos de Adsorción, de Oxidación química y Electroquímica aplicados al tratamiento de aguas en este trabajo de investigación, son muy eficaces para la eliminación de los compuestos farmacéuticos estudiados. Una vez conocidas las variables óptimas de operación de cada uno de los procesos, podría probarse su aplicabilidad a mayor escala. Su alta eficacia, así como la ausencia evidente de compuestos indeseables a la salida del tratamiento, hacen de los POAEs alternativas viables en instalaciones de mayor envergadura. Para dicho cambio de escala queda pendiente la comprobación de la sostenibilidad económica de todo el proceso y su eficacia a niveles reales de contaminación farmacéutica.